ISSUE 05/2026

ISSN 3071-9216

MEBUTRA

SCIENTIFIC JOURNAL OF THE DEPARTMENT OF CIVIL ENGINEERING, DEPARTMENT OF MECHANICAL ENGINEERING, DEPARTMENT OF ELECTRICAL ENGINEERING AND THE DEPARTMENT OF TRANSPORT OF STANISŁAW STASZIC ACADEMY OF APPLIED SCIENCES IN PIŁA

Akademia Nauk Stosowanych
im. Stanisława Staszica w Pile

EDITORIAL STAFF

j.mikolajczyk@ans.pila.pl | wydawnictwo@ans.pila.pl

SCIENTIFIC COMMITTEE

REVIEWERS

ISSN 3071-9216

Foreword

The year 2026 is the fifth year of publication of the MEBUTRA magazine, and this issue is its fifth edition. We are very happy and contented especially because at the turn of December 2025 and January 2026, an agreement was signed between Stanisław Staszic Academy of Applied Sciences in Piła and BAZ-TECH consortium on publishing the issues of MEBUTRA journal. This consortium brings together almost all universities and higher education institutions in Poland. Thus, the availability and reach of articles published in our Journal has increased significantly. Also, there is a potential growth of author citations and all related metrics. I would like to take this opportunity to encourage all students, especially students of the Department of Electrical Engineering, Department of Transport, Department of Mechanical Engineering and the Department of Civil Engineering of Stanisław Staszic Academy of Applied Sciences in Piła, to submit their articles.

ON BEHALF OF THE EDITORIAL STAFF

dr inż. Jarosław Mikołajczyk
jmikolajczyk@ans.pila.pl
(Chief Editor)

ISSN 3071-9216

Wydawca | Published by:
Akademia Nauk Stosowanych im. Stanisława Staszica w Pile, ul. Podchorążych 10, 64-920 Piła
Katedra Inżynierii Mechanicznej, Budynek J, pok. 33
(adres siedziby redakcji)
www.ans.pila.pl
https://wydawnictwo.ans.pila.pl

Spis treści

Continuously Variable Transmission – construction of laboratory device

inż. Agnieszka Noga

Department of Mechanical Engineering

Stanisław Staszic State University of Applied Sciences in Piła, Poland

https://orcid.org/0009-0005-4007-2679

corresponding e-mail: agnieszkajezewska@op.pl

Abstract:

This paper presents the construction of a continuously variable belt transmission test rig. It is driven by a single-phase electric motor found in old "Frania" washing machines. The designed and constructed transmission is characterized by a steady and quiet operation and smooth, manual speed control.

Keywords: continuously variable transmission, belt drive, variator

1. Introduction

Continuously variable transmission is a type of transmission that permits smooth regulation of the rotational speed on the output shaft. Thus, the continuously variable transmission is characterized by an infinitely large number of gear ratios in a certain operating range. There is a maximum and minimum gear ratio here and within these limits an infinitely large number of any gear ratios are possible. The history of the creation of continuously variable transmissions is over 100 years old, but at the beginning the development of this type of design solutions was not dynamic due to the high production cost, not very high durability and complicated control devices regulating the pressure supply to the actuators of the transmission, preventing pressure loss, belt slip, leaks, etc. In 1906, the first vehicles using continuously variable friction transmissions were created and for many years they did not gain recognition, remaining in the shadow of conventional gearboxes. Currently, new design solutions allow better use of the advantages of continuously variable transmissions, which is why they are becoming increasingly popular. The most valuable feature of this type of transmission is that it allows the machine speed to be changed at an unchanging constant engine speed, which can be controlled in correlation with the rotational speed at which, depending on the needs, the greatest power and torque can occur [18].

The contemporary continuous development of technology leads to the emergence of new problems resulting from the requirements placed on technical objects and the way they are operated in complex technical systems. This work aims to build a continuously variable transmission that will provide a smooth change of rotational speed and will allow the observation and recording of the operation of this type of structure.

2. Historical outline of the development and degree of application of continuously variable transmission in vehicles

The first vehicles with a continuously variable transmission appeared already a century ago but this type of gearbox gained wider application thanks to the solution developed by Hub van Doorne, and it was then, in 1965, that DAF vehicles were equipped with continuously variable Variomatic transmissions [4].

In 1877, Charles W. Hunt in the USA patented toroidal gears, in 1920 the first prototypes of these gears were created and a vehicle with such a gear was called a friction drive car.

Currently, CVT gears are characterized by a more interesting design and allow the use of the creep function, full synchronization with the ESP system, and setting driving modes.

Since the 1980s, the development of power transmission systems has been significantly associated with the increase in the number of gear ratios in gearboxes, despite the fact that at the very beginning gearboxes had only 3 or 4 gears. The first cars equipped with a five-speed transmission appeared at the end of the 20th century [11]. Nowadays, we can already see sports cars with nine gears and small city cars with transmissions of six gear ratios [12].

In the 20th century, solutions were used in which automatic transmissions were characterized by a smaller number of gears than manual transmissions, and today it is the other way around. This is due to the development of automation in general. The greater the number of gear ratios, the more often the driver is forced to change gears and

it is not comfortable. In vehicles with a continuously variable transmission, a properly programmed controller is responsible for changing gears, not the driver [3].

The vehicle dynamic index is the ratio of the excess driving force of the vehicle to the current resistance to motion related to the weight of the vehicle. The dynamic characteristics of the vehicle as a function of speed for the same vehicle, but two types of gearboxes, are presented in Fig. 1. The fields on the graph that are hatched in green lines are indicating the loss of power as a result of cooperation with the 5-speed manual gearbox. The overall efficiency of the drive system together with the engine depends on the size of these fields, i.e. on the need to pass through the lower efficiency engine speed zones. Therefore, it is good to use continuously variable transmissions as it will better utilize the characteristics of the combustion engine.

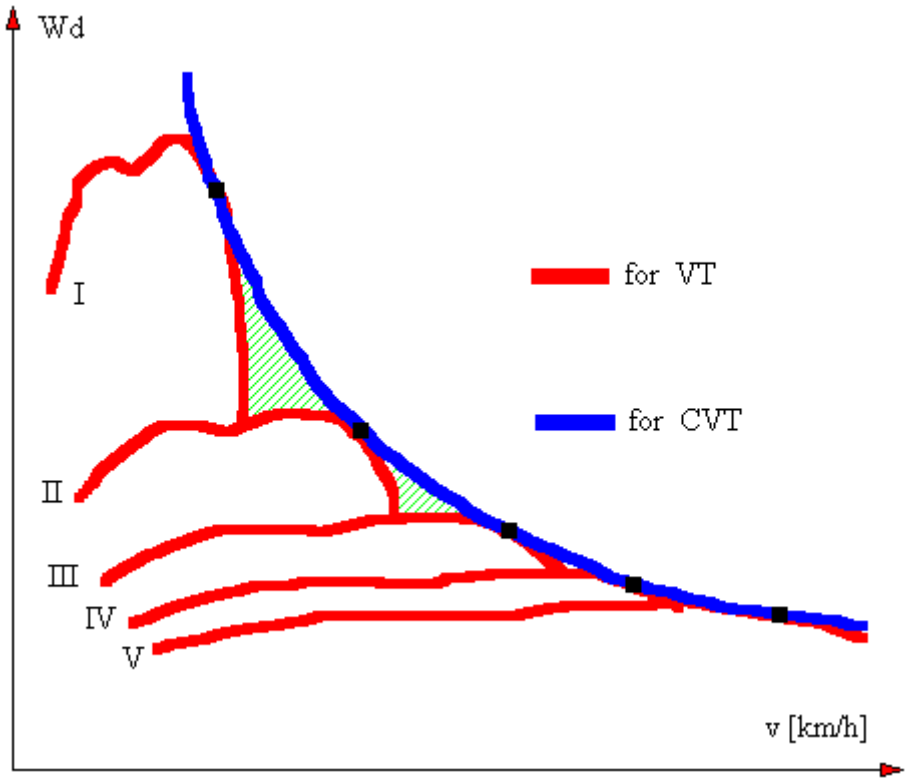

Fig. 1. Dependence of the vehicle dynamic index on the vehicle speed for two types of gearboxes [12]
Wd – vehicle dynamic index; v [km/h] – driving speed; CVT – continuously variable transmission; VT – stepped transmission; I, II, III, IV, V – individual gears of a stepped transmission

The distribution of the global gearbox market is constantly changing. In 2010, about 6% of CVT gearboxes were installed in passenger cars [21], and in 2013 their share increased to 9% [95].

As we already know, gearboxes are mechanisms that allow you to change the ratio of the drive system in order to adapt the engine parameters to changing needs. That is, they allow you to obtain the optimal engine speed depending on the load and driving speed at a given moment [12].

There are several criteria for dividing gearboxes and they can be divided according to the applied transmission, control method and the most commonly used

gearboxes in the automotive industry. One of the more popular criteria is the division of gearboxes according to the control method, where the following gearboxes are distinguished: manual, semi-automatic (sequential) and automatic.

Manual gearboxes are most often gearboxes with stepped transmissions, in which drivers - through a lever system - can operate by switching the appropriate gear (transmission) when pressing the clutch pedal. These gearboxes consist mainly of a set of gear wheels mounted on the main, intermediate and clutch shafts, as well as a mechanism for shifting them. The gear wheel mounted on the clutch shaft transfers the drive to the gear wheel mounted on the intermediate shaft. Pairs of wheels responsible for specific gears are mounted on the main shaft and the last shaft, where activating a given gear disconnects the remaining gear wheels. The gearboxes also contain bearings for securing the shafts, and sealants, the task of which is to prevent oil leakage from the gearbox. Whereas the gear wheels have synchronizers and gear clusters that allow for faster equalization of the rotational speeds of the coupled elements. Nowadays, you can find a reverse gear engagement sensor in newer gearboxes which activates the reversing lights. Manual gearboxes are distinguished by the use of two different solutions for changing gear ratios. They use direct gear ratio and overdrive. In the first case, the clutch shaft is connected directly to the main shaft and in this way their rotational speeds are the same, i.e. the direct gear ratio is 1:1.

In semi-automatic gearboxes, transmisson shifting is automatic and takes place using control devices, and the appropriate gear is selected by the driver. The design of this gearbox is not much different from the manual gearbox, it has most of the same elements, and only differs in design by the control system. It is also equipped with a hydraulic pressure accumulator, an electronic controller, a selected gear ratio sensor, a selector actuator and a selector shaft. The hydraulic actuator is assisted by an electric pump and operates a dry clutch cooperating with the mechanical transmission.

Unlike other gearboxes, automatic ones operate with little involvement of the driver because the optimum gear ratio for the given conditions is selected automatically. And the driver sets the operating range only using a button or lever, e.g. "forward", "reverse" or "park". A gearbox with automatic control differs from a classic automatic in its construction and the method of power transmission. Automatic gearboxes are equipped with a torque converter or a hydrokinetic clutch, while manual gearboxes are equipped with standard clutches. These gearboxes also consist of transmission assemblies and control assemblies. The transmission assemblies constitute planetary gear systems. External electronic systems are usually responsible for control in newer automatic gearboxes, while the actuating elements of the computers that manage the gearbox operation are "internal" solenoid valves. Using the automatic gearbox software, the vehicle speed and other parameters responsible for correct driving can be measured. Based on the collected data, a self-acting and optimal gear change in relation to speed is created.

The DSG dual-clutch gearbox solution combines the best features of a classic automatic gearbox and a manual gearbox. The operating principle of this gearbox is mainly based on a system of two parallel gearboxes placed in one housing. This mechanism has two separate multi-plate clutches (dry or wet), which transmit drive to the appropriate pairs of gears via two separate clutch shafts. When changing gears, one clutch starts working, and the other simultaneously disengages, thus transferring drive to the next gears. When one clutch operates the even gears, the other operates the odd gears.

Changing gears in DSG transmissions takes approximately 300-400 milliseconds, because when driving in a given gear, the next one is always "waiting

ready". The computer determines which gear should be ready for immediate engagement and then activates it using hydraulic actuators.

In CVT gearboxes, the principle of operation is based on the transfer of torque using a belt cooperating with conical pulleys. These continuously variable gearboxes operate similarly to scooter transmissions. The principle of operation and construction of a CVT gearbox is not complicated. The gearbox consists of a metal belt or chain moving along the tracks of two sets of variable-diameter conical pulleys, thereby changing the gear ratio.

3. Changing gear ratios in continuously variable transmissions

The value of the axial force generated in the active wheel and the passive wheel influences the gear ratio change in continuously variable transmissions, the clamping force can be obtained using a hydraulic system (Fig. 2).

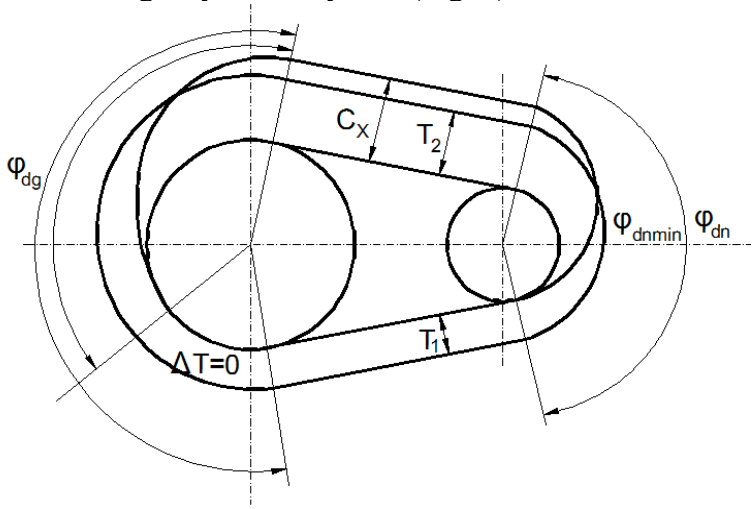

Fig. 2. Distribution of the compressive force for a small-ratio transmission and tension forces in the belt T [97]
C_x - compressive force between segments; T_1, T_2 – belt tension force; φ_{dg} – limiting angle of wrap of the driven pulley; φ_{dn} – angle of wrap of the driving pulley; φ_{dnmin} – minimum angle of wrap of the driving pulley

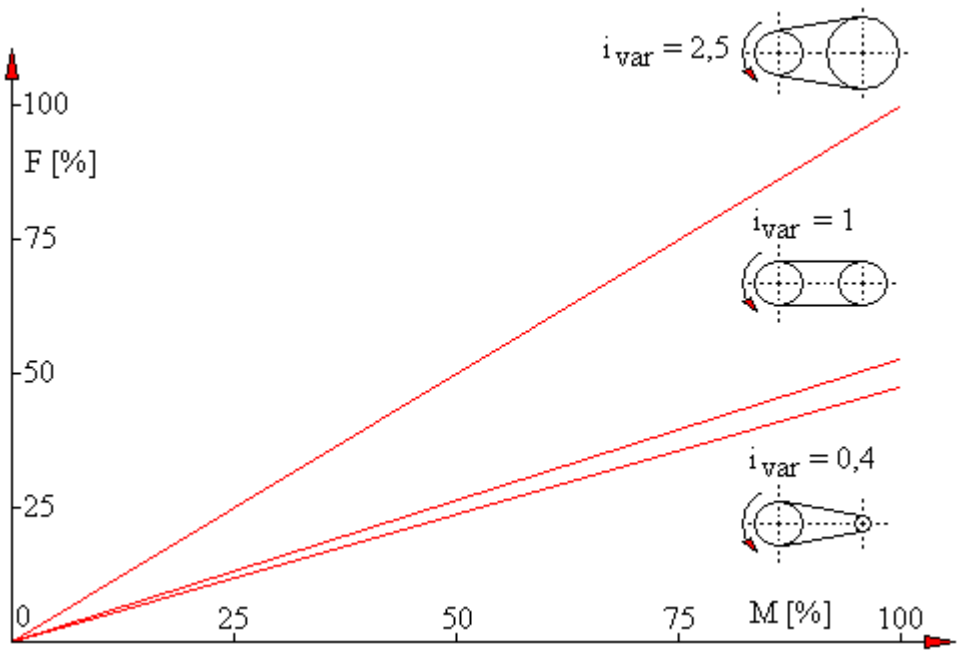

Fig. 3. Relationship between axial force and transmitted torque [18]
i_{var} – variator ratio; F [%] – axial force; M [%] - torque

From the relationship between axial force and transmitted torque, shown in Fig. 3 and marked with red lines, it can be read that with the increase in the transmitted torque, the value of the clamping force increases. To ensure the lowest possible belt slip for large changes in the torques loading the gears, the value of the axial force should be greater than the calculated value of the transmitted torque loading the gears. In addition, resulting also from the variable motion conditions, the value of the clamping force. The greater the clamping force, the greater the safety factor, but the efficiency of the transmission decreases and greater losses occur in the hydraulic system where the clamping force is generated. In a conventional system where clamping forces are generated, there should be no sudden changes in torque, because it is not adapted to this. To eliminate the inertia of the operation of a conventional system, a hydraulic-mechanical torque sensor is used. Fig. 4 shows the relationship of axial force as a function of transmitted torque for conventional solutions consisting of a hydraulic system and for systems with a hydraulic-mechanical sensor. This relationship for the conventional system is described by the green line on the graph, where the axial force for small torques exceeds the force necessary to transmit the torque by 100%. As a result, fuel consumption will be higher even with a partial load of the vehicle.

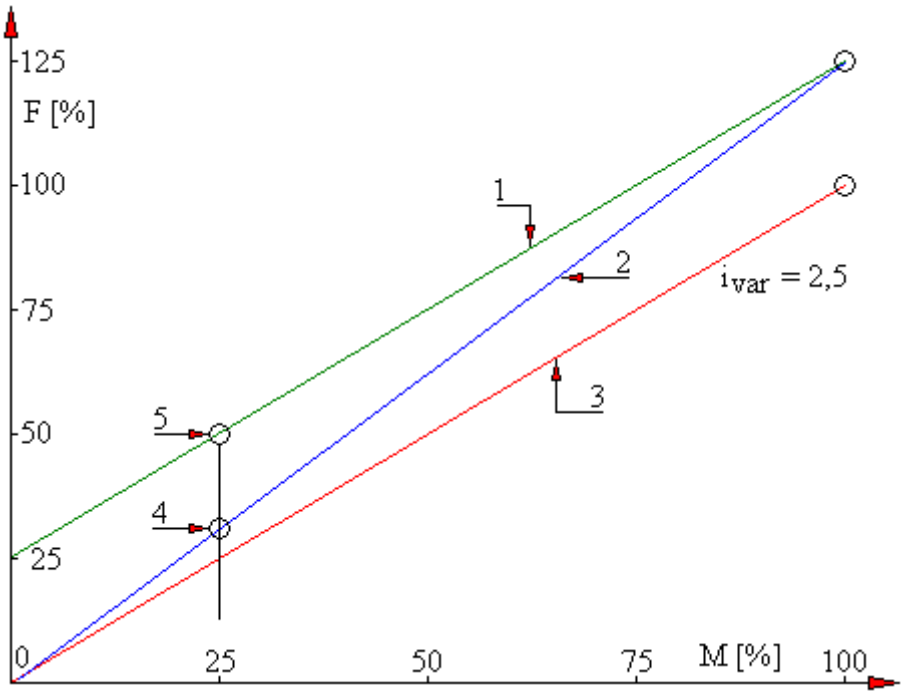

Fig. 4. The relationship between axial force and transmitted torque for conventional system and with torque sensor [3]
i_{var} - variator ratio; 1 – torque peak limitation, 2 – with constant safety factor; 3 – slip limitation; 4 – torque sensor; 5 – conventional system; F [%] – axial force; M [%] - torque

The blue line characterizes the axial force when using a hydraulic-mechanical sensor proposed by LuK. This sensor, shown in Fig. 5, consists of a mechanical part and a hydraulic part with a clamping and sensor chamber. The mechanical part contains a self-locking ball mechanism that transmits the torque and generates a force F, which is then balanced by the force resulting from the pressure p in the sensor chamber.

The flow resistance depends on the movement of the sensor's movable element. The size of the clearance (red) through which oil is supplied by the pump to the sensor chambers is crucial. The movement of the moving element of the sensor takes place until the axial force F is equalized with the force resulting from the pressure. Consequently, the pressures, which are the same in the sensor and clamping chambers, correspond to the transmitted torque and the force F. With a large increase in the transferred torque, the clearance will close, and with a further increase in torque, the moving element of the sensor will move towards the pulley. The oil will then be pumped into the clamping chamber, increasing the pressure there. The sensor works in this situation as a feed pump: activated when needed, without a special drive, quickly responding to torque changes. In a conventional system, the transmission is equipped with two cylinders: one on the driving wheel, one on the driven wheel. Oil flows from the pump to the control device, and from there directly to the cylinders. The obtained clamping forces allow obtaining the appropriate ratio. In order to obtain a high ratio value, the hydraulic pump should provide an appropriate increase in pressure in the cylinder of the driven wheel while at the same time the oil flows out of the cylinder of the driving wheel. Fast ratio changes therefore require a large amounts of energy. The same applies when we want to obtain the lowest possible ratio. Such a conventional system requires a pump with high delivery and therefore high energy demand. The

double piston system developed by LuK enables a reduction in the energy requirement when changing gear ratio.

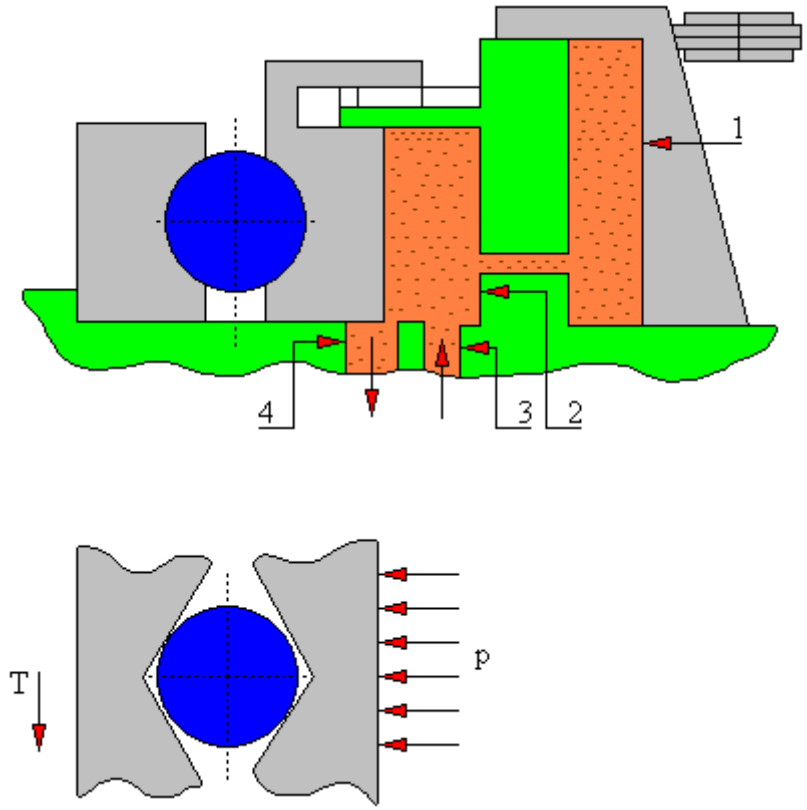

Fig. 5. Hydraulic-mechanical sensor [5]
P – clamping pressure; T – friction force; 1 – clamping chamber; 2 – sensor chamber; 3 – oil supply; 4 – oil drainage

Flow resistance depends on the movement of the moving element of the sensor. The size of the clearance (red) through which the oil is supplied by the pump to the sensor chambers is important. The movement of the moving element of the sensor takes place until the axial force F is equalized with the force resulting from the pressure. Consequently, the pressures, which are the same in the sensor and clamping chambers, correspond to the transmitted torque and the force F. With a large increase in the transferred torque, the clearance will close, and with a further increase in torque, the moving element of the sensor will move towards the pulley. The oil will then be pumped into the clamping chamber, increasing the pressure there. This means that the sensor works on the principle of a feed pump and is activated when necessary, without a special drive, responding quickly to changes in torque. The transmission in a conventional system has two pressure cylinders, one of which is on the driving wheel and the other on the driven wheel. Oil flows from the pump to the control device, and then goes to the cylinders. Obtaining the appropriate ratio depends on the obtained clamping force. The task of the hydraulic pump is to ensure an appropriate increase in pressure in the cylinder of the passive wheel while simultaneously draining oil from the cylinder of the driving wheel in order to achieve a high gear ratio value. Therefore, large energy inputs are needed to obtain fast ratio changes, but also to obtain the smallest possible gear ratios. The pump in such a conventional system must be characterized by high delivery and high energy demand.

In CVT transmission, the gear ratio change depends on takig into account the gear ratio change speed and this is visible in Fig. 6, which shows a simplified physical model of the CVT drive system. The CVT gear ratio can be changed continuously over time. The gear ratio change speed can cause changes in the engine load, and in CVT transmission, the gear ratio can change continuously over time [21].

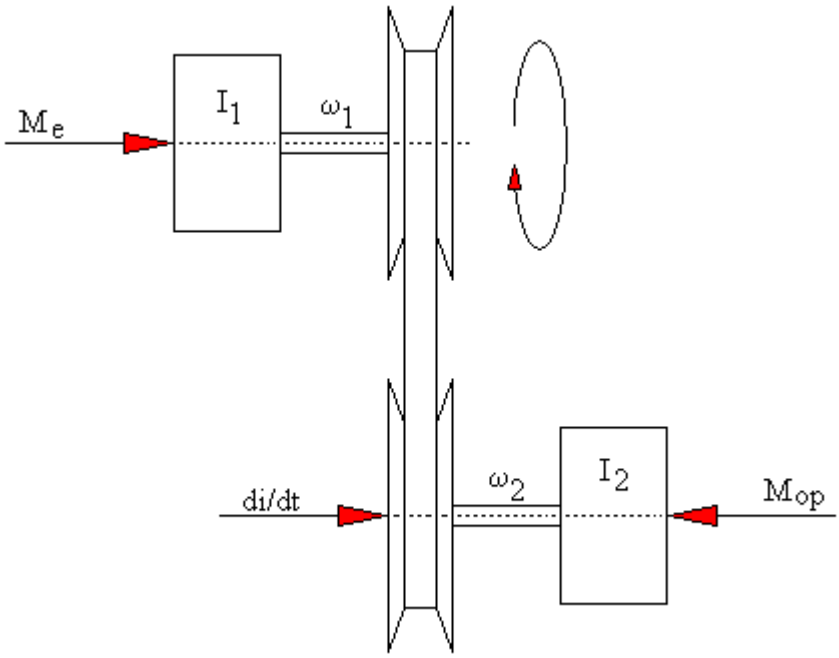

Fig. 6. Physical model of the drive system with CVT transmission [18]
M_e -input torque; I_1 – moment of inertia of the drive wheel; I_2 – moment of inertia of the driven wheel; M_{op} – resistive torque; ω_1 – rotational speed of the drive wheel; ω_2 – rotational speed of the driven wheel; di / dt – speed of gear ratio changes

A simplified physical model of the drive system describes the characteristic phenomena occurring in the drive system during ratio change. This simple model consists of the moment of inertia I_1, rotating at a speed of ω_1, which describes the moment of inertia of the engine and other elements of the drive system before the transmission, together with the moment of inertia of the driving wheel. In turn, the mass of the vehicle and the moment of inertia of the rotating elements on the side of the driven wheel, together with this wheel, are described by the moment of inertia I_2, rotating at a speed of ω_2. A CVT transmission with a ratio of $i(\omega_1 / \omega_2)$ and a speed of ratio change of di/dt is connected by two masses. The acceleration or deceleration of the rotational speed of mass I_1 can be caused by each ratio change performed at a specific speed. The change in the value of the driving force depends on the changes in the engine torque resulting from the change in rotational speed and from the change in gear ratio. If the ratio change is too fast, the vehicle will slow down at the first moment.

The equation of motion for the drive system model is as follows:

$$\left(M_s - I_1 \frac{d\omega_1}{dt}\right) i = M_{op} + I_2 \frac{d\omega_2}{dt} \qquad (1)$$

From equation 1, after transformation, we get:

$$\frac{d\omega_2}{dt} = \frac{M_s i - M_{op}}{I_1 i^2 + I_2} - \frac{I_1 \omega_2 i}{I_1 i^2 + I_2} \frac{di}{dt} \quad (2)$$

From the negative second term of this equation it follows that the speed of ratio changes affects the degree of reduction of the angular acceleration value $d_2\omega$ /dt .
The linear acceleration of the vehicle is described by the following relationship:

$$a = \frac{d\omega_2}{dt} r_k \quad (3)$$

where:

$\frac{d\omega_2}{dt}$ - angular acceleration value

In CVT control systems, taking into account the speed of ratio changes is important, but obtaining the desired gear ratio value is not an easy task, because it depends on two contradictory conditions tkj. Maintaining very good dynamic characteristics of the vehicle while consuming as little fuel as possible. Engine speed, engine torque and CVT gear ratio are engine-related quantities that must be controlled in order to obtain minimum fuel consumption for different values of the required driving torque resulting from the driving conditions.

For specific road conditions, the value of power required to overcome motion resistance is known. This required power can be obtained at different throttle opening angles. The known relationship between the optimal throttle opening angle and the engine's rotational speed allows for the value of this angle for a specific power demand. The driving speed will require the selection of an appropriate CVT gear ratio. In order to meet the requirements described above, i.e. engine operation during vehicle motion with the highest possible efficiency, the required range of gear ratios is very large, so that it is often necessary to use additional transmissions.

The speed of the gear ratio change characteristic in a CVT with a metal belt pushed to develop a controller is usually obtained by experiment. The speed of ratio change plays a significant role during vehicle acceleration, especially if the kick down option is used. The use of a CVT drive system model allows simulation, significantly reducing the time and cost of preparing a controller. The most well-known model is the one developed by Ide et al. In general, the operating conditions of the steel belt - conical pulleys can be described by the following parameters:

-axial force (clamping) on the driving pulley F_{zdg},
-axial force (clamping) on the driven pulley,
-rotational speed of the driving pulley,
- torque on the driving pulley M_{dg},
- transmission ratio,

When the transmission ratio does not change, the axial forces on the driving pulley remain in equilibrium. A ratio change occurs when this equilibrium is disturbed. The axial force F^*_{zdg} on the driving pulley necessary to equalize the equilibrium state (when adjustment is applied to the driving pulley) must be generated. This force depends on the axial force on the driven pulley F_{zdn} and on the value of the transmitted driving torque $M_{dg.}$ The rotational speed also has a significant influence. After

determining the value of the maximum torque that can be transmitted by the transmission without excessive slippage, a map F^*_{zdg}/ F_{zdn} can be drawn on the basis of experimental tests in coordinates $M_{dg}/ M_{max,}$ i.

The experimental studies conducted by Ide [10, 12] allowed the development of the following ratio change model:

$$\frac{di}{dt} = \kappa(i)\,\omega_{dg}(F^*_{zdg} - F_{zdg}) \qquad (4)$$

where:
κ(i) -coefficient obtained experimentally, which is a function of the gear ratio,
F^*_{zdg} - clamping force for the driving pulley
F_{zdg} - clamping force for the driving pulley for the steady state.

The coefficient κ(i) represents the slope of the line that is the relationship of the ratio change speed and the axial force on the driving pulley, regardless of its rotational speed. This coefficient depends only on the transmission ratio. The angular velocity is introduced into equation 3 as an independent parameter.

Based on the dynamic model of the CVT transmission and assuming the engine and vehicle model one can perform simulation calculations of the vehicle dynamic performance.

4. Construction and operation of continuously variable transmissions

Despite the dynamic development of electric drive systems, continuously variable transmissions still have a wide range of applications and are used wherever a large torque must be overcome in the range of low rotational speeds. Currently, they are mainly used in technological devices and in machines powered by combustion engines, especially in vehicles to increase the work of their engines. Due to their construction and operating principle, continuously variable transmissions can be divided into:
- strand-type continuously variable transmissions:
  - continuously variable transmissions with rubber belts,
  - continuously variable transmissions with steel chain,
  - continuously variable transmissions with steel push belt,
- hydraulic and electric transmissions,
- friction transmissions.

5. Strand-type transmissions

Such transmissions consist of two pairs of conical pulleys forming pulleys with changing diameters. Changing the pulley diameters causes a change in the ratio. Each pair of pulleys has one fixed pulley and the other adjustable pulley. The moving pulleys are controlled by hydraulic actuators controlled by an electrovalve block and powered by a hydraulic pump. The actuators perform a smooth movement, so the ratios also change smoothly. Strand-type transmissions can be of belt or chain type. Belt transmissions can be divided into "wet" and "dry". Where "wet" is characterized by torque transferred between the elements of steel belts moistened with oil and the surfaces of the conical pulleys. While "dry" transmissions use the dry friction forces between the V-shaped rubber belt and the conical pulley. In "wet" chain transmissions,

a chain is used instead of a pushed steel belt. In this type of transmission, the chain is lubricated with hydraulic oil [12].

Chain-driven continuously variable transmissions require extensive lubrication and are therefore of limited use. Therefore, taking this fact into account, dry-running belt transmissions can be used more freely, which operate much more quietly, but also have greater energy losses caused by greater elastic slippage, due to the heat generated, which is difficult to dissipate, especially from the middle of the belt. All this translates into a reduction in the power of the belt transmission [20].

Nowadays, the strand-type transmissions mentioned above, i.e. chain and belt transmissions with a pushed belt are undoubtedly very popular in passenger cars.

6. Continuously variable transmissions with rubber belts

Belt transmissions transmit the drive as a result of frictional contact between the pulley and the belt. Between the conical pulleys there is a V-belt, which is loaded with circumferential forces resulting from the transmitted driving torque. In addition, the V-belt is subjected to a compressive axial force, which presses the belt against the surface of the conical pulleys. Figures 7 and 8 show the principle of operation of a CVT with a rubber belt.

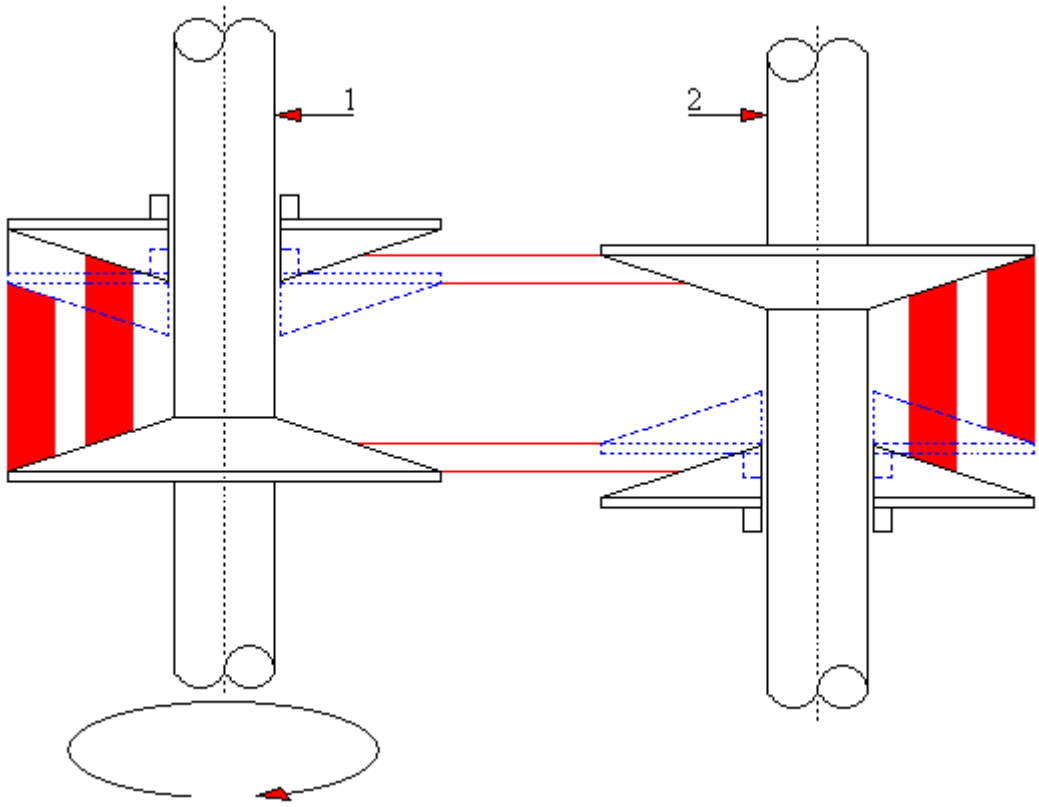

Fig. 7. Belt transmission with conical discs moving on each shaft [18]
1 – driving shaft; 2 – driven shaft

In the transmission shown in Fig. 7, in which there are adjustable gaps between discs on each shaft, the maximum speed is obtained when the driving pulley has a large diameter after the conical discs have come together. On the other hand, when the

driving pulley has a minimum diameter, when the discs are moving apart, the torque is maximum.

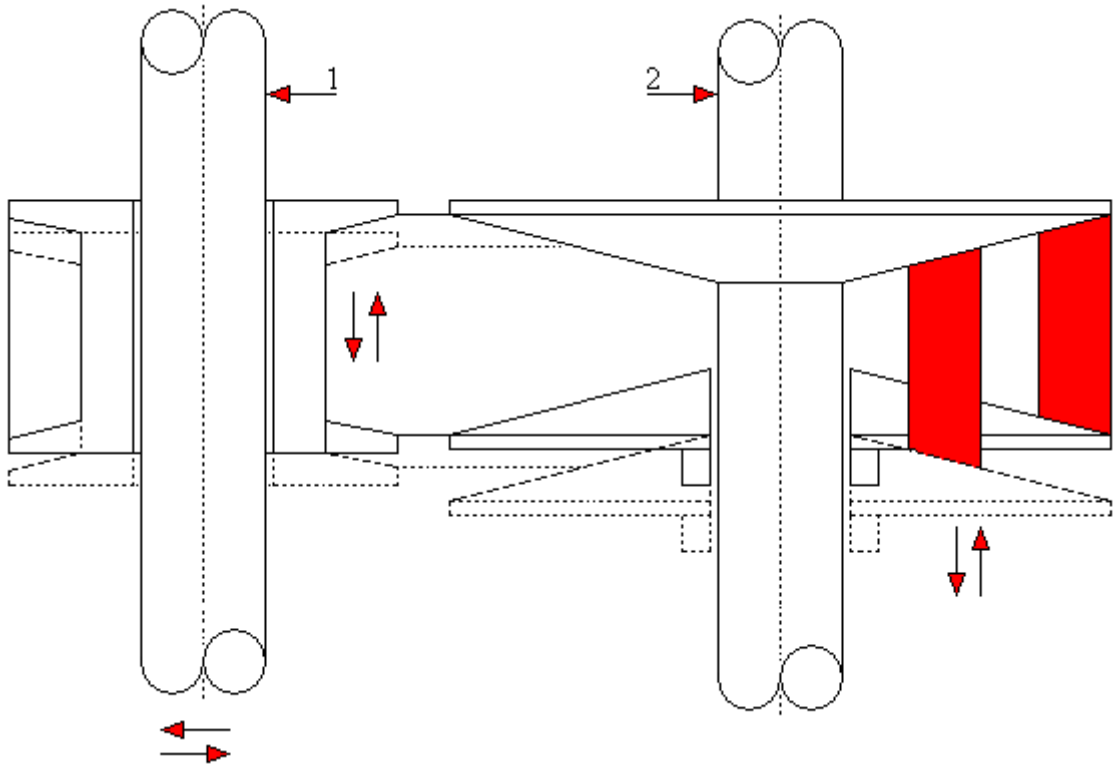

Fig. 8. Belt transmission with adjustable discs only on shaft 2
1 – driving shaft; 2 – driven shaft

The characteristic feature of the transmission illustrated in Fig. 8 is the use of a pulley with a constant diameter moved along shaft 1 and a pulley with adjustable discs that have a variable gap. The change in speed is also related to the change in the distance between the shaft axes.

Comparing the two transmissions shown in Figures 7 and 8, it can be stated that the advantage of the first one is the constant distance between the axles and the possibility of obtaining a much higher gear ratio. The disadvantage, however, is the need to synchronize the smooth adjustment of the gap between the conical discs mounted on both shafts 1 and 2. The disadvantage of the second transmission solution is the need to change the axle distance when changing the gear ratio as well as the requirement for axial movement of the constant-diameter pulley.

The efficiency of a belt transmission depends largely on losses resulting from belt slippage, its bending on the pulleys, as well as aerodynamic drag and internal friction. In order to determine the optimal operating conditions of a belt transmission, tests are performed to determine the so-called drive coefficient [34].

By bringing the conical pulleys closer together, we move the belt radially and change the working radius. However in order to transfer the driving torque, it is necessary to generate an appropriate clamping force of the belt's side surfaces against

the conical pulleys. The axial clamping forces of the pulleys in adjustable belt drives are implemented in various ways, starting from very simple solutions using centrifugal force, up to hydraulic systems and electric actuators [18].

By means of the magnitude and action of axial forces, mechanical properties of the transmission can be determined. So we can, for example, determine the transmitted torque or efficiency of the transmission. Most often, such transmissions are used in small motor vehicles.

The driving torque transmitted by the transmission has an impact on the generation of different circumferential forces in the belt at the input and output of the pulley. In order to determine the principles of operation of belt transmissions, Fig. 9 shows the equilibrium condition for the belt fragment A, which is limited by the angle dφ on the active pulley, and the acting circumferential forces F1 and F2 at the moment when they pass through the pulley.

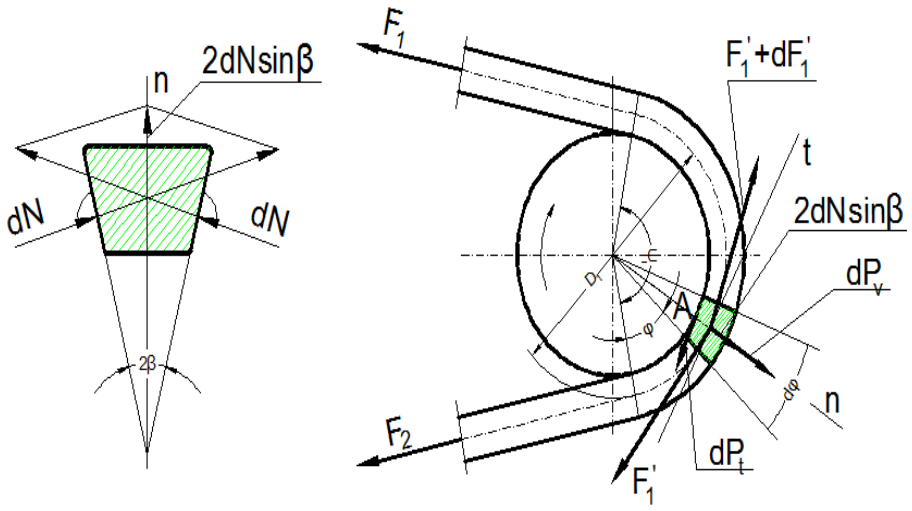

Fig. 9. Distribution of forces acting on the belt element on the driving pulley [18]

As one can see, the belt fragment A marked with green hatching is affected by the pulley pressure forces *dN*, circumferential forces F′1 and F′2 + d F′1, as well as the friction force dP_t, and the centrifugal force dP_v All these forces, passing through the center of segment A, are projected onto the belt's centerline as normal and tangential components.

We can write this as:

$$2dN\ sin\beta + dP_v \approx 2F_1^{'} \sin\frac{d\varphi}{2} \approx F_1^{'} d\varphi \qquad (5)$$

and:

$$dF_1' = (F_1' d\varphi - dP_v)\frac{\mu}{sin\,\beta} \qquad (6)$$

The unit centrifugal force can be written in the following form:

$$dP_v = \frac{qv^2}{g}\, d\varphi \qquad (7)$$

ν - longitudinal belt speed; q/g - unit weight of the belt

The value of the centrifugal force of the entire wrap angle does not change and is dependent on the speed and mass of the belt. This force acts on the belt only when a section of the belt passes over the pulley.

In these transmissions, the stresses in the driven strand are smaller than the stresses in the driving strand, and changes in stress values occur on the arc of contact. Therefore, this affects the change in belt deformation and causes changes in the belt length. But then slippage occurs at the point of contact between the pulley and the belt. There are already many publications and scientific works on the subject of the behavior of belts in belt transmissions, despite the difficulties in explaining the existence of differences in the values of axial forces of the active and passive pulleys at the same rolling radii. This problematic issue was explained precisely by G. Gerbert, who, while describing the belt motion, took into account circumferential and radial slip, thanks to which he found the answer to the previously troubling problem related to the differences in axial forces. The complex analysis presented by Gerbert is supported by the results of the conducted experiments, which confirm the correctness of the assumptions taken into account [10].

The main assumptions adopted in Gerbert's description of the behavior of V-belts in cooperation with pulleys are:

- the belt has a specific width diameter and negligible small thickness (we assume it is equal to 0),
- the belt is characterized by low speed and no mass (inertia forces are omitted),
- the value of the belt's torsional rigidity is zero (no torsional moments),
- the friction coefficient has a constant value,
- the directions of friction forces are opposite to the slip velocity.

Considering the action of axial forces in transmissions, as well as the wedge shape of the belt, it must be expected that the belt will undergo transverse deformation during torque transfer. Then the belt movement will be radial, so that it can adapt to the shape of the pulley, and the belt will undergo longitudinal displacement as a result of the acting variable longitudinal forces. CVT transmissions with a rubber belt should take into account belt deformations and slippages in the basic equations.

The belt resembles materials with linear characteristics, which are distinguished by the fact that their forces are directly proportional to the deformations, which can result in the occurrence of superposition.

The belt is acted on by a force F, which causes longitudinal deformations of the belt ε. This relationship between force and deformation can be written as follows:

$$F = c \cdot B \tag{8}$$

where:

B - the value of longitudinal deformation; c – is the elasticity constant of the belt in the longitudinal direction

This description is only possible for belts composed of lagging, rubber and cords. Each material is characterized by elasticity, that is, the ability to deform under the influence of an acting force.

The properties of cord differ significantly from those of rubber, especially in

terms of rigidity. Because rubber is more than a hundred times less rigid than the cord. So when we load the belt with forces such as the force F causing deformation and the lateral force resulting from the axial force, then the cord carries more force F. The axial force however does not have a major effect on the belt, because the stiffness of the cord excludes the occurrence of longitudinal deformation, the only thing that occurs is transverse deformation.

7. Continuously variable transmissions with steel chain

This type of transmissions with a steel chain transfers the driving torque by using the tension force of the chain. This transmission, compared to the transmission with a pushed steel belt, is characterized by a much greater ability to transfer driving torques. However, its disadvantages include greater noise resulting from the operation of the transmission with a chain. Currently, we can find two types of driving chains that are used in vehicles. These are: chains produced by LuK and involute ones.

The chain built by LuK is equipped with a shackle and two truncated pins. Through the cooperation of the pins with the surfaces of the conical pulleys, it is possible to transfer driving torques of significant values, even over 500 Nm. For steel belts, the surface of the pulleys is distinguished by a different curvature.

The ends of the cooperating pins are shaped in an appropriate way. The mating surface depends on the gear ratio. The angle of inclination of the conical surface also changes. By appropriately selecting the radius of curvature of the conical pulley, we can achieve a reduction in transmission wear. The pins, transferring the torque, roll over each other without slipping. Their movement is greatly influenced by the outline of the conical pulley on which they roll. During mating with the surface of the conical wheel, the pins have to overcome friction forces.

In the construction of an involute chain, three elements are used: a pin, a belt and a connector, where the pin is longer than the belt and only this pin has contact by touching the surface of the conical pulleys. The surface of the belt is in linear contact with the pin and this is how the pin rolls on the belt. The pulleys used to mate with the chain are the same as those used to mate with the steel belt.

8. Steel Push Belt CVT Transmissions

In this type of transmissions with a steel push belt, the gear ratio is changed by creating an appropriate clamping force in the active pulley and the passive pulley. Like other continuously variable gear ratio transmissions, this transmission is made of two pulleys mounted at a constant distance from each other and wrapped in this type of steel belt, which transmits power. The transmission with a pushed steel belt is shown in Fig. 10. Each pulley has one moving part. As you can see, the belt can move tangentially or radially. This mainly depends on the axial forces acting on the pulleys and on the load on the transmission.

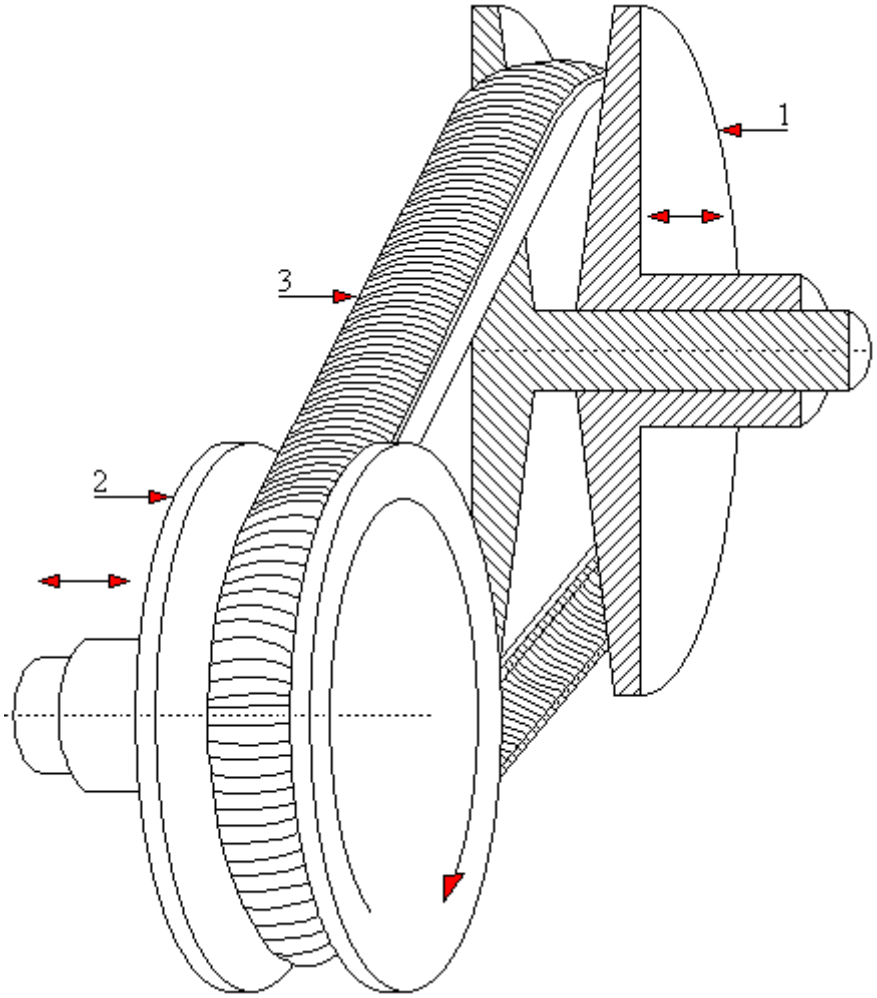

Fig. 10. Transmission with a steel push belt
1 - active pulley; 2 - passive pulley; 3 - steel belt

The transfer of torque from pulley 1 to pulley 2 is carried out by pushing the segments of belt 3. Because this belt is made of 300 to 400 segments connected to each other by means of a thin steel strip in the form of a belt. The thickness of the steel strip used in these belts is in the range of 0.2 [mm] to 0.4 [mm]. The thin steel strip is connected to the segments by means of appropriate cutouts, into which it enters [18].

Each segment has a protrusion that enters the opening of the previous element and therefore it is not possible for the segments to move between each other in an arbitrary way. Moreover, the element has a truncated lower part of the front surface so that it cannot move around the circumference of the pulley [18].

Based on two models of mating between the pulley and the belt surface, the transfer of driving torque through the transmission can be described in practice. The first model uses Coulomb friction and assumes that the compressive force acting

between the segments transfers a significant part of the power for almost all operating conditions, taking into account the friction forces occurring between the strips and between the strip and the belt segment. Whereas, the strips transmit a small part of the power. The friction coefficients most often selected for the contact of the strip surface with the segment are $\mu = 0{,}16$ and $\mu = 0{,}07 \div 0{,}09$ for the contact of the segment surfaces with the pulley. The second simplified model includes shear stresses in the oil film and can be used assuming that there will be an oil film at the contact of the pulley surfaces with the belt segments. This theory was first used by Micklem in 1991 to explain the phenomenon of torque transmission in a steel belt CVT.

At the mating point of the pulley surface with the belt segments, relative movement occurs, which generates shear stresses in the oil.

The following forces act between the parts of the steel belt:

C_x - compressive force between the segments,
T - tension force of the strips,
F_{rad} - radial friction force between the sides of the segment and the pulley surface,
F_R - friction force between the segment cutouts and the strips,
F_T - tangential friction force between the surface of the conical pulley and the side of the segment,
N - normal force to the side surfaces of the segment,
Q - normal force to the surface of the segment cutouts.

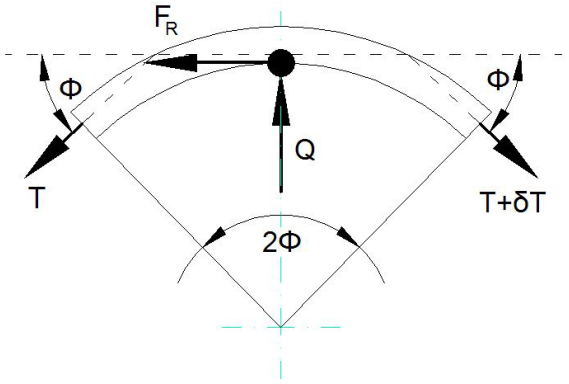

Fig. 11. Fragment of the belt with the distribution of force in the strips [18]

9. Variable ratio hydraulic and electric transmissions

Continuously variable hydraulic transmissions are used to shape the energy flow of medium and higher power. Hydrostatic transmissions are a hydraulic pump system with variable regulated capacity with a hydraulic motor and distributor. In self-adjusting hydrodynamic transmissions, on the other hand, the system is formed by a rotary pump, turbine and a guide vane. In these transmissions, the supplied energy is changed to the kinetic energy of the fluid, and then it is changed to the energy received on the driven shaft. They are also characterized by a narrow range of kinematic ratios, for which the efficiency values of the transmission are high. The weak point of the hydraulic transmission is definitely its low efficiency, especially at extreme values of the ratios and at low powers. Hydrodynamic transmissions which are used, among others, in vehicle drive systems, have become more popular. The use of hydrostatic transmissions in vehicles is limited by higher costs, weight and too low efficiency in a large range of gear ratios. However, they are more widely used in drives of working machines. The efficiency of hydraulic transmissions can be increased by using additional mechanical

transmissions in vehicle drive systems, and a return to the previous range can be achieved by using a reversing gear.

The electric transmission is equipped with an electric generator set and an engine. Just like hydraulic transmissions, they can be adjustable or self-adjusting, depending on whether the gear ratio is determined programmatically or automatically due to the load value. The strength of this transmission is that it is characterized by a large range of gear ratios and high efficiency, much better than the efficiency of a hydraulic transmission. Another advantage is that they can have more stable gear ratio values when the load changes. However, its disadvantage is large dimensions and weight that narrow the range of applications. Transmissions of this type are most often used in diesel locomotives, where weight restrictions are not large due to the traction of the running wheels. They are also used in places where hydraulic transmissions cannot be used for fire protection reasons [20].

10. Friction gears

These gears are the most compact transmissions that change the ratio continuously. Similarly to other transmissions with continuously variable ratio adjustment, they are also called variators. The most important elements of friction gears are their wheels, which transmit energy thanks to mutual frictional contact. This seemingly simple mechanism, in reality, after closer examination, turned out to be very complicated. In a relatively simple way, however, it is possible to obtain in them a change in the ratio, and sometimes a mutual pressure of the friction wheels. An example of this would be a transmission, in which the engine's gravity force is used to mutually press its disc wheels, and the possibility of moving it along the radius of one of these wheels - to change the ratio.

This simple gear is most often used to drive drills. Its efficiency decreases with the decrease of load and with the increase of the distance between the axles of its wheels. This is because, except for the case when the gear ratio value $i_c = 1$, in the entire range of its adjustment on the width of the contact of the friction wheels there is a difference in peripheral speeds called geometric slip. This slip is the main source of energy losses in friction gears [20].

When the pressure of the friction wheels is constant, geometric slip causes losses of transmitted energy that are little dependent on the load. They are also almost constant in the bearings, which causes a decrease in the efficiency of the transmission when it is not fully loaded. In order to increase the efficiency of friction gears, in the event of partial load and to increase the stability of the gear ratio values, mechanisms are used that automatically increase the clamping forces of their wheels along with the load. These are often rolling screw mechanisms, which should be well made. Otherwise, they can cause very large and uncontrolled changes in the clamping force value. This increases the losses in the transmitted energy and the wear of the friction wheels, and may even cause failure.

The speed of pivoting friction caused by geometric slip is equal to the difference in angular velocities in the contact plane of the friction wheels and is the greater the further apart the vertices of their cones are. The torque caused by this friction is the greater the greater the distances of elementary friction forces in the contact area of these wheels from the rolling point. It therefore depends on the dimensions of the contact area and the unloading of pressures on it, and above all on the rigidity of the friction wheels and the shape of their friction surfaces. A higher value of the friction coefficient, which reduces the value of the clamping force

needed to transfer the load, reduces the value of the pivoting torque and the load on the gear bearings. Lubrication, on the other hand, has the opposite effect, but reduces wear, which is especially important when there is point contact, sometimes used in friction wheels made of hardened steel, which can withstand significant loads.

11. Calculation of the designed continuously variable transmission

Calculation of the designed continuously variable transmission consists of:
- determination of all forces acting on the shaft;
- calculation of the values of bending moments for shafts and torsional and equivalent moments at least for the points of application of external forces and for the support points (bearings);
- calculation of shaft diameters in basic sections.

12. Calculation of two-support axles for bending

The axle should be calculated as a beam supported on two supports (bearings). The solution begins with determining the active forces (components) and then the reactions based on equilibrium conditions. In the next step, the bending moments should be determined. Based on the bending strength condition, the minimum axle diameter should then be calculated:

$$\sigma_g = \frac{M_g}{W_x} \approx \frac{M_g}{0{,}1d^3} \leq k_g(k_{gj})(k_{go})$$

where:
σ_g – maximum actual bending stresses [Pa] (in practice in MPa),
M_g – bending moment [Nm],
W_x – index of the section's bending strength relative to the neutral axis [m^3],
k_g, k_{gj}, k_{go} – allowable bending stresses, respectively – general, one-sided, two-sided [MPa].

hence:

$$d \geq \sqrt[3]{\frac{10 \cdot M_g}{k_g}}$$

13. Calculation of double-support shafts

Loading the shafts causes normal (bending) and tangential (torsional) stresses in them, therefore the shafts are calculated using the formula for equivalent stresses based on Huber's hypothesis:

$$\sigma_z = \sqrt{\sigma_g{}^2 + (\alpha \cdot \tau_s)^2} \leq k_{go}$$

The reduction factor α determines the extent to which tangential stresses are taken into account in the calculations. Its value is calculated from the relationship:

$$\alpha = k_{gj} / k_{sj} \quad \text{or} \quad \alpha = k_{go} / k_{so}$$

Because $W_x = -0.1d^3$ hence:

$$d \geq \sqrt[3]{\frac{10 \cdot M_s}{k_{gj}}}$$

14. Calculation of shafts for torsion

We calculate the shafts only for torsion in the following situations;

- When the torsional moment is much greater than the bending moments (e.g. short reducer shafts);
- When the shaft is loaded only with a torsional moment.

The shaft diameter is calculated using the formula:

$$d \geq \sqrt[3]{\frac{5 \cdot M_s}{k_{sj}}}$$

or for a hollow shaft

$$d \geq \sqrt[3]{\frac{5 \cdot M_s}{(1-\beta^4) \cdot k_{sj}}}$$

15. Strength calculations of the shafts of the designed belt variator

The shaft is driven by a pulley with a diameter of D_1=66 [mm] and the power is taken from the shaft by a pulley D_{2max} =70 [mm] and D_{2min}=40 [mm], D_{3max}=100 [mm] and D_{3min}=40 [mm], power on shaft I - P_2=142,5 [W](150Wx0,95), power on shaft II – P_3=135,4 [W] (142,5[W]x0,95). The rotational speed of shaft I is n=1450rpm. Shaft material St3S (S235JR).

The extreme load variant was assumed for the calculations - total power take-off and the efficiency of the belt transmission with a V-belt $\eta = 0{,}95 \div 0{,}96$.

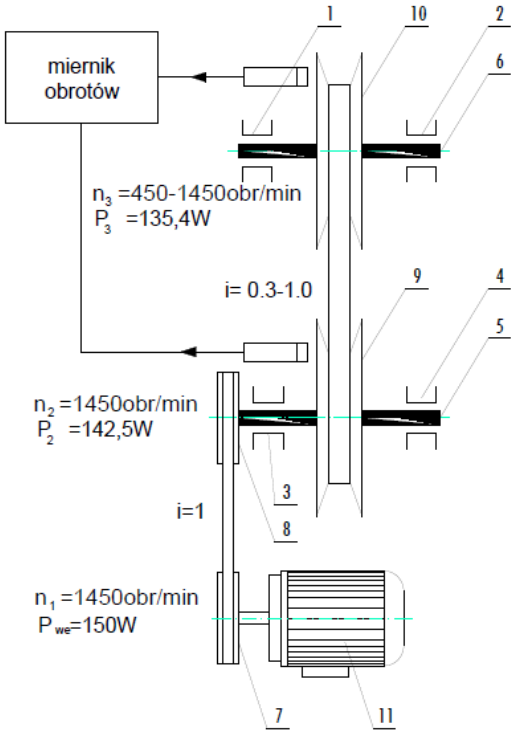

Fig. 12. Diagram of the designed continuously variable transmission
1,2,3,4- bearing units UCPA204/Ø20; 5- shaft I; 6- shaft II; 7,8-drive pulleys D_1; 9- D_2 variator pulley; 10-D_3 variator pulley; 11-electric motor 220V SED110-4BN75 150W.

16. Calculations for shaft I

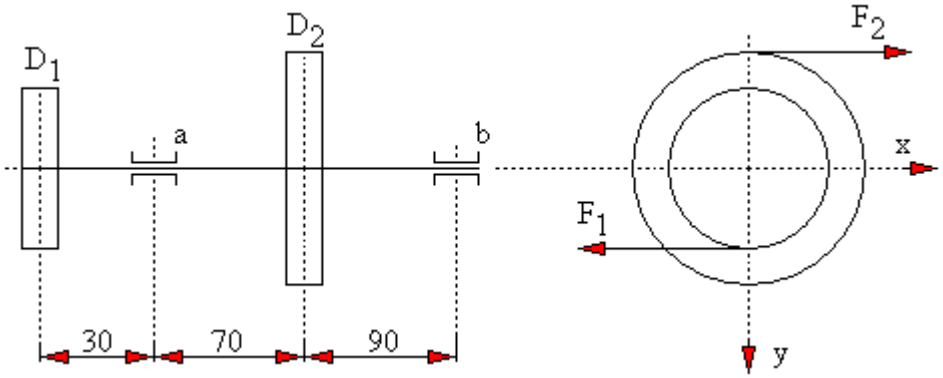

Fig. 13. Distances between supports for shaft I

We calculate the reactions and bending moments:

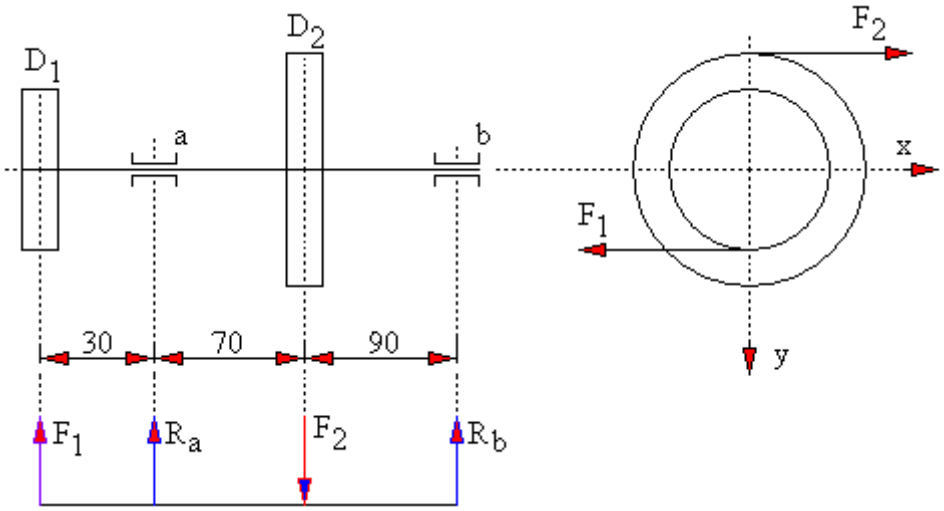

Fig. 14. Distribution of reaction forces on wheels and supports for shaft I

We determine the values of M_s , F_1 ,F_2:

$$M_S = 9554 \cdot \frac{P_1}{n} = 9554 \cdot \frac{0.1425}{1450} = 0.938 \text{ [Nm]}$$

$$F_1 = \frac{M_{s1}}{0.5 \cdot D_1} = \frac{0.938}{0.5 \cdot 0.066} = 28.4 \text{ [N]}$$

$$F_{2max} = \frac{M_s}{0.5 \cdot D_{2min}} = \frac{0.938}{0.5 \cdot 0.04} = 46.9 \text{ [N]}$$

$$F_{2min} = \frac{M_s}{0.5 \cdot D_{2max}} = \frac{0.938}{0.5 \cdot 0.07} = 26.8 \text{ [N]}$$

We write down the equilibrium conditions for the maximum force F_{2max};

$$\begin{cases} \sum F_i = 0 & -F_1 - R_a + F_2 - R_b = 0 \\ \sum M_{ia} = 0 & -F_1 \cdot 0.03\text{m} + R_a \cdot 0\text{m} - F_2 \cdot 0.07\text{m} + R_b \cdot 0.16\text{m} = 0 \end{cases}$$

From the solution we get; R_b= 25,8 [N] , $R_a = -7.3$ [N]

We calculate the bending moments at characteristic points:

$$M_{gl} = F_1 \cdot 0\text{m} = 0$$

$$M_{ga} = -F_1 \cdot 0.03\text{m} + R_a \cdot 0\text{m} = -0.852 \text{ [Nm]}$$

$$M_{g2} = -F_1 \cdot 0.1\text{m} - R_a \cdot 0.07\text{m} + F_2 \cdot 0\text{m} = -2.3 \text{ [Nm]}$$

$$M_{gb} = -F_1 \cdot 0.19\text{m} - R_a \cdot 0.16\text{m} + F_2 \cdot 0.09\text{m} + R_b \cdot 0\text{m} = 0 \text{ [Nm]}$$

We make a diagram of bending moments

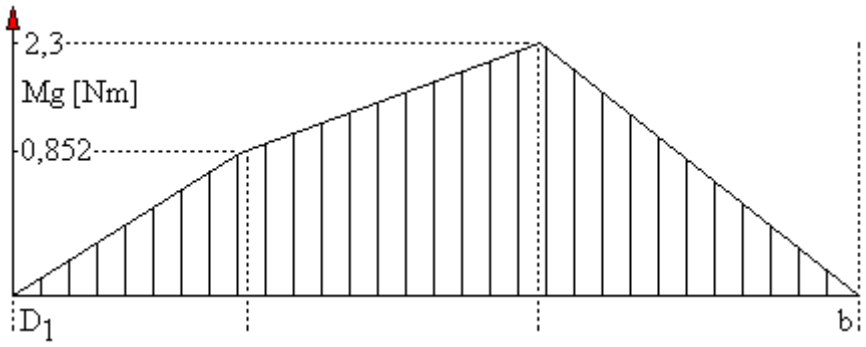

Fig. 15. Diagram of bending moments M_g for shaft I

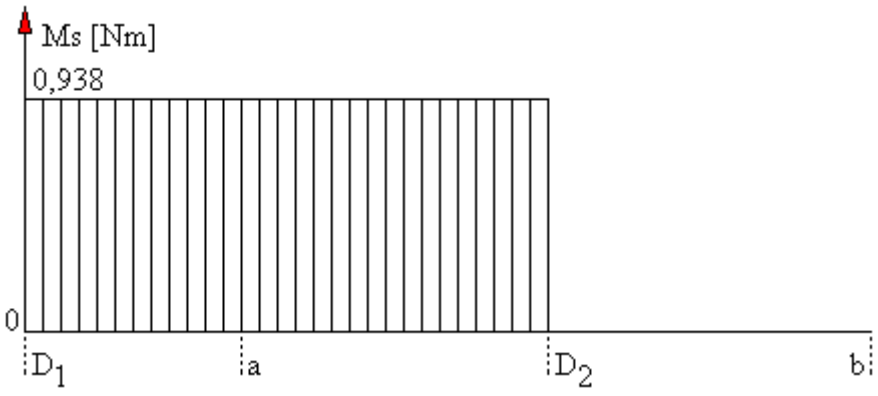

Fig. 16. Torsional moment diagram M_s for shaft I

I calculate equivalent moments at individual points according to the formula:

$$M_z = \sqrt{M_g^2 + \frac{\alpha}{2} M_s^2}$$

Where $\alpha = k_{go} / k_{so} = 50$ [MPa] / 27 [Mpa] = 1,75

$$M_{zD1} = \sqrt{M_{g1}^2 + \frac{\alpha}{2} M_s^2} = \sqrt{0^2 + \frac{1{,}75}{2} \cdot 0.938^2} = 0.877 \text{ [Nm]}$$

$$M_{z\alpha} = \sqrt{M_{g\alpha}^2 + \frac{\alpha}{2} M_s^2} = \sqrt{0.852^2 + \frac{1{,}75}{2} \cdot 0.938^2} = 1.222 \text{ [Nm]}$$

$$M_{zD2} = \sqrt{M_{gD2}^2 + \frac{\alpha}{2} M_s^2} = \sqrt{2.3^2 + \frac{1{,}75}{2} \cdot 0.938^2} = 2.462 \text{ [Nm]}$$

$$M_{zb} = \sqrt{M_{gb}^2 + \frac{\alpha}{2} M_s^2} = \sqrt{0^2 + \frac{1{,}75}{2} \cdot 0^2} = 0 \text{ [Nm]}$$

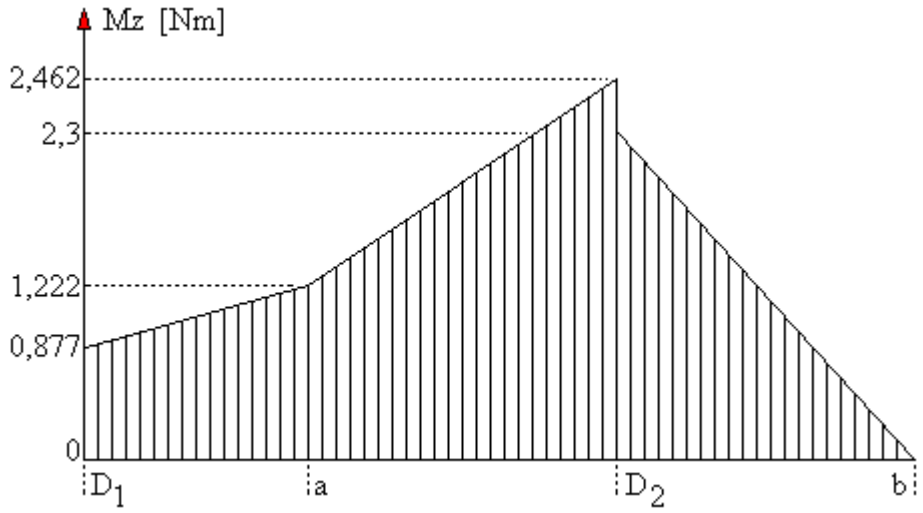

Fig. 17. Diagram of equivalent moments M_z for shaft I

We calculate the diameters of the shaft necks of shaft I for the bearings using the formula;

$$d \geq \sqrt[3]{\frac{10 \cdot M_z}{k_{gj}}}$$

k_{gj} = 75 [MPa] for St3S

Substituting:

$$d_{D1} \geq \sqrt[3]{\frac{10 \cdot 0.877\ [\mathrm{Nm}]}{75000000\ [\mathrm{Pa}]}} = 4{,}9\ [\mathrm{mm}]$$

$$d_A \geq \sqrt[3]{\frac{10 \cdot 1.22\ [\mathrm{Nm}]}{75000000[\mathrm{Pa}]}} = 5{,}4\ [\mathrm{mm}]$$

$$d_{D2} \geq \sqrt[3]{\frac{10 \cdot 2.462\ [\mathrm{Nm}]}{75000000[\mathrm{Pa}]}} = 6{,}8\ [\mathrm{mm}]$$

Due to the adaptation of the variator, the following diameters were adopted: d_{D1}=14 [mm], d_a=20 [mm], d_{D2}=20 [mm], d_b =20 [mm].

17. Calculations for shaft II

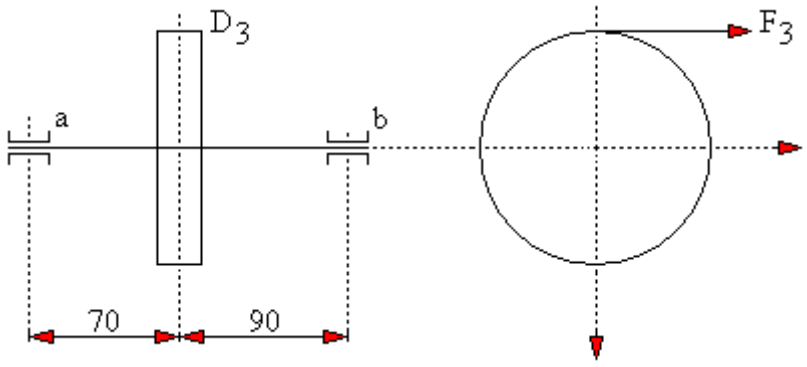

Fig. 18. Distances between supports for shaft II
We calculate the reactions and bending moments on shaft II:

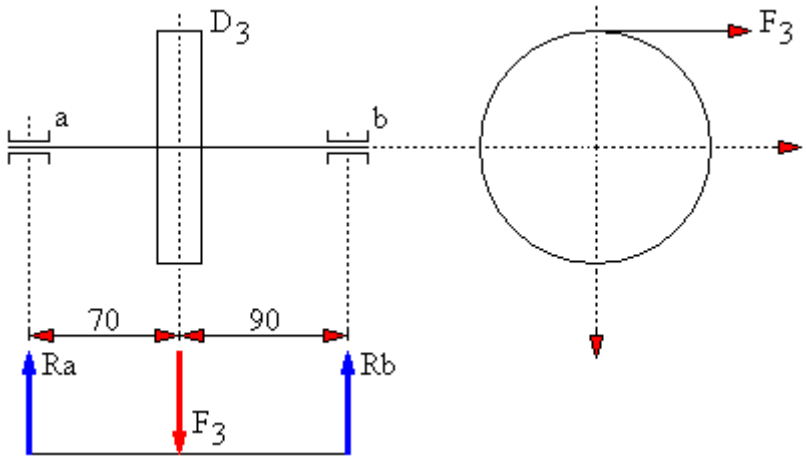

Fig. 19. Distribution of reaction forces on the wheel and on the supports for shaft II

We determine the values of M_s, F_3, for the extreme speed variant n=450 [rpm] and D_{3max}=100 [mm].

$$M_S = 9554 \cdot \frac{P_3}{n} = 9554 \cdot \frac{0.1354}{450} = 2.87 \text{ [Nm]}$$

$$F_3 = \frac{M_s}{0.5 \cdot D_{3max}} = \frac{2.87}{0.5 \cdot 0.100} = 57.4 \text{ [N]}$$

We write down the equilibrium conditions for the maximum force F_{3max}:

$$\begin{cases} \sum F_i = 0 & -R_a + F_3 - R_b = 0 \\ \sum M_{ia} = 0 & R_a \cdot 0\text{m} - F_3 \cdot 0.07\text{m} + R_b \cdot 0.16\text{m} = 0 \end{cases}$$

From the solution we get: R_b= 25,11 [N], R_a = 32.29 [N].

We calculate the bending moments at characteristic points of shaft II:

$$M_{ga} = R_a \cdot 0\text{m} = 0 \text{ [Nm]}$$

$$M_{g3} = -R_a \cdot 0.07\text{m} + F_3 \cdot 0\text{m} = -2.260 \text{ [Nm]}$$

$$M_{gb} = -R_a \cdot 0.16\text{m} + F_3 \cdot 0.09\text{m} + R_b \cdot 0\text{m} = 0 \text{ [Nm]}$$

We make a diagram of bending moments:

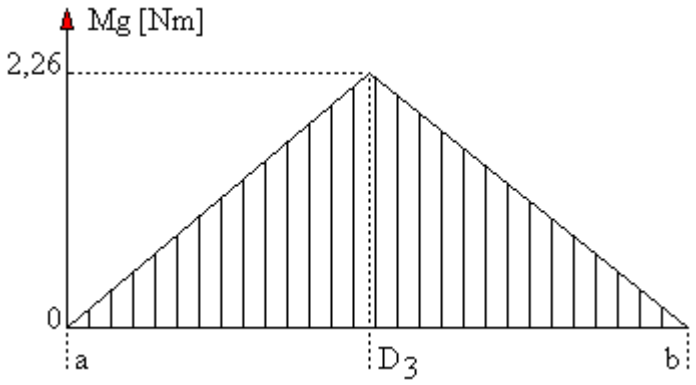

Fig. 20. Diagram of bending moments M_g for shaft II

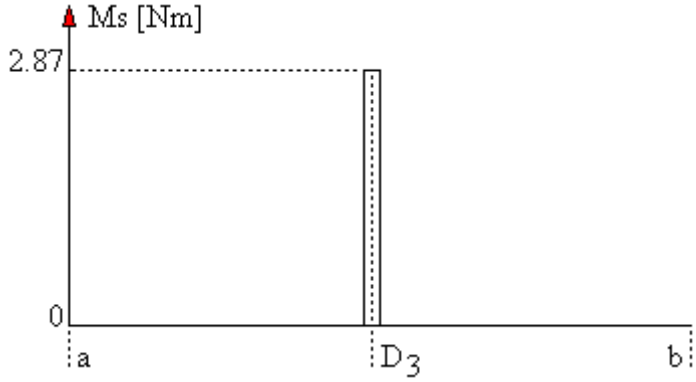

Fig. 21. Diagram of torsional moments M_s for shaft II

We calculate the equivalent moments according to the formula:

$$M_z = \sqrt{M_g^2 + \frac{\alpha}{2} M_s^2}$$

Where $\alpha = k_{go} / k_{so} = 50\text{MPa}/27\text{Mpa} = 1{,}75$

$$M_{za} = \sqrt{M_{ga}^2 + \frac{\alpha}{2} M_s^2} = \sqrt{0^2 + \frac{1{,}75}{2} \cdot 0^2} = 0 \text{ [Nm]}$$

$$M_{zD3} = \sqrt{M_{gD3}^2 + \frac{\alpha}{2} M_s^2} = \sqrt{2.26^2 + \frac{1{,}75}{2} \cdot 2{,}87^2} = 3.509 \text{ [Nm]}$$

$$M_{zb} = \sqrt{M_{gb}^2 + \frac{\alpha}{2} M_s^2} = \sqrt{0^2 + \frac{1{,}75}{2} \cdot 0^2} = 0 \text{ [Nm]}$$

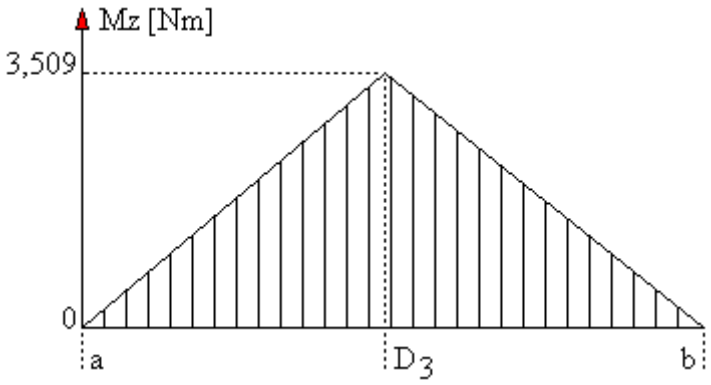

Fig. 22. Diagram of equivalent moments M_z for shaft II

We calculate the diameters of the shaft necks for the bearings using the formula;

$$d \geq \sqrt[3]{\frac{10 \cdot M_z}{k_{gj}}}$$

k_{gj}=75 [MPa] for St3S

Substituting:

$$d_{D3} \geq \sqrt[3]{\frac{10 \cdot 3.509\ [\mathrm{Nm}]}{75000000\ [\mathrm{Pa}]}} = 7{,}8\ [\mathrm{mm}]$$

Due to the adaptation of the variator, the following diameters were adopted: d_a=20 [mm], d_{D2}=25 [mm], d_b =20 [mm].

18. Description of the laboratory device's construction

The continuously variable transmission laboratory device (Fig. 23) was built on the basis of a rubber belt transmission from a 4T GY scooter with an engine capacity of 139 cm^3.

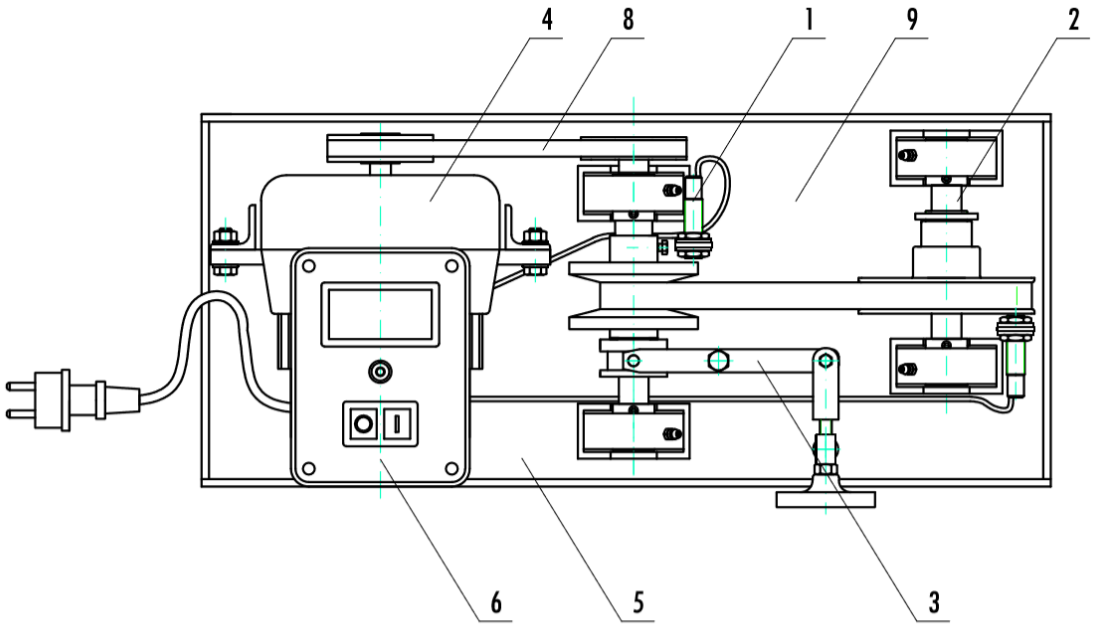

Fig. 23. Continuously variable transmission laboratory device
1 – active unit; 2 – passive unit; 3 – tensioning unit; 4 – drive unit; 5 – base; 6 – power supply and control unit; 8 – 4 T V-belt; 9 – 669x18x30 V-belt

The constructed laboratory device is based on a steel structure 5, made of 4 mm thick sheet metal with dimensions of 570 x 250, thanks to this solution the assembly and disassembly of individual mounted units is facilitated.

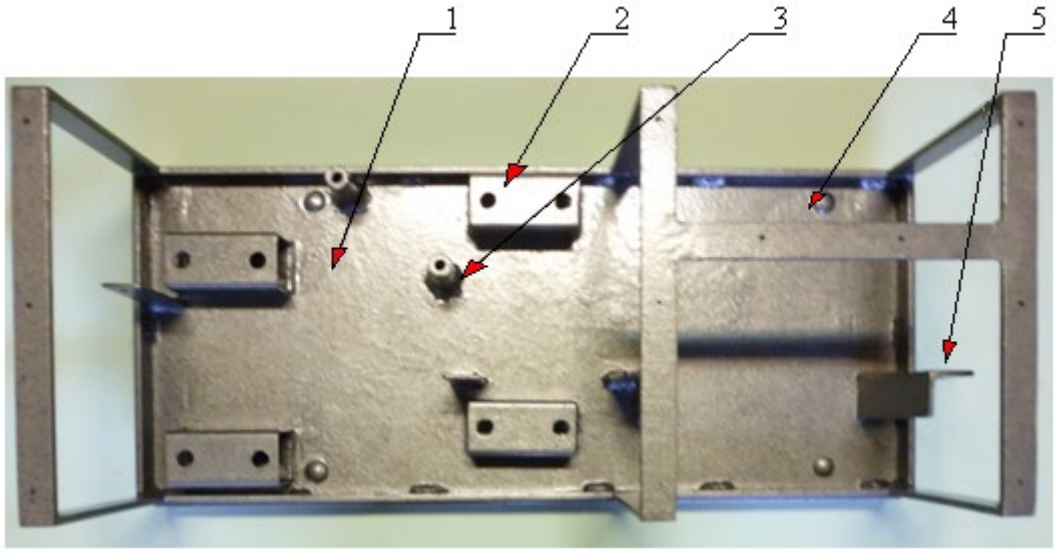

Fig. 24. Steel structure of the laboratory device
1 - steel plate; 2 - bearing housing base; 3 - lever support; 4 - cover supports; 5 - engine support

The laboratory device is equipped with an active unit 1 to which the torque is transferred from the electric motor by means of a belt transmission and a passive unit 2.

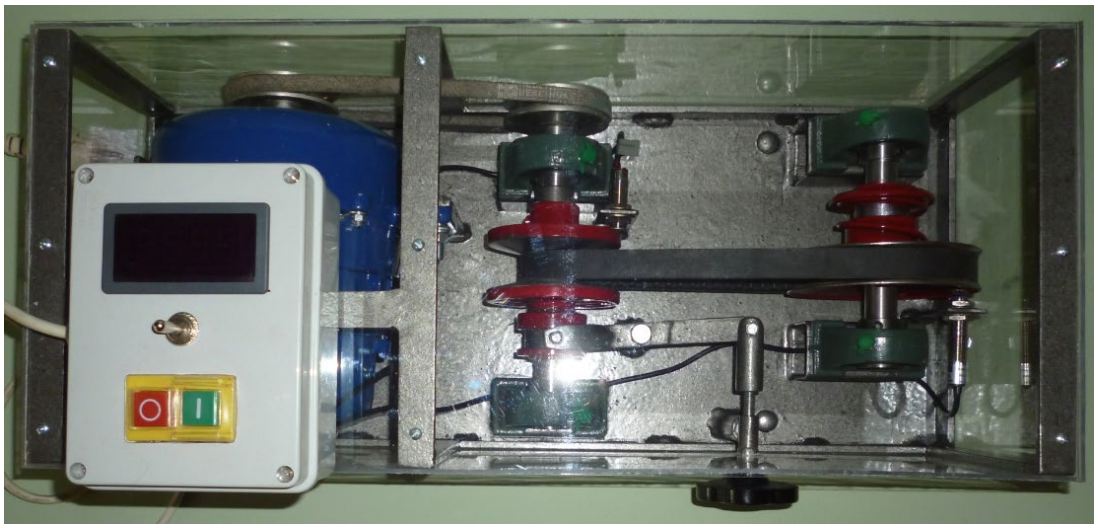

Fig. 26. Continuously variable transmission laboratory device – top view

The driving belt transmission (Fig. 30) is also intended to protect the belt variator against damage. The transmission is driven by a PREDOM SED110-4BN75 150W AC electric motor.

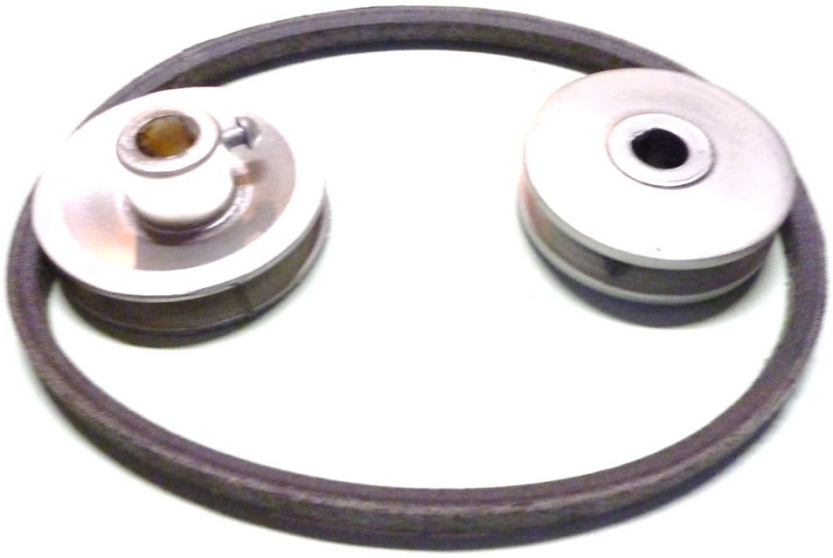

Fig. 30. Parts of the driving transmission

The tested belt variator shown in Fig. 32 used a belt with dimensions of 669x18x30 (Fig. 31) from a 4T GY scooter. One of the tested pulleys (the driving one) is mounted on the active shaft, and the other (the driven one) on the passive shaft.

Fig. 31. Variator V-belt

Fig. 32. Driving set for 4T GY scooter

Fig. 33. Clutch with a 4T GY scooter bell

In the original solution (Fig. 32), the gap between the conical discs in the active unit was regulated by the movement of special rollers through the action of centrifugal force (Fig. 33). In the designed laboratory device, this solution was replaced by a fork lever connected to an adjustment screw.
In the active unit (Fig. 34), one of the discs is permanently mounted on the shaft. The movable disc is moved axially by means of a fork lever. In the constructed system, speed regulation is performed by changing the position of the screw knob connected to the fork lever. The pressure force transferred by the intermediate sleeve causes axial displacement of the disc.

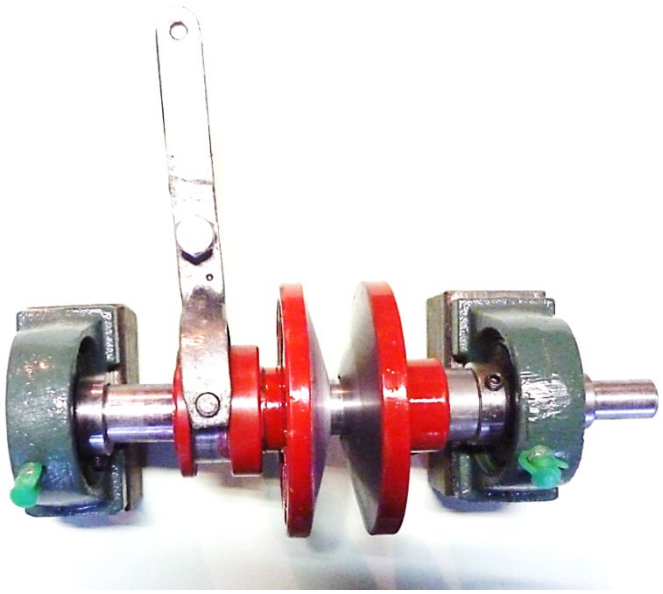

Fig. 34. Active unit

In the passive unit (Fig. 35) of the constructed device, the movable disc can change its position relative to the fixed disc by the axial force generated by the spring pressure. The bell clutch elements were removed from the passive pulley for the 4T GY scooter in order to better observe the change in the position of the movable disc during the speed change.

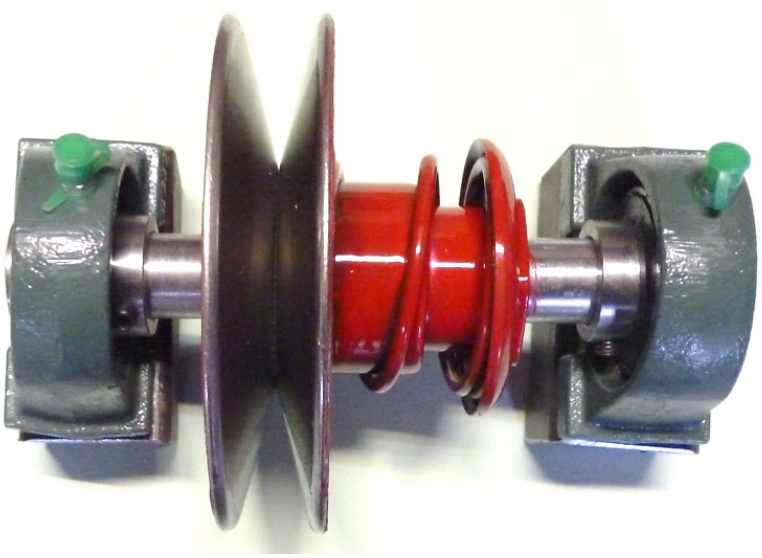

Fig. 35. Passive unit

Both shafts were mounted on bearing units of the UCPA204 type shown in Fig. 36. The unit consists of a UC 204 bearing and a mounting with a standardized PA shape.

The bearing used is maintenance-free, rubber seals protect against moisture and dust and prevent the plastic grease from leaving the working zone of the rolling elements. The plastic grease was introduced by the manufacturer and is sufficient for the entire life of the bearing.

A characteristic feature of the bearing unit is self-alignment, which allows for compensation of assembly errors and shaft deflections. Self-alignment results from the mating of the outer ring of the bearing - a fragment of a sphere together with a mounting of an analogous shape. Self-aligning bearings mounted on the shaft are adapted to drawn shafts with tolerances h6 to h9. UC V self-aligning bearings are fixed on the shaft by two set screws placed every 120° on the inner ring. UC204 bearings are characterized by a dynamic load capacity of Ct=12800 [N] and a static load capacity of Cot=6600 [N].

Fig. 36. UC204 bearing with mounting

The power supply and control unit is designed to read the rotational speeds at the input and output of the transmission. This unit consists of a Hall sensor NPN NO M12 with a 10x2mm neodymium magnet (Fig. 37) with the following parameters:

- supply voltage: 6÷36 V DC,
- detection range: 0÷10 mm,
- max. load current: 300 mA,
- switching frequency: 320 kHz, detected objects - permanent magnet.

Fig. 37. NPN NO M12 Hall sensor with magnet

Digital tachometer (rotating elements speed meter) that measures revolutions in the range of 1÷9999 rpm and enables displaying the current rotational speed using an NPN magnetic sensor cooperating with a magnet mounted on the rotating element. The tachometer (Fig. 38) is characterized by the following parameters:

- supply voltage: 8÷24 VDC,
- current consumption 35 mA,
- measurement range 5÷9999 rpm,
- measurement accuracy +-3 rotations,
- LED display 0.56" (blue),
- meter dimensions 72x36x20 mm.

Fig. 38. Digital tachometer (rotating elements speed meter)

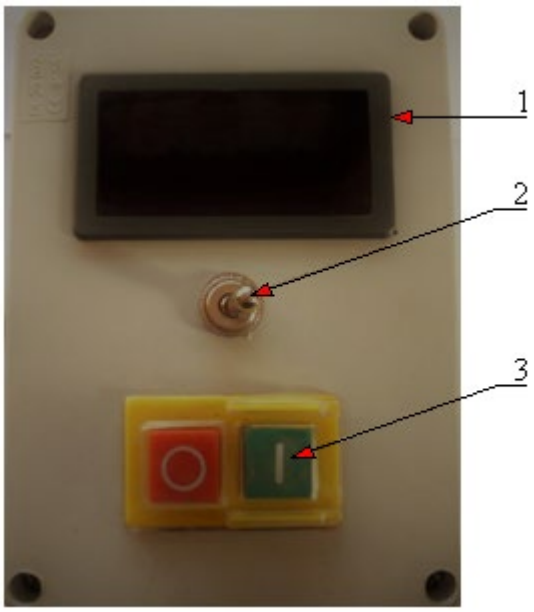

Fig. 39. Control panel: 1 – display (revolution counter); 2 – sensor switch; 3 – power switch

The PREDOM SED110-4BN75 150W engine (Fig. 40) with the following technical parameters was used as the driving unit: voltage: 220V; power: 150W; number of revolutions: 1450 rpm.

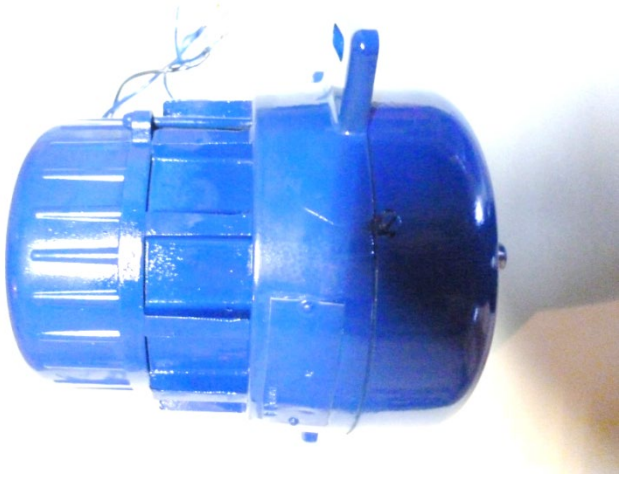

Fig. 40. PREDOM SED110-4BN75 150W engine

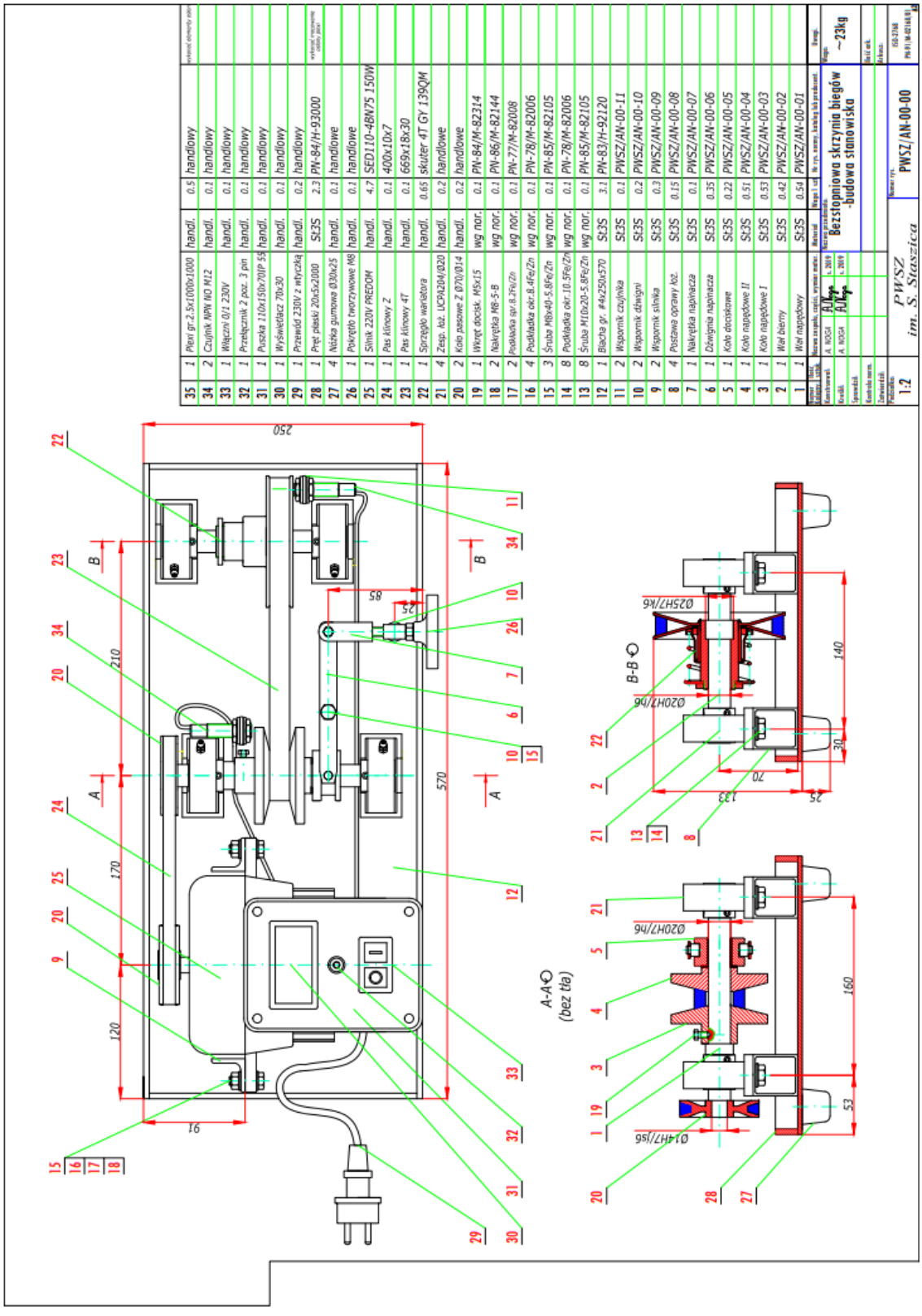

Fig. 41. Assembly drawing of the continuously variable transmission

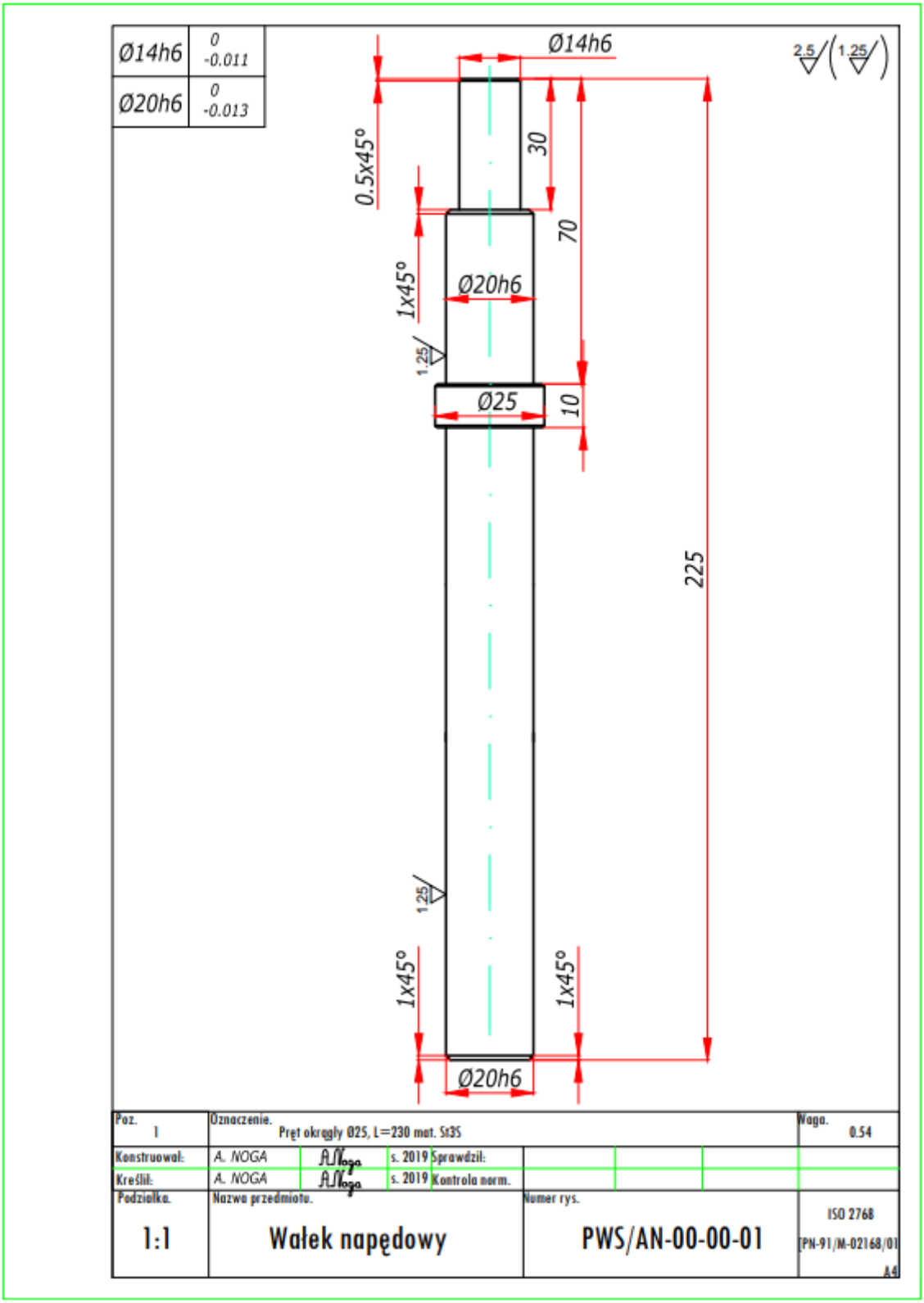

Fig. 42. Production drawing of the driving shaft

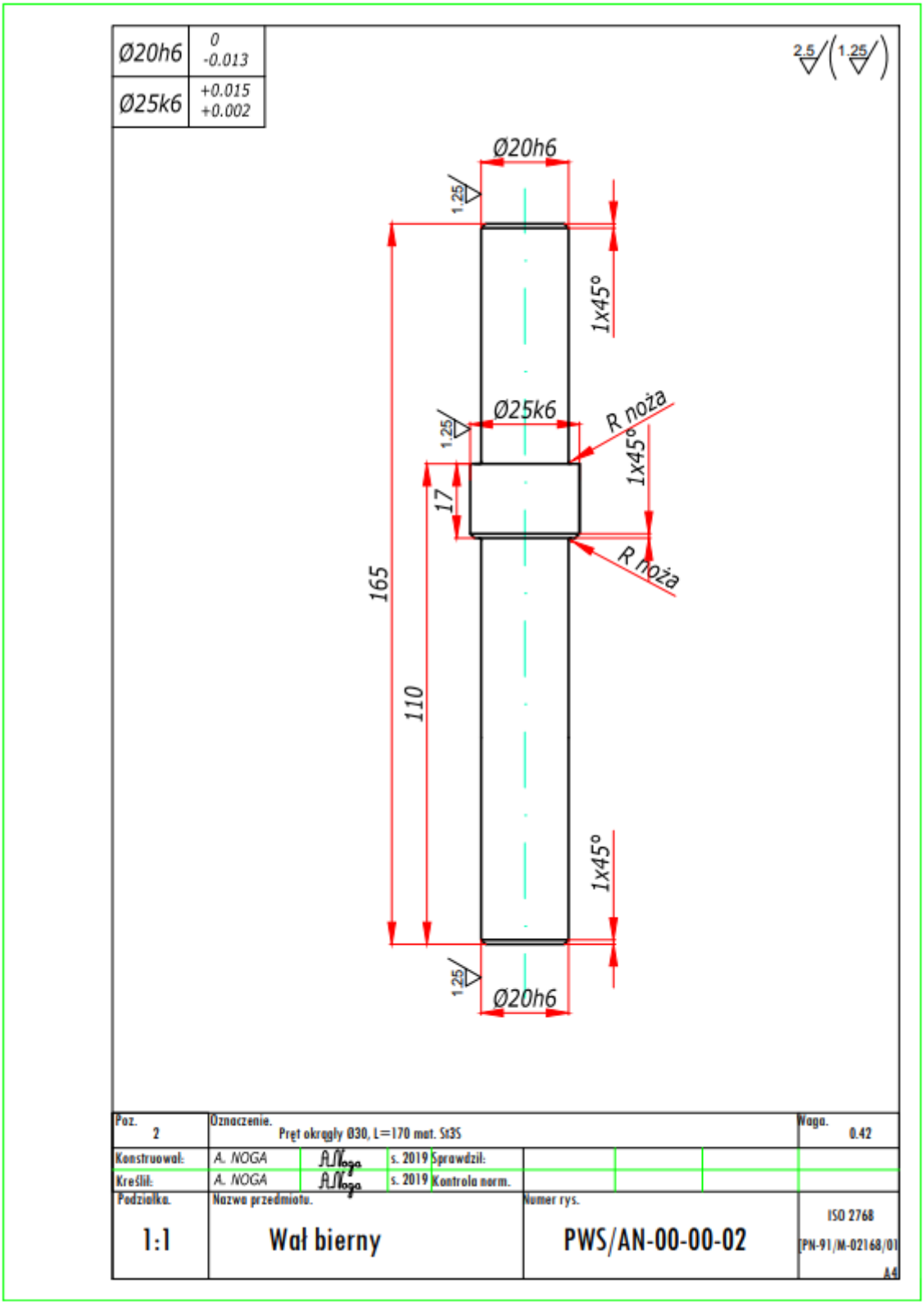

Fig. 43. Production drawing of the driven shaft

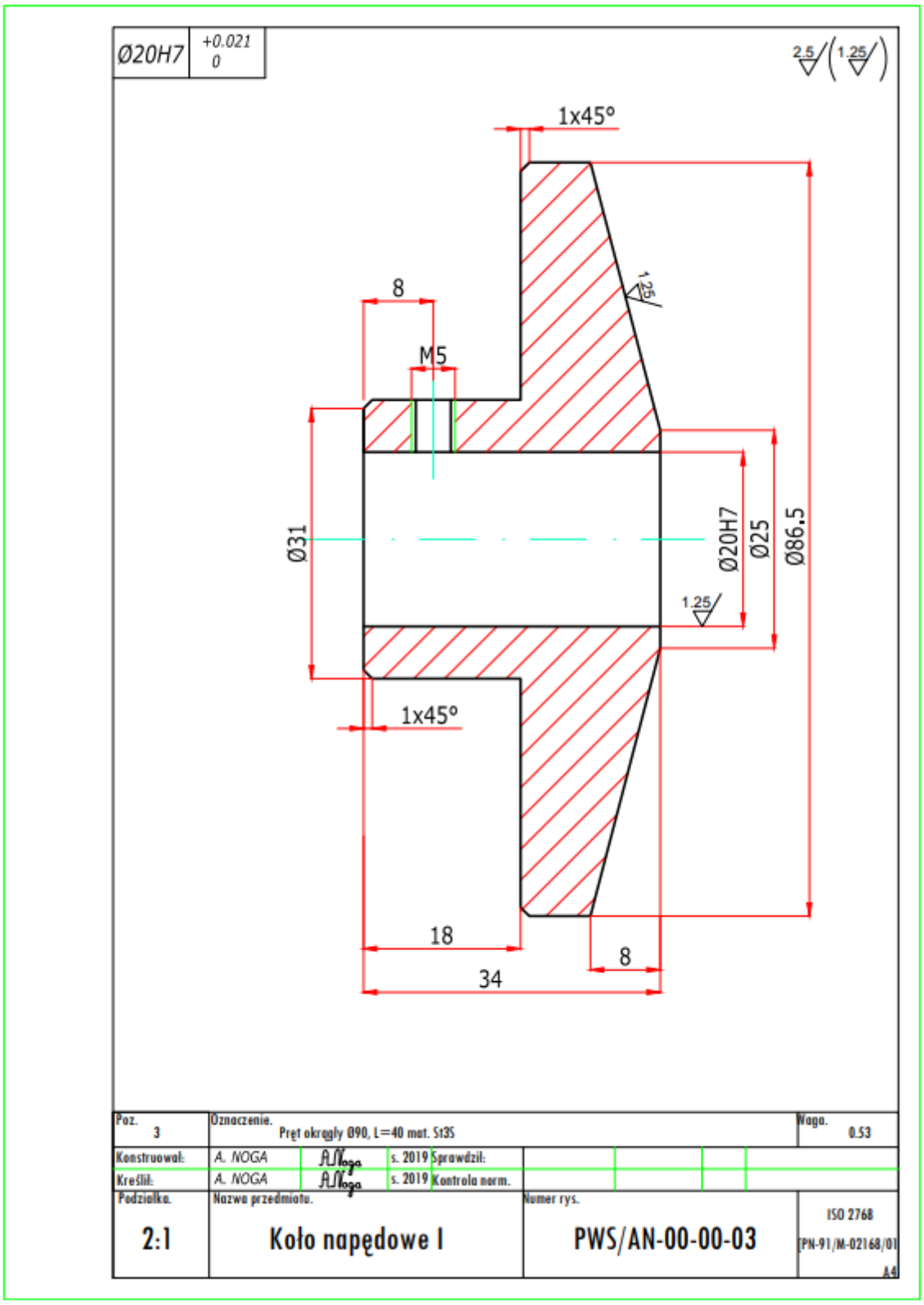

Fig. 44. Production drawing of the drive wheel I

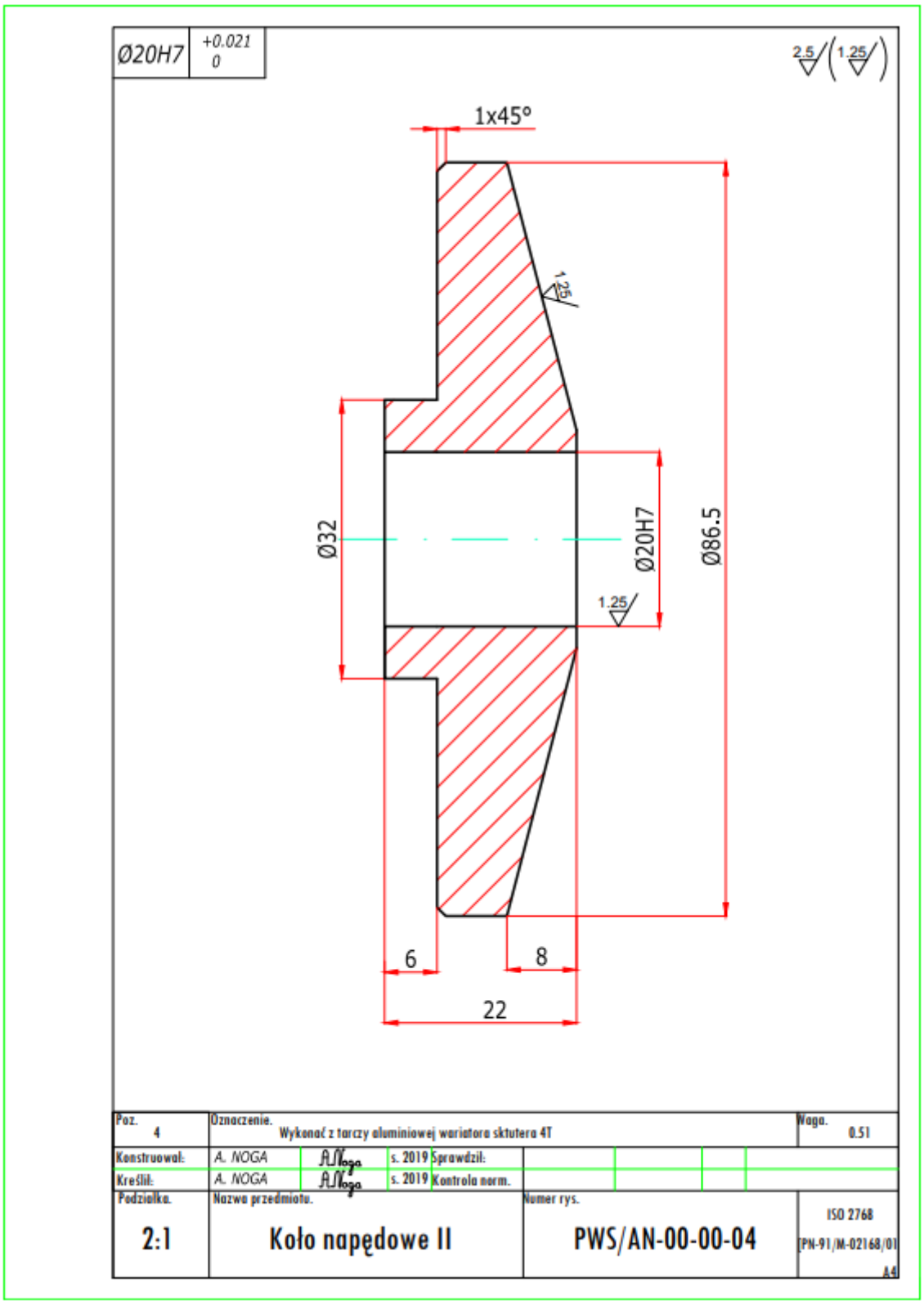

Fig. 45. Production drawing of the drive wheel II

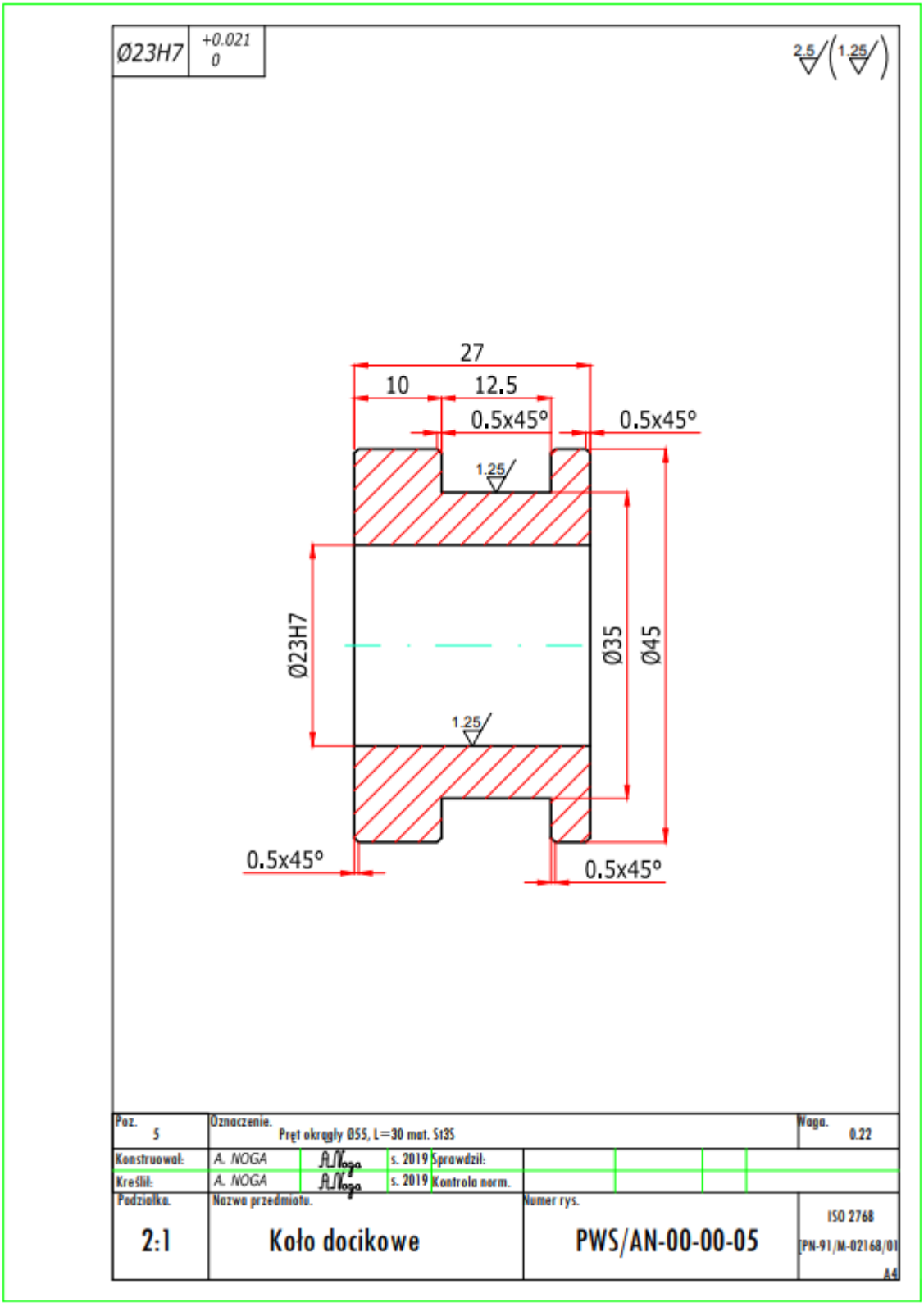

Fig. 46. Production drawing of the pressure wheel

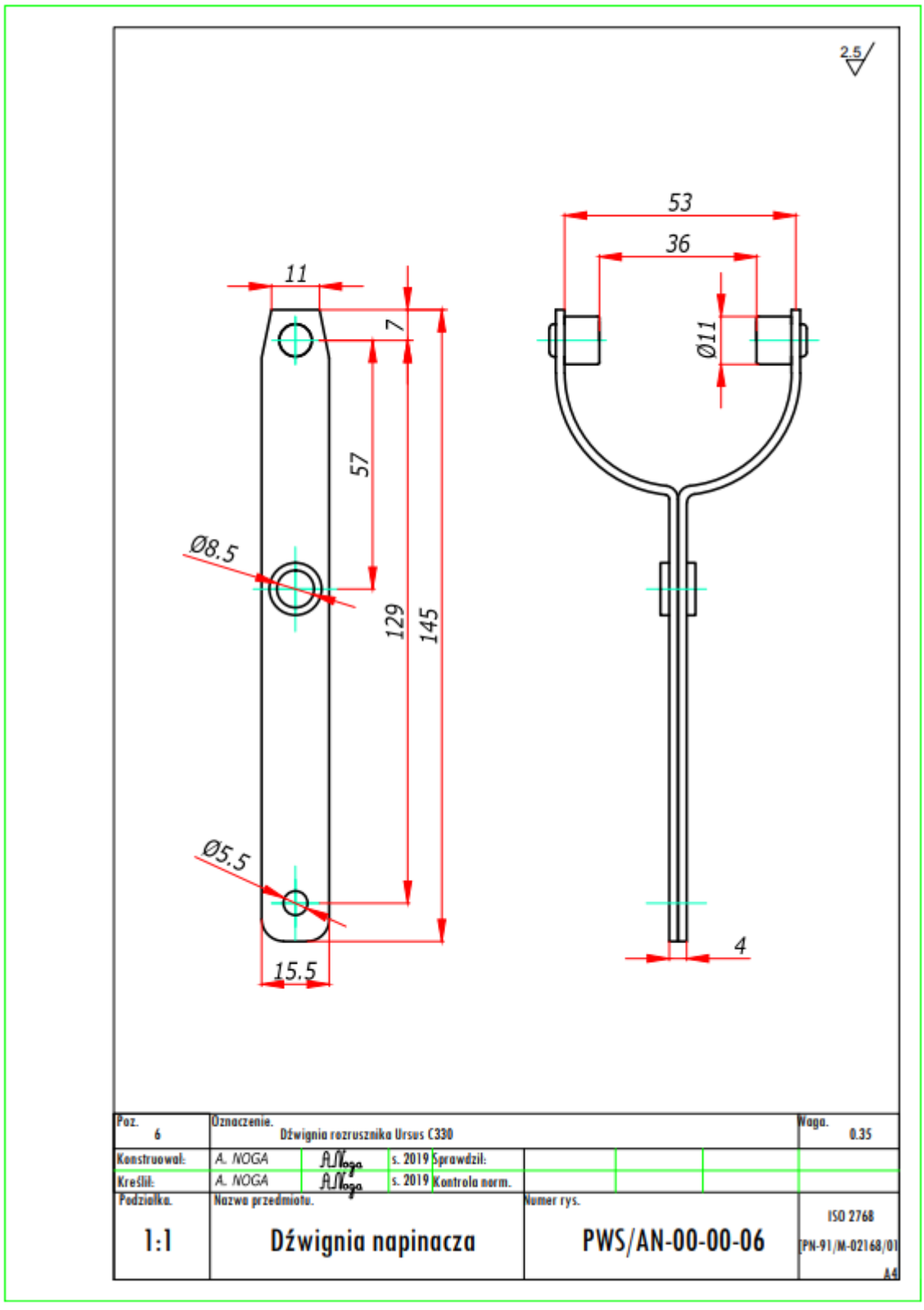

Fig. 47. Production drawing of the tensioner lever

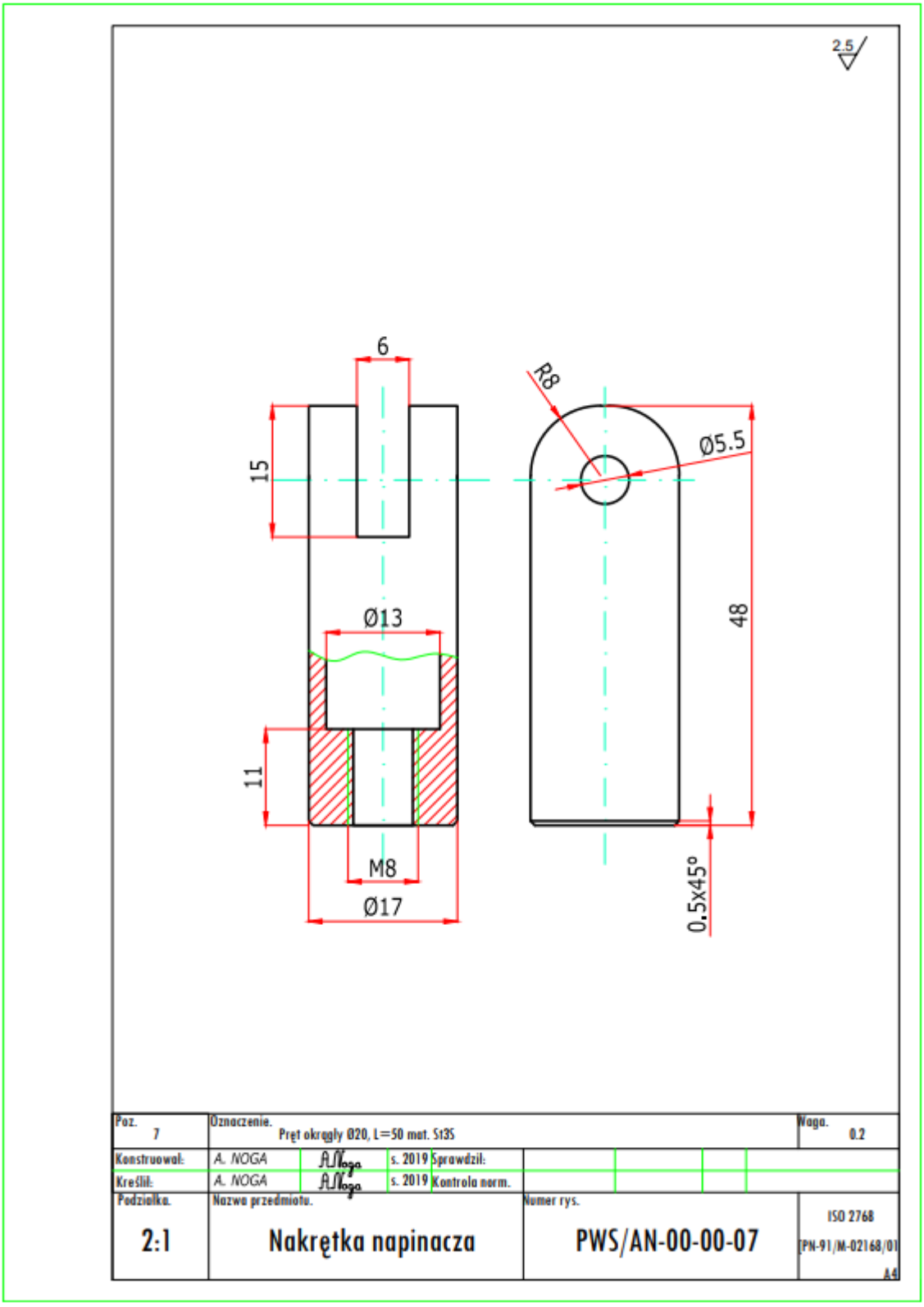

Fig. 48. Production drawing of the tensioner nut

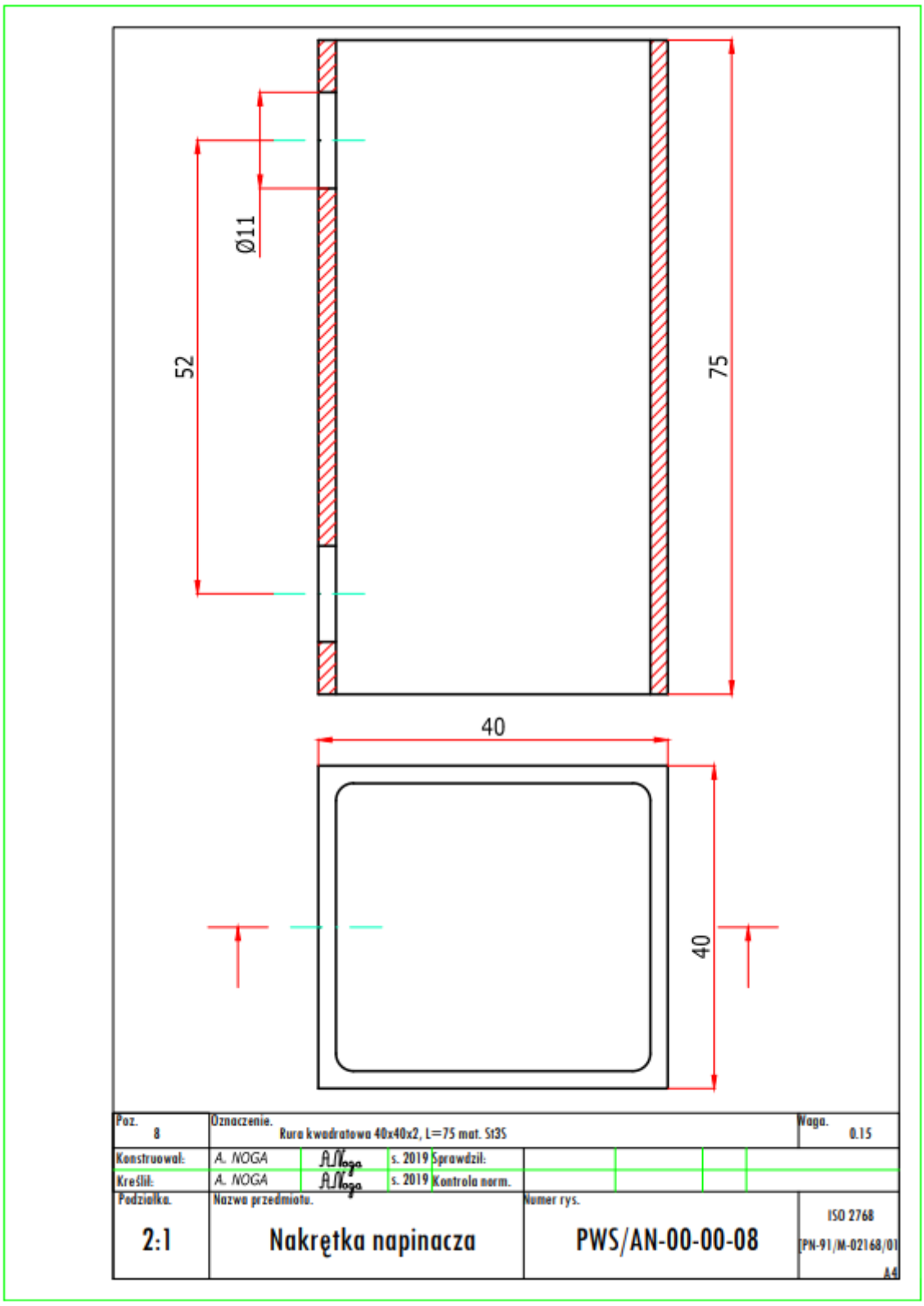

Fig. 49. Production drawing of the tensioner nut profile

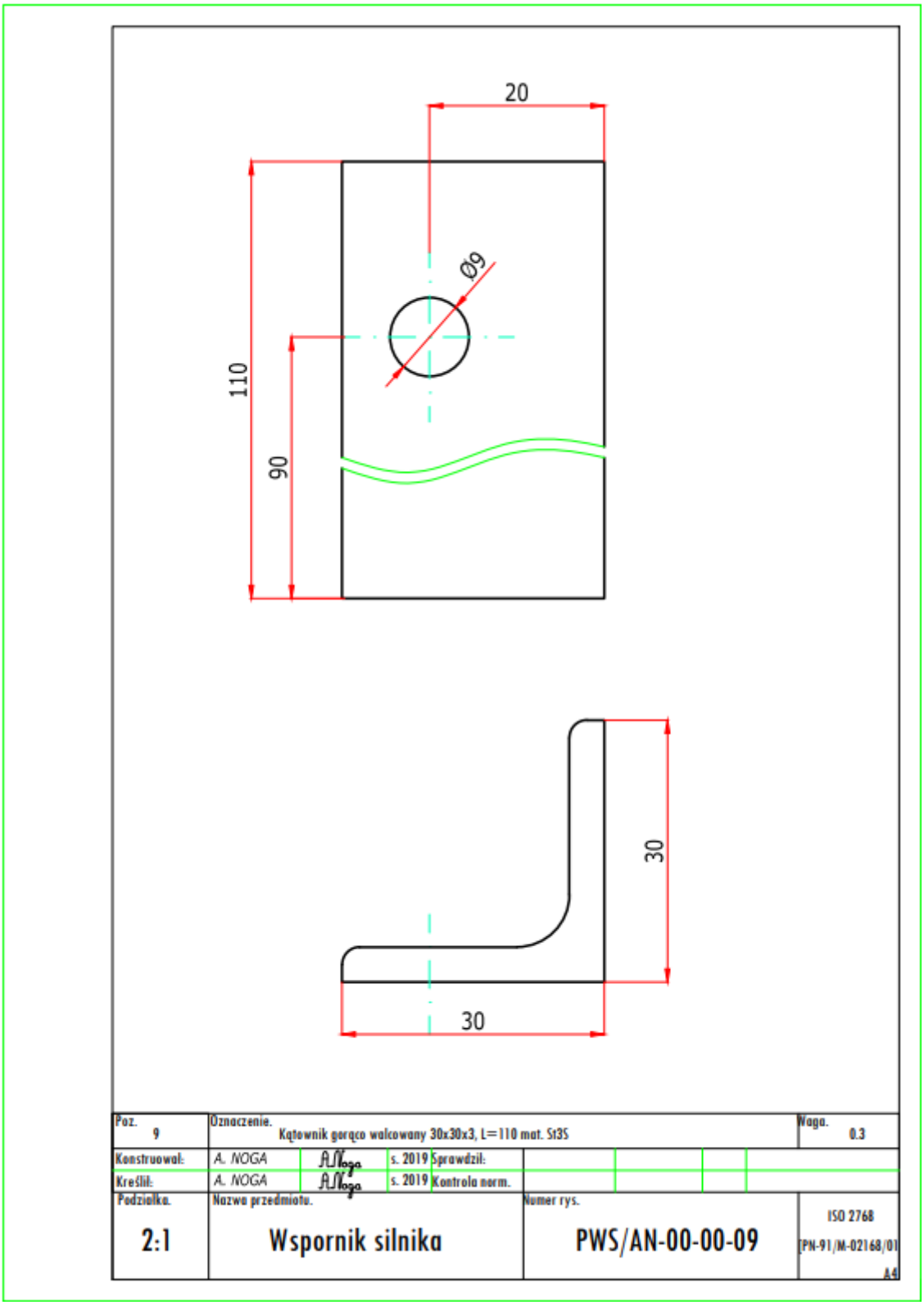

Fig. 50. Production drawing of the engine support

19. Conclusions

The solution for the construction of a continuously variable transmission laboratory device presented in this work shows that in order to obtain optimal power transmission conditions, high transmission reliability and required belt service life, it is necessary to construct the transmission based on calculations aimed at selecting optimal parameters. In the gearbox under consideration, to obtain a better analysis of the parameters, we should use a hydrokinetic clutch on the output shaft and a torque meter. The simple and cheap design of the laboratory device does not require special service or maintenance, which reduces operating costs. Worn V-belts can be quickly and easily replaced without extending the machine's downtime.

Based on the above considerations, one can observe that each transmission has its advantages and disadvantages due to the mechanisms differing in terms of structure and operation, which may affect use and possible repairs. A very important factor in transmissions is the correct belt tension, which affects the quality of power transmission and the service life of belts. Too little tension causes excessive belt slippage on the pulley, too much - a reduction in the service life of the belt and faster wear of the bearings in the driving or driven machine.

The resulting gearbox guarantees calm, quiet and smooth operation. Its advantage is the ability to smooth out sudden load changes and dampen vibrations and is not very sensitive to imperfections in the mutual alignment of the shaft axes. The belt drive allows power distribution, i.e. transferring the drive from one shaft to another.

20. Literature

1. Dobrowolski Z.: Podręcznik spawalnictwa. Wydawnictwo WNT, Warszawa 1978.
2. Domański A., Mikołajczyk J.: Dimensional analysis of the selected type of rolling bearing depending on the manufacturer. **W:** Szkoła Logistyki 2023 / redakcja naukowa Janusz Zawiła-Niedźwiecki, Katarzyna Białczak. Radom: Instytut Naukowo-Wydawniczy "Spatium", 2023, Poland; s. 79-89, p-ISBN: 978-83-67033-75-6; e-ISBN: 978-83-67033-58-9.
3. English A. : *Hochleistung CVT Komponenten,* Vortrag Getriebe in Fahrzeugen, Tagung in Friedrichshafen am 22/23 Juni 2004.
4. Faust H. *: Efficiency Optimised CVT Clamping System*. Luk Symposium, 2002.
5. Faust H .: *CVT Development at LuK*, Luk Symposium, 1998.
6. Fijałkowski K., Mac St.: *Maszynoznawstwo dla ZSZ*. Warszawa 1964.
7. Galon M., Mikołajczyk J.: The effect of laser cutting speed on the bearing surface of peaks and valleys of the cut surface. **W:** Logistyka w ratownictwie 2024 / pod redakcją Andrzeja Chudzikiewicza i Andrzeja Krzyszkowskiego. Radom: Instytut Naukowo-Wydawniczy Spatium, 2024, Poland; s. 71-84, p-ISBN: 978-83-68026-24-5; e-ISBN: 978-83-68026-25-2.
8. Galon M., Mikołajczyk J.: The effect of laser cutting speed on the weight of the workpiece. **W:** Logistyka w ratownictwie 2024 / pod redakcją Andrzeja Chudzikiewicza i Andrzeja Krzyszkowskiego. Radom: Instytut Naukowo-Wydawniczy Spatium, 2024, Poland; s. 85-96, p-ISBN: 978-83-68026-24-5; e-ISBN: 978-83-68026-25-2.
9. Galon M., Mikołajczyk J.: Wpływ wartości posuwu podczas cięcia laserem na chropowatość powierzchni przecięcia. Obróbka Metalu; 2024, nr 3, s. 48-53, p-ISSN: 2081-7002;

https://obrobkametalu.tech/nasze-czasopismo/archiwum/
10. Gerbert B. G.: *Force and Slip Behaviour in V belt Drives*, Acta Polytechnica Scandinavical Engineering Series, No. 67, Helsinki 1972.
11. Goszczak. J.: *Przekładnie o bezstopniowej zmianie przełożenia - charakterystyka i zasosowanie.*
12. Goszczak J., Radzymiński B.: Autobusy: Przekładnie o bezstopniowej zmianie przełożenia - CVT.
13. Goszczak J., Radzymiński B.: *Autobusy: technika, eksploatacja, systemy transportowe.* 2018 | R. 19, nr 6 | 447-451, CD.
14. Grabowska M., Mikołajczyk J.: Zastosowanie tomografii komputerowej CAT w inżynierii materiałowej. Application of CAT scanning for materials engineering. Postępy w Inżynierii Mechanicznej [Developments in Mechanical Engineering]. 2017, nr 9 (5), s. 15-26, p-ISSN: 2300-3383; Wydawnictwa Uczelniane Uniwersytetu Technologiczo-Przyrodniczego w Bydgoszczy, Poland. **http://wu.utp.edu.pl/oferta,8,1**
15. Grabowska M., Mikołajczyk J.: Próba zastosowania tomografii komputerowej CAT do określania struktury grafitu naturalnego w zależności od rozmiaru ziarna. An attempt to apply cat scanning to determine the natural graphite structure depending on the grain size. Postępy w Inżynierii Mechanicznej [Developments in Mechanical Engineering]. 2018, nr 12 (6), s. 5-14, p-ISSN: 2300-3383; Wydawnictwa Uczelniane Uniwersytetu Technologiczno-Przyrodniczego w Bydgoszczy, Poland.
http://wu.utp.edu.pl/oferta,8,1
16. Grabowska M., Mikołajczyk J., Basiak S.: Zastosowanie tomografii komputerowej CAT w nieniszczących badaniach teowych złączy spawanych. Application of cat scanning in non-destructive testing of welded t-joints. Postępy w Inżynierii Mechanicznej [Developments in Mechanical Engineering]; 2018, nr 11 (6), s. 31÷44, p-ISSN: 2300-3383; Wydawnictwa Uczelniane Uniwersytetu Technologiczno-Przyrodniczego w Bydgoszczy, Poland.
http://wu.utp.edu.pl/oferta,8,1
17. Grabowska M., Piochacz A., Mikołajczyk J.: Attempt to use computed tomography CAT to analyze the anodized layer. Postępy w Inżynierii Mechanicznej [Developments in Mechanical Engineering]; 2020, nr 15 (8), s. 25÷33, p-ISSN: 2300-3383; Wydawnictwa Uczelniane Uniwersytetu Technologiczno-Przyrodniczego im. J. J. Śniadeckich w Bydgoszczy, Poland.
https://dme.utp.edu.pl/art/15(8)2020/25.pdf
DOI: 10.37660/dme.2020.15.8.3
18. Grzegożek W.: *Przekładnie o ciągłej zmianie przełożenia (CVT) w układach napędowych pojazdów*. Politechnika Krakowska, Kraków 2011.
19. Hołubowska A., Szałański B., Mikołajczyk J.: Laboratorium termodynamiki. Piła: Wydawnictwo Państwowej Uczelni im. Stanisława Staszica, 2020, Poland; 164 s., e-ISBN: 978-83-62617-93-7;
https://wydawnictwo.puss.pila.pl/files/Laboratorium_termodynamiki_POL_version.pdf
20. Koziarski C.: Bezstopniowe przekładnie cierne ciągła regulacja przełożenia za pomocą tarcia tocznego.
21. Jantos J.*: Control of the Transmision Ratio Derivative In Passenger Car Powertrain with CVT,* Transactions - Journal of Passenger Car , Mechanical System, Vol. 110, 1277 - 1284.
22. Jarmoliński Z., Mikołajczyk J.: Badania wpływu technologii cięcia stali na twardość powierzchni bijaka. Research of the influence of steel cutting technology on the strength of the hammer. Postępy w Inżynierii Mechanicznej [Developments in Mechanical

Engineering]. 2018, nr 12 (6), s. 15-30, p-ISSN: 2300-3383. Wydawnictwa Uczelniane Uniwersytetu Technologiczno-Przyrodniczego w Bydgoszczy, Poland.
http://wu.utp.edu.pl/oferta,8,1
23. Jędrzejczyk D., Mikołajczyk J.: Defining the correlation between the cutting speed and roughness parameter Rz. **W:** MIK-21 : Międzynarodowa Innowacyjność i Konkurencyjność w XXI wieku : aspekty innowacyjne / redakcja naukowa Radosław Luft. Lublin : Fundacja Innowacji i Nowoczesnych Technologii INOTECH, 2022. Radom : nakładem Instytutu Naukowo-Wydawniczego "Spatium", 2022; s. 39-46,
p-ISBN: 978-83-67033-43-5; e-ISBN: 978-83-67033-44-2;
http://inw-spatium.pl/wp-content/uploads/2022/09/MIK-21-2022-Aspekty-innowacyjne-2.pdf
24. Jędrzejczyk D., Mikołajczyk J.: Mathematical models of the influence of cutting speed on Ra parameter. Developments in Mechanical Engineering; 2022, nr 18 (10), s. 115-129, p-ISSN: 2720-0639; Wydawnictwa Uczelniane Uniwersytetu Technologiczno-Przyrodniczego im. J. J. Śniadeckich w Bydgoszczy, Poland.
DOI: 10.37660/dme.2022.18.10.11
25. Jędrzejczyk D., Mikołajczyk J.: Wpływ prędkości skrawania na wybrany parametr warstwy wierzchniej. **W:** Logistyka w ratownictwie 2022 / pod redakcją Andrzeja Chudzikiewicza i Andrzeja Krzyszkowskiego. Radom: Instytut Naukowo-Wydawniczy Spatium, 2022, Poland; s. 75-90,
p-ISBN: 978-83-67033-57-2; e-ISBN: 978-83-67033-70-1
26. Latoś H., Mikołajczyk J.: Effect of partial wear of the tool point on the selected indicator of the machining process. **W:** Logistyka w ratownictwie 2023 / pod redakcją Andrzeja Chudzikiewicza i Anny Stelmach. Radom: Instytut Naukowo-Wydawniczy "Spatium", 2023, Poland; s. 195-210, p-ISBN: 978-83-67033-95-4;
e-ISBN: 978-83-67033-96-1.
27. Latoś H., Mikołajczyk J.: Thickness of the machined layer at milling with single-edge straight blades with an angle of $\lambda s \neq 0°$. **W:** MIK-21 : Międzynarodowa Innowacyjność i Konkurencyjność w XXI wieku : Aspekty innowacyjne / redakcja naukowa dr Łukasz Wojtowicz. Lublin: Fundacja Innowacji i Nowoczesnych Technologii INOTECH : nakładem Instytutu Naukowo-Wydawniczego "Spatium", 2023, Poland; s. 23-27, p-ISBN: 978-83-67033-89-3; e-ISBN: 978-83-67033-90-9.
28. Latoś H., Mikołajczyk J., Konarski J., Mikołajczyk T.: Turning using self-induced vibration. **W:** MIK-21 : Międzynarodowa Innowacyjność i Konkurencyjność w XXI wieku : aspekty innowacyjne / redakcja naukowa dr Łukasz Wojtowicz, 2023, Poland; s. 187-200, p-ISBN: 978-83-67033-89-3; e-ISBN: 978-83-67033-90-9
29. Latoś H., Mikołajczyk J.: Vibration in machining. **W:** Logistyka w ratownictwie 2023 / pod redakcją Andrzeja Chudzikiewicza i Anny Stelmach. Radom: Instytut Naukowo-Wydawniczy "Spatium", 2023, Poland; s. 187-194,
p-ISBN: 978-83-67033-95-4; e-ISBN: 978-83-67033-96-1.
30. Latoś H., Mikołajczyk J.: The effect of feed rate on the roughness of machined surface. **W:** Szkoła Logistyki 2024 / redakcja naukowa Janusz Zawiła-Niedźwiecki, Adam Płaczek. Radom: Instytut Naukowo-Wydawniczy "Spatium", 2024, Poland; s. 217-226, p-ISBN: 978-83-68026-07-8; e-ISBN: 978-83-68026-08-5.
31. Matuszewski M., Mikołajczyk J., Styp-Rekowski M: Modyfikacja cech środka smarującego za pomocą standardowych dodatków smarowych. Modification of lubricants features by means of standard additives. Źródło: Postępy w Inżynierii Mechanicznej [Developments in Mechanical Engineering]. 2013, nr 1 (1), s. 57-65, Wydawnictwo Uczelniane Uniwersytetu Technologiczno-Przyrodniczego w Bydgoszczy; p-ISSN: 2300-3383;

http://wu.utp.edu.pl/uploads/oferta/Postepy_1_1_2013.pdf
32. Matuszewski M., Mikołajczyk J., Mikołajczyk T., Styp-Rekowski M.: Logistyczne aspekty zarządzania procesem naprawy. Logistical aspects of the repair process management. Logistyka, 2015, nr 4, s. 1991-1997, p-ISSN: 1231-5478; **https://www.czasopismologistyka.pl/o-czasopismie/wydania**
33. Matuszewski M., Mikołajczyk J., Mikołajczyk T., Styp-Rekowski M.: The influence of cooling and lubrication liquid quantity on the isotropy of a machine component surface during machining = Wpływ warunków chłodzenia i smarowania podczas obróbki elementów maszyn na stopień izotropowości ich powierzchni. Tribologia. 2016, vol. 265, No. 1, s. 57-65, p-ISSN: 0208-7774; e-ISSN: 1732-422X; **https://t.tribologia.eu/resources/html/article/details?id=158175**
34. Mazanek E. (red.) Przykłady obliczeń z podstaw konstrukcji maszyn. T. 2, WNT, Warszawa 2009.
35. Michalski R.: Zgrzewanie oporowe. Poradnik. Wydawnictwa Naukowo-Techniczne. Warszawa 1970.
36. Mikołajczyk J., Styp-Rekowski M., Świerk K.: Modyfikowanie cech środka smarującego za pomocą dodatków i komputerowe wspomaganie ich doboru. W**:** CAX'2009 : komputerowe wspomaganie nauki i techniki : VI warsztaty naukowe, Bydgoszcz - Duszniki Zdrój 2009 : praca zbiorowa pod redakcją Tadeusza Mikołajczyka. p-ISBN: 978-83-61314-65-3. Wydawnictwa Uczelniane Uniwersytetu Technologiczno-Przyrodniczego w Bydgoszczy, Bydgoszcz 2009.
37. Mikołajczyk J.: Zestawienie porównawcze dodatków depresujących do olejów. W: Zaawansowana tribologia : XXX Ogólnopolska Konferencja Tribologiczna, Nałęczów, 21-24 września 2009 r. Ogólnopolska Konferencja Naukowa XXX Szkoły Tribologicznej "Zaawansowana Tribologia" : Wydział Materiałoznawstwa, Technologii i Wzornictwa Politechniki Radomskiej, Instytut Technologii Eksploatacji - PIB Radom oraz Komitet Budowy Maszyn, Sekcja Podstaw Eksploatacji Maszyn PAN. Wydawnictwo Naukowe Instytutu Technologii Eksploatacji - PIB, Radom, 2009.
38. Mikołajczyk J.: Zestawienie porównawcze własności fizykochemicznych dodatków smarnych w oleju podstawowym SAE-30. W: Terotechnologia 2009 : materiały konferencji na ekspozycji Metal i Control-Tech : Targi - Kielce (29.09-01.10.2009). VI Konferencja Naukowo-Techniczna "Terotechnologia 2009" : Politechnika Świętokrzyska, Centrum Laserowych Technologii Metali, Katedra Inżynierii Eksploatacji, Wydział Mechatroniki i Budowy Maszyn, Polskie Towarzystwo Naukowo-Techniczne, Towarzystwo Eksploatacyjne, Kielce: Wydawnictwo Politechniki Świętokrzyskiej, 2009. Seria: Zeszyty Naukowe - Politechnika Świętokrzyska, nr 13.
39. Mikołajczyk J., Matuszewski M.: Konstrukcja i sterowanie stanowiska do badań tribologicznych. W: CAX'2010 : komputerowe wspomaganie nauki i techniki : VII warsztaty naukowe, Bydgoszcz - Duszniki Zdrój 2010 : praca zbiorowa / pod red. Tadeusza Mikołajczyka. Bydgoszcz : Wydawnictwa Uczelniane Uniwersytetu Technologiczno-Przyrodniczego w Bydgoszczy, 2010. p-ISBN: 9788361314387
40. Mikołajczyk J.: System rejestracji i wizualizacji warunków pracy stanowiska do badań tribologicznych. W: CAX'2011 : komputerowe wspomaganie nauki i techniki : VIII warsztaty naukowe, Bydgoszcz - Duszniki Zdrój 2011 : praca zbiorowa / pod redakcją Tadeusza Mikołajczyka. Bydgoszcz : Wydawnictwa Uczelniane Uniwersytetu Technologiczno-Przyrodniczego w Bydgoszczy, 2011. p-ISBN: 9788361314981.
41. Mikołajczyk J.: Badanie wpływu preparatu eksploatacyjnego Mind M na zmianę własności smarnych oleju bazowego SN-150. Źródło: Inżynieria i aparatura chemiczna

[Chemical Engineering and Equipment]. 2012, nr 5, s. 235-236, p-ISSN: 0368-0827. **http://inzynieria-aparatura-chemiczna.pl/rok-2012-nr-5/**
42. Mikołajczyk J., Styp-Rekowski M., Matuszewski M., Musiał J.: Einfluβ der kompositionen von schmierzusätzen auf die exploitations-eigenschaften der mischung mit Basisöl SN-150. W: Tribologie und mobilität : beiträge der tribotechnik zur optimierung von fertigungsprozessen, wartung, schmierung (reibungskonditionierung) und betriebssicherheit von verkehrsmitteln und verkehrswegen. Wien, 15 November 2012. Symposium 2012 "Tribologie und mobilität" : Österreichische Tribologische Gesellschaft. Österreichische Tribologische Gesellschaft, Wien, 2012.
43. Mikołajczyk J.: Einfluβ der ausgewählten schmierzstoffzusätze auf betriebseigenschaften der mischung mit Basisöl SN-150. **W:** Reibung, schmierung und verschleiβ : forschung und praktische anwendungen. Band 1. Tribologische systeme maschinenelemente und antriebstechnik fahrzeugtechnik prüfen, messen, kontrollieren. Göttingen, 22-24 September 2014. 55. Tribologie Fachtagung "Reibung, Schmierung und Verschleiβ" : Gesellschaft für Tribologie e.V. Stolberg-Venwegen : Gesellschaft für Tribologie e.V., 2014. Germany.
44. Mikołajczyk J.: Einfluss der ausgewählten zusatzschmierstoffe auf die intensivität des verschleiβprozesses (Ra, Rq, Δm) mit Basisöl SN-150. **W:** Tribologie in industrie und forschung : werkstoffe, konstruktion und technologie. Leoben, 26 November 2014. ÖTG Symposium 2014 "Tribologie in industrie und forschung" : Österreichische Tribologische Gesellschaft. Wien : Österreichische Tribologische Gesellschaft, 2014. Austria.
45. Mikołajczyk J., Matuszewski M.: Einfluss der ausgewählten schmierzstoffzusätze auf ΔT und ΔP mit Basisöl SN-150. **W:** Tribologie in industrie und forschung : werkstoffe, schmierstoffe und technologie. Wiener Neustadt, 25 November 2015, Austria. ÖTG Symposium 2015 "Tribologie in industrie und forschung" : Österreichische Tribologische Gesellschaft. Wiener Neustadt : Österreichische Tribologische Gesellschaft, 2015, s. 145-152.
46. Mikołajczyk J.: Vergleich charakteristischer parameter des abbott-firestone-diagramms für ein kinematisches paar mit konformem kontakt. **W:** Tribologie in industrie und forschung : verschleiβschutz, instandhaltung und anlagenzuverlässigkeit. Linz, 22-23 November 2016, Austria. ÖTG Symposium 2016 "Tribologie in industrie und forschung" : Österreichische Tribologische Gesellschaft. Wiener Neustadt : Österreichische Tribologische Gesellschaft, 2016; s. 105-110.
47. Mikołajczyk J.: Wpływ dodatków smarowych na transformację warstwy wierzchniej. Piła : Wydawnictwo Państwowej Wyższej Szkoły Zawodowej im. Stanisława Staszica, 2017 r., Poland. 215, [1] s., p-ISBN: 978-83-62617-76-0; www.ans.pila.pl
48. Mikołajczyk J.: Maszyny tarciowe : budowa, przeznaczenie. Piła, Wydawnictwo Państwowej Wyższej Szkoły Zawodowej im. Stanisława Staszica, 2018, Poland; 256 s., p-ISBN: 978-83-62617-86-9
49. Mikołajczyk J.: Analiza statystyczna zmiany poboru mocy podczas procesu zużywania. Statistical analysis of the power variation of tribotester as a resultat of the wear process. Autobusy. Technika, Eksploatacja, Systemy Transportowe; 2019, nr 10-11, s. 83-88, p-ISSN: 1509-5878; e-ISSN: 2450-7725;
http://yadda.icm.edu.pl/yadda/element/bwmeta1.element.baztech-21189602-884a-4d1a-bb60-9edaeae4af8d
50. Mikołajczyk J.: Influence of consumables on the amount of power consumption of kinematic vapor of conformal contact. Wpływ PE na pobór mocy pary kinematycznej o styku konforemnym. Postępy w Inżynierii Mechanicznej [Developments in Mechanical

Engineering]; 2019, nr 13 (7), s. 39-50, p-ISSN: 2300-3383; Wydawnictwa Uczelniane Uniwersytetu technologiczno-Przyrodniczego im. J. J. Śniadeckich w Bydgoszczy, Poland.
http://yadda.icm.edu.pl/baztech/element/bwmeta1.element.baztech-2faf200b-3010-4192-9fd0-062f53b49d38
51. Mikołajczyk J.: Statistical analysis of the mass variation of samples as a result of the wear process. Analiza statystyczna zmiany masy próbek w wyniku procesu zużywania. Postępy w Inżynierii Mechanicznej [Developments in Mechanical Engineering]; 2019, nr 13 (7), s. 51-61, p-ISSN: 2300-3383; Wydawnictwa Uczelniane Uniwersytetu Technologiczno-Przyrodniczego im. J. J. Śniadeckich w Bydgoszczy, Poland.
http://yadda.icm.edu.pl/baztech/element/bwmeta1.element.baztech-2faf200b-3010-4192-9fd0-062f53b49d38
52. Mikołajczyk J.: Tribotestery : budowa i przeznaczenie. Piła: Wydawnictwo Państwowej Wyższej Szkoły Zawodowej im. Stanisława Staszica, 2019, Poland; 160 s., e-ISBN: 978-83-62617-90-6;
https://wydawnictwo.pwsz.pila.pl/files/Tribotestery.pdf
53. Mikołajczyk J.: Determining the energy validity of the Kostetsky's hypothesis on the basis of models for relative motion velocity v = 0.08 m/sec. Developments in Mechanical Engineering; 2020, nr 16 (8), s. 17-29, p-ISSN: 2720-0639; Wydawnictwa Uczelniane Uniwersytetu Technologiczno-Przyrodniczego im. J. J. Śniadeckich w Bydgoszczy, Poland.
DOI: 10.37660/dme.2020.16.8.2
54. Mikołajczyk J.: Finding the correlation between wear of samples kinematic pair of conformal contact and electric power consumption. Postępy w Inżynierii Mechanicznej [Developments in Mechanical Engineering]; 2020, nr 15 (8), s. 59-68,
p-ISSN: 2300-3383; Wydawnictwa Uczelniane Uniwersytetu Technologiczno-Przyrodniczego im. J. J. Śniadeckich w Bydgoszczy, Poland.
https://dme.utp.edu.pl/art/15(8)2020/59.pdf
DOI: 10.37660/dme.2020.15.8.6
55. Mikołajczyk J.: The effect of temperature lag on the value of power-temperature correlation for frictional pair of conformal contact. Postępy w Inżynierii Mechanicznej [Developments in Mechanical Engineering]; 2020, nr 15 (8), s. 79-86,
p-ISSN: 2300-3383; Wydawnictwa Uczelniane Uniwersytetu Technologiczno-Przyrodniczego im. J. J. Śniadeckich w Bydgoszczy, Poland.
https://dme.utp.edu.pl/art/15(8)2020/79.pdf
DOI: 10.37660/dme.2020.15.8.8
56. Mikołajczyk J.: Określenie na podstawie modeli zmiany masy próbek w wyniku procesu zużywania. **W:** Szkoła Logistyki 2021 / redakcja naukowa Janusz Zawiła-Niedźwiecki, Piotr Korneta. Radom : Instytut Naukowo-Wydawniczy "Spatium", 2021; s. 167-174, Poland; p-ISBN: 978-83-66550-75-9; e-ISBN: 978-83-66550-89-6.
57. Mikołajczyk J.: A method of determining mathematical models of a seizure test of friction pairs. **W:** MIK-21 : Międzynarodowa Innowacyjność i Konkurencyjność w XXI wieku : aspekty innowacyjne / redakcja naukowa Radoslaw Luft. Lublin : Fundacja Innowacji i Nowoczesnych Technologii INOTECH, 2022. Radom : nakładem Instytutu Naukowo-Wydawniczego "Spatium", 2022; s. 7-24, p-ISBN: 978-83-67033-43-5;
e-ISBN: 978-83-67033-44-2.
http://inw-spatium.pl/wp-content/uploads/2022/09/MIK-21-2022-Aspekty-innowacyjne-2.pdf
58. Mikołajczyk J.: Friction machines. Piła: Wydawnictwo Akademii Nauk Stosowanych im. Stanisława Staszica, 2022, Poland; 488 s.,

e-ISBN: 978-83-62617-96-8.
https://wydawnictwo.ans.pila.pl/files/FRICTION_MACHINES.pdf
59. Mikołajczyk J., Jędrzejczyk D.: Określenie korelacji między prędkością skrawania a parametrem chropowatości Ra. Obróbka Metalu; 2022, nr 3, s. 11-15,
p-ISSN: 2081-7002; **https://obrobkametalu.tech/**
60. Mikołajczyk J.: Rolling bearing heating charakter. **W:** Szkoła Logistyki 2022. Radom: Instytut Naukowo-Wydawniczy "Spatium", 2022, Poland; s. 231-239, Materiały z IX Konferencji Naukowej "Szkoła Logistyki 2022";
p-ISBN: 978-83-67033-33-6; e-ISBN: 978-83-67033-34-3.
61. Mikołajczyk J.: Tribological properties of carbon black. **W:** Szkoła Logistyki 2022. Radom: Instytut Naukowo-Wydawniczy "Spatium", 2022, Poland; s. 217-230, Materiały z IX Konferencji Naukowej "Szkoła Logistyki 2022";
p-ISBN: 978-83-67033-33-6; e-ISBN: 978-83-67033-34-3.
62. Mikołajczyk J.: Determination of the modified coefficient of variation from the number of samples. **W:** MIK-21 : Międzynarodowa Innowacyjność i Konkurencyjność w XXI wieku : Aspekty innowacyjne / redakcja naukowa dr Łukasz Wojtowicz. Lublin: Fundacja Innowacji i Nowoczesnych Technologii INOTECH : nakładem Instytutu Naukowo-Wydawniczego "Spatium", 2023, Poland; s. 111-122,
p-ISBN: 978-83-67033-89-3; e-ISBN: 978-83-67033-90-9.
63. Mikołajczyk J.: Effect of cutting speed on the shape of the machined surface profile. Mebutra; 2023, nr 1, s. 47-63, Wydawnictwo Akademii Nauk Stosowanych im. S. Staszica w Pile, Piła 2023, Poland.
https://online.fliphtml5.com/vliuj/yunw/ p=48
64. Mikołajczyk J.: Friction Machines II. Piła: Wydawnictwo Akademii Nauk Stosowanych im. Stanisława Staszica w Pile, 2023, Poland; 598 s.,
p-ISBN: 978-83-67684-00-2;
https://wydawnictwo.ans.pila.pl/files/FRICTION_MACHINES_V_ANS_PILA.pdf
65. Mikołajczyk J.: Oil can talk. **W:** Szkoła Logistyki 2023 / redakcja naukowa Janusz Zawiła-Niedźwiecki, Katarzyna Białczak. Radom: Instytut Naukowo-Wydawniczy "Spatium", 2023, Poland; s. 109-115, p-ISBN: 978-83-67033-75-6;
e-ISBN: 978-83-67033-58-9.
66. Mikołajczyk J.: Pobór mocy elektrycznej przez parę kinematyczną jako parametr oceny jakości oleju. **W:** Logistyka w ratownictwie 2023 / pod redakcją Andrzeja Chudzikiewicza i Anny Stelmach. Radom: Instytut Naukowo-Wydawniczy "Spatium", 2023, Poland; s. 223-230, p-ISBN: 978-83-67033-95-4;
e-ISBN: 978-83-67033-96-1.
67. Mikołajczyk J.: Rola dodatków smarowych w olejach. **W:** Logistyka w ratownictwie 2023 / pod redakcją Andrzeja Chudzikiewicza i Anny Stelmach. Radom: Instytut Naukowo-Wydawniczy "Spatium", 2023, Poland; s. 231-237,
p-ISBN: 978-83-67033-95-4; e-ISBN: 978-83-67033-96-1.
68. Mikołajczyk J.: Temperature as a parameter for assessing the work of a friction pair. **W:** Szkoła Logistyki 2023 / redakcja naukowa Janusz Zawiła-Niedźwiecki, Katarzyna Białczak. Radom: Instytut Naukowo-Wydawniczy "Spatium", 2023, Poland; s. 101-107, p-ISBN: 978-83-67033-75-6; e-ISBN: 978-83-67033-58-9.
69. Mikołajczyk J.: Tire as a selected element of a car subject to diagnostics. **W:** Szkoła Logistyki 2023 / redakcja naukowa Janusz Zawiła-Niedźwiecki, Katarzyna Białczak. Radom: Instytut Naukowo-Wydawniczy "Spatium", 2023, Poland; s. 117-131,
p-ISBN: 978-83-67033-75-6; e-ISBN: 978-83-67033-58-9.

70. Mikołajczyk J.: Wpływ dodatku modyfikującego cechy płynu obróbkowego na zmianę temperatury w strefie kontaktu współpracujących powierzchni. Obróbka Metalu; 2023, nr 2, s. 43-46, p-ISSN: 2081-7002;
https://obrobkametalu.tech/media/2023/05/2023_2_52_ObrobkaMetalu.pdf
71. Mikołajczyk J., Kozłowska M.A., Krasicki K.: Wpływ kompetencji cyfrowych pracowników na poziom rozwoju procesów przemysłowych. **W:** MIK-21 : Międzynarodowa Innowacyjność i Konkurencyjność w XXI wieku : aspekty społeczne / redakcja naukowa Radosław Luft. Lublin-Radom : Fundacja Innowacji i Nowoczesnych Technologii INOTECH : nakładem Instytutu Naukowo-Wydawniczego "Spatium", 2023, Poland; s. 149-169, p-ISBN: 978-83-67033-92-3; e-ISBN: 978-83-67033-93-0.
72. Mikołajczyk J.: Zmiana geometrycznych cech współpracujących powierzchni miarą intensywności procesu zużywania ostrzy skrawających. Obróbka Metalu; 2023, nr 1, s. 50-54, p-ISSN: 2081-7002;
https://yadda.icm.edu.pl/yadda/element/bwmeta1.element.baztech-9e73eb05-2a91-4df5-853b-22abf7a6ee77
73. Mikołajczyk J., Góra F., Jędrzejczyk D.: Analysis of selected surface roughness parameters for wear processes. Analiza wybranych parametrów chropowatości powierzchni pod kątem procesów zużywania. **W:** MIK-21 : Międzynarodowa Innowacyjność i Konkurencyjność w XXI wieku : Aspekty innowacyjne / redakcja naukowa Radosław Luft. Lublin: Wydawnictwo Naukowe FNCE, 2024; s. 93-117,
p-ISBN: 978-83-68074-82-6; e-ISBN: 978-83-68319-03-3.
74. Mikołajczyk J., Galon M.: Mathematical model of straight regression determining the effect of laser cutting speed on the mass of the workpiece. **W:** MIK-21 : Międzynarodowa Innowacyjność i Konkurencyjność w XXI wieku : Aspekty innowacyjne / redakcja naukowa Radosław Luft. Lublin: Wydawnictwo Naukowe FNCE, 2024, Poland; s. 71-92, p-ISBN: 978-83-68074-82-6;
e-ISBN: 978-83-68319-03-3.
75. Mikołajczyk J., Sądej I.: Spinning speed and balancing accuracy. **W:** MIK-21 : Międzynarodowa Innowacyjność i Konkurencyjność w XXI wieku : Aspekty innowacyjne / redakcja naukowa Radosław Luft. Lublin: Wydawnictwo Naukowe FNCE, 2024, Poland; s. 118-132, p-ISBN: 978-83-68074-82-6;
e-ISBN: 978-83-68319-03-3.
76. Mikołajczyk J.: The correlation between the population and number of construction disasters. Mebutra; 2025, nr 3, s. 44-55, Wydawnictwo Akademii Nauk Stosowanych im. S. Staszica w Pile, Poland.
https://wydawnictwo.ans.pila.pl/files/MEBUTRA2025.pdf
77. Mikołajczyk J.: The relationship between the type of structure and the number of construction disasters. Zależność między rodzajem konstrukcji, a liczbą katastrof budowlanych. Mebutra; 2025, 3, s. 30-43, Wydawnictwo Akademii Nauk Stosowanych im. S. Staszica w Pile, Poland.
https://wydawnictwo.ans.pila.pl/files/MEBUTRA2025.pdf
78. Norma PN-86/H-84018. Stal niskostopowa o podwyższonej wytrzymałości. Gatunki.
79. Olechnowicz J., Mikołajczyk J.: Truck scales : the key to safe transport and road protection. Mebutra; 2024, nr 2, s. 03-08, Wydawnictwo Akademii Nauk Stosowanych im. S. Staszica w Pile, Poland.
https://wydawnictwo.ans.pila.pl/files/MEBUTRA2024.pdf
80. Olsza M.: *Projektowanie i dobieranie zespołów maszyn. 311[20].Z2.03.* Instytut Technologii Eksploatacji – Państwowy Instytut Badawczy, Radom 2005.

81. Pikulik K.W., Mikołajczyk J.: The influence of the welding current on the air pollution emissions. Wpływ prądu spawania na emisję zanieczyszczeń powietrza. Postępy w Inżynierii Mechanicznej [Developments in Mechanical Engineering]; 2019, nr 14 (7), s. 33-46, p-ISSN: 2300-3383; Wydawnictwa Uczelniane Uniwersytetu Technologiczno-Przyrodniczego im. J. J. Śniadeckich w Bydgoszczy, Poland.
http://yadda.icm.edu.pl/baztech/element/bwmeta1.element.baztech-2faf200b-3010-4192-9fd0-062f53b49d38
82. Pikulik K.W., Mikołajczyk J.: Determination of emission of iron oxides from the welding process on the basis of mathematical models. Welding Technology Review; 2021, vol. 93, No 2, s. 35-43, p-ISSN: 0033-2364; e-ISSN: 2449-7959; **http://www.pspaw.wip.pw.edu.pl/index.php/pspaw/article/view/1132**
DOI: 10.26628/wtr.v93i2.1132
83. Pikulik J., Pikulik K.W., Mikołajczyk J.: The relationship between the clearance of the coupling mechanism used in uniaxial light car trailers and the date of their production. **W:** MIK-21 : Międzynarodowa Innowacyjność i Konkurencyjność w XXI wieku : aspekty innowacyjne / redakcja naukowa Radosław Luft. Lublin : Fundacja Innowacji i Nowoczesnych Technologii INOTECH, 2022, Poland. Radom : nakładem Instytutu Naukowo-Wydawniczego "Spatium", 2022; s. 221-233,
p-ISBN: 978-83-67033-43-5; e-ISBN: 978-83-67033-44-2;
http://inw-spatium.pl/wp-content/uploads/2022/09/MIK-21-2022-Aspekty-innowacyjne-2.pdf
84. Pikulik J., Pikulik K.W., Mikołajczyk J.: Zależność wielkości luzu mechanizmu sprzęgającego stosowanego w jednoosiowych lekkich przyczepach samochodowych od wartości współczynnika przylegania. **W:** Logistyka w ratownictwie 2022 / pod redakcją Andrzeja Chudzikiewicza i Andrzeja Krzyszkowskiego. Radom: Instytut Naukowo-Wydawniczy "Spatium", 2022, Poland; s. 157-167, p-ISBN: 978-83-67033-57-2;
e-ISBN: 978-83-67033-70-1.
85. Pikulik J., Pikulik K.W., Mikołajczyk J.: Determination of the degree of contact of the movable part of the coupling head with the ball part of the coupling of single-axle light car trailers. **W:** MIK-21 : Międzynarodowa Innowacyjność i Konkurencyjność w XXI wieku : aspekty innowacyjne / redakcja naukowa dr Łukasz Wojtowicz. Lublin: Fundacja Innowacji i Nowoczesnych Technologii INOTECH : nakładem Instytutu Naukowo-Wydawniczego "Spatium", 2023, Poland; s. 97-109,
p-ISBN: 978-83-67033-89-3; e-ISBN: 978-83-67033-90-9.
86. Piochacz A., Mikołajczyk J.: Wpływ czasu trwania procesu anodowania stopu aluminium EN AW-6060 na grubość i twardość otrzymanej warstwy. Influence of aluminium type EN AW-6060 anodizing process duration on the thickness and hardness of the obtained layer. Postępy w Inżynierii Mechanicznej [Developments in Mechanical Engineering], 2018, nr 12 (6), s. 49-56, p-ISSN: 2300-3383; Wydawnictwa Uczelniane Uniwersytetu Technologiczno-Przyrodniczego w Bydgoszczy, Poland. **http://wu.utp.edu.pl/oferta,8,1**
87. Piochacz A., Mikołajczyk J.: Analiza statystyczna wpływu czasu anodowania na grubość otrzymanej powłoki. Statistical analysis of the influence of anodizing time on the thickness of obtained layers. Autobusy. Technika, Eksploatacja, Systemy Transportowe; 2019, vol. 233, nr 9, s. 48-51, p-ISSN: 1509-5878;
e-ISSN: 2450-7725; **http://ceref.pl/index.php/Autobusy/article/view/956**
DOI: 10.24136/atest.2019.201
88. Piochacz A., Mikołajczyk J.: Determination of the thickness of anodized layer on the basis mathematical models. Developments in Mechanical Engineering; 2020, nr 16 (8), s. 31-39, p-ISSN: 2720-0639; Wydawnictwa Uczelniane Uniwersytetu

Technologiczno-Przyrodniczego im. J. J. Śniadeckich w Bydgoszczy, Poland. **DOI: 10.37660/dme.2020.16.8.3**
89. Piotrowski Ł., Góra F., Mikołajczyk J.: Construction of an electric longboard with one-wheel driver. Mebutra; 2024, nr 2, s. 16-27, Wydawnictwo Akademii Nauk Stosowanych im. S. Staszica w Pile, Poland.
https://wydawnictwo.ans.pila.pl/files/MEBUTRA2024.pdf
90. Piotrowski Ł., Góra F., Mikołajczyk J.: Design and construction of an electric longboard. **W:** Logistyka w ratownictwie 2024 / pod redakcją Andrzeja Chudzikiewicza i Andrzeja Krzyszkowskiego. Radom: Instytut Naukowo-Wydawniczy Spatium, 2024, Poland; s. 167-178, p-ISBN: 978-83-68026-24-5; e-ISBN: 978-83-68026-25-2.
91. Praca zbiorowa: Poradnik konstrukcyjny. WNT, Warszawa 2019.
92. Przybył B., Kabat M., Mikołajczyk J.: Wpływ prędkości drukowania 3D na dokładność zarysu kół zębatych. Obróbka Metalu; 2023, nr 4, s. 26-30,
p-ISSN: 2081-7002;
https://obrobkametalu.tech/media/2023/08/2023-4_Nr54_ObrobkaMetalu.pdf
93. Przybył B., Mikołajczyk J.: Efektywność technik przyrostowych. Obróbka Metalu; 2024, nr 1, s. 22-25, p-ISSN: 2081-7002;
https://obrobkametalu.tech/media/2024/03/2024_1_nr55_ObrobkaMetalu-1.pdf
94. Przybył B., Mikołajczyk J.: The influence of 3D printing speed on profile accuracy. **W:** Szkoła Logistyki 2024 / redakcja naukowa Janusz Zawiła-Niedźwiecki, Adam Płaczek. Radom: Instytut Naukowo-Wydawniczy "Spatium", 2024, Poland; s. 199-216, p-ISBN: 978-83-68026-07-8; e-ISBN: 978-83-68026-08-5.
95. Rooij J.H.M.: *The GCI Involute Chain CVT for Torques up to 2500 Nm*, HTAS Presentation Almelo, 22 March 2010.
96. Sądej I., Mikołajczyk J.: Machine tool compensation and mass unbalance measurements. **W:** Logistyka w ratownictwie 2024 / pod redakcją Andrzeja Chudzikiewicza i Andrzeja Krzyszkowskiego. Radom: Instytut Naukowo-Wydawniczy Spatium, 2024, Poland; s. 187-196, p-ISBN: 978-83-68026-24-5;
e-ISBN: 978-83-68026-25-2.
97. Srivastava N. *i in.: A Review on Belt d Chain Continuously Variable Trsnsmission (CVT): Dynamics and Control*
98. Styp-Rekowski M., Mikołajczyk J.: The influence of Mind M preparation on the lubricant properties of base oil SN-150. W**:** Reinung, Schmierung und Verschleiß : forschung und praktische anwendungen : Band 1 : tribologische systeme schmierstoffe und schmierungstechnik zerspanungs : und umformtechnik prüfen, messen, kontrollieren / 53. Tribologie-Fachtagung. 24.bis 26. Septembet 2012 in Göttingen. Aachen : Gesellschaft für Tribologie e.V., 2012. p-ISBN: 978-3-00-039201-6
99. Styp-Rekowski M., Mikołajczyk J.: Wpływ dodatku na własności smarowe oleju bazowego SN-150. Źródło: Tribologia. 2012, vol. 244, No. 4, s. 227-232, p-ISSN: 0208-7774; e-ISSN: 1732-422X;
https://t.tribologia.eu/resources/html/article/details?id=167726
100. Styp-Rekowski M., Mikołajczyk J.: Wpływ preparatu eksploatacyjnego stanowiący kompleks węglowodorowy na zmianę własności smarnych oleju bazowego SN-150. W: Tribologia bliżej praktyki : XXXII Ogólnopolska Konferencja "Jesienna Szkoła Tribologiczna 2012". XXXII Ogólnopolska Konferencja "Jesienna Szkoła Tribologiczna 2012", Kudowa Zdrój, 18-21 września 2012r. Politechnika Wrocławska Wydział Mechaniczny, Instytut Konstrukcji Eksploatacji Maszyn, Polskie Towarzystwo Tribologiczne, Sekcja Podstaw Eksploatacji KBM PAN. Wrocław : Polskie Towarzystwo Tribologiczne, 2012.

101. Styp-Rekowski M., Mikołajczyk J.: Zmiana temperatury na drodze tarcia dla kompozycji olej bazowy SN-150 - preparat eksploatacyjny Mind M. Temperature variability during friction for composition bese oil SN-150 - exploatational preparation Mind M. **W:** III krajowa konferencja nano- i mikromechaniki / Komitet Mechaniki Polskiej Akademii Nauk, Politechnika Rzeszowska im. Ignacego Łukasiewicza, Instytut Podstawowych Problemów Techniki Polskiej Akademii Nauk. Warszawa, 4-6 lipca 2012 r. III Krajowa Konferencja Nano- i Mikromechaniki pod Patronatem Ministra Nauki i Szkolnictwa Wyższego Prof. Barbary Kudryckiej : Komitet Mechaniki Polskiej Akademii Nauk, Politechnika Rzeszowska, Instytut Podstawowych Problemów Techniki Polskiej Akademii Nauk, Warszawa, 2012.
102. Styp-Rekowski M., Mikołajczyk J., Matuszewski M.: Wybrane zagadnienia stosowania płynów obróbkowych w obróbce skrawaniem. W**:** Obróbka Metalu, 2014, nr 3, s. 10-14, p-ISSN: 2081-7002; **http://www.e-obrobkametalu.pl/**
103. Syrek S., Mikołajczyk J.: Analiza matematyczna podstawowych wymiarów złącza spawanego. **W:** Logistyka w ratownictwie 2022 / pod redakcją Andrzeja Chudzikiewicza i Andrzeja Krzyszkowskiego. Radom : Instytut Naukowo-Wydawniczy "Spatium", 2022; s. 169-190, p-ISBN: 978-83-67033-57-2;
e-ISBN: 978-83-67033-70-1.
104. Syrek S., Mikołajczyk J.: Modele liniowe wpływu częstotliwości prądu spawania na grubość spoiny. **W:** MIK-21 : Międzynarodowa Innowacyjność i Konkurencyjność w XXI wieku : aspekty innowacyjne / redakcja naukowa Radosław Luft. Lublin: Fundacja Innowacji i Nowoczesnych Technologii INOTECH, 2022. Radom : nakładem Instytutu Naukowo-Wydawniczego "Spatium", 2022; s. 153-170,
p-ISBN: 978-83-67033-43-5; e-ISBN: 978-83-67033-44-2;
http://inw-spatium.pl/wp-content/uploads/2022/09/MIK-21-2022-Aspekty-innowacyjne-2.pdf
105. Syrek S., Mikołajczyk J.: Modele liniowe wpływu częstotliwości prądu spawania na szerokość spoiny. Obróbka Metalu; 2022, nr 4, s. 24-31,
p-ISSN: 2081-7002; **https://obrobkametalu.tech/**
106. Wesołowski L., Mikołajczyk J.: Hammer mill design and construction analysis. **W:** MIK-21 : Międzynarodowa Innowacyjność i Konkurencyjność w XXI wieku : aspekty innowacyjne / redakcja naukowa dr Łukasz Wojtowicz. Lublin: Fundacja Innowacji i Nowoczesnych Technologii INOTECH : Nakład Instytutu Naukowo-Wydawniczego "Spatium", 2023, Poland; s. 159-185, p-ISBN: 978-83-67033-89-3;
e-ISBN: 978-83-67033-90-9.
107. Zandecki R., Kmita C., Mikołajczyk J.: Mathematical models of the surface layer microhardness for a selected grade of ion nitrided steel. **W:** Szkoła Logistyki 2022. Radom : Instytut Naukowo-Wydawniczy "Spatium", 2022, Poland; s. 203-216, Materiały z IX Konferencji Naukowej "Szkoła Logistyki 2022";
p-ISBN: 978-83-67033-33-6; e-ISBN: 978-83-67033-34-3.

Design and construction of a test rig for measuring the torsional angle of a circular shaft

Julia Dominika Lecka
II Liceum Ogólnokształcące im. Stanisława Staszica w Pile
https://orcid.org/0009-0006-1640-3834

mgr inż. Karol Szudrowicz
Department of Mechanical Engineering
Stanisław Staszic State University of Applied Sciences in Piła, Poland
https://orcid.org/0009-0000-4337-1299
corresponding e-mail: karol-szudrowicz@wp.pl

inż. Paweł Tomasz Lecki
Department of Mechanical Engineering
Stanisław Staszic State University of Applied Sciences in Piła, Poland
https://orcid.org/0009-0001-0714-8118
corresponding e-mail: pt.lecki@wp.pl

Abstract:

Working machines which are currently produced are very complex structures, consisting of many parts, often manufactured in different parts of the world. The element transmitting torque in these machines is most often a shaft. Under the influence of load or external forces, the shaft twists. It is therefore necessary to be able to determine the size of this torsional angle as precisely as possible. This paper, in its first part, presents the construction design and use of shafts. It characterizes the typical loads acting on them, focusing in particular on the phenomenon of torsion. It explains and describes how the torsion is determined based on geometric measurements. The second part contains the design and description of the construction of a test rig for measuring the shaft torsional angle along with an experimental verification of its correct operation. The measurements carried out confirmed the assumptions contained in the theoretical part.

Key words: machine shaft, torque moment, measurement of torsional angle

1. Introduction

The action of torque moments on the shaft during mechanical loads while machine operation may result in improper operation, e.g. in devices with a cam drive or gear mechanisms. Torsional deformations of the drive shaft may cause jamming of components or a lack of synchronization of the device's operation, and in extreme cases they may lead to its destruction. To understand the occurrence of such stresses in a shaft, it will be helpful to perform a test on a test rig for measuring the angle of this torsion.

Shaft - a structural element of a machine, most often circular in section, mounted in the machine by means of bearings, on which working elements are mounted. The main task of shafts is to transmit or change the torque through the components installed on them, assuming that the shaft is an element that is always in rotation during operation. The design of the shaft depends on its purpose and intended working functions, which are characterized by great diversity due to their construction. When we consider the construction, the following can be listed [2]:

- uniform shafts - characterized by a similar section of the element on the entire length; uniform shafts are used in machine units (overhead transmissions) and they are used to transmit rotational motion from the drive unit to the actuator unit, and the drive is transmitted by means of belt or toothed gears (Fig. 1);

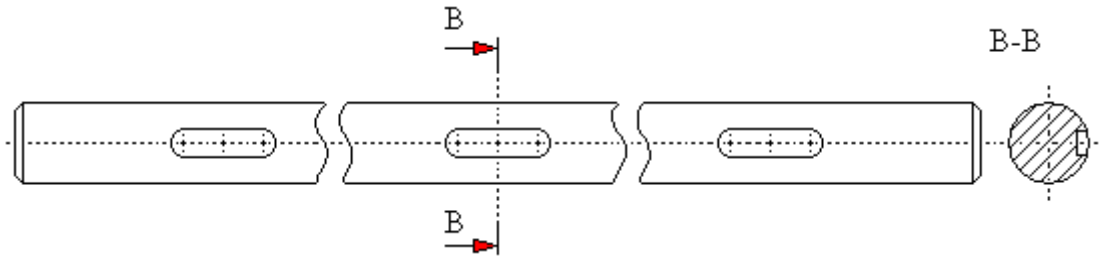

Fig. 1. Example of a uniform shaft

- stepped shafts - the stepped shafts are made for strength reasons and because of the method of mounting the element in the frames. The stepping of shaft diameters from the center (Fig. 2) is used when mounting in split housings, and when mounting the shaft in a non-split housing then used is the stepping of shaft in one direction (Fig. 3); stepped shafts are used, inter alia, in mechanical transmissions, gearboxes, etc.

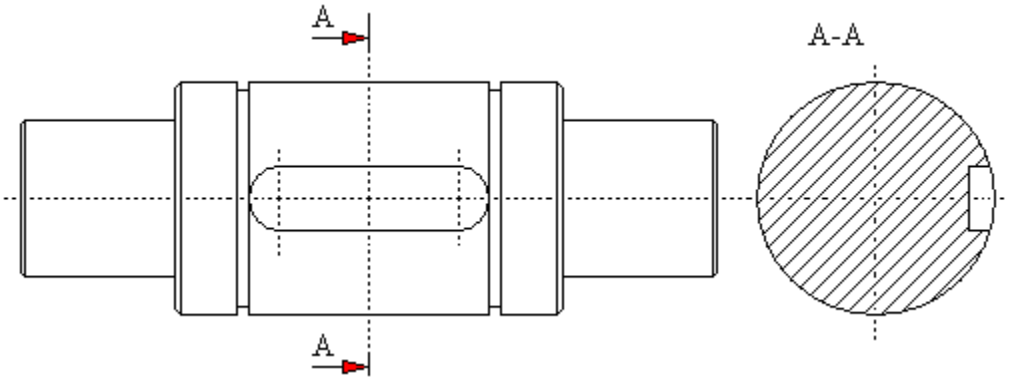

Fig. 2. Example of a shaft stepped from the center

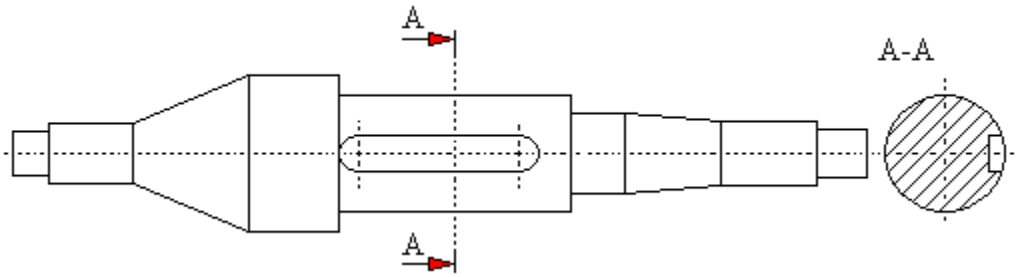

Fig. 3. Example of a shaft stepped in one direction

a) crankshaft - the crankshaft is used to convert rotational motion into reciprocating motion, it is characterized by the displacement of the connecting rod journal axis from the axis of the main journals defining the shaft's axis of rotation. Crankshafts are structural elements of e.g. combustion engines, piston compressors or presses (Fig. 4).

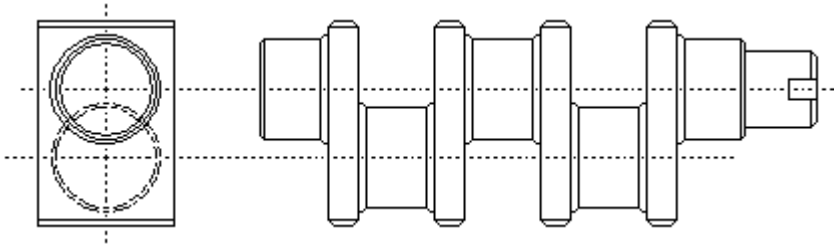

Fig. 4. Example of a crankshaft

2. Working elements of the shafts

Working elements are machine parts mounted on the shaft's resting journals and performing rotational motion with it (gears, pulleys). The working elements of the shaft include, for example:

a) bevel gears - used in mechanical transmissions to transfer torque from the drive shaft to the driven shaft;

b) pulleys, e.g.: pulleys of a continuously variable transmission unit, frictional or otherwise a mechanical variator - used for smooth regulation of the engine speed. This device is used wherever smooth speed regulation is required, e.g. currently used in the scooter drive system (Fig. 5);

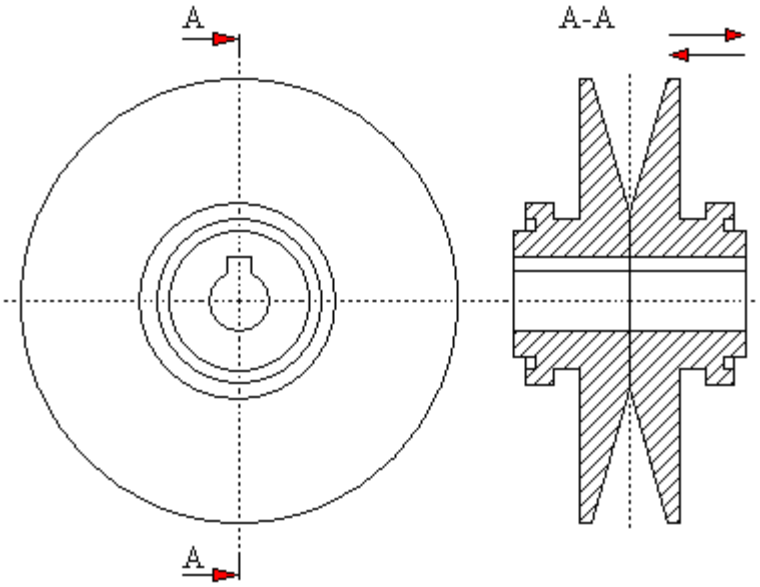

Fig. 5. Example of a variator pulley with extendable discs

c) hub - an element mounted directly on the shaft to which the working elements of shafts are mounted, such as brake discs or drive wheels;

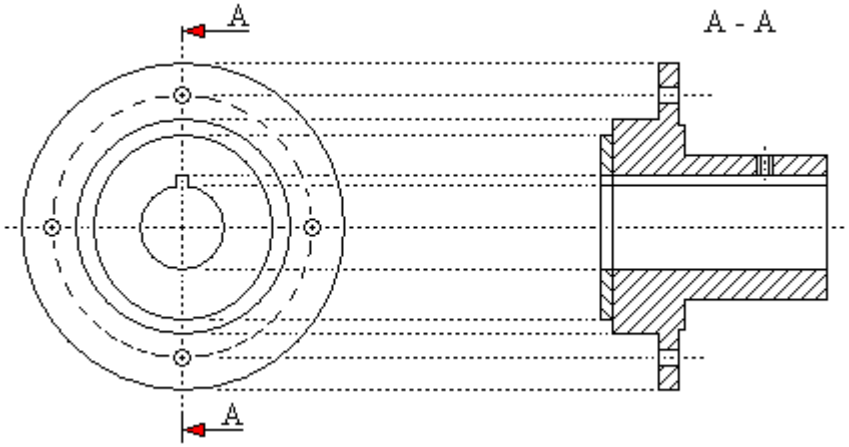

Fig. 6. View of an examplary hub

d) clutch - a part whose task is to connect two independently mounted shafts in order to transmit torque. Through the clutch, the active (drive) shaft transfers the rotational motion to the passive (driven) shaft, setting the driven apparatus in motion. The purpose of the clutch, in addition to transmitting torque, is to compensate for errors in the alignment of the connected shafts, prevent vibrations and protect against overloads.

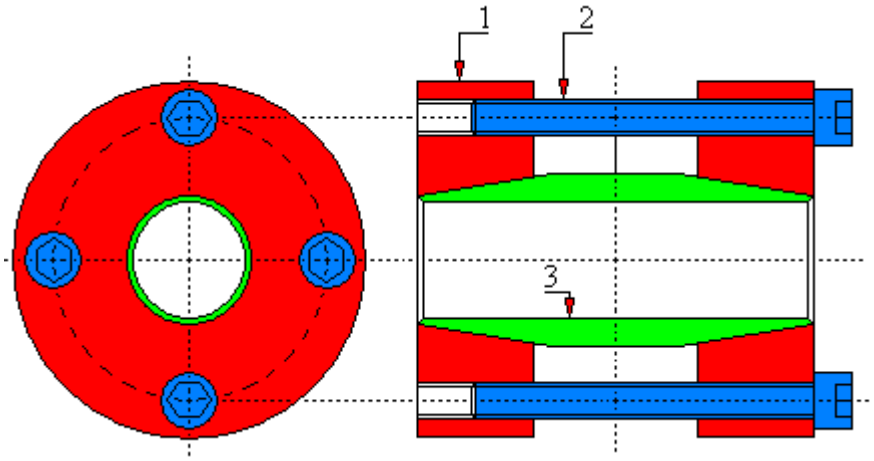

Fig. 7. Example of a rigid clamp coupling
1 – disc, 2 – Allen head screw, 3 – conical sleeve

e) brake discs - structural elements of machines whose purpose is to control speed, stop or prevent rotation of working elements loaded with torque. Brake discs can be mounted on the shaft directly using keyway connections or indirectly using a hub;

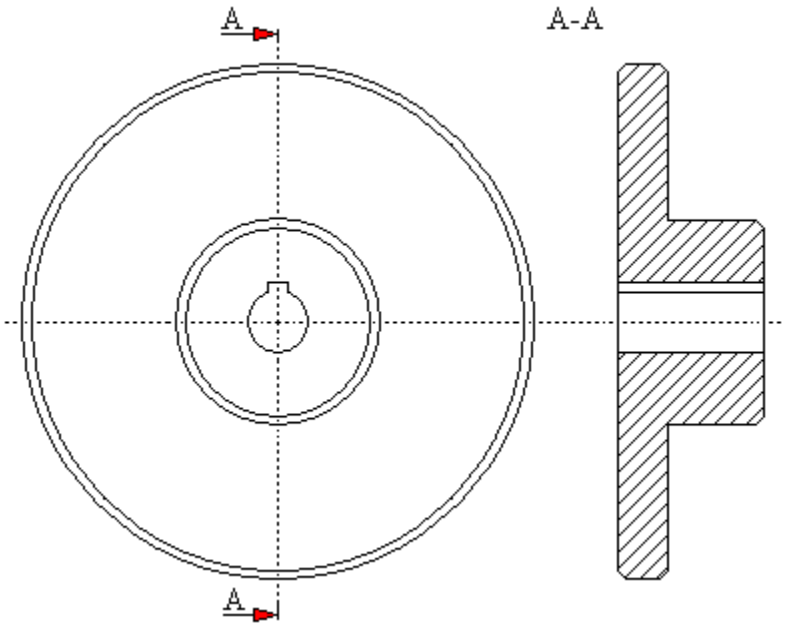

Fig. 8. Example of a brake disc

3. Design assumptions for shaft-type parts

Shaft-type machine parts are elements found in almost every machine and device. Compared to other components in terms of technology, they are the least complicated.

Design solutions used in the shaft construction:

- journals – end or internal, stationary or moveable;

- structural and technological undercuts;
- bearing surfaces;
- journals – smooth, threaded, shaped;
- free surfaces;
- transverse holes, longitudinal holes, center holes.

The journals are shaft sections that are in direct contact with other machine parts (Fig. 9).

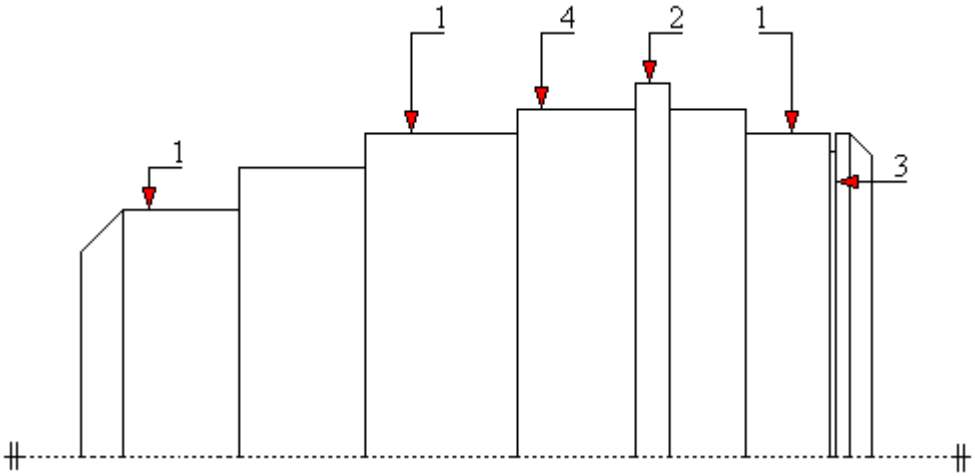

Fig. 9. Examples of surfaces occurring in the construction of a shaft
1 – journals, surfaces where there is contact with other elements; 2 – shaft shoulder; 3 – groove for the external retaining ring; 4 – free surfaces

Depending on their location, the journals are divided into shaft end journals and internal journals. Moveable journals are parts of the shaft on which specific machine elements can move (e.g. a sliding gear). Stationary journals are characterized by ends that have the form of a bearing surface or technological and constructional undercuts.

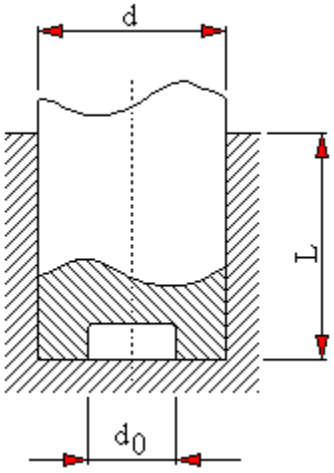

Fig. 10. Stationary journal
d – shaft diameter; d_0 – hole diameter; L – total length of the journal

The diameters of shaft journals and their fits with other machine parts are provided, inter alia, in the following standards [22]:

- PN-EN ISO 286-1:2011: *Geometrical product specifications (GPS). ISO coding system for linear dimensional tolerances. Part 1: Basics of tolerances, deviations and fits;*
- PN-EN 20286-2:1996: *Geometrical product specifications (GPS). ISO coding system for linear dimensional tolerances. Part 2: Tables of normal tolerance classes and limiting deviations for holes and shafts;*
- PN-M-85000:1998: *Cylindrical and tapered shaft ends with 1/10 taper.*

Design undercuts are made in that part of the shaft where the securing elements, e.g. retaining rings, are to be fitted. The bearing surface is that part of the shaft on which the elements mounted on it rest. This surface also prevents machine parts from slipping off. Technological undercuts are used in places where machine parts adhere to bearing surfaces.

These undercuts are described in the standards [22]:

- PN-M-02043:1958: Machining undercuts.
- PN-89/M-82063: Fasteners. Metric thread outlets and undercuts.

The shafts also feature other design details such as center holes, transverse and longitudinal holes, ports and blind holes, splineways and splined elements. Characteristic places on the shaft are shown in Fig. 11.

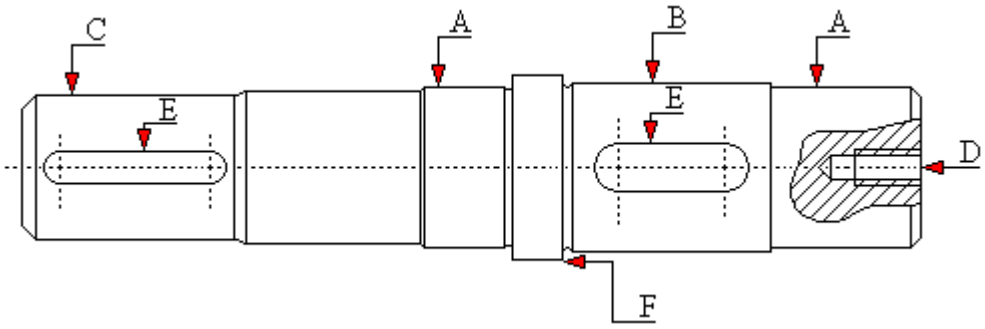

Fig. 11. Examples of characteristic spots on the shaft
A – bearing mounting location; B – wheel mounting location (toothed, pulley); C – shaft-engine connection location; clutch used; D – method of securing bearings against falling out; E – keyway in wheel and clutch mounting locations; F – bearing and wheel bearing surfaces

4. Basic principles of shafts construction

Due to their application characteristics, i.e. the transmission and transfer of torque, shaft-type structural elements are mainly exposed to torsional loads. If the acting forces exceed the permissible value, the element (shaft) may lose its functional properties due to excessive deformation, which may lead to permanent damage or indirectly to the

destruction of the device or machine, and in extreme cases may lead to a threat to the safety of people operating it [25].

Shafts, as structural elements, are subject to strength assessment during design by selecting and calculating appropriate load values, as well as by analyzing the values of resulting deformations. The strength values of the elements are referred to the established design requirements contained in standards, regulations of the Office of Technical Inspection and manufacturer's recommendations in order to ensure proper parameters of the designed parts. The values of stresses and deformations occurring in shafts are influenced by many factors, the leading ones include [4, 8]:

- material type;
- the shape of the element and its dimensions;
- value and category of forces loading the element.

The design of shaft-type machine parts can be divided into the following stages:

- preliminary design – shaping the shaft using strength calculations and preliminary design assumptions;
- selecting places where loads occur and determining their values;
- defining the reactions in the shaft support journals;
- calculation of the reactions occurring in the bearings;
- calculation of bending moments;
- calculation of torque moments;
- determining what material the part will be made of;
- calculation of equivalent moments;
- calculation and selection of shaft diameters;
- shaping the shaft;
- selection and calculation of connections exposed to torsional moments;
- selection of bearings and their strength calculations.

5. Materials used for parts such as shafts

The material intended for the shaft should be selected according to the use, load and type of work of a given part. We typically use the following steel types to produce shafts.

- Unalloyed structural steels for general use [22]

Polish Standard: PN H-84020: 1988 – Unalloyed structural steels for general purposes.
Steel grades: St4W, St5, St6.

European Standard: PN-EN 10025: 2002 – *Hot-rolled products made from unalloyed structural steels*.
Steel grades: S275J0, E295, E335.

Characteristics: steels used for the construction of machine shafts, crankshafts and axles that are lightly loaded and where the stiffness of the part is more important than its strength.

- Unalloyed steels for surface hardening and toughening [22]

Polish Standard: PN H-84019: 1993 - *Unalloyed steels for surface hardening and toughening.*
Steel grades: 35, 45, 55.

European Standard: PN-EN 10083-2+A1: 1999 – *Steels for toughening. Technical conditions of delivery of products made of unalloyed quality steel.*
Steel grades: C35, C45, C55.
Characteristics: This type of steel is used in the production of shafts that are loaded with greater forces and exposed to higher temperatures, up to 500°C. These steels are subjected to heat treatment which is characterized by a combination of hardening and tempering.

- Special alloy steels for toughening [22]

Polish Standard: PN H-84030/04: 1989 - *Alloy steels for toughening and surface hardening.*
Steel grades: 45HN, 30G2, 35HGS.

European Standard: PN-EN 10083-1: 1999 – *Steels for toughening. Technical conditions of delivery of special steel products.*
Steel grades: 42CrMo4, 28Mn6, 50CrMo4.
Characteristics: steels of this type are characterized by high impact strength and resistance. We use them to produce forged crankshafts, shafts for motor vehicles and separable shafts.

- Structural alloy steels for case-hardening [22]

Polish Standard: PN H-84030/02: 1989 – *Alloyed structural steels for case-hardening.*

Steel grades: 15H, 18H2N2, 12HN3A.

European Standard: PN-EN 10084: 2002 – *Case-hardening steels. Technical delivery conditions.*

Steel grades: 17Cr3, 14NiCrMo13-4, 10NiCr5-4.

Characteristics: this material is used to produce camshafts, centrifuge shafts and machine parts subjected to higher-order rotations and frequently changing loads. The hardness of the surface layer that can be obtained is in the range of 58-62 HRC.

In addition, there are cases where the technical requirements of the shaft construction require the use of materials such as ductile iron, cast steel or bronze.

6. Basic knowledge of material strength

Strength of materials is a part of engineering knowledge based on the laws of general mechanics and dealing with the study of changes occurring in real bodies caused by external loads in materials and structural elements [107].

The basis on which the strength of materials is based is, on the one hand, experimental tests and, on the other, methods of related sciences. These sciences include, for example:

- theory of elasticity;
- theory of plasticity.

The task of the science of strength of materials is to solve the following problems:

- will the material used to make the structural element of machines not be damaged as a result of external forces acting on the designed structural element?
- will the type of material selected, as well as the designed structural shape of the element, ensure the durability and correct operation of the machine, taking into account the economic aspect of saving the materials used?

Construction materials are characterized by:

- deformability - the ability to change geometric shapes as a result of external forces;
- plasticity - the ability to undergo permanent deformations caused by external forces;
- strength - defining the maximum load value which - if exceeded - will result in damage to the constructed element;
- elasticity - the ability to recover (return) to its original shape after the forces causing deformation cease.

Typical deformations caused by external forces acting on machine components include:

- axial compression and tension (Fig. 12, Fig. 13) – is a condition induced in an element by the application of forces lying on the shaft axis with opposite directions. The action of tensile forces after exceeding the conventional elastic limit causes an irreversible change in the geometric dimensions of the element [18]:

- during tension - elongation and deformation (reduction) of the cross-section,
- during compression - shortening and deformation (increase) of the cross-section;

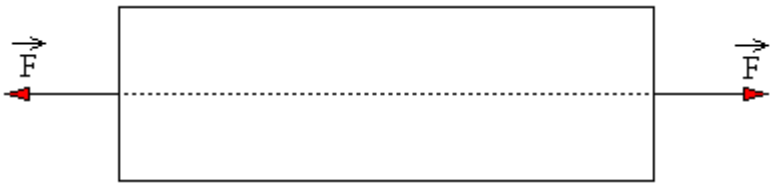

Fig. 12. Scheme of applying tensile forces in the element

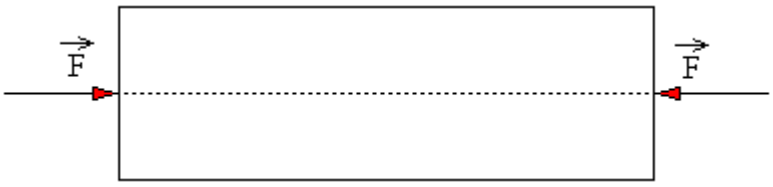

Fig. 13. Schematic diagram of the application of compressive forces in the element

- bending - a condition caused by loading with a force directed perpendicularly to the axis of the supported element (Fig. 14). The action of bending forces after exceeding the conventional elastic limit causes a change in the shape and geometric dimensions of the element.

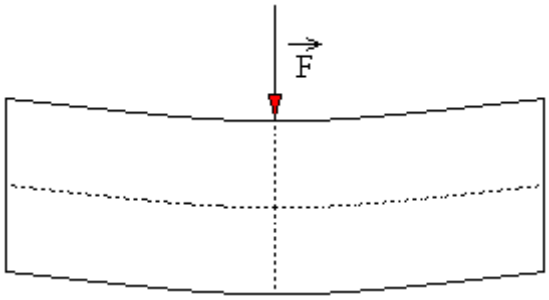

Fig. 14. Schematic diagram of the application of bending forces in the element

7. Shaft torsion

Shaft torsion is a state of deformation caused by loading the element with a couple of forces, acting in a plane perpendicular to the shaft axis, which cause the shaft cross-sectional planes to rotate in accordance with its axis by a certain angle φ. The value of the torsional forces is called the torsional moment M_s, and the value of the torsional moment in each considered section of the element is the same.

$$M_S = F \cdot a \quad (1)$$

M_s - torsional moment; F - loading force; a - arm of the force couple

Experience shows that for very small deformations (for shafts, depending on the design, the permissible torsional angle is up to two degrees over a length of one meter). The action of a torsional moment on a circular shaft (Fig. 15) causes deformations in which it can be observed that [3]:

- the *Y* shaft axis remains straight and is not deformed;
- the lines forming on the shaft envelope parallel to the axis during the action of the torsional moment take the form of a *PR* helix with a constant value of the inclination angle γ along the length of the element;
- when the shaft is twisted, there is no change in the volume of the element body (the diameter and length remain constant and the section is flat);
- when the shaft is twisted, the circumferential lines do not change their initial circular shape;
- when the shaft is loaded with torsional moments, the sectional radius of the element is not deformed, it only rotates by the torsional angle φ [4].

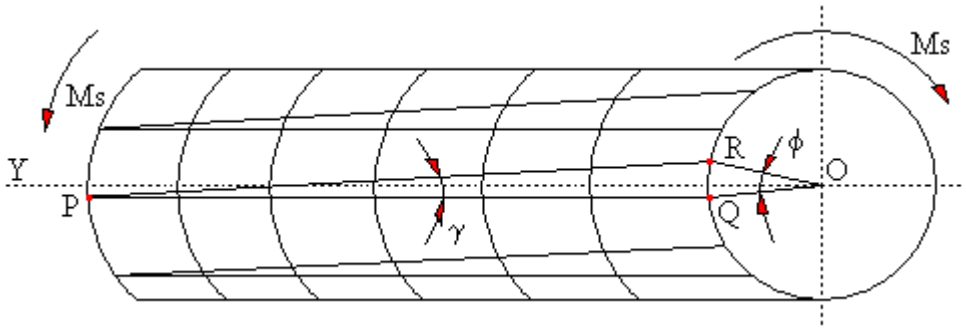

Fig. 15. Shaft deformation under the influence of torque moment [109]

Observations show that when the shaft is twisted, only tangential stresses occur in individual sections. The magnitude of the shear stresses in the section of a circular shaft varies depending on the center (value equal to zero) of the shaft section to its outer layer (maximum value), so [29]:

- the magnitude of the shear stresses depends proportionally on the distance from the center of the shaft section. (Fig. 16);
- the highest shear stresses occur in the outer layer of the section (Fig. 16) located at a distance of radius *r* from the shaft axis, and the value of these stresses decreases towards the shaft symmetry axis, assuming a zero value there [29].

The equation, therefore, shows the relationship:

$$\frac{\tau}{\tau_{max}} = \frac{\rho}{r} \qquad (2)$$

where: τ – stress in the inner layers; τ_{max} – maximum stress (outer layer); ρ – any radius on the rod section; r – shaft radius

The maximum shear stress τ_{max} caused by the torque moment M_s is equal to the ratio of the torque moment to the torsional section modulus W_o. Maximum stresses occur in the outer layer of the shaft section for $\rho = r$ (Fig. 16) thus [5]:

$$\tau_{max} = \frac{M_S}{W_o} = \frac{M_S}{J_o \cdot \frac{\rho}{r}} \qquad (3)$$

where:

- J_o - polar moment of inertia

For a circular cross-section:

$$J_o = \frac{\pi \cdot d^4}{32} \qquad (4)$$

- W_o - torsional strength modulus of a section is the ratio of the polar moment of inertia to the radius of the shaft cross-section

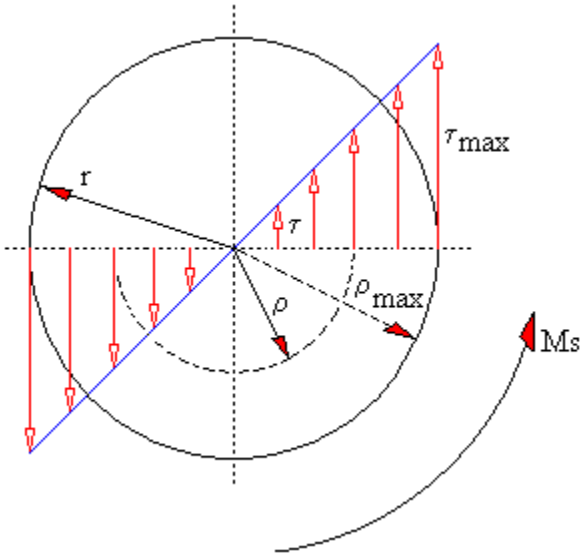

Fig. 16. Distribution of shear stresses in a circular shaft [109]

In mechanics, the torsional strength modulus of a section is a quantity which characterizes the resistance of a shaft to torsion. The W_o index expresses the quotient of the shaft torque moment and shear stress in the shaft [18]:

$$W_o = \frac{\pi \cdot d^3}{16} \qquad (5)$$

- d - diameter of the shaft cross-section

The torsional strength modulus of a circular shaft has an approximate value of:

$$W_o \approx 0.2 \cdot d^3 \qquad (6)$$

Under the influence of a torque moment acting on a circular shaft, it twists around its own axis (Fig. 17), and the ones forming PQ are deformed, taking the form of a helical line PR with an inclination angle φ (Fig. 17), this angle is the torsional angle of the shaft.

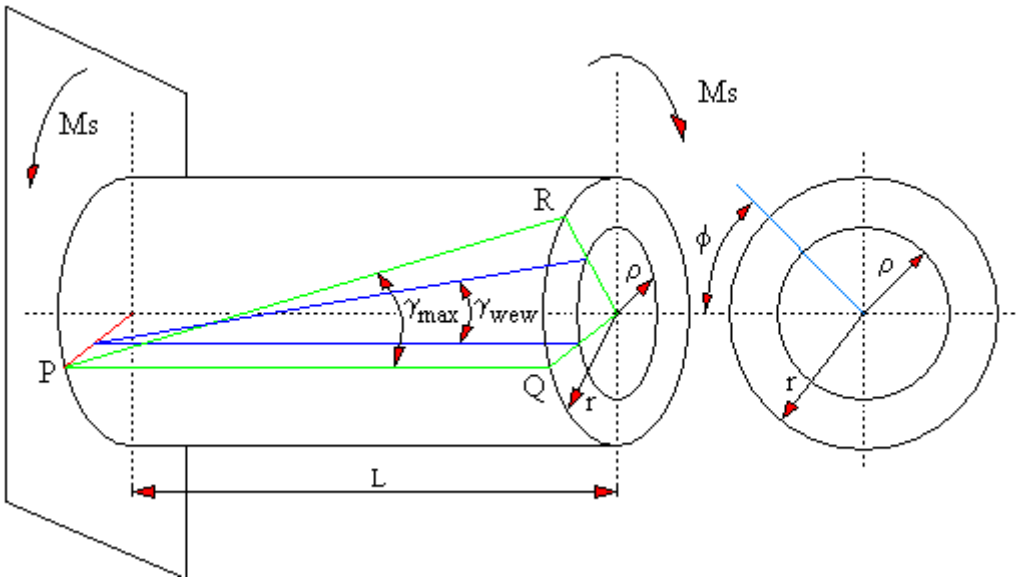

Fig. 17. Deformation angle of inner layers [109]
φ – torsional angle [rad]; γ – deformation angle (this is the value of the angle γ of rotation of layers parallel to the shaft axis; L – shaft length [m]; PQ – generator along the shaft length [mm]; r – shaft diameter (mm); ρ – section diameter of the inner layer [mm]

As a result of the action of the torque moment, the final section of the shaft is rotated relative to the fixed section by the torsional angle φ (Fig. 16). The total torsional angle of the shaft is proportional to the product of the torque moment Ms and the shaft length l, and inversely proportional to the product of the shear modulus of elasticity G and the polar moment of inertia [88]:

$$\emptyset = \frac{M_S \cdot l}{J_o \cdot G} \qquad (7)$$

- G - Kirchhoff modulus - modulus of shear elasticity depending on the type of material from which the element is made;
- Jo - polar moment of inertia;
- GJo - shaft stiffness in torsion, the higher the value of the product, the smaller the shaft deformation

8. Discussion of strength assumptions for a uniform shaft with a circular section

The main task of a structural element of a shaft-type part is to transmit and transfer torque moments that cause torsional deformations. If the forces or loads exceed the permissible value, the element may lose its functional properties due to excessive deformation which may lead to permanent damage to the element or indirectly to the

destruction of the device or machine, and in extreme cases may lead to a threat to the safety of people operating the machine [6].

Shafts, as structural elements, are subject to strength assessment during design by selecting the material and calculating appropriate values for a given type of load, as well as by analyzing the values of the resulting deformations. The strength values of the elements are referred to the established design requirements contained in the standards and the manufacturer's recommendations in order to ensure correct parameters of the designed parts. The values of stresses and deformations occurring in shafts are influenced by many factors, the main ones include [4, 8]:

- material type;
- the shape of the element and its dimensions;
- value and category of forces loading the element.

In a simplified approach, the design of shafts exposed to torsion involves selecting the material type and size of element sections so that the strength condition (tangential stresses) and the operating condition (torsional angle) of the shaft do not exceed the permissible values [8].

The condition of the shaft's torsional strength determines the value of the greatest stress caused by the action of the torque moment which will not cause permanent deformation of the element during operation [119]:

$$\tau = \frac{M_S}{W_O} \leq k_S \qquad k_S = (0.5 \div 0.6)\, k_t \tag{8}$$

- k_t - permissible shear stress;
- k_s - permissible torsional stress

From the strength condition (8) we obtain the formula for the shaft torsional strength index from which we can calculate what torque moment the shaft can safely transfer without undergoing elastic-plastic deformations [28]:

$$\frac{M_S}{k_S} \leq W_O \tag{9}$$

When designing a shaft, we are guided by its intended purpose, taking into account the torsional stiffness of the element. The torsional stiffness parameter *k* of the shaft is the ratio of the torque moment to the shaft torsional angle which must meet the condition of not exceeding the permissible value of the torsional angle φ calculated over the length of one meter of the designed shaft, length which is assumed for machine shafts [1, 10]:

$$\emptyset_{dop} \leq 0.25^{\circ} = 0.0044\ rad \tag{10}$$

where: φ_{dop} - permissible value of the torsional angle

$$\emptyset_{max} = \frac{M_S \cdot l}{J_O \cdot G} \leq \emptyset_{dop} \tag{11}$$

- φ_{max} - maximum value of the shaft torsional angle;
- Ms - torque moment [Nm];

- l – length of the element [m];
- G - Kirchhoff modulus (modulus of elasticity);
- Jo - polar moment of inertia for a uniform solid shaft with a circular section;
- φ_{dop} - permissible value of the torsional angle

9. Determining the shaft torsional angle based on geometric measurements

To determine the value of the shaft torsional angle, an experimental method can be used which involves measuring the linear displacements of measuring levers mounted on the tested element. To read the displacement values, use two analog dial gauges (Fig. 18).

The first gauge should be mounted at a rigid shaft mounting, and the second one should be mounted as close as possible to the point of action of the torque moment. Based on the values of changes in linear displacements of measuring levers measured by dial gauges.

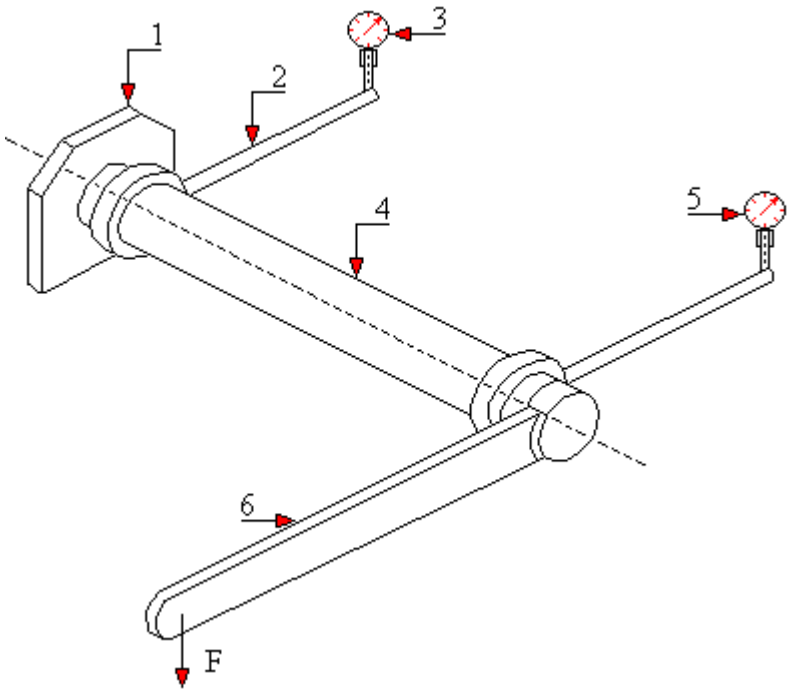

Fig. 18. Schematic diagram of the measuring test rig
1 – shaft mounting plate; 2 – measuring lever; 3 – dial gauge I; 4 – shaft subjected to a torque moment; 5 – dial gauge II; 6 – load arm; F – load force

Assuming that the shaft torsional stiffness parameter is correct for torsional angles of small values [4]:

$$tg\alpha = \frac{L_y}{L} \qquad (12)$$

- Ly - linear displacement [m];
- L - length of the measuring lever [m];
- α - angle of change of the measuring lever position [°], [rad]

The torsional angle of a round shaft can be determined (Fig. 19).

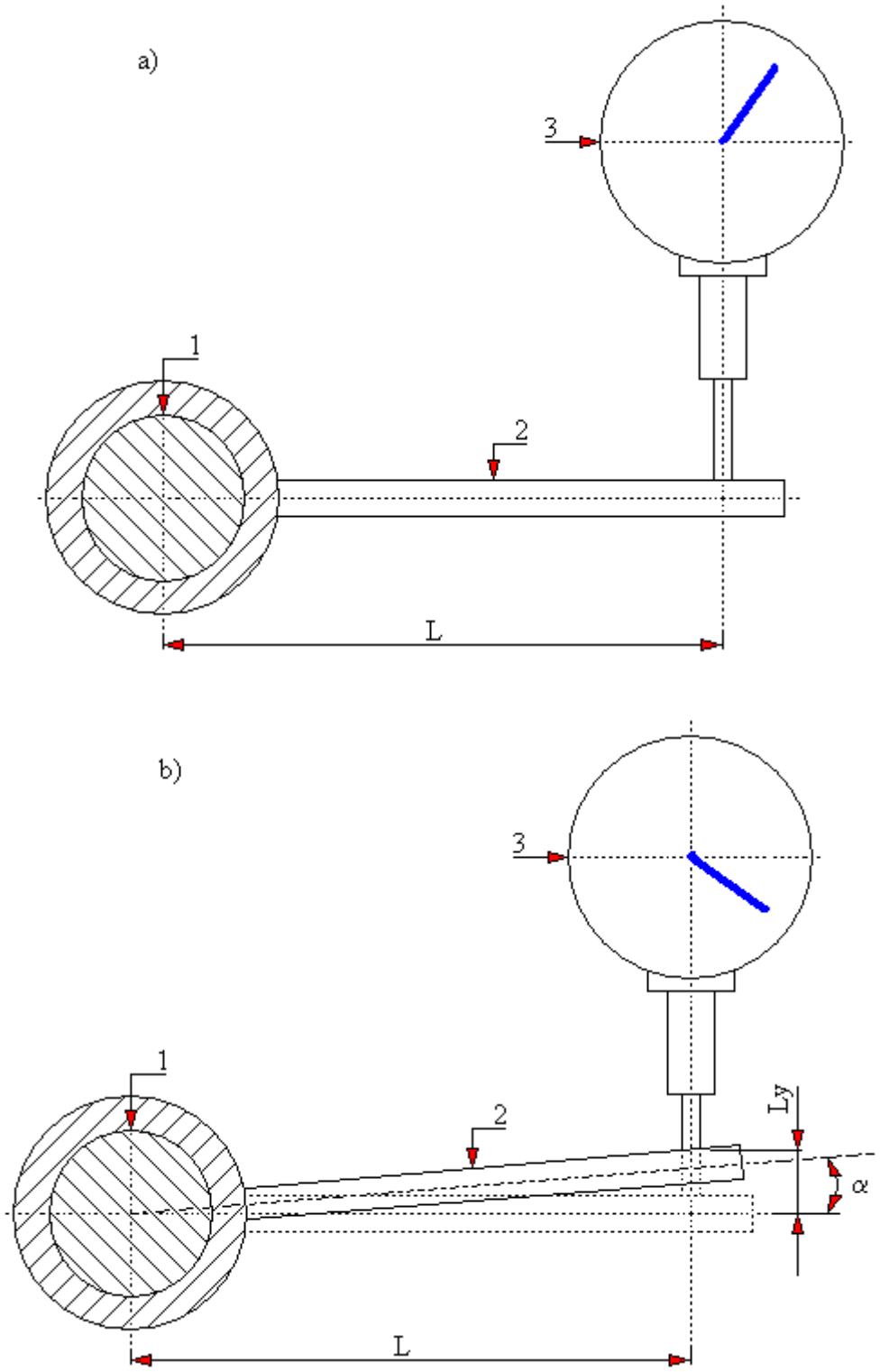

Fig. 19. Changing the position of the measuring gauge lever before (Fig. a) and after (Fig. b) loading the shaft with a torque moment

1 – twisted shaft; 2 – lever arm; 3 – measuring quage; L – lever arm length; Ly - difference in dial gauge readings [mm]; L - measuring lever length [m]; α - angle of change of the measuring lever position [°], [rad]

10. Variants of the measuring test rig

When starting to build a rig for measuring the deformation angle of a round shaft during a static torsion test, a basic conceptual diagram of its construction was developed. The assumptions were:

- simple design;
- cheap to make;
- simple operation;
- operational reliability.

During the initial design, it was found that the main design assumptions of the test rig (Fig. 20) and the selected materials were optimal:

- steel base 8÷10 mm thick;
- Rigid shaft mounting made of 8÷12 mm steel plate;
- Mounting bracket for the twisting mechanism made of 8÷12 mm steel plate;
- Round steel rod Ø25÷30 mm;
- Self-aligning bearings in the housing;
- Measuring handles or levers.

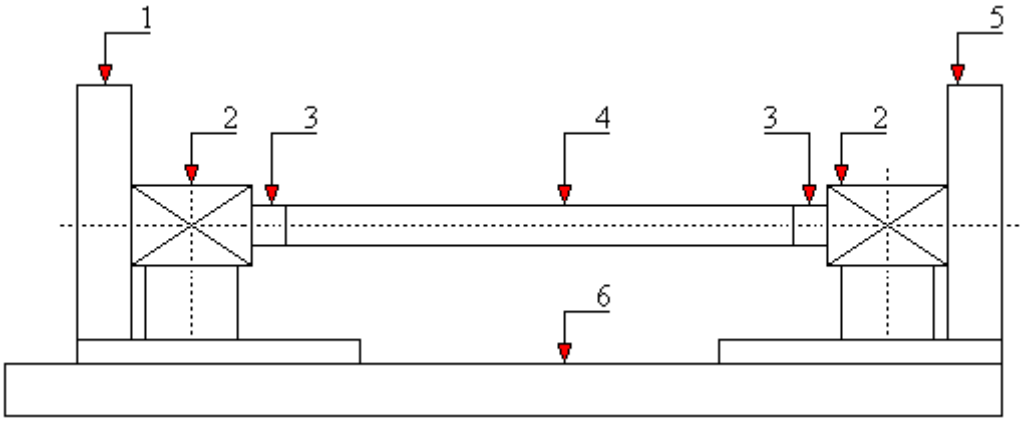

Fig. 20. General concept of the test rig for measuring the shaft torsion angle
1 – holder for rigid shaft mounting; 2 – bearing; 3 – measuring holder; 4 – shaft; 5 – holder for mounting the twisting mechanism; 6 – base

Based on the design assumptions,prepared were four variants of the test rig for measuring the shaft torsion angle.

In the first variant (Fig. 21), the shaft angle measurement rig consists of a steel or aluminum wheel. A groove was bored around its circumference in which a strong cord was placed, at the end of which an appropriate number of weights were put.

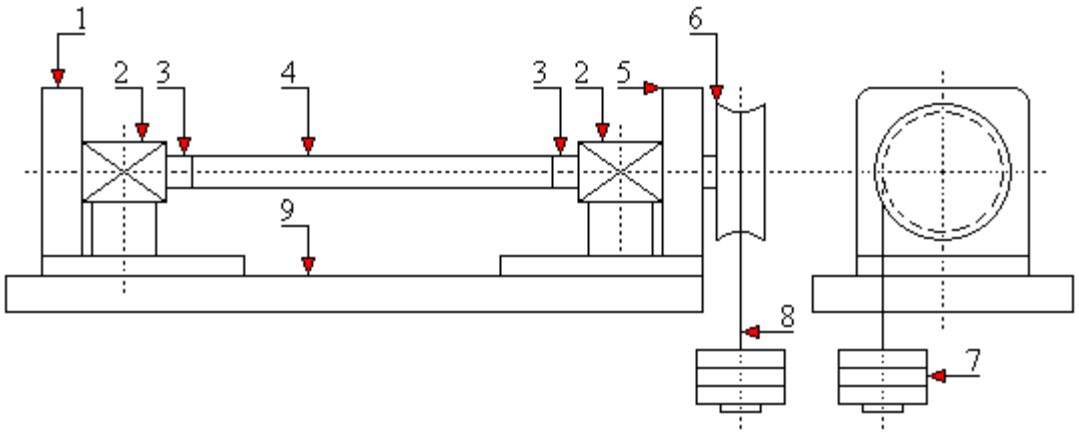

Fig. 21. The first variant of the test rig for measuring the torsional angle of the shaft
1 – holder for rigid mounting of the shaft; 2 – bearing; 3 – measuring holder; 4 – shaft; 5 – holder for mounting the twisting wheel; 6 – twisting wheel; 7 – weights; 8 – cord for mounting the weights; 9 – base

The second variant (Fig. 22) also uses weights during the twisting test but they are fitted in a different way. The initial assumptions remain the same as in the first variant, instead of a twisting wheel, an arm in a horizontal position is used, at the end of which there is a handle on which steel weights are put. The torsion arm will be made of steel flat bar.

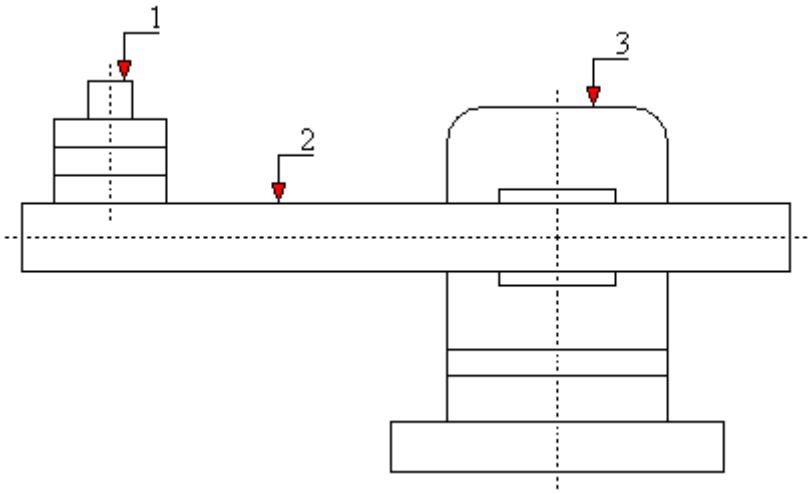

Fig. 22. The second variant of the test rig for measuring the torsional angle of the shaft
1 – weight mounting bracket; 2 – torsion arm; 3 – twisting arm mounting bracket

In the third variant (Fig. 23), the method of loading the beam was changed – instead of applying weights, it is twisted using a hydraulic actuator. Due to the use of an additional element, which is a hydraulic pump, the width of the base will be adjucted.

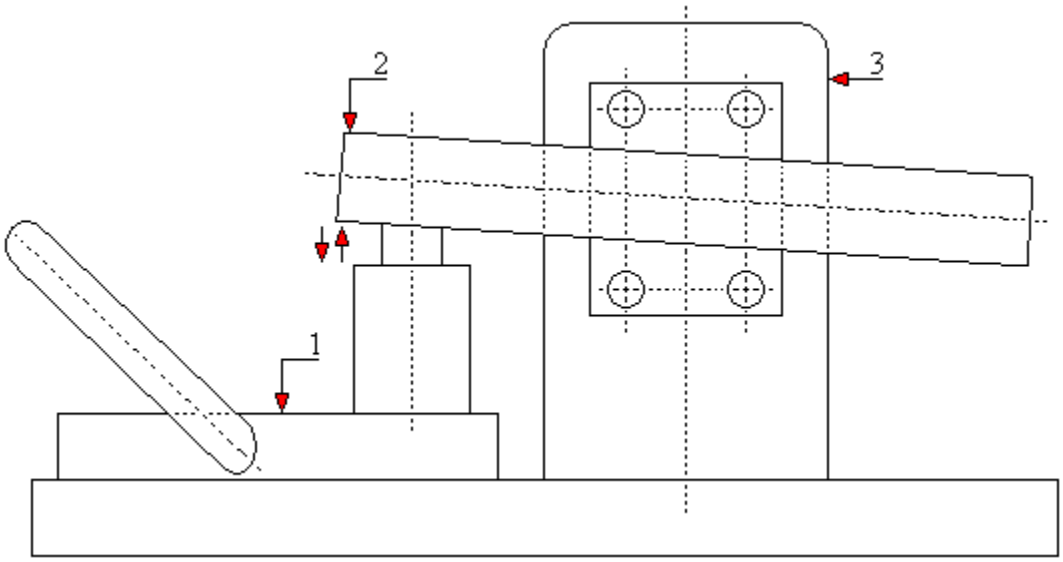

Fig. 23. The third variant of the test rig for measuring the torsional angle of the shaft
1 – hydraulic pump; 2 – torsion beam; 3 – torsion arm mounting bracket

In the fourth variant (Fig. 24), the torsion beam is mounted at an angle to the base and the weights are suspended directly below it on a special holder made of a steel rod.

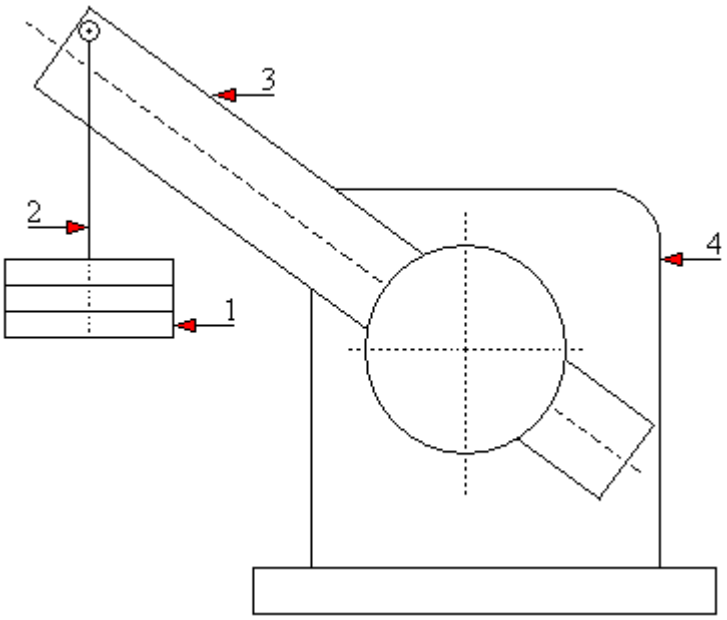

Fig. 24. The fourth variant of the test rig for measuring the torsional angle of the shaft
1 – weights; 2 – weight holder; 3 – torsion arm; 4 – torsion arm mounting bracket

After verifying all four test rigs, the second variant was considered the best and was implemented for further design work.

11. Making the designed test rig

In line with the assumptions established in the initial design phase and the selected second variant of the rig, the following parts of its construction were agreed:

- test rig base made of 10 mm thick S235JR steel with dimensions of 200 mm by 910 mm;
- rigid shaft mounting made of S235JR steel plate, 10 mm thick and measuring 76 mm by 200 mm;
- arm twisting the shaft made of S235JR steel, 8 mm thick, 42 mm wide and 700 mm long;
- weights mounting pin on the torsion arm made of S235 steel;
- S235 steel weights weighing 1kg (2 pieces), 2kg (4 pieces), 3kg (2 pieces);
- round shaft Ø25h6 made of 55 steel, 1000 mm long;
- the torsion arm mounting bracket of steel plate was replaced with a BK 95/25x55 expansion and clamping sleeve (2 pieces);
- self-aligning bearings in UCP 205 housing (4 pieces);
- measuring handles (2 pieces);
- dial gauges on a stand (2 pieces);
- test rig table made of S235 steel sections with dimensions of 30x30 mm.

The dimensions of the rig and its components were selected so as to maintain its full stability during the torsion test. Model of the test rig for measuring the shaft torsional angle (Fig. 25) was made in CAD – AUTODESK INVENTOR 2022.

Fig. 25. Model of the test rig for measuring the shaft torsional angle

The first stage of work was laser cutting of the following parts:

a) test rig base;
b) torsion arm;
c) back plate securing the shaft.

The contours of elements (a) and (b) were cut to dimensions, and element (c) was a semi-finished product ready for further processing (Fig. 26).

Fig. 26. Laser-cut elements of the test rig for measuring the shaft torsional angle

Then the rig plate was put on the table of the CNC column milling machine (Fig. 27) and four Ø6.2 mm holes and six Ø12.2 mm holes were drilled (Fig. 28) which are used to fix bearings in the housing and the back wall mounting the end of the shaft.

Fig. 27. Base plate mounted on a CNC milling machine

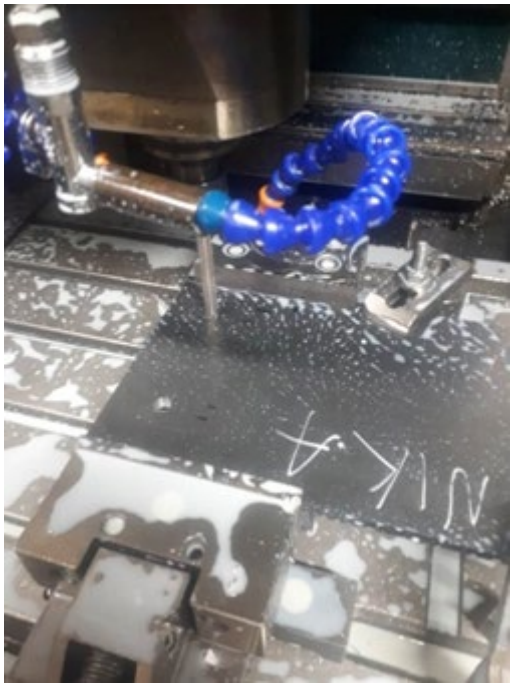

Fig. 28. Drilling Ø12.2mm holes in the rig plate

The next step is to drill six Ø7.5mm holes in the torsion arm on a CNC milling machine (Fig. 29) which are used to fix the BK 95/25x55 mounting sleeve. The holes were deburred manually using a countersink.

Fig. 29. Drilling Ø7.5mm holes in the torsion arm

The back plate of the rig, whose task is to rigidly mount the shaft, was first laser-cut from 10 mm thick S235JR steel sheet. The element was intended for further processing on a CNC milling machine, so it was made with 5 mm allowances around its

entire circumference. In the first clamping, the element was machined with an end mill to a dimension of 76 mm (Fig. 30) and thus the base surface was obtained. The second mounting has four M5 threads whose purpose is to attach the back plate to the base of the rig (Fig. 31). In the third and last mounting, the shape of the plate was milled to the size (Fig. 32), and a Ø30 mm hole was made using linear interpolation and six Ø6.5 mm holes were drilled, the purpose of which was to attach the BK 95/25x55 sleeve with the shaft to the back wall of the test rig. The final shape of the back plate securing the shaft is shown in (Fig. 33).

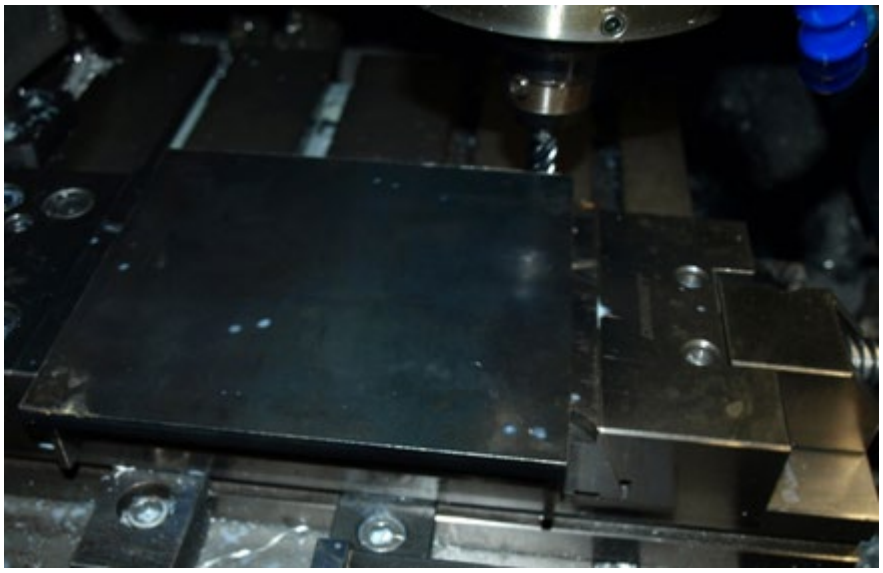

Fig. 30. Milling the base surface of the back wall of the rig

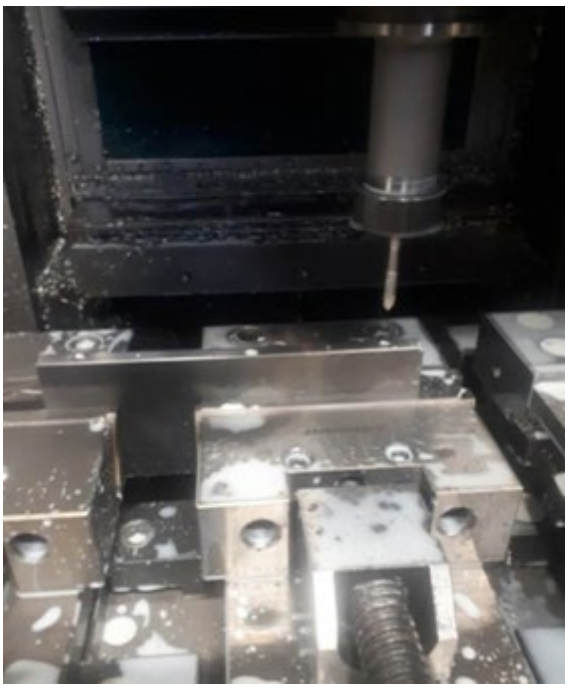

Fig. 31. Making four M5 threads in the base of the back plate securing the shaft

Fig. 32. Finish milling of the shape of the shaft mounting plate

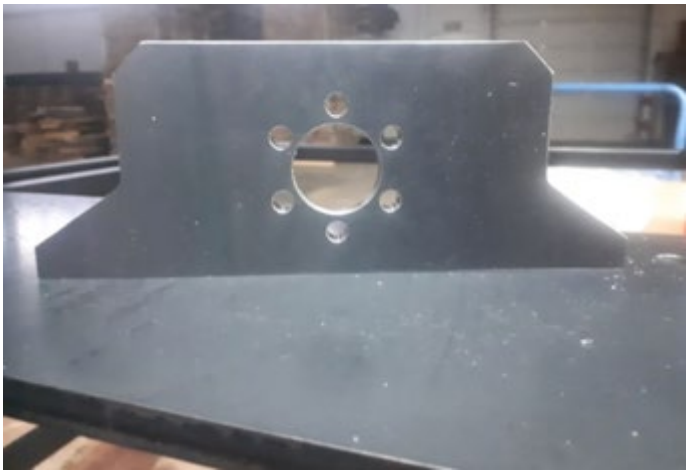

Fig. 33. Back plate for securing the shaft after all machining operations are completed

Next, we made the weight mounting pin and a set of weights which together with the torsion arm create a system for twisting the shaft and thus enabling the measurement of the angle of this twist. In the first machining operation of the pin, the finished shape was turned from Ø 40 mm S235 steel shaft on an engine lathe (Fig. 34). The second operation is milling a groove 8.2 mm wide and 42 mm deep on a CNC milling machine (Fig. 35) which will enable the connection of the element with the twisting arm. In the third operation, the sides of the handle were milled to a thickness of 23 mm (Fig. 36). In the fourth operation and the first fmounting, a Ø8.2mm hole was drilled on this plane. In the second mounting an M8 thread was made (Fig. 37) which is used to screw the pin to the load arm.

Fig. 34. A weight mounting pin turned on an engine lathe

Fig. 35. Milling a groove on the pin, 8.2 mm wide and 42 mm deep

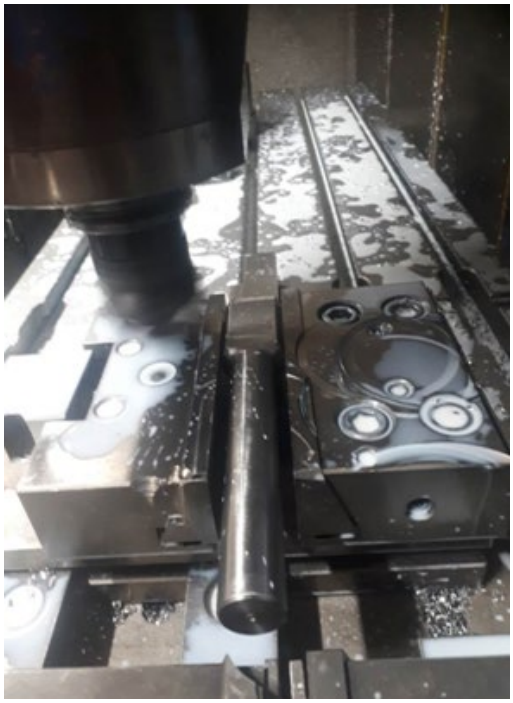

Fig. 36. Milling the sides of the weight mounting pin

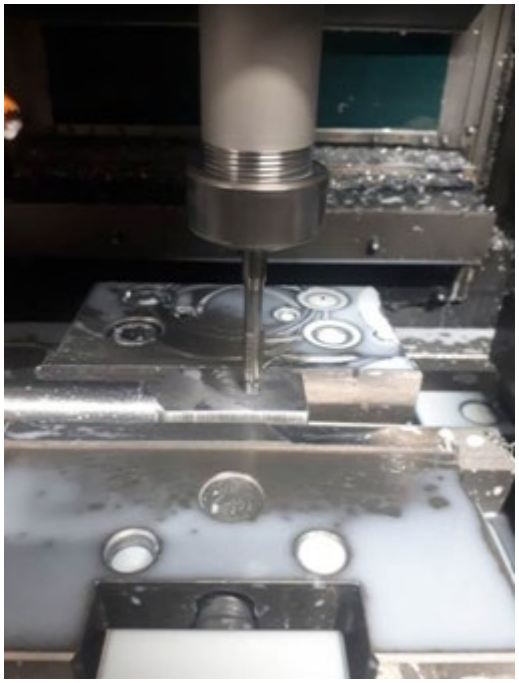

Fig. 37. Making an M8 thread in the side part of the weight mounting pin

The next step was to turn the weights from S235 steel. They were designed using AUTODESK INVENTOR software and their weight was checked in a simulation after entering data such as dimensions and material from which they were made. The weights were turned on a engine lathe (Fig. 38) and control weighed on an industrial scale.

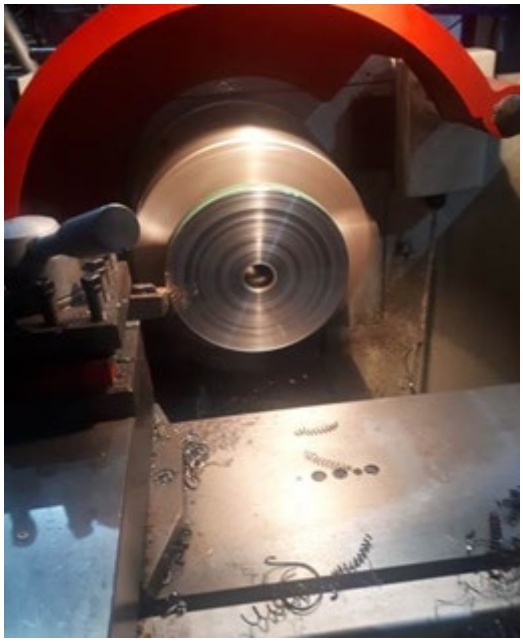

Fig. 38. Turning steel weights on an engine lathe

The set was painted so that each color corresponded to a given weight (Fig. 39):

- blue weight 3 kg – 2 pieces;

- green weight 2 kg – 4 pieces;
- red weight 1 kg – 2 pieces;

Fig. 39. A set of weights used on the test rig to measure the torsional angle of the shaft

In the design used were standardized elements such as:

- linear shaft Ø25h6 made of C55 steel;
- mounting sleeves BK 95/25x55;
- self-aligning bearings in UCP 205 housing.

The precision guide shaft Ø25h6 made of C55 steel (Fig. 40) was selected due to its high manufacturing accuracy, load resistance and high stiffness. This structural element is used, inter alia, in: machine tools, industrial machines, circular saws and industrial robots.

The basic parameters of the linear shaft include:

- surface hardness – 59 HRC;
- shaft diameter accuracy class – ISO h6;
- roughness of the ground surface – max. 0.3 Ra;
- hardening depth: 0.9÷1.8mm.

Fig. 40. Linear shaft Ø25h6 made of C55 steel

The BK 95/25x55 expansion and clamping sleeve (Fig. 41) is used for rigid connection of rotating elements with the shaft without using any keyway or key. This type of solution was used in the rig design because of a quick and easy assembly and disassembly of parts.

Fig. 41. Expansion and clamping sleeve BK 95/25x55

Technical data of the BK 95/25x55 expansion and clamping sleeve:

- material – C45E steel;
- transmitted torque – 394 Nm;
- axial force – 32 kN.

Self-aligning bearings in a cast iron housing UCP 205 (Fig. 42) – are a design variant of ball bearings. They are characterized by a spherical outer ring surface, a built-in seal and a grease filling. This design effectively minimizes the phenomenon of shaft bending. The housing allows the bearing to be screwed to the bearing surface. Their very simple design, ease of assembly and disassembly, and possibly easy replacement of the self-aligning bearing have led to their use in agricultural, construction, mining, textile machines, conveyors, fans, and in the food and woodworking industries.

Fig. 42. Self-aligning bearing in a cast iron housing UCP 205

Basic technical data of the bearing:

- nominal dynamic load capacity (C) – 14 kN;
- nominal static load capacity (C_0) – 7.8 kN;
- fatigue load limit (P_u) – 0.335 kN;
- limiting speed (n_{max}) – 5,850 rpm;
- bearing material – bearing steel;

- housing material – cast iron.

The final result after assembling all parts is a rig for measuring the shaft torsional angle (Fig. 43).

Fig. 43. Test rig for measuring the torsional angle of a uniform shaft with a circular section

12. Conclusion

The designed and constructed test rig for measuring the shaft torsional angle was verified for correctness of construction and operation.

1) Verification of elements made and their assembly at the test rig:
- checking the seating of the motherboard on the rig table;
- checking the attachment of bearings to the rig base;
- checking the alignment of the shaft and bearings in the housing;
- checking the attachment of the clamping sleeve to the back plate of the test rig;
- checking the stiffness and correctness of the entire shaft mounting node;
- checking the entire node connecting the twisting mechanism with the shaft;
- checking the correct mounting of the measuring lever rings;
- checking the correct setting of dial gauges.

2) The verification of the correct operation of the shaft torsional angle measuring rig consisted in gradually loading the shaft twisting beam with steel discs of a total mass of 16 kg and reading - using a dial gauge - the increase in the linear displacement of the measuring lever (mounted near the point of force application). The results were

recorded in Table 1 and a graph (Fig. 44) of the beam load function to the displacement of the measuring sensors was prepared in an Excel spreadsheet.

Table 1. Results of the displacement of the measuring lever during the twisting of beam loaded with steel discs

No.	Load	Disc weight [kg]	Total beam load [kg]	Sensor measurement [mm]
1	Beam without weight	0	0	0
2	Disc 1	3	3	0,76
3	Disc 2	3	6	1.89
4	Disc 3	2	8	2.51
5	Disc 4	2	10	3.17
6	Disc 5	2	12	3.84
7	Disc 6	2	14	4.47
8	Disc 7	1	15	4.93
9	Disc 8	1	16	5.18

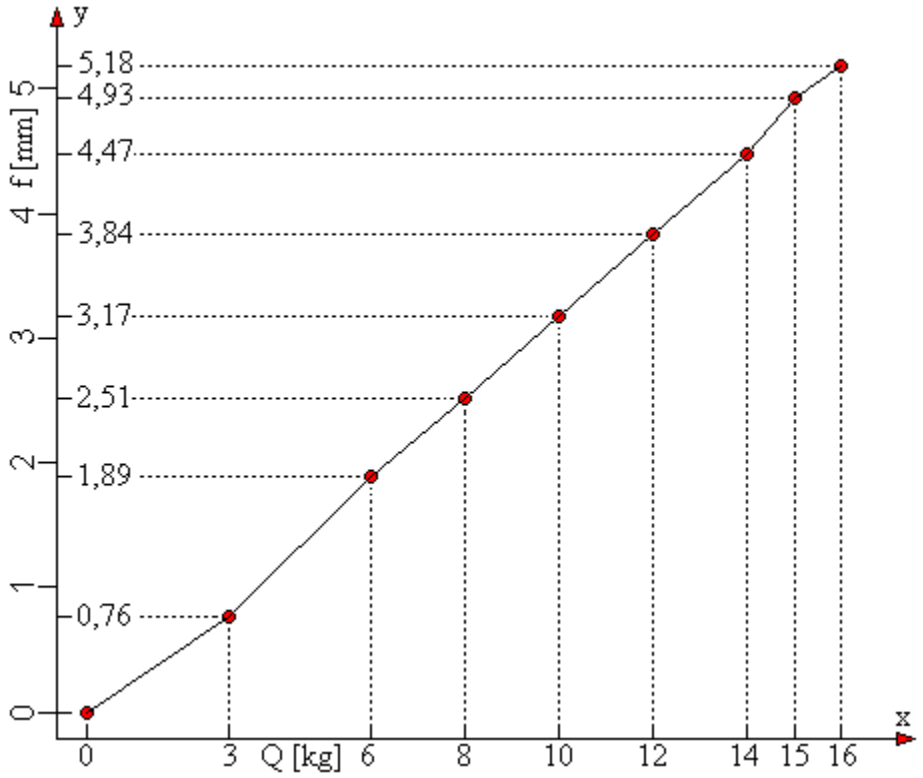

Fig. 44. Graph of the displacement of the measuring holder to the load value of the twisting beam
x axis – load Q [kg]; y axis – displacement of the measuring holder [mm]

The verification of the test rig demonstrated the correctness of design, construction and operation of the rig for measuring the shaft torsional angle and confirmed the theoretical assumptions.

13. Literature

1. Banaszek J, Jonak. J.: *„Podstawy konstrukcji maszyn”.* Wydawnictwo Politechniki Lubelskiej, Lublin 2008.
2. Bąk R., Burzyński T.: Wytrzymałość materiałów z elementami ujęcia komputerowego. WNT, Warszawa 2013.
3. Brzoska Z.: Wytrzymałość materiałów. Wydawnictwo PWN, Warszawa 1972.
4. Chwiej M.: Podstawy konstrukcji maszyn. Zeszyt I. Wydawnictwo Politechniki Warszawskiej, Warszawa 1982.
5. Dąbrowski Z., Maksymiuk M.: Wały i osie. PWN, Warszawa 1984.
6. Ditrich M.: Podstawy konstrukcji maszyn. Wydawnictwo Naukowo-Techniczne, Warszawa 1999.
7. Dobrowolski Z.: Podręcznik spawalnictwa. Wydawnictwo WNT, Warszawa 1978.
8. Dobrzański T.: Rysunek techniczny maszynowy. WNT, Warszawa, 1995.
9. Domański A., Mikołajczyk J.: Dimensional analysis of the selected type of rolling bearing depending on the manufacturer. **W:** Szkoła Logistyki 2023 / redakcja naukowa Janusz Zawiła-Niedźwiecki, Katarzyna Białczak. Radom: Instytut Naukowo-Wydawniczy "Spatium", 2023, Poland; s. 79-89, p-ISBN: 978-83-67033-75-6; e-ISBN: 978-83-67033-58-9.
10. Dyląg Z., Jakubowicz A., Orłoś. Z.: Wytrzymałość materiałów. WNT, Warszawa 1997.
11. Galon M., Mikołajczyk J.: The effect of laser cutting speed on the bearing surface of peaks and valleys of the cut surface. **W:** Logistyka w ratownictwie 2024 / pod redakcją Andrzeja Chudzikiewicza i Andrzeja Krzyszkowskiego. Radom: Instytut Naukowo-Wydawniczy Spatium, 2024, Poland; s. 71-84, p-ISBN: 978-83-68026-24-5; e-ISBN: 978-83-68026-25-2.
12. Galon M., Mikołajczyk J.: The effect of laser cutting speed on the weight of the workpiece. **W:** Logistyka w ratownictwie 2024 / pod redakcją Andrzeja Chudzikiewicza i Andrzeja Krzyszkowskiego. Radom: Instytut Naukowo-Wydawniczy Spatium, 2024, Poland; s. 85-96, p-ISBN: 978-83-68026-24-5; e-ISBN: 978-83-68026-25-2.
13. Galon M., Mikołajczyk J.: Wpływ wartości posuwu podczas cięcia laserem na chropowatość powierzchni przecięcia. Obróbka Metalu; 2024, nr 3, s. 48-53, p-ISSN: 2081-7002; **https://obrobkametalu.tech/nasze-czasopismo/archiwum/**
14. Grabowska M., Mikołajczyk J.: Zastosowanie tomografii komputerowej CAT w inżynierii materiałowej. Application of CAT scanning for materials engineering. Postępy w Inżynierii Mechanicznej [Developments in Mechanical Engineering]. 2017, nr 9 (5), s. 15-26, p-ISSN: 2300-3383; Wydawnictwa Uczelniane Uniwersytetu Technologiczo-Przyrodniczego w Bydgoszczy, Poland. **http://wu.utp.edu.pl/oferta,8,1**
15. Grabowska M., Mikołajczyk J.: Próba zastosowania tomografii komputerowej CAT do określania struktury grafitu naturalnego w zależności od rozmiaru ziarna. An attempt to apply cat scanning to determine the natural graphite structure depending on the grain size. Postępy w Inżynierii Mechanicznej [Developments in Mechanical Engineering]. 2018, nr 12 (6), s. 5-14, p-ISSN: 2300-3383; Wydawnictwa Uczelniane Uniwersytetu Technologiczno-Przyrodniczego w Bydgoszczy, Poland. **http://wu.utp.edu.pl/oferta,8,1**
16. Grabowska M., Mikołajczyk J., Basiak S.: Zastosowanie tomografii komputerowej CAT w nieniszczących badaniach teowych złączy spawanych. Application of cat

scanning in non-destructive testing of welded t-joints. Postępy w Inżynierii Mechanicznej [Developments in Mechanical Engineering]; 2018, nr 11 (6), s. 31-44, p-ISSN: 2300-3383; Wydawnictwa Uczelniane Uniwersytetu Technologiczno-Przyrodniczego w Bydgoszczy, Poland.
http://wu.utp.edu.pl/oferta,8,1
17. Grabowska M., Piochacz A., Mikołajczyk J.: Attempt to use computed tomography CAT to analyze the anodized layer. Postępy w Inżynierii Mechanicznej [Developments in Mechanical Engineering]; 2020, nr 15 (8), s. 25-33, p-ISSN: 2300-3383; Wydawnictwa Uczelniane Uniwersytetu Technologiczno-Przyrodniczego im. J. J. Śniadeckich w Bydgoszczy, Poland.
https://dme.utp.edu.pl/art/15(8)2020/25.pdf
DOI: 10.37660/dme.2020.15.8.3
18. Grzelak K., Telega J., Korzewski J.: Podstawy konstrukcji maszyn. Wydawnictwa Szkolne i Pedagogiczne, Warszawa, 2013.
19. Hillar J., Jarmoszuk S.: Technologia. Spawalnictwo. Wydawnictwa Szkolne i Pedagogiczne, Warszawa 1987.
20. Hillar J.: Spawanie gazowe. Wiadomości specjalistyczne. Wydawnictwo ZZDZ, nr M-120.
21. Hołubowska A., Szałański B., Mikołajczyk J.: Laboratorium termodynamiki. Piła: Wydawnictwo Państwowej Uczelni im. Stanisława Staszica, 2020, Poland; 164 s., e-ISBN: 978-83-62617-93-7;
https://wydawnictwo.puss.pila.pl/files/Laboratorium_termodynamiki_POL_version.pdf
22. Jakubowicz A., Orłoś A.: Wytrzymałość materiałów. Wydawnictwa Naukowo-Techniczne, Warszawa, 1978.
23. Jarmoliński Z., Mikołajczyk J.: Badania wpływu technologii cięcia stali na twardość powierzchni bijaka. Research of the influence of steel cutting technology on the strength of the hammer. Postępy w Inżynierii Mechanicznej [Developments in Mechanical Engineering]. 2018, nr 12 (6), s. 15-30, p-ISSN: 2300-3383. Wydawnictwa Uczelniane Uniwersytetu Technologiczno-Przyrodniczego w Bydgoszczy, Poland.
http://wu.utp.edu.pl/oferta,8,1
24. Jarmoszuk S.: Spawanie elektryczne. Wiadomości specjalistyczne. Wydawnictwo ZZDZ, nr M-121.
25. Jastrzębowski P., Mutermilch J., Orłowski W.: Wytrzymałość materiałów. Wydawnictwo Arkady, Warszawa, 1986.
26. Jędrzejczyk D., Mikołajczyk J.: Defining the correlation between the cutting speed and roughness parameter Rz. **W:** MIK-21 : Międzynarodowa Innowacyjność i Konkurencyjność w XXI wieku : aspekty innowacyjne / redakcja naukowa Radosław Luft. Lublin : Fundacja Innowacji i Nowoczesnych Technologii INOTECH, 2022. Radom : nakładem Instytutu Naukowo-Wydawniczego "Spatium", 2022; s. 39-46, p-ISBN: 978-83-67033-43-5; e-ISBN: 978-83-67033-44-2;
http://inw-spatium.pl/wp-content/uploads/2022/09/MIK-21-2022-Aspekty-innowacyjne-2.pdf
27. Jędrzejczyk D., Mikołajczyk J.: Mathematical models of the influence of cutting speed on Ra parameter. Developments in Mechanical Engineering; 2022, nr 18 (10), s. 115-129, p-ISSN: 2720-0639; Wydawnictwa Uczelniane Uniwersytetu Technologiczno-Przyrodniczego im. J. J. Śniadeckich w Bydgoszczy, Poland.
DOI: 10.37660/dme.2022.18.10.11
28. Jędrzejczyk D., Mikołajczyk J.: Wpływ prędkości skrawania na wybrany parametr warstwy wierzchniej. **W:** Logistyka w ratownictwie 2022 / pod redakcją Andrzeja

Chudzikiewicza i Andrzeja Krzyszkowskiego. Radom: Instytut Naukowo-Wydawniczy Spatium, 2022, Poland; s. 75-90, p-ISBN: 978-83-67033-57-2;
e-ISBN: 978-83-67033-70-1.
29. Knosala R., Gwiazda A., Raier A., Gentarz P.: PKM. Przykłady obliczeń. Wydawnictwa Naukowo-Techniczne, Warszawa, 2000.
30. Kocanda S., Szala J.: Podstawy obliczeń zmęczeniowych. Państwowe Wydawnictwa Naukowe, Warszawa, 1991
31. Korewa W.: Podstawy konstrukcji maszyn, tom I. Państwowe Wydawnictwa Naukowe, Warszawa, 1976.
32. Kurmaz L.W.: Podstawy konstrukcji maszyn. Projektowanie. Państwowe Wydawnictwa Naukowe, Warszawa, 1999.
33. Kurmaz L.W., Kurmaz O.L.: Podstawy konstruowania węzłów i części maszyn. Politechnika Świętokrzyska, Kielce, 2011.
34. Latoś H., Mikołajczyk J.: Effect of partial wear of the tool point on the selected indicator of the machining process. **W:** Logistyka w ratownictwie 2023 / pod redakcją Andrzeja Chudzikiewicza i Anny Stelmach. Radom: Instytut Naukowo-Wydawniczy "Spatium", 2023, Poland; s. 195-210, p-ISBN: 978-83-67033-95-4;
e-ISBN: 978-83-67033-96-1.
35. Latoś H., Mikołajczyk J.: Thickness of the machined layer at milling with single-edge straight blades with an angle of $\lambda s \neq 0°$. **W:** MIK-21 : Międzynarodowa Innowacyjność i Konkurencyjność w XXI wieku : Aspekty innowacyjne / redakcja naukowa dr Łukasz Wojtowicz. Lublin: Fundacja Innowacji i Nowoczesnych Technologii INOTECH : nakładem Instytutu Naukowo-Wydawniczego "Spatium", 2023, Poland; s. 23-27, p-ISBN: 978-83-67033-89-3; e-ISBN: 978-83-67033-90-9.
36. Latoś H., Mikołajczyk J., Konarski J., Mikołajczyk T.: Turning using self-induced vibration. **W:** MIK-21 : Międzynarodowa Innowacyjność i Konkurencyjność w XXI wieku : aspekty innowacyjne / redakcja naukowa dr Łukasz Wojtowicz, 2023, Poland; s. 187-200, p-ISBN: 978-83-67033-89-3; e-ISBN: 978-83-67033-90-9.
37. Latoś H., Mikołajczyk J.: Vibration in machining. **W:** Logistyka w ratownictwie 2023 / pod redakcją Andrzeja Chudzikiewicza i Anny Stelmach. Radom: Instytut Naukowo-Wydawniczy "Spatium", 2023, Poland; s. 187-194,
p-ISBN: 978-83-67033-95-4; e-ISBN: 978-83-67033-96-1.
38. Latoś H., Mikołajczyk J.: The effect of feed rate on the roughness of machined surface. **W:** Szkoła Logistyki 2024 / redakcja naukowa Janusz Zawiła-Niedźwiecki, Adam Płaczek. Radom: Instytut Naukowo-Wydawniczy "Spatium", 2024, Poland; s. 217-226, p-ISBN: 978-83-68026-07-8; e-ISBN: 978-83-68026-08-5.
39. Lewiński J., Wilczyński A. P., Witemberg-Perzyk D.: Podstawy wytrzymałości materiałów. Oficyna Wydawnicza Politechniki Warszawskiej, Warszawa, 2010.
40. Lisowski A., Siemieniec A.: Wytrzymałość materiałów. Przykłady obliczeń – zadania. Państwowe Wydawnictwa Naukowe, Warszawa, 1973.
41. Łączkowski R.: Wytrzymałość materiałów. Wydawnictwo Politechniki Gdańskiej, Gdańsk, 1999.
42. Matuszewski M., Mikołajczyk J., Styp-Rekowski M: Modyfikacja cech środka smarującego za pomocą standardowych dodatków smarowych. Modification of lubricants features by means of standard additives. Postępy w Inżynierii Mechanicznej [Developments in Mechanical Engineering]. 2013, nr 1 (1), s. 57-65, Wydawnictwo Uczelniane Uniwersytetu Technologiczno-Przyrodniczego w Bydgoszczy;
p-ISSN: 2300-3383;
http://wu.utp.edu.pl/uploads/oferta/Postepy_1_1_2013.pdf

43. Matuszewski M., Mikołajczyk J., Mikołajczyk T., Styp-Rekowski M.: Logistyczne aspekty zarządzania procesem naprawy. Logistical aspects of the repair process management. Logistyka, 2015, nr 4, s. 1991-1997, p-ISSN: 1231-5478; **https://www.czasopismologistyka.pl/o-czasopismie/wydania**
44. Matuszewski M., Mikołajczyk J., Mikołajczyk T., Styp-Rekowski M.: The influence of cooling and lubrication liquid quantity on the isotropy of a machine component surface during machining = Wpływ warunków chłodzenia i smarowania podczas obróbki elementów maszyn na stopień izotropowości ich powierzchni. Tribologia. 2016, vol. 265, No. 1, s. 57-65, p-ISSN: 0208-7774; e-ISSN: 1732-422X; **https://t.tribologia.eu/resources/html/article/details?id=158175**
45. Mikołajczyk J., Styp-Rekowski M., Świerk K.: Modyfikowanie cech środka smarującego za pomocą dodatków i komputerowe wspomaganie ich doboru. W**:** CAX'2009 : komputerowe wspomaganie nauki i techniki : VI warsztaty naukowe, Bydgoszcz - Duszniki Zdrój 2009 : praca zbiorowa pod redakcją Tadeusza Mikołajczyka. p-ISBN: 978-83-61314-65-3. Wydawnictwa Uczelniane Uniwersytetu Technologiczno-Przyrodniczego w Bydgoszczy, Bydgoszcz 2009.
46. Mikołajczyk J.: Zestawienie porównawcze dodatków depresujących do olejów. W: Zaawansowana tribologia : XXX Ogólnopolska Konferencja Tribologiczna, Nałęczów, 21-24 września 2009 r. Ogólnopolska Konferencja Naukowa XXX Szkoły Tribologicznej "Zaawansowana Tribologia" : Wydział Materiałoznawstwa, Technologii i Wzornictwa Politechniki Radomskiej, Instytut Technologii Eksploatacji - PIB Radom oraz Komitet Budowy Maszyn, Sekcja Podstaw Eksploatacji Maszyn PAN. Wydawnictwo Naukowe Instytutu Technologii Eksploatacji - PIB, Radom, 2009.
47. Mikołajczyk J.: Zestawienie porównawcze własności fizykochemicznych dodatków smarnych w oleju podstawowym SAE-30. W: Terotechnologia 2009 : materiały konferencji na ekspozycji Metal i Control-Tech : Targi - Kielce (29.09-01.10.2009). VI Konferencja Naukowo-Techniczna "Terotechnologia 2009" : Politechnika Świętokrzyska, Centrum Laserowych Technologii Metali, Katedra Inżynierii Eksploatacji, Wydział Mechatroniki i Budowy Maszyn, Polskie Towarzystwo Naukowo-Techniczne, Towarzystwo Eksploatacyjne, Kielce: Wydawnictwo Politechniki Świętokrzyskiej, 2009. Seria: Zeszyty Naukowe - Politechnika Świętokrzyska, nr 13.
48. Mikołajczyk J., Matuszewski M.: Konstrukcja i sterowanie stanowiska do badań tribologicznych. W: CAX'2010 : komputerowe wspomaganie nauki i techniki : VII warsztaty naukowe, Bydgoszcz - Duszniki Zdrój 2010 : praca zbiorowa / pod red. Tadeusza Mikołajczyka. Bydgoszcz : Wydawnictwa Uczelniane Uniwersytetu Technologiczno-Przyrodniczego w Bydgoszczy, 2010. p-ISBN: 9788361314387
49. Mikołajczyk J.: System rejestracji i wizualizacji warunków pracy stanowiska do badań tribologicznych. W: CAX'2011 : komputerowe wspomaganie nauki i techniki : VIII warsztaty naukowe, Bydgoszcz - Duszniki Zdrój 2011 : praca zbiorowa / pod redakcją Tadeusza Mikołajczyka. Bydgoszcz : Wydawnictwa Uczelniane Uniwersytetu Technologiczno-Przyrodniczego w Bydgoszczy, 2011. p-ISBN: 9788361314981
50. Mikołajczyk J.: Badanie wpływu preparatu eksploatacyjnego Mind M na zmianę własności smarnych oleju bazowego SN-150. Źródło: Inżynieria i aparatura chemiczna [Chemical Engineering and Equipment]. 2012, nr 5, s. 235-236, p-ISSN: 0368-0827. **http://inzynieria-aparatura-chemiczna.pl/rok-2012-nr-5/**
51. Mikołajczyk J., Styp-Rekowski M., Matuszewski M., Musiał J.: Einfluβ der kompositionen von schmierzusätzen auf die exploitations-eigenschaften der mischung mit Basisöl SN-150. W: Tribologie und mobilität : beiträge der tribotechnik zur optimierung von fertigungsprozessen, wartung, schmierung (reibungskonditionierung)

und betriebssicherheit von verkehrsmitteln und verkehrswegen. Wien, 15 November 2012. Symposium 2012 "Tribologie und mobilität" : Österreichische Tribologische Gesellschaft. Österreichische Tribologische Gesellschaft, Wien, 2012.
52. Mikołajczyk J.: Einfluβ der ausgewählten schmierzstoffzusätze auf betriebseigenschaften der mischung mit Basisöl SN-150. **W:** Reibung, schmierung und verschleiβ : forschung und praktische anwendungen. Band 1. Tribologische systeme maschinenelemente und antriebstechnik fahrzeugtechnik prüfen, messen, kontrollieren. Göttingen, 22-24 September 2014. 55. Tribologie Fachtagung "Reibung, Schmierung und Verschleiβ" : Gesellschaft für Tribologie e.V. Stolberg-Venwegen : Gesellschaft für Tribologie e.V., 2014. Germany.
53. Mikołajczyk J.: Einfluss der ausgewählten zusatzschmierstoffe auf die intensivität des verschleiβprozesses (Ra, Rq, Δm) mit Basisöl SN-150. **W:** Tribologie in industrie und forschung : werkstoffe, konstruktion und technologie. Leoben, 26 November 2014. ÖTG Symposium 2014 "Tribologie in industrie und forschung" : Österreichische Tribologische Gesellschaft. Wien : Österreichische Tribologische Gesellschaft, 2014. Austria.
54. Mikołajczyk J., Matuszewski M.: Einfluss der ausgewählten schmierzstoffzusätze auf ΔT und ΔP mit Basisöl SN-150. **W:** Tribologie in industrie und forschung : werkstoffe, schmierstoffe und technologie. Wiener Neustadt, 25 November 2015, Austria. ÖTG Symposium 2015 "Tribologie in industrie und forschung" : Österreichische Tribologische Gesellschaft. Wiener Neustadt : Österreichische Tribologische Gesellschaft, 2015, s. 145-152.
55. Mikołajczyk J.: Vergleich charakteristischer parameter des abbott-firestone-diagramms für ein kinematisches paar mit konformem kontakt. **W:** Tribologie in industrie und forschung : verschleiβschutz, instandhaltung und anlagenzuverlässigkeit. Linz, 22-23 November 2016, Austria. ÖTG Symposium 2016 "Tribologie in industrie und forschung" : Österreichische Tribologische Gesellschaft. Wiener Neustadt : Österreichische Tribologische Gesellschaft, 2016; s. 105-110.
56. Mikołajczyk J.: Wpływ dodatków smarowych na transformację warstwy wierzchniej. Piła : Wydawnictwo Państwowej Wyższej Szkoły Zawodowej im. Stanisława Staszica, 2017r., Poland , p-ISBN: 978-83-62617-76-0; www.ans.pila.pl
57. Mikołajczyk J.: Maszyny tarciowe : budowa, przeznaczenie. Piła, Wydawnictwo Państwowej Wyższej Szkoły Zawodowej im. Stanisława Staszica, 2018, Poland; 256 s., p-ISBN: 978-83-62617-86-9.
58. Mikołajczyk J.: Analiza statystyczna zmiany poboru mocy podczas procesu zużywania. Statistical analysis of the power variation of tribotester as a resultat of the wear process. Autobusy. Technika, Eksploatacja, Systemy Transportowe; 2019, nr 10-11, s. 83-88, p-ISSN: 1509-5878; e-ISSN: 2450-7725;
http://yadda.icm.edu.pl/yadda/element/bwmeta1.element.baztech-21189602-884a-4d1a-bb60-9edaeae4af8d
59. Mikołajczyk J.: Influence of consumables on the amount of power consumption of kinematic vapor of conformal contact. Wpływ PE na pobór mocy pary kinematycznej o styku konforemnym. Postępy w Inżynierii Mechanicznej [Developments in Mechanical Engineering]; 2019, nr 13 (7), s. 39-50, p-ISSN: 2300-3383; Wydawnictwa Uczelniane Uniwersytetu Technologiczno-Przyrodniczego im. J. J. Śniadeckich w Bydgoszczy, Poland.
http://yadda.icm.edu.pl/baztech/element/bwmeta1.element.baztech-2faf200b-3010-4192-9fd0-062f53b49d38
60. Mikołajczyk J.: Statistical analysis of the mass variation of samples as a result of the wear process. Analiza statystyczna zmiany masy próbek w wyniku procesu zużywania.

Postępy w Inżynierii Mechanicznej [Developments in Mechanical Engineering]; 2019, nr 13 (7), s. 51-61, p-ISSN: 2300-3383; Wydawnictwa Uczelniane Uniwersytetu Technologiczno-Przyrodniczego im. J. J. Śniadeckich w Bydgoszczy, Poland.
http://yadda.icm.edu.pl/baztech/element/bwmeta1.element.baztech-2faf200b-3010-4192-9fd0-062f53b49d38
61. Mikołajczyk J.: Tribotestery : budowa i przeznaczenie. Piła: Wydawnictwo Państwowej Wyższej Szkoły Zawodowej im. Stanisława Staszica, 2019, Poland; 160 s., e-ISBN: 978-83-62617-90-6;
https://wydawnictwo.pwsz.pila.pl/files/Tribotestery.pdf
62. Mikołajczyk J.: Determining the energy validity of the Kostetsky's hypothesis on the basis of models for relative motion velocity v = 0.08 m/sec. Developments in Mechanical Engineering; 2020, nr 16 (8), s. 17-29, p-ISSN: 2720-0639; Wydawnictwa Uczelniane Uniwersytetu Technologiczno-Przyrodniczego im. J. J. Śniadeckich w Bydgoszczy, Poland.
DOI: 10.37660/dme.2020.16.8.2
63. Mikołajczyk J.: Finding the correlation between wear of samples kinematic pair of conformal contact and electric power consumption. Postępy w Inżynierii Mechanicznej [Developments in Mechanical Engineering]; 2020, nr 15 (8), s. 59-68,
p-ISSN: 2300-3383; Wydawnictwa Uczelniane Uniwersytetu Technologiczno-Przyrodniczego im. J. J. Śniadeckich w Bydgoszczy, Poland.
https://dme.utp.edu.pl/art/15(8)2020/59.pdf
DOI: 10.37660/dme.2020.15.8.6
64. Mikołajczyk J.: The effect of temperature lag on the value of power-temperature correlation for frictional pair of conformal contact. Postępy w Inżynierii Mechanicznej [Developments in Mechanical Engineering]; 2020, nr 15 (8), s. 79-86,
p-ISSN: 2300-3383; Wydawnictwa Uczelniane Uniwersytetu Technologiczno-Przyrodniczego im. J. J. Śniadeckich w Bydgoszczy, Poland.
https://dme.utp.edu.pl/art/15(8)2020/79.pdf
DOI: 10.37660/dme.2020.15.8.8
65. Mikołajczyk J.: Określenie na podstawie modeli zmiany masy próbek w wyniku procesu zużywania. **W:** Szkoła Logistyki 2021 / redakcja naukowa Janusz Zawiła-Niedźwiecki, Piotr Korneta. Radom : Instytut Naukowo-Wydawniczy "Spatium", 2021; s. 167-174, Poland; p-ISBN: 978-83-66550-75-9; e-ISBN: 978-83-66550-89-6.
66. Mikołajczyk J.: A method of determining mathematical models of a seizure test of friction pairs. **W:** MIK-21 : Międzynarodowa Innowacyjność i Konkurencyjność w XXI wieku : aspekty innowacyjne / redakcja naukowa Radoslaw Luft. Lublin : Fundacja Innowacji i Nowoczesnych Technologii INOTECH, 2022. Radom : nakładem Instytutu Naukowo-Wydawniczego "Spatium", 2022; s. 7-24, p-ISBN: 978-83-67033-43-5;
e-ISBN: 978-83-67033-44-2.
http://inw-spatium.pl/wp-content/uploads/2022/09/MIK-21-2022-Aspekty-innowacyjne-2.pdf
67. Mikołajczyk J.: Friction machines. Piła: Wydawnictwo Akademii Nauk Stosowanych im. Stanisława Staszica, 2022, Poland; 488 s.,
e-ISBN: 978-83-62617-96-8.
https://wydawnictwo.ans.pila.pl/files/FRICTION_MACHINES.pdf
68. Mikołajczyk J., Jędrzejczyk D.: Określenie korelacji między prędkością skrawania a parametrem chropowatości Ra. Obróbka Metalu; 2022, nr 3, s. 11-15,
p-ISSN: 2081-7002; **https://obrobkametalu.tech/**

69. Mikołajczyk J.: Rolling bearing heating charakter. **W:** Szkoła Logistyki 2022. Radom: Instytut Naukowo-Wydawniczy "Spatium", 2022, Poland; s. 231-239, Materiały z IX Konferencji Naukowej "Szkoła Logistyki 2022";
p-ISBN: 978-83-67033-33-6; e-ISBN: 978-83-67033-34-3.
70. Mikołajczyk J.: Tribological properties of carbon black. **W:** Szkoła Logistyki 2022. Radom: Instytut Naukowo-Wydawniczy "Spatium", 2022, Poland; s. 217-230, Materiały z IX Konferencji Naukowej "Szkoła Logistyki 2022";
p-ISBN: 978-83-67033-33-6; e-ISBN: 978-83-67033-34-3.
71. Mikołajczyk J.: Determination of the modified coefficient of variation from the number of samples. **W:** MIK-21 : Międzynarodowa Innowacyjność i Konkurencyjność w XXI wieku : Aspekty innowacyjne / redakcja naukowa dr Łukasz Wojtowicz. Lublin: Fundacja Innowacji i Nowoczesnych Technologii INOTECH : nakładem Instytutu Naukowo-Wydawniczego "Spatium", 2023, Poland; s. 111-122,
p-ISBN: 978-83-67033-89-3; e-ISBN: 978-83-67033-90-9.
72. Mikołajczyk J.: Effect of cutting speed on the shape of the machined surface profile. Mebutra; 2023, nr 1, s. 47-63, Wydawnictwo Akademii Nauk Stosowanych im. S. Staszica w Pile, Piła 2023, Poland.
https://online.fliphtml5.com/vliuj/yunw/ p=48
73. Mikołajczyk J.: Friction Machines II. Piła: Wydawnictwo Akademii Nauk Stosowanych im. Stanisława Staszica w Pile, 2023, Poland; 598 s.,
p-ISBN: 978-83-67684-00-2;
https://wydawnictwo.ans.pila.pl/files/FRICTION_MACHINES_V_ANS_PILA.pdf
74. Mikołajczyk J.: Oil can talk. **W:** Szkoła Logistyki 2023 / redakcja naukowa Janusz Zawiła-Niedźwiecki, Katarzyna Białczak. Radom: Instytut Naukowo-Wydawniczy "Spatium", 2023, Poland; s. 109-115, p-ISBN: 978-83-67033-75-6;
e-ISBN: 978-83-67033-58-9.
75. Mikołajczyk J.: Pobór mocy elektrycznej przez parę kinematyczną jako parametr oceny jakości oleju. **W:** Logistyka w ratownictwie 2023 / pod redakcją Andrzeja Chudzikiewicza i Anny Stelmach. Radom: Instytut Naukowo-Wydawniczy "Spatium", 2023, Poland; s. 223-230, p-ISBN: 978-83-67033-95-4;
e-ISBN: 978-83-67033-96-1.
76. Mikołajczyk J.: Rola dodatków smarowych w olejach. **W:** Logistyka w ratownictwie 2023 / pod redakcją Andrzeja Chudzikiewicza i Anny Stelmach. Radom: Instytut Naukowo-Wydawniczy "Spatium", 2023, Poland; s. 231-237,
p-ISBN: 978-83-67033-95-4; e-ISBN: 978-83-67033-96-1.
77. Mikołajczyk J.: Temperature as a parameter for assessing the work of a friction pair. **W:** Szkoła Logistyki 2023 / redakcja naukowa Janusz Zawiła-Niedźwiecki, Katarzyna Białczak. Radom: Instytut Naukowo-Wydawniczy "Spatium", 2023, Poland; s. 101-107, p-ISBN: 978-83-67033-75-6; e-ISBN: 978-83-67033-58-9.
66. Mikołajczyk J.: Tire as a selected element of a car subject to diagnostics. **W:** Szkoła Logistyki 2023 / redakcja naukowa Janusz Zawiła-Niedźwiecki, Katarzyna Białczak. Radom: Instytut Naukowo-Wydawniczy "Spatium", 2023, Poland; s. 117-131,
p-ISBN: 978-83-67033-75-6; e-ISBN: 978-83-67033-58-9.
78. Mikołajczyk J.: Wpływ dodatku modyfikującego cechy płynu obróbkowego na zmianę temperatury w strefie kontaktu współpracujących powierzchni. Obróbka Metalu; 2023, nr 2, s. 43-46, p-ISSN: 2081-7002;
https://obrobkametalu.tech/media/2023/05/2023_2_52_ObrobkaMetalu.pdf
79. Mikołajczyk J., Kozłowska M.A., Krasicki K.: Wpływ kompetencji cyfrowych pracowników na poziom rozwoju procesów przemysłowych. **W:** MIK-21 : Międzynarodowa Innowacyjność i Konkurencyjność w XXI wieku : aspekty społeczne /

redakcja naukowa Radosław Luft. Lublin-Radom : Fundacja Innowacji i Nowoczesnych Technologii INOTECH : nakładem Instytutu Naukowo-Wydawniczego "Spatium", 2023, Poland; s. 149-169, p-ISBN: 978-83-67033-92-3; e-ISBN: 978-83-67033-93-0.
80. Mikołajczyk J.: Zmiana geometrycznych cech współpracujących powierzchni miarą intensywności procesu zużywania ostrzy skrawających; Obróbka Metalu; 2023, nr 1, s. 50-54, p-ISSN: 2081-7002;
https://yadda.icm.edu.pl/yadda/element/bwmeta1.element.baztech-9e73eb05-2a91-4df5-853b-22abf7a6ee77
81. Mikołajczyk J., Góra F., Jędrzejczyk D.: Analysis of selected surface roughness parameters for wear processes. Analiza wybranych parametrów chropowatości powierzchni pod kątem procesów zużywania. **W:** MIK-21 : Międzynarodowa Innowacyjność i Konkurencyjność w XXI wieku : Aspekty innowacyjne / redakcja naukowa Radosław Luft. Lublin: Wydawnictwo Naukowe FNCE, 2024; s. 93-117,
p-ISBN: 978-83-68074-82-6; e-ISBN: 978-83-68319-03-3.
82. Mikołajczyk J., Galon M.: Mathematical model of straight regression determining the effect of laser cutting speed on the mass of the workpiece. **W:** MIK-21 : Międzynarodowa Innowacyjność i Konkurencyjność w XXI wieku : Aspekty innowacyjne / redakcja naukowa Radosław Luft. Lublin: Wydawnictwo Naukowe FNCE, 2024, Poland; s. 71-92, p-ISBN: 978-83-68074-82-6;
e-ISBN: 978-83-68319-03-3.
83. Mikołajczyk J., Sądej I.: Spinning speed and balancing accuracy. **W:** MIK-21 : Międzynarodowa Innowacyjność i Konkurencyjność w XXI wieku : Aspekty innowacyjne / redakcja naukowa Radosław Luft. Lublin: Wydawnictwo Naukowe FNCE, 2024, Poland; s. 118-132, p-ISBN: 978-83-68074-82-6;
e-ISBN: 978-83-68319-03-3.
84. Mikołajczyk J.: The correlation between the population and number of construction disasters. Mebutra; 2025, nr 3, s. 44-55, Wydawnictwo Akademii Nauk Stosowanych im. S. Staszica w Pile, Poland.
https://wydawnictwo.ans.pila.pl/files/MEBUTRA2025.pdf
85. Mikołajczyk J.: The relationship between the type of structure and the number of construction disasters. Zależność między rodzajem konstrukcji, a liczbą katastrof budowlanych. Mebutra; 2025, 3, s. 30-43, Wydawnictwo Akademii Nauk Stosowanych im. S. Staszica w Pile, Poland.
https://wydawnictwo.ans.pila.pl/files/MEBUTRA2025.pdf
86. Niezgodziński M., Niezgodziński T.: Wytrzymałość materiałów. Wydawnictwo PWN, Warszawa, 2009.
87. Olechnowicz J., Mikołajczyk J.: Truck scales : the key to safe transport and road protection. Mebutra; 2024, nr 2, s. 03-08, Wydawnictwo Akademii Nauk Stosowanych im. S. Staszica w Pile, Poland.
https://wydawnictwo.ans.pila.pl/files/MEBUTRA2024.pdf
88. Orlik Z., Surowiak W.: Części maszyn. Cz. I. Wydawnictwa Szkolne i Pedagogiczne, Warszawa, 1980.
89. Osiński Z., Bajon W., Szucki T.: Podstawy konstrukcji maszyn. Wydawnictwo PWN, Warszawa, 1975.
90. Pałasz J.: Poradnik spawacza gazowego. Wydawnictwa Naukowo-Techniczne. Warszawa, 1986.
91. Piwowar S.: Spawanie i zgrzewanie elektryczne. Wydawnictwa Szkolne i Pedagogiczne. Warszawa, 1981.
92. Pikulik K.W., Mikołajczyk J.: The influence of the welding current on the air pollution emissions. Wpływ prądu spawania na emisję zanieczyszczeń powietrza.

Postępy w Inżynierii Mechanicznej [Developments in Mechanical Engineering]; 2019, nr 14 (7), s. 33-46, p-ISSN: 2300-3383; Wydawnictwa Uczelniane Uniwersytetu Technologiczno-Przyrodniczego im. J. J. Śniadeckich w Bydgoszczy, Poland.
http://yadda.icm.edu.pl/baztech/element/bwmeta1.element.baztech-2faf200b-3010-4192-9fd0-062f53b49d38
93. Pikulik K.W., Mikołajczyk J.: Determination of emission of iron oxides from the welding process on the basis of mathematical models. Welding Technology Review; 2021, vol. 93, No 2, s. 35-43, p-ISSN: 0033-2364; e-ISSN: 2449-7959;
http://www.pspaw.wip.pw.edu.pl/index.php/pspaw/article/view/1132
DOI: 10.26628/wtr.v93i2.1132
94. Pikulik J., Pikulik K.W., Mikołajczyk J.: The relationship between the clearance of the coupling mechanism used in uniaxial light car trailers and the date of their production. **W:** MIK-21 : Międzynarodowa Innowacyjność i Konkurencyjność w XXI wieku : aspekty innowacyjne / redakcja naukowa Radosław Luft. Lublin : Fundacja Innowacji i Nowoczesnych Technologii INOTECH, 2022, Poland. Radom : nakładem Instytutu Naukowo-Wydawniczego "Spatium", 2022; s. 221-233,
p-ISBN: 978-83-67033-43-5; e-ISBN: 978-83-67033-44-2;
http://inw-spatium.pl/wp-content/uploads/2022/09/MIK-21-2022-Aspekty-innowacyjne-2.pdf
95. Pikulik J., Pikulik K.W., Mikołajczyk J.: Zależność wielkości luzu mechanizmu sprzęgającego stosowanego w jednoosiowych lekkich przyczepach samochodowych od wartości współczynnika przylegania. **W:** Logistyka w ratownictwie 2022 / pod redakcją Andrzeja Chudzikiewicza i Andrzeja Krzyszkowskiego. Radom: Instytut Naukowo-Wydawniczy "Spatium", 2022, Poland; s. 157-167, p-ISBN: 978-83-67033-57-2;
e-ISBN: 978-83-67033-70-1.
96. Pikulik J., Pikulik K.W., Mikołajczyk J.: Determination of the degree of contact of the movable part of the coupling head with the ball part of the coupling of single-axle light car trailers. **W:** MIK-21 : Międzynarodowa Innowacyjność i Konkurencyjność w XXI wieku : aspekty innowacyjne / redakcja naukowa dr Łukasz Wojtowicz. Lublin: Fundacja Innowacji i Nowoczesnych Technologii INOTECH : nakładem Instytutu Naukowo-Wydawniczego "Spatium", 2023, Poland; s. 97-109,
p-ISBN: 978-83-67033-89-3; e-ISBN: 978-83-67033-90-9.
97. Piochacz A., Mikołajczyk J.: Wpływ czasu trwania procesu anodowania stopu aluminium EN AW-6060 na grubość i twardość otrzymanej warstwy. Influence of aluminium type EN AW-6060 anodizing process duration on the thickness and hardness of the obtained layer. Postępy w Inżynierii Mechanicznej [Developments in Mechanical Engineering]; 2018, nr 12 (6), s. 49-56, p-ISSN: 2300-3383; Wydawnictwa Uczelniane Uniwersytetu Technologiczno-Przyrodniczego w Bydgoszczy, Poland.
http://wu.utp.edu.pl/oferta,8,1
98. Piochacz A., Mikołajczyk J.: Analiza statystyczna wpływu czasu anodowania na grubość otrzymanej powłoki. Statistical analysis of the influence of anodizing time on the thickness of obtained layers. Autobusy. Technika, Eksploatacja, Systemy Transportowe; 2019, vol. 233, nr 9, s. 48-51, p-ISSN: 1509-5878;
e-ISSN: 2450-7725; **http://ceref.pl/index.php/Autobusy/article/view/956**
DOI: 10.24136/atest.2019.201
99. Piochacz A., Mikołajczyk J.: Determination of the thickness of anodized layer on the basis mathematical models. Developments in Mechanical Engineering; 2020, nr 16 (8), s. 31-39, p-ISSN: 2720-0639; Wydawnictwa Uczelniane Uniwersytetu Technologiczno-Przyrodniczego im. J. J. Śniadeckich w Bydgoszczy, Poland.
DOI: 10.37660/dme.2020.16.8.3

100. Piotrowski Ł., Góra F., Mikołajczyk J.: Construction of an electric longboard with one-wheel driver. Mebutra; 2024, nr 2, s. 16-27, Wydawnictwo Akademii Nauk Stosowanych im. S. Staszica w Pile, Poland.
https://wydawnictwo.ans.pila.pl/files/MEBUTRA2024.pdf
101. Piotrowski Ł., Góra F., Mikołajczyk J.: Design and construction of an electric longboard. **W:** Logistyka w ratownictwie 2024 / pod redakcją Andrzeja Chudzikiewicza i Andrzeja Krzyszkowskiego. Radom: Instytut Naukowo-Wydawniczy Spatium, 2024, Poland; s. 167-178, p-ISBN: 978-83-68026-24-5; e-ISBN: 978-83-68026-25-2.
102. Praca zbiorowa: Poradnik inżyniera spawalnictwa. Wydawnictwa Naukowo-Techniczne. Warszawa 1983.
103. Przybył B., Kabat M., Mikołajczyk J.: Wpływ prędkości drukowania 3D na dokładność zarysu kół zębatych. Obróbka Metalu; 2023, nr 4, s. 26-30,
p-ISSN: 2081-7002;
https://obrobkametalu.tech/media/2023/08/2023-4_Nr54_ObrobkaMetalu.pdf
104. Przybył B., Mikołajczyk J.: Efektywność technik przyrostowych. Obróbka Metalu; 2024, nr 1, s. 22-25, p-ISSN: 2081-7002;
https://obrobkametalu.tech/media/2024/03/2024_1_nr55_ObrobkaMetalu-1.pdf
105. Przybył B., Mikołajczyk J.: The influence of 3D printing speed on profile accuracy. **W:** Szkoła Logistyki 2024 / redakcja naukowa Janusz Zawiła-Niedźwiecki, Adam Płaczek. Radom: Instytut Naukowo-Wydawniczy "Spatium", 2024, Poland; s. 199-216, p-ISBN: 978-83-68026-07-8; e-ISBN: 978-83-68026-08-5.
106. Przybyłowicz P.: Mechanika techniczna. Wydawnictwo Politechniki Warszawskiej, Warszawa, 2012
107. Rutkowski A.: Części maszyn. Wydawnictwa Szkolne i Pedagogiczne, Warszawa, 1986.
108. Sądej I., Mikołajczyk J.: Machine tool compensation and mass unbalance measurements. **W:** Logistyka w ratownictwie 2024 / pod redakcją Andrzeja Chudzikiewicza i Andrzeja Krzyszkowskiego. Radom: Instytut Naukowo-Wydawniczy Spatium, 2024, Poland; s. 187-196, p-ISBN: 978-83-68026-24-5;
e-ISBN: 978-83-68026-25-2.
109. Siuta W.: Wytrzymałość materiałów. Wydawnictwa Szkolne i Pedagogiczne, Warszawa, 1954.
110. Styp-Rekowski M., Mikołajczyk J.: The influence of Mind M preparation on the lubricant properties of base oil SN-150. W**:** Reinung, Schmierung und Verschleiβ : forschung und praktische anwendungen : Band 1 : tribologische systeme schmierstoffe und schmierungstechnik zerspanungs : und umformtechnik prüfen, messen, kontrollieren / 53. Tribologie-Fachtagung. 24.bis 26. Septembet 2012 in Göttingen. Aachen : Gesellschaft für Tribologie e.V., 2012. p-ISBN: 978-3-00-039201-6.
111. Styp-Rekowski M., Mikołajczyk J.: Wpływ dodatku na własności smarowe oleju bazowego SN-150. Tribologia. 2012, vol. 244, No. 4, s. 227-232, p-ISSN: 0208-7774; e-ISSN: 1732-422X;
https://t.tribologia.eu/resources/html/article/details?id=167726
112. Styp-Rekowski M., Mikołajczyk J.: Wpływ preparatu eksploatacyjnego stanowiący kompleks węglowodorowy na zmianę własności smarnych oleju bazowego SN-150. W: Tribologia bliżej praktyki : XXXII Ogólnopolska Konferencja "Jesienna Szkoła Tribologiczna 2012". XXXII Ogólnopolska Konferencja "Jesienna Szkoła Tribologiczna 2012", Kudowa Zdrój, 18-21 września 2012r. Politechnika Wrocławska Wydział Mechaniczny, Instytut Konstrukcji Eksploatacji Maszyn, Polskie Towarzystwo Tribologiczne, Sekcja Podstaw Eksploatacji KBM PAN. Wrocław : Polskie Towarzystwo Tribologiczne, 2012

Functional changes to 3D printer

inż. Michał Seńko
Department of Mechanical Engineering
Stanisław Staszic State University of Applied Sciences in Piła, Poland
https://orcid.org/0009-0003-5648-5895
corresponding e-mail: michalsenko@wp.pl

Abstract:

This paper presents a project of modernizing a 3D printer and introducing functional changes. It consists of two parts: the first, a theoretical introduction to the project, and the second, presenting the practical implementation of the project. Further, this paper presents an analysis of the feasibility of implementing design changes to the 3D printer. Finally, the paper ends with a description and documentation of the design process for the laser head and engraving head, as well as functional testing and determining the performance characteristics of these print heads.

Key words: CNC machines, 3D printers, CNC machine programming

1. Introduction

The concept of sustainable development sets many requirements for contemporary technical projects in which particular attention is paid to the rational and economical management of raw materials and energy necessary to produce the product.
The global market for devices used in home applications such as 3D printers, laser cutters and CNC engravers is full of devices designed for only one purpose. A general analysis of these devices shows that they share many common design features and the same components are used in their production. Thanks to these features, it is possible to modernize a 3D printer with functional changes that broaden its scope of application. The advantages of using devices with extended functionality means, above all, reducing the consumption of raw materials. This applies to rare earth metals such as neodymium which is the main component of permanent magnets used in stepper motors. Equally important is the reduction of energy consumption necessary for the production of devices (instead of 3, produced is 1), as well as the reduction of costs of disposal of devices after their service life (instead of 3, disposed is 1). Additionally, there are lower costs of possible maintenance and repair (instead of 3, servicing needs 1), lower requirements for storage space in warehouses, and also at users' homes.

The project of modernizing a 3D printer with changes in functionality is a complex topic combining many fields of technology, with particular emphasis on mechanical engineering and electronics, designing in the Auto CAD environment and machine code programming. It is also a project with a wide scope of implementation, starting from acquiring the necessary knowledge about the subject of work, through the implementation of modernization projects, to practical testing of the implemented structural changes.

This paper aims at presenting the idea of building machines and devices that are based on similar technical solutions but can be modernized to be used for many applications.

The subject of this paper is the modernization of a 3D printer with functional changes enabling the use of additional print heads. It was planned to build a laser head intended for engraving and cutting with a laser beam, and a mechanical engraving head for removing material with micro-mills.

The aim of the paper is to modernize the structure of a 3D printer using minimal design changes to enable safe operation and proper functioning of all print heads.

Modernization of a 3D printer with functional changes was chosen as the topic of the paper because of possibility of integrating the theoretical knowledge and manual skills for machine construction in one project. Currently, the latest technologies for manufacturing consumer items, machine parts, and even entire components are additive technologies. A 3D printing technology is a very interesting example of this, showing a wide spectrum of applications from simple home applications to highly specialized ones in modern military and space technology. This technology already makes it possible to eliminate the need to carry a stock of necessary parts which can be printed on site at any time. This is especially important in space, where the cost of launching objects into space is extremely high. The possibility of expanding the functionality of 3D printers is the next step in the development of universal machines, so exploring such possibilities is a valuable experience. Gaining additional knowledge and experience in the construction and design of CNC machines can be very useful in further education and professional work.

The development of modern methods of manufacturing consumer items, spare parts and machine components through the use of numerically controlled machines creates

many new possibilities that expand the scope of their functionality. The additive manufacturing method, including 3D printing, is currently the technology which undergoes the greatest changes. Reviewing new 3D printing technologies and 3D printer designs is important for identifying new applications and increasing functionality. Therefore, there is a need to conduct appropriate research and specify conclusions in this regard.

The main goal put forward in the paper is to modernize the Creality CR10 printer with changes in functionality in the use of additional print heads.

The specific objectives are:

a) analyzing the design solutions of 3D printers,
b) designing a system for expanding the basic print head with interchangeable accessories in the form of a laser head and an engraving head,
c) preparation of technical documentation of the project,
d) conducting functionality tests of a 3D printer with extended functionality,
e) analyzing the possibilities of further development of the structure.

In order to achieve the assumed objectives, the following scope of work was planned:

a) analyzing the design of 3D printers,
b) designing structural changes to the 3D printer,
c) production of the necessary details and electronic systems enabling the mounting and control of the print heads,
d) testing the functional properties of individual print heads mounted on the 3D printer structure,
e) preparation of a detailed design documentation.

Two main methods are used in the manufacturing of consumer goods: the decremental method and the additive method, also known as the incremental method. The decremental method involves removing unnecessary elements, called allowance, from the material until the geometry assumed in the design is achieved. This method has been used since the dawn of human history to produce the necessary tools and weapons [76, 89, 124, 128, 129, 134, 135, 139]. Thanks to this method, primitive people used sharp-edged stone tools to remove successive layers of wood and thus produce spears, clubs, hammers and other objects necessary for life. Over the centuries, the decremental method has developed and evolved into modern types such as:

- machining,
- electrcal discharge machining,
- heat treatment,
- plastic working.

Machining is the removal of chips generated by using a tool equipped with cutting edges of an appropriate shape and hardness greater than the material itself. The main methods are: milling, turning, chiseling, drilling, grinding [43, 46, 99, 100, 101, 102, 120, 134] .

Electrical discharge machining of a material involves removing part of its volume using the erosion process, i.e. removing subsequent layers of material in the form of very small chips or spalls.

Heat treatment involves the use of high temperatures, which allows the metal to liquefy and be given the appropriate form, as well as changing its functional properties by affecting the internal structure of the material.

Plastic working is the application of force to metal, which gives permanent deformation of the material. This is possible thanks to the use of its properties related to plasticity, i.e. the ability to assume and retain the shape obtained after exceeding the elastic limit. Plastic working includes bending, cutting, and forging.

Additive manufacturing (3D printing) is the opposite of subtractive manufacturing. Instead of formatting an object from a large, unshaped element, the element is produced by adding successive layers [123]. The biggest advantage of additive manufacturing is the saving of material – it is not cut, as is the case with the subtractive method. Additive manufacturing (AM) is a relatively new method as its origins date back to the 1980s [97]. Currently, the following additive manufacturing methods are as follows:

- Extrusion,
- Photopolymerization,
- sintered powder method.

Additive manufacturing by thermoplastic extrusion begins with the thermoplastic being taken from a spool and then passed through a die where it is heated and melted. This allows the material to pass through the nozzle, allowing subsequent layers of the printed component to be formed. Then, cooling takes place and all layers merge – and the finished product is obtained.

Photopolymerization is an additive manufacturing method that uses UV resin, i.e.a light-curing material. The main technique classified as photopolymerization is SLA (stereolithography). The UV resin is placed in the tank, while the platform on which the desired component will be formed in the first phase of production is placed at the level of the resin tank. The laser system, together with lenses and mirrors, heats the resin which forms the first layer of the manufactured item. After its creation, the platform with the object being produced is lowered to a level equal to the thickness of the next layer and the whole process is repeated until we reach the object produced by the photopolymerization technique.

Additive manufacturing using sintered powders is a category of technologies that use metal or plastic in powder form and a laser or electron beam to form the powder into the desired object. The production process takes place in one of the powder containers where the platform is located. The powder is continuously replenished from the second powder container – this happens systematically as production progresses. The laser, as a heat source, fuses powder particles together, which, based on the design, create subsequent layers of the printed object.

The implementation of metal 3D printing shortens production time, speeds up the work of engineers, reduces material losses and enables the construction of durable metal structures with fewer welded joints. Metal 3D printing also allows to create complex and unique structures that were previously too time-consuming or impossible to produce.

Manufacturing products in the pre-Industrial Revolution era of the 18th century using hand tools was generally unproductive and imprecise, so new methods were sought that could eliminate these disadvantages. This solution was the use of mechanical machines, which contributed to a significant increase in accuracy, efficiency and scale of production. Initially, these were machines powered by a steam engine using transmission belts.

These were mostly drills, lathes, milling machines, slotting machines, saws and grinders. The accuracy of work performed on them was sufficient to produce spare parts but a big amount of work involved in their operation limited production efficiency and generated high costs. The next step in the development of production machines was the

use, at the end of the 19th century, of electric motors to drive them. These motors enabled better control of the spindle speed and more precise tool guidance. Thus, the electric drive contributed to reducing the dimensions of machine tools, simplifying their construction, and increasing the precision of the work performed [43, 46, 99, 100, 101, 102, 120].

As technology advanced, opportunities arose to automate machining processes. In the 1950s, the first numerically controlled (NC) machines were introduced which allowed the programming of tool and spindle movement sequences using special punched cards. This allowed operators to focus on supervising the machining process rather than manually guiding the tools. Further development occurred in the 1970s when the use of microprocessors and personal computers led to the development of computer numerical control technology, i.e. the creation of CNC lathes. CNC machine tools have enabled even greater precision and control over machining processes, making it possible to perform complex operations such as 3D machining and interpolation. Furthermore, the introduction of CAD/CAM systems allowed engineering designs to be directly converted into instructions for CNC machines, which significantly improved production processes. Currently, industrial machine tool technologies allow to carry out operations on multiple axes simultaneously, which enables to implement complex geometries and shortens processing times. Adaptive systems are being developed that enable machines to independently optimize machining processes based on data collected during operation. This allows machine tools to adapt to changing conditions and maintain a high quality of manufactured components. The emergence of 3D printing technology also led to the development of printers which evolved from simple three-axis printers to multi-axis machining centers [25].

The latest technological solution is the use of hybrid machines, i.e. combining a 3D printer and a CNC machine into one machining center. The hybrid 3D printing system uses the mechanical base of standard CNC machines. The print head is moved by the axes of the CNC machine. This allows the machine to be used normally in 3- and 5-axis operations such as milling, drilling, cutting, tapping, etc., while the extruder is in storage outside the work area. Adapting a CNC machine for 3D printing is done by hanging the print head next to the spindle or adding an additional print beam.

A CNC machine is a mechanized maneuvering tool that is controlled by a computer according to detailed input instructions. CNC is an abbreviation of the English phrase Computerized Numerical Control which means computer control of numerical devices. Instructions are delivered to the CNC machine in the form of a sequential program of machine control instructions such as G code and M code and then executed.
The main parts of a CNC machine are:

- Input/output devices: These are devices that are used to load the program of the machined part into the CNC machine. There are three commonly used input devices: punched tape reader, magnetic tape reader, SD card reader. Additionally, there is communication with the computer via USB and RS-232-C connectors.
- Central Processing Unit (CPU): It is the heart of the CNC machine. It performs all control activities of the CNC machine; CPU fulfills various functions:
  - reads the encoded instructions entered into it,
  - decodes the encoded instruction;
  - implements interpolation (linear, circular and helical) to generate axis travel commands;
  - transmits axis movement commands to the amplifier circuits that control axle mechanisms;

- receives position and speed feedback for each drive axle;

- performs auxiliary control functions such as turning the coolant or spindle on/off and changing tools.

- A CNC machine always has a sliding table and a spindle. The machine table is controlled in the X and Y axes direction and the spindle is controlled in the Z axis direction.
- Drive system: The drive system of a CNC machine consists of control circuits and stepper motors. The CPU transmits signals (i.e., positions and speeds) of each axis to the stepper motor controller circuits that position the machine table and spindle.
- Measurement system: This system consists of transducers that act as sensors. It contains position and speed transducers that continuously monitor the position and speed of the cutting tool at any given time. The CPU receives signals from these transducers and uses the difference between the reference and feedback signals to generate control signals to correct position and velocity errors.
- Information display unit: The monitor is used to display programs, commands and other useful CNC machine data.

Unlike a conventional machine tool, where the employee manually controls the machining process based on the technological process or manufacturing drawing, in a numerically controlled machine tool, the control system processes the appropriate control signals and controls the individual machine units. Each support is equipped with a motor with variable speed control. A similar solution is used to drive the machine tool spindle. Conventional machine tools most often use motors that provide a constant rotational speed, and the speed change is achieved via gearboxes. Dimensional accuracy in conventional machine tools is achieved by setting appropriate scales using handwheels. In numerically controlled machine tools used are position measurement systems which continuously read the position of the controlled unit. This information is transmitted as feedback to the control system and already during operation it allow to ensure the dimensional accuracy of the workpiece. The use of numerically controlled machines has many advantages over conventional machines:

- increased efficiency thanks to shorter machining time (concentration of machining on one machine, shortening the time of preparation and finishing),
- increased dimensional and shape accuracy (feedback to the control system, measurement with a resolution of 0.001 mm),
- geometric repeatability of manufactured items,
- increased production flexibility,
- operators can easily make changes and improvements and thus reduce delay times,
- possibility to produce complex designs with high accuracy in the shortest possible time,
- modern design software allows the designer to simulate the manufacturer of his idea. this eliminates the need to create a prototype or model and saves time and money,
- fewer workers are needed to operate a CNC machine, which reduces labor costs.

These advantages, as well as many other beneficial features, make numerically controlled machines increasingly popular in industry.

CNC machine programming involves creating a control program in the appropriate language and format on the required information medium. Such a program contains the information necessary to perform technological operations, processing or individual passes in the machining process. There are many different criteria for classifying CNC machine programming methods, but the most important one is the division based on the method of data processing. Therefore, a distinction is made between manual programming and automatic programming.

Manual programming involves directly creating a control program in a language and format adapted to a given CNC machine with a specific control system. Such a language is G-Code which in Poland is standardized by the ISO 6983 and DIN 66025 standards. In manual programming, the programmer/technologist, while performing the activities that make up the creation of the control program, directly uses the information that makes up the technological knowledge bases (manuals, material tables, technical and operational documentation of machine tools, tool catalogs, electronic tool databases, etc.) [25].

The control program called the **Technological Operation Program** is a set of instructions in the language and format required by the automatic control system. It is stored on a suitable medium to perform the intended actions by the automatic control system. Instructions in the control program determine the magnitudes and speeds of the shifts. The program may also contain subprograms which are fragments of the technological operation program. They are called for execution by appropriate control commands. Programs are divided into data blocks describing subsequent sequences of the machining process. The structure of the program provisions is presented in Table 1. The blocks, in turn, consist of **words**. The first block of data is called the header block and contains information about the name of the program or subprogram and a label identifying the type of data. The last data block is also characteristic - the final block - which necessarily contains an auxiliary function defining the end of the program (M 2 or M 3( )) or subprogram (M 17).

Table 1. Structure of the control program [25]

%_N_PROGRAM_MPF	Header block
N10 G90 G94 G71	Data block
N20 DI M3 S250	Data block
N30 GO X50 Z40	Data block
N40Gl X20 Z38 F200 ; WORKING MOVEMENT	Data block
…	…
N120 M30	Final block

Code words consist of a letter specifying its type, the so-called address, followed by a number specifying the value expressed by the word or the number of the function, subprogram, tool, parameter, etc. The address identifies the data contained in the word. How to edit the codeword address is shown in Table 2.

Table 2. Data block structure [25]

Data block								
N40	G1	X20		Z38		F200	OPERATIONS MOTION	
Word	Word	Word		Word		Word	Comment	
N	40	G	1	X	20	Z	38	….
Address	Numerical value	Address	Numerical value	Address	Numerical value	Address	Numerical value	

Words defined by address and numerical value define data specifying auxiliary and preparatory functions. The operation of these functions may vary depending on the activity and order of execution of the data block.
Depending on their activity, words can be divided into:

- modal words (inter-block) - these words remain active until another numerical value is written to the address of this word, e.g. the feed specified by the word **Fxx** remains active until its new value is entered.
- non-modal (block) words - these words are active only in a given block.

Non-modal words, depending on the order in which they are executed in the data block, can be further divided into:

- pre-block words - e.g. function M3 (enabling rotation in the positive direction) is executed before the execution of the remaining words in the block,
- post-block words - e.g. the M30 function (program stop) is executed after all words in the block have been executed.

Manual programming is very time-consuming and requires knowledge of how to properly edit individual lines of code. Even simple details can require hundreds or thousands of lines of code to work together flawlessly and achieve the intended result. Because G-Code works as a series of points and instructions line by line, it is possible to produce the same detail using different paths and instructions. They may depend, for example, on the type of machine tool, the number of axes, the type of tools, the material, etc. . The name G-Code is short for "geometric code", which is a record of simple, logical commands in the form of phrases starting with the letter G followed by a number. It is a command to change the geometry, e.g. "G00" is a rapid movement command. The Gcode instruction list contains several hundred items.

Automatic programming is characterized by two-stage data processing. In the first stage (processor), intermediate data is created which constitutes the input of the second stage (post-processor). Only at the post-processor stage, when intermediate data is adapted to a specific machine tool, the control program is created. In the processor stage, based on the source program or CAD (Computer Aided Design) model of the workpiece, geometric and technological calculations are performed, often using databases and automatic selection of cutting parameters. Source programs are created in a specific programming language (APT, EXAPT, GTJ,..), in which such a program is written using appropriate geometric and technological instructions. Source programs

can be processed in applications designed for a given language, which also enable interactive programming.

Automatic CAD/CAM programming requires the creation of a model of the workpiece in an appropriate CAD system. An example of such a system is Autodesk Fusion 360 software thanks to which it is possible to create a part model. The model thus created is imported into the CAM (Computer Aided Manufacturing) system. The next step is to import or automatically create a blank model and determine the geometry, in the form of machining features (e.g. pockets, punches), profiles and points, necessary for the automatic creation of tool paths. Creating tool paths comes down to selecting a specific tool and defining the appropriate machining cycle.

At this stage, in addition to the geometric calculations performed by the system, it is also possible to automatically select cutting parameters. Thanks to the program's extensive functions, it is also possible to quickly change the dimensions and shapes of the model and immediately update previously generated tool paths. The movement of these tools can be visualized to detect any possible collisions between the tool and the workpiece.

Modern computer-aided manufacturing (CAM) systems are characterized by great flexibility in the selection of machining cycles. Simultaneous virtual machining is also possible, which gives the machine greater security when the program is first run on a real CNC machine.

3D printing technology, as a relatively simple tool, is currently used in many industries, including aviation, automotive, clothing companies, medicine, and architecture. The widespread use of 3D printers results in their constant development and specialization depending on the industry in which they are used.

There are many types of 3D printers on the market, differing in purpose, printing technology, construction layout, and size. Despite the differences, all printers have common design features such as: computer control of the operation of components, frame construction, use of stepper motors, presence of a work table and print head. The construction of 3D printers includes, among others:

- DC power supplies are designed to power the computer control unit, stepper motors, as well as the heating elements of the work table and print head. Most often, the DC voltage is 12 or 24 [V], and the power, depending on the printer size, ranges from 300 [W] to several kW;
- the computer control unit for the operation of components manages the operation of all printer components, starting from loading the digital model of the printed object into the computer's memory, through monitoring all operating parameters, as well as communication with the device operator;
- the data input and output interface is a component that enables the user to communicate with the printer control system. It has connectors and sockets for connecting external memory or data transmission as well as control manipulators and screens displaying messages;
- the structural frame is the base for mounting all printer components. Frame structures can be open, made of aluminum profiles, or closed made of aluminum sheet or plastic. Closed frames are designed to protect the inside of the printer from dust, dirt and other contaminants. In addition, they maintain the proper temperature of printed objects, which has a significant impact on the quality of prints;
- guides are the elements on which the print head and the work table move using bearing rollers. These may be frame elements in the case of open frames or

separate linear guides intended solely for the movement of the head and work table;
- the work table is a component on which designed objects are printed. The table is heated to prevent material shrinkage and provide the model with greater stability;
- stepper motors provide drive for the head, extruder and the work table surface. The stepper motor is characterized by the ability to perform very precise rotations and can also, on the basis of feedback, maintain a constant position in response to the applied mechanical load on the rotor shaft;
- the extruder is a filament extruder that takes the appropriate amount of filament and then transports it to the head. There it is heated to the appropriate temperature, obtaining a liquid form that allows printing of any models;
- the print head is responsible for melting the filament supplied by the extruder and for forcing it out through the nozzle. the head is equipped with heat sinks and fans that regulate the filament heating temperature so that the filament does not heat up too quickly, which could lead to nozzle clogging.

3D printers are devices capable of printing three-dimensional objects according to special designs created in specialized computer programs. Templates for printed items can be created independently or, for example, downloaded from the Internet. The process of printing a 3D object is carried out by applying multiple layers of material, which, after hardening, retain the desired shape and have properties typical of the material used.

Currently, there are 5 basic 3D printing technologies:
- Fused Filament Fabrication (FFF)
- Selective Laser Sintering (SLS)
- Stereolithography (SLA)
- Direct Metal Laser Sintering (DMLS)
- PolyJet

Fused Filament Fabrication (FFF) technology is one of the oldest and most widespread additive technologies in the world. This method involves laying down successive layers of melted material, allowing adjacent layers to cool and bond together before applying the next layer. One of the biggest advantages of FDM is a quick adjustment of the infill of 3D printed models. This means it is very easy to print a prototype just to check fitting and finish. With a low internal filling, or even empty, you save on material costs. Once the design phase is complete, final checks can be carried out or small and medium production runs can be launched with the target infills of a given 3D print.

Selective Laser Sintering technology involves joining polyamide molecules together using a high-energy laser beam. This process begins by filling the chamber with powder material. As printing progresses, the build surface goes down and a new layer of powder is added. The sintering of the polyamide powder is carried out precisely layer by layer. The 3D SLS technology does not require the use of supports because the created models are naturally supported by excess loose material tightly surrounding the print. The above relationship makes it possible to produce geometrically complex elements that maintain high dimensional accuracy, greater than when using other 3D printing methods.

Stereolithography technology is a 3D printing technique using liquid photopolymer resin. Stereolithography is a precision 3D printing technology where the model material is hardened with an ultraviolet (UV) laser beam to create the target geometry. The material needed for SLA printing, i.e. liquid resin, is stored in a tub into which a work table is immersed, which is then spot-illuminated (in places where the model is to be created) by a UV laser. Curing of the resin by exposure is repeated until the finished part is obtained which is then rinsed with isopropyl alcohol to remove any uncured photopolymer. After cleaning, the print goes to a specialized imagesetter where it acquires its final properties.

Direct Metal Laser Sintering is a technology that uses a high-power laser in the 3D printing process to weld metals and alloys on a micro scale. The main applications of DMLS include the production of metal parts with complex geometry. Parts produced after the 3D printing process are fully functional (heat-resistant, strong and durable). These parts are usually better than cast parts in terms of density and therefore their mechanical properties. This technology has enormous advantages over traditional production techniques. Eeven complex objects can be manufactured in a single production cycle, thus reducing production costs. Combined with topological analysis, it enables the production of lighter parts compared to conventional manufacturing methods. Metal parts manufactured using DMLS technology are exceptionally durable and have a high strength-to-weight ratio. Usually used are High strength materials such as 316L tool steel, aluminum alloy, titanium, or Inconel (a nickel-chromium alloy).

PolyJet technology is one of the most precise 3D printing technologies. The operating principle is similar to SLA technology, as it is based on the curing of liquid resin, with the difference that photopolymer resins are cured with UV lamp light. A single printing layer in this technology is only 0.016 mm thick (less than the thickness of a human hair). The accuracy of this technology is unattainable with any other additive technology. PolyJet technology, due to the use of resins with different properties, especially mechanical properties, and a soluble support material, is well suited for the production of precise elements where there is no room for large deviations. It is dedicated to rapid prototyping and creating final prototypes of high quality and smooth surfaces.

Programming a 3D printer requires having a three-dimensional model of the object that will then be printed, previously designed in an IT environment. For this purpose, specialized 3D modeling software is used, such as: T-Wings 3D, Blender, 3DCrafter, 3ds Max, Netfabb or AutoCAD software such as: Autodesk Fusion 360, Solid Edge or Free CAD. 3D printing requires saving the object in the standard STL format.

3D object models can be designed independently, and can also be obtained as ready-made STL files from numerous websites. Ready-made models can be obtained from online portals such as Thingiverse, Cults, GrabCAD, Fab 365, Yeggi or My Mini Factory. The proper process of programming a 3D printer is to use slicer programs to "cut" the 3D object model into thin slices (layers) and position them in three-dimensional space.

The most popular programs for generating Gcode for commercial printers include Cura, Ultimaker, Prusa Slicer, Bambu Studio, ChiTuBox, Luchee, and many others. Industrial printers have special software that is dedicated to the machines manufactured by companies.

Thanks to this software, machine operators can influence many factors occurring during printing. The temperature of the printing nozzle and the work table can be adjusted, the printing speed can be set and additional supports can be used to stabilize the printed element. Other parameters can be changed, such as the height of the printed

layer, the type and density of the infill, and the number of embossed layers. These parameters vary depending on the filament materials used for printing, as well as the type of 3D object designed and how it is set up for printing.

2. Analysis of the possibilities of upgrading the functionality of the Creality CR 10 3D printer

The Creality CR10 printer shown in Fig. 1 is a printer working in the FDM (Fused Deposition Modeling) printing technology, commonly called "3D printing from plastic", as well as the FFF technology, which stands for Fused Filament Fabrication (depositing of melted material). It has a modular structure in which the control module is separated as an independent unit, and the executive module is a structure screwed together from T-slot aluminum profiles. It has a print head with a heating element that reaches a temperature of 300°C. The work platform on which the print is created is also heated and can reach a temperature of 110°C. The temperature of the print head and platform can be adjusted, depending on the filament material, by the control unit. Two fans reaching a speed of 12,000 [rpm] are used to cool the print. The movement of the guides is carried out by means of rubber wheels with ball bearings with a low coefficient of friction, which is only 0.04.

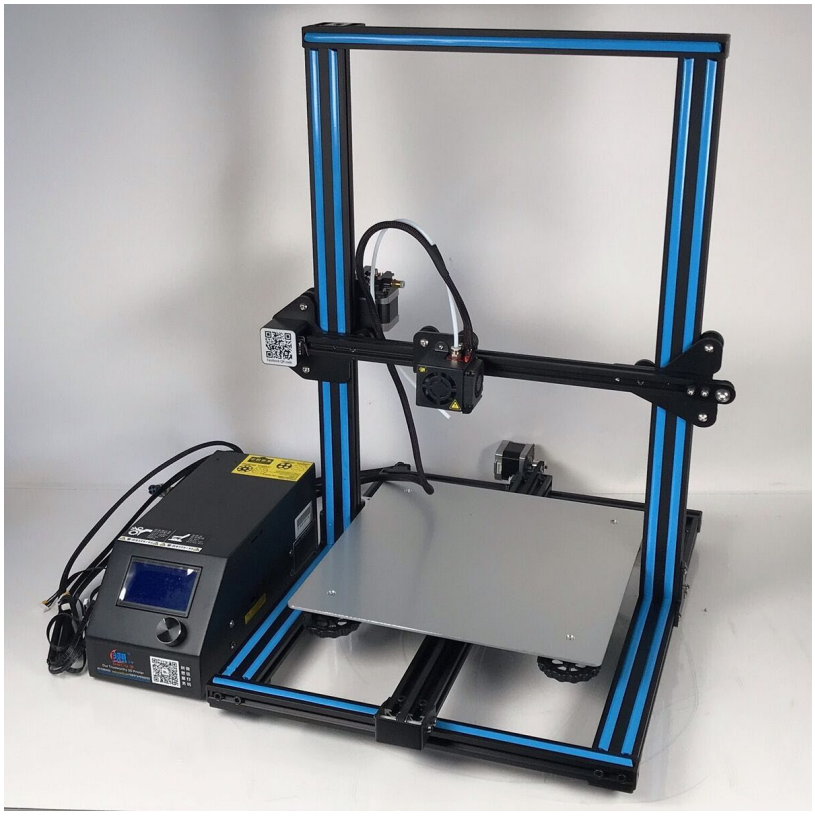

Fig. 1. Creality CR10 3D printer

The drive of the print head in the X, Y, Z axes is provided by three JK 42HS40 stepper motors. The drive from motors is transmitted via toothed belts. The extruder drive is also implemented using a JK 42HS40 stepper motor. The main component of the Creality CR10 printer is the CNC control motherboard based on the 32-bit ARM STM32 F103 microcomputer and integrated stepper motor controllers for the X, Y, Z

working axes and the extruder drive. The view of the motherboard and the arrangement of individual components is shown in Fig. 2. The board also includes: micro SD memory port and type 2 USB port. Additionally, the motherboard has outputs for controlling fans and inputs for signals from limit switches.

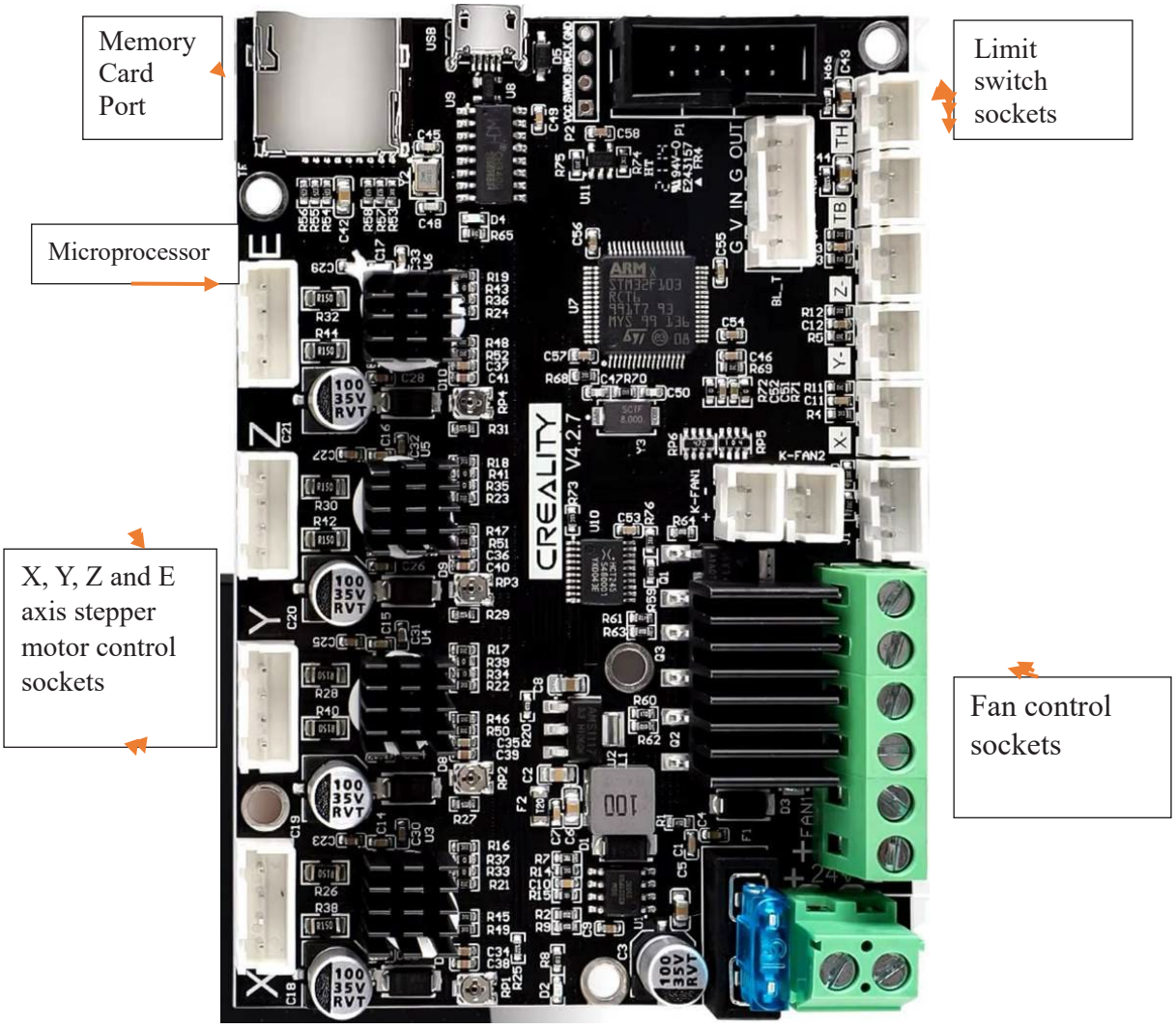

Fig. 2. Creality CR10 Printer Motherboard

The element responsible for powering the individual components is the Creality CMS 350-24C2 power supply with a power of 350 [W], voltage of 12 [V] and a maximum current of 14.5 [A]. Its appearance is presented in Fig. 3 which shows the connection strip and the cooling fan.

Fig. 3. Creality CR 10 3D Printer Power Supply

Table 3. Creality CR 10 Printer Specifications

No.	Item	Description
1.	Working field	300x300x400 [mm]
2.	X-axis movement range	300 [mm]
3.	Y-axis movement range	300 [mm]
4.	Z-axis movement range	400 [mm]
5.	Device power	260 [W]
6.	Filament diameter	1.75 [mm]
7.	Maximum head temperature	300 °C
8.	Maximum platform temperature	110 °C
9.	Print speed	600 [mm/s]
10.	Filament extrusion force	65 [N]
11.	Supply voltage	230 [V]
12.	Printer dimensions	600x510x610 [mm]
13.	Weight	9 [kg]

Stepper motors perform rotary motion in specific, precise steps. Each electrical pulse causes the motor to rotate one step. This enables precise positioning of mechanical elements. The Creality CR 10 printer uses four JK 42HS40 motors. The technical data of the engine are presented in Table 4, and its view is illustrated in Fig. 4.

Fig. 4. JK 42HS40 stepper motor

Table 4. JK 42HS40 motor specifications

No.	Item	Data
1.	Resolution:	200 steps/rev (1.8° per step)
2.	Current consumption per coil:	0.5 A
3.	Nominal voltage:	12 V
4.	Holding torque:	4.4 kg·cm (0.43 Nm)
5.	Coil resistance:	24 Ω
6.	Winding inductance:	36 mH
7.	Shaft diameter:	5 mm
8.	Type of shaft:	round
9.	Dimensions:	42 x 42 x 40 mm
10.	Weight:	280 g

The heating element control signals are routed from the central unit outside the housing via GX16 quick connectors, while the motor control signals are routed directly to the connectors on the stepper motors. The limit switches are also connected directly to the controller motherboard.

The Creality CR 10 printer can be programmed manually or automatically using specialized software. In manual mode, due to the time-consuming nature of programming, only simple geometric bodies can be programmed by editing the G code using a regular text editor such as Word or specialized editors such as Brackets, Visual Studio Code, Notepad++ and similar ones. This involves designing single solid layers with a height of 0.2 mm. Depending on the size of the block, there may be from several hundred to several thousand such layers, so it is a very labor-intensive and complicated process. To design complex solid shapes one needs solid design software such as Autodesk Fusjon 360, Autodesk Inventor, Solid Works or FreeCAD.

After designing the shape, a 3D printing preparation process called slicing should be used. This involves "slicing" the designed solid into layers 0.2 mm high. Such functions are available in programs such as AutoCAD, as well as specialized programs that are used exclusively for operating 3D printers. These include programs like Creality Print, UltiMaker Cura, PrusaSlicer and many others. These programs not only cut solids into layers but also set printing parameters such as filament type, nozzle temperature, bed temperature, print speed and density. There are many more parameters for determining print quality and they include, among others, the degree of print cooling, the idle speed of the head, the provision of supports to stabilize the printed block, and the increase of adhesion of the table on which the block is printed. These programs have the ability to simulate and visualize the print from a single print layer to its entirety. The visualization of the generated print head movement paths is presented in Fig. 5.

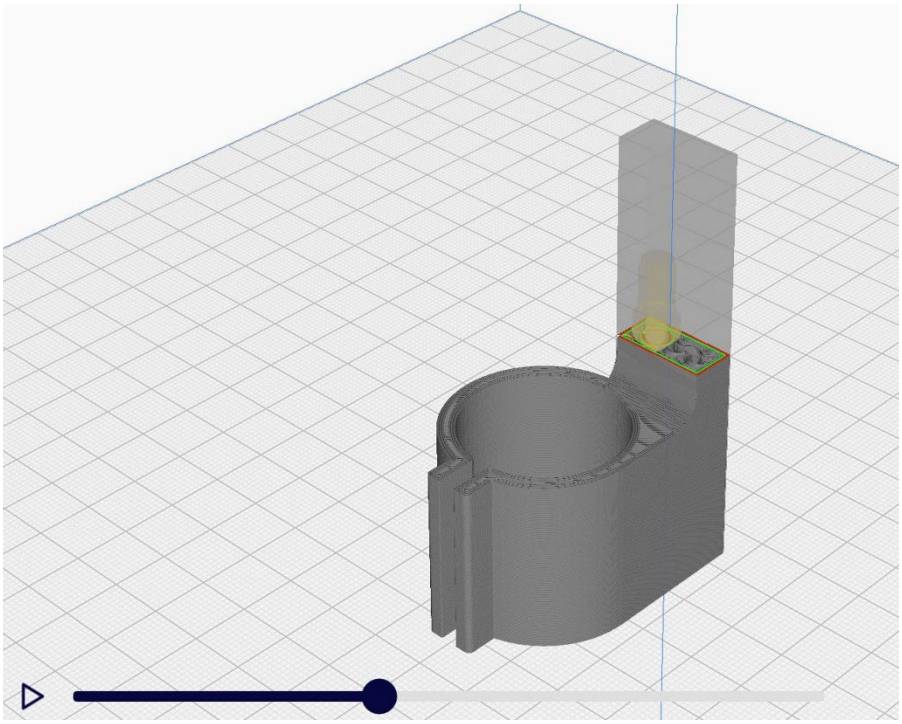

Fig. 5. 3D printing simulation in UltiMaker Cura

In order to test the Creality CR10 3D printer for the possibility of expanding its functionality with additional working modules, the "reverse engineering" method was used. For this purpose, the control module was disassembled and then the electronic components and their connection to the working module were identified. The interior view of the control module is shown in Fig. 6.

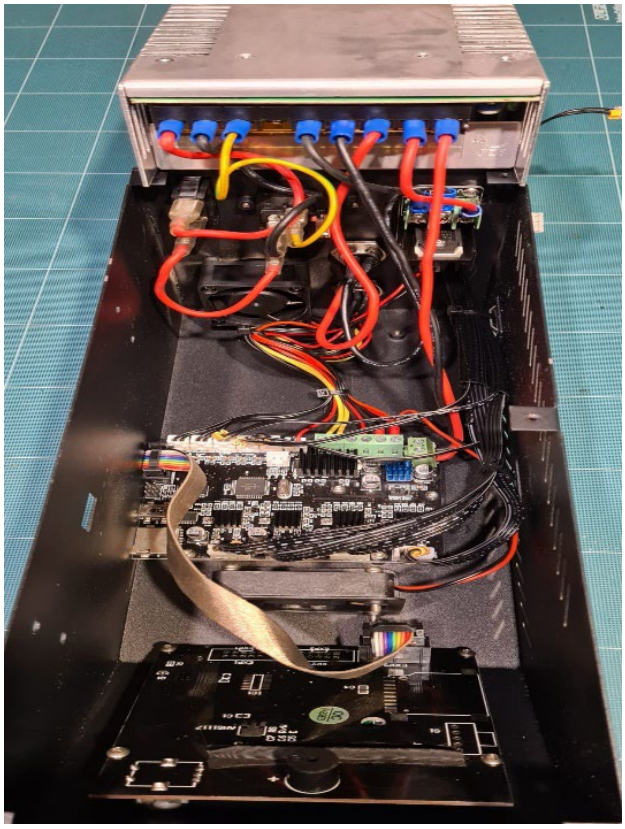

Fig. 6. Control module after disassembly

It was established that the X, Y, Z axes control channels as well as the extruder stepper motor together with the limit switches of these channels are connected to the controller motherboard via JST-XH type connectors. From the motherboard, the control channel wires run through a hole in the rear of the housing to the individual stepper motors and limit switches. It was then determined that the power cables for the printing nozzle heating elements were connected to the electronic quick connector type GX16 No. 1. The cables controlling the fans installed in the print head are connected to the same connector. The wiring arrangement in the GX16 connector is shown in Fig. 7.

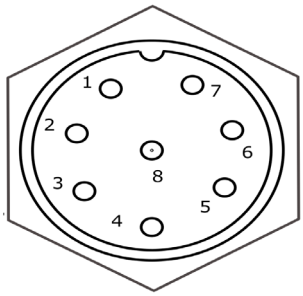

Fig. 7. Wiring connection system in the GX16 connector socket No. 1

As a result of examining the layout of connectors and the cable routing, the method of connecting the motherboard with GX16 connectors was determined, and the results are presented in Table 5.

Table 5. Description of the GX16 type quick connector socket No. 1

Pin No.	Description	Wire color	Comments
1	Plus power supply to the printing nozzle heating element	red	+12 V
2	Print nozzle heating element power supply mass	red	-12 V
3	Print nozzle temperature sensor	white	Digital system
4	Print nozzle temperature sensor	white	Digital system
5	Plus power supply for fan No. 1	red	+12 V without modulation
6	Fan No. 1 weight	black	- 12 V without modulation
7	Plus power supply for fan No. 2	red	+12 V PWM modulation
8	Fan No. 2 weight	black	- 12 V PWM modulation

The heating cables of the working plate and the temperature sensor of this plate are connected to the GX16 No. 2 quick connector. The wiring arrangement in the GX16 connector is shown in Fig. 8, and the description of the connections is presented in Table 6.

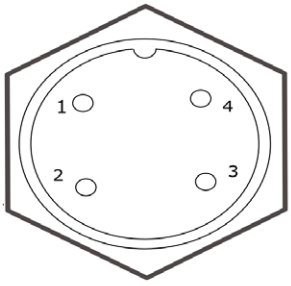

Fig. 8. Wiring connection system in the GX16 quick connector socket No. 2

Table 6. Description of the GX16 type quick connector socket No. 2

Pin No.	Description	Color of the wire	Comments
1	Plus power supply for the work table heating element	red	+12 V
2	Power supply mass of the work table heating element	black	-12 V
3	Work table temperature sensor	white	Digital system
4	Work table temperature sensor	white	Digital system

Next, the arrangement of components on the rear wall of the control module housing was checked and measurements were taken to find convenient places for mounting additional GX16 quick connectors. These quick connectors could be installed as detachable elements of cables which, in the factory version, are permanently connected to the working module. It was determined that it was possible to safely and permanently place four additional GX16 quick connectors on the rear wall of the control module housing as shown in Fig. 9.

Fig. 9. Hole layout for additional GX16 quick connectors

The last element of the testing was to determine the parameters of the signal controlling the power of fans cooling the printout. These parameters are important due to the possibility of using the fan power control channel to power and control the laser module and potentially other working modules. The Metex M3850 universal meter and the FNIRSI-1014D oscilloscope [121] were used for the test according to the diagram shown in Fig. 10.

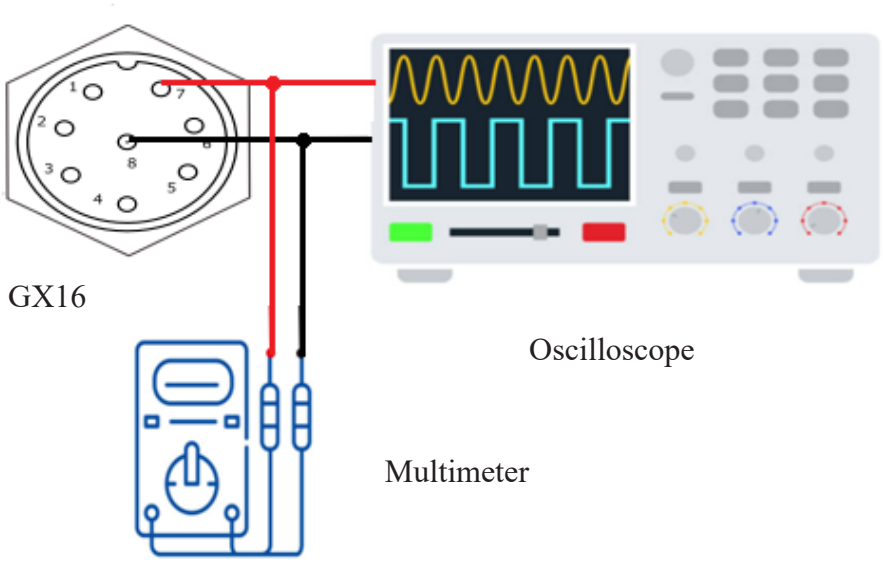

Fig. 10. Diagram of the measuring system for the power supply of fan No. 2

The fan power is controlled via software or manually via the printer interface in the "Control" directory. The power level can be adjusted using the knob on a scale from 0 to 255. The measurement results are presented in Table 7.

Table 7. Fan No. 2 control voltage measurement results

Measurement No.	Power level	Voltage value read [V]
1	0	0.12
2	50	3.3
3	100	5.4
4	150	7.6
5	200	10.1
6	255	12.3

After examining the voltages, the shape of the signal controlling the operation of fan No. 2 was checked using an oscilloscope. The shape of the examined signal shows that it is a PWM (pulse-width modulation) signal. The course of the tested signal is shown in Fig. 11.

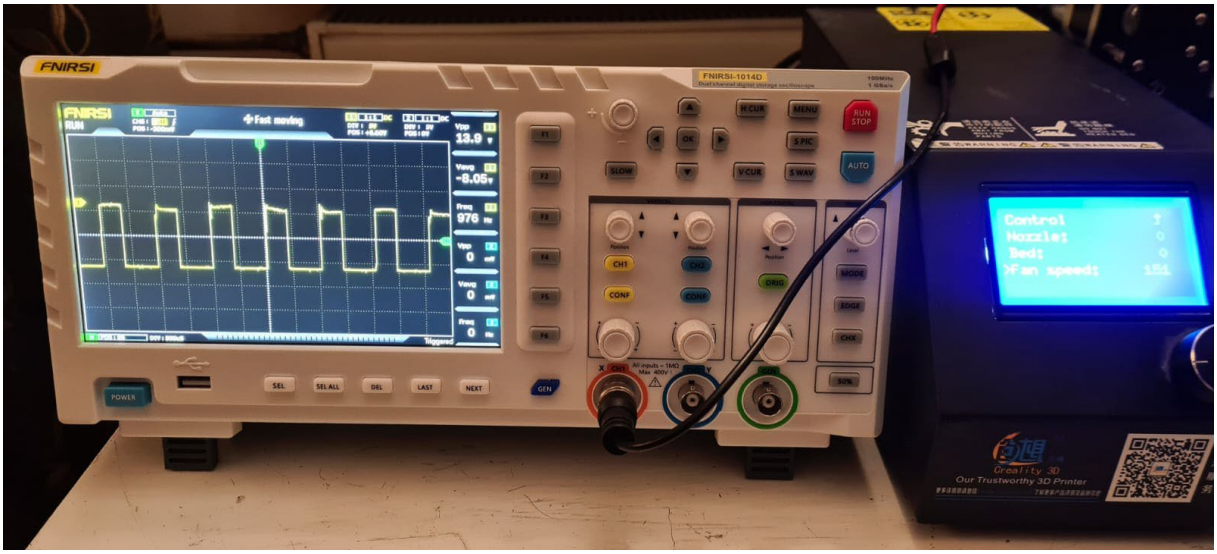

Fig. 11. The waveform of the signal controlling fan No. 2

The inspection, measurements and analyses of components of the Creality CR10 3D printer led us to draw the following conclusions:

1. The arrangement of elements on the control module housing allows of the creation of space for additional GX16 quick connectors which enable the separation of the control module from the printer's working module. This modification will allow the control module to be used with other designed CNC machines, e.g. a plasma cutter for metal or a thermal cutter for polystyrene. Additionally, it will be possible to more easily move printer modules, e.g. to other rooms.
2. The use of additional print heads requires the design and manufacture of a new mounting bracket to which these heads will be screwed.
3. It is possible to control the power of other working modules by using the power control channel of the print cooling fans. The limitation in this case is the need to adapt additional working modules for the control voltage of 12 [V] and the shape of the PWM control signal.
4. The implementation of design changes should be graded in terms of the complexity of the problems that need to be solved. The following sequence was adopted for implementation:
   a) design and manufacture of a mounting bracket for working modules,
   b) separation of the control module from the working module by using GX16 quick connectors,
   c) design and manufacture of the laser head,
   d) design and manufacture of the engraving head,
5. Any changes must be made with particular caution due to the high voltages supplying the printer, as well as the possibility of damaging sensitive electronic components, e.g. by short circuit or touching with an ungrounded tool or hand.

Based on the literature studied regarding CNC machines, as well as the conclusions from the analysis of the possibilities of expanding the functionality of the Creality CR10 printer, the following modifications were planned:

- separation of the control module from the printer's operating module by using GX16 type electrical quick connectors on the connections of the printer's power and control cables,
- making a new bracket for mounting the printer's print heads,
- manufacturing of the laser head,
- making the engraving head.

The order in which design changes are implemented results from the adopted principle of grading the complexity of projects from simple to more complex.

To increase the scope of use of the control module for other CNC machines and its mobility when moving to other places, GX 16 quick connectors were used. All power and control cables have been cut and re-soldered to GX 16 quick-connect sockets and plugs. In order to avoid incorrect connection sequence, before assembly the correctness and proper order of soldered wires were checked with a multimeter. The control module housing has four additional holes with a diameter of 16 mm intended for mounting GX 16 quick-connect sockets. The location of the holes for installing GX 16 quick connectors is shown in Fig. 12.

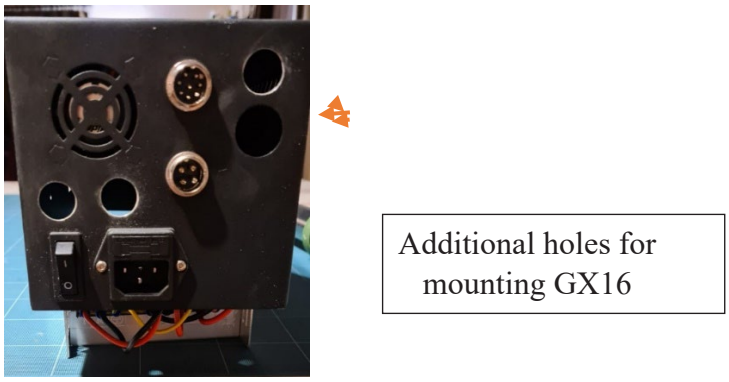

Fig. 12. Additional holes made for mounting GX16 sockets

Drilling holes for quick connectors was done with particular care to avoid possible short circuits in electronic systems caused by chips generated during drilling. The inside of the housing was dusted and visually inspected using a magnifying glass. The method and location for mounting additional GX16 quick connector sockets are shown in Fig. 13.

Fig. 13. Location of additional GX16 quick-connect sockets

After mounting and connecting the plugs, the correct operation of the printer was checked by performing a control 3D print. The produced cube with a side length of 10 mm showed that the Creality CR10 printer did not change its properties, and the cube mapping parameters were correct in all working axes X, Y, Z.

Analysis of the construction of Creality CR10 printer's working module showed that the printhead mounting bracket is too small to accommodate additional printheads. To make a new bracket, the original bracket was disassembled and then dimensioned. Based on the obtained dimensions, the design was carried out using Autodesk Fusion 360 software [29, 35, 36, 37, 45]. This program was used to design the support structure as shown in Fig. 14, and then a technical drawing was prepared according to the dimensions shown in Fig. 15.

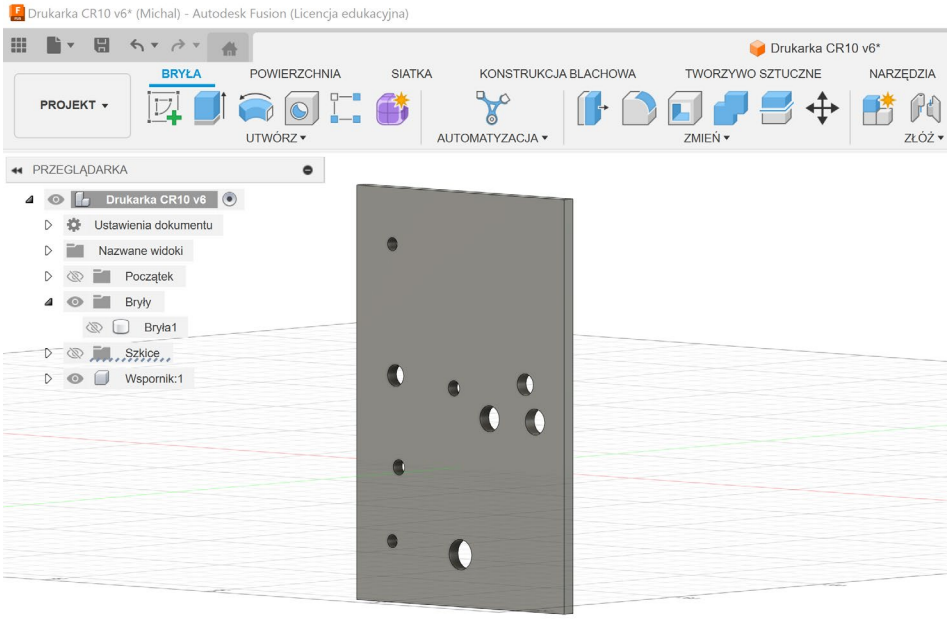

Fig. 14. Design of the mounting bracket for print heads

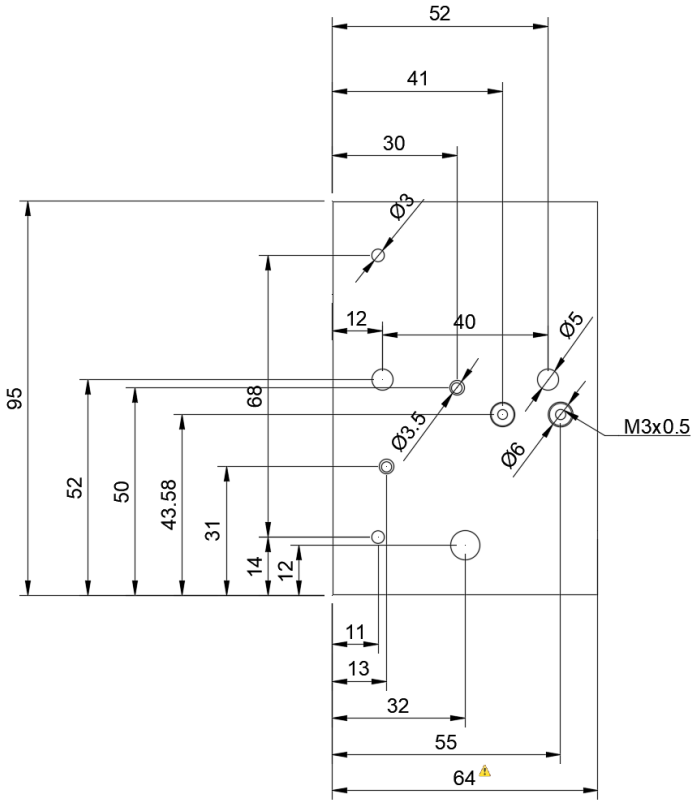

Fig. 15. Dimensions of the new printer workhead mounting bracket

The mounting bracket is made of PA6 aluminum on a milling and drilling machine equipped with a DRO (Dynamic Rotation Offset) measuring system. Digital Readout is a digital reading system which is used to indicate the position of the cutting tool relative to the workpiece. This was due to the need to precisely make holes and threads. Shifting or skewing the hole patterns could affect the accuracy of prints made with Creality CR10 printer. After manufacturing and installing a new mounting bracket and the printer's printhead, the correct printing was checked again, with particular attention paid to any possible collisions with other parts of the printer. No such collisions were found and the control print was performed correctly.

{0><}0{>The laser head was designed based on the Neje 20 diode laser.<0} It is a diode laser with blue light of 450 nm wavelength and diode power of 6 W. It is mounted directly to the mounting bracket on the left side of the printhead at a height of 3mm above the print nozzle of the Creality CR 10 printer. The method of attaching the laser to the bracket is shown in Fig. 16.

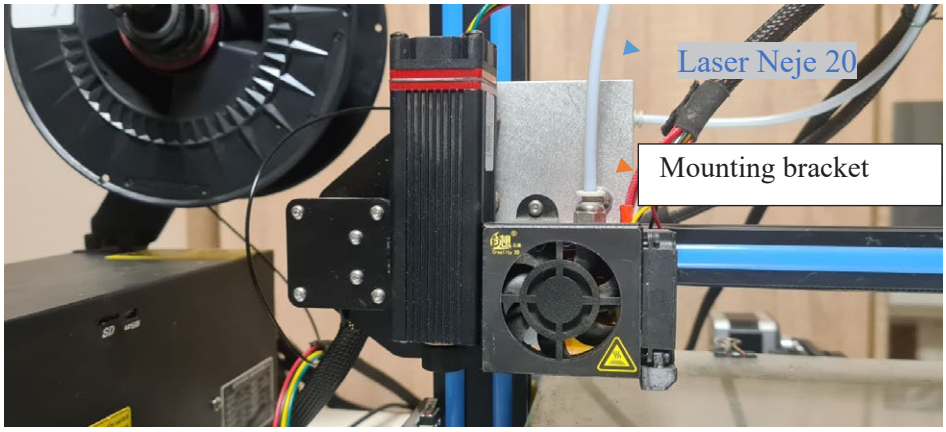

Fig. 16. Neje 20 laser installation method

After installing the laser module, tests were carried out on the movements of the printer's print head to detect any possible collisions with other printer components. No such collisions were observed, so the next step was to design and implement the laser power supply and develop a method of controlling its power. The Neje 20 laser module is powered by 12 [V] and consumes a maximum power of 20 [W]. It is controlled by a PWM signal with a voltage of 5 [V]. To control the laser power, it was decided to use the control channel of the 3D print cooling fans. The Creality CR10 printer control module has a control channel that can regulate the receiver power by specifying its level in the control program in values from 0 to 255. Whereas power 0 means the receiver is completely turned off, and 255 means full power. The problem in this case was the control voltage, which is 12 [V], while the laser module requires a voltage of 5 [V]. In order to adjust the voltage, a simple voltage divider was made according to the diagram in Fig. 17.

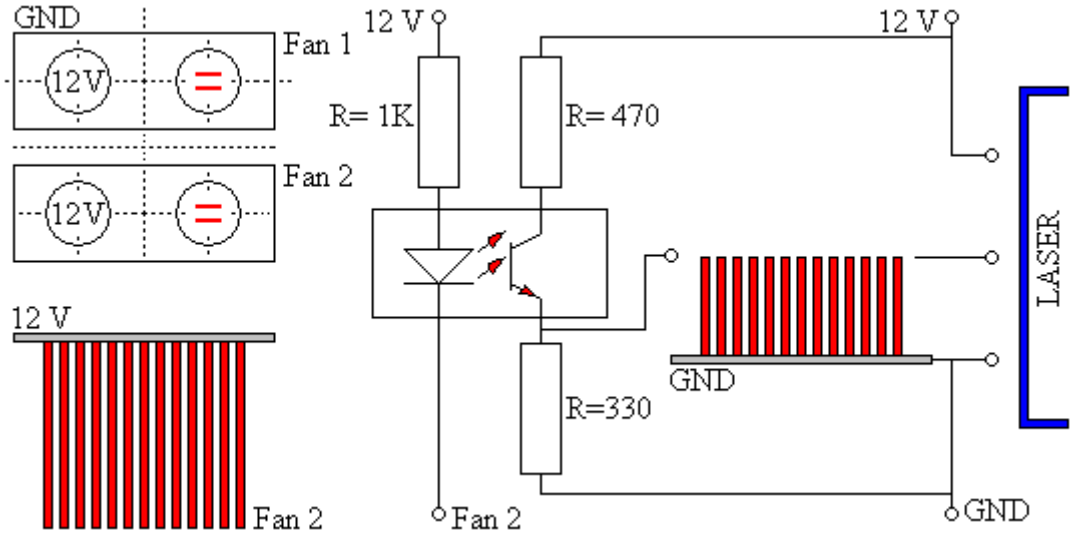

Fig. 17. Voltage divider that reduces the PWM signal voltage from 12 [V] to 5 [V]

Then, a PCB (Printed Circuit Board) prototype board was designed according to the diagram and manufactured using the etching method in an iron trichloride solution.

After soldering the electronic components, measurements were carried out using a multimeter and an oscilloscope to check the compliance of the designed voltages and the shape of the laser control signal. The course and magnitude of the control signals are presented in Fig. 18.

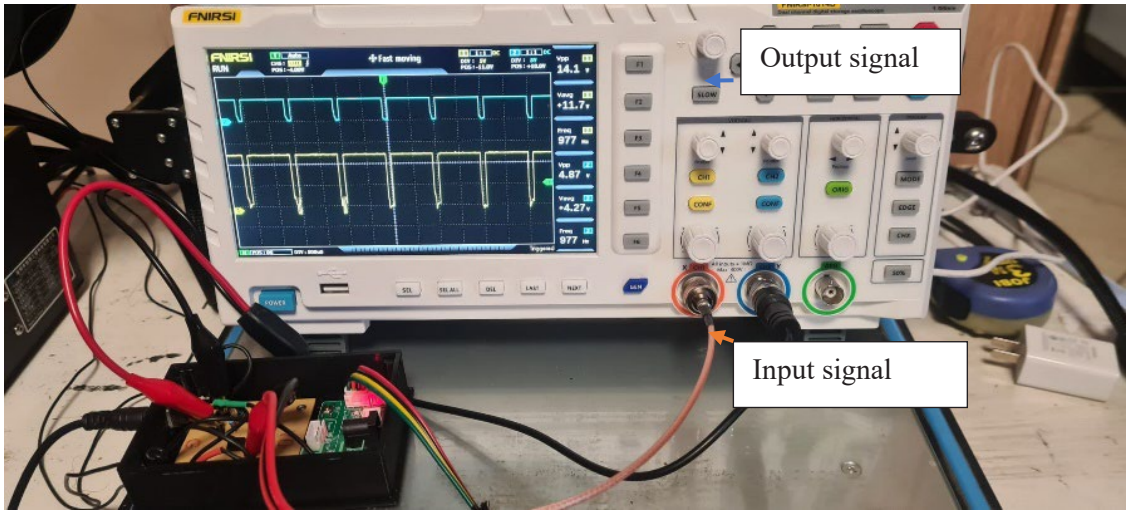

Fig. 18. Oscilloscope measurement of the shape of the laser power control signal

Correct measurement results allowed to make first attempts to connect the Creality CR10 printer control module to the laser module. In this case, the control signal was connected to pins 6 and 7 of the GX16 quick connector of channel E, which controls the supply of filament to the printing nozzle. This solution was used due to the lack of space for installing an additional GX16 quick connector. The laser is powered by a separate 12V 5A power supply to separate the direct connection of the control module from the laser module. This separation is made using a PC 817 optical coupler system, which protects the control module main board against possible overvoltages or short circuits. The system was assembled and installed in a separate housing as shown in Fig. 19.

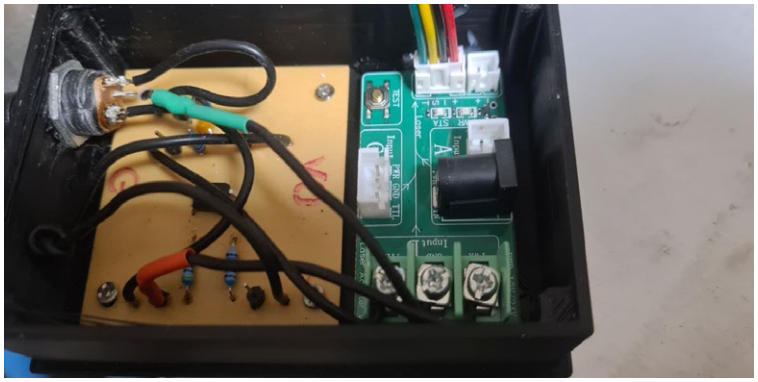

Fig. 19. PWM signal voltage reduction system with laser driver

The engraving head design consists of a brushless direct-current motor (BLDC) and an ER8 milling chuck mounted on its shaft. The whole thing is powered by a 12[V] DC power supply. The NEEBRC 2838 motor is attached to the mounting bracket using a holder (Fig. 20) which was designed in Autodesk Fusion 360 software and then printed with a Creality CR10 printer. The technical data and operating parameters of the NEEBRC 2838 motor are presented in Table 8. In order to increase the stiffness of the

holder, a carbon tube with a diameter of 4 [mm] was glued into its core. The printing material was PLA filament which is a polymer from the group of aliphatic polyesters. It is a biodegradable material made from, among others, corn meal. It is characterized by low processing shrinkage and simple use, making it one of the easiest materials for 3D print.

Table 8. NEEBRC 2838 Motor Specifications

Supply voltage	Maximum current	Power	Maximum revs	No-load current	Number of rotor fields
<16 [V]	35 [A]	600 [W]	50000 [rpm]	2.7 [A]	4

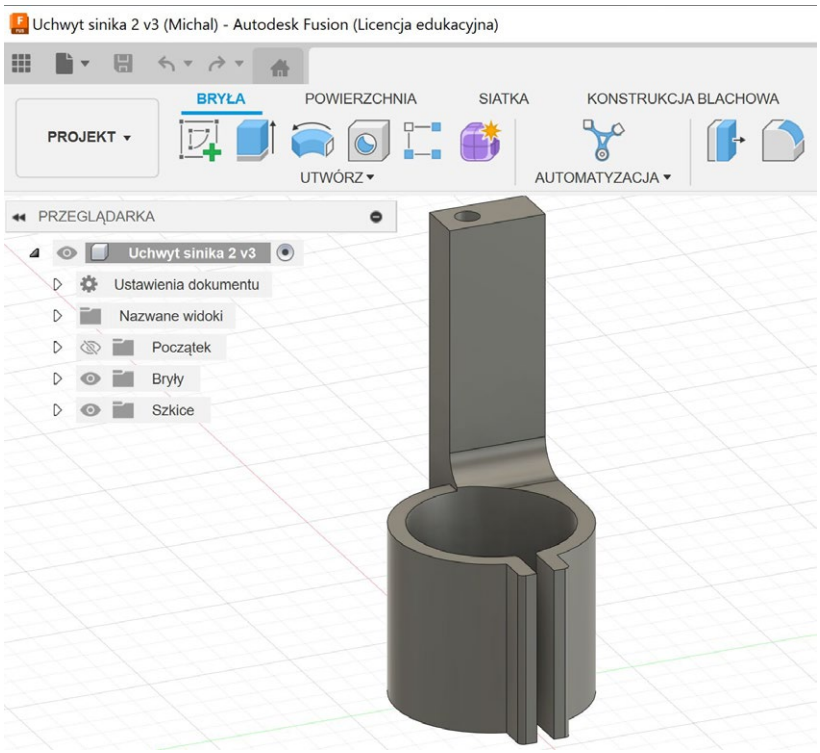

Fig. 20. Engraving head motor holder design

After printing the holder and mounting it in the mounting bracket, the printer's operation in the workspace was checked, with particular attention paid to any possible collisions of the mounted holder with other parts of the printer. After confirming there was no collision, the engraving head motor with the ER 8 milling chuck was mounted in the mounting bracket.

The method of mounting the engraving head on the mounting bracket is shown in Fig. 21.

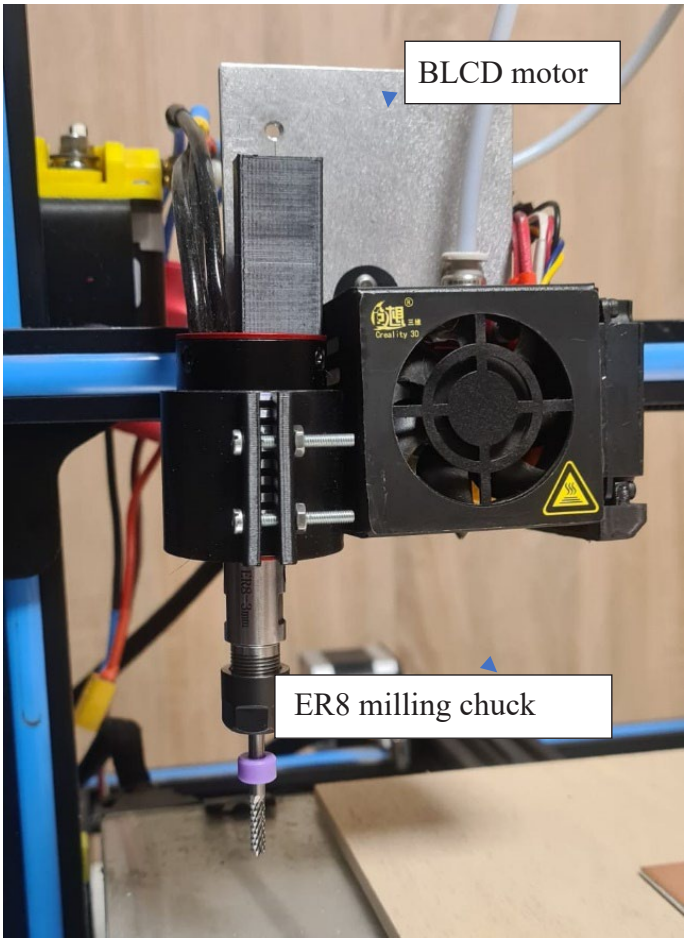

Fig. 21. Creality CR10 Printer Engraving Head

After assembling everything, the printer was checked again for proper operation. No collisions between individual components were detected and, as a result, connected to the motor was a 12 V DC power supply with a current of 5 A connected to the motor speed governor. The speed governor is controlled by a 12V PWM signal, so in this case there was no need to adjust the control and power supply voltages of the motor. The final test was to start up the 3D printer with the engraving head and observe any possible structural problems that could affect the proper operation of the whole thing. The system worked correctly and was suitable for further testing.

In order to verify the correct operation and determine the functional characteristics of individual print heads extending the functionality of the Creality CR10 3D printer, the following tests were planned:

- determining the dimensions of the work space;
- measuring the amount of energy consumed by individual heads and the entire device;
- determining the accuracy of the execution of programmed projects.

Originally, the Creality CR10 3D printer has a build work table with dimensions of 310 x 310 [mm], however, the workspace has the following dimensions: X axis=300 mm, Y axis=300 mm, Z axis=400 mm. Since the individual work modules are mounted on the side of the main work module of the printer, their workspace is different. In terms of power supply for working modules, the tests covered the power consumption from an external power supply with a voltage of 12 [V] and a maximum current of 5 [A], as well as the total power consumption of the entire device. In order to compare the accuracy of

work performed by individual heads, it was planned to have measurements of dimensions of geometric figures such as: a square 60x60 [mm], a circle with a diameter of 60 mm and an equilateral triangle with a side of 60 mm.

The laser head is designed to cut soft materials such as: paper, cardboard, textiles, PCF foil or polyester foam, as well as for engraving graphics on harder materials. Such materials may be: wood, plywood, polycarbonate or aluminum. It is planned that office clips will be used to mount objects on the work table in the case of thin materials and double-sided adhesive tape or hot glue in the case of thicker materials.

To determine the working space of the laser head, measurements were taken using the internal software of the Creality CR10 printer control module. After setting the "AUTO HOME" position, i.e. the absolute zero position for each axis (X=0, Y=0, Z=0), the activated laser was moved to the minimum and maximum positions using the knob. A 5 mm margin of the printer's work table dimensions was maintained. The following coordinates of the individual working axes were determined:

- X from 50 to 304 [mm]
- Y from 10 to 305 [mm]
- Z from 0 to 370 [mm]

Based on the measurements, the maximum dimensions in the X-Y axes were determined to be 254 x 295 [mm], and in the X-Z axes 254 x 350 [mm]. When determining the height of the Z axis, a height of 20 mm was subtracted, which is necessary to properly focus the laser beam on the cut object. Fig. 22 presents the principle of focusing the laser beam and the need to determine a smaller maximum height of the working space.

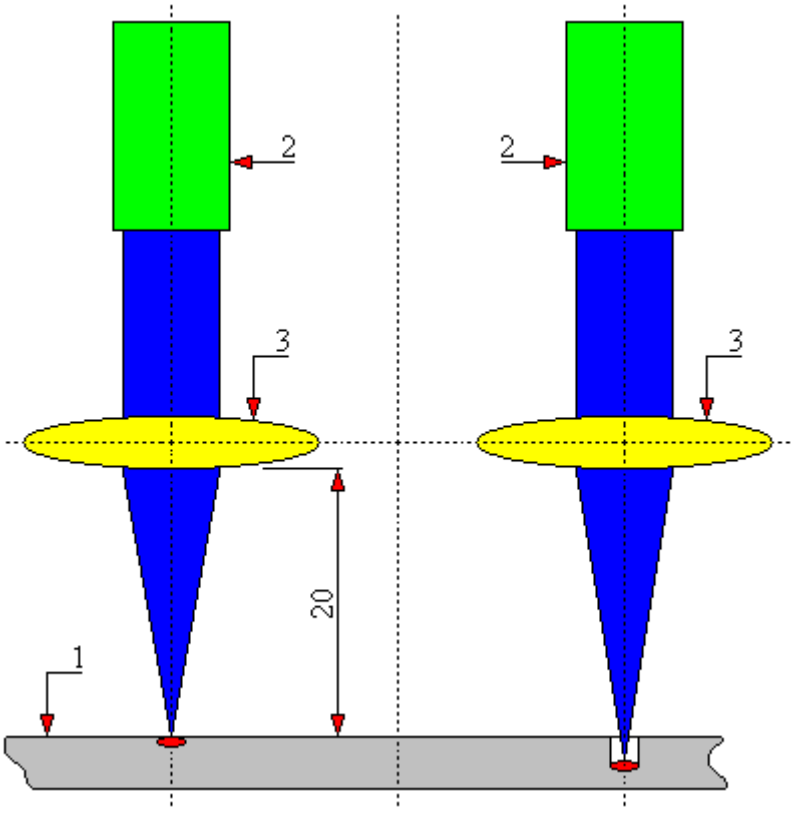

Fig. 22. Height of the laser lens above the material being cut
1 – etched material; 2 – laser; 3 – lens

The calculated maximum dimensions of the cuboid that can be mounted in this case are: width 254 mm, depth 295 mm and height 350 mm. The limitation is the weight which cannot exceed 0.5 kg.

The method of determining the laser head position parameters in the individual working axes X, Y, Z is shown in Fig. 23.

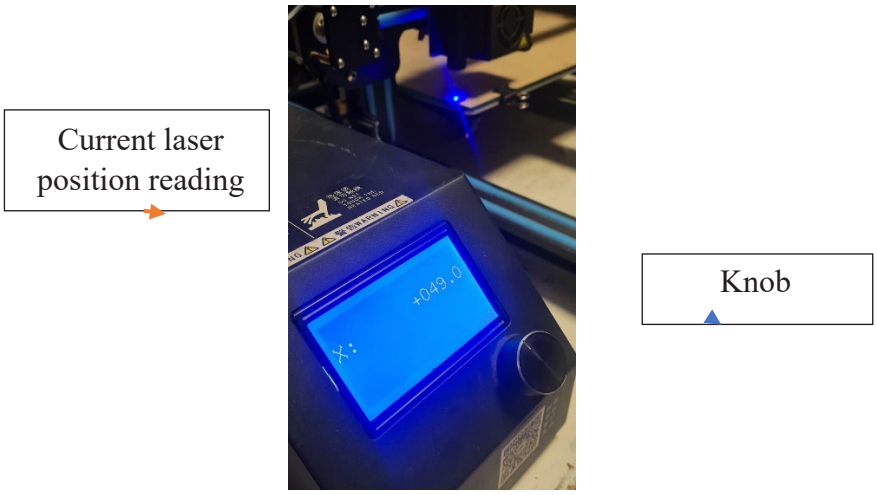

Fig. 23. Determining the minimum X-axis value that allows the laser to work on the work table

The power consumption of the printer with a laser head was measured using an MFC Technology E 246 meter, and the results are summarized in Table 9.

.

Table 9. Power consumption measurement results for the Creality CR10 laser printer

No.	Printer operation type	Read value [W]
1.	Printer no-load running without laser	10.6
2.	Laser no-load running without a printer	0.8
3.	Laser printer 25% power	31.5
4.	Laser printer 50% power	36.5
5.	Laser printer 75% power	41.4
6.	Laser printer 100% power	46.6

Then the accuracy of the laser head was measured. For the test purposes, drawings of simple geometric figures were designed with Inkscape, along with dimensions and the text "LASER TEST". The test was performed on a 3 mm thick MDF board using the following laser power: 25%, 50%, 75% and 100%. In each case the figures were made according to the design. The lines were straight without breaks in their continuity and the angles without distortions. The circle was made while

maintaining its full shape without any distortions, e.g. oval type. Line visibility was good when using 25% laser power, and very good at 50%, 75% and 100% power. The measurements taken showed that dimensions of figures were 0.5 mm smaller than those designed. This is probably caused by the Inkscape software used to generate the Gcode which is not a professional software like e.g. Autodesk Fusion 360, but it is free software (unpaid). The letters of the text were also etched without distortions or breaks in the line continuity. The quality of the etched figures and inscriptions is illustrated in Fig. 24 and Fig. 25.

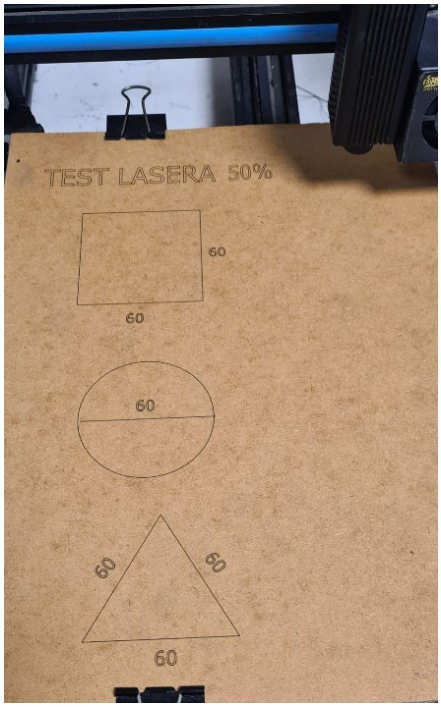

Fig. 24. Laser test at 50% power

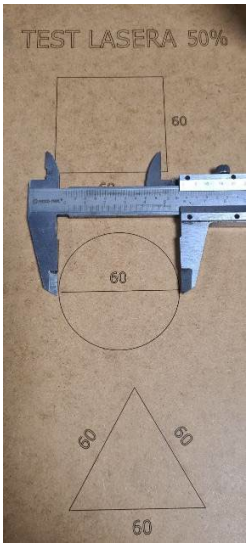

Fig. 25. Measurement of the accuracy of geometric figures

The next test was an attempt to cut a 3 mm thick MDF board with a laser beam. It was made using a hand-designed program that cut 10 mm squares successively using

multiple passes of the laser beam. Etching involved applying a number of laser passes equal to the sequence number of the square being cut. Square No. 1 was cut with a single pass, square No. 2 was cut twice, square No. 3 three times, and so on until square No. 7, which was etched with seven passes of the laser beam. To etch through an MDF board, 7 laser passes were needed, while for a 2 mm thick pine board, 3 passes were enough. A comparison of the cutting capacity of different materials is shown in Fig. 26.

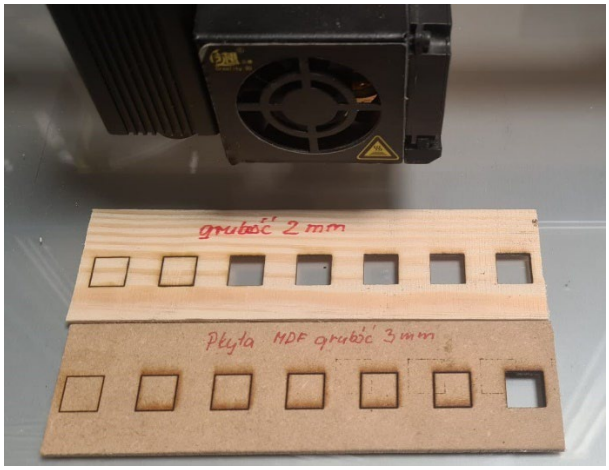

Fig. 26. A comparison of the cutting capacity of different materials

Then, tested were functional and operational features of the engraving head. The engraving head is designed for engraving and milling in soft materials such as: wood, plastic, aluminum and brass. The specific purpose of the head is to mill tracks in prototype boards for mounting electronic components. For mounting them on the work table, an additional holder with clamps was designed to ensure a stable position of the board.

To determine the working space of the engraving head, measurements were made using the same method as for the laser head. A 5 mm margin of the printer's work table dimensions was maintained. Following the reading, the coordinates of the individual working axes were determined:

- X from 55 to 305 [mm]
- Y from 25 to 305 [mm]
- Z from 0 to 370 [mm]

The maximum working space calculated based on the measurements is: width 250 mm, depth 280 mm and height 370 mm.

The power consumption of the 3D printer with an engraving head was measured using an MFC Technology E 246 meter, and the results are summarized in the Table 10.

Table 10. Power consumption measurement results of the printer with an engraving head

No.	Printer operation type	Read value
1.	Printer no-load running without engraving head	10.6 [W]
2.	No-load running of the engraving head without a printer	4 [W]
3.	Working under load of the printer and head	22.4 [W]
4.	Working under load of the engraving head	9 [W]
5.	Total consumption of the unit under load	31.4 [W]

During the measurements, minor vibrations of the spindle were observed. These vibrations were dependent on the spindle speed. In order to determine the optimal speed of the engraving head spindle, the speed at which the module vibrations were the lowest was set using a regulator. Next, the set speed was measured using a DT-2234C tachometer. The optimal speed was determined to be 12,500 rpm. During the tests, the temperature of the engraving head motor housing and the bracket attaching it to the print head were measured. Measurements showed that there was no risk of deformation of the plastic bracket securing the motor because after 30 minutes of continuous operation under load the motor temperature rose from 27.3°C to 30.5°C, and the plastic temperature rose from 25.6°C to 27.8°C. The PLA filament from which the bracket was printed has a thermal resistance of 65°C and is sufficient for this application. The measurements were performed with a GM 320 digital infrared thermometer. The measurement method and the place of the highest temperature marked with a laser spot are shown in Fig. 27.

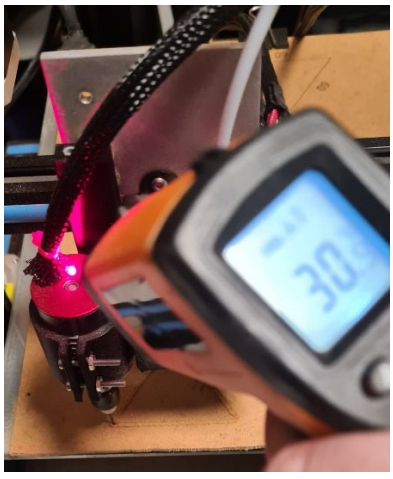

Fig. 27. Measuring the temperature of the milling machine motor

To measure the accuracy and quality of engraved designs, a system of geometric figures was used, the same as in the case of the laser head. The test was performed on a 3 mm thick MDF board using a 1 mm diameter shell end mill, and the milling depth

was set at 0.4 mm. The quality of the first test engraving on MDF board is shown in Fig. 28.

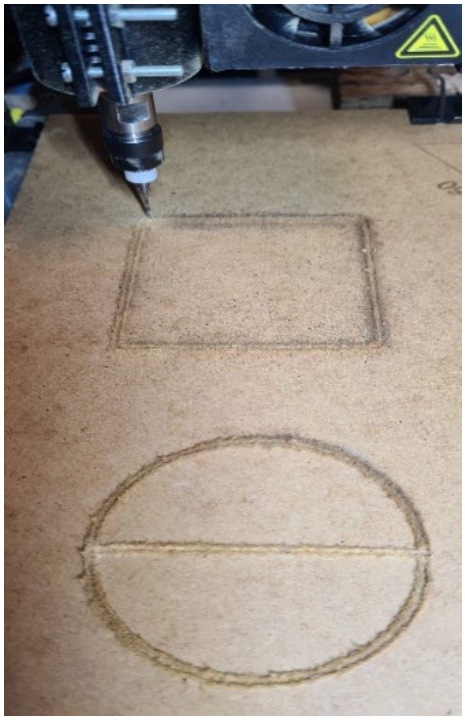

Fig. 28. Quality of engraving with a Ø1mm cutter

The overall shapes of the designed geometric figures were executed correctly but the edges were uneven and jagged. This made it impossible to measure the geometry of the figures, so a second test was carried out using a Ø 2 mm milling cutter. In this case, the edges of the figures were sharp and allowed measurements to be taken. Measurements showed that the dimensions of the square and circle were smaller than those set in the Inkscape program. Instead of a side length of 60 mm, a square with a side length of 57 mm was obtained. This difference occurred despite declaring the correct diameter (2 mm) of the cutter in the program settings. The same difference in dimensions occurred in the design of the circle whose assumed diameter was 60 mm, but the actual diameter obtained was 57 mm. In order to determine the cause of the discrepancy, a new test was manually programmed in the Gcode editor, taking into account the diameter of the cutter. The dimensions of the square and circle obtained differed by +0.1 mm from the assumed 60 mm, so it seems that in the previous test the fault lay with the Inkscape program. The geometry of the figures and the clarity of the engraving with a 2 mm diameter cutter are shown in Fig. 29.

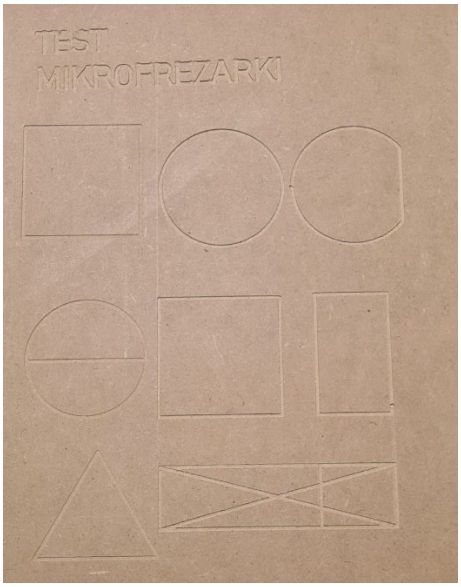

Fig. 29. Engraving head test for the accuracy of geometric figures

Another test conducted with the engraving head was to cut a 120 mm diameter circle from a 3 mm thick MDF board using a Ø3 mm cutter. For this purpose, the editor was manually programmed to produce a circle with a radius of 60 mm in six passes with the cutter's penetration into the material of 0.5 mm each. After executing the program, it turned out that the circle had not been cut out, so another pass was added to the program with a cutter depth of 0.2 mm. The final result of cutting with a milling cutter is shown in Fig. 30.

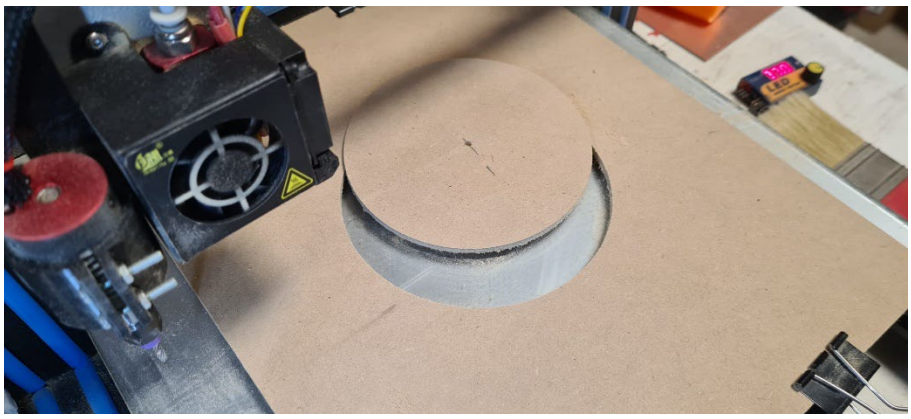

Fig. 30. Final result of cutting with an engraving head cutter

Following this procedure, the circle was cut out correctly. The shape of the wheel was very well made, and the edges of the wheel and the hole were sharp, with no burrs or tears in the material. The total cutting time using the engraving head of the programmed wheel was 32 minutes.

An additional test was conducted involving the milling of soft metals such as copper. In this case, for the purpose of testing, used was a laminate with a copper layer used in the construction of backplanes for electronic circuits. Several tests were carried out experimenting with the selection of parameters for milling depth, cutter speed and shape, as well as the working feed rate of the head. The results of the first tests are

presented in Fig. 31 which shows milling imperfections such as incomplete milling of tracks and local copper tearing.

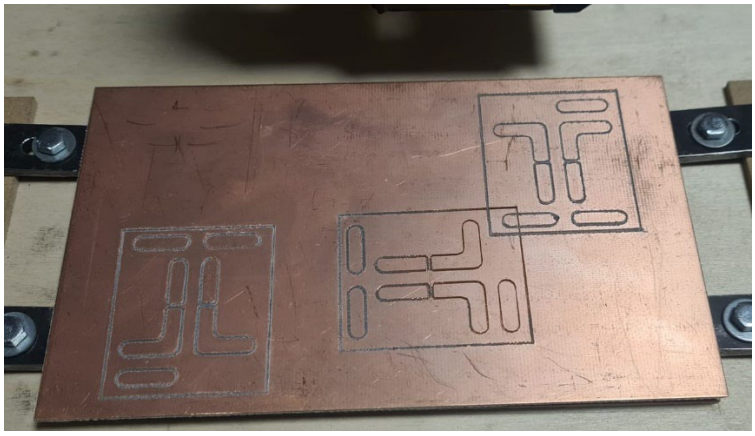

Fig. 31. Tests of milling electronic tracks on a PCB board

After gaining experience, it was determined that the best parameters for milling PCB tracks are with a milling depth of 0.08 mm at a milling speed of 12,000 rpm and a working feed of 80 mm/min. Additionally, an attempt was made to drill holes for electronic components. In this case, a drilling feed rate of 10 mm/min was used with positive results. Fig. 32 shows correctly milled electronic tracks as well as holes drilled with an engraving head with a 0.8 mm diameter drill.

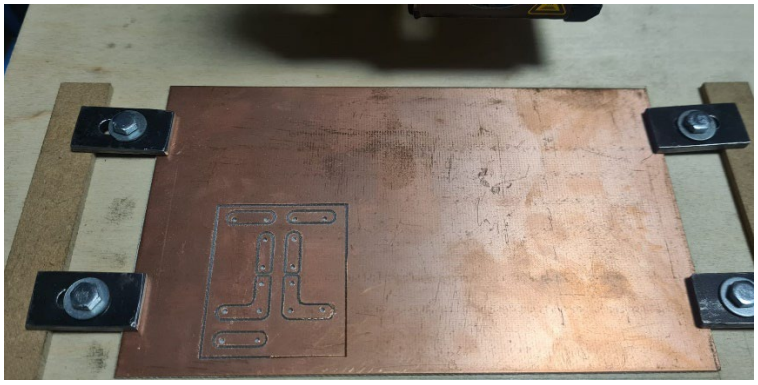

Fig. 32. A PCB with milled tracks and drilled holes for mounting electronic components

3. Conclusion

1. The main goal presented in the paper was to modernize the Creality CR10 printer to include changes in functionality in the scope of using additional print heads. This goal was achieved in full because two additional print heads were designed and built, which confirmed their functionality during testing. The laser head correctly performs the work programmed for it. It has the ability to etch with laser and cut soft materials, executing the program with high accuracy and speed. The engraving head also executes programs correctly with high accuracy but given the lightweight construction of the Creality CR10 printer frame, it does so only with a sufficient speed. It can engrave on materials that are harder than the laser head. In addition,

it can be used to precisely cut wood and soft metals with a milling cutter. It should be emphasized that the operation of additional heads does not adversely affect the quality of the main print head.

2. Analysis of the project's implementation leads to the conclusion that the adopted assumptions and plans were developed at a good level. Proper selection of working methods made it possible to carry out structural changes to the printer safely and without failure. No printer components or additional print heads used were damaged during work on the project. The risk of such damage was high because the structural changes involved interference with the printer's electronic components.

3. The examination of workspace available for additional print heads showed that it was only slightly smaller than the workspace required for 3D printing. Originally, it presents a hypothetical cuboid with dimensions in individual working axes: X=300, Y=300, Z=400 [mm]. The working space for additional heads is:
   a) laser head - X= 254, Y=295, Z=350 [mm],
   b) engraving head - X= 250, Y=280, Z=370 [mm],
   The workspace of the upgraded Creality CR10 printer is significantly larger in the Z axis range than that available in similar devices available for sale.

4. In terms of measuring the power consumed by individual print heads, it was found to be at a low level, amounting to 46.6 W for the laser head and 34.4 W for the engraving head, respectively. Power of additionally consumed electricity does not significantly burden the performance of the internal power supply of the Creality CR10 printer, which is 350 W.

5. The general conclusion from the accuracy test of the print heads is that there are discrepancies between the dimensions declared in the automatic software and those actually obtained in the tools' operation. For the laser head, this error was 0.5 mm, and for the engraving head, it was 3 mm. This error is probably due to the fact that the Inkscape program parameters do not take into account the diameter of the cutter used, despite this diameter being declared in the code editor settings. This hypothesis is confirmed by the fact that dimensional accuracy of 0.1 mm was achieved for jobs programmed manually using the Gcode editor, taking into account the diameter of the cutter used.

The design work was performed using Auto CAD software, and the actual production of the parts was carried out using a 3D printer, a milling and drilling machine, and tools for soldering electronic components. When analyzing the results achieved with individual devices, it should be emphasized that additional print heads have practical applications especially for home and hobby uses. The laser head is a particularly useful device because it has many applications, especially in tasks requiring high accuracy and speed. This module can be used to engrave various objects at very high speeds. Thanks to a big possible working height of the module on the Z axis, engraving can be performed on high objects, which is not possible with popular low-cost laser engravers. In addition, it can be used to cut foil, foam, plastic, and soft wood at high speeds. These features of the device may be useful in model making or other hobby fields. The disadvantage of the device is that it produces a large amount of smoke which can be unpleasant for people in closed rooms.

The engraving head proved to be the most complex design requiring special attention. This was because of the need to find lightweight components that would not place too much strain on the mechanics of the Creality CR10 printer, while at the same time guaranteeing precision in operation. Therefore, a lightweight model motor and an ER 8 micro milling chuck were used. In addition to having no face run-out, this motor must ensure a high rotational speed of several thousand revolutions per minute, which is necessary for the operation of milling cutters. An additional problem was to ensure durable mechanics that would guarantee tool stability when the milled material experienced resistance. During the first tests, the originally designed motor holder was broken, so a carbon tube reinforcement was used to provide adequate rigidity and strength. The engraving head can be used for engraving soft materials such as plastic, wood, plywood, aluminum, or brass. It can be used to mill these materials and cut out various elements with high precision. In addition, it can be used to make prototype boards for use in electronics projects. The disadvantage of the device is its relatively slow operation and the dust generated during milling.

The completed project is a prototype and it may be improved and developed to include other functions. The next step in modernization could be the design of a thermal cutter module for polystyrene foam and extruded polystyrene, which could be used to cut out letters and shapes for artistic or modeling projects. Another possible modification is to use the 3D printer control module for a separate CNC machine such as a plasma metal cutter.

Finally, it is worth adding that the best solution is to have two 3D printers. Why? Converting a 3D printer from a laser head to an engraving head or vice versa is both difficult and time-consuming. If we want to work with both of these tools at the same time it is necessary to have two 3D printers. Preferably identical ones, then it would be easier to use them. And the third 3D printer would be useful for 3D printing.

4. Literature

1. Azarow A. S.: Mechanizacja i automatyzacja obróbki skrawaniem. Państwowe Wydawnictwo Techniczne, Warszawa, 1957 r.
2. Adamczak S.: Pomiary geometryczne powierzchni. Zarysy kształtu, falistości i chropowatości. Wydawnictwa Naukowo-Techniczne, Warszawa, 2008 r.
3. Brodowicz W.: Skrawanie i narzędzia, cz. I i II. Wydawnictwa Szkolne i Pedagogiczne. Warszawa, 1975.
4. Brzozowski D., Wieczorowski M., Gapiński B.: Pomiar geometrii i ocena powierzchni narzędzi za pomocą mikroskopu różnicowania ogniskowego. Mechanik 11/2017, s. 1020÷1022.
5. Dietrych J. i inni: Podstawy konstrukcji maszyn. Wydawnictwa Naukowo-Techniczne, Warszawa, 1968 r.
6. Dobrowolski Z.: Podręcznik spawalnictwa. Wydawnictwo WNT, Warszawa 1978.
7. Dobrzański T.: Poradnik konstruktora. Przyrządy i uchwyty obróbkowe. Wydawnictwa Naukowo-Techniczne, Warszawa, 1964 r.
8. Dobrzański T.: Uchwyty obróbkowe. Wydawnictwa Naukowo-Techniczne, Warszawa, 1967 r.
9. Dudik K.: Poradnik tokarza. Wydawnictwa Naukowo-Techniczne, Warszawa, 1958 r.

10. Domański A., Mikołajczyk J.: Dimensional analysis of the selected type of rolling bearing depending on the manufacturer. **W:** Szkoła Logistyki 2023 / redakcja naukowa Janusz Zawiła-Niedźwiecki, Katarzyna Białczak. Radom: Instytut Naukowo-Wydawniczy "Spatium", 2023, Poland; s. 79-89, p-ISBN: 978-83-67033-75-6; e-ISBN: 978-83-67033-58-9.
11. Galon M., Mikołajczyk J.: The effect of laser cutting speed on the bearing surface of peaks and valleys of the cut surface. **W:** Logistyka w ratownictwie 2024 / pod redakcją Andrzeja Chudzikiewicza i Andrzeja Krzyszkowskiego. Radom: Instytut Naukowo-Wydawniczy Spatium, 2024, Poland; s. 71÷84, p-ISBN: 978-83-68026-24-5; e-ISBN: 978-83-68026-25-2.
12. Galon M., Mikołajczyk J.: The effect of laser cutting speed on the weight of the workpiece. **W:** Logistyka w ratownictwie 2024 / pod redakcją Andrzeja Chudzikiewicza i Andrzeja Krzyszkowskiego. Radom: Instytut Naukowo-Wydawniczy Spatium, 2024, Poland; s. 85÷96, p-ISBN: 978-83-68026-24-5; e-ISBN: 978-83-68026-25-2.
13. Galon M., Mikołajczyk J.: Wpływ wartości posuwu podczas cięcia laserem na chropowatość powierzchni przecięcia. Obróbka Metalu; 2024, nr 3, s. 48÷53, p-ISSN: 2081-7002; **https://obrobkametalu.tech/nasze-czasopismo/archiwum/**
14. Górski E.: Frezerstwo. Wydawnictwa Szkolne i Pedagogiczne, Warszawa, 1975 r.
15. Górski E.: Obróbka gładkościowa. Wydawnictwa Naukowo-Techniczne, Warszawa, 1963 r.
16. Górski E.: Poradnik narzędziowca. Wydawnictwa Naukowo-Techniczne, Warszawa, 1980.
17. Górski E.: Poradnik frezera. Wydawnictwa Naukowo-Techniczne, Warszawa, 1974.
18. Górski E.: Narzędzia i oprzyrządowanie narzędziowe. Automatyzacja obróbki skrawaniem. Wydawnictwa Naukowo-Techniczne, Warszawa, 1977 r.
19. Górski E.: Narzędzia do wiercenia i roztaczania głębokich otworów. Wydawnictwa Naukowo-Techniczne, Warszawa, 1962 r.
20. Grabowska M., Mikołajczyk J.: Zastosowanie tomografii komputerowej CAT w inżynierii materiałowej. Application of CAT scanning for materials engineering. Postępy w Inżynierii Mechanicznej [Developments in Mechanical Engineering]. 2017, nr 9 (5), s. 15÷26, p-ISSN: 2300-3383; Wydawnictwa Uczelniane Uniwersytetu Technologiczo-Przyrodniczego w Bydgoszczy, Poland. **http://wu.utp.edu.pl/oferta,8,1**
21. Grabowska M., Mikołajczyk J.: Próba zastosowania tomografii komputerowej CAT do określania struktury grafitu naturalnego w zależności od rozmiaru ziarna. An attempt to apply cat scanning to determine the natural graphite structure depending on the grain size. Postępy w Inżynierii Mechanicznej [Developments in Mechanical Engineering]. 2018, nr 12 (6), s. 5÷14, p-ISSN: 2300-3383; Wydawnictwa Uczelniane Uniwersytetu Technologiczno-Przyrodniczego w Bydgoszczy, Poland. **http://wu.utp.edu.pl/oferta,8,1**
22. Grabowska M., Mikołajczyk J., Basiak S.: Zastosowanie tomografii komputerowej CAT w nieniszczących badaniach teowych złączy spawanych. Application of cat scanning in non-destructive testing of welded t-joints. Postępy w Inżynierii Mechanicznej [Developments in Mechanical Engineering]; 2018, nr 11 (6), s. 31÷44, p-ISSN: 2300-3383; Wydawnictwa Uczelniane Uniwersytetu Technologiczno-Przyrodniczego w Bydgoszczy, Poland. **http://wu.utp.edu.pl/oferta,8,1**
23. Grabowska M., Piochacz A., Mikołajczyk J.: Attempt to use computed tomography CAT to analyze the anodized layer. Postępy w Inżynierii Mechanicznej [Developments in Mechanical Engineering]; 2020, nr 15 (8), s. 25÷33, p-ISSN: 2300-3383; Wydawnictwa Uczelniane Uniwersytetu Technologiczno-Przyrodniczego im. J. J. Śniadeckich w Bydgoszczy, Poland. **https://dme.utp.edu.pl/art/15(8)2020/25.pdf**

DOI: 10.37660/dme.2020.15.8.3
24. Grzesik W.: Podstawy skrawania materiałów konstrukcyjnych. Wydawnictwa Naukowo-Techniczne, Warszawa, 2010.
25. Habrat W.: Obsługa i programowanie obrabiarek CNC. Podręcznik operatora. Wydawnictwo KaBe, Krosno, 2015.
26. Hołubowska A., Szałański B., Mikołajczyk J.: Laboratorium termodynamiki. Piła: Wydawnictwo Państwowej Uczelni im. Stanisława Staszica, 2020, Poland.; s. 164 , e-ISBN: 978-83-62617-93-7;
https://wydawnictwo.puss.pila.pl/files/Laboratorium_termodynamiki_POL_version.pdf
27. Honczrenko J.: Obrabiarki sterowane numerycznie. Wydawnictwa Naukowe PWN, Warszawa, 2017.
28. Jarmoliński Z., Mikołajczyk J.: Badania wpływu technologii cięcia stali na twardość powierzchni bijaka. Research of the influence of steel cutting technology on the strength of the hammer. Postępy w Inżynierii Mechanicznej [Developments in Mechanical Engineering]. 2018, nr 12 (6), s. 15÷30, p-ISSN: 2300-3383. Wydawnictwa Uczelniane Uniwersytetu Technologiczno-Przyrodniczego w Bydgoszczy, Poland.
http://wu.utp.edu.pl/oferta,8,1
29. Jaworski Z.: Obrabiarki. Wydawnictwa Szkolne i Pedagogiczne, Warszawa, 1975.
30. Jaworski Z.: Tokarstwo. Państwowe Wydawnictwo Szkolnictwa Zawodowego, Warszawa, 1972 r.
31. Jaworski Z.: Toczenie kształtowe. Państwowe Wydawnictwa Techniczne, Warszawa, 1958 r.
32. Jędrzejczyk D., Mikołajczyk J.: Defining the correlation between the cutting speed and roughness parameter Rz. **W:** MIK-21 : Międzynarodowa Innowacyjność i Konkurencyjność w XXI wieku : aspekty innowacyjne / redakcja naukowa Radosław Luft. Lublin : Fundacja Innowacji i Nowoczesnych Technologii INOTECH, 2022. Radom : nakładem Instytutu Naukowo-Wydawniczego "Spatium", 2022; s. 39÷46, p-ISBN: 978-83-67033-43-5; e-ISBN: 978-83-67033-44-2;
http://inw-spatium.pl/wp-content/uploads/2022/09/MIK-21-2022-Aspekty-innowacyjne-2.pdf
33. Jędrzejczyk D., Mikołajczyk J.: Mathematical models of the influence of cutting speed on Ra parameter. Developments in Mechanical Engineering; 2022, nr 18 (10), s. 115÷129, p-ISSN: 2720-0639; Wydawnictwa Uczelniane Uniwersytetu Technologiczno-Przyrodniczego im. J. J. Śniadeckich w Bydgoszczy, Poland.
DOI: 10.37660/dme.2022.18.10.11
34. Jędrzejczyk D., Mikołajczyk J.: Wpływ prędkości skrawania na wybrany parametr warstwy wierzchniej. **W:** Logistyka w ratownictwie 2022 / pod redakcją Andrzeja Chudzikiewicza i Andrzeja Krzyszkowskiego. Radom: Instytut Naukowo-Wydawniczy Spatium, 2022, Poland; s. 75÷90, p-ISBN: 978-83-67033-57-2; e-ISBN: 978-83-67033-70-1.
35. Kania L.: Podstawy programu Auto CAD. Wydawnictwo Politechniki Częstochowskiej, Częstochowa, 2007.
36. Kiepuszewski B.: Technologia budowy maszyn. Państwowe Wydawnictwa Techniczne, Warszawa, 1960 r.
37. Kornberger Z.: Technologia budowy maszyn. Wydawnictwa Naukowo-Techniczne, Warszawa, 1965 r.
38. Latoś H., Mikołajczyk J.: Effect of partial wear of the tool point on the selected indicator of the machining process. **W:** Logistyka w ratownictwie 2023 / pod redakcją

Andrzeja Chudzikiewicza i Anny Stelmach. Radom: Instytut Naukowo-Wydawniczy "Spatium", 2023, Poland; s. 195÷210, p-ISBN: 978-83-67033-95-4; e-ISBN: 978-83-67033-96-1.
39. Latoś H., Mikołajczyk J.: Thickness of the machined layer at milling with single-edge straight blades with an angle of λs≠0°. **W:** MIK-21 : Międzynarodowa Innowacyjność i Konkurencyjność w XXI wieku : Aspekty innowacyjne / redakcja naukowa dr Łukasz Wojtowicz. Lublin: Fundacja Innowacji i Nowoczesnych Technologii INOTECH : nakładem Instytutu Naukowo-Wydawniczego "Spatium", 2023, Poland; s. 23÷27, p-ISBN: 978-83-67033-89-3; e-ISBN: 978-83-67033-90-9.
40. Latoś H., Mikołajczyk J., Konarski J., Mikołajczyk T.: Turning using self-induced vibration. **W:** MIK-21 : Międzynarodowa Innowacyjność i Konkurencyjność w XXI wieku : aspekty innowacyjne / redakcja naukowa dr Łukasz Wojtowicz, 2023, Poland; s. 187÷200, p-ISBN: 978-83-67033-89-3; e-ISBN: 978-83-67033-90-9.
41. Latoś H., Mikołajczyk J.: Vibration in machining. **W:** Logistyka w ratownictwie 2023 / pod redakcją Andrzeja Chudzikiewicza i Anny Stelmach. Radom: Instytut Naukowo-Wydawniczy "Spatium", 2023, Poland; s. 187÷194, p-ISBN: 978-83-67033-95-4; e-ISBN: 978-83-67033-96-1.
42. Latoś H., Mikołajczyk J.: The effect of feed rate on the roughness of machined surface. **W:** Szkoła Logistyki 2024 / redakcja naukowa Janusz Zawiła-Niedźwiecki, Adam Płaczek. Radom: Instytut Naukowo-Wydawniczy "Spatium", 2024, Poland; s. 217÷226, p-ISBN: 978-83-68026-07-8; e-ISBN: 978-83-68026-08-5.
43. Latour A.: Skrawalność metali i metody jej określania. Wydawnictwa Naukowo-Techniczne, Warszawa, 1962.
44. Lisowski E.: Integracja modelowania 3D, kinematyki i wytrzymałości w programie CReo Parametric. Wydawnictwo Politechniki Krakowskiej, Kraków, 2013.
45. Makowski T., Jałowiec M., Święcicka A.: Modelowanie w Fusion 360. Praktyczne przykłady. Wydawnictwo Helion, Gliwice, 2024.
46. Matuszak J., Zalewski K.: Podstawy obróbki ubytkowej. Wydawnictwo Politechniki Lubelskiej, Lublin, 2016.
47. Matuszak J., Skoczylas A., Zalewski K.: Narzędzia skrawające. Ćwiczenia laboratoryjne. Wydawnictwo Politechniki Lubelskiej, Lublin, 2014.
48. Matuszewski M., Mikołajczyk J., Styp-Rekowski M: Modyfikacja cech środka smarującego za pomocą standardowych dodatków smarowych. Modification of lubricants features by means of standard additives. Postępy w Inżynierii Mechanicznej [Developments in Mechanical Engineering]. 2013, nr 1 (1), s. 57÷65, Wydawnictwo Uczelniane Uniwersytetu Technologiczno-Przyrodniczego w Bydgoszczy; p-ISSN: 2300-3383; **http://wu.utp.edu.pl/uploads/oferta/Postepy_1_1_2013.pdf**
49. Matuszewski M., Mikołajczyk J., Mikołajczyk T., Styp-Rekowski M.: Logistyczne aspekty zarządzania procesem naprawy. Logistical aspects of the repair process management. Logistyka, 2015, nr 4, s. 1991÷1997, p-ISSN: 1231-5478; **https://www.czasopismologistyka.pl/o-czasopismie/wydania**
50. Matuszewski M., Mikołajczyk J., Mikołajczyk T., Styp-Rekowski M.: The influence of cooling and lubrication liquid quantity on the isotropy of a machine component surface during machining = Wpływ warunków chłodzenia i smarowania podczas obróbki elementów maszyn na stopień izotropowości ich powierzchni. Tribologia. 2016, vol. 265, No. 1, s. 57÷65, p-ISSN: 0208-7774; e-ISSN: 1732-422X; **https://t.tribologia.eu/resources/html/article/details?id=158175**
51. Matyszkiewicz H., Szymanowicz T.: Ćwiczenia z technologii obróbki skrawaniem. Wydawnictwa Naukowo-Techniczne, Warszawa, 1963.

52. Miernik M.: Skrawalność metali. Metody określania i prognozowania. Oficyna Wydawnicza Politechniki Wrocławskiej, Wrocław, 2000.
53. Mikołajczyk J., Styp-Rekowski M., Świerk K.: Modyfikowanie cech środka smarującego za pomocą dodatków i komputerowe wspomaganie ich doboru. W**:** CAX' 2009 : Komputerowe Wspomaganie Nauki i Techniki : VI warsztaty naukowe, Bydgoszcz - Duszniki Zdrój 2009 : praca zbiorowa pod redakcją Tadeusza Mikołajczyka; p-ISBN: 978-83-61314-65-3. Wydawnictwa Uczelniane Uniwersytetu Technologiczno-Przyrodniczego w Bydgoszczy, Bydgoszcz 2009.
54. Mikołajczyk J.: Zestawienie porównawcze dodatków depresujących do olejów. W: Zaawansowana tribologia : XXX Ogólnopolska Konferencja Tribologiczna, Nałęczów, 21-24 września 2009 r. Ogólnopolska Konferencja Naukowa XXX Szkoły Tribologicznej "Zaawansowana Tribologia" : Wydział Materiałoznawstwa, Technologii i Wzornictwa Politechniki Radomskiej, Instytut Technologii Eksploatacji - PIB Radom oraz Komitet Budowy Maszyn, Sekcja Podstaw Eksploatacji Maszyn PAN. Wydawnictwo Naukowe Instytutu Technologii Eksploatacji - PIB, Radom, 2009.
55. Mikołajczyk J.: Zestawienie porównawcze własności fizykochemicznych dodatków smarnych w oleju podstawowym SAE-30. W: Terotechnologia 2009 : materiały konferencji na ekspozycji Metal i Control-Tech : Targi - Kielce (29.09-01.10.2009). VI Konferencja Naukowo-Techniczna "Terotechnologia 2009" : Politechnika Świętokrzyska, Centrum Laserowych Technologii Metali, Katedra Inżynierii Eksploatacji, Wydział Mechatroniki i Budowy Maszyn, Polskie Towarzystwo Naukowo-Techniczne, Towarzystwo Eksploatacyjne, Kielce: Wydawnictwo Politechniki Świętokrzyskiej, 2009. Seria: Zeszyty Naukowe - Politechnika Świętokrzyska, Nr 13.
56. Mikołajczyk J., Matuszewski M.: Konstrukcja i sterowanie stanowiska do badań tribologicznych. W: CAX'2010 : komputerowe wspomaganie nauki i techniki : VII warsztaty naukowe, Bydgoszcz - Duszniki Zdrój 2010 : praca zbiorowa / pod red. Tadeusza Mikołajczyka. Bydgoszcz : Wydawnictwa Uczelniane Uniwersytetu Technologiczno-Przyrodniczego w Bydgoszczy, 2010; p-ISBN: 9788361314387.
57. Mikołajczyk J.: System rejestracji i wizualizacji warunków pracy stanowiska do badań tribologicznych. W: CAX'2011 : komputerowe wspomaganie nauki i techniki : VIII warsztaty naukowe, Bydgoszcz - Duszniki Zdrój 2011 : praca zbiorowa / pod redakcją Tadeusza Mikołajczyka. Bydgoszcz : Wydawnictwa Uczelniane Uniwersytetu Technologiczno-Przyrodniczego w Bydgoszczy, 2011; p-ISBN: 9788361314981.
58. Mikołajczyk J.: Badanie wpływu preparatu eksploatacyjnego Mind M na zmianę własności smarnych oleju bazowego SN-150. Inżynieria i aparatura chemiczna [Chemical Engineering and Equipment]. 2012, nr 5, s. 235÷236, p-ISSN: 0368-0827.
http://inzynieria-aparatura-chemiczna.pl/rok-2012-nr-5/
59. Mikołajczyk J., Styp-Rekowski M., Matuszewski M., Musiał J.: Einfluβ der kompositionen von schmierzusätzen auf die exploitations-eigenschaften der mischung mit Basisöl SN-150. W: Tribologie und mobilität : beiträge der tribotechnik zur optimierung von fertigungsprozessen, wartung, schmierung (reibungskonditionierung) und betriebssicherheit von verkehrsmitteln und verkehrswegen. Wien, 15 November 2012. Symposium 2012 "Tribologie und mobilität" : Österreichische Tribologische Gesellschaft. Österreichische Tribologische Gesellschaft, Wien, 2012.
60. Mikołajczyk J.: Einfluβ der ausgewählten schmierzstoffzusätze auf betriebseigenschaften der mischung mit Basisöl SN-150. **W:** Reibung, schmierung und verschleiβ : forschung und praktische anwendungen. Band 1. Tribologische systeme maschinenelemente und antriebstechnik fahrzeugtechnik prüfen, messen, kontrollieren. Göttingen, 22-24 September 2014. 55. Tribologie Fachtagung "Reibung, Schmierung

und Verschleiß" : Gesellschaft für Tribologie e.V. Stolberg-Venwegen : Gesellschaft für Tribologie e.V., 2014. Germany.
61. Mikołajczyk J.: Einfluss der ausgewählten zusatzschmierstoffe auf die intensivität des verschleißprozesses (Ra, Rq, Δm) mit Basisöl SN-150. **W:** Tribologie in industrie und forschung : werkstoffe, konstruktion und technologie. Leoben, 26 November 2014. ÖTG Symposium 2014 "Tribologie in industrie und forschung" : Österreichische Tribologische Gesellschaft. Wien : Österreichische Tribologische Gesellschaft, 2014. Austria.
62. Mikołajczyk J., Matuszewski M.: Einfluss der ausgewählten schmierzstoffzusätze auf ΔT und ΔP mit Basisöl SN-150. **W:** Tribologie in industrie und forschung : werkstoffe, schmierstoffe und technologie. Wiener Neustadt, 25 November 2015, Austria. ÖTG Symposium 2015 "Tribologie in industrie und forschung" : Österreichische Tribologische Gesellschaft. Wiener Neustadt : Österreichische Tribologische Gesellschaft, 2015, s. 145-152.
63. Mikołajczyk J.: Vergleich charakteristischer parameter des abbott-firestone-diagramms für ein kinematisches paar mit konformem kontakt. **W:** Tribologie in industrie und forschung : verschleißschutz, instandhaltung und anlagenzuverlässigkeit. Linz, 22-23 November 2016, Austria. ÖTG Symposium 2016 "Tribologie in industrie und forschung" : Österreichische Tribologische Gesellschaft. Wiener Neustadt : Österreichische Tribologische Gesellschaft, 2016; s. 105-110.
64. Mikołajczyk J.: Wpływ dodatków smarowych na transformację warstwy wierzchniej. Piła : Wydawnictwo Państwowej Wyższej Szkoły Zawodowej im. Stanisława Staszica, 2017r., Poland; 215 s., p-ISBN: 978-83-62617-76-0; www.ans.pila.pl
65. Mikołajczyk J.: Maszyny tarciowe : budowa, przeznaczenie. Piła, Wydawnictwo Państwowej Wyższej Szkoły Zawodowej im. Stanisława Staszica, 2018, Poland; 256 s., p-ISBN: 978-83-62617-86-9.
66. Mikołajczyk J.: Analiza statystyczna zmiany poboru mocy podczas procesu zużywania. Statistical analysis of the power variation of tribotester as a resultat of the wear process. Autobusy. Technika, Eksploatacja, Systemy Transportowe; 2019, nr 10-11, s. 83÷88, p-ISSN: 1509-5878; e-ISSN: 2450-7725;
http://yadda.icm.edu.pl/yadda/element/bwmeta1.element.baztech-21189602-884a-4d1a-bb60-9edaeae4af8d
67. Mikołajczyk J.: Influence of consumables on the amount of power consumption of kinematic vapor of conformal contact. Wpływ PE na pobór mocy pary kinematycznej o styku konforemnym. Postępy w Inżynierii Mechanicznej [Developments in Mechanical Engineering]; 2019, nr 13 (7), s. 39÷50, p-ISSN: 2300-3383; Wydawnictwa Uczelniane Uniwersytetu technologiczno-Przyrodniczego im. J. J. Śniadeckich w Bydgoszczy, Poland.
http://yadda.icm.edu.pl/baztech/element/bwmeta1.element.baztech-2faf200b-3010-4192-9fd0-062f53b49d38
68. Mikołajczyk J.: Statistical analysis of the mass variation of samples as a result of the wear process. Analiza statystyczna zmiany masy próbek w wyniku procesu zużywania. Postępy w Inżynierii Mechanicznej [Developments in Mechanical Engineering]; 2019, nr 13 (7), s. 51÷61, p-ISSN: 2300-3383; Wydawnictwa Uczelniane Uniwersytetu Technologiczno-Przyrodniczego im. J. J. Śniadeckich w Bydgoszczy, Poland.
http://yadda.icm.edu.pl/baztech/element/bwmeta1.element.baztech-2faf200b-3010-4192-9fd0-062f53b49d38
69. Mikołajczyk J.: Tribotestery : budowa i przeznaczenie. Piła: Wydawnictwo Państwowej Wyższej Szkoły Zawodowej im. Stanisława Staszica, 2019, Poland; 160 s.,

e-ISBN: 978-83-62617-90-6; https://wydawnictwo.pwsz.pila.pl/files/Tribotestery.pdf
70. Mikołajczyk J.: Determining the energy validity of the Kostetsky's hypothesis on the basis of models for relative motion velocity v = 0.08 m/sec. Developments in Mechanical Engineering; 2020, nr 16 (8), s. 17÷29, p-ISSN: 2720-0639; Wydawnictwa Uczelniane Uniwersytetu Technologiczno-Przyrodniczego im. J. J. Śniadeckich w Bydgoszczy, Poland. **DOI: 10.37660/dme.2020.16.8.2**
71. Mikołajczyk J.: Finding the correlation between wear of samples kinematic pair of conformal contact and electric power consumption. Postępy w Inżynierii Mechanicznej [Developments in Mechanical Engineering]; 2020, nr 15 (8), s. 59÷68,
p-ISSN: 2300-3383; Wydawnictwa Uczelniane Uniwersytetu Technologiczno-Przyrodniczego im. J. J. Śniadeckich w Bydgoszczy, Poland.
https://dme.utp.edu.pl/art/15(8)2020/59.pdf
DOI: 10.37660/dme.2020.15.8.6
72. Mikołajczyk J.: The effect of temperature lag on the value of power-temperature correlation for frictional pair of conformal contact. Postępy w Inżynierii Mechanicznej [Developments in Mechanical Engineering]; 2020, nr 15 (8), s. 79÷86,
p-ISSN: 2300-3383; Wydawnictwa Uczelniane Uniwersytetu Technologiczno-Przyrodniczego im. J. J. Śniadeckich w Bydgoszczy, Poland.
https://dme.utp.edu.pl/art/15(8)2020/79.pdf
DOI: 10.37660/dme.2020.15.8.8
73. Mikołajczyk J.: Określenie na podstawie modeli zmiany masy próbek w wyniku procesu zużywania. **W:** Szkoła Logistyki 2021 / redakcja naukowa Janusz Zawiła-Niedźwiecki, Piotr Korneta. Radom : Instytut Naukowo-Wydawniczy "Spatium", 2021; s. 167÷174, Poland; p-ISBN: 978-83-66550-75-9; e-ISBN: 978-83-66550-89-6.
74. Mikołajczyk J.: A method of determining mathematical models of a seizure test of friction pairs. **W:** MIK-21 : Międzynarodowa Innowacyjność i Konkurencyjność w XXI wieku : aspekty innowacyjne / redakcja naukowa Radoslaw Luft. Lublin : Fundacja Innowacji i Nowoczesnych Technologii INOTECH, 2022. Radom : nakładem Instytutu Naukowo-Wydawniczego "Spatium", 2022; s. 7÷24, p-ISBN: 978-83-67033-43-5;
e-ISBN: 978-83-67033-44-2.
http://inw-spatium.pl/wp-content/uploads/2022/09/MIK-21-2022-Aspekty-innowacyjne-2.pdf
75. Mikołajczyk J.: Friction machines. Wydawnictwo Akademii Nauk Stosowanych im. Stanisława Staszica, Piła, 2022, Poland; 488 s., e-ISBN: 978-83-62617-96-8.
https://wydawnictwo.ans.pila.pl/files/FRICTION_MACHINES.pdf
76. Mikołajczyk J., Jędrzejczyk D.: Określenie korelacji między prędkością skrawania a parametrem chropowatości Ra. Obróbka Metalu; 2022, nr 3, s. 11÷15,
p-ISSN: 2081-7002; https://obrobkametalu.tech/
77. Mikołajczyk J.: Rolling bearing heating charakter. **W:** Szkoła Logistyki 2022. Radom: Instytut Naukowo-Wydawniczy "Spatium", 2022, Poland; s. 231÷239, Materiały z IX Konferencji Naukowej "Szkoła Logistyki 2022";
p-ISBN: 978-83-67033-33-6; e-ISBN: 978-83-67033-34-3.
78. Mikołajczyk J.: Tribological properties of carbon black. **W:** Szkoła Logistyki 2022. Radom: Instytut Naukowo-Wydawniczy "Spatium", 2022, Poland; s. 217-230, Materiały z IX Konferencji Naukowej "Szkoła Logistyki 2022";
p-ISBN: 978-83-67033-33-6; e-ISBN: 978-83-67033-34-3.
79. Mikołajczyk J.: Determination of the modified coefficient of variation from the number of samples. **W:** MIK-21 : Międzynarodowa Innowacyjność i Konkurencyjność w XXI wieku : Aspekty innowacyjne / redakcja naukowa dr Łukasz Wojtowicz. Lublin:

Fundacja Innowacji i Nowoczesnych Technologii INOTECH : nakładem Instytutu Naukowo-Wydawniczego "Spatium", 2023, Poland; s. 111÷122,
p-ISBN: 978-83-67033-89-3; e-ISBN: 978-83-67033-90-9.
80. Mikołajczyk J.: Effect of cutting speed on the shape of the machined surface profile. Mebutra; 2023, nr 1, s. 47÷63, Wydawnictwo Akademii Nauk Stosowanych im. S. Staszica w Pile, Piła 2023, Poland. **https://online.fliphtml5.com/vliuj/yunw/ p=48**
81. Mikołajczyk J.: Friction Machines II. Piła: Wydawnictwo Akademii Nauk Stosowanych im. Stanisława Staszica w Pile, 2023, Poland; s. 598;
p-ISBN: 978-83-67684-00-2;
https://wydawnictwo.ans.pila.pl/files/FRICTION_MACHINES_V_ANS_PILA.pdf
82. Mikołajczyk J.: Oil can talk. **W:** Szkoła Logistyki 2023 / redakcja naukowa Janusz Zawiła-Niedźwiecki, Katarzyna Białczak. Radom: Instytut Naukowo-Wydawniczy "Spatium", 2023, Poland; s. 109÷115, p-ISBN: 978-83-67033-75-6;
e-ISBN: 978-83-67033-58-9.
83. Mikołajczyk J.: Pobór mocy elektrycznej przez parę kinematyczną jako parametr oceny jakości oleju. **W:** Logistyka w ratownictwie 2023 / pod redakcją Andrzeja Chudzikiewicza i Anny Stelmach. Radom: Instytut Naukowo-Wydawniczy "Spatium", 2023, Poland; s. 223-230, p-ISBN: 978-83-67033-95-4; e-ISBN: 978-83-67033-96-1.
84. Mikołajczyk J.: Rola dodatków smarowych w olejach. **W:** Logistyka w ratownictwie 2023 /pod redakcją Andrzeja Chudzikiewicza i Anny Stelmach/; Radom: Instytut Naukowo-Wydawniczy "Spatium", 2023, Poland; s. 231÷237, p-ISBN: 978-83-67033-95-4; e-ISBN: 978-83-67033-96-1.
85. Mikołajczyk J.: Temperature as a parameter for assessing the work of a friction pair. **W:** Szkoła Logistyki 2023 / redakcja naukowa Janusz Zawiła-Niedźwiecki, Katarzyna Białczak. Radom: Instytut Naukowo-Wydawniczy "Spatium", 2023, Poland; s. 101-107, p-ISBN: 978-83-67033-75-6; e-ISBN: 978-83-67033-58-9.
86. Mikołajczyk J.: Tire as a selected element of a car subject to diagnostics. **W:** Szkoła Logistyki 2023 / redakcja naukowa Janusz Zawiła-Niedźwiecki, Katarzyna Białczak. Radom: Instytut Naukowo-Wydawniczy "Spatium", 2023, Poland; s. 117÷131,
p-ISBN: 978-83-67033-75-6; **e-ISBN:** 978-83-67033-58-9.
87. Mikołajczyk J.: Wpływ dodatku modyfikującego cechy płynu obróbkowego na zmianę temperatury w strefie kontaktu współpracujących powierzchni. Obróbka Metalu; 2023, nr 2, s. 43÷46, p-ISSN: 2081-7002;
https://obrobkametalu.tech/media/2023/05/2023_2_52_ObrobkaMetalu.pdf
88. Mikołajczyk J., Kozłowska M.A., Krasicki K.: Wpływ kompetencji cyfrowych pracowników na poziom rozwoju procesów przemysłowych. **W:** MIK-21 : Międzynarodowa Innowacyjność i Konkurencyjność w XXI wieku : aspekty społeczne /redakcja naukowa Radosław Luft/; Lublin-Radom : Fundacja Innowacji i Nowoczesnych Technologii INOTECH : nakładem Instytutu Naukowo-Wydawniczego "Spatium", 2023, Poland; s. 149÷169, p-ISBN: 978-83-67033-92-3;
e-ISBN: 978-83-67033-93-0.
89. Mikołajczyk J.: Zmiana geometrycznych cech współpracujących powierzchni miarą intensywności procesu zużywania ostrzy skrawających. Obróbka Metalu; 2023, nr 1, s. 50÷54, p-ISSN: 2081-7002;
https://yadda.icm.edu.pl/yadda/element/bwmeta1.element.baztech-9e73eb05-2a91-4df5-853b-22abf7a6ee77
90. Mikołajczyk J., Góra F., Jędrzejczyk D.: Analysis of selected surface roughness parameters for wear processes. Analiza wybranych parametrów chropowatości powierzchni pod kątem procesów zużywania. **W:** MIK-21 : Międzynarodowa

Innowacyjność i Konkurencyjność w XXI wieku : Aspekty innowacyjne / redakcja naukowa Radosław Luft. Lublin: Wydawnictwo Naukowe FNCE, 2024; s. 93-117, p-ISBN: 978-83-68074-82-6; e-ISBN: 978-83-68319-03-3.
91. Mikołajczyk J., Galon M.: Mathematical model of straight regression determining the effect of laser cutting speed on the mass of the workpiece. **W:** MIK-21 : Międzynarodowa Innowacyjność i Konkurencyjność w XXI wieku : Aspekty innowacyjne / redakcja naukowa Radosław Luft. Lublin: Wydawnictwo Naukowe FNCE, 2024, Poland; s. 71÷92, p-ISBN: 978-83-68074-82-6; e-ISBN: 978-83-68319-03-3.
92. Mikołajczyk J., Sądej I.: Spinning speed and balancing accuracy. **W:** MIK-21 : Międzynarodowa Innowacyjność i Konkurencyjność w XXI wieku : Aspekty innowacyjne / redakcja naukowa Radosław Luft. Lublin: Wydawnictwo Naukowe FNCE, 2024, Poland; s. 118÷132, p-ISBN: 978-83-68074-82-6; e-ISBN: 978-83-68319-03-3.
93. Mikołajczyk J.: The correlation between the population and number of construction disasters. Mebutra; 2025, nr 3, s. 44-55, Wydawnictwo Akademii Nauk Stosowanych im. S. Staszica w Pile, Poland.
https://wydawnictwo.ans.pila.pl/files/MEBUTRA2025.pdf
94. Mikołajczyk J.: The relationship between the type of structure and the number of construction disasters. Zależność między rodzajem konstrukcji, a liczbą katastrof budowlanych. Mebutra; 2025, 3, s. 30÷43, Wydawnictwo Akademii Nauk Stosowanych im. S. Staszica w Pile, Poland.
https://wydawnictwo.ans.pila.pl/files/MEBUTRA2025.pdf
95. Miracki J.: Przeciąganie. Wydawnictwa Naukowo-Techniczne, Warszawa, 1969 r.
96. Niemczewska-Wójcik M.: Dualny system charakteryzowania powierzchni technologicznej i eksploatacyjnej warstwy wierzchniej elementów trących. Wydawnictwo Naukowe Instytutu Technologii Eksploatacji PIB, Kraków, 2018.
97. Noga B., Budzik G.: Inventor. Pierwsze kroki. Wydawnictwo Helion, Gliwice, 2018.
98. Norma PN-EN ISO 3274:2011. Specyfikacja geometrii wyrobów (GPS) – Struktura geometryczna powierzchni: Metoda profilowa – Charakterystyki nominalne przyrządów stykowych (z ostrzem odwzorowującym).
99. Okoniewski S.: Technologia metali, cz. I. Wydawnictwa Szkolne i Pedagogiczne, Warszawa, 1980.
100. Okoniewski S.: Technologia metali, cz. II. Wydawnictwa Szkolne i Pedagogiczne, Warszawa, 1980.
101. Okoniewski S.: Technologia metali, cz. III. Wydawnictwa Szkolne i Pedagogiczne, Warszawa, 1980.
102. Okoniewski S.: Technologia metali, cz. IV. Wydawnictwa Szkolne i Pedagogiczne, Warszawa, 1980.
103. Olechnowicz J., Mikołajczyk J.: Truck scales : the key to safe transport and road protection. Mebutra; 2024, nr 2, s. 3÷8, Wydawnictwo Akademii Nauk Stosowanych im. S. Staszica w Pile, Poland.
https://wydawnictwo.ans.pila.pl/files/MEBUTRA2024.pdf
104. Pikulik K.W., Mikołajczyk J.: The influence of the welding current on the air pollution emissions. Wpływ prądu spawania na emisję zanieczyszczeń powietrza. Postępy w Inżynierii Mechanicznej [Developments in Mechanical Engineering]; 2019, nr 14 (7), s. 33÷46, p-ISSN: 2300-3383; Wydawnictwa Uczelniane Uniwersytetu Technologiczno-Przyrodniczego im. J. J. Śniadeckich w Bydgoszczy, Poland.
http://yadda.icm.edu.pl/baztech/element/bwmeta1.element.baztech-2faf200b-3010-4192-9fd0-062f53b49d38

105. Pikulik K.W., Mikołajczyk J.: Determination of emission of iron oxides from the welding process on the basis of mathematical models. Welding Technology Review; 2021, vol. 93, No 2, s. 35÷43, p-ISSN: 0033-2364; e-ISSN: 2449-7959;
http://www.pspaw.wip.pw.edu.pl/index.php/pspaw/article/view/1132
DOI: 10.26628/wtr.v93i2.1132
106. Pikulik J., Pikulik K.W., Mikołajczyk J.: The relationship between the clearance of the coupling mechanism used in uniaxial light car trailers and the date of their production. **W:** MIK-21 : Międzynarodowa Innowacyjność i Konkurencyjność w XXI wieku : aspekty innowacyjne / redakcja naukowa Radosław Luft. Lublin : Fundacja Innowacji i Nowoczesnych Technologii INOTECH, 2022, Poland. Radom : nakładem Instytutu Naukowo-Wydawniczego "Spatium"; 2022; s. 221÷233,
p-ISBN: 978-83-67033-43-5; e-ISBN: 978-83-67033-44-2;
http://inw-spatium.pl/wp-content/uploads/2022/09/MIK-21-2022-Aspekty-innowacyjne-2.pdf
107. Pikulik J., Pikulik K.W., Mikołajczyk J.: Zależność wielkości luzu mechanizmu sprzęgającego stosowanego w jednoosiowych lekkich przyczepach samochodowych od wartości współczynnika przylegania. **W:** Logistyka w ratownictwie 2022 / pod redakcją Andrzeja Chudzikiewicza i Andrzeja Krzyszkowskiego. Radom: Instytut Naukowo-Wydawniczy "Spatium", 2022, Poland; s. 157÷167, p-ISBN: 978-83-67033-57-2;
e-ISBN: 978-83-67033-70-1.
108. Pikulik J., Pikulik K.W., Mikołajczyk J.: Determination of the degree of contact of the movable part of the coupling head with the ball part of the coupling of single-axle light car trailers. **W:** MIK-21 : Międzynarodowa Innowacyjność i Konkurencyjność w XXI wieku : aspekty innowacyjne / redakcja naukowa dr Łukasz Wojtowicz. Lublin: Fundacja Innowacji i Nowoczesnych Technologii INOTECH : nakładem Instytutu Naukowo-Wydawniczego "Spatium", 2023, Poland; s. 97÷109,
p-ISBN: 978-83-67033-89-3; e-ISBN: 978-83-67033-90-9.
109. Pilarczyk J.: Poradnik inżyniera. Spawalnictwo. t. 2. Wydawnictwa Naukowo-Techniczne, Warszawa, 2005.
110. Piochacz A., Mikołajczyk J.: Wpływ czasu trwania procesu anodowania stopu aluminium EN AW-6060 na grubość i twardość otrzymanej warstwy. Influence of aluminium type EN AW-6060 anodizing process duration on the thickness and hardness of the obtained layer. Postępy w Inżynierii Mechanicznej [Developments in Mechanical Engineering]; 2018, nr 12 (6), s. 49÷56, p-ISSN: 2300-3383; Wydawnictwa Uczelniane Uniwersytetu Technologiczno-Przyrodniczego w Bydgoszczy, Poland.
http://wu.utp.edu.pl/oferta,8,1
111. Piochacz A., Mikołajczyk J.: Analiza statystyczna wpływu czasu anodowania na grubość otrzymanej powłoki. Statistical analysis of the influence of anodizing time on the thickness of obtained layers. Autobusy. Technika, Eksploatacja, Systemy Transportowe; 2019, vol. 233, nr 9, s. 48÷51, p-ISSN: 1509-5878; e-ISSN: 2450-7725;
http://ceref.pl/index.php/Autobusy/article/view/956
DOI: 10.24136/atest.2019.201
112. Piochacz A., Mikołajczyk J.: Determination of the thickness of anodized layer on the basis mathematical models. Developments in Mechanical Engineering; 2020, nr 16 (8), s. 31÷39, p-ISSN: 2720-0639; Wydawnictwa Uczelniane Uniwersytetu Technologiczno-Przyrodniczego im. J. J. Śniadeckich w Bydgoszczy, Poland.
DOI: 10.37660/dme.2020.16.8.3
113. Piotrowski Ł., Góra F., Mikołajczyk J.: Construction of an electric longboard with one-wheel driver. Mebutra; 2024, nr 2, s. 16÷27, Wydawnictwo Akademii Nauk Stosowanych im. S. Staszica w Pile, Poland.

https://wydawnictwo.ans.pila.pl/files/MEBUTRA2024.pdf
114. Piotrowski Ł., Góra F., Mikołajczyk J.: Design and construction of an electric longboard. **W:** Logistyka w ratownictwie 2024 / pod redakcją Andrzeja Chudzikiewicza i Andrzeja Krzyszkowskiego. Radom: Instytut Naukowo-Wydawniczy Spatium, 2024, Poland; s. 167÷178, p-ISBN: 978-83-68026-24-5; e-ISBN: 978-83-68026-25-2.
115. Pokutycki J.: Podstawy automatyki. Państwowe Wydawnictwo Szkolnictwa Zawodowego, Warszawa, 1970 r.
116. Praca zbiorowa: Poradnik inżyniera spawalnictwa. Wydawnictwa Naukowo-Techniczne. Warszawa 1983.
117. Przybył B., Kabat M., Mikołajczyk J.: Wpływ prędkości drukowania 3D na dokładność zarysu kół zębatych. Obróbka Metalu; 2023, nr 4, s. 26÷30,
p-ISSN: 2081-7002;
https://obrobkametalu.tech/media/2023/08/2023-4_Nr54_ObrobkaMetalu.pdf
118. Przybył B., Mikołajczyk J.: Efektywność technik przyrostowych. Obróbka Metalu; 2024, nr 1, s. 22÷25, p-ISSN: 2081-7002;
https://obrobkametalu.tech/media/2024/03/2024_1_nr55_ObrobkaMetalu-1.pdf
119. Przybył B., Mikołajczyk J.: The influence of 3D printing speed on profile accuracy. **W:** Szkoła Logistyki 2024 / redakcja naukowa Janusz Zawiła-Niedźwiecki, Adam Płaczek. Radom: Instytut Naukowo-Wydawniczy "Spatium", 2024, Poland; s. 199÷216, p-ISBN: 978-83-68026-07-8; e-ISBN: 978-83-68026-08-5.
120. Rodziewicz M.: Wygładzanie luźnym ścierniwem w pojemnikach. Wydawnictwa Naukowo-Techniczne, Warszawa, 1964 r.
121. Rydzewski J.: Pomiary oscyloskopowe. Wydawnictwa Naukowo-Techniczne, Warszawa, 1994.
122. Sądej I., Mikołajczyk J.: Machine tool compensation and mass unbalance measurements. **W:** Logistyka w ratownictwie 2024 / pod redakcją Andrzeja Chudzikiewicza i Andrzeja Krzyszkowskiego. Radom: Instytut Naukowo-Wydawniczy Spatium, 2024, Poland; s. 187÷196, p-ISBN: 978-83-68026-24-5;
e-ISBN: 978-83-68026-25-2.
123. Siemiński P., Budzik G.: Techniki przyrostowe, druk 3D, drukarki 3D. Oficyna Wydawnicza Politechniki Warszawskiej, Warszawa, 2015.
124. Storch B.: Podstawy obróbki skrawaniem. Wydawnictwo Uczelniane Politechniki Koszalińskiej, Koszalin, 2001.
125. Styp-Rekowski M., Mikołajczyk J.: The influence of Mind M preparation on the lubricant properties of base oil SN-150. W**:** Reinung, Schmierung und Verschleiβ : forschung und praktische anwendungen : Band 1 : tribologische systeme schmierstoffe und schmierungstechnik zerspanungs : und umformtechnik prüfen, messen, kontrollieren / 53. Tribologie-Fachtagung. 24. bis 26. Septembet 2012 in Göttingen. Aachen : Gesellschaft für Tribologie e.V., 2012. p-ISBN: 978-3-00-039201-6.
126. Styp-Rekowski M., Mikołajczyk J.: Wpływ dodatku na własności smarowe oleju bazowego SN-150. Tribologia. 2012, vol. 244, No. 4, s. 227-232, p-ISSN: 0208-7774;
e-ISSN: 1732-422X; https://t.tribologia.eu/resources/html/article/details?id=167726
127. Styp-Rekowski M., Mikołajczyk J.: Wpływ preparatu eksploatacyjnego stanowiący kompleks węglowodorowy na zmianę własności smarnych oleju bazowego SN-150. W: Tribologia bliżej praktyki : XXXII Ogólnopolska Konferencja "Jesienna Szkoła Tribologiczna 2012". XXXII Ogólnopolska Konferencja "Jesienna Szkoła Tribologiczna 2012", Kudowa Zdrój, 18-21 września 2012r. Politechnika Wrocławska Wydział Mechaniczny, Instytut Konstrukcji Eksploatacji Maszyn, Polskie Towarzystwo Tribologiczne, Sekcja Podstaw Eksploatacji KBM PAN. Wrocław : Polskie Towarzystwo Tribologiczne, 2012.

128. Styp-Rekowski M., Mikołajczyk J.: Zmiana temperatury na drodze tarcia dla kompozycji olej bazowy SN-150 - preparat eksploatacyjny Mind M. Temperature variability during friction for composition bese oil SN-150 - exploatational preparation Mind M. **W:** III krajowa konferencja nano- i mikromechaniki / Komitet Mechaniki Polskiej Akademii Nauk, Politechnika Rzeszowska im. Ignacego Łukasiewicza, Instytut Podstawowych Problemów Techniki Polskiej Akademii Nauk. Warszawa, 4-6 lipca 2012 r. III Krajowa Konferencja Nano- i Mikromechaniki pod Patronatem Ministra Nauki i Szkolnictwa Wyższego Prof. Barbary Kudryckiej : Komitet Mechaniki Polskiej Akademii Nauk, Politechnika Rzeszowska, Instytut Podstawowych Problemów Techniki Polskiej Akademii Nauk, Warszawa, 2012.
129. Styp-Rekowski M., Mikołajczyk J., Matuszewski M.: Wybrane zagadnienia stosowania płynów obróbkowych w obróbce skrawaniem. W**:** Obróbka Metalu, 2014, nr 3, s. 10÷14, p-ISSN: 2081-7002; **http://www.e-obrobkametalu.pl/**
130. Syrek S., Mikołajczyk J.: Analiza matematyczna podstawowych wymiarów złącza spawanego. **W:** Logistyka w ratownictwie 2022/ pod redakcją Andrzeja Chudzikiewicza i Andrzeja Krzyszkowskiego. Radom : Instytut Naukowo-Wydawniczy "Spatium", 2022; s. 169÷190, p-ISBN: 978-83-67033-57-2; e-ISBN: 978-83-67033-70-1.
131. Syrek S., Mikołajczyk J.: Modele liniowe wpływu częstotliwości prądu spawania na grubość spoiny. **W:** MIK-21 : Międzynarodowa Innowacyjność i Konkurencyjność w XXI wieku : aspekty innowacyjne / redakcja naukowa Radosław Luft. Lublin: Fundacja Innowacji i Nowoczesnych Technologii INOTECH, 2022. Radom : nakładem Instytutu Naukowo-Wydawniczego "Spatium", 2022; s. 153÷170, p-ISBN: 978-83-67033-43-5; e-ISBN: 978-83-67033-44-2;
http://inw-spatium.pl/wp-content/uploads/2022/09/MIK-21-2022-Aspekty-innowacyjne-2.pdf
132. Syrek S., Mikołajczyk J.: Modele liniowe wpływu częstotliwości prądu spawania na szerokość spoiny. Obróbka Metalu; 2022, nr 4, s. 24÷31, p-ISSN: 2081-7002; **https://obrobkametalu.tech/**
133. Terczyński S.: Buduję swoją pierwszą drukarkę 3D. Wydawnictwo IT START, Warszawa, 2018.
134. Tubielewicz K.: Technologia maszyn i metrologia warstwy wierzchniej. Wydawnictwo Wyższej Szkoły Pedagogicznej w Częstochowie, Częstochowa, 1998.
135. Tymowski J.: Automatyzacja procesów technologicznych w przemyśle maszynowym. Wydawnictwa naukowo-Techniczne, Warszawa, 1966 r.
136. Wesołowski L., Mikołajczyk J.: Hammer mill design and construction analysis. **W:** MIK-21 : Międzynarodowa Innowacyjność i Konkurencyjność w XXI wieku : aspekty innowacyjne / redakcja naukowa dr Łukasz Wojtowicz. Lublin: Fundacja Innowacji i Nowoczesnych Technologii INOTECH : nakładem Instytutu Naukowo-Wydawniczego "Spatium", 2023, Poland; s. 159÷185, p-ISBN: 978-83-67033-89-3; e-ISBN: 978-83-67033-90-9.
137. Wieczorowski M.: Digitalizacja powierzchni w aplikacjach mikro, mezo i makro. Mechanik 11/2018, s. 944÷949.
138. Wieczorowski M.: Kierunki rozwoju metrologii nierówności powierzchni. Mechanik 8-9/2014, s. 467÷479.
139. Wrotny L.: Podstawy budowy obrabiarek. Wydawnictwa Naukowo-Techniczne, Warszawa, 1964.
140. Zalewski A., Grzesik W.: Obrabiarki CNC. Podstawy funkcjonowania i programowania. Wydawnictwa Naukowe PWN, Warszawa, 2024.
141. Zandecki R., Kmita C., Mikołajczyk J.: Mathematical models of the surface layer microhardness for a selected grade of ion nitrided steel. **W:** Szkoła Logistyki 2022.

Radom : Instytut Naukowo-Wydawniczy "Spatium", 2022, Poland; s. 203÷216, Materiały z IX Konferencji Naukowej "Szkoła Logistyki 2022".
p-ISBN: 978-83-67033-33-6; e-ISBN: 978-83-67033-34-3.

Methods and conditions of neutralizing the bending of strips resulting from milling of one of their sides

inż. Tomasz Krugiołka

Department of Mechanical Engineering

Stanisław Staszic State University of Applied Sciences in Piła, Poland

https://orcid.org/0009-0005-1500-4594

corresponding e-mail: tomaszkrugiolka@wp.pl

Abstract:

The paper describes the problem of deformation of a strip that occurs when one of its sides is milled. Particular attention is paid to the residual stress occurring in the surface layer of the machined objects. Analyzed were causes of residual stress and its influence on deformations. Furthermore, experimental verification was carried out. Strips milling tests were carried out and then deformation measurements were taken. Attempts were made to find cutting parameters that ensure neutralization of deformations in the workpieces being machined.

As a result of the Author's many years of experience in the field of machining it was noticed that when milling one side of the strip there is a problem of deformation of the workpiece. Plastic deformation significantly changes the geometric dimensions and shape of the machined strip. In order to obtain the desired dimensions the workpiece must be subjected to additional operations which extends the production process and its costs.

Key words: machining, milling, cutters

1. Introduction

Subtractive machining is a technique commonly used in industry that involves shaping parts of machines and devices by removing a specific volume of material which is called machining allowance [1, 2, 3, 5]. Depending on the type of method used to remove machining allowance we have machining and erosion machining [41, 94, 96, 98].

Machining is a process in which the movement of cutting edges causes that a layer of machining allowance is converted into chips. The concept of machining includes chip processing which is performed using cutting tools with a defined geometry and a specific number of cutting edges. The chips formed during cutting are visible to the naked eye, and their shape depends on the specified machining parameters. The second type of machining is abrasive machining, which, unlike machining, is performed with a tool of undefined cutting edges, and the chips generated during cutting are in the form of dust [14, 15, 16, 17, 18, 19, 41].

The precision of machining and the quality of manufactured products are influenced by the interaction of the machine tool – workpiece – tool system. During the cutting process, a number of phenomena occur that influence the course of the machining process. These include high temperature in the cutting zone, the occurrence of friction forces, and abrasion of the cutting blade. Therefore, a very important factor in the process of manufacturing an item is a properly designed technological process.

Milling is a type of machining used mainly for machining surfaces, shaped surfaces, straight and helical grooves and threads. Additionally, milling is also used to cut gear teeth. Milling is performed using multi-blade tools called milling cutters. They perform a working rotary motion. The feed movement is usually performed by a workpiece mounted on the table of a machine called a milling machine.

When working on a keyway milling machine both the working motion and feed motion are performed by the tool.

Depending on the direction of the feed motion in relation to the working motion, we have down milling and up milling (Fig. 1 and Fig. 2) [111, 112, 113, 114]. If the direction of the table feed motion is consistent with the direction of the milling cutter work motion, such process is called down milling (Fig. 1). In the opposite case, i.e. when the table feed motion takes place in the direction opposite to the working direction of the milling cutter, such process is called up milling (Fig. 2).

During down milling the forces acting on the workpiece press it against the milling table. Particularly strong pressure occurs when the cutter blade starts working. It then begins to cut a layer of considerable thickness which decreases to zero as the cutting progresses. This type of work causes the machine to vibrate. If there is play in the table feed mechanism, then the milling machines will operate unevenly and the tool or machine may be damaged. Down milling is mainly used for machining layered materials, e.g. wood, laminates, because then the individual layers are pressed against each other during machining [15, 16, 18, 19].

Up milling is more commonly used. During up milling, the forces acting on the workpiece try to tear it away from the table. The cutting layer is very thin at the beginning of the blade's operation but becomes thicker as the cutting progresses.

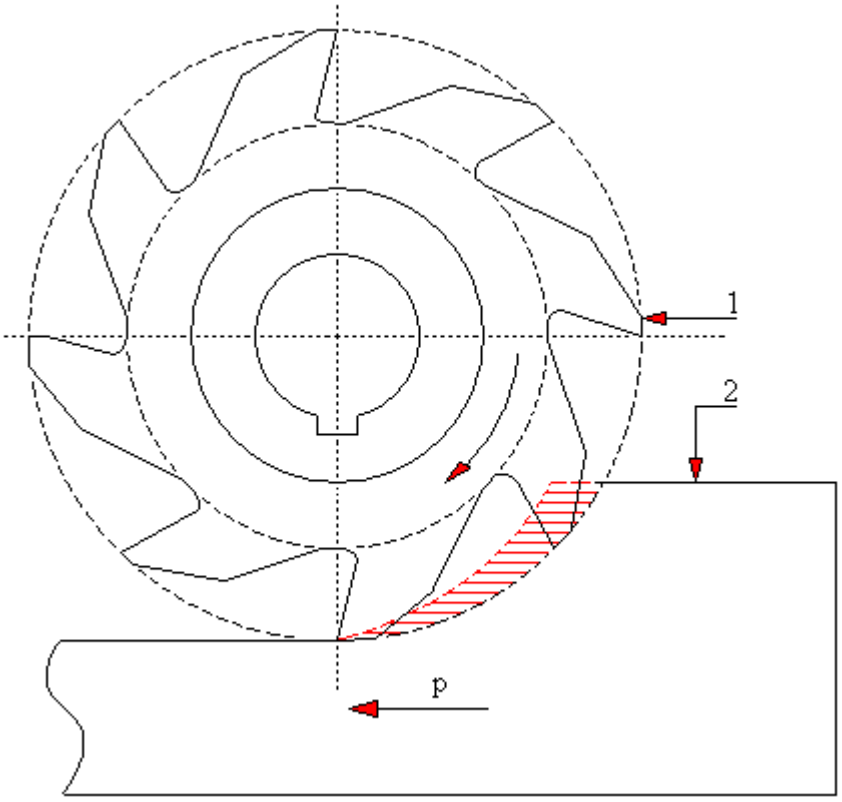

Fig. 1. Down milling
1 – milling cutter; 2 – workpiece; p – workpiece feed

Depending on the type of milling operation, there are the following types of milling [41, 134]:

- face milling (Fig. 4, Fig. 5, Fig. 6), realized when the tool rotation axis is perpendicular to the workpiece; the cutting blades are on the face of the cutter;
- peripheral milling (Fig. 3), realized when the axis of rotation of the tool is parallel to the workpiece; the cutting blades are located on the circumference of the cutter;
- end milling; this is a combination of cutting with blades on the face and on the circumference of the cutter.

If we take the tool positioning relative to the workpiece as the criterion for differentiating the milling process, then face milling can be divided into [41]:

- full milling (Fig. 4) – the width of the workpiece is greater than the diameter of the milling cutter;
- incomplete symmetric milling (Fig. 5) – the width of the workpiece is smaller than the diameter of the cutter; the cutter is located in the axis of symmetry of the workpiece;
- incomplete asymmetric milling (Fig. 6) – the width of the workpiece is smaller than the diameter of the cutter; the cutter is not located in the axis of symmetry of the workpiece;

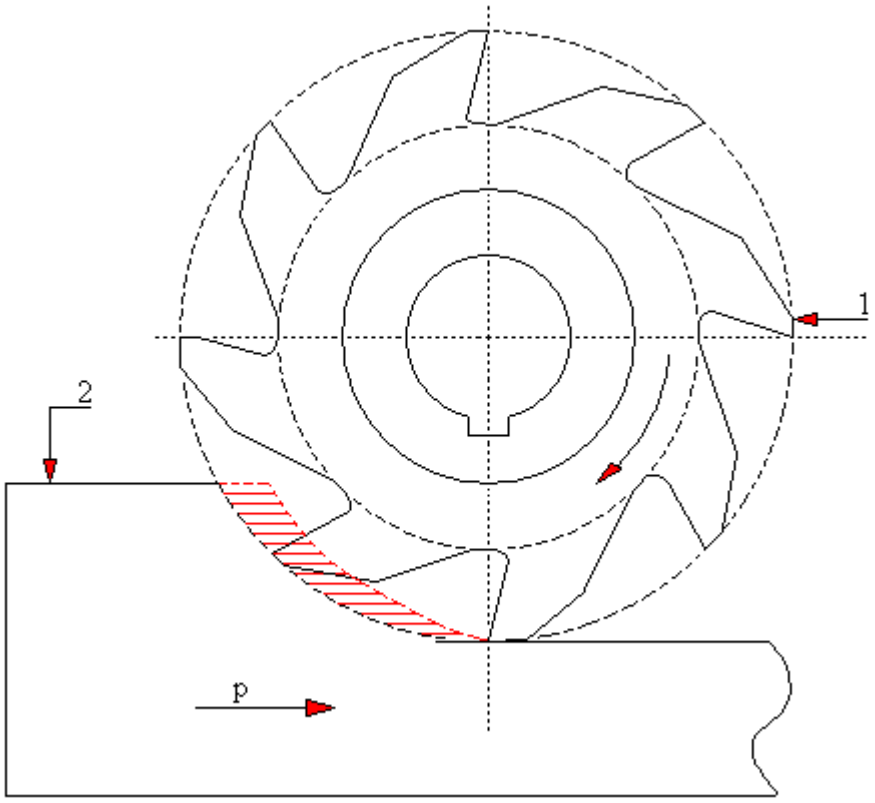

Fig. 2. Up milling
1 – milling cutter; 2 – workpiece; p – workpiece feed

It is estimated that most of the work done during cutting is converted into heat. This heat has a negative effect on the workpiece and the tool. Therefore, it is necessary to use cutting-tool lubricants. Cutting-tool lubricants generally have two purposes. First, absorb large amounts of heat from the cutting zone. Second, minimize the effects of friction. Moreover, cutting-tool lubricants protect the workpiece, to some extent, gainst corrosion and support the washing away of cutting products (dust, chips) from the machined surface. There are three basic groups of cutting fluids [14, 16, 18, 41, 134]:

- oil;
- emulsion;
- water-soluble.

Oil cutting fluids are characterized by good lubricating properties [67, 68, 69, 70]. This group includes mineral oils, vegetable oils and warm animal fats.

Emulsion cutting fluids are a mixture of water and emulsifying oil. They are characterized by good cooling and lubricating properties [43, 44, 45, 48].

Water-based cutting fluid is a mixture of water and synthetic compounds. It has good cooling properties but poor lubricating properties.

The cutting tool material plays an extremely important role in the cutting process. This material should be characterized by high hardness which should be at least 20 HRC higher than the hardness of the material being machined. Moreover, this material should be resistant to high temperatures and should be bend-resistant. In industry, cutting tools are made of unalloyed tool steel, alloyed tool steel, cermets, sintered carbides, ceramic sintered materials and superhard materials.

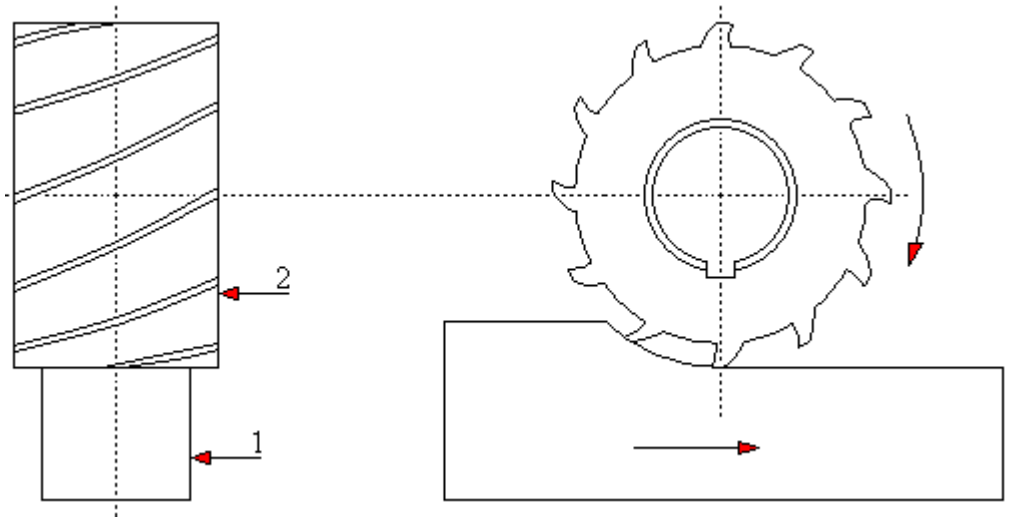

Fig. 3. Peripheral milling
1 – workpiece; 2 – milling cutter

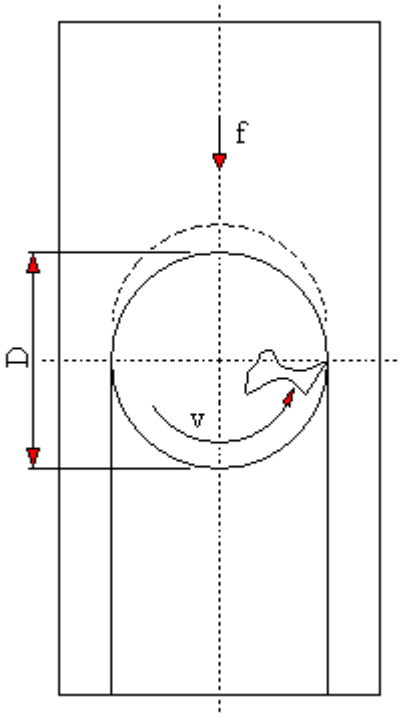

Fig. 4. Full face milling
D – cutter diameter; v – cutter rotational speed; f – workpiece feed

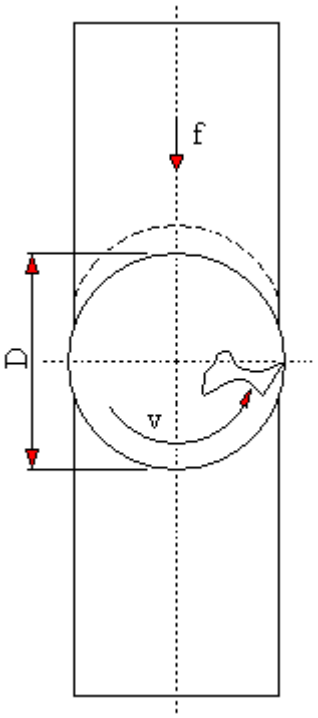

Fig. 5. Incomplete symmetric face milling
D – cutter diameter; v – cutter rotational speed; f – workpiece feed

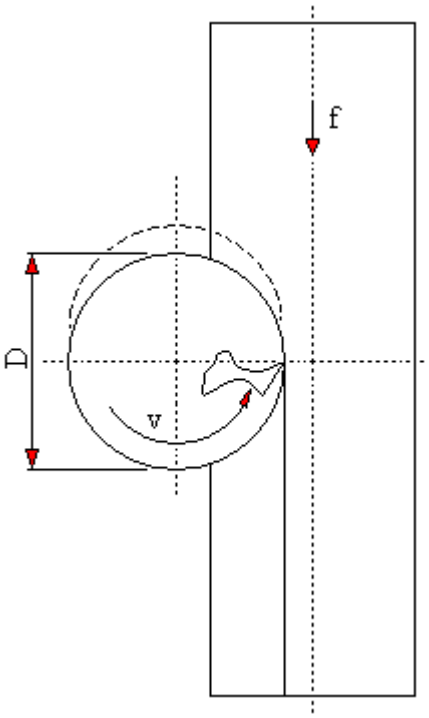

Fig. 6. Incomplete asymmetric face milling
D – cutter diameter; v – cutter rotational speed; f – workpiece feed

HSS high-speed steel is defined in the PN-EN ISO 4957 standard: 2018-09. There are several grades of HSS steel available in the industry. They fall into four main groups: cobalt-free, cobalt-free with increased carbon concentration, cobalt, cobalt with increased carbon concentration. Tools made of high-speed steel are characterized by very good cutting properties up to a temperature of 650°C. HSS steel is mainly used to produce multi-edge cutting tools such as milling cutters, reamers, drills and taps.

Sintered carbide is currently one of the most commonly used materials for cutting tools. This group includes tungsten carbides, tantalum carbides, titanium carbides and niobium carbides. The binding metal is cobalt. Due to their application, most sintered carbides are divided into three basic groups:

- group P (blue) – intended for machining steel, cast steel and malleable cast irons that produce long chips;
- group K (red) – intended for cutting cast iron, hardened steel giving a short chip and for cutting non-metallic materials;
- group M (yellow) – intended for processing non-ferrous metals, stainless steel, heat-resistant steel and creep-resistant steel.

Sintered carbides are characterized by thermal resistance up to a temperature of approx. 1000°C. Carbide sinters are most often found in the form of plates that are mounted in cutting tools [24, 134].

The purpose of machining processes is to give the machined material specific shapes and dimensions. As a result of these actions, a surface layer is created on the workpiece, which is characterized by properties different from the deeper layers of the material, referred to as the material core. The surface layer is defined, inter alia, in the PN-87/M-045250 standard: "Surface layer - the outer layer of a material bounded by the actual surface of an object, including this surface and the part of the material deeper than the actual surface which exhibits changed physical and sometimes chemical properties in relation to the properties of the core material."

The surface layer has a structural structure. It can be divided into several characteristic zones that differ in their physical characteristics. The number, location and thickness of individual zones depend on the machining process parameters [93, 95, 97, 99]. Individual zones can interpenetrate each other and occupy a common space. The simplest model of the surface layer consists of three layers. A single layer includes, inter alia: phases, grains, grain arrangements, crystallites [93, 94, 95, 98, 110].

The layers or zones in the basic three-zone model are defined as follows [24, 67, 68, 69, 70]:

- outer zone; has a thickness of 0.001 μm to 0.02 μm; it consists mainly of residues of machining processes, such as coolant particles, elements of the tool material and foreign components (dust, moisture, dirt);
- middle zone; has a thickness from 0.5 μm to 500 μm; it consists of deformed grains of native material; the properties and structure of the middle zone influence the operational properties of the technological surface layer;
- inner zone; it consists of less deformed grains, however, it has a structure that differs from the structure of material core; in reality, there is no clear boundary between the inner zone and the material core; the inner boundary is determined mainly by the distribution of residual stress.

Fig. 7 shows the simplest, structural, three-layer model of the surface layer structure.

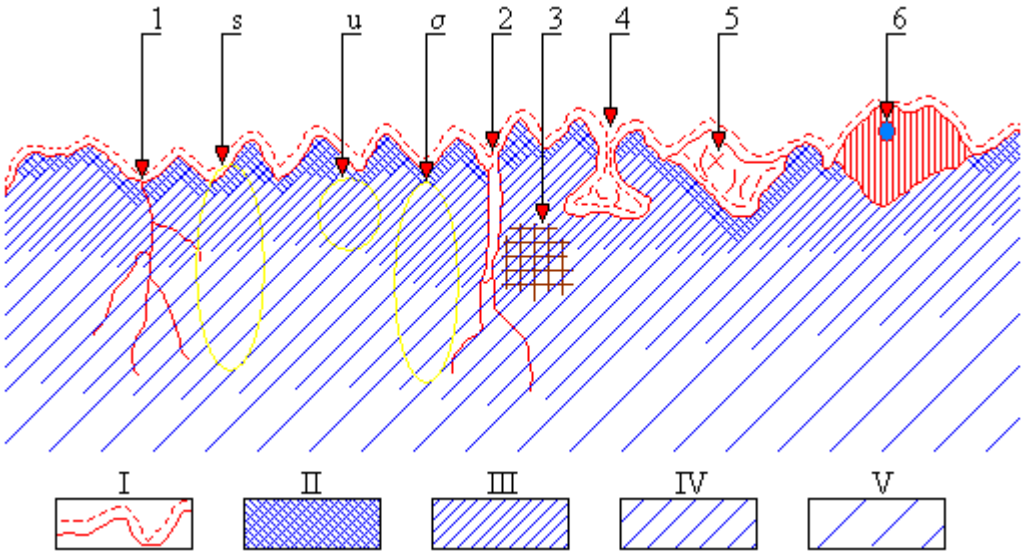

Fig. 7. Zones characterizing the surface layer of a solid body in a three-layer model [24, 67, 68, 69, 70]
1 – microcrack; 2 – crack; 3 – microshrinkage; 4 – porosity; 5 – void; 6 – inclusion; s – structure of the surface layer; u – strengthening of the middle zone; σ – residual stress in the surface layer; I – gas shell; II – outer zone; III – middle zone; IV – inner zone; V – core

It should be stressed that there is a strengthened zone on the surface of the machined workpiece. In the atmospheric environment, an oxidized layer is formed on it, which consists of adsorbed gases, moisture and pollutants [67, 68, 69, 70]. A cross-section of such a model of the surface layer structure is shown in Fig. 8.

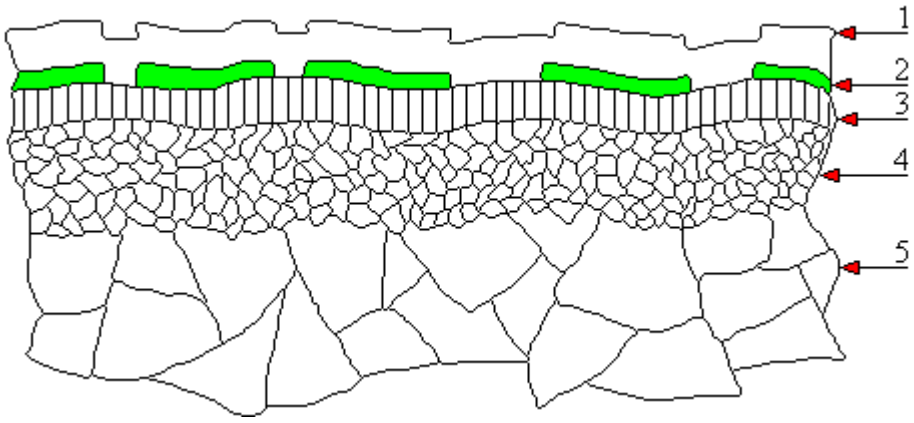

Fig. 8. Cross-section of the surface layer in metalworking [24]
1 – impurities; 2 – adsorbed gas; 3 – oxides; 4 – strengthening zone; 5 – core

Fig. 9 and Fig. 10 shows the appearance of an example of a formed cutter and a gear cutter often used in the milling process.

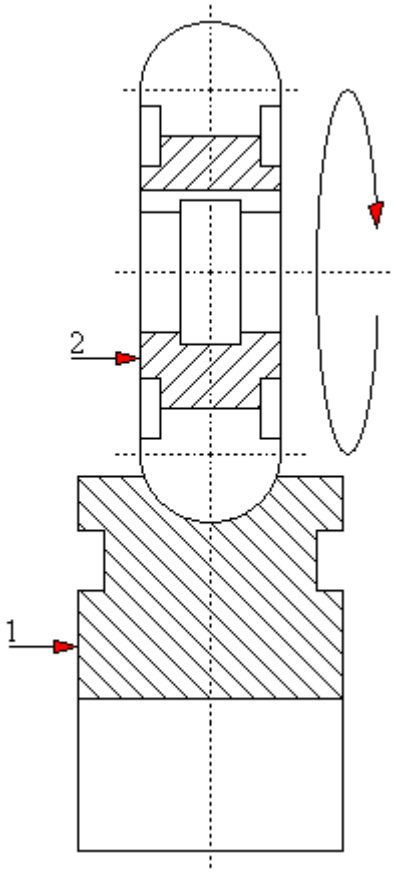

Fig. 9. Formed cutter
1 – workpiece; 2 – formed cutter

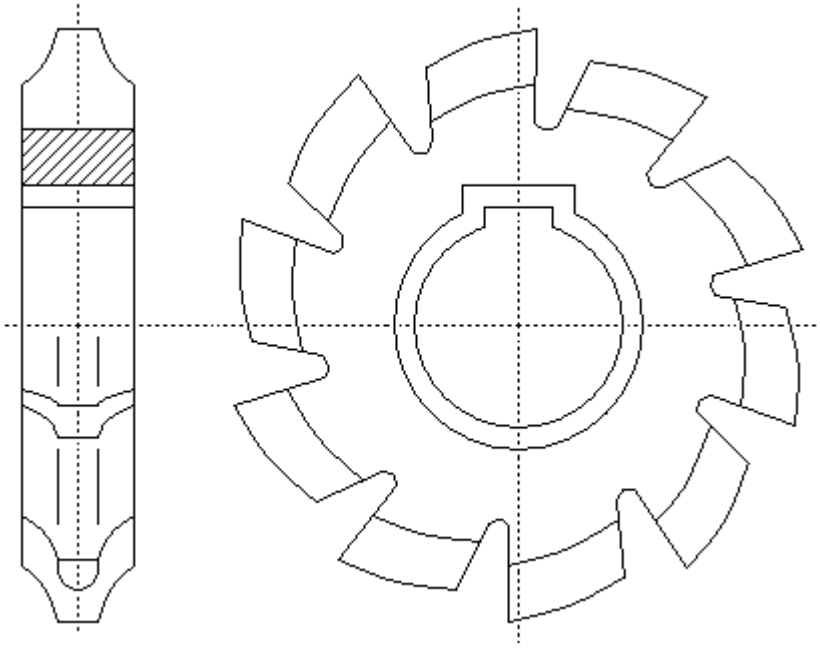

Fig. 10. Gear cutter

The most well-known method for assessing the residual stress distribution is the Weissmann-Philips method of removing material layers. This device allows the examination

of elements with a constant rectangular cross-section along their entire length. The diagram of the stress measuring device is shown in Fig. 11. Stress measurement involves removing the surface layer in an etching process. The test sample, placed on two supports, is immersed in a tank with electrolyte, and then part of the material is removed in an electrochemical reaction. During this process, the deflection is continuously recorded using an inductive sensor. In the next step, the data from the inductive sensor, together with information about the thickness of the removed material layer, are transferred to the calculation program on the computer which uses a calculation algorithm to determine the distribution of residual stress in the surface layer. During this test, some interference may occur. The interference may be due to the heating of the sample and electrolyte or a sudden change in the deflection value when the power is turned on. Therefore, it is advisable to use a cooling system for the electrolyte tank [46, 47, 143].

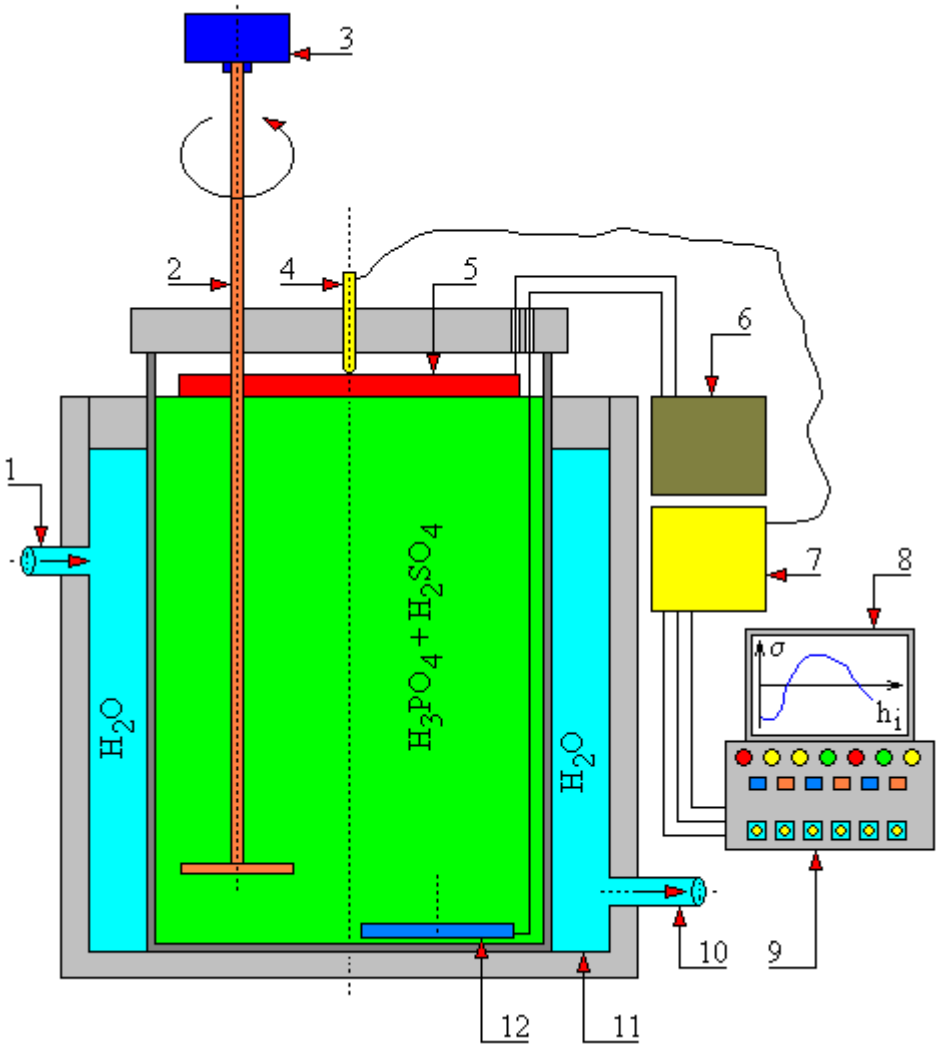

Fig. 11. Schematic diagram of the station for measuring residual stress on thin rectangular samples machined electrochemically
1 – cooling water inlet; 2 – stirrer; 3 – electric motor; 4 – small displacement electric sensor; 5 – tested sample (anode); 6 – current stabilizer; 7 – analog signal amplifier; 8 – monitor; 9 – computer; 10 – cooling water outlet; 11 – cooling water tank; 12 – cathode; h_i – thickness of the removed layer in the tested sample; σ – stress in the tested sample

2. Author's own testing

During machining of a given element, certain deformations occur in it resulting from the impact of residual stress occurring in the newly created surface layer of the machined object. The size of deformation depends on the state of residual stress and the dimensions of the workpiece. It should be assumed that in objects of relatively small thickness (thin), these stress will have the greatest influence on deformation.

The experimental test was carried out on a strip with dimensions of 30x10x320 mm (Fig. 14) made of unalloyed structural steel S 235JR. This material was chosen because of its widespread use in mechanical engineering. The chemical composition of S 235JR steel is presented in Table 1, and its mechanical properties in Table 2.

Table 1. Chemical composition of unalloyed structural steel S235JR

Steel grade	Chemical composition [%]				
	C	Mn	Si	P_{max}	S_{max}
S 235JR	0.17	1.4	------	0.045	0.045

where: C – carbon; Mn – manganese; Si – silicon; Pmax – phosphorus; Smax - sulfur

Table 2. Mechanical properties of unalloyed structural steel S235JR

Impact strength at 20°C	Tensile strength	Yield point	Elongation
[J/cm^2]	[MPa]	[MPa]	[%]
27	340÷470	235	26

Machining was performed on a 6P82 conventional milling machine (Fig. 12) with NFPc 40 DIN 845 BKN HSS milling cutter (Fig. 13) [143, 146, 147, 148]. The technical data of the 6P82 conventional milling machine are presented in Table 3. And Table 4 presents technical data of the milling cutter NFPc 40 DIN 845 BKN HSS.

Table 3. Technical data of the 6P82 conventional milling machine

Overall dimensions of the table	1350x320 mm
Working dimensions of the table	1250x320 mm
Maximum table displacement	• lengthwise: 800 mm; • crosswise: 250 mm; • vertical: 370 mm.
Spindle revolutions	• minimum: 31.5 rpm • 1600 rpm
Main engine power	5.5 kW

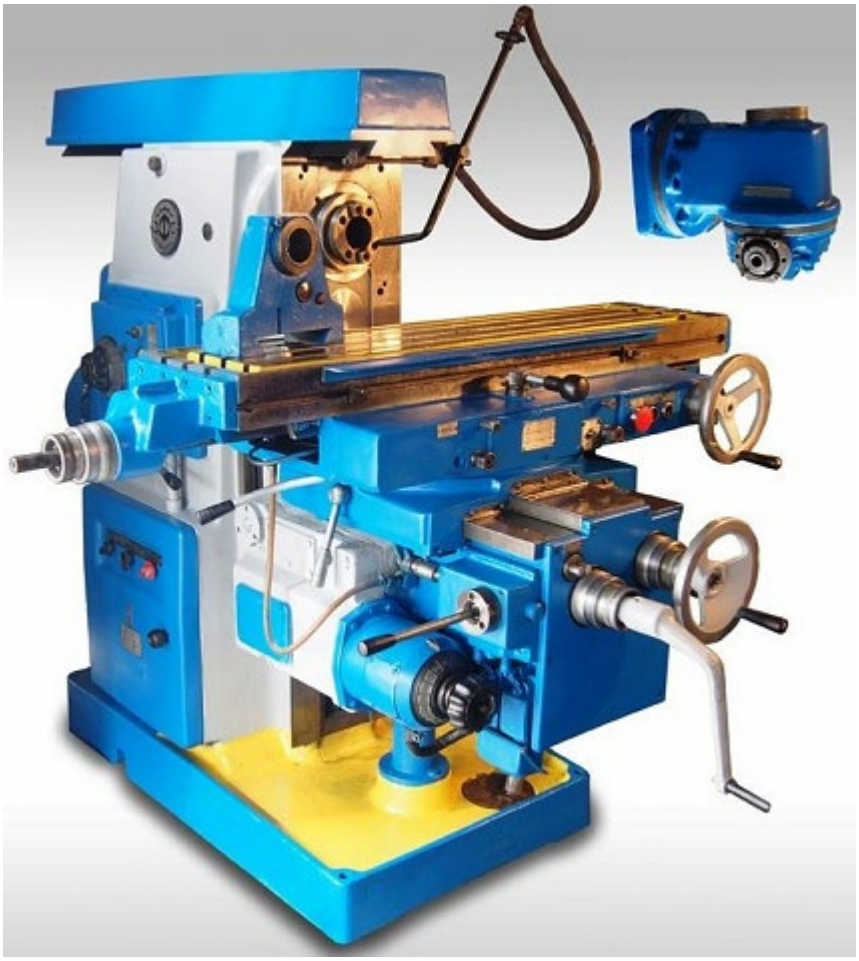

Fig. 12. General view of the 6P82 conventional milling machine

Fig. 13. NFPc 845 DIN BKN HSS milling cutter

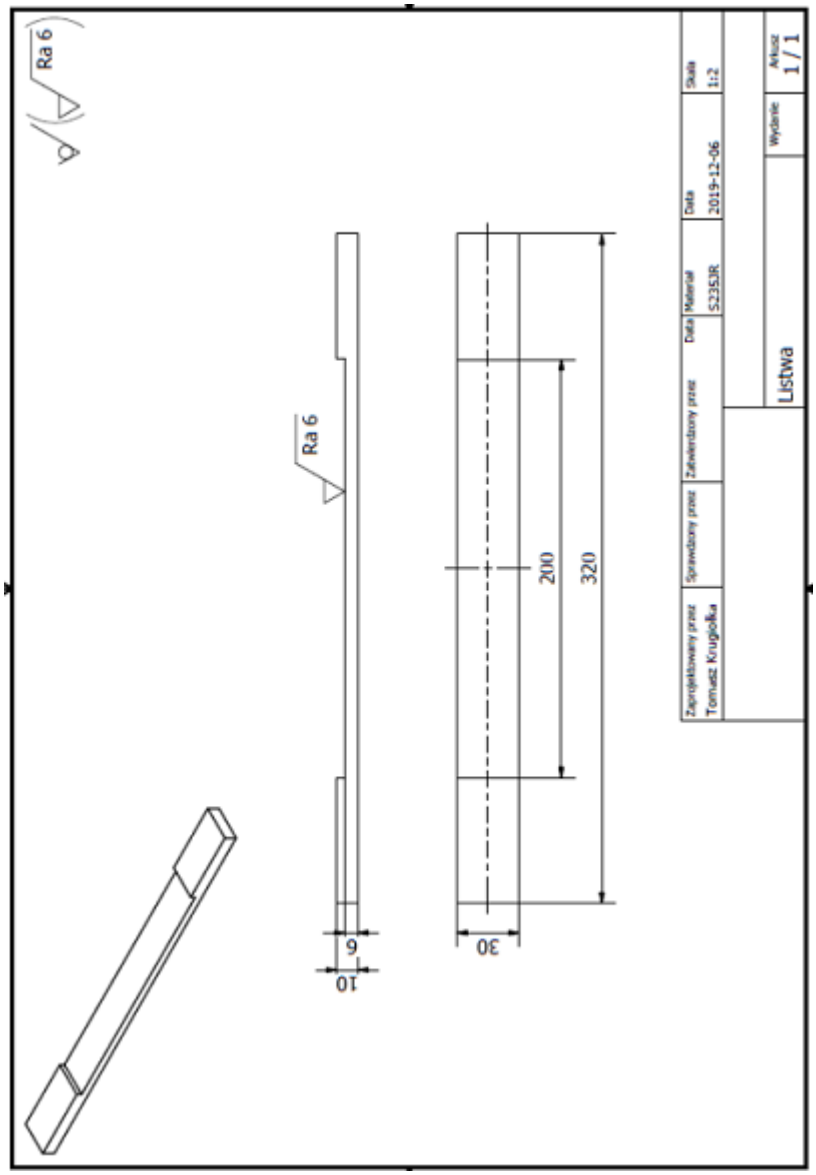

Fig. 14. Tested strip

Table 4. Technical data of the milling cutter NFPc 845 DIN BKN HSS

Working diameter D	Ø 40 mm
Length of working part l	53 mm
Total length L	178 mm
Morse taper number	4
Number of blades Z	6
Flutes inclination angle λ's	30°

The strip was machined using the peripheral, counter-rotating milling method. To improve cutting conditions, an emulsion cutting fluid was used. The tool (milling cutter) made of HSS high-speed steel used for machining showed no signs of wear on the blades. While milling the strip, the ambient temperature was +20°C. The workpiece strip material was mounted on the machine using two clamping lugs located at the ends of the workpiece. Fig.

15 shows a view of the milled strip. And Table 5 shows the cutting parameters of the machined strip.

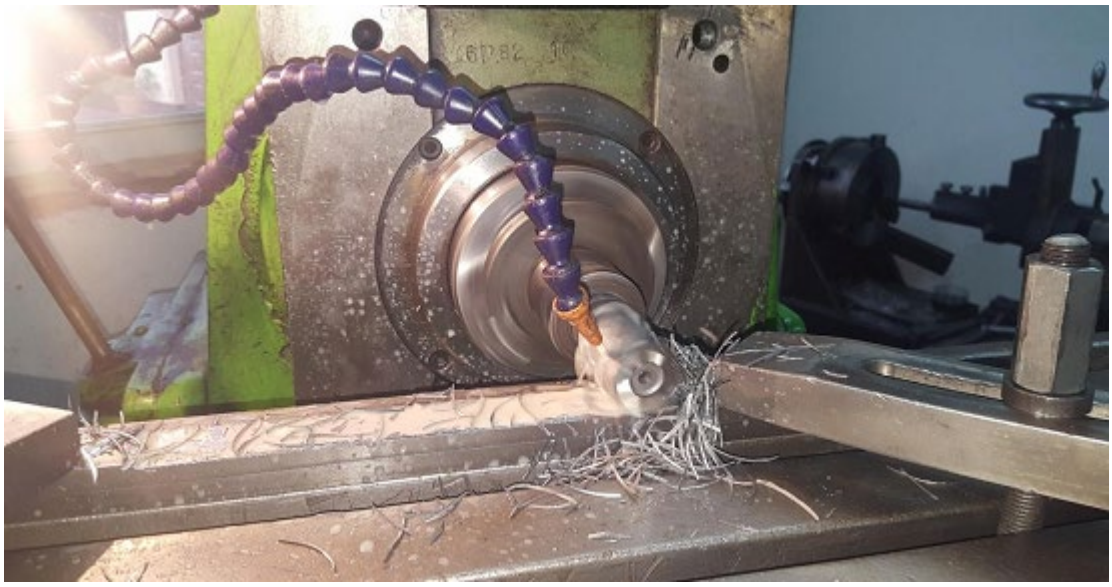

Fig. 15. Milling of the tested strip

Table 5. Cutting parameters of the machined strip

Cutting speed [Vc]	39.6 m/min
Revolutions [n]	315 rpm
Rate of feed [f]	250 mm/min
Cutting depth [a_p]	2 mm
Number of tool passes [i]	2

As a result of the milling process we got a deformed strip. Its greatest deflection was located in the middle of its length (Fig. 16). The deflection f was measured three times (Fig. 17). The measurement results of the maximum deflection f [mm] are presented in Table 6.

Fig. 16. View of the deformed element after milling

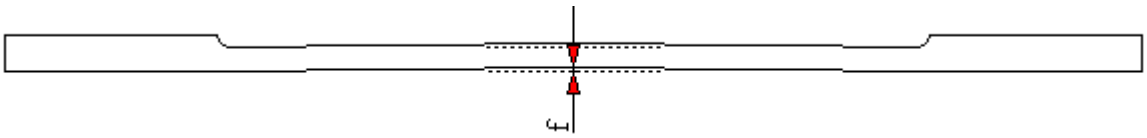

Fig. 17. Measurement of the deflection f [mm] of the milled strip

Table 6. Measurement results of the maximum deflection f [mm] of the milled strip

Measurement 1	2.30 mm
Measurement 2	2.34 mm
Measurement 3	2.30 mm
Average value	2.31(3) mm

Then, an attempt was made to find cutting parameters that would allow to obtain the smallest possible deformation of the workpiece. The magnitude and distribution of internal stress in the cut element depend on two factors: cutting forces and temperature in the cutting zone. Therefore, three types of milling tests were carried out on identical elements (Fig. 14) by changing: cutting speed, machining method and type of tool used. For each test, three measurements of the deflection f were made.

Type I tests concern peripheral milling in reverse rotation using an NFPc 40 DIN 845 BKN HSS milling cutter. Machined was a strip (Fig. 14) made of S 235 JR steel with dimensions of 30x10x320 mm. The tests were carried out on a 6P82 conventional milling machine. To improve cutting conditions, an emulsion cutting fluid was used. The tool (milling cutter) used for machining made of HSS high-speed steel showed no signs of wear on the

blades. During tests of milling the strip, the ambient temperature was +20°C. The milled strip material was mounted on the machine using two clamping lugs located at the ends of the workpiece.
Fig. 18 shows a view of milling for type I tests. Table 7 presents the cutting parameters for type I tests. Table 8 presents a summary of the deflection measurements for individual type I tests. And Table 9 presents average values of the deflection f for the individual speeds V_c of type I tests.

Fig. 18. View of milling for type I tests

Table 7. Cutting parameters for type I tests

Parameter	Test A	Test B	Test C
Cutting speed [Vc]	5 [m/min]	39.6 [m/min]	79.2 [m/min]
Revolutions [n]	40 rpm	315 rpm	630 rpm
Rate of feed [f]	48 [mm/min]	250 [mm/min]	750 [mm/min]
Cutting depth [a_p]	2 [mm]	2 [mm]	2 [mm]
Number of tool passes [i]	2	2	2

Table 8. Deflection measurements for individual type I tests

Test	Measurement No. 1	Measurement No. 2	Measurement No. 3	Average value
Test IA	2.30 mm	2.28 mm	2.32 mm	2.30 mm
Test IB	2.30 mm	2.34 mm	2.30 mm	2.31 mm
Test IC	2.34 mm	2.44 mm	2.40 mm	2.39 mm

Table 9. Average values of the deflection f for the individual speeds V_c of type I tests.

Test	Cutting speed [V_c]	Deflection f (average value)
IA	5 [m/min]	2.30 mm
IB	39.6 [m/min]	2.31 mm
IC	79.2 [m/min]	2.39 mm

Type II tests concern up face milling using an NFPc 40 DIN 845 BKN HSS milling cutter. Applied was the method of partial symmetrical milling. Machined was a strip (Fig. 14) made of S 235 JR steel with dimensions of 30x10x320 mm. The tests were carried out on a 6P82 conventional milling machine. To improve cutting conditions, an emulsion cutting fluid was used. The tool (milling cutter) used for machining, which was made of HSS high-speed steel, showed no signs of wear on the blades. During tests of milling the strip, the ambient temperature was +20°C. The milled strip material was mounted on the machine using two clamping lugs located at the ends of the workpiece.

Fig. 19 shows a view of milling for type II tests. Table 10 presents the cutting parameters for type II tests. Table 11 presents a summary of the deflection measurements for individual type II tests. And Table 12 presents average values of the deflection f for the individual speeds V_c of type II tests.

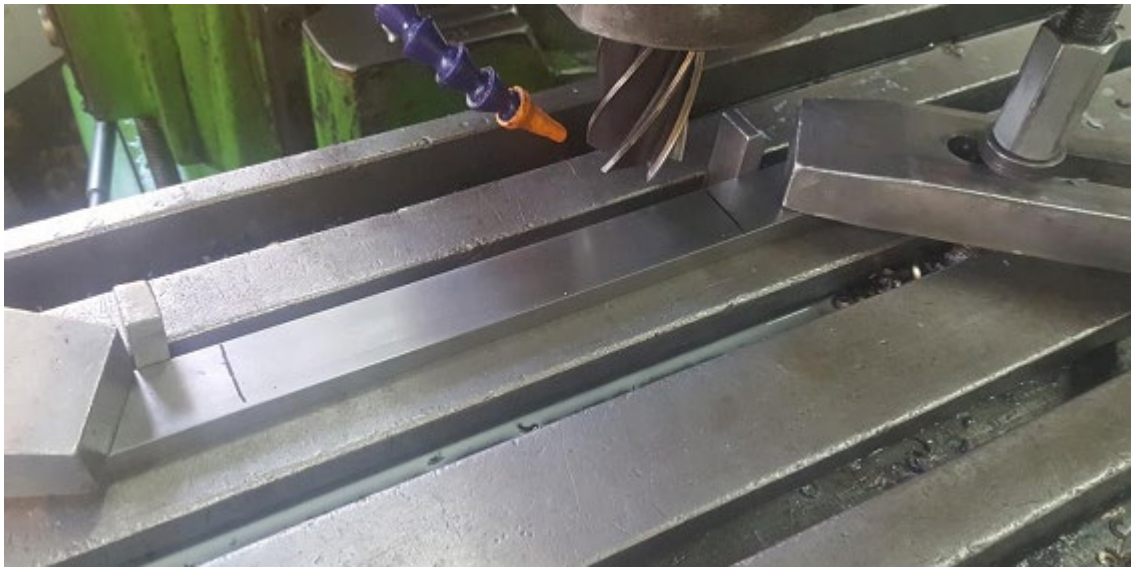

Fig. 19. View of milling for type II tests

Table 10. Cutting parameters for type II tests

Parameter	Test A	Test B	Test C	Test D
Cutting speed [Vc]	5 [m/min]	39.6 [m/min]	79.2 [m/min]	100.5 [m/min]
Revolutions [n]	40 rpm	315 rpm	630 rpm	800 rpm
Rate of feed [f]	48 [mm/min]	250 [mm/min]	750 [mm/min]	950 [mm/min]
Cutting depth [a_p]	2 [mm]	2 [mm]	2 [mm]	2 [mm]
Number of tool passes [i]	2	2	2	2

Table 11. Deflection measurements for individual type II tests

Test	Measurement No. 1	Measurement No. 2	Measurement No. 3	Average value
Test IIA	2.26 mm	2.28 mm	2.24 mm	2.26 mm
Test IIB	2.30 mm	2.30 mm	2.30 mm	2.30 mm
Test IIC	2.32 mm	2.30 mm	2.30 mm	2.31 mm
Test IID	2.26 mm	2.24 mm	2.24 mm	2.25 mm

Table 12. Results of the average values of the deflection f for the individual speeds V_c of type II tests.

Test	Cutting speed [V_c]	Deflection f (average value)
IIA	5 [m/min]	2.26 mm
IIB	39.6 [m/min]	2.30 mm
IIC	79.2 [m/min]	2.31 mm
IID	100.5 [m/min]	2.25 mm

Type III tests concern upstream face milling. Applied was the method of partial symmetrical milling. Machined was a strip (Fig. 14) made of S 235 JR steel with dimensions of 30x10x320 mm. The tests were carried out on a 6P82 conventional milling machine and an 80 mm TRI-SQ Indexa IND 1393420 milling head with multi-edge inserts. To improve cutting conditions, an emulsion cutting fluid was used. The tool used for machining is a milling head in which mounted are multi-edge inserts made of sintered carbide. No signs of blade wear were found. During tests of milling the strip, the ambient temperature was +20°C. The milled strip material was mounted on the machine using two clamping lugs located at the ends of the workpiece.

Fig. 20 shows a view of the milling head used. And Fig. 21 shows a view of performer milling for type III tests. Table 13 presents cutting parameters for type III tests. Table 14 presents a summary of the deflection measurements for individual type III tests. And Table 15 presents average values of the deflection f for individual speeds Vc of type III tests.

Fig. 20. View of the 80mm TRI-SQ Indexa IND1393420 milling head with SM25T multi-edge inserts

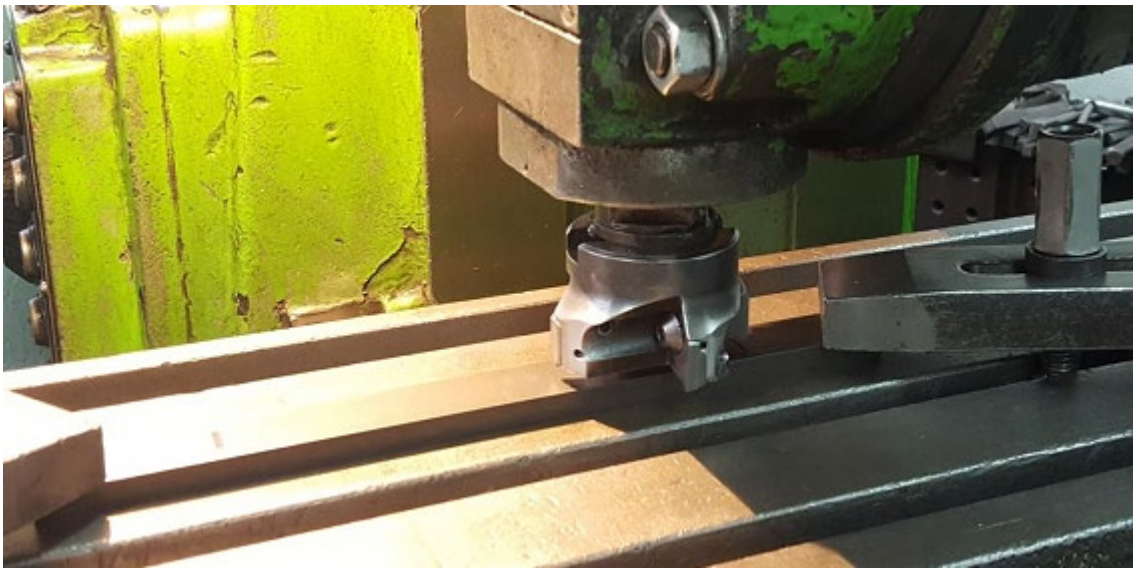

Fig. 21. View of milling for type III tests

Table 13. Cutting parameters for type III tests

Parameter	Test A	Test B
Cutting speed [Vc]	63 [m/min]	201 [m/min]
Revolutions [n]	250 rpm	800 rpm
Rate of feed [f]	200 [mm/min]	640 [mm/min]
Cutting depth [a_p]	2 [mm]	2 [mm]
Number of tool passes [i]	2	2

Table 14. Deflection measurements for individual type III tests

Test	Measurement No. 1	Measurement No. 2	Measurement No. 3	Average value
Test IIIA	2.34 mm	2.36 mm	2.38 mm	2.36 mm
Test IIIB	2.44 mm	2.44 mm	2.44 mm	2.44 mm

Table 15. Average values of the deflection f for individual speeds V_c of type III tests

Test	Cutting speed [V_c]	Deflection f (average value)
IIIA	63 [m/min]	2.36 mm
IIIB	201 [m/min]	2.44 mm

3. Conclusion

The experimental verification carried out by milling one side of the strip confirmed the thesis that the machined element got deformed. Attempts to find cutting conditions that would ensure the absence of deformation have failed. Despite the change in machining conditions, the deformations of all machined elements were of similar magnitude.

This paper presents the problem of deformation of thin strips as a result of milling of one of their sides. It should be recognized that what impacts plastic deformation of the workpiece is the state of residual stress. The magnitude and distribution of residual stress depend on the forces that occur during the cutting process. and on the temperature in the cutting zone. Cutting forces create a mechanical model that generates compressive stress. However, high temperature in the cutting zone creates a thermal model responsible for tensile stress. In articles on machining it can be found that in most cases tensile stress occurs (dominates) in the newly formed surface layer. This may indicate that the influence of temperature is more important than the influence of cutting forces.

The lowest up peripheral cutting speed V_c=5 [m/min] turned out to be too high to generate compressive stress in the surface layer of the workpiece under test conditions. The influence of heat release was dominant. Further reduction of the cutting speed was considered pointless because of reduced efficiency of the milling process. Unfortunately, to get rid of

unwanted stress in the surface layer either heat treatment or straightening process must be applied.

4. Literature

1. Azarow A. S.: Mechanizacja i automatyzacja obróbki skrawaniem. Państwowe Wydawnictwo Techniczne, Warszawa, 1957 r.
2. Adamczak S.: Pomiary geometryczne powierzchni. Zarysy kształtu, falistości i chropowatości. Wydawnictwa Naukowo-Techniczne, Warszawa, 2008 r.
3. Brodowicz W.: Skrawanie i narzędzia, cz. I i II. Wydawnictwa Szkolne i Pedagogiczne. Warszawa, 1975.
4. Brzozowski D., Wieczorowski M., Gapiński B.: Pomiar geometrii i ocena powierzchni narzędzi za pomocą mikroskopu różnicowania ogniskowego. Mechanik 11/2017, s. 1020÷1022.
5. Dietrych J. i inni: Podstawy konstrukcji maszyn. Wydawnictwa Naukowo-Techniczne, Warszawa, 1968 r.
6. Dobrowolski Z.: Podręcznik spawalnictwa. Wydawnictwo WNT, Warszawa 1978.
7. Dobrzański T.: Poradnik konstruktora. Przyrządy i uchwyty obróbkowe. Wydawnictwa Naukowo-Techniczne, Warszawa, 1964 r.
8. Dobrzański T.: Uchwyty obróbkowe. Wydawnictwa Naukowo-Techniczne, Warszawa, 1967 r.
9. Dudik K.: Poradnik tokarza. Wydawnictwa Naukowo-Techniczne, Warszawa, 1958 r.
10. Domański A., Mikołajczyk J.: Dimensional analysis of the selected type of rolling bearing depending on the manufacturer. **W:** Szkoła Logistyki 2023 / redakcja naukowa Janusz Zawiła-Niedźwiecki, Katarzyna Białczak. Radom: Instytut Naukowo-Wydawniczy "Spatium", 2023, Poland; s. 79-89, p-ISBN: 978-83-67033-75-6;
e-ISBN: 978-83-67033-58-9.
11. Galon M., Mikołajczyk J.: The effect of laser cutting speed on the bearing surface of peaks and valleys of the cut surface. **W:** Logistyka w ratownictwie 2024 / pod redakcją Andrzeja Chudzikiewicza i Andrzeja Krzyszkowskiego. Radom: Instytut Naukowo-Wydawniczy Spatium, 2024, Poland; s. 71÷84, p-ISBN: 978-83-68026-24-5;
e-ISBN: 978-83-68026-25-2.
12. Galon M., Mikołajczyk J.: The effect of laser cutting speed on the weight of the workpiece. **W:** Logistyka w ratownictwie 2024 / pod redakcją Andrzeja Chudzikiewicza i Andrzeja Krzyszkowskiego. Radom: Instytut Naukowo-Wydawniczy Spatium, 2024, Poland; s. 85÷96, p-ISBN: 978-83-68026-24-5; e-ISBN: 978-83-68026-25-2.
13. Galon M., Mikołajczyk J.: Wpływ wartości posuwu podczas cięcia laserem na chropowatość powierzchni przecięcia. Obróbka Metalu; 2024, nr 3, s. 48÷53,
p-ISSN: 2081-7002; **https://obrobkametalu.tech/nasze-czasopismo/archiwum/**
14. Górski E.: Frezerstwo. Wydawnictwa Szkolne i Pedagogiczne, Warszawa, 1975 r.
15. Górski E.: Obróbka gładkościowa. Wydawnictwa Naukowo-Techniczne, Warszawa, 1963 r.
16. Górski E.: Poradnik narzędziowca. Wydawnictwa Naukowo-Techniczne, Warszawa, 1980 r.
17. Górski E.: Poradnik frezera. Wydawnictwa Naukowo-Techniczne, Warszawa, 1974 r.

18. Górski E.: Narzędzia i oprzyrządowanie narzędziowe. Automatyzacja obróbki skrawaniem. Wydawnictwa Naukowo-Techniczne, Warszawa, 1977 r.
19. Górski E.: Narzędzia do wiercenia i roztaczania głębokich otworów. Wydawnictwa Naukowo-Techniczne, Warszawa, 1962 r.
20. Grabowska M., Mikołajczyk J.: Zastosowanie tomografii komputerowej CAT w inżynierii materiałowej. Application of CAT scanning for materials engineering. Postępy w Inżynierii Mechanicznej [Developments in Mechanical Engineering]. 2017, nr 9 (5), s. 15÷26, p-ISSN: 2300-3383; Wydawnictwa Uczelniane Uniwersytetu Technologiczno-Przyrodniczego w Bydgoszczy, Poland. **http://wu.utp.edu.pl/oferta,8,1**
21. Grabowska M., Mikołajczyk J.: Próba zastosowania tomografii komputerowej CAT do określania struktury grafitu naturalnego w zależności od rozmiaru ziarna. An attempt to apply cat scanning to determine the natural graphite structure depending on the grain size. Postępy w Inżynierii Mechanicznej [Developments in Mechanical Engineering]. 2018, nr 12 (6), s. 5÷14, p-ISSN: 2300-3383; Wydawnictwa Uczelniane Uniwersytetu Technologiczno-Przyrodniczego w Bydgoszczy, Poland.
http://wu.utp.edu.pl/oferta,8,1
22. Grabowska M., Mikołajczyk J., Basiak S.: Zastosowanie tomografii komputerowej CAT w nieniszczących badaniach teowych złączy spawanych. Application of cat scanning in non-destructive testing of welded t-joints. Postępy w Inżynierii Mechanicznej [Developments in Mechanical Engineering]; 2018, nr 11 (6), s. 31÷44, p-ISSN: 2300-3383; Wydawnictwa Uczelniane Uniwersytetu Technologiczno-Przyrodniczego w Bydgoszczy, Poland. **http://wu.utp.edu.pl/oferta,8,1**
23. Grabowska M., Piochacz A., Mikołajczyk J.: Attempt to use computed tomography CAT to analyze the anodized layer. Postępy w Inżynierii Mechanicznej [Developments in Mechanical Engineering]; 2020, nr 15 (8), s. 25÷33, p-ISSN: 2300-3383; Wydawnictwa Uczelniane Uniwersytetu Technologiczno-Przyrodniczego im. J. J. Śniadeckich w Bydgoszczy, Poland. **https://dme.utp.edu.pl/art/15(8)2020/25.pdf**
DOI: 10.37660/dme.2020.15.8.3
24. Grzesik W.: Podstawy skrawania materiałów konstrukcyjnych. Wydawnictwa Naukowo-Techniczne, Warszawa, 2010.
25. Hołubowska A., Szałański B., Mikołajczyk J.: Laboratorium termodynamiki. Piła: Wydawnictwo Państwowej Uczelni im. Stanisława Staszica, 2020, Poland.; s. 164 , e-ISBN: 978-83-62617-93-7;
https://wydawnictwo.puss.pila.pl/files/Laboratorium_termodynamiki_POL_version.pdf
26. Jarmoliński Z., Mikołajczyk J.: Badania wpływu technologii cięcia stali na twardość powierzchni bijaka. Research of the influence of steel cutting technology on the strength of the hammer. Postępy w Inżynierii Mechanicznej [Developments in Mechanical Engineering]. 2018, nr 12 (6), s. 15÷30, p-ISSN: 2300-3383. Wydawnictwa Uczelniane Uniwersytetu Technologiczno-Przyrodniczego w Bydgoszczy, Poland.
http://wu.utp.edu.pl/oferta,8,1
27. Jaworski Z.: Obrabiarki. Wydawnictwa Szkolne i Pedagogiczne, Warszawa, 1975.
28. Jaworski Z.: Tokarstwo. Państwowe Wydawnictwo Szkolnictwa Zawodowego, Warszawa, 1972 r.
29. Jaworski Z.: Toczenie kształtowe. Państwowe Wydawnictwa Techniczne, Warszawa, 1958 r.
30. Jędrzejczyk D., Mikołajczyk J.: Defining the correlation between the cutting speed and roughness parameter Rz. **W:** MIK-21 : Międzynarodowa Innowacyjność i Konkurencyjność w XXI wieku : aspekty innowacyjne / redakcja naukowa Radosław Luft. Lublin : Fundacja Innowacji i Nowoczesnych Technologii INOTECH, 2022. Radom : nakładem Instytutu Naukowo-Wydawniczego "Spatium", 2022; s. 39÷46, p-ISBN: 978-83-67033-43-5;

e-ISBN: 978-83-67033-44-2;
http://inw-spatium.pl/wp-content/uploads/2022/09/MIK-21-2022-Aspekty-innowacyjne-2.pdf
31. Jędrzejczyk D., Mikołajczyk J.: Mathematical models of the influence of cutting speed on Ra parameter. Developments in Mechanical Engineering; 2022, nr 18 (10), s. 115÷129, p-ISSN: 2720-0639; Wydawnictwa Uczelniane Uniwersytetu Technologiczno-Przyrodniczego im. J.J. Śniadeckich w Bydgoszczy, Poland.
DOI: 10.37660/dme.2022.18.10.11
32. Jędrzejczyk D., Mikołajczyk J.: Wpływ prędkości skrawania na wybrany parametr warstwy wierzchniej. **W:** Logistyka w ratownictwie 2022 / pod redakcją Andrzeja Chudzikiewicza i Andrzeja Krzyszkowskiego. Radom: Instytut Naukowo-Wydawniczy Spatium, 2022, Poland; s. 75÷90, p-ISBN: 978-83-67033-57-2; e-ISBN: 978-83-67033-70-1.
33. Kiepuszewski B.: Technologia budowy maszyn. Państwowe Wydawnictwa Techniczne, Warszawa, 1960 r.
34. Kornberger Z.: Technologia budowy maszyn. Wydawnictwa Naukowo-Techniczne, Warszawa, 1965 r.
35. Latoś H., Mikołajczyk J.: Effect of partial wear of the tool point on the selected indicator of the machining process. **W:** Logistyka w ratownictwie 2023 / pod redakcją Andrzeja Chudzikiewicza i Anny Stelmach. Radom: Instytut Naukowo-Wydawniczy "Spatium", 2023, Poland; s. 195÷210, p-ISBN: 978-83-67033-95-4; e-ISBN: 978-83-67033-96-1.
36. Latoś H., Mikołajczyk J.: Thickness of the machined layer at milling with single-edge straight blades with an angle of $\lambda s \neq 0°$. **W:** MIK-21 : Międzynarodowa Innowacyjność i Konkurencyjność w XXI wieku : Aspekty innowacyjne / redakcja naukowa dr Łukasz Wojtowicz. Lublin: Fundacja Innowacji i Nowoczesnych Technologii INOTECH : nakładem Instytutu Naukowo-Wydawniczego "Spatium", 2023, Poland; s. 23÷27, p-ISBN: 978-83-67033-89-3; e-ISBN: 978-83-67033-90-9.
37. Latoś H., Mikołajczyk J., Konarski J., Mikołajczyk T.: Turning using self-induced vibration. **W:** MIK-21 : Międzynarodowa Innowacyjność i Konkurencyjność w XXI wieku : aspekty innowacyjne / redakcja naukowa dr Łukasz Wojtowicz, 2023, Poland; s. 187÷200, p-ISBN: 978-83-67033-89-3; e-ISBN: 978-83-67033-90-9.
38. Latoś H., Mikołajczyk J.: Vibration in machining. **W:** Logistyka w ratownictwie 2023 / pod redakcją Andrzeja Chudzikiewicza i Anny Stelmach. Radom: Instytut Naukowo-Wydawniczy "Spatium", 2023, Poland; s. 187÷194, p-ISBN: 978-83-67033-95-4; e-ISBN: 978-83-67033-96-1.
39. Latoś H., Mikołajczyk J.: The effect of feed rate on the roughness of machined surface. **W:** Szkoła Logistyki 2024 / redakcja naukowa Janusz Zawiła-Niedźwiecki, Adam Płaczek. Radom: Instytut Naukowo-Wydawniczy "Spatium", 2024, Poland; s. 217÷226, p-ISBN: 978-83-68026-07-8; e-ISBN: 978-83-68026-08-5.
40. Latour A.: Skrawalność metali i metody jej określania. Wydawnictwa Naukowo-Techniczne, Warszawa, 1962.
41. Matuszak J., Zalewski K.: Podstawy obróbki ubytkowej. Wydawnictwo Politechniki Lubelskiej, Lublin, 2016.
42. Matuszak J., Skoczylas A., Zalewski K.: Narzędzia skrawające. Ćwiczenia laboratoryjne. Wydawnictwo Politechniki Lubelskiej, Lublin, 2014.
43. Matuszewski M., Mikołajczyk J., Styp-Rekowski M: Modyfikacja cech środka smarującego za pomocą standardowych dodatków smarowych. Modification of lubricants features by means of standard additives. Postępy w Inżynierii Mechanicznej [Developments in Mechanical Engineering]. 2013, nr 1 (1), s. 57÷65, Wydawnictwo Uczelniane Uniwersytetu Technologiczno-Przyrodniczego w Bydgoszczy; p-ISSN: 2300-3383; http://wu.utp.edu.pl/uploads/oferta/Postepy_1_1_2013.pdf

44. Matuszewski M., Mikołajczyk J., Mikołajczyk T., Styp-Rekowski M.: Logistyczne aspekty zarządzania procesem naprawy. Logistical aspects of the repair process management. Logistyka, 2015, nr 4, s. 1991÷1997, p-ISSN: 1231-5478;
https://www.czasopismologistyka.pl/o-czasopismie/wydania
45. Matuszewski M., Mikołajczyk J., Mikołajczyk T., Styp-Rekowski M.: The influence of cooling and lubrication liquid quantity on the isotropy of a machine component surface during machining = Wpływ warunków chłodzenia i smarowania podczas obróbki elementów maszyn na stopień izotropowości ich powierzchni. Tribologia. 2016, vol. 265, No. 1, s. 57÷65, p-ISSN: 0208-7774; e-ISSN: 1732-422X;
https://t.tribologia.eu/resources/html/article/details?id=158175
46. Matyszkiewicz H., Szymanowicz T.: Ćwiczenia z technologii obróbki skrawaniem. Wydawnictwa Naukowo-Techniczne, Warszawa, 1963.
47. Miernik M.: Skrawalność metali. Metody określania i prognozowania. Oficyna Wydawnicza Politechniki Wrocławskiej, Wrocław, 2000.
48. Mikołajczyk J., Styp-Rekowski M., Świerk K.: Modyfikowanie cech środka smarującego za pomocą dodatków i komputerowe wspomaganie ich doboru. W: CAX' 2009 : Komputerowe Wspomaganie Nauki i Techniki : VI warsztaty naukowe, Bydgoszcz - Duszniki Zdrój 2009 : praca zbiorowa pod redakcją Tadeusza Mikołajczyka; p-ISBN: 978-83-61314-65-3. Wydawnictwa Uczelniane Uniwersytetu Technologiczno-Przyrodniczego w Bydgoszczy, Bydgoszcz 2009.
49. Mikołajczyk J.: Zestawienie porównawcze dodatków depresujących do olejów. W: Zaawansowana tribologia : XXX Ogólnopolska Konferencja Tribologiczna, Nałęczów, 21-24 września 2009 r. Ogólnopolska Konferencja Naukowa XXX Szkoły Tribologicznej "Zaawansowana Tribologia" : Wydział Materiałoznawstwa, Technologii i Wzornictwa Politechniki Radomskiej, Instytut Technologii Eksploatacji - PIB Radom oraz Komitet Budowy Maszyn, Sekcja Podstaw Eksploatacji Maszyn PAN. Wydawnictwo Naukowe Instytutu Technologii Eksploatacji - PIB, Radom, 2009.
50. Mikołajczyk J.: Zestawienie porównawcze własności fizykochemicznych dodatków smarnych w oleju podstawowym SAE-30. W: Terotechnologia 2009 : materiały konferencji na ekspozycji Metal i Control-Tech : Targi - Kielce (29.09-01.10.2009). VI Konferencja Naukowo-Techniczna "Terotechnologia 2009" : Politechnika Świętokrzyska, Centrum Laserowych Technologii Metali, Katedra Inżynierii Eksploatacji, Wydział Mechatroniki i Budowy Maszyn, Polskie Towarzystwo Naukowo-Techniczne, Towarzystwo Eksploatacyjne, Kielce: Wydawnictwo Politechniki Świętokrzyskiej, 2009. Seria: Zeszyty Naukowe - Politechnika Świętokrzyska, nr 13.
51. Mikołajczyk J., Matuszewski M.: Konstrukcja i sterowanie stanowiska do badań tribologicznych. W: CAX'2010 : komputerowe wspomaganie nauki i techniki : VII warsztaty naukowe, Bydgoszcz - Duszniki Zdrój 2010 : praca zbiorowa / pod red. Tadeusza Mikołajczyka. Bydgoszcz : Wydawnictwa Uczelniane Uniwersytetu Technologiczno-Przyrodniczego w Bydgoszczy, 2010; p-ISBN: 9788361314387.
52. Mikołajczyk J.: System rejestracji i wizualizacji warunków pracy stanowiska do badań tribologicznych. W: CAX'2011 : komputerowe wspomaganie nauki i techniki : VIII warsztaty naukowe, Bydgoszcz - Duszniki Zdrój 2011 : praca zbiorowa / pod redakcją Tadeusza Mikołajczyka. Bydgoszcz : Wydawnictwa Uczelniane Uniwersytetu Technologiczno-Przyrodniczego w Bydgoszczy, 2011; p-ISBN: 9788361314981.
53. Mikołajczyk J.: Badanie wpływu preparatu eksploatacyjnego Mind M na zmianę własności smarnych oleju bazowego SN-150. Inżynieria i aparatura chemiczna [Chemical Engineering and Equipment]. 2012, nr 5, s. 235÷236, p-ISSN: 0368-0827.
http://inzynieria-aparatura-chemiczna.pl/rok-2012-nr-5/

54. Mikołajczyk J., Styp-Rekowski M., Matuszewski M., Musiał J.: Einfluβ der kompositionen von schmierzusätzen auf die exploitations-eigenschaften der mischung mit Basisöl SN-150. W: Tribologie und mobilität : beiträge der tribotechnik zur optimierung von fertigungsprozessen, wartung, schmierung (reibungskonditionierung) und betriebssicherheit von verkehrsmitteln und verkehrswegen. Wien, 15 November 2012. Symposium 2012 "Tribologie und mobilität" : Österreichische Tribologische Gesellschaft. Österreichische Tribologische Gesellschaft, Wien, 2012.
55. Mikołajczyk J.: Einfluβ der ausgewählten schmierzstoffzusätze auf betriebseigenschaften der mischung mit Basisöl SN-150. **W:** Reibung, schmierung und verschleiβ : forschung und praktische anwendungen. Band 1. Tribologische systeme maschinenelemente und antriebstechnik fahrzeugtechnik prüfen, messen, kontrollieren. Göttingen, 22-24 September 2014. 55. Tribologie Fachtagung "Reibung, Schmierung und Verschleiβ" : Gesellschaft für Tribologie e.V. Stolberg-Venwegen : Gesellschaft für Tribologie e.V., 2014. Germany.
56. Mikołajczyk J.: Einfluss der ausgewählten zusatzschmierstoffe auf die intensivität des verschleiβprozesses (Ra, Rq, Δm) mit Basisöl SN-150. **W:** Tribologie in industrie und forschung : werkstoffe, konstruktion und technologie. Leoben, 26 November 2014. ÖTG Symposium 2014 "Tribologie in industrie und forschung" : Österreichische Tribologische Gesellschaft. Wien : Österreichische Tribologische Gesellschaft, 2014. Austria.
57. Mikołajczyk J., Matuszewski M.: Einfluss der ausgewählten schmierzstoffzusätze auf ΔT und ΔP mit Basisöl SN-150. **W:** Tribologie in industrie und forschung : werkstoffe, schmierstoffe und technologie. Wiener Neustadt, 25 November 2015, Austria. ÖTG Symposium 2015 "Tribologie in industrie und forschung" : Österreichische Tribologische Gesellschaft. Wiener Neustadt : Österreichische Tribologische Gesellschaft, 2015, s. 145-152.
58. Mikołajczyk J.: Vergleich charakteristischer parameter des abbott-firestone-diagramms für ein kinematisches paar mit konformem kontakt. **W:** Tribologie in industrie und forschung : verschleiβschutz, instandhaltung und anlagenzuverlässigkeit. Linz, 22-23 November 2016, Austria. ÖTG Symposium 2016 "Tribologie in industrie und forschung" : Österreichische Tribologische Gesellschaft. Wiener Neustadt : Österreichische Tribologische Gesellschaft, 2016; s. 105-110.
59. Mikołajczyk J.: Wpływ dodatków smarowych na transformację warstwy wierzchniej. Piła : Wydawnictwo Państwowej Wyższej Szkoły Zawodowej im. Stanisława Staszica, 2017r., Poland; 215 s., p-ISBN: 978-83-62617-76-0; www.ans.pila.pl
60. Mikołajczyk J.: Maszyny tarciowe : budowa, przeznaczenie. Piła, Wydawnictwo Państwowej Wyższej Szkoły Zawodowej im. Stanisława Staszica, 2018, Poland; 256 s., p-ISBN: 978-83-62617-86-9.
61. Mikołajczyk J.: Analiza statystyczna zmiany poboru mocy podczas procesu zużywania. Statistical analysis of the power variation of tribotester as a resultat of the wear process. Autobusy. Technika, Eksploatacja, Systemy Transportowe; 2019, nr 10-11, s. 83÷88, p-ISSN: 1509-5878; e-ISSN: 2450-7725; **http://yadda.icm.edu.pl/yadda/element/bwmeta1.element.baztech-21189602-884a-4d1a-bb60-9edaeae4af8d**
62. Mikołajczyk J.: Influence of consumables on the amount of power consumption of kinematic vapor of conformal contact. Wpływ PE na pobór mocy pary kinematycznej o styku konforemnym. Postępy w Inżynierii Mechanicznej [Developments in Mechanical Engineering]; 2019, nr 13 (7), s. 39÷50, p-ISSN: 2300-3383; Wydawnictwa Uczelniane Uniwersytetu technologiczno-Przyrodniczego im. J. J. Śniadeckich w Bydgoszczy, Poland. **http://yadda.icm.edu.pl/baztech/element/bwmeta1.element.baztech-2faf200b-3010-4192-9fd0-062f53b49d38**
63. Mikołajczyk J.: Statistical analysis of the mass variation of samples as a result of the wear process. Analiza statystyczna zmiany masy próbek w wyniku procesu zużywania. Postępy w

Inżynierii Mechanicznej [Developments in Mechanical Engineering]; 2019, nr 13 (7), s. 51÷61, p-ISSN: 2300-3383; Wydawnictwa Uczelniane Uniwersytetu Technologiczno-Przyrodniczego im. J. J. Śniadeckich w Bydgoszczy, Poland.
http://yadda.icm.edu.pl/baztech/element/bwmeta1.element.baztech-2faf200b-3010-4192-9fd0-062f53b49d38
64. Mikołajczyk J.: Tribotestery : budowa i przeznaczenie. Piła: Wydawnictwo Państwowej Wyższej Szkoły Zawodowej im. Stanisława Staszica, 2019, Poland; 160 s.,
e-ISBN: 978-83-62617-90-6; https://wydawnictwo.pwsz.pila.pl/files/Tribotestery.pdf
65. Mikołajczyk J.: Determining the energy validity of the Kostetsky's hypothesis on the basis of models for relative motion velocity v = 0.08 m/sec. Developments in Mechanical Engineering; 2020, nr 16 (8), s. 17÷29, p-ISSN: 2720-0639; Wydawnictwa Uczelniane Uniwersytetu Technologiczno-Przyrodniczego im. J.J. Śniadeckich w Bydgoszczy, Poland.
DOI: 10.37660/dme.2020.16.8.2
66. Mikołajczyk J.: Finding the correlation between wear of samples kinematic pair of conformal contact and electric power consumption. Postępy w Inżynierii Mechanicznej [Developments in Mechanical Engineering]; 2020, nr 15 (8), s. 59÷68,
p-ISSN: 2300-3383; Wydawnictwa Uczelniane Uniwersytetu Technologiczno-Przyrodniczego im. J. J. Śniadeckich w Bydgoszczy, Poland.
https://dme.utp.edu.pl/art/15(8)2020/59.pdf
DOI: 10.37660/dme.2020.15.8.6
67. Mikołajczyk J.: The effect of temperature lag on the value of power-temperature correlation for frictional pair of conformal contact. Postępy w Inżynierii Mechanicznej [Developments in Mechanical Engineering]; 2020, nr 15 (8), s. 79÷86,
p-ISSN: 2300-3383; Wydawnictwa Uczelniane Uniwersytetu Technologiczno-Przyrodniczego im. J. J. Śniadeckich w Bydgoszczy, Poland.
https://dme.utp.edu.pl/art/15(8)2020/79.pdf
DOI: 10.37660/dme.2020.15.8.8
68. Mikołajczyk J.: Określenie na podstawie modeli zmiany masy próbek w wyniku procesu zużywania. **W:** Szkoła Logistyki 2021 / redakcja naukowa Janusz Zawiła-Niedźwiecki, Piotr Korneta. Radom : Instytut Naukowo-Wydawniczy "Spatium", 2021; s. 167÷174, Poland;
p-ISBN: 978-83-66550-75-9; e-ISBN: 978-83-66550-89-6.
69. Mikołajczyk J.: A method of determining mathematical models of a seizure test of friction pairs. **W:** MIK-21 : Międzynarodowa Innowacyjność i Konkurencyjność w XXI wieku : aspekty innowacyjne / redakcja naukowa Radoslaw Luft. Lublin : Fundacja Innowacji i Nowoczesnych Technologii INOTECH, 2022. Radom : nakładem Instytutu Naukowo-Wydawniczego "Spatium", 2022; s. 7÷24, p-ISBN: 978-83-67033-43-5;
e-ISBN: 978-83-67033-44-2.
http://inw-spatium.pl/wp-content/uploads/2022/09/MIK-21-2022-Aspekty-innowacyjne-2.pdf
70. Mikołajczyk J.: Friction machines. Wydawnictwo Akademii Nauk Stosowanych im. Stanisława Staszica, Piła, 2022, Poland; 488 s., e-ISBN: 978-83-62617-96-8.
https://wydawnictwo.ans.pila.pl/files/FRICTION_MACHINES.pdf
71. Mikołajczyk J., Jędrzejczyk D.: Określenie korelacji między prędkością skrawania a parametrem chropowatości Ra. Obróbka Metalu; 2022, nr 3, s. 11÷15,
p-ISSN: 2081-7002; https://obrobkametalu.tech/
72. Mikołajczyk J.: Rolling bearing heating charakter. **W:** Szkoła Logistyki 2022. Radom: Instytut Naukowo-Wydawniczy "Spatium", 2022, Poland; s. 231÷239, Materiały z IX Konferencji Naukowej "Szkoła Logistyki 2022"; p-ISBN: 978-83-67033-33-6;
e-ISBN: 978-83-67033-34-3.
73. Mikołajczyk J.: Tribological properties of carbon black. **W:** Szkoła Logistyki 2022.

Radom: Instytut Naukowo-Wydawniczy "Spatium", 2022, Poland; s. 217-230, Materiały z IX Konferencji Naukowej "Szkoła Logistyki 2022"; p-ISBN: 978-83-67033-33-6;
e-ISBN: 978-83-67033-34-3.
74. Mikołajczyk J.: Determination of the modified coefficient of variation from the number of samples. **W:** MIK-21 : Międzynarodowa Innowacyjność i Konkurencyjność w XXI wieku : Aspekty innowacyjne / redakcja naukowa dr Łukasz Wojtowicz. Lublin: Fundacja Innowacji i Nowoczesnych Technologii INOTECH : nakładem Instytutu Naukowo-Wydawniczego "Spatium", 2023, Poland; s. 111÷122, p-ISBN: 978-83-67033-89-3;
e-ISBN: 978-83-67033-90-9.
75. Mikołajczyk J.: Effect of cutting speed on the shape of the machined surface profile. Mebutra; 2023, nr 1, s. 47÷63, Wydawnictwo Akademii Nauk Stosowanych im. S. Staszica w Pile, Piła 2023, Poland.
https://online.fliphtml5.com/vliuj/yunw/ p=48
76. Mikołajczyk J.: Friction Machines II. Piła: Wydawnictwo Akademii Nauk Stosowanych im. Stanisława Staszica w Pile, 2023, Poland; s. 598;
p-ISBN: 978-83-67684-00-2;
https://wydawnictwo.ans.pila.pl/files/FRICTION_MACHINES_V_ANS_PILA.pdf
77. Mikołajczyk J.: Oil can talk. **W:** Szkoła Logistyki 2023 / redakcja naukowa Janusz Zawiła-Niedźwiecki, Katarzyna Białczak. Radom: Instytut Naukowo-Wydawniczy "Spatium", 2023, Poland; s. 109÷115, p-ISBN: 978-83-67033-75-6;
e-ISBN: 978-83-67033-58-9.
78. Mikołajczyk J.: Pobór mocy elektrycznej przez parę kinematyczną jako parametr oceny jakości oleju. **W:** Logistyka w ratownictwie 2023 / pod redakcją Andrzeja Chudzikiewicza i Anny Stelmach. Radom: Instytut Naukowo-Wydawniczy "Spatium", 2023, Poland; s. 223-230, p-ISBN: 978-83-67033-95-4; e-ISBN: 978-83-67033-96-1.
79. Mikołajczyk J.: Rola dodatków smarowych w olejach. **W:** Logistyka w ratownictwie 2023 /pod redakcją Andrzeja Chudzikiewicza i Anny Stelmach/; Radom: Instytut Naukowo-Wydawniczy "Spatium", 2023, Poland; s. 231÷237, p-ISBN: 978-83-67033-95-4;
e-ISBN: 978-83-67033-96-1.
80. Mikołajczyk J.: Temperature as a parameter for assessing the work of a friction pair. **W:** Szkoła Logistyki 2023 / redakcja naukowa Janusz Zawiła-Niedźwiecki, Katarzyna Białczak. Radom: Instytut Naukowo-Wydawniczy "Spatium", 2023, Poland; s. 101-107,
p-ISBN: 978-83-67033-75-6; e-ISBN: 978-83-67033-58-9.
81. Mikołajczyk J.: Tire as a selected element of a car subject to diagnostics. **W:** Szkoła Logistyki 2023 / redakcja naukowa Janusz Zawiła-Niedźwiecki, Katarzyna Białczak. Radom: Instytut Naukowo-Wydawniczy "Spatium", 2023, Poland; s. 117÷131,
p-ISBN: 978-83-67033-75-6; e-ISBN: 978-83-67033-58-9.
82. Mikołajczyk J.: Wpływ dodatku modyfikującego cechy płynu obróbkowego na zmianę temperatury w strefie kontaktu współpracujących powierzchni. Obróbka Metalu; 2023, nr 2,
s. 43÷46, p-ISSN: 2081-7002;
https://obrobkametalu.tech/media/2023/05/2023_2_52_ObrobkaMetalu.pdf
83. Mikołajczyk J., Kozłowska M.A., Krasicki K.: Wpływ kompetencji cyfrowych pracowników na poziom rozwoju procesów przemysłowych. **W:** MIK-21 : Międzynarodowa Innowacyjność i Konkurencyjność w XXI wieku : aspekty społeczne /redakcja naukowa Radosław Luft/; Lublin-Radom : Fundacja Innowacji i Nowoczesnych Technologii INOTECH : nakładem Instytutu Naukowo-Wydawniczego "Spatium", 2023, Poland;
s. 149÷169, p-ISBN: 978-83-67033-92-3; e-ISBN: 978-83-67033-93-0.
84. Mikołajczyk J.: Zmiana geometrycznych cech współpracujących powierzchni miarą intensywności procesu zużywania ostrzy skrawających. Obróbka Metalu; 2023, nr 1, s. 50÷54, p-ISSN: 2081-7002;

https://yadda.icm.edu.pl/yadda/element/bwmeta1.element.baztech-9e73eb05-2a91-4df5-853b-22abf7a6ee77
85. Mikołajczyk J., Góra F., Jędrzejczyk D.: Analysis of selected surface roughness parameters for wear processes. Analiza wybranych parametrów chropowatości powierzchni pod kątem procesów zużywania. **W:** MIK-21 : Międzynarodowa Innowacyjność i Konkurencyjność w XXI wieku : Aspekty innowacyjne / redakcja naukowa Radosław Luft. Lublin: Wydawnictwo Naukowe FNCE, 2024; s. 93-117, p-ISBN: 978-83-68074-82-6; e-ISBN: 978-83-68319-03-3.
86. Mikołajczyk J., Galon M.: Mathematical model of straight regression determining the effect of laser cutting speed on the mass of the workpiece. **W:** MIK-21 : Międzynarodowa Innowacyjność i Konkurencyjność w XXI wieku : Aspekty innowacyjne / redakcja naukowa Radosław Luft. Lublin: Wydawnictwo Naukowe FNCE, 2024, Poland; s. 71÷92, p-ISBN: 978-83-68074-82-6; e-ISBN: 978-83-68319-03-3.
87. Mikołajczyk J., Sądej I.: Spinning speed and balancing accuracy. **W:** MIK-21 : Międzynarodowa Innowacyjność i Konkurencyjność w XXI wieku : Aspekty innowacyjne / redakcja naukowa Radosław Luft. Lublin: Wydawnictwo Naukowe FNCE, 2024, Poland; s. 118÷132, p-ISBN: 978-83-68074-82-6; e-ISBN: 978-83-68319-03-3.
88. Mikołajczyk J.: The correlation between the population and number of construction disasters. Mebutra; 2025, nr 3, s. 44-55, Wydawnictwo Akademii Nauk Stosowanych im. S. Staszica w Pile, Poland.
https://wydawnictwo.ans.pila.pl/files/MEBUTRA2025.pdf
89. Mikołajczyk J.: The relationship between the type of structure and the number of construction disasters. Zależność między rodzajem konstrukcji, a liczbą katastrof budowlanych. Mebutra; 2025, 3, s. 30÷43, Wydawnictwo Akademii Nauk Stosowanych im. S. Staszica w Pile, Poland.
https://wydawnictwo.ans.pila.pl/files/MEBUTRA2025.pdf
90. Miracki J.: Przeciąganie. Wydawnictwa Naukowo-Techniczne, Warszawa, 1969 r.
79. Niemczewska-Wójcik M.: Dualny system charakteryzowania powierzchni technologicznej i eksploatacyjnej warstwy wierzchniej elementów trących. Wydawnictwo Naukowe Instytutu Technologii Eksploatacji PIB, Kraków, 2018.
91. Norma PN-86/H-84018. Stal niskostopowa o podwyższonej wytrzymałości. Gatunki.
92. Norma PN-75/H-84019. Stal węglowa konstrukcyjne wyższej jakości ogólnego przeznaczenia. Gatunki.
93. Norma PN-EN ISO 25178-1. Specyfikacje geometrii wyrobów (GPS) - Struktura geometryczna powierzchni: Przestrzenna – Część 1: Oznaczanie struktury geometrycznej powierzchni.
94. Norma PN-EN ISO 25178-2. Specyfikacje geometrii wyrobów (GPS) – Struktura geometryczna powierzchni: Przestrzenna – Część 2: Terminy, definicje i parametry struktury geometrycznej powierzchni.
95. Norma PN-EN ISO 25178-6. Specyfikacje geometrii wyrobów (GPS) – Struktura geometryczna powierzchni: Przestrzenna – Część 6: Klasyfikacja metod pomiaru struktury geometrycznej powierzchni.
96. Norma PN-EN ISO 25178-70. Specyfikacje geometrii wyrobów (GPS) – Struktura geometryczna powierzchni: Przestrzenna – Część 70: Wzorce materialne.
97. Norma PN-EN ISO 25178-73. Specyfikacje geometrii wyrobów (GPS) – Struktura geometryczna powierzchni: Przestrzenna – Część 73: Wady powierzchni na obiektach materialnych; terminy i definicje.
98. Norma PN-EN ISO 1302:2004. Specyfikacje geometrii wyrobów (GPS) – Oznaczanie struktury geometrycznej powierzchni w dokumentacji technicznej wyrobu.

99. Norma PN-EN ISO 3274:2011. Specyfikacja geometrii wyrobów (GPS) – Struktura geometryczna powierzchni: Metoda profilowa – Charakterystyki nominalne przyrządów stykowych (z ostrzem odwzorowującym).
100. Norma PN-EN ISO 4287: 1999. Specyfikacje geometrii wyrobów – Struktura geometryczna powierzchni: Metoda profilowa – Terminy, definicje i parametry struktury geometrycznej powierzchni.
101. Norma PN-EN ISO 4288: 2011. Specyfikacje geometrii wyrobów (GPS) – Struktura geometryczna powierzchni: Metoda profilowa – Zasady i procedury oceny struktury geometrycznej powierzchni.
102. Norma PN-EN ISO 5436-1: 2002. Specyfikacje geometrii wyrobów (GPS) – Struktura geometryczna powierzchni: Metoda profilowa – Wzorce – Część 1: Wzorce materialne.
103. Norma PN-EN ISO 5436-1: 2013-04. Specyfikacje geometrii wyrobów (GPS) – Struktura geometryczna powierzchni: Metoda profilowa; Wzorce – część 2: Wzorce programowane.
104. Norma PN-EN ISO 8785: 2000. Specyfikacje geometrii wyrobów – Skazy powierzchni – Terminy, definicje i parametry.
105. Norma PN-EN ISO 16610-21: 2013-02. Specyfikacje geometrii wyrobów (GPS) – Filtrowanie – Część 21: Liniowe filtry profilu: Filtry Gaussa.
106. Norma PN-EN ISO 16610-30: 2017-04. Specyfikacje geometrii wyrobów (GPS) – Filtrowanie – Część 30: Odporne filtry profilu: Podstawowe pojęcia.
107. Norma PN-EN ISO 12085: 1999. Specyfikacje geometrii wyrobów – Struktura geometryczna powierzchni: Metoda profilowa – Parametry metody motywów.
108. Norma PN-EN ISO 12179: 2002. Specyfikacje geometrii wyrobów (GPS) – Struktura geometryczna powierzchni: Metoda profilowa – Wzorcowanie przyrządów stykowych (z ostrzem odwzorowującym).
109. Norma PN-EN ISO 13565-1: 1999. Specyfikacje geometrii wyrobów – Struktura geometryczna powierzchni – metoda profilowa – Powierzchnie o warstwowych właściwościach funkcjonalnych – Filtrowanie i ogólne warunki pomiaru.
110. Norma PN-EN ISO 13565-2: 1999. Specyfikacje geometrii wyrobów – Struktura geometryczna powierzchni – Metoda profilowa – Powierzchnie o warstwowych właściwościach funkcjonalnych – Opis wysokości za pomocą linearyzacji krzywej udziału materiałowego.
111. Okoniewski S.: Technologia metali, cz. I. Wydawnictwa Szkolne i Pedagogiczne, Warszawa, 1980.
112. Okoniewski S.: Technologia metali, cz. II. Wydawnictwa Szkolne i Pedagogiczne, Warszawa, 1980.
113. Okoniewski S.: Technologia metali, cz. III. Wydawnictwa Szkolne i Pedagogiczne, Warszawa, 1980.
114. Okoniewski S.: Technologia metali, cz. IV. Wydawnictwa Szkolne i Pedagogiczne, Warszawa, 1980.
115. Olechnowicz J., Mikołajczyk J.: Truck scales : the key to safe transport and road protection. Mebutra; 2024, nr 2, s. 3÷8, Wydawnictwo Akademii Nauk Stosowanych im. S. Staszica w Pile, Poland.
https://wydawnictwo.ans.pila.pl/files/MEBUTRA2024.pdf
116. Pikulik K.W., Mikołajczyk J.: The influence of the welding current on the air pollution emissions. Wpływ prądu spawania na emisję zanieczyszczeń powietrza. Postępy w Inżynierii Mechanicznej [Developments in Mechanical Engineering]; 2019, nr 14 (7), s. 33÷46, p-ISSN: 2300-3383; Wydawnictwa Uczelniane Uniwersytetu Technologiczno-Przyrodniczego im. J. J. Śniadeckich w Bydgoszczy, Poland.

http://yadda.icm.edu.pl/baztech/element/bwmeta1.element.baztech-2faf200b-3010-4192-9fd0-062f53b49d38
117. Pikulik K.W., Mikołajczyk J.: Determination of emission of iron oxides from the welding process on the basis of mathematical models. Welding Technology Review; 2021, vol. 93, No 2, s. 35÷43, p-ISSN: 0033-2364; e-ISSN: 2449-7959;
http://www.pspaw.wip.pw.edu.pl/index.php/pspaw/article/view/1132
DOI: 10.26628/wtr.v93i2.1132
118. Pikulik J., Pikulik K.W., Mikołajczyk J.: The relationship between the clearance of the coupling mechanism used in uniaxial light car trailers and the date of their production. **W:** MIK-21 : Międzynarodowa Innowacyjność i Konkurencyjność w XXI wieku : aspekty innowacyjne / redakcja naukowa Radosław Luft. Lublin : Fundacja Innowacji i Nowoczesnych Technologii INOTECH, 2022, Poland. Radom : nakładem Instytutu Naukowo-Wydawniczego "Spatium"; 2022; s. 221÷233, p-ISBN: 978-83-67033-43-5;
e-ISBN: 978-83-67033-44-2;
http://inw-spatium.pl/wp-content/uploads/2022/09/MIK-21-2022-Aspekty-innowacyjne-2.pdf
119. Pikulik J., Pikulik K.W., Mikołajczyk J.: Zależność wielkości luzu mechanizmu sprzęgającego stosowanego w jednoosiowych lekkich przyczepach samochodowych od wartości współczynnika przylegania. **W:** Logistyka w ratownictwie 2022 / pod redakcją Andrzeja Chudzikiewicza i Andrzeja Krzyszkowskiego. Radom: Instytut Naukowo-Wydawniczy "Spatium", 2022, Poland; s. 157÷167, p-ISBN: 978-83-67033-57-2;
e-ISBN: 978-83-67033-70-1.
120. Pikulik J., Pikulik K.W., Mikołajczyk J.: Determination of the degree of contact of the movable part of the coupling head with the ball part of the coupling of single-axle light car trailers. **W:** MIK-21 : Międzynarodowa Innowacyjność i Konkurencyjność w XXI wieku : aspekty innowacyjne / redakcja naukowa dr Łukasz Wojtowicz. Lublin: Fundacja Innowacji i Nowoczesnych Technologii INOTECH : nakładem Instytutu Naukowo-Wydawniczego "Spatium", 2023, Poland; s. 97÷109, p-ISBN: 978-83-67033-89-3;
e-ISBN: 978-83-67033-90-9.
121. Pilarczyk J.: Poradnik inżyniera. Spawalnictwo. t. 2. Wydawnictwa Naukowo-Techniczne, Warszawa, 2005.
122. Piochacz A., Mikołajczyk J.: Wpływ czasu trwania procesu anodowania stopu aluminium EN AW-6060 na grubość i twardość otrzymanej warstwy. Influence of aluminium type EN AW-6060 anodizing process duration on the thickness and hardness of the obtained layer. Postępy w Inżynierii Mechanicznej [Developments in Mechanical Engineering]; 2018, nr 12 (6), s. 49÷56, p-ISSN: 2300-3383; Wydawnictwa Uczelniane Uniwersytetu Technologiczno-Przyrodniczego w Bydgoszczy, Poland.
http://wu.utp.edu.pl/oferta,8,1
123. Piochacz A., Mikołajczyk J.: Analiza statystyczna wpływu czasu anodowania na grubość otrzymanej powłoki. Statistical analysis of the influence of anodizing time on the thickness of obtained layers. Autobusy. Technika, Eksploatacja, Systemy Transportowe; 2019, vol. 233, nr 9, s. 48÷51, p-ISSN: 1509-5878; e-ISSN: 2450-7725;
http://ceref.pl/index.php/Autobusy/article/view/956
DOI: 10.24136/atest.2019.201
124. Piochacz A., Mikołajczyk J.: Determination of the thickness of anodized layer on the basis mathematical models. Developments in Mechanical Engineering; 2020, nr 16 (8), s. 31÷39, p-ISSN: 2720-0639; Wydawnictwa Uczelniane Uniwersytetu Technologiczno-Przyrodniczego im. J.J. Śniadeckich w Bydgoszczy, Poland.
DOI: 10.37660/dme.2020.16.8.3

125. Piotrowski Ł., Góra F., Mikołajczyk J.: Construction of an electric longboard with one-wheel driver. Mebutra; 2024, nr 2, s. 16÷27, Wydawnictwo Akademii Nauk Stosowanych im. S. Staszica w Pile, Poland.
https://wydawnictwo.ans.pila.pl/files/MEBUTRA2024.pdf
126. Piotrowski Ł., Góra F., Mikołajczyk J.: Design and construction of an electric longboard. **W:** Logistyka w ratownictwie 2024 / pod redakcją Andrzeja Chudzikiewicza i Andrzeja Krzyszkowskiego. Radom: Instytut Naukowo-Wydawniczy Spatium, 2024, Poland; s. 167÷178, p-ISBN: 978-83-68026-24-5; e-ISBN: 978-83-68026-25-2.
127. Pokutycki J.: Podstawy automatyki. Państwowe Wydawnictwo Szkolnictwa Zawodowego, Warszawa, 1970 r.
128. Praca zbiorowa: Poradnik inżyniera spawalnictwa. Wydawnictwa Naukowo-Techniczne. Warszawa 1983.
129. Przybył B., Kabat M., Mikołajczyk J.: Wpływ prędkości drukowania 3D na dokładność zarysu kół zębatych. Obróbka Metalu; 2023, nr 4, s. 26÷30, p-ISSN: 2081-7002;
https://obrobkametalu.tech/media/2023/08/2023-4_Nr54_ObrobkaMetalu.pdf
130. Przybył B., Mikołajczyk J.: Efektywność technik przyrostowych. Obróbka Metalu; 2024, nr 1, s. 22÷25, p-ISSN: 2081-7002;
https://obrobkametalu.tech/media/2024/03/2024_1_nr55_ObrobkaMetalu-1.pdf
131. Przybył B., Mikołajczyk J.: The influence of 3D printing speed on profile accuracy. **W:** Szkoła Logistyki 2024 / redakcja naukowa Janusz Zawiła-Niedźwiecki, Adam Płaczek. Radom: Instytut Naukowo-Wydawniczy "Spatium", 2024, Poland; s. 199÷216, p-ISBN: 978-83-68026-07-8; e-ISBN: 978-83-68026-08-5.
132. Rodziewicz M.: Wygładzanie luźnym ścierniwem w pojemnikach. Wydawnictwa Naukowo-Techniczne, Warszawa, 1964 r.
133. Sądej I., Mikołajczyk J.: Machine tool compensation and mass unbalance measurements. **W:** Logistyka w ratownictwie 2024 / pod redakcją Andrzeja Chudzikiewicza i Andrzeja Krzyszkowskiego. Radom: Instytut Naukowo-Wydawniczy Spatium, 2024, Poland; s. 187÷196, p-ISBN: 978-83-68026-24-5; e-ISBN: 978-83-68026-25-2.
134. Storch B.: Podstawy obróbki skrawaniem. Wydawnictwo Uczelniane Politechniki Koszalińskiej, Koszalin, 2001.
135. Styp-Rekowski M., Mikołajczyk J.: The influence of Mind M preparation on the lubricant properties of base oil SN-150. W**:** Reinung, Schmierung und Verschleiβ : forschung und praktische anwendungen : Band 1 : tribologische systeme schmierstoffe und schmierungstechnik zerspanungs : und umformtechnik prüfen, messen, kontrollieren / 53. Tribologie-Fachtagung. 24.bis 26. Septembet 2012 in Göttingen. Aachen : Gesellschaft für Tribologie e.V., 2012. p-ISBN: 978-3-00-039201-6.
136. Styp-Rekowski M., Mikołajczyk J.: Wpływ dodatku na własności smarowe oleju bazowego SN-150. Tribologia. 2012, vol. 244, No. 4, s. 227-232, p-ISSN: 0208-7774;
e-ISSN: 1732-422X; https://t.tribologia.eu/resources/html/article/details?id=167726
137. Styp-Rekowski M., Mikołajczyk J.: Wpływ preparatu eksploatacyjnego stanowiący kompleks węglowodorowy na zmianę własności smarnych oleju bazowego SN-150. W: Tribologia bliżej praktyki : XXXII Ogólnopolska Konferencja "Jesienna Szkoła Tribologiczna 2012". XXXII Ogólnopolska Konferencja "Jesienna Szkoła Tribologiczna 2012", Kudowa Zdrój, 18-21 września 2012r. Politechnika Wrocławska Wydział Mechaniczny, Instytut Konstrukcji Eksploatacji Maszyn, Polskie Towarzystwo Tribologiczne, Sekcja Podstaw Eksploatacji KBM PAN. Wrocław : Polskie Towarzystwo Tribologiczne, 2012.
138. Styp-Rekowski M., Mikołajczyk J.: Zmiana temperatury na drodze tarcia dla kompozycji olej bazowy SN-150 - preparat eksploatacyjny Mind M. Temperature variability during friction for composition bese oil SN-150 - exploatational preparation Mind M. **W:** III krajowa

konferencja nano- i mikromechaniki / Komitet Mechaniki Polskiej Akademii Nauk, Politechnika Rzeszowska im. Ignacego Łukasiewicza, Instytut Podstawowych Problemów Techniki Polskiej Akademii Nauk. Warszawa, 4-6 lipca 2012 r. III Krajowa Konferencja Nano- i Mikromechaniki pod Patronatem Ministra Nauki i Szkolnictwa Wyższego Prof. Barbary Kudryckiej : Komitet Mechaniki Polskiej Akademii Nauk, Politechnika Rzeszowska, Instytut Podstawowych Problemów Techniki Polskiej Akademii Nauk, Warszawa, 2012.
139. Styp-Rekowski M., Mikołajczyk J., Matuszewski M.: Wybrane zagadnienia stosowania płynów obróbkowych w obróbce skrawaniem. W**:** Obróbka Metalu, 2014, nr 3, s. 10÷14, p-ISSN: 2081-7002; **http://www.e-obrobkametalu.pl/**
140. Syrek S., Mikołajczyk J.: Analiza matematyczna podstawowych wymiarów złącza spawanego. **W:** Logistyka w ratownictwie 2022 / pod redakcją Andrzeja Chudzikiewicza i Andrzeja Krzyszkowskiego. Radom : Instytut Naukowo-Wydawniczy "Spatium", 2022; s. 169÷190, p-ISBN: 978-83-67033-57-2; e-ISBN: 978-83-67033-70-1.
141. Syrek S., Mikołajczyk J.: Modele liniowe wpływu częstotliwości prądu spawania na grubość spoiny. **W:** MIK-21 : Międzynarodowa Innowacyjność i Konkurencyjność w XXI wieku : aspekty innowacyjne / redakcja naukowa Radosław Luft. Lublin: Fundacja Innowacji i Nowoczesnych Technologii INOTECH, 2022. Radom : nakładem Instytutu Naukowo-Wydawniczego "Spatium", 2022; s. 153÷170, p-ISBN: 978-83-67033-43-5;
e-ISBN: 978-83-67033-44-2;
http://inw-spatium.pl/wp-content/uploads/2022/09/MIK-21-2022-Aspekty-innowacyjne-2.pdf
142. Syrek S., Mikołajczyk J.: Modele liniowe wpływu częstotliwości prądu spawania na szerokość spoiny. Obróbka Metalu; 2022, nr 4, s. 24÷31,
p-ISSN: 2081-7002; **https://obrobkametalu.tech/**
143. Tubielewicz K.: Technologia maszyn i metrologia warstwy wierzchniej. Wydawnictwo Wyższej Szkoły Pedagogicznej w Częstochowie, Częstochowa, 1998.
144. Tymowski J.: Automatyzacja procesów technologicznych w przemyśle maszynowym. Wydawnictwa naukowo-Techniczne, Warszawa, 1966 r.
145. Wesołowski L., Mikołajczyk J.: Hammer mill design and construction analysis. **W:** MIK-21 : Międzynarodowa Innowacyjność i Konkurencyjność w XXI wieku : aspekty innowacyjne / redakcja naukowa dr Łukasz Wojtowicz. Lublin: Fundacja Innowacji i Nowoczesnych Technologii INOTECH : nakładem Instytutu Naukowo-Wydawniczego "Spatium", 2023, Poland; s. 159÷185, p-ISBN: 978-83-67033-89-3;
e-ISBN: 978-83-67033-90-9.
146. Wieczorowski M.: Digitalizacja powierzchni w aplikacjach mikro, mezo i makro. Mechanik 11/2018, s. 944÷949.
147. Wieczorowski M.: Kierunki rozwoju metrologii nierówności powierzchni. Mechanik 8-9/2014, s. 467÷479.
148. Wrotny L.: Podstawy budowy obrabiarek. Wydawnictwa Naukowo-Techniczne, Warszawa, 1964.
149. Zandecki R., Kmita C., Mikołajczyk J.: Mathematical models of the surface layer microhardness for a selected grade of ion nitrided steel. **W:** Szkoła Logistyki 2022. Radom : Instytut Naukowo-Wydawniczy "Spatium", 2022, Poland; s. 203÷216, Materiały z IX Konferencji Naukowej "Szkoła Logistyki 2022". p-ISBN: 978-83-67033-33-6;
e-ISBN: 978-83-67033-34-3.

Design and construction of a welding workstation

inż. Leszek Klaryński

Department of Mechanical Engineering

Stanisław Staszic State University of Applied Sciences in Piła, Poland

https://orcid.org/0009-0002-2554-3549

inż. Mariusz Morenc

Department of Mechanical Engineering

Stanisław Staszic State University of Applied Sciences in Piła, Poland

https://orcid.org/0009-0006-5064-886X

corresponding e-mail: morenc28101982@onet.pl

Abstract:

The paper presents the design and construction of an innovative welding workstation which enables more efficient performance of welding operations.

Key words: welding, weld, welding table

1. Introduction

The history of joining metals is very old and dates back to ancient Egypt. At that time, metals with a low melting point, such as silver and gold, were welded and soldered. In order to obtain the appropriate temperature, bellows were used to direct the flame onto the elements being joined. Over time, new materials (e.g. steel) and new methods of joining them have emerged, such as electron beam welding, diffusion or plasma welding. Among the many types of welding processes currently used according to the PN-EN ISO 4063 standard is arc welding with a non-consumable (tungsten) electrode in an inert gas shield TIG 141 (Tungsten Inert Gas) [5, 6, 239, 240, 241].

TIG welding (Fig. 1) involves joining two elements using an electric arc generated by a non-consumable tungsten electrode in a protective gas shield, melting the edges of the joined elements and adding a binder in the form of an electrode wire. This method can be used to weld low-alloy and high-alloy steels, aluminum, copper, titanium, and their alloys. Welding is carried out in an inert gas shield. Most often, pure argon is used, less often helium or a mixture of these two gases. A reducing mixture (argon with added hydrogen) can also be used for welding austenitic steels.

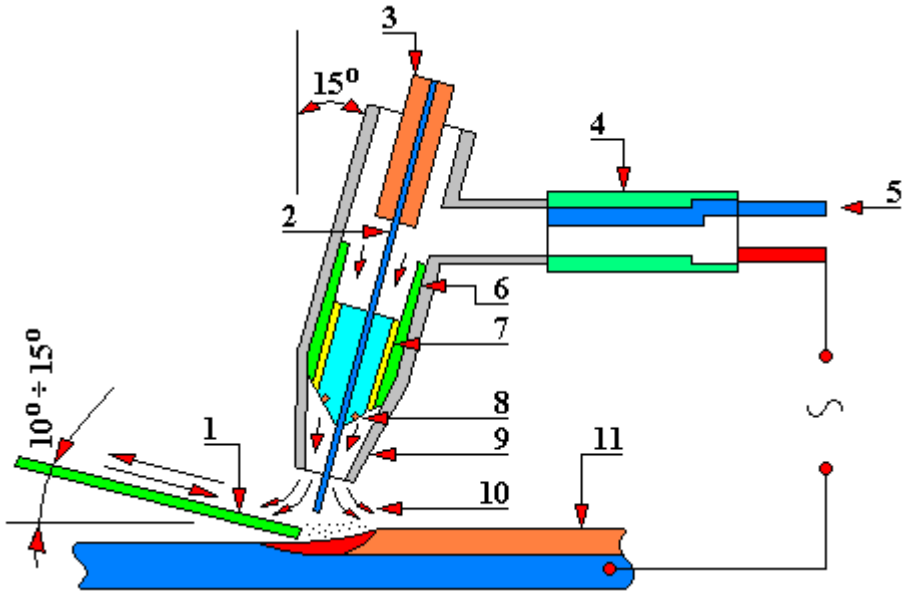

Fig. 1. TIG welding diagram [239, 240, 241]
1 – filler metal; 2 – tungsten electrode; 3 – mounting and adjustment of the tungsten electrode position; 4 – electrode holder; 5 – shielding gas; 6 – current cable; 7 – contact tip; 8 – gas channels; 9 – gas nozzle; 10 – shielding gas; 11 – weld

During TIG welding, the filler metal fed at an angle of 10° ÷ 15° melts with the materials being joined in the weld pool which is produced by an electric arc. This arc is an electric discharge with a voltage of 10V to 50V and a current of 0.1A to 2000A. The phenomenon of gas ionization causes the electric arc to be focused and maintained, the arc simultaneously removes the oxide layer from the surface of the joined elements (so-called cathodic cleaning). An electric arc glowing in an atmosphere of inert gas (argon) is an open arc. The tungsten electrode used is a non-consumable electrode and allows the emission of

electrons to a specific place of the welded joint [14, 18, 19, 20]. Electron emission depends on the type and method of its termination (beveling) – Figure 9. Fig. 2 shows an example of a welded joint. Fig. 3 shows sample dimensions of the joined sheets. Fig. 4 shows a view of some joint elements. And Fig. 5 and Fig. 6 shows how to measure the width and thickness of the joint. Fig. 7 shows examples of places where weld dimensions (thickness and width) can be read.

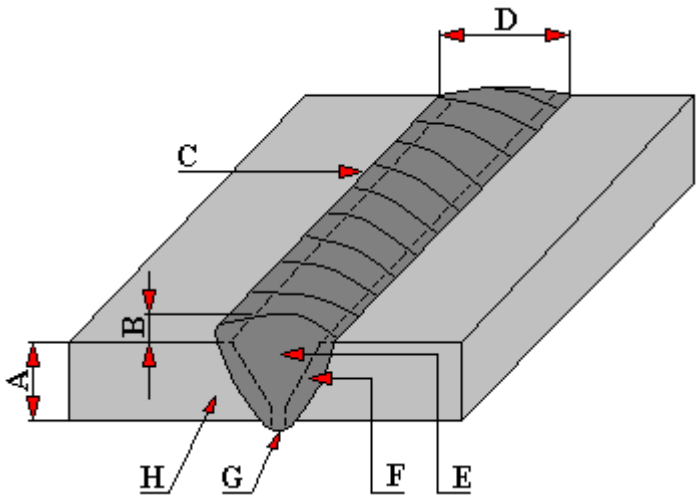

Fig. 2. Welded joint [239, 240, 241]
A – material thickness; B – riser head height; C – weld face; D – weld width; E – weld (melted metal); F – fusion zone; G – weld root; H – heat affected zone

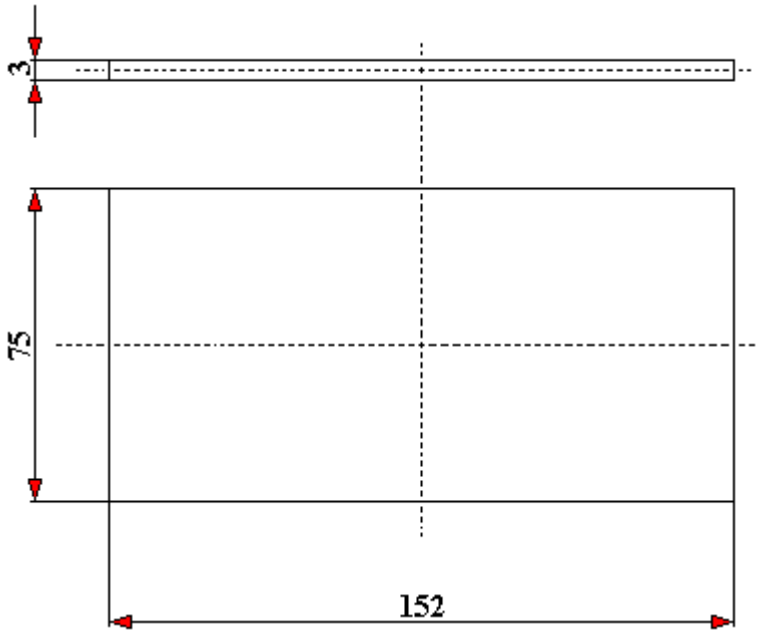

Fig. 3. Example dimensions of joined sheets (both with the same dimensions) [239, 240, 241]

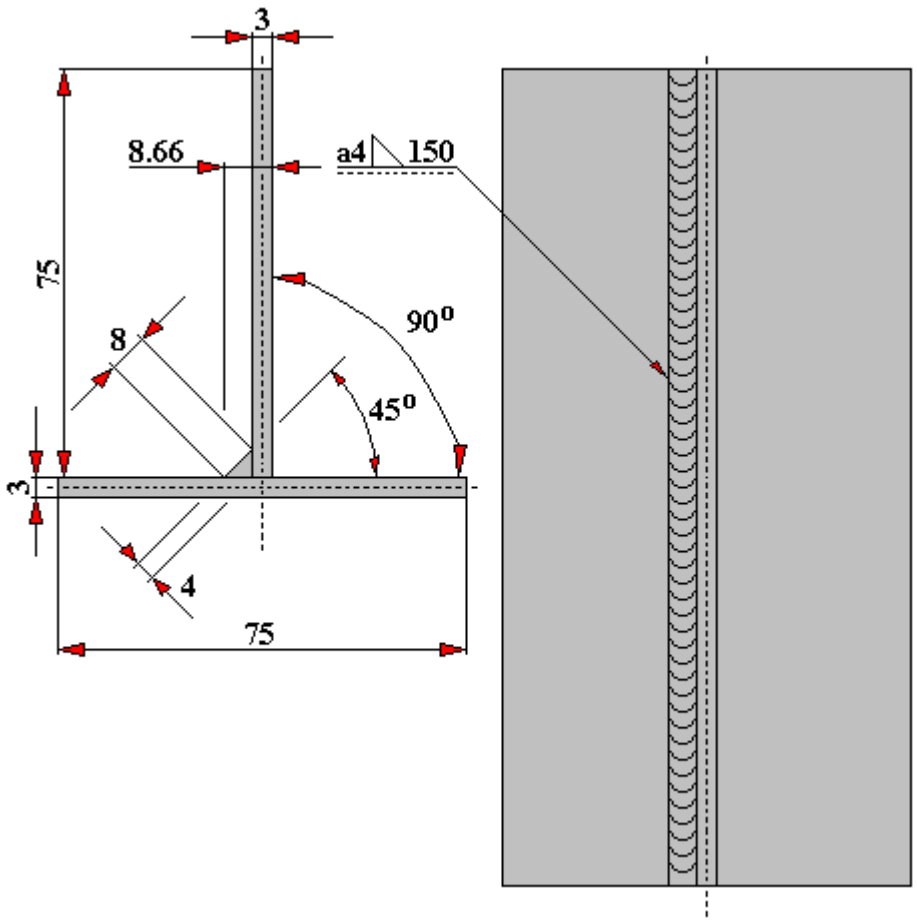

Fig. 4. View of some joint elements [239, 240, 241]

Fig. 5. Method of measuring the weld width [239, 240, 241]

Fig. 6. Method of measuring the weld thickness [239, 240, 241]

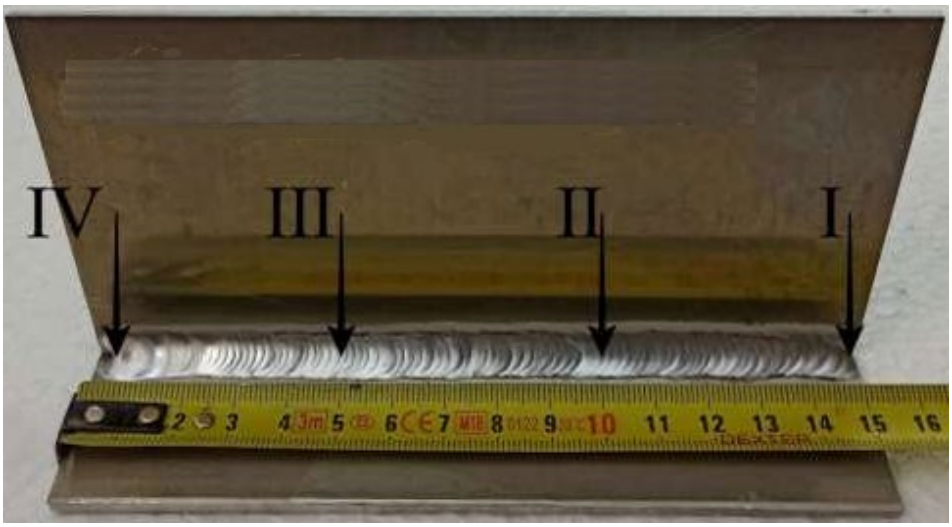

Fig. 7. Examples of places where weld dimensions (thickness and width) [239, 240, 241] can be read
I – number of the first measurement (beginning of the weld); II – number of the second measurement; III – number of the third measurement; IV – number of the fourth measurement (end of the weld)

The TIG method is very versatile, it is used for welding both thin and thick elements. However, due to its low efficiency, in practice it is more used for welding thin elements. When welding thick sheets, e.g. 15 mm and thicker, the root pass (joint penetration) is performed using the TIG method, and the remaining weld groove beads are filled using more efficient methods, e.g. MAG. Using this method one can weld in any position, and the process itself can be fully automated.

The TIG welding process is carried out using both direct current and alternating current. Direct current is mainly used for welding steel, copper and titanium. Alternating

current, on the other hand, is used when welding materials such as aluminum, magnesium and their alloys.

The polarity of the current we use has a very significant impact on the tungsten electrode itself, the depth of penetration and the amount of heat released. Figure 8 shows the effect of DC polarity during TIG welding on the amount of heat Q released in the base material and on the tungsten electrode. If a negative pole is connected to the tungsten electrode, the heat balance is distributed 30% to 70%, respectively. This means that 30% of the heat is released on the electrode (the electrode then becomes the cathode, which emits a stream of electrons towards the anode), and 70% of the heat is released in the welded material (the welded material then becomes the anode). This condition is shown in Fig. 8a. We then obtain much deeper penetration and reduce electrode wear. It is with negative polarity that welding is most common in practice. However, when the polarity is positive (Fig. 8b), 30% of the heat is released in the welded material, which results in the reduction of the penetration depth. Moreover, the wear of the tungsten electrode is very high [25].

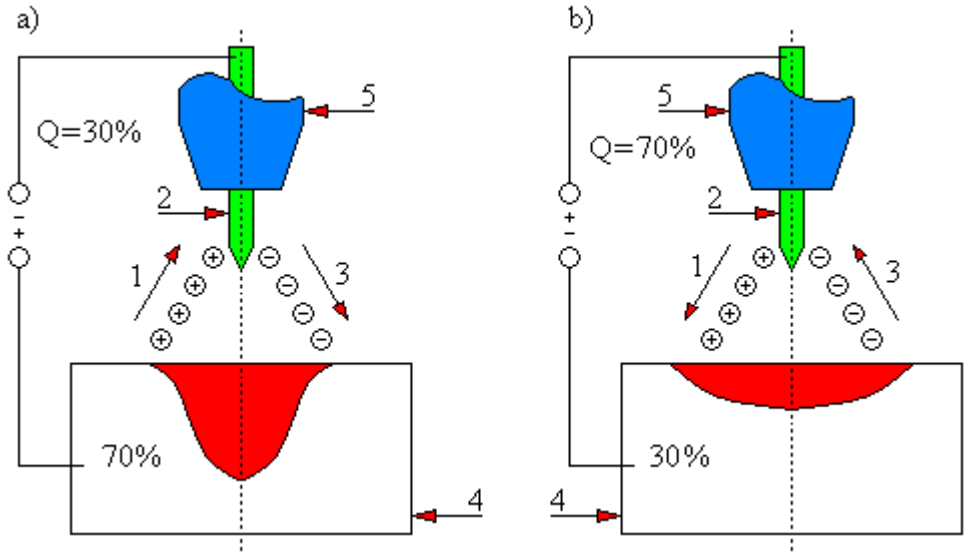

Fig. 8. The effect of DC polarity during TIG welding on the amount of heat Q released in the base material and on the tungsten electrode. a) with negative polarity; b) with positive polarity [25]
1 – ions; 2 – tungsten electrode; 3 – electrons; 4 – base material; 5 – tungsten electrode holder

AC welding is used to join aluminum, magnesium and their alloys (Fig. 1 and Fig. 10). In this case, when the tungsten electrode is positively polarized, negatively polarized electrons flow from the workpiece to the tungsten electrode, which results in breaking down the oxide layer. Then the electrode polarity changes to negative and the electrons flowing to the workpiece generate heat, which is necessary to form a weld pool and, consequently, a weld. The influence of alternating current on the heat balance is 50% to 50%, i.e. half on the electrode and half on the welded piece.

The effect of alternating current on the heat balance results in that the end of the tungsten electrode gets rounded. Modern welding machines are equipped with the so-called "balance" which allows the heat on the tungsten electrode to be adjusted within the range of 50% to 10%. This adjustment affects the penetration depth, the width of the welding arc and the degree of rounding of the tungsten electrode terminal.

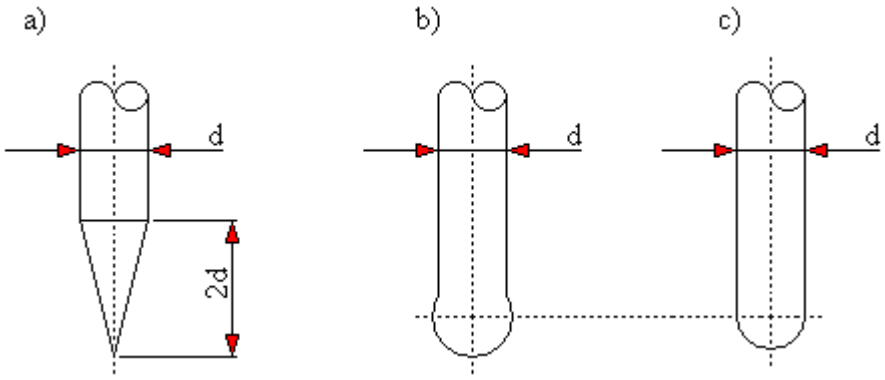

Fig. 9. Examples of electrode terminal shapes for TIG welding [1]
a) negative polarity, b) positive polarity, c) for alternating current

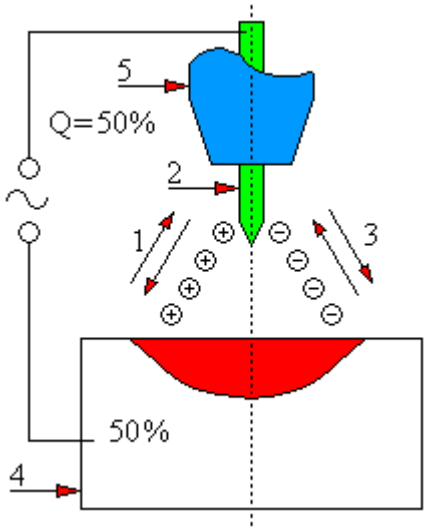

Fig. 10. The effect of AC polarity during TIG welding on the amount of heat Q released in the base material and on the tungsten electrode [25]
1 – ions; 2 – tungsten electrode; 3 – electrons; 4 – base material; 5 – tungsten electrode holder

Basic parameters during TIG welding are:

- welding current intensity [A];
- amount of protective gas [l/min];
- arc voltage [V];
- binder wire diameter [mm];
- electrode diameter [mm].

Currently, the most common welding method is arc welding with a consumable electrode in an active gas shield, the MAG 135 method (Fig. 11). It is mainly used for welding carbon, low-alloy and high-alloy steels. This method involves connecting two elements using an electrode wire extending from a contact tip. The electrode wire is wound on a spool and fed continuously using a wire feeder. When the wire touches the material being welded there is arcing which causes the wire to melt and enter the weld pool, solidify, and form a weld. This

welding process takes place in an atmosphere of protective gases such as carbon dioxide (CO2) or a mixture of carbon dioxide with argon (CO2 + Ar) or carbon dioxide with argon and oxygen (CO2 + Ar + O2), less often a mixture of carbon dioxide with argon, oxygen and hydrogen (CO2 + Ar + O2 + H2). The MAG welding process is most often carried out using direct current of positive polarity (plus connected to the electrode wire, minus to the welded element) [2].

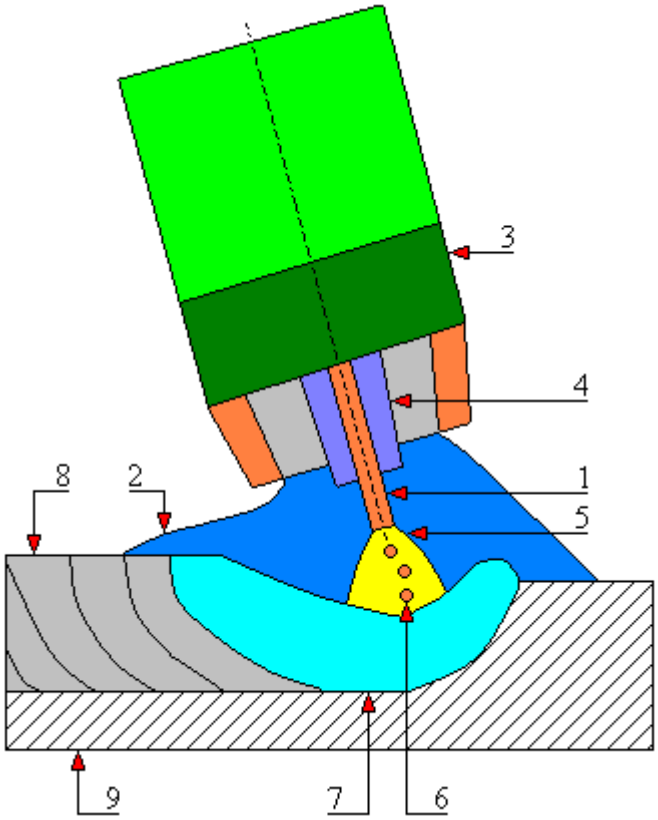

Fig. 11. Diagram of the MAG 135 welding method
1 – electrode wire; 2 – shielding gas; 3 – gas nozzle; 4 – current contact (contact tip); 5 – welding arc; 6 – electrode metal drops; 7 – weld pool; 8 – solidified weld; 9 – welded element

In MAG welding we have three types of welding arcs (Fig. 12) [2]:

- short circuit arc– is created at low current intensity, molten wire drops pass into the weld pool during short circuits when the electrode wire touches the workpiece; this type of arc is used when welding thin materials (up to 4 mm thick) with electrode wires with a diameter of up to 1 mm;
- spray arc – liquid metal drops pass into the weld in the form of a very large number of fine droplets, without causing short circuits; this is the so-called non-fusing arc; this arc is generated at a high welding current (above 200 A), causes deep penetration, low spatter and a smooth weld face; mainly used in the downward (PA) or side (PB) position; in this case we use electrode wires with a diameter of 1.2 mm or 1.6 mm;
- short circuit spray arc – a combination of short circuit arc and spray arc; it is created at a current intensity above 100 A; then we use electrode wire diameters of 1.0 mm or 1.2 mm.

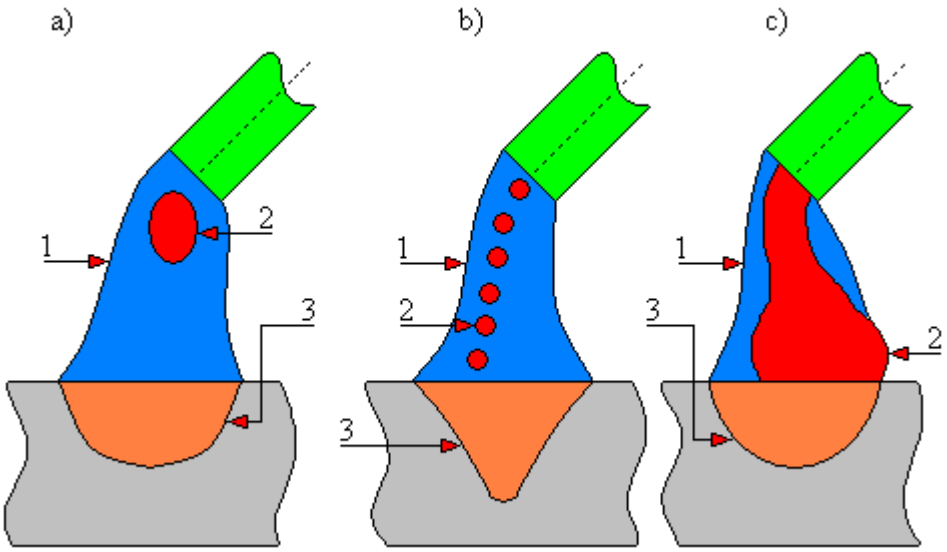

Fig. 12. A method of transferring metal through a gas-shielded arc
a) globular transfer; b) spray; c) short circuit
1 – welding arc; 2 – drops of liquid metal; 3 – weld pool

A variation of the MAG 135 method is arc welding with a consumable electrode in an inert gas shield – the MIG 131 method, in which the inert gases argon (Ar), helium (He) or a mixture of these gases are used. The materials that can be welded using this method are aluminum and its alloys, as well as micro-alloy steel.

Another welding method is arc welding with coated electrodes, MMA 111 method (Fig. 13). Coated arc welding involves joining metals using an electric arc that ignites between a coated electrode and the material being welded. This process is most often performed manually, which is why this method is inefficient. We can use coated electrodes to weld, pad or cut material. When selecting a coated electrode, one should consider parameters such as the chemical composition of the electrode, the tensile strength of the electrode material, the type of electrode coating, and the type of welding current.

Laser welding (Fig. 14) involves melting the contact area of two elements using a very narrow, high-density laser beam. The joining of welded materials can be done either with the laser beam itself or by adding an additional wire as a binder. Welds that can be made using laser welding can be divided into three groups (Fig. 15) depending on the energy density and the size of the laser focus point.

Gas welding (Fig. 16 and Fig. 17) is the oldest welding method. The heat source here is a flame from the combustion of acetylene and oxygen. The flame temperature is approximately 3100°C. By adding a wire (binder) to the melted edges of the joined elements, a weld is formed [26, 79, 213]. Sometimes propane, butane, natural gas, hydrogen, and methane are used as gases. Then the resulting flame temperature is usually much lower [2, 222, 243]. However, for economic reasons, these types of gases are used for cutting (most often in scrap yards), soldering or heating. Gas welding is used only for butt joints of both sheets and pipes.

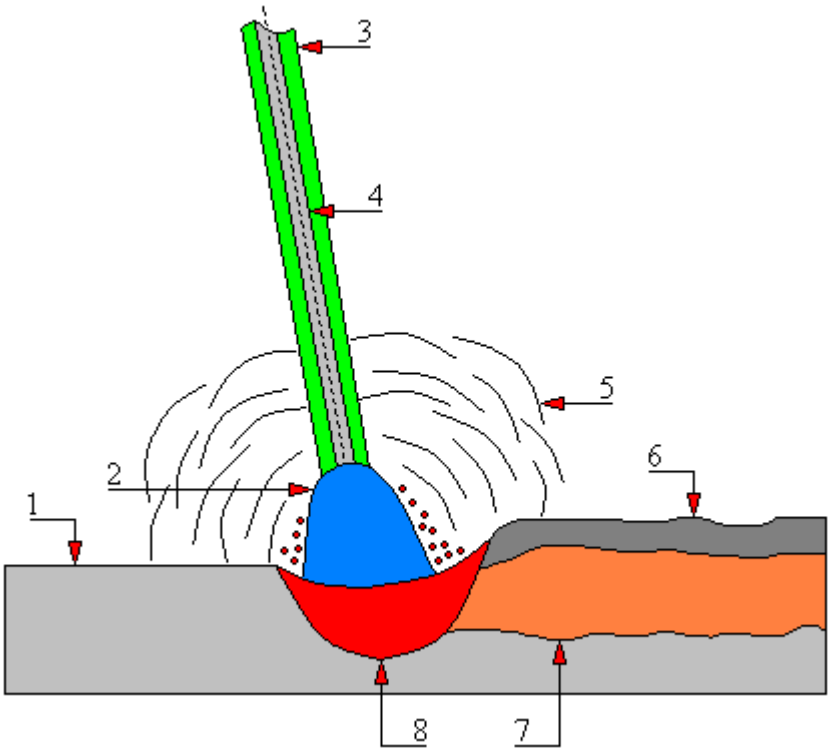

Fig. 13. The process of electric arc welding with a coated electrode
1 – welded material; 2 – electric arc; 3 – electrode coating; 4 – electrode core; 5 – gas atmosphere (protective); 6 – slag; 7 – weld; 8 – weld pool

Electrode wires used in MAG or MIG methods can be solid (Fig. 18) or flux-cored (Fig. 19 and Fig. 20) and have a circular cross-section. Flux-cored wire consists of an outer metal coating in the form of a tube filled inside with flux, metal powder or alloy additions. Flux-cored wires, unlike solid wires, may have different weld metal properties due to different powder composition. During welding, the powder components create their own protective atmosphere that prevents ambient air from entering the weld pool. In cored wires, rutile, basic or metallic filler powder is used [2, 3, 26, 27, 242].

During welding, the unprotected eye is exposed to harmful light radiation. The welder's eyes are protected by a welding helmet. However, people working around the welding station or passing by are also exposed to this harmful radiation. Therefore, protection in the form of screens is used (Fig. 21). Typically, it is a curtain made of non-flammable or flame-retardant material that blocks harmful optical radiation. The minimum height of such a screen according to the relevant regulations is two meters, while maintaining a ventilation gap at the floor. This break is necessary because some of the gases used during welding are heavier than air and can accumulate near the floor, which can be dangerous to human life.

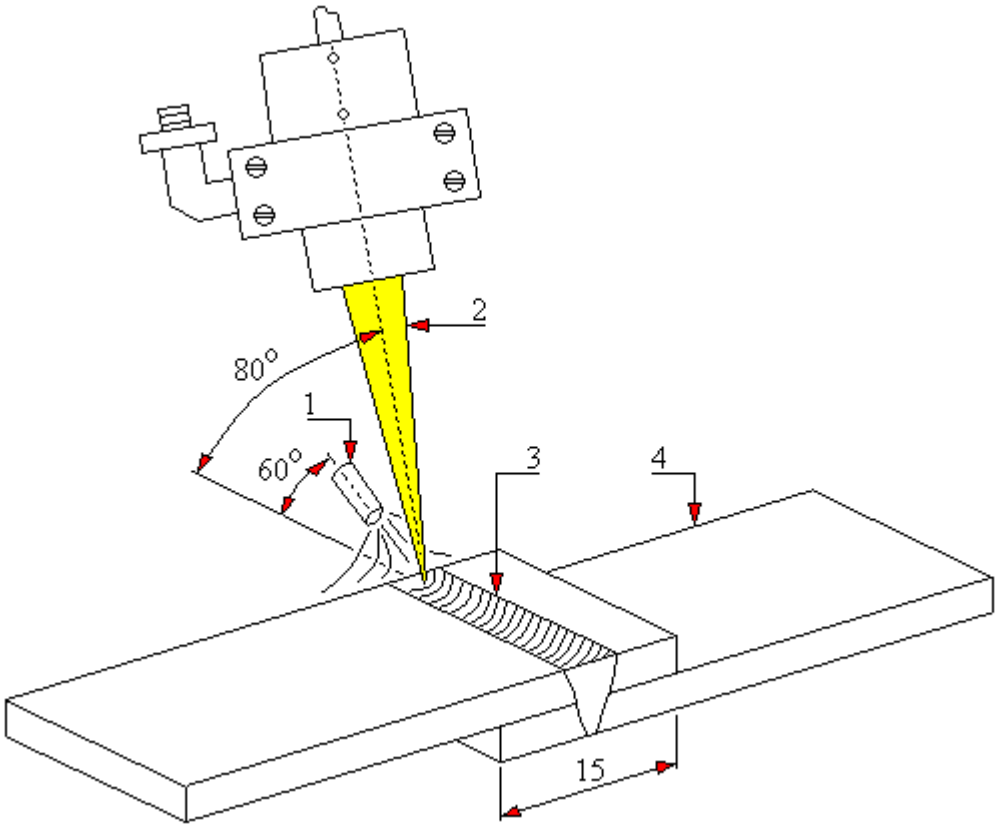

Fig. 14. Laser welding
1 – shielding gas; 2 – laser beam; 3 – weld; 4 – welded material

The welding process produces a large amount of fumes or gaseous products that can enter the human body. That is why fume extractors are used at welding stations. However, it should be remembered that such pollutants can be inhaled by humans or enter the body through pores in the skin (respirable pollutants) [218, 219, 220, 221]. A certain solution to this problem is for the welder to use personal protective equipment, e.g. welding helmets with a filtered air supply.

Among the many regulations regarding welding stations, there is also a requirement that each welding workstation must have at least 2m^2 of free floor space not occupied by devices and equipment. In addition, a permanent welding station should be equipped with a welding table or appropriate equipment enabling safe performance of welding work. Currently, there are many companies on the market offering this type of products ensuring ergonomics and work safety. There are design solutions for welding tables with adjustable height, electrically or hydraulically, and with lower or upper fume extraction. Such an extraction system is often integrated with the welding table. In addition, these tables are often equipped with welding positioners or turnover fixtures (manual or electric). The relevant welding regulations are regulated by standards [80÷211]. The literature on welding is very extensive [14, 18, 19, 20, 26, 79, 213, 214, 215, 216, 228, 232].

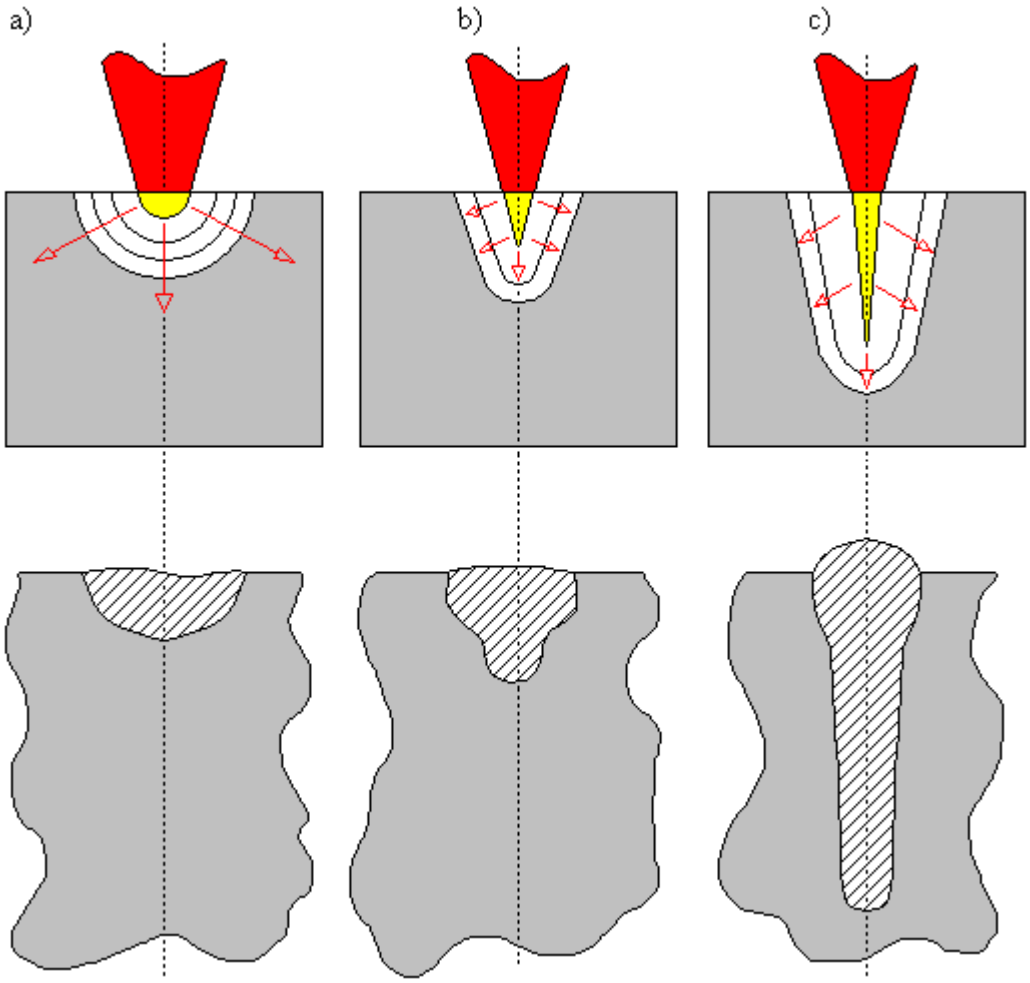

Fig. 15. Types of laser welds [23]
a) conductive (energy density 0.4÷0.6 MW/cm^2); b) transient (energy density approx. 1 MW/cm^2); c) penetrating (energy density 1.4÷1.6 MW/cm^2)

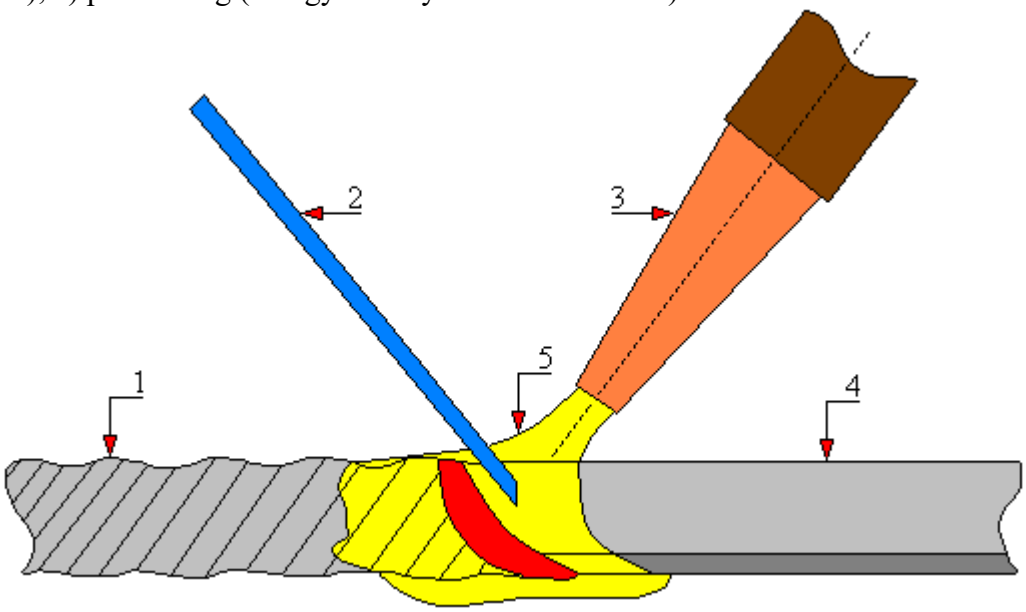

Fig. 16. Gas welding diagram
1 – weld; 2 – filler metal; 3 – welding torch; 4 – edge of the welded material; 5 – gas flame

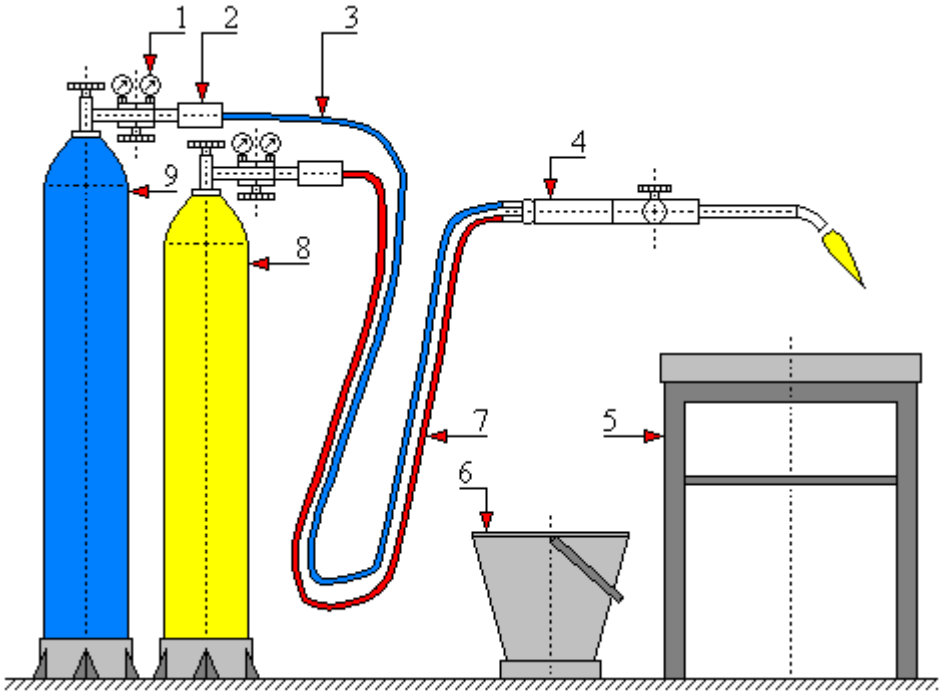

Fig. 17. Gas welding station
1 – reducer; 2 – dry fuse; 3 – oxygen hose; 4 – torch; 5 – welding table; 6 – water container; 7 – acetylene hose; 8 – acetylene cylinder; 9 – oxygen cylinder

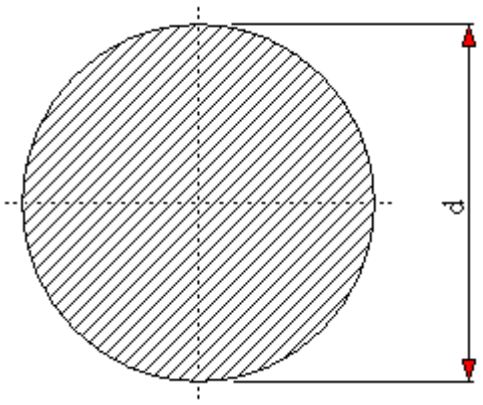

Fig. 18. Solid wire cross-section
d – wire diameter

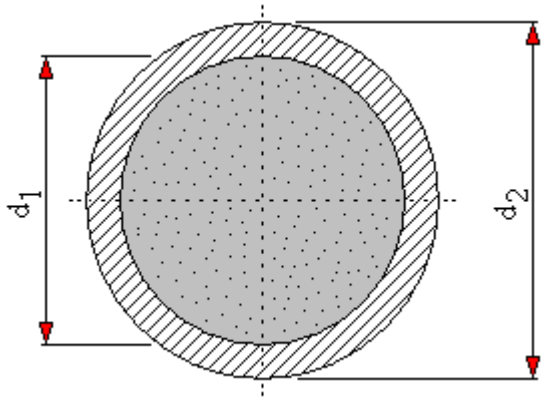

Fig. 19. Cross-section of a solid-tube flux-cored wire
d_1 – inner diameter of the tube; d_2 – outer diameter of the tube

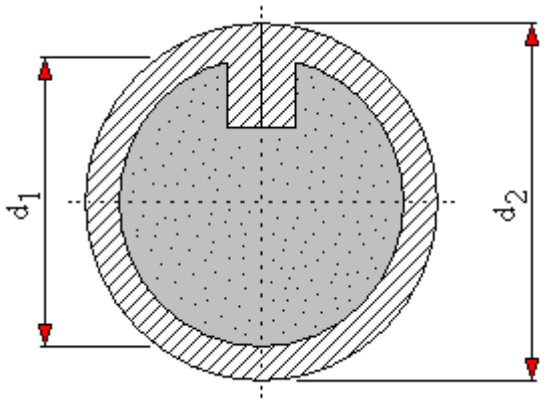

Fig. 20. Cross-section of a coiled flux-cored wire
d_1 – inner diameter of the wire; d_2 – outer diameter of the wire

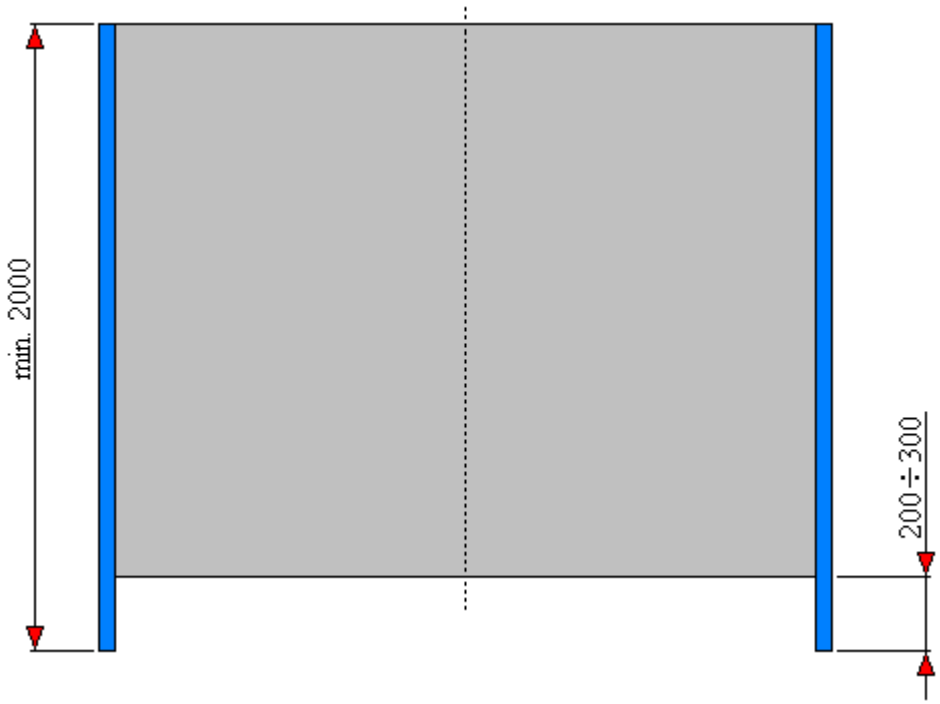

Fig. 21. Screen - visualization

2. Design and construction of a welding workstation

The design assumptions for the construction of this welding station include the following requirements:

- the workstation should be mobile;
- it should enable working in any position;
- it should have an adjustable welding table height adapted to the individual needs of the welder;
- it should have a turntable installed to improve the pipe welding process;
- it should be equipped with adjustable LED lighting;
- it should be possible to connect a lower exhaust system;
- it should have protection of the external environment through the use of adjustable screens.

Based on the above-mentioned guidelines, in order to build it, a welding table was designed in the Fusion 360 computer program (Fig. 22).

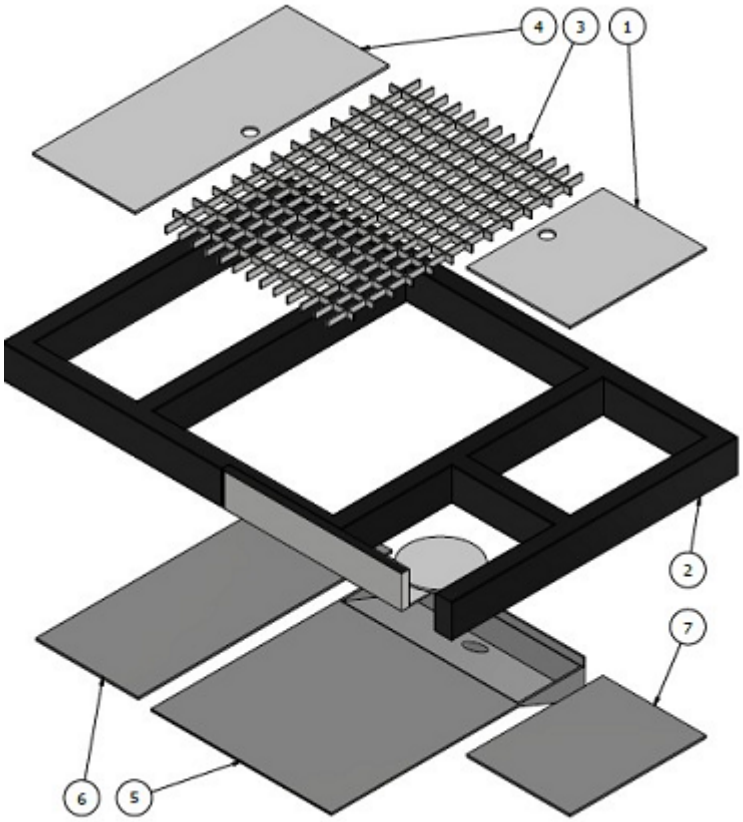

Fig. 22. Assembly drawing of the welding table
1 – small storage compartment cover (aluminum sheet ≠ 5 mm); 2 – main frame (steel profile 80x40x2 mm); 3 – truss (galvanized flat bar 20x2 mm); 4 – large storage compartment cover (aluminum sheet ≠ 1.5 mm); 5 – lower cover with exhaust (aluminum sheet ≠ 1.5 mm); 6 – lower storage compartment cover (aluminum sheet ≠ 1.5 mm); 7 – lower storage compartment cover (aluminum sheet ≠ 5 mm)

To raise the welding table according to the welder's needs used are two electric actuators with synchronized uniformity of extending pistons (Fig. 23) controlled via the control panel. The table is equipped with a commercial turntable enabling the clamping and rotation of the welded element, especially pipes. The entire system (lighting, welding table lifting or lowering height and turntable operation) is controlled by an intuitive and easy-to-use control panel (Fig. 24).

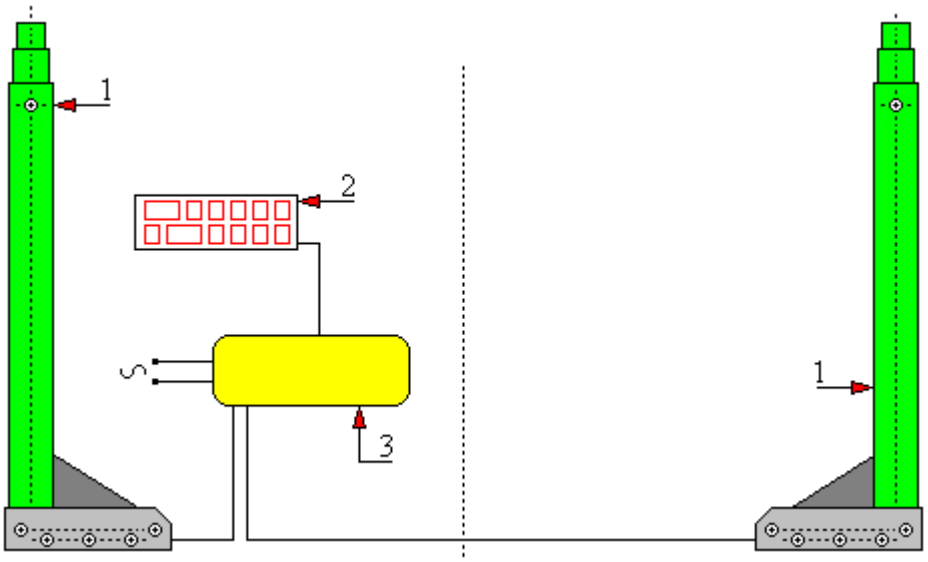

Fig. 23. Diagram of the welding table lifting system
1 – electric actuator (2 pcs.); 2 – control panel; 3 – controller

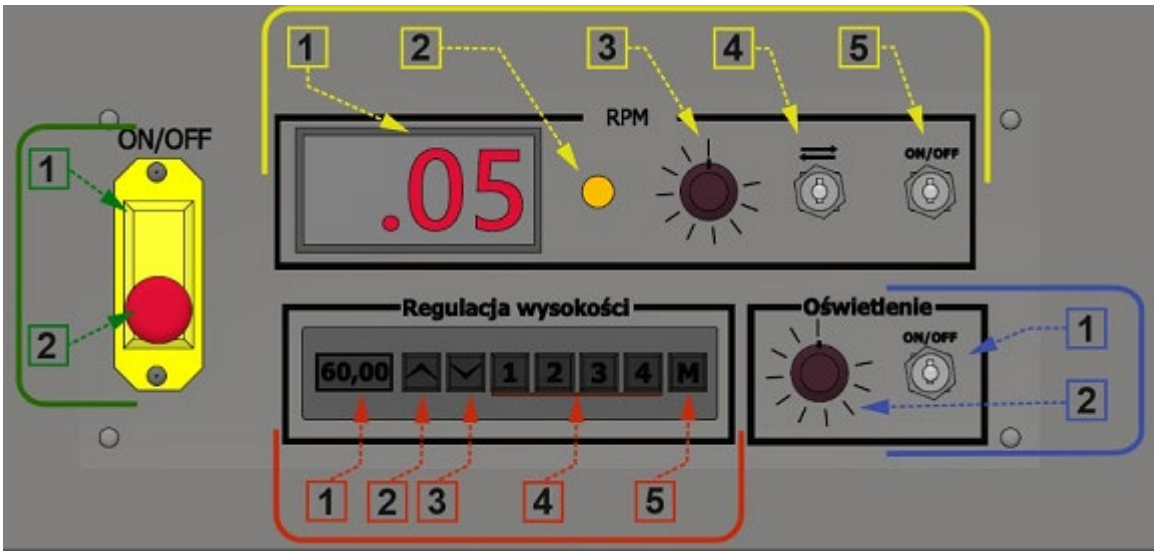

Fig. 24. Control panel for the turntable, lighting and the height of raising or lowering the welding table

The control panel (Fig. 24) is divided into the following zones:

- the green zone concerns the main power switch of the welding table: 1 – power on/off button; 2 – safety switch;
- the blue zone is for lighting: 1 – welding table lighting on/off button; 2 – light intensity adjustment potentiometer;
- the yellow zone is for controlling the turntable operation: 1 – rotational speed display; 2 – power indicator light; 3 – rotational speed adjustment potentiometer; 4 – rotation direction reversal switch; 5 – turntable power on/off button;
- the red zone is for controlling the height of the welding table: 1 – current table height display; 2 – table up button; 3 – table down button; 4 – controller memory button (allows to store four table setting heights); 5 – table height memory saving button.

The welding table is equipped with upper and lower extraction of welding fumes and dust (Fig. 25).

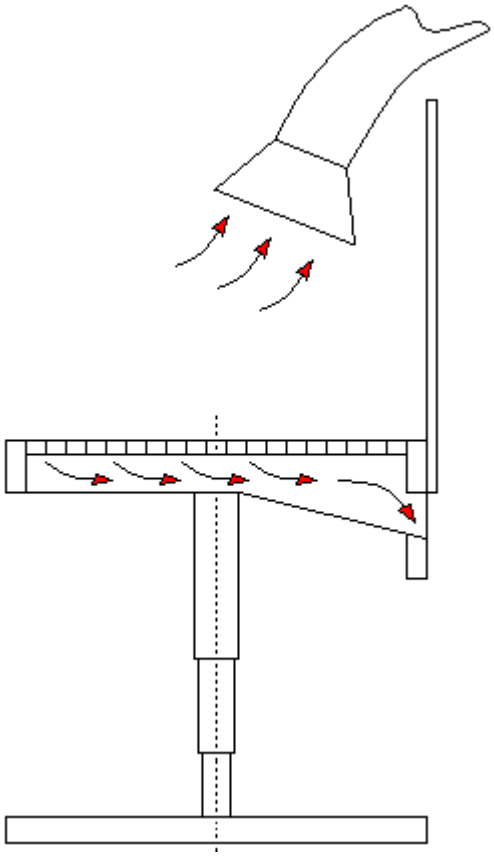

Fig. 25. Schematic diagram of the welding table system with upper and lower extraction of welding fumes and dust

Part of the welding table is made of a grid which serves as a tabletop but also as a cover for the exhaust hood through which the welding fumes is drawn. The welding table top has several storage compartments for all necessary tools. The components purchased for this welding workstation include, inter alia, a holder (manual positioner) designed for welding in forced positions (Fig. 26).

Fig. 26. Welding holder designed for welding in forced positions

Fig. 27 and Fig. 28 show a visualization of the designed welding table. Based on the prepared technical and drawing documentation of the designed welding table carried out was the process of cutting steel profiles 80x40x2, 80x20x2 and 30x30x2 of the S235 JRH grade on a band saw (Fig. 29). Then, after preparing the cut profiles (deburring sharp edges, grafting) (Fig. 30), they were welded using the TIG method (Fig. 31) and ground (Fig. 32). The following drawings from Fig. 29 to Fig. 53 show the subsequent stages of work on the construction of this welding station. And Fig. 55 shows a test run – TIG welding of a pipe in the HL-045 position using a turntable.

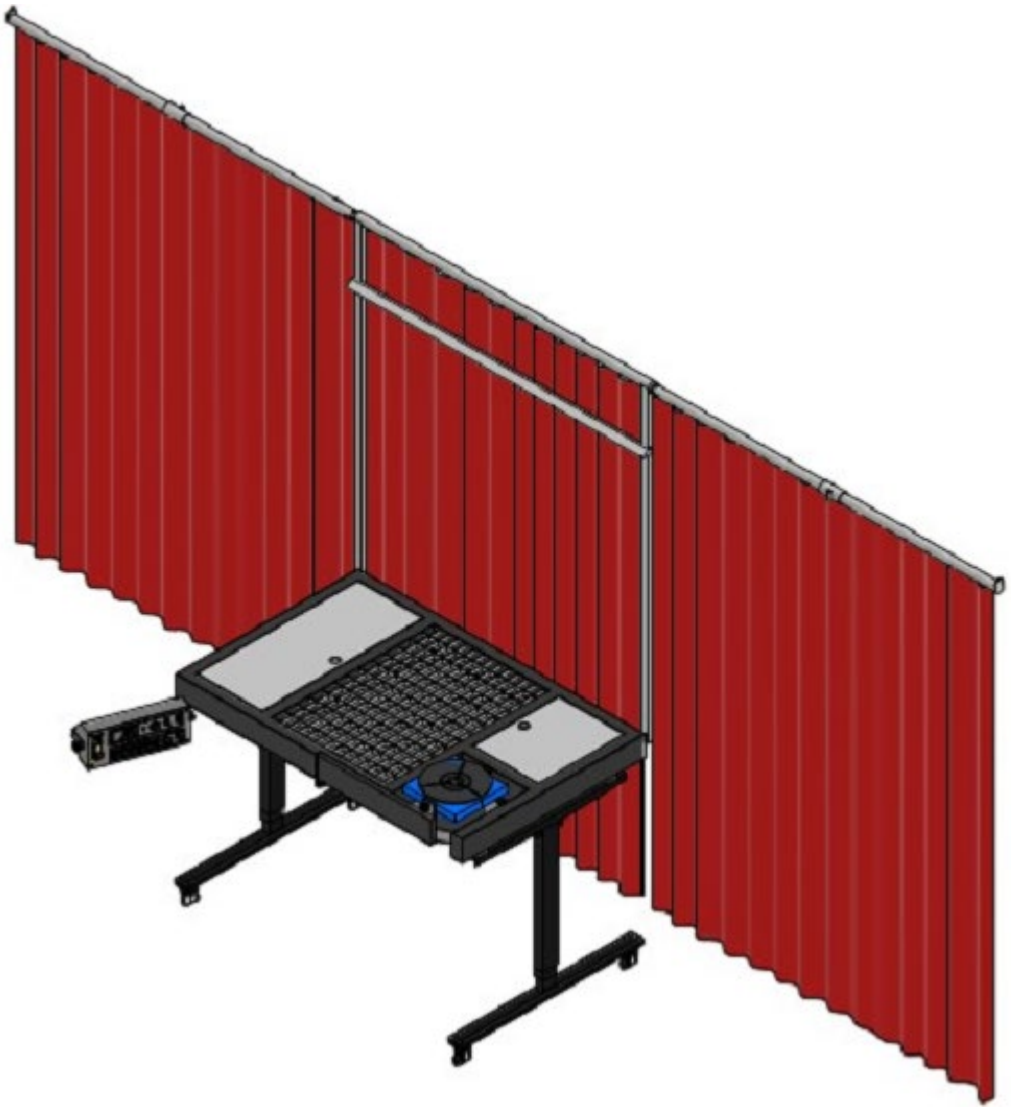

Fig. 27. An overview drawing of the welding table designed in Fusion 360

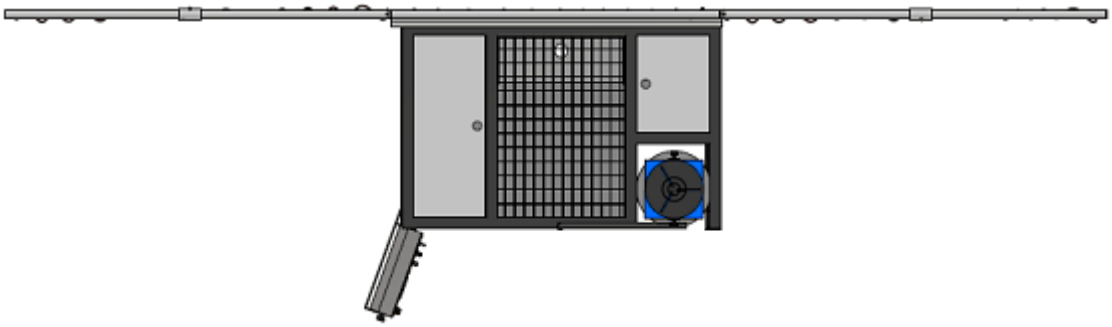

Fig. 28. Designed welding table – top view

Fig. 29. The process of cutting profiles of the supporting frame of the welding table

Fig. 30. Preparation of cut profiles for welding

Fig. 31. The process of welding the cut profiles of the supporting frame of the welding table

Fig. 32. Welded profiles of the welding table support frame after the process of grinding

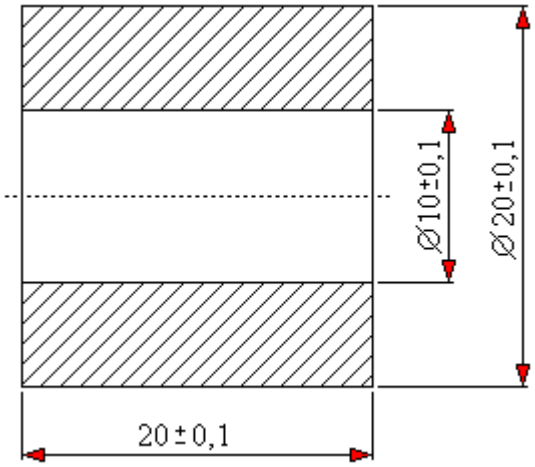

Fig. 33. Bushing for the turntable arm made of S355J2 steel grade

Fig. 34. Welding the bushing into the turntable arm and into welding table arm

Fig. 35. Welding the pin into the bushing plate and of the sleeve into the turntable arm

Fig. 36. Making welded joints of 80x20x2 profiles of the truss frame separating the ventilation space of the lower exhaust from the space for tool storage

Fig. 37. Table covers made of 1.5 mm thick aluminum sheets

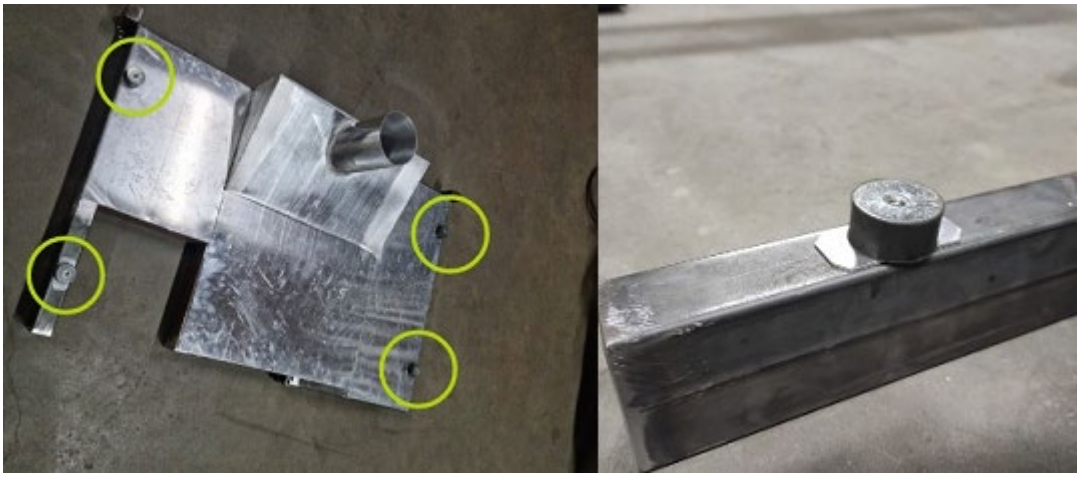

Fig. 37. Making insulators (marked with yellow circles) for the table top to protect the electronics against overvoltage

Fig. 38. Commercial ERB-1 frame as a supporting structure for the welding table top

Fig. 39. Mounting the arm for the welding table control panel on the ERB-1 frame

Fig. 40. Mounting the welding table top to the ERB-1 frame

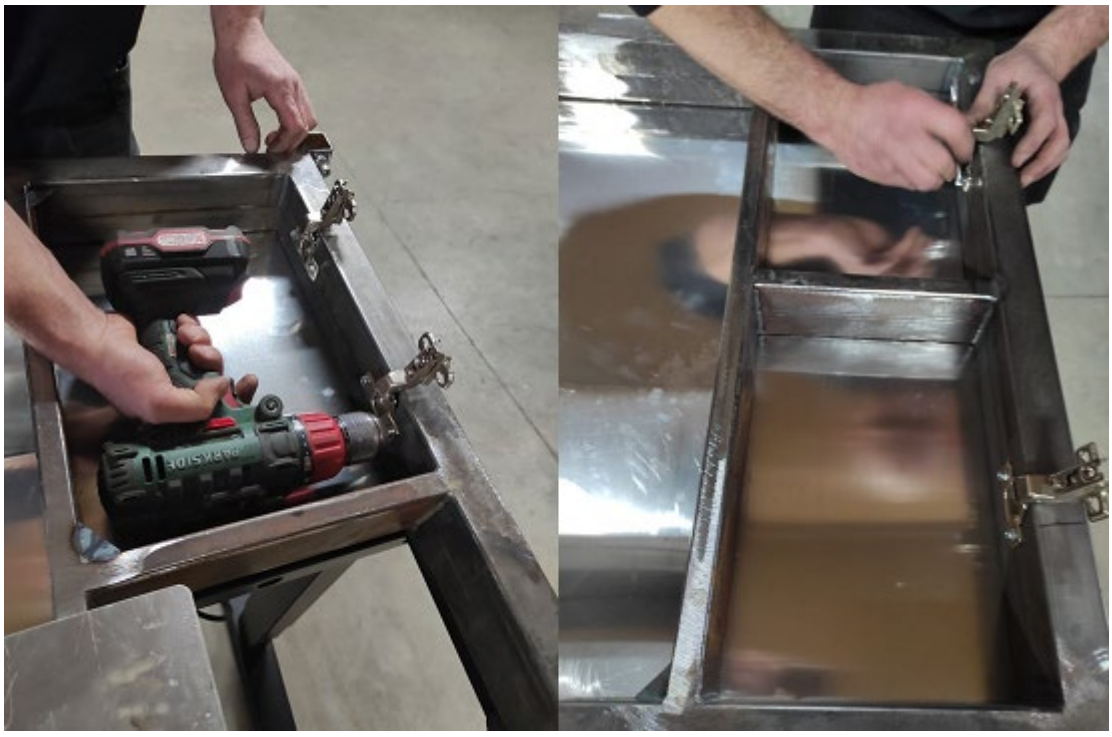

Fig. 41. Installing the tool compartment door hinges

Fig. 42. Installation of furniture accessories for the welding table structure

Fig. 43. Assembly of the welding table top truss

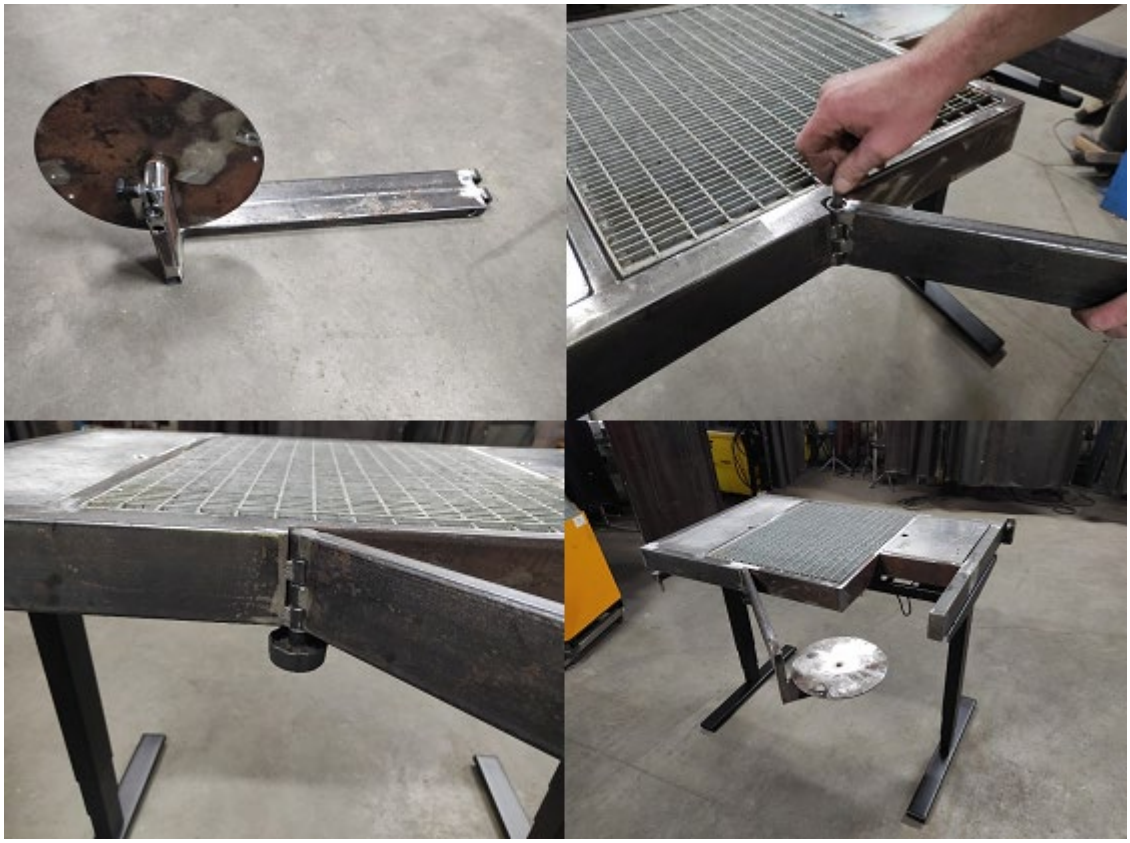

Fig. 44. Mounting the turntable arm to the welding table

Fig. 45. Mounting the turntable on the arm

Fig. 46. Welding and assembly of the control panel support structure

Fig. 47. Mounting the control panel to the welding table structure

Fig. 48. Construction of a protective screen frame made of 30x30x2 steel profiles

Fig. 49. Installing the protective screen frame for the welding table

Fig. 50. View of the welding curtain (screen) with mounting hooks (right)

Fig. 51. Assembling of all components of the welding table to check their fitting

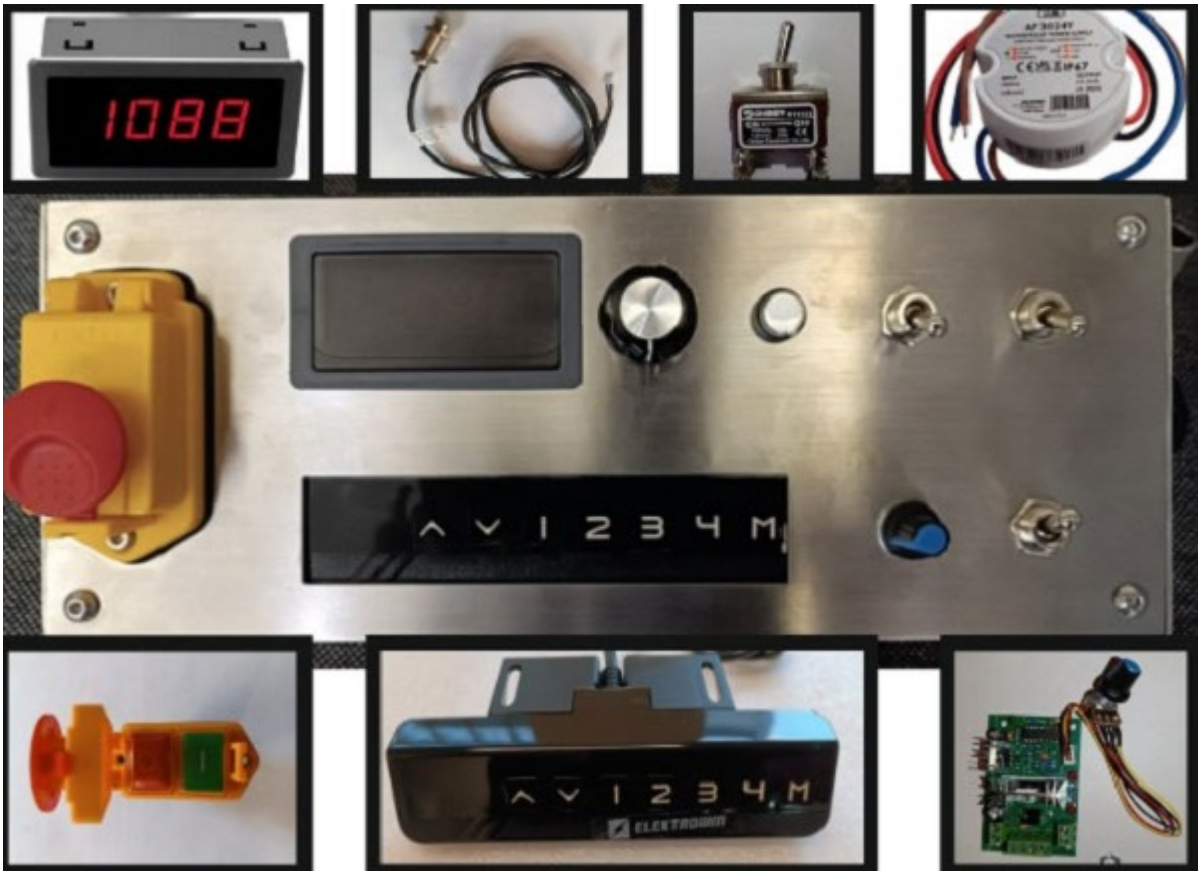

Fig. 52. Assembly of components of the welding table control panel

Fig. 53. View of the finished welding table after powder coating (table frame color: graphite RAL 7016, frame color: black RAL 9005)

Fig. 54. Possible combinations of protective screen settings

Fig. 55. Operational test of the designed and constructed welding table. TIG welding of a pipe in the HL-045 position using a turntable

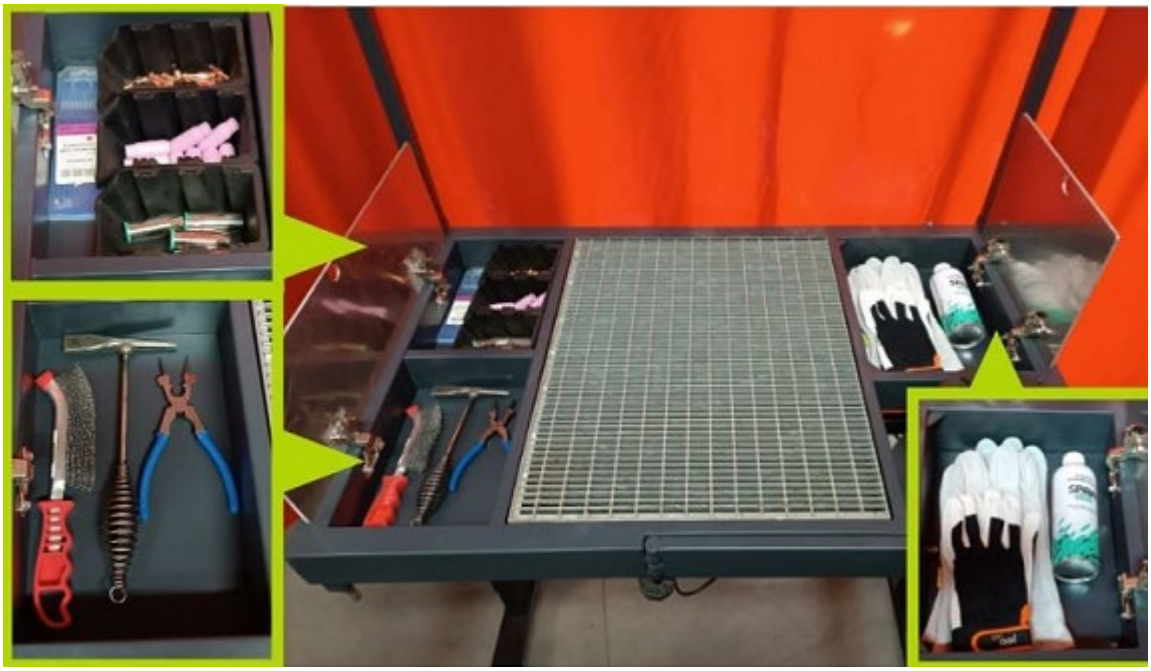

Fig. 56. Example of tool storage arrangement for a designed and constructed welding table

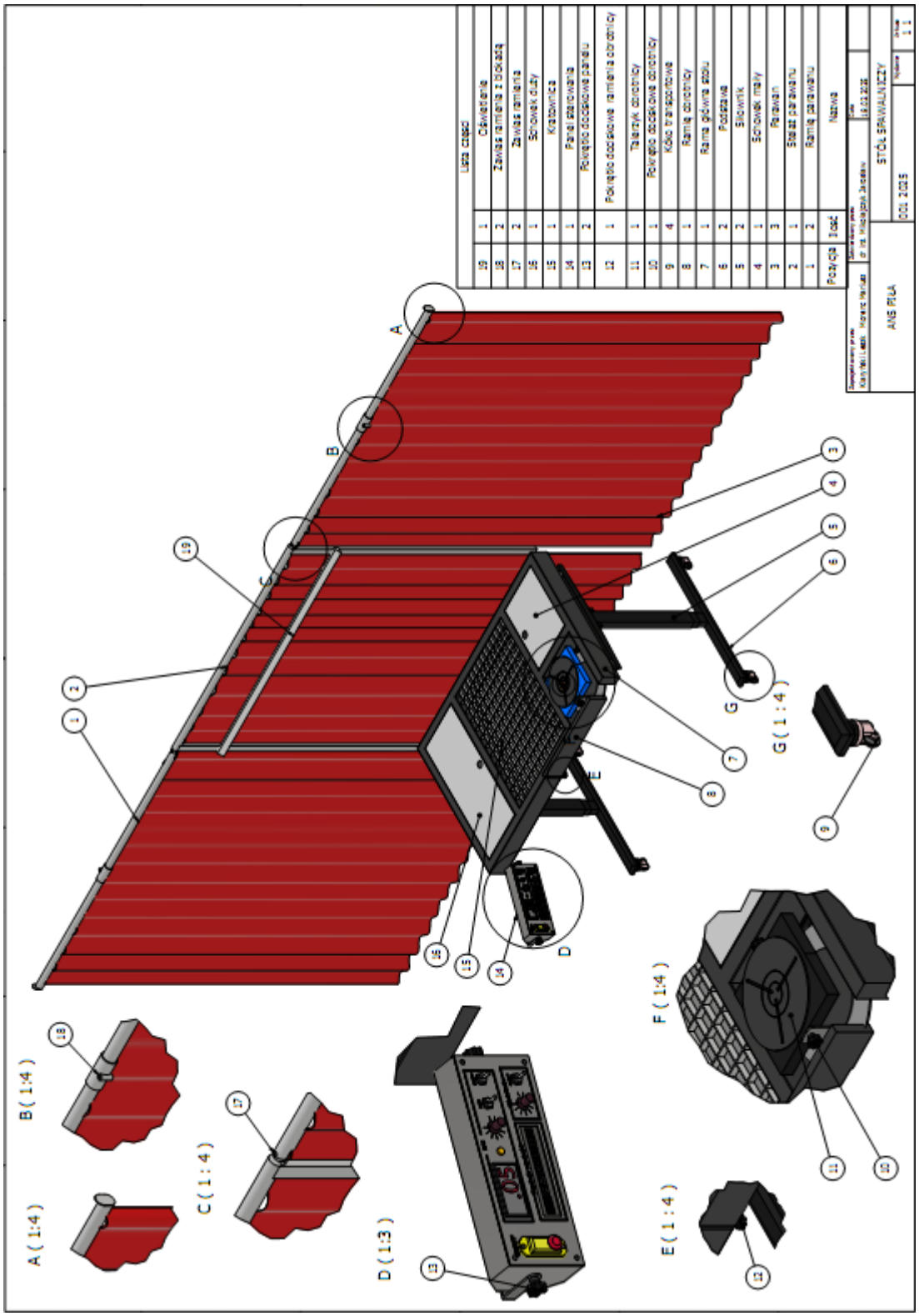

Fig. 57. Assembly drawing of the designed and constructed welding table

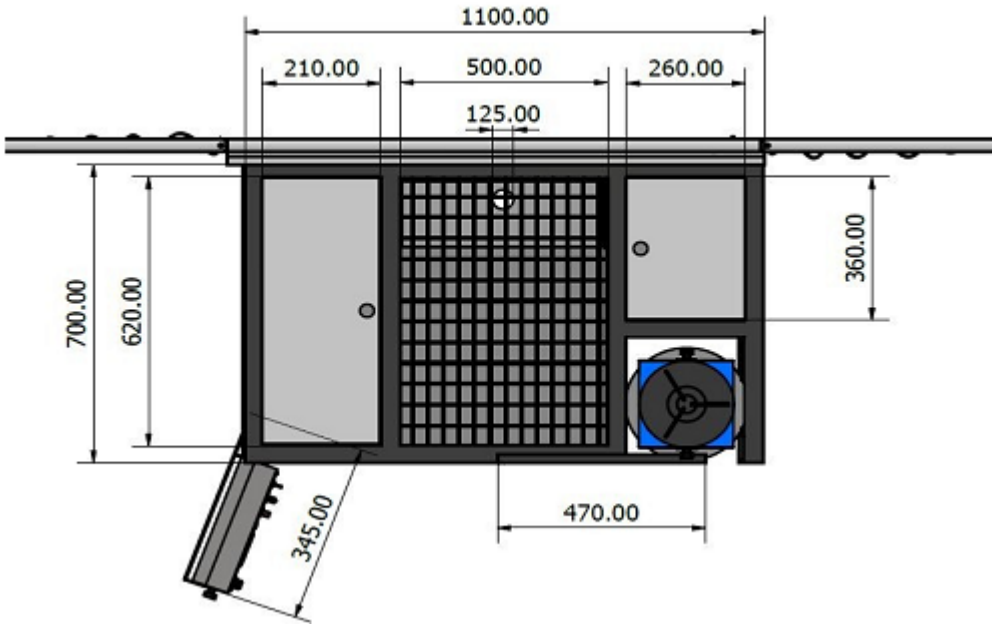

Fig. 58. Basic dimensions of the welding table (top view)

Fig. 59. Basic dimensions of the welding table (main view)

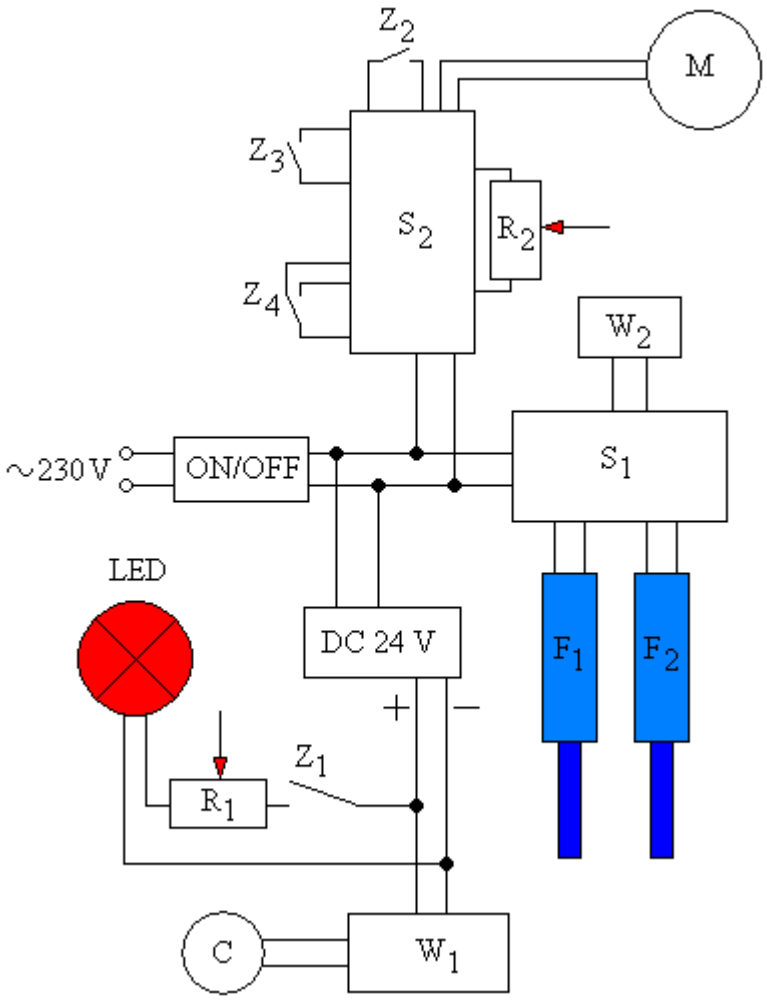

Fig. 60. Block diagram of the welding table's electrical installation
M – turntable motor; S_1 – welding table height adjustment controller; S_2 – turntable controller; W_1 – turntable speed display; W_2 – table height display; C – rotation sensor; R_1 – light intensity adjustment potentiometer; R_2 – turntable speed adjustment potentiometer; LED – LED lamp; DC 24V – DC power supply; Z_1 – lighting switch; Z_2 – turntable power manual switch; Z_3 – turntable power foot switch; Z_4 – turntable rotation direction change switch; F_1 – left welding table lifting actuator; F_2 – right welding table lifting actuator

3. Conclusion

The designed and constructed welding station enables, among other things:

- welding table height adjustment;
- mobility of the welding workbench thanks to the mounted wheels;
- storing welding tools in appropriate drawers;
- insulation of the welding table from any voltage and current interference;
- installation of lower and upper extraction of gases and fumes generated during the welding process;
- making welds in virtually any position;
- conducting welding courses or teaching classes for students;
- performing experiments and tests of the welding process.

4. Literature

1. Adamiec P., Dziubiński J.: Techniki wytwarzania. Spawalnictwo. Wydawnictwo Politechniki Śląskiej, Gliwice, 1996.
2. Ambroziak A.: Techniki wytwarzania – spawalnictwo. Wydawnictwo Politechniki Wrocławskiej, Wrocław, 2010.
3. Dobrowolski Z.: Podręcznik spawalnictwa. Wydawnictwo WNT, Warszawa 1978.
4. Domański A., Mikołajczyk J.: Dimensional analysis of the selected type of rolling bearing depending on the manufacturer. **W:** Szkoła Logistyki 2023 / redakcja naukowa Janusz Zawiła-Niedźwiecki, Katarzyna Białczak. Radom: Instytut Naukowo-Wydawniczy "Spatium", 2023, Poland; s. 79-89, p-ISBN: 978-83-67033-75-6;
e-ISBN: 978-83-67033-58-9.
5. Ferenc K.: Spawalnictwo. Wydawnictwa Naukowo-Techniczne, Warszawa, 2007.
6. Ferenc K., Ferenc J.: Konstrukcje spawane – połączenia. Wydawnictwa Naukowo-Techniczne, Warszawa, 2006.
7. Galon M., Mikołajczyk J.: The effect of laser cutting speed on the bearing surface of peaks and valleys of the cut surface. **W:** Logistyka w ratownictwie 2024 / pod redakcją Andrzeja Chudzikiewicza i Andrzeja Krzyszkowskiego. Radom: Instytut Naukowo-Wydawniczy Spatium, 2024, Poland; s. 71-84, p-ISBN: 978-83-68026-24-5;
e-ISBN: 978-83-68026-25-2.
8. Galon M., Mikołajczyk J.: The effect of laser cutting speed on the weight of the workpiece. **W:** Logistyka w ratownictwie 2024 / pod redakcją Andrzeja Chudzikiewicza i Andrzeja Krzyszkowskiego. Radom: Instytut Naukowo-Wydawniczy Spatium, 2024, Poland; s. 85-96, p-ISBN: 978-83-68026-24-5; e-ISBN: 978-83-68026-25-2.
9. Galon M., Mikołajczyk J.: Wpływ wartości posuwu podczas cięcia laserem na chropowatość powierzchni przecięcia. Obróbka Metalu; 2024, nr 3, s. 48-53,
p-ISSN: 2081-7002; **https://obrobkametalu.tech/nasze-czasopismo/archiwum/**
10. Grabowska M., Mikołajczyk J.: Zastosowanie tomografii komputerowej CAT w inżynierii materiałowej. Application of CAT scanning for materials engineering. Postępy w Inżynierii Mechanicznej [Developments in Mechanical Engineering]. 2017, nr 9 (5), s. 15-26,
p-ISSN: 2300-3383; Wydawnictwa Uczelniane Uniwersytetu Technologiczno-Przyrodniczego w Bydgoszczy, Poland. **http://wu.utp.edu.pl/oferta,8,1**
11. Grabowska M., Mikołajczyk J.: Próba zastosowania tomografii komputerowej CAT do określania struktury grafitu naturalnego w zależności od rozmiaru ziarna. An attempt to apply cat scanning to determine the natural graphite structure depending on the grain size. Postępy w Inżynierii Mechanicznej [Developments in Mechanical Engineering]. 2018, nr 12 (6), s. 5-14, p-ISSN: 2300-3383; Wydawnictwa Uczelniane Uniwersytetu Technologiczno-Przyrodniczego w Bydgoszczy, Poland.
http://wu.utp.edu.pl/oferta,8,1
12. Grabowska M., Mikołajczyk J., Basiak S.: Zastosowanie tomografii komputerowej CAT w nieniszczących badaniach teowych złączy spawanych. Application of cat scanning in non-destructive testing of welded t-joints. Postępy w Inżynierii Mechanicznej [Developments in Mechanical Engineering]; 2018, nr 11 (6), s. 31-44, p-ISSN: 2300-3383; Wydawnictwa Uczelniane Uniwersytetu Technologiczno-Przyrodniczego w Bydgoszczy, Poland. **http://wu.utp.edu.pl/oferta,8,1**
13. Grabowska M., Piochacz A., Mikołajczyk J.: Attempt to use computed tomography CAT to analyze the anodized layer. Postępy w Inżynierii Mechanicznej [Developments in

Mechanical Engineering]; 2020, nr 15 (8), s. 25-33, p-ISSN: 2300-3383; Wydawnictwa Uczelniane Uniwersytetu Technologiczno-Przyrodniczego im. J. J. Śniadeckich w Bydgoszczy, Poland. https://dme.utp.edu.pl/art/15(8)2020/25.pdf
DOI: 10.37660/dme.2020.15.8.3
14. Hillar J., Jarmoszuk S.: Technologia. Spawalnictwo. Wydawnictwa Szkolne i Pedagogiczne, Warszawa 1987.
15. Hillar J.: Spawanie gazowe. Wiadomości specjalistyczne. Wydawnictwo ZZDZ, nr M-120.
16. Hołubowska A., Szałański B., Mikołajczyk J.: Laboratorium termodynamiki. Piła: Wydawnictwo Państwowej Uczelni im. Stanisława Staszica, 2020, Poland.; s. 164 , e-ISBN: 978-83-62617-93-7;
https://wydawnictwo.puss.pila.pl/files/Laboratorium_termodynamiki_POL_version.pdf
17. Jarmoliński Z., Mikołajczyk J.: Badania wpływu technologii cięcia stali na twardość powierzchni bijaka. Research of the influence of steel cutting technology on the strength of the hammer. Postępy w Inżynierii Mechanicznej [Developments in Mechanical Engineering]. 2018, nr 12 (6), s. 15-30, p-ISSN: 2300-3383. Wydawnictwa Uczelniane Uniwersytetu Technologiczno-Przyrodniczego w Bydgoszczy, Poland.
http://wu.utp.edu.pl/oferta,8,1
18. Jarmoszuk S.: Spawanie elektryczne. Wiadomości specjalistyczne. Wydawnictwo ZZDZ, nr M-121.
19. Jarmoszuk S.: Spawanie w osłonie argonu elektrodą wolframową. Wydawnictwo ZZDZ, nr M-158.
20. Jarmoszuk S.: Spawanie w osłonie dwutlenku węgla. Wydawnictwo ZZDZ, nr M-157.
21. Jędrzejczyk D., Mikołajczyk J.: Defining the correlation between the cutting speed and roughness parameter Rz. **W:** MIK-21 : Międzynarodowa Innowacyjność i Konkurencyjność w XXI wieku : aspekty innowacyjne / redakcja naukowa Radosław Luft. Lublin : Fundacja Innowacji i Nowoczesnych Technologii INOTECH, 2022. Radom : nakładem Instytutu Naukowo-Wydawniczego "Spatium", 2022; s. 39-46, p-ISBN: 978-83-67033-43-5; e-ISBN: 978-83-67033-44-2;
http://inw-spatium.pl/wp-content/uploads/2022/09/MIK-21-2022-Aspekty-innowacyjne-2.pdf
22. Jędrzejczyk D., Mikołajczyk J.: Mathematical models of the influence of cutting speed on Ra parameter. Developments in Mechanical Engineering; 2022, nr 18 (10), s. 115-129, p-ISSN: 2720-0639; Wydawnictwa Uczelniane Uniwersytetu Technologiczno-Przyrodniczego im. J.J. Śniadeckich w Bydgoszczy, Poland.
DOI: 10.37660/dme.2022.18.10.11
23. Jędrzejczyk D., Mikołajczyk J.: Wpływ prędkości skrawania na wybrany parametr warstwy wierzchniej. **W:** Logistyka w ratownictwie 2022 / pod redakcją Andrzeja Chudzikiewicza i Andrzeja Krzyszkowskiego. Radom: Instytut Naukowo-Wydawniczy Spatium, 2022, Poland; s. 75-90, p-ISBN: 978-83-67033-57-2; e-ISBN: 978-83-67033-70-1.
24. Kaczmar W.: Techniki wytwarzania. Spawalnictwo. Wydawnictwo Politechniki Wrocławskiej, Wrocław, 1979.
25. Karpiński S., Moszumański J., Radwan-Wiatrowski K.: Laboratorium z podstaw spawalnictwa. Wydawnictwo Uczelniane Politechniki Koszalińskiej, Koszalin, 2001.
26. Klimpel A.: Spawanie, zgrzewanie i cięcie metali. Wydawnictwa Naukowo-Techniczne, Warszawa, 1999.
27. Klimpel A.: Technologia spawania i cięcia metali. Wydawnictwo Politechniki Śląskiej, Gliwice, 1997.
28. Latoś H., Mikołajczyk J.: Effect of partial wear of the tool point on the selected indicator of the machining process. **W:** Logistyka w ratownictwie 2023 / pod redakcją Andrzeja

Chudzikiewicza i Anny Stelmach. Radom: Instytut Naukowo-Wydawniczy "Spatium", 2023, Poland; s. 195-210, p-ISBN: 978-83-67033-95-4; e-ISBN: 978-83-67033-96-1.
29. Latoś H., Mikołajczyk J.: Thickness of the machined layer at milling with single-edge straight blades with an angle of λs≠0°. **W:** MIK-21 : Międzynarodowa Innowacyjność i Konkurencyjność w XXI wieku : Aspekty innowacyjne / redakcja naukowa dr Łukasz Wojtowicz. Lublin: Fundacja Innowacji i Nowoczesnych Technologii INOTECH : nakładem Instytutu Naukowo-Wydawniczego "Spatium", 2023, Poland; s. 23-27,
p-ISBN: 978-83-67033-89-3; e-ISBN: 978-83-67033-90-9.
30. Latoś H., Mikołajczyk J., Konarski J., Mikołajczyk T.: Turning using self-induced vibration. **W:** MIK-21 : Międzynarodowa Innowacyjność i Konkurencyjność w XXI wieku : aspekty innowacyjne / redakcja naukowa dr Łukasz Wojtowicz, 2023, Poland; s. 187-200,
p-ISBN: 978-83-67033-89-3; e-ISBN: 978-83-67033-90-9.
31. Latoś H., Mikołajczyk J.: Vibration in machining. **W:** Logistyka w ratownictwie 2023 / pod redakcją Andrzeja Chudzikiewicza i Anny Stelmach. Radom: Instytut Naukowo-Wydawniczy "Spatium", 2023, Poland; s. 187-194, p-ISBN: 978-83-67033-95-4; e-ISBN: 978-83-67033-96-1.
32. Latoś H., Mikołajczyk J.: The effect of feed rate on the roughness of machined surface. **W:** Szkoła Logistyki 2024 / redakcja naukowa Janusz Zawiła-Niedźwiecki, Adam Płaczek. Radom: Instytut Naukowo-Wydawniczy "Spatium", 2024, Poland; s. 217-226, p-ISBN: 978-83-68026-07-8; e-ISBN: 978-83-68026-08-5.
33. Matuszewski M., Mikołajczyk J., Styp-Rekowski M: Modyfikacja cech środka smarującego za pomocą standardowych dodatków smarowych. Modification of lubricants features by means of standard additives. Źródło: Postępy w Inżynierii Mechanicznej [Developments in Mechanical Engineering]. 2013, nr 1 (1), s. 57-65, Wydawnictwo Uczelniane Uniwersytetu Technologiczno-Przyrodniczego w Bydgoszczy; p-ISSN: 2300-3383; **http://wu.utp.edu.pl/uploads/oferta/Postepy_1_1_2013.pdf**
34. Matuszewski M., Mikołajczyk J., Mikołajczyk T., Styp-Rekowski M.: Logistyczne aspekty zarządzania procesem naprawy. Logistical aspects of the repair process management. Logistyka, 2015, nr 4, s. 1991-1997, p-ISSN: 1231-5478;
https://www.czasopismologistyka.pl/o-czasopismie/wydania
35. Matuszewski M., Mikołajczyk J., Mikołajczyk T., Styp-Rekowski M.: The influence of cooling and lubrication liquid quantity on the isotropy of a machine component surface during machining = Wpływ warunków chłodzenia i smarowania podczas obróbki elementów maszyn na stopień izotropowości ich powierzchni. Tribologia. 2016, vol. 265, No. 1, s. 57-65,
p-ISSN: 0208-7774; e-ISSN: 1732-422X;
https://t.tribologia.eu/resources/html/article/details?id=158175
36. Michalski R.: Zgrzewanie oporowe. Poradnik. Wydawnictwa Naukowo-Techniczne. Warszawa 1970.
37. Mikołajczyk J., Styp-Rekowski M., Świerk K.: Modyfikowanie cech środka smarującego za pomocą dodatków i komputerowe wspomaganie ich doboru. W**:** CAX'2009 : komputerowe wspomaganie nauki i techniki : VI warsztaty naukowe, Bydgoszcz - Duszniki Zdrój 2009 : praca zbiorowa pod redakcją Tadeusza Mikołajczyka. p-ISBN: 978-83-61314-65-3. Wydawnictwa Uczelniane Uniwersytetu Technologiczno-Przyrodniczego w Bydgoszczy, Bydgoszcz 2009.
38. Mikołajczyk J.: Zestawienie porównawcze dodatków depresujących do olejów. W: Zaawansowana tribologia : XXX Ogólnopolska Konferencja Tribologiczna, Nałęczów, 21-24 września 2009 r. Ogólnopolska Konferencja Naukowa XXX Szkoły Tribologicznej "Zaawansowana Tribologia" : Wydział Materiałoznawstwa, Technologii i Wzornictwa Politechniki Radomskiej, Instytut Technologii Eksploatacji - PIB Radom oraz Komitet

Budowy Maszyn, Sekcja Podstaw Eksploatacji Maszyn PAN. Wydawnictwo Naukowe Instytutu Technologii Eksploatacji - PIB, Radom, 2009.
39. Mikołajczyk J.: Zestawienie porównawcze własności fizykochemicznych dodatków smarnych w oleju podstawowym SAE-30. W: Terotechnologia 2009 : materiały konferencji na ekspozycji Metal i Control-Tech : Targi - Kielce (29.09-01.10.2009). VI Konferencja Naukowo-Techniczna "Terotechnologia 2009" : Politechnika Świętokrzyska, Centrum Laserowych Technologii Metali, Katedra Inżynierii Eksploatacji, Wydział Mechatroniki i Budowy Maszyn, Polskie Towarzystwo Naukowo-Techniczne, Towarzystwo Eksploatacyjne, Kielce: Wydawnictwo Politechniki Świętokrzyskiej, 2009. Seria: Zeszyty Naukowe - Politechnika Świętokrzyska, nr 13.
40. Mikołajczyk J., Matuszewski M.: Konstrukcja i sterowanie stanowiska do badań tribologicznych. W: CAX'2010 : komputerowe wspomaganie nauki i techniki : VII warsztaty naukowe, Bydgoszcz - Duszniki Zdrój 2010 : praca zbiorowa / pod red. Tadeusza Mikołajczyka. Bydgoszcz : Wydawnictwa Uczelniane Uniwersytetu Technologiczno-Przyrodniczego w Bydgoszczy, 2010. p-ISBN: 9788361314387.
41. Mikołajczyk J.: System rejestracji i wizualizacji warunków pracy stanowiska do badań tribologicznych. W: CAX'2011 : komputerowe wspomaganie nauki i techniki : VIII warsztaty naukowe, Bydgoszcz - Duszniki Zdrój 2011 : praca zbiorowa / pod redakcją Tadeusza Mikołajczyka. Bydgoszcz : Wydawnictwa Uczelniane Uniwersytetu Technologiczno-Przyrodniczego w Bydgoszczy, 2011. p-ISBN: 9788361314981.
42. Mikołajczyk J.: Badanie wpływu preparatu eksploatacyjnego Mind M na zmianę własności smarnych oleju bazowego SN-150. Źródło: Inżynieria i aparatura chemiczna [Chemical Engineering and Equipment]. 2012, nr 5, s. 235-236, p-ISSN: 0368-0827. **http://inzynieria-aparatura-chemiczna.pl/rok-2012-nr-5/**
43. Mikołajczyk J., Styp-Rekowski M., Matuszewski M., Musiał J.: Einfluβ der kompositionen von schmierzusätzen auf die exploitations-eigenschaften der mischung mit Basisöl SN-150. W: Tribologie und mobilität : beiträge der tribotechnik zur optimierung von fertigungsprozessen, wartung, schmierung (reibungskonditionierung) und betriebssicherheit von verkehrsmitteln und verkehrswegen. Wien, 15 November 2012. Symposium 2012 "Tribologie und mobilität" : Österreichische Tribologische Gesellschaft. Österreichische Tribologische Gesellschaft, Wien, 2012.
44. Mikołajczyk J.: Einfluβ der ausgewählten schmierzstoffzusätze auf betriebseigenschaften der mischung mit Basisöl SN-150. **W:** Reibung, schmierung und verschleiβ : forschung und praktische anwendungen. Band 1. Tribologische systeme maschinenelemente und antriebstechnik fahrzeugtechnik prüfen, messen, kontrollieren. Göttingen, 22-24 September 2014. 55. Tribologie Fachtagung "Reibung, Schmierung und Verschleiβ" : Gesellschaft für Tribologie e.V. Stolberg-Venwegen : Gesellschaft für Tribologie e.V., 2014. Germany.
45. Mikołajczyk J.: Einfluss der ausgewählten zusatzschmierstoffe auf die intensivität des verschleiβprozesses (Ra, Rq, Δm) mit Basisöl SN-150. **W:** Tribologie in industrie und forschung : werkstoffe, konstruktion und technologie. Leoben, 26 November 2014. ÖTG Symposium 2014 "Tribologie in industrie und forschung" : Österreichische Tribologische Gesellschaft. Wien : Österreichische Tribologische Gesellschaft, 2014. Austria.
46. Mikołajczyk J., Matuszewski M.: Einfluss der ausgewählten schmierzstoffzusätze auf ΔT und ΔP mit Basisöl SN-150. **W:** Tribologie in industrie und forschung : werkstoffe, schmierstoffe und technologie. Wiener Neustadt, 25 November 2015, Austria. ÖTG Symposium 2015 "Tribologie in industrie und forschung" : Österreichische Tribologische Gesellschaft. Wiener Neustadt : Österreichische Tribologische Gesellschaft, 2015, s. 145-152.
47. Mikołajczyk J.: Vergleich charakteristischer parameter des abbott-firestone-diagramms für ein kinematisches paar mit konformem kontakt. **W:** Tribologie in industrie und forschung : verschleiβschutz, instandhaltung und anlagenzuverlässigkeit. Linz, 22-23 November 2016,

Austria. ÖTG Symposium 2016 "Tribologie in industrie und forschung" : Österreichische Tribologische Gesellschaft. Wiener Neustadt : Österreichische Tribologische Gesellschaft, 2016; s. 105-110.
48. Mikołajczyk J.: Wpływ dodatków smarowych na transformację warstwy wierzchniej. Piła: Wydawnictwo Państwowej Wyższej Szkoły Zawodowej im. Stanisława Staszica, 2017r., Poland. 215, [1] s., p-ISBN: 978-83-62617-76-0; www.ans.pila.pl
49. Mikołajczyk J.: Maszyny tarciowe : budowa, przeznaczenie. Piła, Wydawnictwo Państwowej Wyższej Szkoły Zawodowej im. Stanisława Staszica, 2018, Poland; 256 s., p-ISBN: 978-83-62617-86-9.
50. Mikołajczyk J.: Analiza statystyczna zmiany poboru mocy podczas procesu zużywania. Statistical analysis of the power variation of tribotester as a resultat of the wear process. Autobusy. Technika, Eksploatacja, Systemy Transportowe; 2019, nr 10-11, s. 83-88, p-ISSN: 1509-5878; e-ISSN: 2450-7725;
http://yadda.icm.edu.pl/yadda/element/bwmeta1.element.baztech-21189602-884a-4d1a-bb60-9edaeae4af8d
51. Mikołajczyk J.: Influence of consumables on the amount of power consumption of kinematic vapor of conformal contact. Wpływ PE na pobór mocy pary kinematycznej o styku konforemnym. Postępy w Inżynierii Mechanicznej [Developments in Mechanical Engineering]; 2019, nr 13 (7), s. 39-50, p-ISSN: 2300-3383; Wydawnictwa Uczelniane Uniwersytetu technologiczno-Przyrodniczego im. J. J. Śniadeckich w Bydgoszczy, Poland.
http://yadda.icm.edu.pl/baztech/element/bwmeta1.element.baztech-2faf200b-3010-4192-9fd0-062f53b49d38
52. Mikołajczyk J.: Statistical analysis of the mass variation of samples as a result of the wear process. Analiza statystyczna zmiany masy próbek w wyniku procesu zużywania. Postępy w Inżynierii Mechanicznej [Developments in Mechanical Engineering]; 2019, nr 13 (7), s. 51-61, p-ISSN: 2300-3383; Wydawnictwa Uczelniane Uniwersytetu Technologiczno-Przyrodniczego im. J. J. Śniadeckich w Bydgoszczy, Poland.
http://yadda.icm.edu.pl/baztech/element/bwmeta1.element.baztech-2faf200b-3010-4192-9fd0-062f53b49d38
53. Mikołajczyk J.: Tribotestery : budowa i przeznaczenie. Piła: Wydawnictwo Państwowej Wyższej Szkoły Zawodowej im. Stanisława Staszica, 2019, Poland; 160 s., e-ISBN: 978-83-62617-90-6; **https://wydawnictwo.pwsz.pila.pl/files/Tribotestery.pdf**
54. Mikołajczyk J.: Determining the energy validity of the Kostetsky's hypothesis on the basis of models for relative motion velocity v = 0.08 m/sec. Developments in Mechanical Engineering; 2020, nr 16 (8), s. 17-29, p-ISSN: 2720-0639; Wydawnictwa Uczelniane Uniwersytetu Technologiczno-Przyrodniczego im. J. J. Śniadeckich w Bydgoszczy, Poland.
DOI: 10.37660/dme.2020.16.8.2
55. Mikołajczyk J.: Finding the correlation between wear of samples kinematic pair of conformal contact and electric power consumption. Postępy w Inżynierii Mechanicznej [Developments in Mechanical Engineering]; 2020, nr 15 (8), s. 59-68, p-ISSN: 2300-3383; Wydawnictwa Uczelniane Uniwersytetu Technologiczno-Przyrodniczego im. J. J. Śniadeckich w Bydgoszczy, Poland.
https://dme.utp.edu.pl/art/15(8)2020/59.pdf
DOI: 10.37660/dme.2020.15.8.6
56. Mikołajczyk J.: The effect of temperature lag on the value of power-temperature correlation for frictional pair of conformal contact. Postępy w Inżynierii Mechanicznej [Developments in Mechanical Engineering]; 2020, nr 15 (8), s. 79-86, p-ISSN: 2300-3383; Wydawnictwa Uczelniane Uniwersytetu Technologiczno-Przyrodniczego im. J. J. Śniadeckich w Bydgoszczy, Poland.
https://dme.utp.edu.pl/art/15(8)2020/79.pdf

DOI: 10.37660/dme.2020.15.8.8
57. Mikołajczyk J.: Określenie na podstawie modeli zmiany masy próbek w wyniku procesu zużywania. **W:** Szkoła Logistyki 2021 / redakcja naukowa Janusz Zawiła-Niedźwiecki, Piotr Korneta. Radom : Instytut Naukowo-Wydawniczy "Spatium", 2021; s. 167-174, Poland;
p-ISBN: 978-83-66550-75-9; e-ISBN: 978-83-66550-89-6.
58. Mikołajczyk J.: A method of determining mathematical models of a seizure test of friction pairs. **W:** MIK-21 : Międzynarodowa Innowacyjność i Konkurencyjność w XXI wieku : aspekty innowacyjne / redakcja naukowa Radoslaw Luft. Lublin : Fundacja Innowacji i Nowoczesnych Technologii INOTECH, 2022. Radom : nakładem Instytutu Naukowo-Wydawniczego "Spatium", 2022; s. 7-24, p-ISBN: 978-83-67033-43-5;
e-ISBN: 978-83-67033-44-2.
http://inw-spatium.pl/wp-content/uploads/2022/09/MIK-21-2022-Aspekty-innowacyjne-2.pdf
59. Mikołajczyk J.: Friction machines. Piła: Wydawnictwo Akademii Nauk Stosowanych im. Stanisława Staszica, 2022, Poland; 488 s., e-ISBN: 978-83-62617-96-8.
https://wydawnictwo.ans.pila.pl/files/FRICTION_MACHINES.pdf
60. Mikołajczyk J., Jędrzejczyk D.: Określenie korelacji między prędkością skrawania a parametrem chropowatości Ra. Obróbka Metalu; 2022, nr 3, s. 11-15,
p-ISSN: 2081-7002; **https://obrobkametalu.tech/**
61. Mikołajczyk J.: Rolling bearing heating charakter. **W:** Szkoła Logistyki 2022. Radom: Instytut Naukowo-Wydawniczy "Spatium", 2022, Poland; s. 231-239, Materiały z IX Konferencji Naukowej "Szkoła Logistyki 2022"; p-ISBN: 978-83-67033-33-6;
e-ISBN: 978-83-67033-34-3.
62. Mikołajczyk J.: Tribological properties of carbon black. **W:** Szkoła Logistyki 2022. Radom: Instytut Naukowo-Wydawniczy "Spatium", 2022, Poland; s. 217-230, Materiały z IX Konferencji Naukowej "Szkoła Logistyki 2022"; p-ISBN: 978-83-67033-33-6;
e-ISBN: 978-83-67033-34-3.
63. Mikołajczyk J.: Determination of the modified coefficient of variation from the number of samples. **W:** MIK-21 : Międzynarodowa Innowacyjność i Konkurencyjność w XXI wieku : Aspekty innowacyjne / redakcja naukowa dr Łukasz Wojtowicz. Lublin: Fundacja Innowacji i Nowoczesnych Technologii INOTECH : nakładem Instytutu Naukowo-Wydawniczego "Spatium", 2023, Poland; s. 111-122, p-ISBN: 978-83-67033-89-3;
e-ISBN: 978-83-67033-90-9.
64. Mikołajczyk J.: Effect of cutting speed on the shape of the machined surface profile. Mebutra; 2023, nr 1, s. 47-63, Wydawnictwo Akademii Nauk Stosowanych im. S. Staszica w Pile, Piła 2023, Poland.
https://online.fliphtml5.com/vliuj/yunw/ p=48
65. Mikołajczyk J.: Friction Machines II. Piła: Wydawnictwo Akademii Nauk Stosowanych im. Stanisława Staszica w Pile, 2023, Poland; s. 598; p-ISBN: 978-83-67684-00-2;
https://wydawnictwo.ans.pila.pl/files/FRICTION_MACHINES_V_ANS_PILA.pdf
66. Mikołajczyk J.: Oil can talk. **W:** Szkoła Logistyki 2023 / redakcja naukowa Janusz Zawiła-Niedźwiecki, Katarzyna Białczak. Radom: Instytut Naukowo-Wydawniczy "Spatium", 2023, Poland; s. 109-115, p-ISBN: 978-83-67033-75-6;
e-ISBN: 978-83-67033-58-9.
67. Mikołajczyk J.: Pobór mocy elektrycznej przez parę kinematyczną jako parametr oceny jakości oleju. **W:** Logistyka w ratownictwie 2023 / pod redakcją Andrzeja Chudzikiewicza i Anny Stelmach. Radom: Instytut Naukowo-Wydawniczy "Spatium", 2023, Poland; s. 223-230, p-ISBN: 978-83-67033-95-4; e-ISBN: 978-83-67033-96-1.

68. Mikołajczyk J.: Rola dodatków smarowych w olejach. **W:** Logistyka w ratownictwie 2023 /pod redakcją Andrzeja Chudzikiewicza i Anny Stelmach/; Radom: Instytut Naukowo-Wydawniczy "Spatium", 2023, Poland; s. 231-237, p-ISBN: 978-83-67033-95-4; e-ISBN: 978-83-67033-96-1.
69. Mikołajczyk J.: Temperature as a parameter for assessing the work of a friction pair. **W:** Szkoła Logistyki 2023 / redakcja naukowa Janusz Zawiła-Niedźwiecki, Katarzyna Białczak. Radom: Instytut Naukowo-Wydawniczy "Spatium", 2023, Poland; s. 101-107, p-ISBN: 978-83-67033-75-6; e-ISBN: 978-83-67033-58-9.
70. Mikołajczyk J.: Tire as a selected element of a car subject to diagnostics. **W:** Szkoła Logistyki 2023 / redakcja naukowa Janusz Zawiła-Niedźwiecki, Katarzyna Białczak. Radom: Instytut Naukowo-Wydawniczy "Spatium", 2023, Poland; s. 117-131, p-ISBN: 978-83-67033-75-6; e-ISBN: 978-83-67033-58-9.
71. Mikołajczyk J.: Wpływ dodatku modyfikującego cechy płynu obróbkowego na zmianę temperatury w strefie kontaktu współpracujących powierzchni. Obróbka Metalu; 2023, nr 2, s. 43-46, p-ISSN: 2081-7002; **https://obrobkametalu.tech/media/2023/05/2023_2_52_ObrobkaMetalu.pdf**
72. Mikołajczyk J., Kozłowska M.A., Krasicki K.: Wpływ kompetencji cyfrowych pracowników na poziom rozwoju procesów przemysłowych. **W:** MIK-21 : Międzynarodowa Innowacyjność i Konkurencyjność w XXI wieku : aspekty społeczne /redakcja naukowa Radosław Luft/; Lublin-Radom : Fundacja Innowacji i Nowoczesnych Technologii INOTECH : nakładem Instytutu Naukowo-Wydawniczego "Spatium", 2023, Poland; s. 149-169, p-ISBN: 978-83-67033-92-3; e-ISBN: 978-83-67033-93-0.
73. Mikołajczyk J.: Zmiana geometrycznych cech współpracujących powierzchni miarą intensywności procesu zużywania ostrzy skrawających. Obróbka Metalu; 2023, nr 1, s. 50-54, p-ISSN: 2081-7002; **https://yadda.icm.edu.pl/yadda/element/bwmeta1.element.baztech-9e73eb05-2a91-4df5-853b-22abf7a6ee77**
74. Mikołajczyk J., Góra F., Jędrzejczyk D.: Analysis of selected surface roughness parameters for wear processes. Analiza wybranych parametrów chropowatości powierzchni pod kątem procesów zużywania. **W:** MIK-21 : Międzynarodowa Innowacyjność i Konkurencyjność w XXI wieku : Aspekty innowacyjne / redakcja naukowa Radosław Luft. Lublin: Wydawnictwo Naukowe FNCE, 2024; s. 93-117, p-ISBN: 978-83-68074-82-6; e-ISBN: 978-83-68319-03-3.
75. Mikołajczyk J., Galon M.: Mathematical model of straight regression determining the effect of laser cutting speed on the mass of the workpiece. **W:** MIK-21 : Międzynarodowa Innowacyjność i Konkurencyjność w XXI wieku : Aspekty innowacyjne / redakcja naukowa Radosław Luft. Lublin: Wydawnictwo Naukowe FNCE, 2024, Poland; s. 71-92, p-ISBN: 978-83-68074-82-6; e-ISBN: 978-83-68319-03-3.
76. Mikołajczyk J., Sądej I.: Spinning speed and balancing accuracy. **W:** MIK-21 : Międzynarodowa Innowacyjność i Konkurencyjność w XXI wieku : Aspekty innowacyjne / redakcja naukowa Radosław Luft. Lublin: Wydawnictwo Naukowe FNCE, 2024, Poland; s. 118-132, p-ISBN: 978-83-68074-82-6; e-ISBN: 978-83-68319-03-3.
77. Mikołajczyk J.: The correlation between the population and number of construction disasters. Mebutra; 2025, nr 3, s. 44-55, Wydawnictwo Akademii Nauk Stosowanych im. S. Staszica w Pile, Poland. **https://wydawnictwo.ans.pila.pl/files/MEBUTRA2025.pdf**
78. Mikołajczyk J.: The relationship between the type of structure and the number of construction disasters. Zależność między rodzajem konstrukcji, a liczbą katastrof budowlanych. Mebutra; 2025, 3, s. 30-43, Wydawnictwo Akademii Nauk Stosowanych im. S. Staszica w Pile, Poland.

https://wydawnictwo.ans.pila.pl/files/MEBUTRA2025.pdf
79. Mistur L.: Spawanie gazowe i elektryczne. Wydawnictwa Szkolne i Pedagogiczne. Warszawa 1983.
80. Norma PN-86/H-84018. Stal niskostopowa o podwyższonej wytrzymałości. Gatunki.
81. Norma PN-75/H-84019. Stal węglowa konstrukcyjne wyższej jakości ogólnego przeznaczenia. Gatunki.
82. Norma PN-72/H-84020. Stal węglowa konstrukcyjna zwykłej jakości ogólnego przeznaczenia. Gatunki.
83. Norma PN-75/H-84024. Stal do pracy przy podwyższonych temperaturach. Gatunki.
84. Norma PN-71/H-86020. Stal odporna na korozję (nierdzewna i kwasoodporna). Gatunki.
85. Norma PN-71/H-86022. Stal żaroodporna. Gatunki.
86. Norma PN-75/M-69703. Spawalnictwo. Wady złączy spawanych. Nazwy i określenia (zmiana 1, Biul. PKNiM nr 9/76, poz. 85).
87. Norma PN-78/M-69760. Spawalnictwo. Badania skłonności do tworzenia zimnych pęknięć w złączach spawanych łukowo.
88. Norma PN-79/M-69761. Spawalnictwo. Metody badań skłonności do tworzenia pęknięć krystalizacyjnych w spoinach stalowych złączy spawanych łukowo.
89. Norma PN-72/M—69770. Radiografia przemysłowa. Radiogramy spoin czołowych w złączach doczołowych ze stali. Wymagania jakościowe i wytyczne wykonania.
90. Norma PN-74/M-69771. Spawanie. Wady złączy doczołowych wykrywane badaniami radiograficznymi. Nazwy i określenia (zmiana 1, Biul. PKNiM nr 9/76, poz. 85).
91. Norma PN-87/M-69772. Spawalnictwo. Klasyfikacja wadliwości złączy spawanych na podstawie radiogramów.
92. Norma PN-85/M-69775. Spawalnictwo. Wadliwość złączy spawanych. Oznaczenia klasy wadliwości na podstawie oględzin zewnętrznych.
93. Norma PN-77/M-70001. Przemysłowe badania radiograficzne. Wskaźniki jakości obrazu. Wymagania.
94. Norma PN-75/M-70020. Badania nie niszczące. Metody radiologiczne. Nazwy i określenia.
95. Norma PN-76/M-70050. Badania nie niszczące. Metody ultradźwiękowe. Nazwy i określenia.
96. Norma PN-75/M-70051. Badania nie niszczące metodami ultradźwiękowymi. Wzorzec kontrolny W1.
97. Norma PN-74/M-70052. Badania nie niszczące. Metody penetracyjne. Nazwy i określenia.
98. Norma PN-75/M-70054. Badania nie niszczące metodami ultradźwiękowymi. Wzorzec kontrolny W2.
99. Norma PN-77/M-70055. Badania nie niszczące. Metody ultradźwiękowe. Badanie spoin w złączach doczołowych.
100. Norma PN-75/M-70056. Badania nie niszczące metodami ultradźwiękowymi. Wzorce mikrosekundowe.
101. Norma PN-86/M-69707. Spawalnictwo. Zasady wykonywania próbnych złączy spawanych lub zgrzewanych.
102. Norma PN-78/M-69710. Spawalnictwo. Próba statyczna rozciągania doczołowych złączy spawanych lub zgrzewanych.
103. Norma PN-80/M-69714. Spawalnictwo. Próba statyczna rozciągania złączy ze spoinami pachwinowymi.
104. Norma PN-57/M-69715. Spawanie. Próba statyczna rozciągania złącza nakładkowego z pachwinowymi spoinami poprzecznymi.

105. Norma PN-57/M-69716. Spawanie. Próba statyczna rozciągania złącza nakładkowego z pachwinowymi spoinami podłużnymi.
106. Norma PN-78/M-69720. Spawalnictwo. Próby zginania doczołowych złączy spawanych lub zgrzewanych.
107. Norma PN-70/M69733. Spawalnictwo. Próba udarności złączy spawanych lub zgrzewanych doczołowo.
108. Norma PN-69/M-69734. Próba starzenia stalowych płaskich złączy spawanych doczołowo.
109. Norma PN-58/M69740. Spawanie. Próba łamania płaskiego złącza doczołowego o grubości powyżej 4 mm.
110. Norma PN-58/M-69741. Spawanie. Próba łamania złącza kątowego ze spoiną pachwinową.
111. Norma PN-58/M-69742. Spawanie. Próba łamania złącza nakładkowego ze spoiną pachwinową.
112. Norma PN-64/M-69751. Próba twardości złączy spawanych i zgrzewanych.
113. Norma PN-76/M-69783. Spawalnictwo. Próby statyczne ścinania i rozciągania zgrzein liniowych.
114. Norma PN-67/M-69790. Próby statyczne rozciągania i ścinania złączy lutowanych.
115. Norma PN-65/M-69013. Spawanie gazowe stali niskowęglowych i niskostopowych. Rowki do spawania.
116. Norma PN-75/M-69014. Spawanie lukowe elektrodami otulonymi stali węglowych i niskostopowych. Przygotowanie brzegów do spawania.
117. Norma PN-73/M-69015. Spawanie łukiem krytym stali węglowych i niskostopowych. Przygotowanie brzegów do spawania.
118. Norma PN-74/M-69016. Spawanie w osłonie dwutlenku węgla stali węglowych i niskostopowych. Przygotowanie brzegów do spawania.
119. Norma PN-65/M-69017. Spawanie argonowe elektroda nietopliwą stali stopowych. Rowki do spawania.
120. Norma PN-67/M-69018. Spawanie żużlowe stali węglowych i niskostopowych. Rowki do spawania.
121. Norma PN-69/M-69019. Spawanie doczołowe rur stalowych. Rowki do spawania.
122. Norma PN-70/M-69023. Spawanie łukowe stali platerowanych stalą odporną na korozje. Wytyczne projektowania i wykonywania złączy spawanych.
123. Norma PN-70/M-69024. Spawanie łukowe aluminium i jego stopów elektrodą wolframową w osłonie argonu. Przygotowanie brzegów do spawania.
124. Norma PN-70/M-69025. Spawanie gazowe miedzi. Przygotowanie brzegów do spawania.
125. Norma PN-72/M-69026. Spawanie łukowe miedzi w osłonie argonu elektrodą wolframową. Przygotowanie brzegów do spawania.
126. Norma PN-73/M-69027. Spawanie łukowe aluminium i jego stopów elektrodą topliwą w osłonie argonu. Przygotowanie brzegów do spawania.
127. Norma PN-78/M-69028. Spawalnictwo. Spawanie łukowe miedzi w osłonie argonu elektrodą topliwą. Przygotowanie brzegów do spawania.
128. Norma PN-76/M-69070. Spawalnictwo. Urządzenia do mechanizacji spawania. Nazwy i określenia.
129. Norma PN-61/M-69100. Spawalnictwo. Źródła prądu do ręcznego spawania łukowego. Klasyfikacja.
130. Norma PN-75/M-69101. Spawalnictwo. Szpule elektrodowe do automatów i półautomatów spawalniczych. Główne wymiary.

131. Norma PN-75/M-69104. Automaty i półautomaty do spawania łukiem krytym i w osłonie gazów ochronnych elektrodą topliwą. Nazwy i określenia.
132. Norma PN-75/M-69105. Spawalnictwo. Półautomaty spawalnicze do spawania łukowego w osłonie gazu ochronnego elektrodą topliwą. Ogólne wymagania i badania.
133. Norma PN-79/M-69106. Spawalnictwo. Automaty spawalnicze. Ogólne wymagania i badania.
134. Norma PN-83/M-69108. Spawalnictwo. Źródło energii elektrycznej do spawania łukowego. Nazwy i określenia.
135. Norma PN-69/M-69124. Elektrody wolframowe do celów spawalniczych.
136. Norma PN-76/M-69160. Spawalnictwo. Osłony twarzy przed promieniowaniem łuku spawalniczego. Tarcze spawalnicze.
137. Norma PN-80/M-69161. Spawalnictwo. Uchwyty elektrodowe do spawania ręcznego izolowane.
138. Norma PN-79/M-69010. Wyroby z węgli uszlachetnionych. Elektrody spawalnicze.
139. Norma PN-85/E-81106. Spawalnictwo. Jednostanowiskowe transformatory spawalnicze. Wymagania i badania.
140. Norma PN-74/M-69102. Spawalnictwo. Przecinarki do cięcia termicznego. Dokładność odwzorowania.
141. Norma PN-74/M-69103. Spawalnictwo. Przecinarki półautomatyczne do cięcia tlenem stali. Wymagania i badania.
142. Norma PN-80/M-69107. Spawalnictwo. Przecinarki do cięcia termicznego. Nazwy i określenia.
143. Norma PN-80/M-69180. Spawalnictwo. Palniki, oznaczenia i cechowanie.
144. Norma PN-81/M-69181. Spawalnictwo. Dysze palników gazowych. Określenia, podział i oznaczenia.
145. Norma PN-76/M69182. Spawalnictwo. Palniki do spawania gazowego i cięcia tlenem. Wymagania i badania.
146. Norma PN-75/M-69200. Spawalnictwo. Wytwornice acetylenowe. Podział.
147. Norma PN-76/M-69202. Spawalnictwo. Zawory bezpieczeństwa.
148. Norma PN-75/M-69210. Zbiorniki transportowe do gazów. Barwy rozpoznawcze i oznakowanie.
149. Norma PN-79/M-69221. Butle do gazów. Butle stalowe do gazów.
150. Norma PN-76/M-69222. Butle do gazów. Butle stalowe bez szwu.
151. Norma PN-82/M-69223. Butle do gazów. Gwinty stożkowe. Wymiary i tolerancje.
152. Norma PN-60/M-69224. Butle do gazów. Gwinty Whitwortha o średnicach 21,8 i 24,3 mm.
153. Norma PN-80/M-69225. Butle do gazów. Gwint Whitwortha o średnicy 80 mm.
154. Norma PN-63/M-69226. Butle do gazów. Gwint stożkowy metryczny.
155. Norma PN-67/M-69227. Zawory butlowe do acetylenu VA1.
156. Norma PN-81/M-69228. Butle do gazów. Zawory do butli. Wymagania i badania.
157. Norma PN-81/M-69229. Butle do gazów. Złącza zaworów butlowych.
158. Norma PN-74/M-69240. Reduktory spawalnicze. Główne wskaźniki.
159. Norma PN-80/M-69242. Spawalnictwo. Reduktory do tlenu.
160. Norma PN-77/M-69243. Spawalnictwo. Reduktory butlowe do gazów płynnych.
161. Norma PN-78/M-69244. Spawalnictwo. Reduktory do acetylenu.
162. Norma PN-72/M-69260. Spawalnictwo. Króćce do przyłączenia węży gumowych. Główne wymiary.
163. Norma PN-71/M-69261. Spawalnictwo. Przyłączki i złączki do węży gumowych.
164. Norma PN-76/M-69774. Spawalnictwo. Cięcie gazowe stali węglowych o grubości 5÷100 mm. Jakość powierzchni cięcia.

165. Norma PN-63/M-74905. Opaski zaciskowe przewodów giętkich.
166. Norma PN-77/C-94250.47. Węże gumowe. Węże tłoczne gumowe ze wzmocnieniem tekstylnym do tlenu.
167. Norma PN-77/C-94250.48. Węże gumowe. Węże tłoczne ze wzmocnieniem tekstylnym do acetylenu.
168. Norma BN-68/4122-02. Zawory butlowe do tlenu technicznego VT1.
169. Norma PN-67/M-69350. Topniki spawalnicze. Klasyfikacja.
170. Norma PN-81/M-69354. Spawalnictwo. Topniki do gazowego spawania miedzi, mosiądzów, brązów, aluminium i stopów aluminium.
171. Norma PN-73/M-69355. Topniki do spawania i napawania łukiem krytym.
172. Norma PN-67/M-69356. Topniki do spawania żużlowego.
173. Norma PN-76/M-69400. Spoiwa cynowo-ołowiowe do lutowania miękkiego. Gatunki.
174. Norma PN-80/M-69411. Spawalnictwo. Spoiwa srebrne do lutowania.
175. Norma PN-73/M-69412. Spawalnictwo. Druty do gazowego i łukowego metalizowania natryskowego.
176. Norma PN-70/M-69413. Spoiwa miedziane, mosiężne, brązowe i niklowe do spawania i lutowania.
177. Norma PN-75/M-69414. Spawalnictwo. Spoiwa do spawania aluminium i stopów aluminium.
178. Norma PN-77/M-69420. Spawalnictwo. Spoiwa stalowe do spawania i napawania.
179. Norma PN-74/M-69430. Spawalnictwo. Elektrody stalowe otulone do spawania i napawania. Ogólne wymagania i badania.
180. Norma PN-77/M-69433. Spawalnictwo. Elektrody stalowe otulone do spawania stali węglowych i niskostopowych.
181. Norma PN-74/M-69434. Elektrody otulone do spawania stali niskostopowych przeznaczonych do pracy w podwyższonych temperaturach.
182. Norma PN-79/M-69435. Spawalnictwo. Elektrody stalowe do spawania stali wysokostopowych.
183. Norma PN-74/M-69436. Elektrody stalowe do napawania.
184. Norma PN-57/M-69451. Spawanie. Spoiwa. Pręty żeliwne.
185. Norma PN-64/M-69708. Spawalnictwo. Próby mechaniczne stopiwa.
186. Norma PN-57/M-69712. Spawanie. Próba statyczna rozciągania materiału spoiny.
187. norma PN-58/M-69717. Spawanie gazowe. Próba statyczna rozciągania stopiwa.
188. Norma PN-58/M-69730. Spawanie gazowe. Próba udarności stopiwa.
189. Norma PN-82/C-23050. Karbid.
190. Norma PN-71/C-84905. Acetylen rozpuszczony.
191. Norma PN-61/C-84908. Wodór techniczny sprężony.
192. Norma PN-70/C-84910. Tlen sprężony (zmiana Biul. PKNiM nr 10/76, poz. 93).
193. Norma PN-72/C-84912. Azot sprężony techniczny.
194. Norma PN-82/C-96000. Przetwory naftowe. Gazy węglowodorowe (płynne C_3-C_4).
195. Norma PN-77/M-69000. Spawalnictwo. Spawanie metali. Nazwy i określenia.
196. Norma PN-84/M-69001. Spawalnictwo. Spajanie metali i procesy pokrewne. Podział.
197. Norma PN-75/M-69002. Spawalnictwo. Pozycje spawania. Klasyfikacja i oznaczenia.
198. Norma PN-87/M-69008. Spawalnictwo. Klasyfikacja konstrukcji spawanych.
199. Norma PN-87/M-6990/01. Spawalnictwo. Egzaminy spawaczy i zgrzewaczy. Postanowienia ogólne.
200. Norma PN-87/M-69900/02. Spawalnictwo. Podstawowy egzamin spawacza.
201. Norma PN-87/M-69900/03. Spawalnictwo. Ponadpodstawowy egzamin spawacza.
202. Norma PN-87/M-69900/04. Spawalnictwo. Egzamin spawacza-operatora.
203. Norma PN-87/M-69900/05. Spawalnictwo. Egzamin zgrzewacza.

204. Norma PN-87/M-69900/06. Spawalnictwo. Egzamin rozszerzający oraz sprawdzający spawacza i zgrzewacza.
205. Norma PN-79/M- 01134. Rysunek techniczny maszynowy. Uproszczenia rysunkowe. Zasady oznaczania spoin.
206. Norma PN-64/M-01138. Rysunek techniczny maszynowy. Połączenia spawane i powierzchnie napawane (zmiana Biul. PKN nr 6/67, poz. 67).
207. Norma PN-64/M-01139. Rysunek techniczny maszynowy. Połączenia zgrzewane i lutowane (bez lutowania). Biul. PKNiM nr 28/76.
208. Norma PN-83/N-01635. Rysunek techniczny. Uproszczenia rysunkowe. Połączenia nitowane, lutowane, klejone i zszywane.
209. Norma PN-64/B-01043. Rysunek konstrukcyjny budowlany. Konstrukcje stalowe.
210. Norma PN-81/M-Z-53201. Sprzęt ochrony osobistej oczu. Optyczne filtry i szybki ochronne. Ogólne wymagania i badania.
211. Norma PN-73/Z-53205. Sprzęt ochrony osobistej oczu. Szybki ochronne przeciwodpryskowe.
212. Olechnowicz J., Mikołajczyk J.: Truck scales : the key to safe transport and road protection. Mebutra; 2024, nr 2, s. 03-08, Wydawnictwo Akademii Nauk Stosowanych im. S. Staszica w Pile, Poland.
https://wydawnictwo.ans.pila.pl/files/MEBUTRA2024.pdf
213. Pałasz J.: Poradnik spawacza gazowego. Wydawnictwa Naukowo-Techniczne. Warszawa 1986.
214. Piwowar S.: Spawanie i zgrzewanie elektryczne. Wydawnictwa Szkolne i Pedagogiczne. Warszawa 1981.
215. Piwowar S.: Kontrola procesów spawalniczych. Wydawnictwa Naukowo-Techniczne, Warszawa 1979.
216. Piątek P.: Spawanie (materiały dydaktyczne). Wydawnictwo SANNORT, Sandomierz, 2014.
217. Pikulik K.W., Mikołajczyk J.: The influence of the welding current on the air pollution emissions. Wpływ prądu spawania na emisję zanieczyszczeń powietrza. Postępy w Inżynierii Mechanicznej [Developments in Mechanical Engineering]; 2019, nr 14 (7), s. 33-46, p-ISSN: 2300-3383; Wydawnictwa Uczelniane Uniwersytetu Technologiczno-Przyrodniczego im. J. J. Śniadeckich w Bydgoszczy, Poland.
http://yadda.icm.edu.pl/baztech/element/bwmeta1.element.baztech-2faf200b-3010-4192-9fd0-062f53b49d38
218. Pikulik K.W., Mikołajczyk J.: Determination of emission of iron oxides from the welding process on the basis of mathematical models. Welding Technology Review; 2021, vol. 93, No 2, s. 35-43, p-ISSN: 0033-2364; e-ISSN: 2449-7959;
http://www.pspaw.wip.pw.edu.pl/index.php/pspaw/article/view/1132
DOI: 10.26628/wtr.v93i2.1132
219. Pikulik J., Pikulik K.W., Mikołajczyk J.: The relationship between the clearance of the coupling mechanism used in uniaxial light car trailers and the date of their production. **W:** MIK-21 : Międzynarodowa Innowacyjność i Konkurencyjność w XXI wieku : aspekty innowacyjne / redakcja naukowa Radosław Luft. Lublin : Fundacja Innowacji i Nowoczesnych Technologii INOTECH, 2022, Poland. Radom : nakładem Instytutu Naukowo-Wydawniczego "Spatium"; 2022; s. 221-233, p-ISBN: 978-83-67033-43-5; e-ISBN: 978-83-67033-44-2;
http://inw-spatium.pl/wp-content/uploads/2022/09/MIK-21-2022-Aspekty-innowacyjne-2.pdf
220. Pikulik J., Pikulik K.W., Mikołajczyk J.: Zależność wielkości luzu mechanizmu sprzęgającego stosowanego w jednoosiowych lekkich przyczepach samochodowych od

wartości współczynnika przylegania. **W:** Logistyka w ratownictwie 2022 / pod redakcją Andrzeja Chudzikiewicza i Andrzeja Krzyszkowskiego. Radom: Instytut Naukowo-Wydawniczy "Spatium", 2022, Poland; s. 157-167, p-ISBN: 978-83-67033-57-2;
e-ISBN: 978-83-67033-70-1.
221. Pikulik J., Pikulik K.W., Mikołajczyk J.: Determination of the degree of contact of the movable part of the coupling head with the ball part of the coupling of single-axle light car trailers. **W:** MIK-21 : Międzynarodowa Innowacyjność i Konkurencyjność w XXI wieku : aspekty innowacyjne / redakcja naukowa dr Łukasz Wojtowicz. Lublin: Fundacja Innowacji i Nowoczesnych Technologii INOTECH : nakładem Instytutu Naukowo-Wydawniczego "Spatium", 2023, Poland; s. 97-109, p-ISBN: 978-83-67033-89-3;
e-ISBN: 978-83-67033-90-9.
222. Pilarczyk J.: Poradnik inżyniera. Spawalnictwo. t. 2. Wydawnictwa Naukowo-Techniczne, Warszawa, 2005.
223. Piochacz A., Mikołajczyk J.: Wpływ czasu trwania procesu anodowania stopu aluminium EN AW-6060 na grubość i twardość otrzymanej warstwy. Influence of aluminium type EN AW-6060 anodizing process duration on the thickness and hardness of the obtained layer. Postępy w Inżynierii Mechanicznej [Developments in Mechanical Engineering]; 2018, nr 12 (6), s. 49-56, p-ISSN: 2300-3383; Wydawnictwa Uczelniane Uniwersytetu Technologiczno-Przyrodniczego w Bydgoszczy, Poland.
http://wu.utp.edu.pl/oferta,8,1
224. Piochacz A., Mikołajczyk J.: Analiza statystyczna wpływu czasu anodowania na grubość otrzymanej powłoki. Statistical analysis of the influence of anodizing time on the thickness of obtained layers. Autobusy. Technika, Eksploatacja, Systemy Transportowe; 2019, vol. 233, nr 9, s. 48-51, p-ISSN: 1509-5878; e-ISSN: 2450-7725;
http://ceref.pl/index.php/Autobusy/article/view/956
DOI: 10.24136/atest.2019.201
225. Piochacz A., Mikołajczyk J.: Determination of the thickness of anodized layer on the basis mathematical models. Developments in Mechanical Engineering; 2020, nr 16 (8), s. 31-39, p-ISSN: 2720-0639; Wydawnictwa Uczelniane Uniwersytetu Technologiczno-Przyrodniczego im. J. J. Śniadeckich w Bydgoszczy, Poland.
DOI: 10.37660/dme.2020.16.8.3
226. Piotrowski Ł., Góra F., Mikołajczyk J.: Construction of an electric longboard with one-wheel driver. Mebutra; 2024, nr 2, s. 16-27, Wydawnictwo Akademii Nauk Stosowanych im. S. Staszica w Pile, Poland.
https://wydawnictwo.ans.pila.pl/files/MEBUTRA2024.pdf
227. Piotrowski Ł., Góra F., Mikołajczyk J.: Design and construction of an electric longboard. **W:** Logistyka w ratownictwie 2024 / pod redakcją Andrzeja Chudzikiewicza i Andrzeja Krzyszkowskiego. Radom: Instytut Naukowo-Wydawniczy Spatium, 2024, Poland; s. 167-178, p-ISBN: 978-83-68026-24-5; e-ISBN: 978-83-68026-25-2.
228. Praca zbiorowa: Poradnik inżyniera spawalnictwa. Wydawnictwa Naukowo-Techniczne. Warszawa 1983.
229. Przybył B., Kabat M., Mikołajczyk J.: Wpływ prędkości drukowania 3D na dokładność zarysu kół zębatych. Obróbka Metalu; 2023, nr 4, s. 26-30, p-ISSN: 2081-7002;
https://obrobkametalu.tech/media/2023/08/2023-4_Nr54_ObrobkaMetalu.pdf
230. Przybył B., Mikołajczyk J.: Efektywność technik przyrostowych. Obróbka Metalu; 2024, nr 1, s. 22-25, p-ISSN: 2081-7002;
https://obrobkametalu.tech/media/2024/03/2024_1_nr55_ObrobkaMetalu-1.pdf
231. Przybył B., Mikołajczyk J.: The influence of 3D printing speed on profile accuracy. **W:** Szkoła Logistyki 2024 / redakcja naukowa Janusz Zawiła-Niedźwiecki, Adam Płaczek.

Radom: Instytut Naukowo-Wydawniczy "Spatium", 2024, Poland; s. 199-216, p-ISBN: 978-83-68026-07-8; e-ISBN: 978-83-68026-08-5.
232. Radomski T., Ciszewski A.: Lutowanie. Wydawnictwa Naukowo-Techniczne. Warszawa 1985.
233. Sądej I., Mikołajczyk J.: Machine tool compensation and mass unbalance measurements. **W:** Logistyka w ratownictwie 2024 / pod redakcją Andrzeja Chudzikiewicza i Andrzeja Krzyszkowskiego. Radom: Instytut Naukowo-Wydawniczy Spatium, 2024, Poland; s. 187-196, p-ISBN: 978-83-68026-24-5; e-ISBN: 978-83-68026-25-2.
234. Styp-Rekowski M., Mikołajczyk J.: The influence of Mind M preparation on the lubricant properties of base oil SN-150. W**:** Reinung, Schmierung und Verschleiβ : forschung und praktische anwendungen : Band 1 : tribologische systeme schmierstoffe und schmierungstechnik zerspanungs : und umformtechnik prüfen, messen, kontrollieren / 53. Tribologie-Fachtagung. 24.bis 26. Septembet 2012 in Göttingen. Aachen : Gesellschaft für Tribologie e.V., 2012. p-ISBN: 978-3-00-039201-6.
235. Styp-Rekowski M., Mikołajczyk J.: Wpływ dodatku na własności smarowe oleju bazowego SN-150. Źródło: Tribologia. 2012, vol. 244, No. 4, s. 227-232, p-ISSN: 0208-7774; e-ISSN: 1732-422X; **https://t.tribologia.eu/resources/html/article/details?id=167726**
236. Styp-Rekowski M., Mikołajczyk J.: Wpływ preparatu eksploatacyjnego stanowiący kompleks węglowodorowy na zmianę własności smarnych oleju bazowego SN-150. W: Tribologia bliżej praktyki : XXXII Ogólnopolska Konferencja "Jesienna Szkoła Tribologiczna 2012". XXXII Ogólnopolska Konferencja "Jesienna Szkoła Tribologiczna 2012", Kudowa Zdrój, 18-21 września 2012r. Politechnika Wrocławska Wydział Mechaniczny, Instytut Konstrukcji Eksploatacji Maszyn, Polskie Towarzystwo Tribologiczne, Sekcja Podstaw Eksploatacji KBM PAN. Wrocław : Polskie Towarzystwo Tribologiczne, 2012.
237. Styp-Rekowski M., Mikołajczyk J.: Zmiana temperatury na drodze tarcia dla kompozycji olej bazowy SN-150 - preparat eksploatacyjny Mind M. Temperature variability during friction for composition bese oil SN-150 - exploatational preparation Mind M. **W:** III krajowa konferencja nano- i mikromechaniki / Komitet Mechaniki Polskiej Akademii Nauk, Politechnika Rzeszowska im. Ignacego Łukasiewicza, Instytut Podstawowych Problemów Techniki Polskiej Akademii Nauk. Warszawa, 4-6 lipca 2012 r. III Krajowa Konferencja Nano- i Mikromechaniki pod Patronatem Ministra Nauki i Szkolnictwa Wyższego Prof. Barbary Kudryckiej : Komitet Mechaniki Polskiej Akademii Nauk, Politechnika Rzeszowska, Instytut Podstawowych Problemów Techniki Polskiej Akademii Nauk, Warszawa, 2012.
238. Styp-Rekowski M., Mikołajczyk J., Matuszewski M.: Wybrane zagadnienia stosowania płynów obróbkowych w obróbce skrawaniem. W**:** Obróbka Metalu, 2014, nr 3, s. 10-14, p-ISSN: 2081-7002; **http://www.e-obrobkametalu.pl/**
239. Syrek S., Mikołajczyk J.: Analiza matematyczna podstawowych wymiarów złącza spawanego. **W:** Logistyka w ratownictwie 2022 / pod redakcją Andrzeja Chudzikiewicza i Andrzeja Krzyszkowskiego. Radom : Instytut Naukowo-Wydawniczy "Spatium", 2022; s. 169-190, p-ISBN: 978-83-67033-57-2; e-ISBN: 978-83-67033-70-1.
240. Syrek S., Mikołajczyk J.: Modele liniowe wpływu częstotliwości prądu spawania na grubość spoiny. **W:** MIK-21 : Międzynarodowa Innowacyjność i Konkurencyjność w XXI wieku : aspekty innowacyjne / redakcja naukowa Radosław Luft. Lublin: Fundacja Innowacji i Nowoczesnych Technologii INOTECH, 2022. Radom : nakładem Instytutu Naukowo-Wydawniczego "Spatium", 2022; s. 153-170, p-ISBN: 978-83-67033-43-5;
e-ISBN: 978-83-67033-44-2;
http://inw-spatium.pl/wp-content/uploads/2022/09/MIK-21-2022-Aspekty-innowacyjne-2.pdf

241. Syrek S., Mikołajczyk J.: Modele liniowe wpływu częstotliwości prądu spawania na szerokość spoiny. Obróbka Metalu; 2022, nr 4, s. 24-31, p-ISSN: 2081-7002; **https://obrobkametalu.tech/**
242. Szustakowski J.: Poradnik spawacza elektrycznego. Wydawnictwa Naukowo-Techniczne, Warszawa 1977.
243. Śledziewski E.: Projektowanie stalowych konstrukcji spawanych. Wydawnictwa Naukowo-Techniczne, Warszawa, 1972.
244. Wesołowski L., Mikołajczyk J.: Hammer mill design and construction analysis. **W:** MIK-21 : Międzynarodowa Innowacyjność i Konkurencyjność w XXI wieku : aspekty innowacyjne / redakcja naukowa dr Łukasz Wojtowicz. Lublin: Fundacja Innowacji i Nowoczesnych Technologii INOTECH : nakładem Instytutu Naukowo-Wydawniczego "Spatium", 2023, Poland; s. 159-185, p-ISBN: 978-83-67033-89-3;
e-ISBN: 978-83-67033-90-9.
245. Zandecki R., Kmita C., Mikołajczyk J.: Mathematical models of the surface layer microhardness for a selected grade of ion nitrided steel. **W:** Szkoła Logistyki 2022. Radom : Instytut Naukowo-Wydawniczy "Spatium", 2022, Poland; s. 203-216, Materiały z IX Konferencji Naukowej "Szkoła Logistyki 2022". p-ISBN: 978-83-67033-33-6;
e-ISBN: 978-83-67033-34-3.

Correlation of cutting speed and deflection in milling processing

dr inż. Jarosław Mikołajczyk

Department of Mechanical Engineering

Stanisław Staszic State University of Applied Sciences in Piła, Poland

https://orcid.org/0000-0001-9196-0039

corresponding e-mail: jmikolajczyk@ans.pila.pl

inż. Tomasz Krugiołka

Department of Mechanical Engineering

Stanisław Staszic State University of Applied Sciences in Piła, Poland

https://orcid.org/0009-0005-1500-4594

Abstract:

The paper determines the correlation between cutting speed and deflection during milling processing. The tests performed on milling the strips and the subsequent deformation measurements made it possible to calculate the relationship between both variables. Based on the actual tests performed, determined were also mathematical models for the studied variables

Key words: machining, milling, cutters

1. Introduction

Data science is a dynamically developing discipline. It combines issues from the field of programming and data analysis. Currently, the demand for this type of analysis is very high. The data streams that are processed are very large in terms of quantity. Therefore, appropriate tools are necessary to process them. One of such tools is the R language [37, 40, 42, 43, 45, 48, 60, 62, 67, 71, 72, 75, 85, 86, 87, 89]. There are, of course, many programming languages, but R enables faster and more accurate data processing than other languages. At the address http://bit.ly/2fXfWV2 there is an introduction to the potential of the R program prepared by Microsoft. In this paper, analyzed are deformation results of a steel strip subjected to milling. Subtractive machining is a technique commonly used in industry. It involves shaping parts of machines and devices by removing a specific volume of material which is called machining allowance. Depending on the type of method used to remove machining allowance we can distinguish machining and erosion machining.

Machining is a process in which the movement of cutting edges causes that a layer of machining allowance is converted into chips. The concept of machining includes chip processing which is performed using cutting tools with a defined geometry and a specific number of cutting edges. The chips formed during cutting are visible to the naked eye, and their shape depends on the specified machining parameters. The second type of machining is abrasive machining, which, unlike machining, is performed with a tool of undefined cutting edges, and the chips generated during cutting are in the form of dust.

2. Test conditions and results

The experimental test was carried out on a strip with dimensions of 30x10x320 mm made of unalloyed structural steel S 235JR. This material was chosen because of its widespread use in mechanical engineering. Machining was performed on a 6P82 conventional milling machine. The cutting depth was 2 mm in two passes of the cutting tool. Three types of tests were performed using the following tools:

- NFPc 40 DIN 845 BKN HSS milling cutter, peripheral up milling;
- NFPc 40 DIN 845 BKN HSS milling cutter, up-cut face milling;
- 80 mm TRI-SQ Indexa IND 1393420 milling head with multi-edge inserts, up-cut face milling.

As a result of machining, the processed strip got deformed. The greatest deformation of the strip was located halfway along the strip length (in the middle).

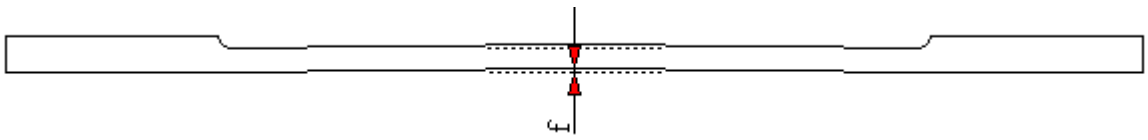

Fig. 1. Measurement of the deflection f [mm] of the milled strip

Table 1. Technical data of the milling cutter NFPc 845 DIN BKN HSS

Working diameter D	Ø 40 mm
Length of working part l	53 mm
Total length L	178 mm
Morse taper number	4
Number of blades Z	6
Flutes inclination angle λ's	30°

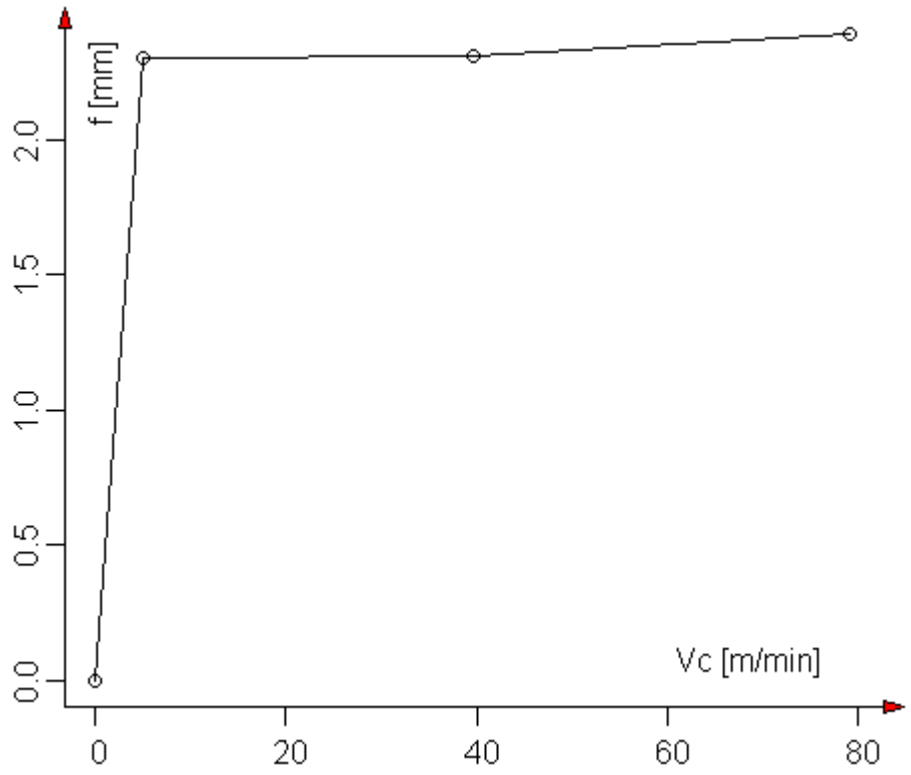

Fig. 2. Graphical representation of the dependence of the deflection f [mm] on the cutting speed Vc [m/min] for up-cut peripheral milling with the NFPc 40 DIN 845 BKN HSS cutter (actual data)

Table 2. Summary of the correlations, calculated using the Pearson's and Spearman's methods, between the cutting speed V_c and the deflection f for up-cut peripheral milling with NFPc 40 DIN 845 BKN HSS cutter

Pearson correlation	Spearman correlation	Cutting speed V_c [m/min]	Deflection f [mm]
0.5887867	1.0	0	0
		5	2.30
		39.6	2.31
		79.2	2.39

The first-degree regression formula is given by:

$$y = 0.01874 \cdot x + 1.1699$$

where: y – deflection [mm]; x – cutting speed [m/min]

For such a mathematical model, the relationship between the deflection f and cutting speed V_c takes the following values (Table 3):

Table 3. The values of the deflection f [mm] depending on the cutting speed V_c [m/min] calculated according to the mathematical model of simple regression

Cutting speed V_c [m/min]	Deflection f [mm]
0	1.1899
5	1.2636
39.6	1.912004
79.2	2.654108

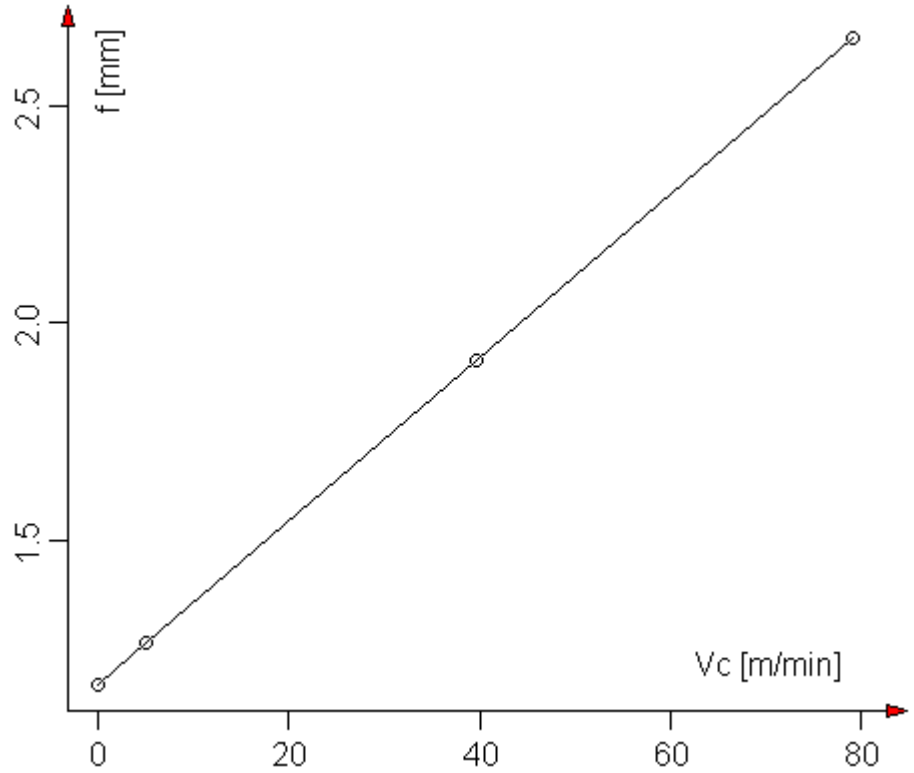

Fig. 3. Graphical representation of the dependence of the deflection f [mm] on the cutting speed V_c [m/min] for up-cut peripheral milling using NFPc 40 DIN 845 BKN HSS cutter (data according to the mathematical model)

Table 4. Summary of the correlations, calculated using the Pearson's and Spearman's methods, between the cutting speed and the deflection for up-cut face milling using NFPc 40 DIN 845 BKN HSS cutter

Pearson correlation	Spearman correlation	Cutting speed V_c [m/min]	Deflection f [mm]
0.5642628	0.4	0	0
		5	2.26
		39.6	2.30
		79.2	2.31
		100.5	2.25

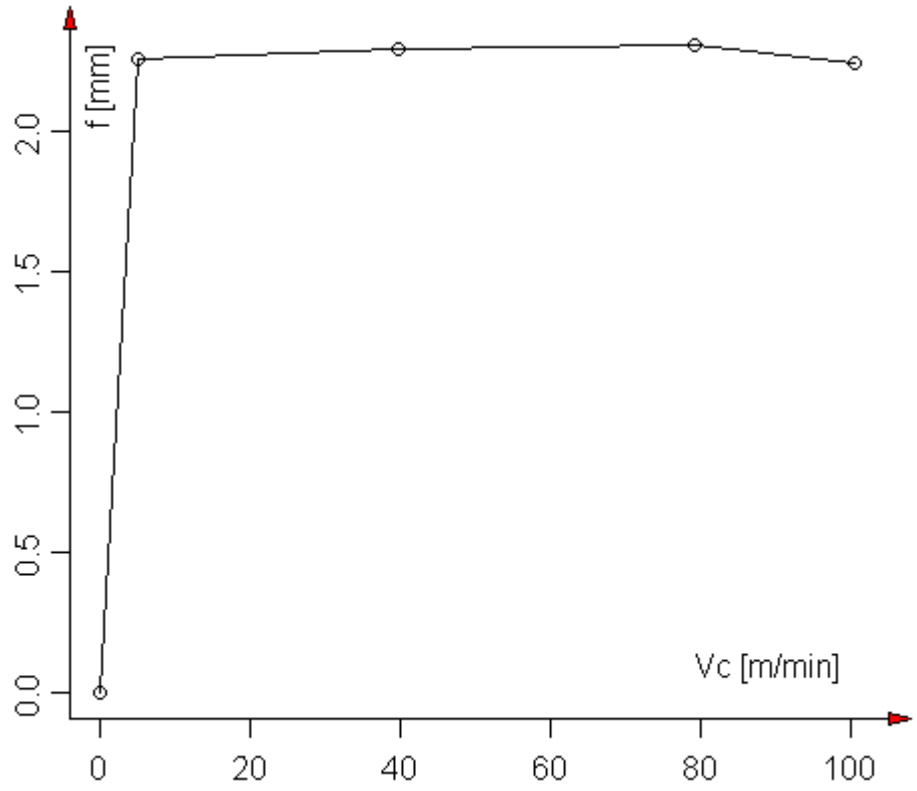

Fig. 4. Graphical representation of the dependence of the deflection f [mm] on the cutting speed V_c [m/min] for up-cut face milling with the NFPc 40 DIN 845 BKN HSS cutter (actual data)

The first-degree regression formula is given by:

$$y = 0.01295 \cdot x + 1.24319$$

where: y – deflection [mm]; x – cutting speed [m/min]

For such a mathematical model, the relationship between the deflection f and cutting speed V_c takes the following values (Table 5):

Table 5. The values of the deflection f [mm] depending on the cutting speed V_c [m/min] calculated according to the mathematical model of simple regression

Cutting speed V_c [m/min]	Deflection f [mm]
0	1.24319
5	1.30794
39.6	1.75601
79.2	2.26883
100.5	2.544665

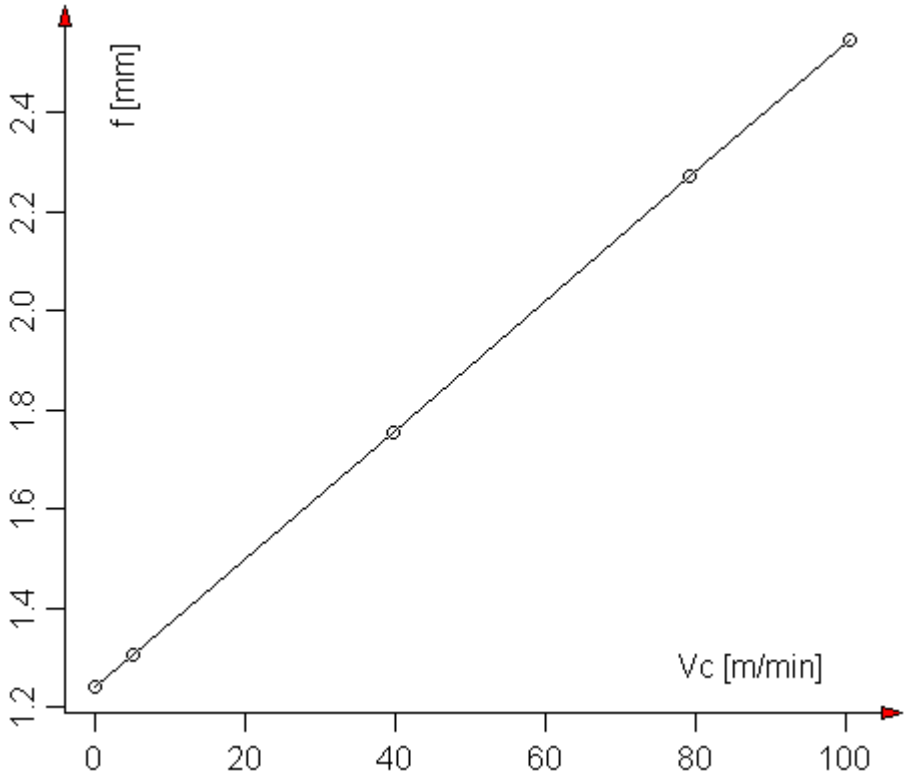

Fig. 5. Graphical representation of the dependence of the deflection f [mm] on the cutting speed V_c [m/min] for up-cut face milling using NFPc 40 DIN 845 BKN HSS cutter (data according to the mathematical model)

The final part of this analysis is to determine the correlation between the deflection f [mm] and cutting speed V_c [m/min] during machining using an 80 mm TRI-SQ Indexa IND 1393420 milling head with multi-edge inserts, up-cut face milling.

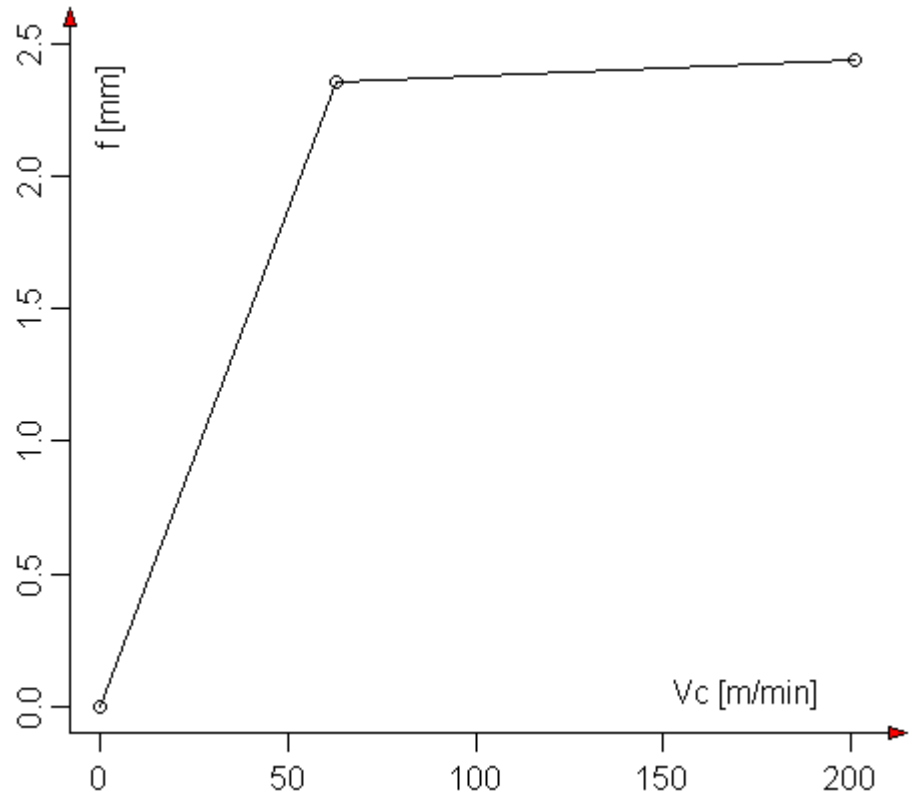

Fig. 6. Graphical representation of the dependence of the deflection f [mm] on the cutting speed V_c [m/min] for up-cut face milling using an 80 mm TRI-SQ Indexa IND 1393420 milling head with multi-edge inserts (actual data)

Table 6. Summary of the correlations calculated using the Pearson's and Spearman's methods between the cutting speed V_c and the deflection f for up-cut face milling using an 80 mm TRI-SQ Indexa IND 1393420 milling head with multi-edge inserts

Pearson correlation	Spearman correlation	Cutting speed V_c [m/min]	Deflection f [mm]
0.7603623	1.0	0	0
		63	2.36
		201	2.44

The first-degree regression formula is given by:

$$y = 0.010025 \cdot x + 0.69777$$

where: y – deflection [mm]; x – cutting speed [m/min]

For such a mathematical model, the relationship between the deflection f and cutting speed Vc takes the following values (Table 7):

Table 7. The values of the deflection f [mm] depending on the cutting speed V_c [m/min] calculated according to the mathematical model of simple regression

Cutting speed V_c [m/min]	Deflection f [mm]
0	0.69777
63	1.34352
201	2.75802

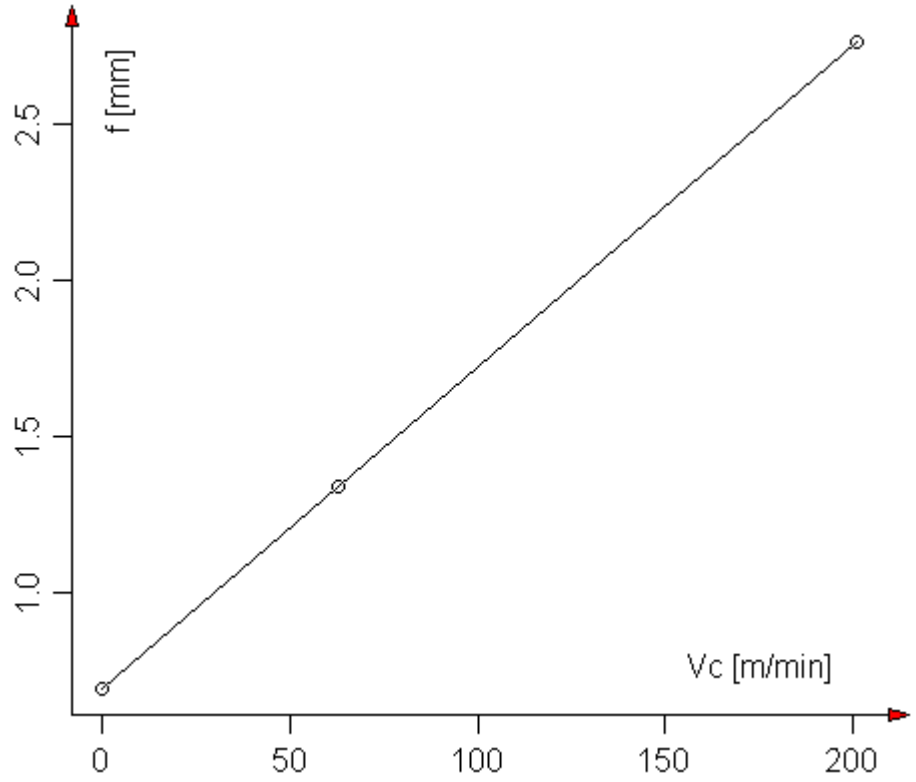

Fig. 7. Graphical representation of the dependence of the deflection f [mm] on the cutting speed V_c [m/min] for up-cut face milling using an 80 mm TRI-SQ Indexa IND 1393420 milling head with multi-edge inserts (data according to the mathematical model)

3. Conclusion

The correlations between the deflection f [mm] and cutting speed V_c [m/min], calculated using the Pearson method, for the tested types of samples range from 0.5642628 to

0.7603623. These are positive and strong dependencies. This means that there is a real relationship between the tested variables.

However, the correlations calculated using the Spearman method between the deflection f [mm] and cutting speed V_c [m/min] for the tested types of samples have a quite large range of values and take values from 0.4 to 1.0. These are positive dependencies of medium strength, or functional (very strong). This proves that there is a real relationship between the tested variables.

Unfortunately, the calculated correlations are for a small data set (three or four samples). Therefore, it will be necessary to continue this study topic with a larger number of tests, so that to perform machining for a greater number of cutting speeds and determine the deflection for them.

4. Literature

1. Domański A., Mikołajczyk J.: Dimensional analysis of the selected type of rolling bearing depending on the manufacturer. **W:** Szkoła Logistyki 2023 / redakcja naukowa Janusz Zawiła-Niedźwiecki, Katarzyna Białczak. Radom: Instytut Naukowo-Wydawniczy "Spatium", 2023, Poland; s. 79-89, p-ISBN: 978-83-67033-75-6;
e-ISBN: 978-83-67033-58-9.
2. Galon M., Mikołajczyk J.: The effect of laser cutting speed on the bearing surface of peaks and valleys of the cut surface. **W:** Logistyka w ratownictwie 2024 / pod redakcją Andrzeja Chudzikiewicza i Andrzeja Krzyszkowskiego. Radom: Instytut Naukowo-Wydawniczy Spatium, 2024, Poland; s. 71÷84, p-ISBN: 978-83-68026-24-5;
e-ISBN: 978-83-68026-25-2.
3. Galon M., Mikołajczyk J.: The effect of laser cutting speed on the weight of the workpiece. **W:** Logistyka w ratownictwie 2024 / pod redakcją Andrzeja Chudzikiewicza i Andrzeja Krzyszkowskiego. Radom: Instytut Naukowo-Wydawniczy Spatium, 2024, Poland; s. 85÷96, p-ISBN: 978-83-68026-24-5; e-ISBN: 978-83-68026-25-2.
4. Galon M., Mikołajczyk J.: Wpływ wartości posuwu podczas cięcia laserem na chropowatość powierzchni przecięcia. Obróbka Metalu; 2024, nr 3, s. 48÷53,
p-ISSN: 2081-7002; **https://obrobkametalu.tech/nasze-czasopismo/archiwum/**
5. Grabowska M., Mikołajczyk J.: Zastosowanie tomografii komputerowej CAT w inżynierii materiałowej. Application of CAT scanning for materials engineering. Postępy w Inżynierii Mechanicznej [Developments in Mechanical Engineering]. 2017, nr 9 (5), s. 15÷26,
p-ISSN: 2300-3383; Wydawnictwa Uczelniane Uniwersytetu Technologiczno-Przyrodniczego w Bydgoszczy, Poland. **http://wu.utp.edu.pl/oferta,8,1**
6. Grabowska M., Mikołajczyk J.: Próba zastosowania tomografii komputerowej CAT do określania struktury grafitu naturalnego w zależności od rozmiaru ziarna. An attempt to apply cat scanning to determine the natural graphite structure depending on the grain size. Postępy w Inżynierii Mechanicznej [Developments in Mechanical Engineering]. 2018, nr 12 (6), s. 5÷14, p-ISSN: 2300-3383; Wydawnictwa Uczelniane Uniwersytetu Technologiczno-Przyrodniczego w Bydgoszczy, Poland.
http://wu.utp.edu.pl/oferta,8,1
7. Grabowska M., Mikołajczyk J., Basiak S.: Zastosowanie tomografii komputerowej CAT w nieniszczących badaniach teowych złączy spawanych. Application of cat scanning in non-destructive testing of welded t-joints. Postępy w Inżynierii Mechanicznej [Developments in Mechanical Engineering]; 2018, nr 11 (6), s. 31÷44, p-ISSN: 2300-3383; Wydawnictwa

Uczelniane Uniwersytetu Technologiczno-Przyrodniczego w Bydgoszczy, Poland. http://wu.utp.edu.pl/oferta,8,1
8. Grabowska M., Piochacz A., Mikołajczyk J.: Attempt to use computed tomography CAT to analyze the anodized layer. Postępy w Inżynierii Mechanicznej [Developments in Mechanical Engineering]; 2020, nr 15 (8), s. 25÷33, p-ISSN: 2300-3383; Wydawnictwa Uczelniane Uniwersytetu Technologiczno-Przyrodniczego im. J. J. Śniadeckich w Bydgoszczy, Poland. https://dme.utp.edu.pl/art/15(8)2020/25.pdf
DOI: 10.37660/dme.2020.15.8.3
9. Hołubowska A., Szałański B., Mikołajczyk J.: Laboratorium termodynamiki. Piła: Wydawnictwo Państwowej Uczelni im. Stanisława Staszica, 2020, Poland.; s. 164 , e-ISBN: 978-83-62617-93-7;
https://wydawnictwo.puss.pila.pl/files/Laboratorium_termodynamiki_POL_version.pdf
10. Jarmoliński Z., Mikołajczyk J.: Badania wpływu technologii cięcia stali na twardość powierzchni bijaka. Research of the influence of steel cutting technology on the strength of the hammer. Postępy w Inżynierii Mechanicznej [Developments in Mechanical Engineering]. 2018, nr 12 (6), s. 15÷30, p-ISSN: 2300-3383. Wydawnictwa Uczelniane Uniwersytetu Technologiczno-Przyrodniczego w Bydgoszczy, Poland.
http://wu.utp.edu.pl/oferta,8,1
11. Jędrzejczyk D., Mikołajczyk J.: Defining the correlation between the cutting speed and roughness parameter Rz. **W:** MIK-21 : Międzynarodowa Innowacyjność i Konkurencyjność w XXI wieku : aspekty innowacyjne / redakcja naukowa Radosław Luft. Lublin : Fundacja Innowacji i Nowoczesnych Technologii INOTECH, 2022. Radom : nakładem Instytutu Naukowo-Wydawniczego "Spatium", 2022; s. 39÷46, p-ISBN: 978-83-67033-43-5; e-ISBN: 978-83-67033-44-2;
http://inw-spatium.pl/wp-content/uploads/2022/09/MIK-21-2022-Aspekty-innowacyjne-2.pdf
12. Jędrzejczyk D., Mikołajczyk J.: Mathematical models of the influence of cutting speed on Ra parameter. Developments in Mechanical Engineering; 2022, nr 18 (10), s. 115÷129, p-ISSN: 2720-0639; Wydawnictwa Uczelniane Uniwersytetu Technologiczno-Przyrodniczego im. J. J. Śniadeckich w Bydgoszczy, Poland.
DOI: 10.37660/dme.2022.18.10.11
13. Jędrzejczyk D., Mikołajczyk J.: Wpływ prędkości skrawania na wybrany parametr warstwy wierzchniej. **W:** Logistyka w ratownictwie 2022 / pod redakcją Andrzeja Chudzikiewicza i Andrzeja Krzyszkowskiego. Radom: Instytut Naukowo-Wydawniczy Spatium, 2022, Poland; s. 75÷90, p-ISBN: 978-83-67033-57-2; e-ISBN: 978-83-67033-70-1.
14. Latoś H., Mikołajczyk J.: Effect of partial wear of the tool point on the selected indicator of the machining process. **W:** Logistyka w ratownictwie 2023 / pod redakcją Andrzeja Chudzikiewicza i Anny Stelmach. Radom: Instytut Naukowo-Wydawniczy "Spatium", 2023, Poland; s. 195÷210, p-ISBN: 978-83-67033-95-4; e-ISBN: 978-83-67033-96-1.
15. Latoś H., Mikołajczyk J.: Thickness of the machined layer at milling with single-edge straight blades with an angle of $\lambda s \neq 0°$. **W:** MIK-21 : Międzynarodowa Innowacyjność i Konkurencyjność w XXI wieku : Aspekty innowacyjne / redakcja naukowa dr Łukasz Wojtowicz. Lublin: Fundacja Innowacji i Nowoczesnych Technologii INOTECH : nakładem Instytutu Naukowo-Wydawniczego "Spatium", 2023, Poland; s. 23÷27, p-ISBN: 978-83-67033-89-3; e-ISBN: 978-83-67033-90-9.
16. Latoś H., Mikołajczyk J., Konarski J., Mikołajczyk T.: Turning using self-induced vibration. **W:** MIK-21 : Międzynarodowa Innowacyjność i Konkurencyjność w XXI wieku : aspekty innowacyjne / redakcja naukowa dr Łukasz Wojtowicz, 2023, Poland; s. 187÷200, p-ISBN: 978-83-67033-89-3; e-ISBN: 978-83-67033-90-9.

17. Latoś H., Mikołajczyk J.: Vibration in machining. **W:** Logistyka w ratownictwie 2023 / pod redakcją Andrzeja Chudzikiewicza i Anny Stelmach. Radom: Instytut Naukowo-Wydawniczy "Spatium", 2023, Poland; s. 187÷194, p-ISBN: 978-83-67033-95-4; e-ISBN: 978-83-67033-96-1.
18. Latoś H., Mikołajczyk J.: The effect of feed rate on the roughness of machined surface. **W:** Szkoła Logistyki 2024 / redakcja naukowa Janusz Zawiła-Niedźwiecki, Adam Płaczek. Radom: Instytut Naukowo-Wydawniczy "Spatium", 2024, Poland; s. 217÷226, p-ISBN: 978-83-68026-07-8; e-ISBN: 978-83-68026-08-5.19. Matuszewski M., Mikołajczyk J., Styp-Rekowski M: Modyfikacja cech środka smarującego za pomocą standardowych dodatków smarowych. Modification of lubricants features by means of standard additives. Postępy w Inżynierii Mechanicznej [Developments in Mechanical Engineering]. 2013, nr 1 (1), s. 57÷65, Wydawnictwo Uczelniane Uniwersytetu Technologiczno-Przyrodniczego im. J. J. Śniadeckich w Bydgoszczy; p-ISSN: 2300-3383;
http://wu.utp.edu.pl/uploads/oferta/Postepy_1_1_2013.pdf
20. Matuszewski M., Mikołajczyk J., Mikołajczyk T., Styp-Rekowski M.: Logistyczne aspekty zarządzania procesem naprawy. Logistical aspects of the repair process management. Logistyka, 2015, nr 4, s. 1991÷1997, p-ISSN: 1231-5478;
https://www.czasopismologistyka.pl/o-czasopismie/wydania
21. Matuszewski M., Mikołajczyk J., Mikołajczyk T., Styp-Rekowski M.: The influence of cooling and lubrication liquid quantity on the isotropy of a machine component surface during machining = Wpływ warunków chłodzenia i smarowania podczas obróbki elementów maszyn na stopień izotropowości ich powierzchni. Tribologia. 2016, vol. 265, No. 1, s. 57÷65, p-ISSN: 0208-7774; e-ISSN: 1732-422X;
https://t.tribologia.eu/resources/html/article/details?id=158175
22. Mikołajczyk J., Styp-Rekowski M., Świerk K.: Modyfikowanie cech środka smarującego za pomocą dodatków i komputerowe wspomaganie ich doboru. W: CAX' 2009 : Komputerowe Wspomaganie Nauki i Techniki : VI warsztaty naukowe, Bydgoszcz - Duszniki Zdrój 2009 : praca zbiorowa pod redakcją Tadeusza Mikołajczyka; p-ISBN: 978-83-61314-65-3. Wydawnictwa Uczelniane Uniwersytetu Technologiczno-Przyrodniczego w Bydgoszczy, Bydgoszcz 2009.
23. Mikołajczyk J.: Zestawienie porównawcze dodatków depresujących do olejów. W: Zaawansowana tribologia : XXX Ogólnopolska Konferencja Tribologiczna, Nałęczów, 21-24 września 2009 r. Ogólnopolska Konferencja Naukowa XXX Szkoły Tribologicznej "Zaawansowana Tribologia" : Wydział Materiałoznawstwa, Technologii i Wzornictwa Politechniki Radomskiej, Instytut Technologii Eksploatacji - PIB Radom oraz Komitet Budowy Maszyn, Sekcja Podstaw Eksploatacji Maszyn PAN. Wydawnictwo Naukowe Instytutu Technologii Eksploatacji - PIB, Radom, 2009.
24. Mikołajczyk J.: Zestawienie porównawcze własności fizykochemicznych dodatków smarnych w oleju podstawowym SAE-30. W: Terotechnologia 2009 : materiały konferencji na ekspozycji Metal i Control-Tech : Targi - Kielce (29.09-01.10.2009). VI Konferencja Naukowo-Techniczna "Terotechnologia 2009" : Politechnika Świętokrzyska, Centrum Laserowych Technologii Metali, Katedra Inżynierii Eksploatacji, Wydział Mechatroniki i Budowy Maszyn, Polskie Towarzystwo Naukowo-Techniczne, Towarzystwo Eksploatacyjne, Kielce: Wydawnictwo Politechniki Świętokrzyskiej, 2009. Seria: Zeszyty Naukowe - Politechnika Świętokrzyska, nr 13.
25. Mikołajczyk J., Matuszewski M.: Konstrukcja i sterowanie stanowiska do badań tribologicznych. W: CAX'2010 : komputerowe wspomaganie nauki i techniki : VII warsztaty naukowe, Bydgoszcz - Duszniki Zdrój 2010 : praca zbiorowa / pod red. Tadeusza Mikołajczyka. Bydgoszcz : Wydawnictwa Uczelniane Uniwersytetu Technologiczno-Przyrodniczego w Bydgoszczy, 2010; p-ISBN: 9788361314387.

26. Mikołajczyk J.: System rejestracji i wizualizacji warunków pracy stanowiska do badań tribologicznych. W: CAX'2011 : komputerowe wspomaganie nauki i techniki : VIII warsztaty naukowe, Bydgoszcz - Duszniki Zdrój 2011 : praca zbiorowa / pod redakcją Tadeusza Mikołajczyka. Bydgoszcz : Wydawnictwa Uczelniane Uniwersytetu Technologiczno-Przyrodniczego w Bydgoszczy, 2011; p-ISBN: 9788361314981.
27. Mikołajczyk J.: Badanie wpływu preparatu eksploatacyjnego Mind M na zmianę własności smarnych oleju bazowego SN-150. Inżynieria i aparatura chemiczna [Chemical Engineering and Equipment]. 2012, nr 5, s. 235÷236, p-ISSN: 0368-0827.
http://inzynieria-aparatura-chemiczna.pl/rok-2012-nr-5/
28. Mikołajczyk J., Styp-Rekowski M., Matuszewski M., Musiał J.: Einfluβ der kompositionen von schmierzusätzen auf die exploitations-eigenschaften der mischung mit Basisöl SN-150. W: Tribologie und mobilität : beiträge der tribotechnik zur optimierung von fertigungsprozessen, wartung, schmierung (reibungskonditionierung) und betriebssicherheit von verkehrsmitteln und verkehrswegen. Wien, 15 November 2012. Symposium 2012 "Tribologie und mobilität" : Österreichische Tribologische Gesellschaft. Österreichische Tribologische Gesellschaft, Wien, 2012.
29. Mikołajczyk J.: Einfluβ der ausgewählten schmierzstoffzusätze auf betriebseigenschaften der mischung mit Basisöl SN-150. **W:** Reibung, schmierung und verschleiβ : forschung und praktische anwendungen. Band 1. Tribologische systeme maschinenelemente und antriebstechnik fahrzeugtechnik prüfen, messen, kontrollieren. Göttingen, 22-24 September 2014. 55. Tribologie Fachtagung "Reibung, Schmierung und Verschleiβ" : Gesellschaft für Tribologie e.V. Stolberg-Venwegen : Gesellschaft für Tribologie e.V., 2014. Germany.
30. Mikołajczyk J.: Einfluss der ausgewählten zusatzschmierstoffe auf die intensivität des verschleiβprozesses (Ra, Rq, Δm) mit Basisöl SN-150. **W:** Tribologie in industrie und forschung : werkstoffe, konstruktion und technologie. Leoben, 26 November 2014. ÖTG Symposium 2014 "Tribologie in industrie und forschung" : Österreichische Tribologische Gesellschaft. Wien : Österreichische Tribologische Gesellschaft, 2014. Austria.
31. Mikołajczyk J., Matuszewski M.: Einfluss der ausgewählten schmierzstoffzusätze auf ΔT und ΔP mit Basisöl SN-150. **W:** Tribologie in industrie und forschung : werkstoffe, schmierstoffe und technologie. Wiener Neustadt, 25 November 2015, Austria. ÖTG Symposium 2015 "Tribologie in industrie und forschung" : Österreichische Tribologische Gesellschaft. Wiener Neustadt : Österreichische Tribologische Gesellschaft, 2015, s. 145-152.
32. Mikołajczyk J.: Vergleich charakteristischer parameter des abbott-firestone-diagramms für ein kinematisches paar mit konformem kontakt. **W:** Tribologie in industrie und forschung : verschleiβschutz, instandhaltung und anlagenzuverlässigkeit. Linz, 22-23 November 2016, Austria. ÖTG Symposium 2016 "Tribologie in industrie und forschung" : Österreichische Tribologische Gesellschaft. Wiener Neustadt : Österreichische Tribologische Gesellschaft, 2016; s. 105-110.
33. Mikołajczyk J.: Wpływ dodatków smarowych na transformację warstwy wierzchniej. Piła: Wydawnictwo Państwowej Wyższej Szkoły Zawodowej im. Stanisława Staszica, 2017r., Poland; 215 s., p-ISBN: 978-83-62617-76-0; www.ans.pila.pl
34. Mikołajczyk J.: Maszyny tarciowe : budowa, przeznaczenie. Piła, Wydawnictwo Państwowej Wyższej Szkoły Zawodowej im. Stanisława Staszica, 2018, Poland; 256 s., p-ISBN: 978-83-62617-86-9.
35. Mikołajczyk J.: Analiza statystyczna zmiany poboru mocy podczas procesu zużywania. Statistical analysis of the power variation of tribotester as a resultat of the wear process. Autobusy. Technika, Eksploatacja, Systemy Transportowe; 2019, nr 10-11, s. 83÷88, p-ISSN: 1509-5878; e-ISSN: 2450-7725;
http://yadda.icm.edu.pl/yadda/element/bwmeta1.element.baztech-21189602-884a-4d1a-bb60-9edaeae4af8d

36. Mikołajczyk J.: Influence of consumables on the amount of power consumption of kinematic vapor of conformal contact. Wpływ PE na pobór mocy pary kinematycznej o styku konforemnym. Postępy w Inżynierii Mechanicznej [Developments in Mechanical Engineering]; 2019, nr 13 (7), s. 39÷50, p-ISSN: 2300-3383; Wydawnictwa Uczelniane Uniwersytetu technologiczno-Przyrodniczego im. J. J. Śniadeckich w Bydgoszczy, Poland.
http://yadda.icm.edu.pl/baztech/element/bwmeta1.element.baztech-2faf200b-3010-4192-9fd0-062f53b49d38
37. Mikołajczyk J.: Statistical analysis of the mass variation of samples as a result of the wear process. Analiza statystyczna zmiany masy próbek w wyniku procesu zużywania. Postępy w Inżynierii Mechanicznej [Developments in Mechanical Engineering]; 2019, nr 13 (7), s. 51÷61, p-ISSN: 2300-3383; Wydawnictwa Uczelniane Uniwersytetu Technologiczno-Przyrodniczego im. J. J. Śniadeckich w Bydgoszczy, Poland.
http://yadda.icm.edu.pl/baztech/element/bwmeta1.element.baztech-2faf200b-3010-4192-9fd0-062f53b49d38
38. Mikołajczyk J.: Tribotestery : budowa i przeznaczenie. Piła: Wydawnictwo Państwowej Wyższej Szkoły Zawodowej im. Stanisława Staszica, 2019, Poland; 160 s.,
e-ISBN: 978-83-62617-90-6; **https://wydawnictwo.pwsz.pila.pl/files/Tribotestery.pdf**
39. Mikołajczyk J.: Determining the energy validity of the Kostetsky's hypothesis on the basis of models for relative motion velocity v = 0.08 m/sec. Developments in Mechanical Engineering; 2020, nr 16 (8), s. 17÷29, p-ISSN: 2720-0639; Wydawnictwa Uczelniane Uniwersytetu Technologiczno-Przyrodniczego im. J.J. Śniadeckich w Bydgoszczy, Poland.
DOI: 10.37660/dme.2020.16.8.2
40. Mikołajczyk J.: Finding the correlation between wear of samples kinematic pair of conformal contact and electric power consumption. Postępy w Inżynierii Mechanicznej [Developments in Mechanical Engineering]; 2020, nr 15 (8), s. 59÷68,
p-ISSN: 2300-3383; Wydawnictwa Uczelniane Uniwersytetu Technologiczno-Przyrodniczego im. J. J. Śniadeckich w Bydgoszczy, Poland.
https://dme.utp.edu.pl/art/15(8)2020/59.pdf
DOI: 10.37660/dme.2020.15.8.6
41. Mikołajczyk J.: The effect of temperature lag on the value of power-temperature correlation for frictional pair of conformal contact. Postępy w Inżynierii Mechanicznej [Developments in Mechanical Engineering]; 2020, nr 15 (8), s. 79÷86,
p-ISSN: 2300-3383; Wydawnictwa Uczelniane Uniwersytetu Technologiczno-Przyrodniczego im. J. J. Śniadeckich w Bydgoszczy, Poland.
https://dme.utp.edu.pl/art/15(8)2020/79.pdf
DOI: 10.37660/dme.2020.15.8.8
42. Mikołajczyk J.: Określenie na podstawie modeli zmiany masy próbek w wyniku procesu zużywania. **W:** Szkoła Logistyki 2021 / redakcja naukowa Janusz Zawiła-Niedźwiecki, Piotr Korneta. Radom : Instytut Naukowo-Wydawniczy "Spatium", 2021; s. 167÷174, Poland;
p-ISBN: 978-83-66550-75-9; e-ISBN: 978-83-66550-89-6.
43. Mikołajczyk J.: A method of determining mathematical models of a seizure test of friction pairs. **W:** MIK-21 : Międzynarodowa Innowacyjność i Konkurencyjność w XXI wieku : aspekty innowacyjne / redakcja naukowa Radoslaw Luft. Lublin : Fundacja Innowacji i Nowoczesnych Technologii INOTECH, 2022. Radom : nakładem Instytutu Naukowo-Wydawniczego "Spatium", 2022; s. 7÷24, p-ISBN: 978-83-67033-43-5;
e-ISBN: 978-83-67033-44-2.
http://inw-spatium.pl/wp-content/uploads/2022/09/MIK-21-2022-Aspekty-innowacyjne-2.pdf
44. Mikołajczyk J.: Friction machines. Wydawnictwo Akademii Nauk Stosowanych im. Stanisława Staszica, Piła, 2022, Poland; 488 s., e-ISBN: 978-83-62617-96-8.

https://wydawnictwo.ans.pila.pl/files/FRICTION_MACHINES.pdf
45. Mikołajczyk J., Jędrzejczyk D.: Określenie korelacji między prędkością skrawania a parametrem chropowatości Ra. Obróbka Metalu; 2022, nr 3, s. 11÷15,
p-ISSN: 2081-7002; **https://obrobkametalu.tech/**
46. Mikołajczyk J.: Rolling bearing heating charakter. **W:** Szkoła Logistyki 2022. Radom: Instytut Naukowo-Wydawniczy "Spatium", 2022, Poland; s. 231÷239, Materiały z IX Konferencji Naukowej "Szkoła Logistyki 2022"; p-ISBN: 978-83-67033-33-6;
e-ISBN: 978-83-67033-34-3.
47. Mikołajczyk J.: Tribological properties of carbon black. **W:** Szkoła Logistyki 2022. Radom: Instytut Naukowo-Wydawniczy "Spatium", 2022, Poland; s. 217-230, Materiały z IX Konferencji Naukowej "Szkoła Logistyki 2022"; p-ISBN: 978-83-67033-33-6;
e-ISBN: 978-83-67033-34-3.
48. Mikołajczyk J.: Determination of the modified coefficient of variation from the number of samples. **W:** MIK-21 : Międzynarodowa Innowacyjność i Konkurencyjność w XXI wieku : Aspekty innowacyjne / redakcja naukowa dr Łukasz Wojtowicz. Lublin: Fundacja Innowacji i Nowoczesnych Technologii INOTECH : nakładem Instytutu Naukowo-Wydawniczego "Spatium", 2023, Poland; s. 111÷122, p-ISBN: 978-83-67033-89-3;
e-ISBN: 978-83-67033-90-9.
49. Mikołajczyk J.: Effect of cutting speed on the shape of the machined surface profile. Mebutra; 2023, nr 1, s. 47÷63, Wydawnictwo Akademii Nauk Stosowanych im. S. Staszica w Pile, Piła 2023, Poland.
https://online.fliphtml5.com/vliuj/yunw/ p=48
50. Mikołajczyk J.: Friction Machines II. Piła: Wydawnictwo Akademii Nauk Stosowanych im. Stanisława Staszica w Pile, 2023, Poland; s. 598;
p-ISBN: 978-83-67684-00-2;
https://wydawnictwo.ans.pila.pl/files/FRICTION_MACHINES_V_ANS_PILA.pdf
51. Mikołajczyk J.: Oil can talk. **W:** Szkoła Logistyki 2023 / redakcja naukowa Janusz Zawiła-Niedźwiecki, Katarzyna Białczak. Radom: Instytut Naukowo-Wydawniczy "Spatium", 2023, Poland; s. 109÷115, p-ISBN: 978-83-67033-75-6;
e-ISBN: 978-83-67033-58-9.
52. Mikołajczyk J.: Pobór mocy elektrycznej przez parę kinematyczną jako parametr oceny jakości oleju. **W:** Logistyka w ratownictwie 2023 / pod redakcją Andrzeja Chudzikiewicza i Anny Stelmach. Radom: Instytut Naukowo-Wydawniczy "Spatium", 2023, Poland; s. 223-230, p-ISBN: 978-83-67033-95-4; e-ISBN: 978-83-67033-96-1.
53. Mikołajczyk J.: Rola dodatków smarowych w olejach. **W:** Logistyka w ratownictwie 2023 /pod redakcją Andrzeja Chudzikiewicza i Anny Stelmach/; Radom: Instytut Naukowo-Wydawniczy "Spatium", 2023, Poland; s. 231÷237, p-ISBN: 978-83-67033-95-4;
e-ISBN: 978-83-67033-96-1.
54. Mikołajczyk J.: Temperature as a parameter for assessing the work of a friction pair. **W:** Szkoła Logistyki 2023 / redakcja naukowa Janusz Zawiła-Niedźwiecki, Katarzyna Białczak. Radom: Instytut Naukowo-Wydawniczy "Spatium", 2023, Poland; s. 101-107,
p-ISBN: 978-83-67033-75-6; e-ISBN: 978-83-67033-58-9.
55. Mikołajczyk J.: Tire as a selected element of a car subject to diagnostics. **W:** Szkoła Logistyki 2023 / redakcja naukowa Janusz Zawiła-Niedźwiecki, Katarzyna Białczak. Radom: Instytut Naukowo-Wydawniczy "Spatium", 2023, Poland; s. 117÷131,
p-ISBN: 978-83-67033-75-6; e-ISBN: 978-83-67033-58-9.
56. Mikołajczyk J.: Wpływ dodatku modyfikującego cechy płynu obróbkowego na zmianę temperatury w strefie kontaktu współpracujących powierzchni. Obróbka Metalu; 2023, nr 2,
s. 43÷46, p-ISSN: 2081-7002;
https://obrobkametalu.tech/media/2023/05/2023_2_52_ObrobkaMetalu.pdf

57. Mikołajczyk J., Kozłowska M.A., Krasicki K.: Wpływ kompetencji cyfrowych pracowników na poziom rozwoju procesów przemysłowych. **W:** MIK-21 : Międzynarodowa Innowacyjność i Konkurencyjność w XXI wieku : aspekty społeczne /redakcja naukowa Radosław Luft/; Lublin-Radom : Fundacja Innowacji i Nowoczesnych Technologii INOTECH : nakładem Instytutu Naukowo-Wydawniczego "Spatium", 2023, Poland; s. 149÷169, p-ISBN: 978-83-67033-92-3; e-ISBN: 978-83-67033-93-0.
58. Mikołajczyk J.: Zmiana geometrycznych cech współpracujących powierzchni miarą intensywności procesu zużywania ostrzy skrawających. Obróbka Metalu; 2023, nr 1, s. 50÷54, p-ISSN: 2081-7002;
https://yadda.icm.edu.pl/yadda/element/bwmeta1.element.baztech-9e73eb05-2a91-4df5-853b-22abf7a6ee77
59. Mikołajczyk J., Góra F., Jędrzejczyk D.: Analysis of selected surface roughness parameters for wear processes. Analiza wybranych parametrów chropowatości powierzchni pod kątem procesów zużywania. **W:** MIK-21 : Międzynarodowa Innowacyjność i Konkurencyjność w XXI wieku : Aspekty innowacyjne / redakcja naukowa Radosław Luft. Lublin: Wydawnictwo Naukowe FNCE, 2024; s. 93-117, p-ISBN: 978-83-68074-82-6; e-ISBN: 978-83-68319-03-3.
60. Mikołajczyk J., Galon M.: Mathematical model of straight regression determining the effect of laser cutting speed on the mass of the workpiece. **W:** MIK-21 : Międzynarodowa Innowacyjność i Konkurencyjność w XXI wieku : Aspekty innowacyjne / redakcja naukowa Radosław Luft. Lublin: Wydawnictwo Naukowe FNCE, 2024, Poland; s. 71÷92, p-ISBN: 978-83-68074-82-6; e-ISBN: 978-83-68319-03-3.
61. Mikołajczyk J., Sądej I.: Spinning speed and balancing accuracy. **W:** MIK-21 : Międzynarodowa Innowacyjność i Konkurencyjność w XXI wieku : Aspekty innowacyjne / redakcja naukowa Radosław Luft. Lublin: Wydawnictwo Naukowe FNCE, 2024, Poland; s. 118÷132, p-ISBN: 978-83-68074-82-6; e-ISBN: 978-83-68319-03-3.
62. Mikołajczyk J.: The correlation between the population and number of construction disasters. MEBUTRA; 2025, nr 3, s. 44-55, Wydawnictwo Akademii Nauk Stosowanych im. S. Staszica w Pile, Poland.
https://wydawnictwo.ans.pila.pl/files/MEBUTRA2025.pdf
63. Mikołajczyk J.: The relationship between the type of structure and the number of construction disasters. Zależność między rodzajem konstrukcji, a liczbą katastrof budowlanych. MEBUTRA; 2025, 3, s. 30÷43, Wydawnictwo Akademii Nauk Stosowanych im. S. Staszica w Pile, Poland.
https://wydawnictwo.ans.pila.pl/files/MEBUTRA2025.pdf
64. Olechnowicz J., Mikołajczyk J.: Truck scales : the key to safe transport and road protection. Mebutra; 2024, nr 2, s. 3÷8, Wydawnictwo Akademii Nauk Stosowanych im. S. Staszica w Pile, Poland.
https://wydawnictwo.ans.pila.pl/files/MEBUTRA2024.pdf
65. Pikulik K.W., Mikołajczyk J.: The influence of the welding current on the air pollution emissions. Wpływ prądu spawania na emisję zanieczyszczeń powietrza. Postępy w Inżynierii Mechanicznej [Developments in Mechanical Engineering]; 2019, nr 14 (7), s. 33÷46, p-ISSN: 2300-3383; Wydawnictwa Uczelniane Uniwersytetu Technologiczno-Przyrodniczego im. J. J. Śniadeckich w Bydgoszczy, Poland.
http://yadda.icm.edu.pl/baztech/element/bwmeta1.element.baztech-2faf200b-3010-4192-9fd0-062f53b49d38
66. Pikulik K.W., Mikołajczyk J.: Determination of emission of iron oxides from the welding process on the basis of mathematical models. Welding Technology Review; 2021, vol. 93, No 2, s. 35÷43, p-ISSN: 0033-2364; e-ISSN: 2449-7959;
http://www.pspaw.wip.pw.edu.pl/index.php/pspaw/article/view/1132

DOI: 10.26628/wtr.v93i2.1132
67. Pikulik J., Pikulik K.W., Mikołajczyk J.: The relationship between the clearance of the coupling mechanism used in uniaxial light car trailers and the date of their production. **W:** MIK-21 : Międzynarodowa Innowacyjność i Konkurencyjność w XXI wieku : aspekty innowacyjne / redakcja naukowa Radosław Luft. Lublin : Fundacja Innowacji i Nowoczesnych Technologii INOTECH, 2022, Poland. Radom : nakładem Instytutu Naukowo-Wydawniczego "Spatium"; 2022; s. 221÷233, p-ISBN: 978-83-67033-43-5;
e-ISBN: 978-83-67033-44-2;
http://inw-spatium.pl/wp-content/uploads/2022/09/MIK-21-2022-Aspekty-innowacyjne-2.pdf
68. Pikulik J., Pikulik K.W., Mikołajczyk J.: Zależność wielkości luzu mechanizmu sprzęgającego stosowanego w jednoosiowych lekkich przyczepach samochodowych od wartości współczynnika przylegania. **W:** Logistyka w ratownictwie 2022 / pod redakcją Andrzeja Chudzikiewicza i Andrzeja Krzyszkowskiego. Radom: Instytut Naukowo-Wydawniczy "Spatium", 2022, Poland; s. 157÷167, p-ISBN: 978-83-67033-57-2;
e-ISBN: 978-83-67033-70-1.
69. Pikulik J., Pikulik K.W., Mikołajczyk J.: Determination of the degree of contact of the movable part of the coupling head with the ball part of the coupling of single-axle light car trailers. **W:** MIK-21 : Międzynarodowa Innowacyjność i Konkurencyjność w XXI wieku : aspekty innowacyjne / redakcja naukowa dr Łukasz Wojtowicz. Lublin: Fundacja Innowacji i Nowoczesnych Technologii INOTECH : nakładem Instytutu Naukowo-Wydawniczego "Spatium", 2023, Poland; s. 97÷109, p-ISBN: 978-83-67033-89-3;
e-ISBN: 978-83-67033-90-9.
70. Piochacz A., Mikołajczyk J.: Wpływ czasu trwania procesu anodowania stopu aluminium EN AW-6060 na grubość i twardość otrzymanej warstwy. Influence of aluminium type EN AW-6060 anodizing process duration on the thickness and hardness of the obtained layer. Postępy w Inżynierii Mechanicznej [Developments in Mechanical Engineering]; 2018, nr 12 (6), s. 49÷56, p-ISSN: 2300-3383; Wydawnictwa Uczelniane Uniwersytetu Technologiczno-Przyrodniczego w Bydgoszczy, Poland.
http://wu.utp.edu.pl/oferta,8,1
71. Piochacz A., Mikołajczyk J.: Analiza statystyczna wpływu czasu anodowania na grubość otrzymanej powłoki. Statistical analysis of the influence of anodizing time on the thickness of obtained layers. Autobusy. Technika, Eksploatacja, Systemy Transportowe; 2019, vol. 233, nr 9, s. 48÷51, p-ISSN: 1509-5878; e-ISSN: 2450-7725;
http://ceref.pl/index.php/Autobusy/article/view/956
DOI: 10.24136/atest.2019.201
72. Piochacz A., Mikołajczyk J.: Determination of the thickness of anodized layer on the basis mathematical models. Developments in Mechanical Engineering; 2020, nr 16 (8), s. 31÷39, p-ISSN: 2720-0639; Wydawnictwa Uczelniane Uniwersytetu Technologiczno-Przyrodniczego im. J. J. Śniadeckich w Bydgoszczy, Poland.
DOI: 10.37660/dme.2020.16.8.3
73. Piotrowski Ł., Góra F., Mikołajczyk J.: Construction of an electric longboard with one-wheel driver. Mebutra; 2024, nr 2, s. 16÷27, Wydawnictwo Akademii Nauk Stosowanych im. S. Staszica w Pile, Poland.
https://wydawnictwo.ans.pila.pl/files/MEBUTRA2024.pdf
74. Piotrowski Ł., Góra F., Mikołajczyk J.: Design and construction of an electric longboard. **W:** Logistyka w ratownictwie 2024 / pod redakcją Andrzeja Chudzikiewicza i Andrzeja Krzyszkowskiego. Radom: Instytut Naukowo-Wydawniczy Spatium, 2024, Poland; s. 167÷178, p-ISBN: 978-83-68026-24-5; e-ISBN: 978-83-68026-25-2.

75. Przybył B., Kabat M., Mikołajczyk J.: Wpływ prędkości drukowania 3D na dokładność zarysu kół zębatych. Obróbka Metalu; 2023, nr 4, s. 26÷30, p-ISSN: 2081-7002; **https://obrobkametalu.tech/media/2023/08/2023-4_Nr54_ObrobkaMetalu.pdf**
76. Przybył B., Mikołajczyk J.: Efektywność technik przyrostowych. Obróbka Metalu; 2024, nr 1, s. 22÷25, p-ISSN: 2081-7002; **https://obrobkametalu.tech/media/2024/03/2024_1_nr55_ObrobkaMetalu-1.pdf**
77. Przybył B., Mikołajczyk J.: The influence of 3D printing speed on profile accuracy. **W:** Szkoła Logistyki 2024 / redakcja naukowa Janusz Zawiła-Niedźwiecki, Adam Płaczek. Radom: Instytut Naukowo-Wydawniczy "Spatium", 2024, Poland; s. 199÷216, p-ISBN: 978-83-68026-07-8; e-ISBN: 978-83-68026-08-5.
78. Sądej I., Mikołajczyk J.: Machine tool compensation and mass unbalance measurements. **W:** Logistyka w ratownictwie 2024 / pod redakcją Andrzeja Chudzikiewicza i Andrzeja Krzyszkowskiego. Radom: Instytut Naukowo-Wydawniczy Spatium, 2024, Poland; s. 187÷196, p-ISBN: 978-83-68026-24-5; e-ISBN: 978-83-68026-25-2.
79. Storch B.: Podstawy obróbki skrawaniem. Wydawnictwo Uczelniane Politechniki Koszalińskiej, Koszalin, 2001.
80. Styp-Rekowski M., Mikołajczyk J.: The influence of Mind M preparation on the lubricant properties of base oil SN-150. W**:** Reinung, Schmierung und Verschleiβ : forschung und praktische anwendungen : Band 1 : tribologische systeme schmierstoffe und schmierungstechnik zerspanungs : und umformtechnik prüfen, messen, kontrollieren / 53. Tribologie-Fachtagung. 24.bis 26. Septembet 2012 in Göttingen. Aachen : Gesellschaft für Tribologie e.V., 2012. p-ISBN: 978-3-00-039201-6.
81. Styp-Rekowski M., Mikołajczyk J.: Wpływ dodatku na własności smarowe oleju bazowego SN-150. Tribologia. 2012, vol. 244, No. 4, s. 227-232, p-ISSN: 0208-7774; e-ISSN: 1732-422X; **https://t.tribologia.eu/resources/html/article/details?id=167726**
82. Styp-Rekowski M., Mikołajczyk J.: Wpływ preparatu eksploatacyjnego stanowiący kompleks węglowodorowy na zmianę własności smarnych oleju bazowego SN-150. W: Tribologia bliżej praktyki : XXXII Ogólnopolska Konferencja "Jesienna Szkoła Tribologiczna 2012". XXXII Ogólnopolska Konferencja "Jesienna Szkoła Tribologiczna 2012", Kudowa Zdrój, 18-21 września 2012r. Politechnika Wrocławska Wydział Mechaniczny, Instytut Konstrukcji Eksploatacji Maszyn, Polskie Towarzystwo Tribologiczne, Sekcja Podstaw Eksploatacji KBM PAN. Wrocław : Polskie Towarzystwo Tribologiczne, 2012.
83. Styp-Rekowski M., Mikołajczyk J.: Zmiana temperatury na drodze tarcia dla kompozycji olej bazowy SN-150 - preparat eksploatacyjny Mind M. Temperature variability during friction for composition bese oil SN-150 - exploatational preparation Mind M. **W:** III krajowa konferencja nano- i mikromechaniki / Komitet Mechaniki Polskiej Akademii Nauk, Politechnika Rzeszowska im. Ignacego Łukasiewicza, Instytut Podstawowych Problemów Techniki Polskiej Akademii Nauk. Warszawa, 4-6 lipca 2012 r. III Krajowa Konferencja Nano- i Mikromechaniki pod Patronatem Ministra Nauki i Szkolnictwa Wyższego Prof. Barbary Kudryckiej : Komitet Mechaniki Polskiej Akademii Nauk, Politechnika Rzeszowska, Instytut Podstawowych Problemów Techniki Polskiej Akademii Nauk, Warszawa, 2012.
84. Styp-Rekowski M., Mikołajczyk J., Matuszewski M.: Wybrane zagadnienia stosowania płynów obróbkowych w obróbce skrawaniem. W**:** Obróbka Metalu, 2014, nr 3, s. 10÷14, p-ISSN: 2081-7002; **http://www.e-obrobkametalu.pl/**
85. Syrek S., Mikołajczyk J.: Analiza matematyczna podstawowych wymiarów złącza spawanego. **W:** Logistyka w ratownictwie 2022 / pod redakcją Andrzeja Chudzikiewicza i Andrzeja Krzyszkowskiego. Radom : Instytut Naukowo-Wydawniczy "Spatium", 2022; s. 169÷190, p-ISBN: 978-83-67033-57-2; e-ISBN: 978-83-67033-70-1.

86. Syrek S., Mikołajczyk J.: Modele liniowe wpływu częstotliwości prądu spawania na grubość spoiny. **W:** MIK-21 : Międzynarodowa Innowacyjność i Konkurencyjność w XXI wieku : aspekty innowacyjne / redakcja naukowa Radosław Luft. Lublin: Fundacja Innowacji i Nowoczesnych Technologii INOTECH, 2022. Radom : nakładem Instytutu Naukowo-Wydawniczego "Spatium", 2022; s. 153÷170, p-ISBN: 978-83-67033-43-5;
e-ISBN: 978-83-67033-44-2;
http://inw-spatium.pl/wp-content/uploads/2022/09/MIK-21-2022-Aspekty-innowacyjne-2.pdf
87. Syrek S., Mikołajczyk J.: Modele liniowe wpływu częstotliwości prądu spawania na szerokość spoiny. Obróbka Metalu; 2022, nr 4, s. 24÷31,
p-ISSN: 2081-7002; **https://obrobkametalu.tech/**
88. Wesołowski L., Mikołajczyk J.: Hammer mill design and construction analysis. **W:** MIK-21 : Międzynarodowa Innowacyjność i Konkurencyjność w XXI wieku : aspekty innowacyjne / redakcja naukowa dr Łukasz Wojtowicz. Lublin: Fundacja Innowacji i Nowoczesnych Technologii INOTECH : nakładem Instytutu Naukowo-Wydawniczego "Spatium", 2023, Poland; s. 159÷185, p-ISBN: 978-83-67033-89-3;
e-ISBN: 978-83-67033-90-9.
89. Zandecki R., Kmita C., Mikołajczyk J.: Mathematical models of the surface layer microhardness for a selected grade of ion nitrided steel. **W:** Szkoła Logistyki 2022. Radom : Instytut Naukowo-Wydawniczy "Spatium", 2022, Poland; s. 203÷216, Materiały z IX Konferencji Naukowej "Szkoła Logistyki 2022". p-ISBN: 978-83-67033-33-6;
e-ISBN: 978-83-67033-34-3.

Visual and macroscopic examinations of sample welded joints

inż. Tomasz Dokudowicz

Department of Mechanical Engineering

Stanisław Staszic State University of Applied Sciences in Piła, Poland

https://orcid.org/0009-0001-9348-6702

corresponding e-mail: tomaszdok706@gmail.com

Abstract: This paper presents the results of visual and macroscopic examinations of an example of a finished product in production. Discussed in it are features of the above-mentioned examinations and their applications. Characterized are types of discrepancies that may occur in this type of examinations.

Key words: welding, design process, visual examination of welds, macroscopic examination of welds

1. Introduction

Welding is a process of joining materials (mainly metals) by locally melting their edges with or without the addition of a filler metal. The joined elements are not pressed against each other during the welding process [1, 4, 8, 9, 10, 12, 145, 147, 148]. The document containing information on the welding process of a given product is the Welding Technology Manual. It contains, inter alia, guidelines such as:

- type of joint;
- type of weld;
- welding position;
- blowpipe angle;
- welding method;
- joint details;
- method of preparing and cleaning the material;
- name of the machine (welding machine);
- diameter of additional material (filler metal);
- wire feed speed (m/min);
- arc intensity;
- arc voltage;
- welding speed;
- type of additional material;
- type of shielding gas.

The second important document for the welding process of a given product is the Welding Plan which is an instruction for the assembly of elements. This manual shows, step by step, where the weld should be placed to properly complete the product. The use of such a plan is expected to bring benefits in the form of reduced training time for welders and increased control of welds [148, 149, 151, 153, 156]. This document contains, inter alia, information such as:

- number of the welding drawing;
- type of joint testing;
- regulations, standards and related documents;
- degree of welding mechanization: manual or robotic welding;
- number of the welding fixture;
- order of the assembly;
- welding sequence.

Because of the fact that welded joints are subjected to high loads and work in difficult conditions associated with changes in stresses resulting from variable forces acting on a given product, they should be subjected to thorough tests in terms of strength and compliance with technological requirements. Testing of welded joints can be divided into destructive testing and non-destructive testing. Destructive testing includes:

- breaking test;
- impact test;
- hardness test;
- bending test;
- tensile test;
- macroscopic tests;
- microscopic tests;
- metallographic tests.

Non-destructive testing includes:

- LT leaktightness tests;
- VT visual testing;
- UT ultrasonic testing;
- MT magnetic-particle testing ;
- PT penetration testing;
- RT radiographic testing.

One of the above-mentioned methods of destructive testing of welded joints is macroscopic examination. It involves cutting a sample and observing its cross-section without magnification or with magnification up to thirty times. The preparation of a sample involves cutting the element perpendicularly to the weld axis and polishing the surface with sandpaper of various granulations. The prepared polished section is etched with a strong acid in order to reveal the weld, its shape, and the number of layers in the weld. We can also obtain information on internal defects that occurred on the polished section, e.g. gas bubbles, sticking, non-metallic inclusions [1, 4, 8, 10, 12, 156]. An example of a macroscopic examination is shown in Fig. 1.

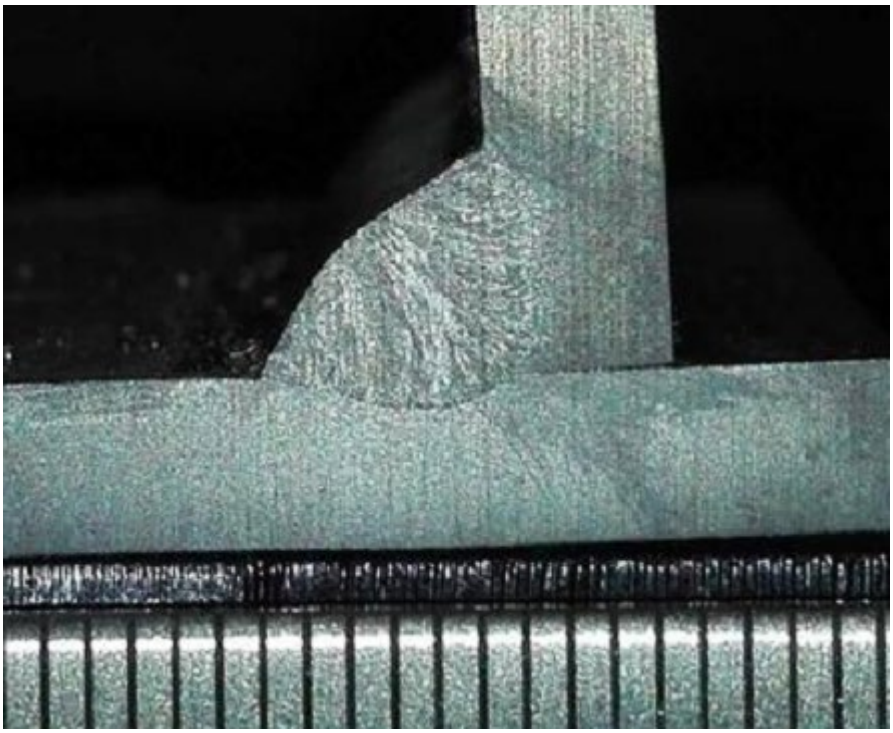

Fig. 1. Example of macroscopic examination

The most common non-destructive testing method is visual testing (VT) (Fig. 2), also called external inspection. This test involves a thorough visual observation of the weld, and taking its measurements. The tools used for this test are a slide caliper and a weld gauge. VT tests are mainly aimed at determining the dimensions of the weld and detecting most of the external defects of the welded joint, such as: [10, 12, 145, 147, 153, 156]:

- weld asymmetry;
- craters;
- cracks;
- undercut of the welded material on both the face and root sides.

Fig. 2. Example of a sample subjected to visual inspection

A welded product with imperfections may be repaired (the imperfections may be removed) by means of technological procedures (e.g. grinding, electro-air gouging). An item that has irreparable welding defects after the welding process is unfortunately usually not suitable for use [212].

The PN-EN- ISO 5817 standard lists the following external (surface) welding imperfections and defects:

- cracks;
- surface blowholes;
- crater pipe end discordance;
- incomplete fusion;
- undercut;
- excessive weld protrusion;
- excess penetration bead;
- improper toe of weld;
- excessive weld asymmetry;
- root concavity;
- improper restart of welding;
- insufficient throat of fillet weld;
- excessive weld throat thickness;
- erratic arc;
- weld overlap;
- weld sagging;
- incompletely filled groove;
- melt-through.

The above-mentioned standard also enumerates the following types of internal imperfections and welding defects:

- gas cavities;
- cracks;
- metallic inclusions;
- copper inclusions;
- incomplete fusion;
- no weld penetration.

A very important feature of steel is its weldability, i.e. the ability to create strong and durable welded joints without the occurrence of welding defects such as cracks, lack of joint

penetration, or porosity. To determine the weldability of steel, the carbon equivalent index CE is used.

Information on the chemical composition and the CE carbon equivalent index should be included in the material certificate delivered together with the steel products [1, 4, 8, 9, 10, 12, 151, 153, 156].

Welding is one of the most important methods of joining metals [13÷144]. In order to ensure high quality of manufactured elements and precision of joints, in addition to the welder's experience, it is also necessary to prepare the process, including the use of appropriate welding equipment. Designing and implementing these devices is an important step in optimizing the production process.

2. Visual and macroscopic examination of welded joints of the "LEG" finished product

For the purpose of this paper, a product called "LEG" was subjected to visual and macroscopic tests – a construction element that can be used, for example, in public transport. "LEG" performs a key load-bearing function ensuring the stability and durability of the structure, e.g. a seat, and ensures the possibility of its safe attachment to the vehicle (chassis).

The type of material used for this construction of the product called "NOGA" was S235JR structural steel, selected for its good plastic properties and ease of welding.

S235JR steel is a material that is widely used in the construction and machinery industry due to its universal properties such as [14]:

- strength;
- plasticity;
- ease of machining.

The individual steel abbreviations are:

- S – structural steel;
- 235 – minimum yield strength expressed in [MPa] for samples up to 16 mm thick;
- JR – indicates that the steel meets the impact strength requirements at 20°C.

Concentrations of chemical elements in S235JR steel are included in Table 1 based on the material certificate 3.1 EN10204.

Table 1. Concentrations of chemical elements in S235JR steel based on the material certificate EN10204 .

Concentration of elements		
Chemical element	Symbol	Concentration value [%]
carbon	C	0.12
silicon	Si	0.014
phosphorus	P	0.006
manganese	Mn	0.42
sulfur	S	0.006
copper	Cu	0.02
vanadium	V	0.001
aluminium	Al	0.034
molybdenum	Mo	0.002
titanium	Ti	0.001
boron	B	0.0002
niobium	Nb	0.001
nickel	Ni	0.005
nitrogen	N	0.0059
chromium	Cr	0.02

The mechanical properties of steel grade S235JR according to material certificate 3.1 EN10204 are presented in Table 2.

Table 2. The mechanical properties of steel grade S235JR according to material certificate 3.1 EN10204

Mechanical properties	
Property	Value
Yield point	259 MPa
Tensile strength	371 MPa
Elongation	34,5%

Based on the material certificate 3.1 EN10204 the CE carbon equivalent index is 0.2%, and the CE carbon equivalent index value calculated using the formula given in the standard is 0.196%. The above results confirm the good weldability of S235JR steel.

Overall dimensions of the “LEG” type product (Fig. 3) are:

- height: 361mm;
- length: 672.4mm;
- width: 240mm.

The production process of the above-mentioned product includes the following operations:

- 2D and 3D laser cutting;
- bending;
- welding;
- shot peening;
- powder coating.

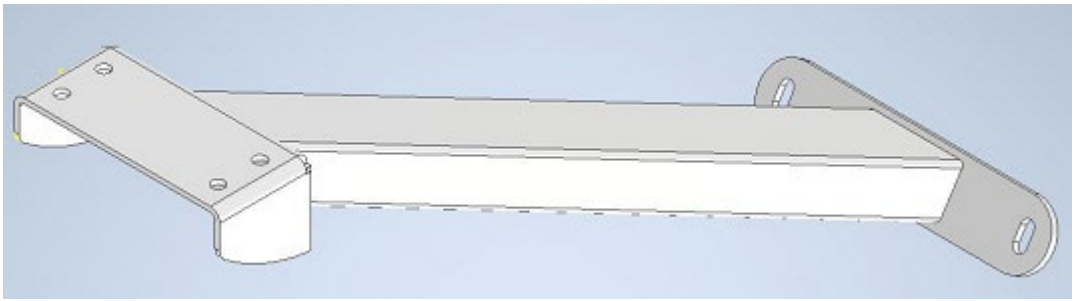

Fig. 3. 3D model of "LEG" product designed in Solid Works

Visual tests were carried out at a laboratory rig with an operating lamp (Fig. 4). The evaluation of the welded joint was performed at a light intensity of 600 lx. The following tools were used to carry out the tests:

- Stanley tape measure, 3m;
- SPD-1weld gauge.

Fig. 4. View of the finished "LEG" product prepared for visual inspection

And macroscopic examinations were carried out on a test rig equipped with the following devices:

- band cutter for metal;
- grinder-polisher.

The joints of the tested element were cut. Then, surfaces of the samples were polished. In the next step, the cross-section was etched with Adler's reagent.

The dimensions of the finished element of “LEG” are presented in the manufacturing drawing ANS-12015-0003-02-00-01 (Fig. 5).

Fig. 6÷10 shows the results of visual and macroscopic examinations. And Fig. 11. presents the designation of welds subject to visual and macroscopic examination of the finished product.

Based on the results of visual inspection of VT No. 1 (Fig. 6) one can conclude that:

- the tested joint has no visible mechanical damage;
- the width of the weld is uniform along its entire length;
- there is a smooth transition of the weld into the welded material;
- face of weld is regular along the entire length;
- the overall result of the examination is positive.

Similar test results were obtained for weld No. 2 (Fig. 7).

Based on macroscopic examination No. 1 (Fig. 8) it can be concluded that:

- the required protrusion of the tested weld should be 3 mm, however, the measured protrusion value is 4.76 mm;
- the measured weld protrusion indication is acceptable.

Based on macroscopic examination No. 2 (Fig. 9) one can state that the tested weld meets the requirements of the PN-EN ISO 5817 standard.

Based on macroscopic examination No. 3 (Fig. 10) it can be concluded that:

- the required protrusion of the tested weld should be 4 mm, however, the measured protrusion value is 5.14 mm;

- protrusion indication acceptable.

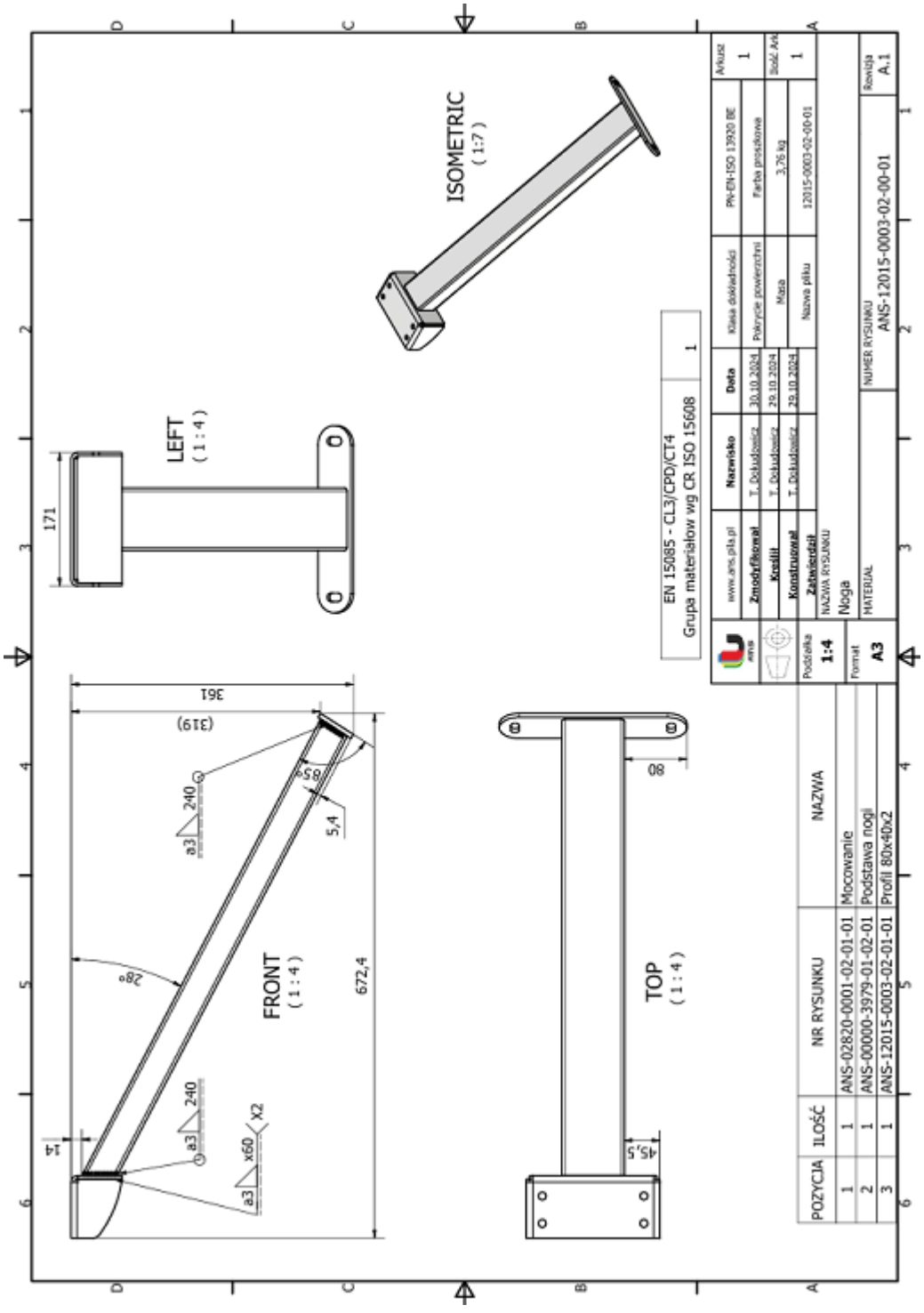

Fig. 5. Manufacturing drawing of the "LEG" finished element

BADANIE WIZUALNE VT NR 1			
Parametry spawania	**Wartość**	**Parametry spawania**	**Wartość**
Proces spawania	135	Korekta długości łuku	2,0
Nazwa maszyny	Fronius TPS 270i	Korekta dynamiki łuku	-2,0
Łączone grubości [mm]	2+4	Natężenie przepływu gazu [l/min]	14
Prędkość posuwu drutu [m/min]	10,7	Wolny wylot elektrody [mm]	10
Natężenie prądu [A]	215	Kąt pochylenia palnika α [stopnie]	45
Napięcie łuku [V]	18,1	Kąt pochylenia palnika β [stopnie]	90
Średnica drutu [mm]	1,0	Program pracy	CMT

Zdjęcie złącza

Pytania kontrolne do oceny wizualnej	**TAK**	**NIE**	
Czy złącze posiada widoczne uszkodzenia mechaniczne?		X	**Poziom jakości wg PN-EN ISO 5817**
Czy na całej długości spoiny jej szerokość jest równomierna?	X		
Czy spoina przechodzi łagodnie w materiał spawany?	X		
Czy lico spoiny jest regularne na całej długości?	X		**Pozytywny "B"**
Ocena: Spełnia wymagania, brak wskazań.			

Fig. 6. Results of visual testing VT No. 1

BADANIE WIZUALNE VT NR 2			
Parametry spawania	**Wartość**	**Parametry spawania**	**Wartość**
Proces spawania	135	Korekta długości łuku	2,0
Nazwa maszyny	Fronius TPS 270i	Korekta dynamiki łuku	-2,0
Łączone grubości [mm]	2+6	Natężenie przepływu gazu [l/min]	14
Prędkość posuwu drutu [m/min]	12	Wolny wylot elektrody [mm]	10
Natężenie prądu [A]	240	Kąt pochylenia palnika α [stopnie]	45
Napięcie łuku [V]	18,5	Kąt pochylenia palnika β [stopnie]	90
Średnica drutu [mm]	1,0	Program pracy	CMT

Zdjęcie złącza

Pytania kontrolne do oceny wizualnej	**TAK**	**NIE**	
Czy złącze posiada widoczne uszkodzenia mechaniczne?		X	**Poziom jakości wg PN-EN ISO 5817**
Czy na całej długości spoiny jej szerokość jest równomierna?	X		
Czy spoina przechodzi łagodnie w materiał spawany?	X		
Czy lico spoiny jest regularne na całej długości?	X		**Pozytywny "B"**
Ocena: Spełnia wymagania, brak wskazań.			

Fig. 7. Results of visual testing VT No. 2

BADANIE MAKROSKOPOWE NR 1

Parametry spawania	Wartość	Parametry spawania	Wartość
Proces spawania	135	Korekta długości łuku	2,0
Nazwa maszyny	Fronius TPS 270i	Korekta dynamiki łuku	-2,0
Łączone grubości [mm]	2+4	Natężenie przepływu gazu [l/min]	14
Prędkość posuwu drutu [m/min]	10,7	Wolny wylot elektrody [mm]	10
Natężenie prądu [A]	215	Kąt pochylenia palnika α [stopnie]	45
Napięcie łuku [V]	18,1	Kąt pochylenia palnika β [stopnie]	90
Średnica drutu [mm]	1,0	Program pracy	CMT

Zdjęcie złącza

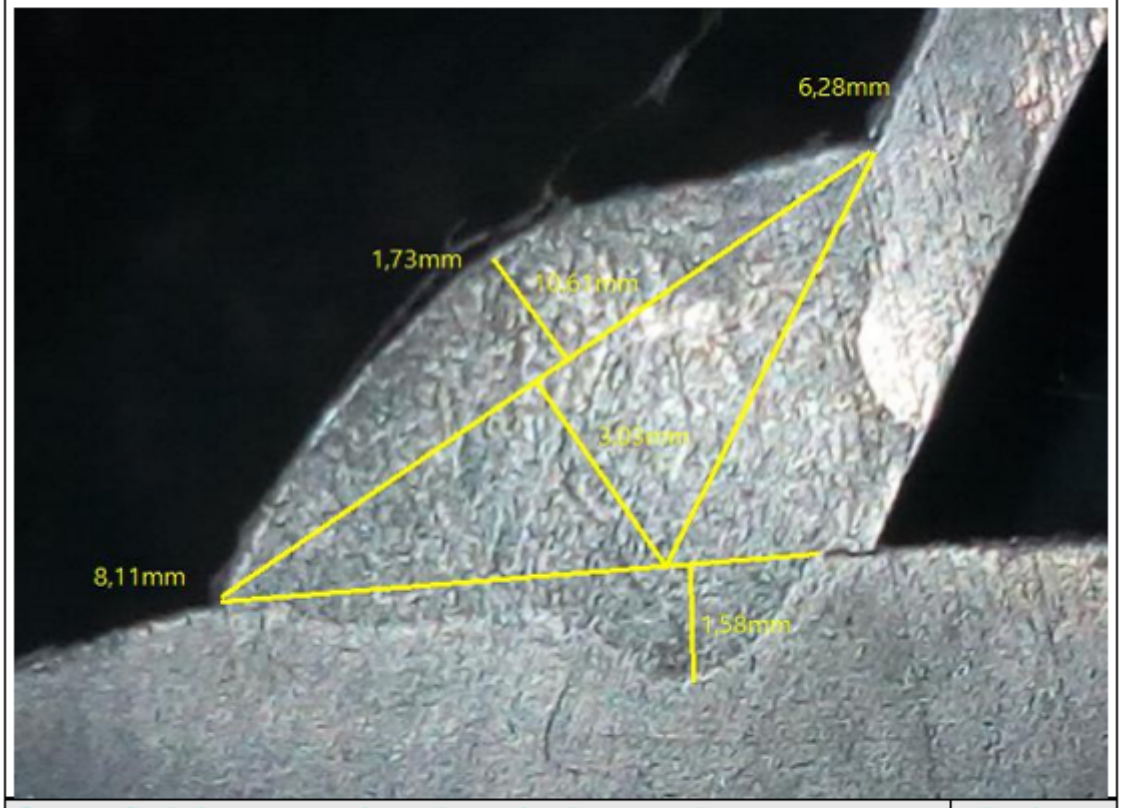

Ocena: Spełnia wymagania, wskazania akceptowalne.

Poziom jakości wg PN-EN ISO 5817

Typ niezgodności	Wymiar [mm]	Wymagania [mm]	
Nadmierna wypukłość	4,76	3	**POZIOM "B"**

Fig. 8. Macroscopic examination result No. 1

BADANIE MAKROSKOPOWE NR 2			
Parametry spawania	**Wartość**	**Parametry spawania**	**Wartość**
Proces spawania	135	Korekta długości łuku	2,0
Nazwa maszyny	Fronius TPS 270i	Korekta dynamiki łuku	-2,0
Łączone grubości [mm]	2+4	Natężenie przepływu gazu [l/min]	14
Prędkość posuwu drutu [m/min]	10,7	Wolny wylot elektrody [mm]	10
Natężenie prądu [A]	215	Kąt pochylenia palnika α [stopnie]	45
Napięcie łuku [V]	18,1	Kąt pochylenia palnika β [stopnie]	90
Średnica drutu [mm]	1,0	Program pracy	CMT
Zdjęcie złącza			
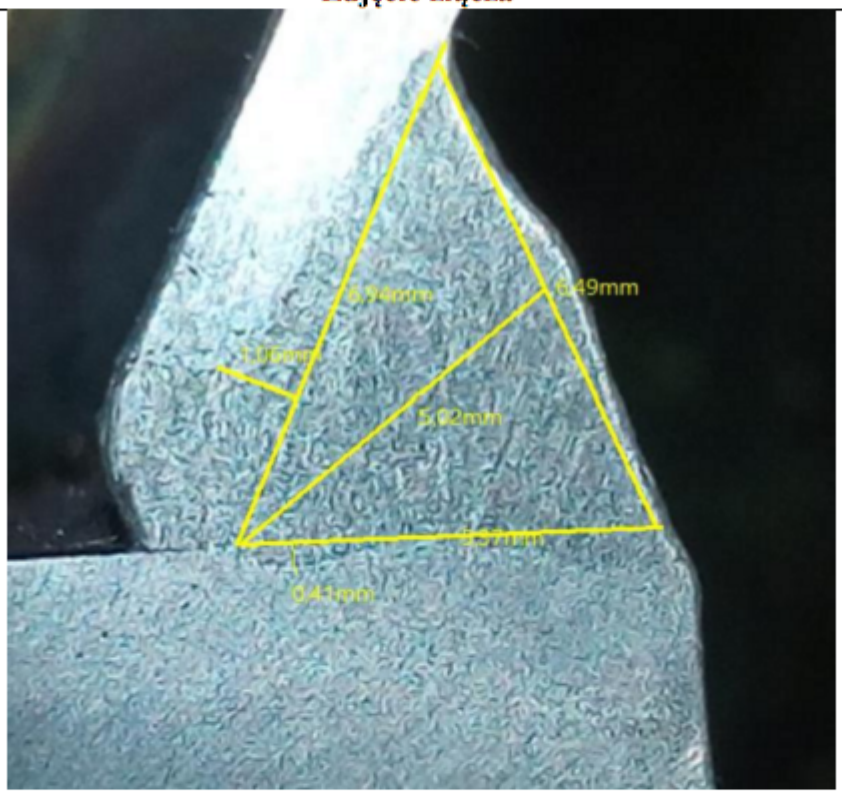			
Ocena: Spełnia wymagania, brak wskazań.			**Poziom jakości wg PN-EN ISO 5817**
Typ niezgodności	**Wymiar [mm]**	**Wymagania [mm]**	**POZIOM "B"**
ND	ND	ND	

Fig. 9. Macroscopic examination results No. 2

BADANIE MAKROSKOPOWE NR 3			
Parametry spawania	**Wartość**	**Parametry spawania**	**Wartość**
Proces spawania	135	Korekta długości łuku	2,0
Nazwa maszyny	Fronius TPS 270i	Korekta dynamiki łuku	-2,0
Łączone grubości [mm]	2+6	Natężenie przepływu gazu [l/min]	14
Prędkość posuwu drutu [m/min]	12	Wolny wylot elektrody [mm]	10
Natężenie prądu [A]	240	Kąt pochylenia palnika α [stopnie]	45
Napięcie łuku [V]	18,5	Kąt pochylenia palnika β [stopnie]	90
Średnica drutu [mm]	1,0	Program pracy	CMT
Zdjęcie złącza			

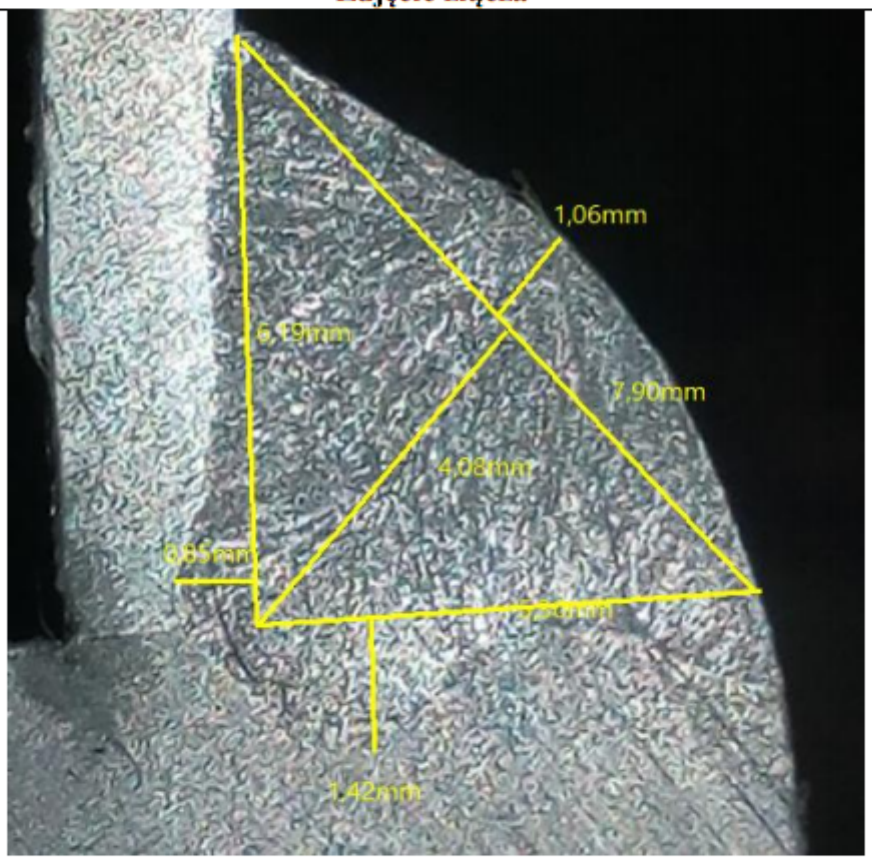

Ocena: Spełnia wymagania, wskazania akceptowalne.			**Poziom jakości wg PN-EN ISO 5817**
Typ niezgodności	**Wymiar [mm]**	**Wymagania [mm]**	**POZIOM "B"**
Nadmierna wypukłość	5,14	4	

Fig. 10. Macroscopic examination results No. 3

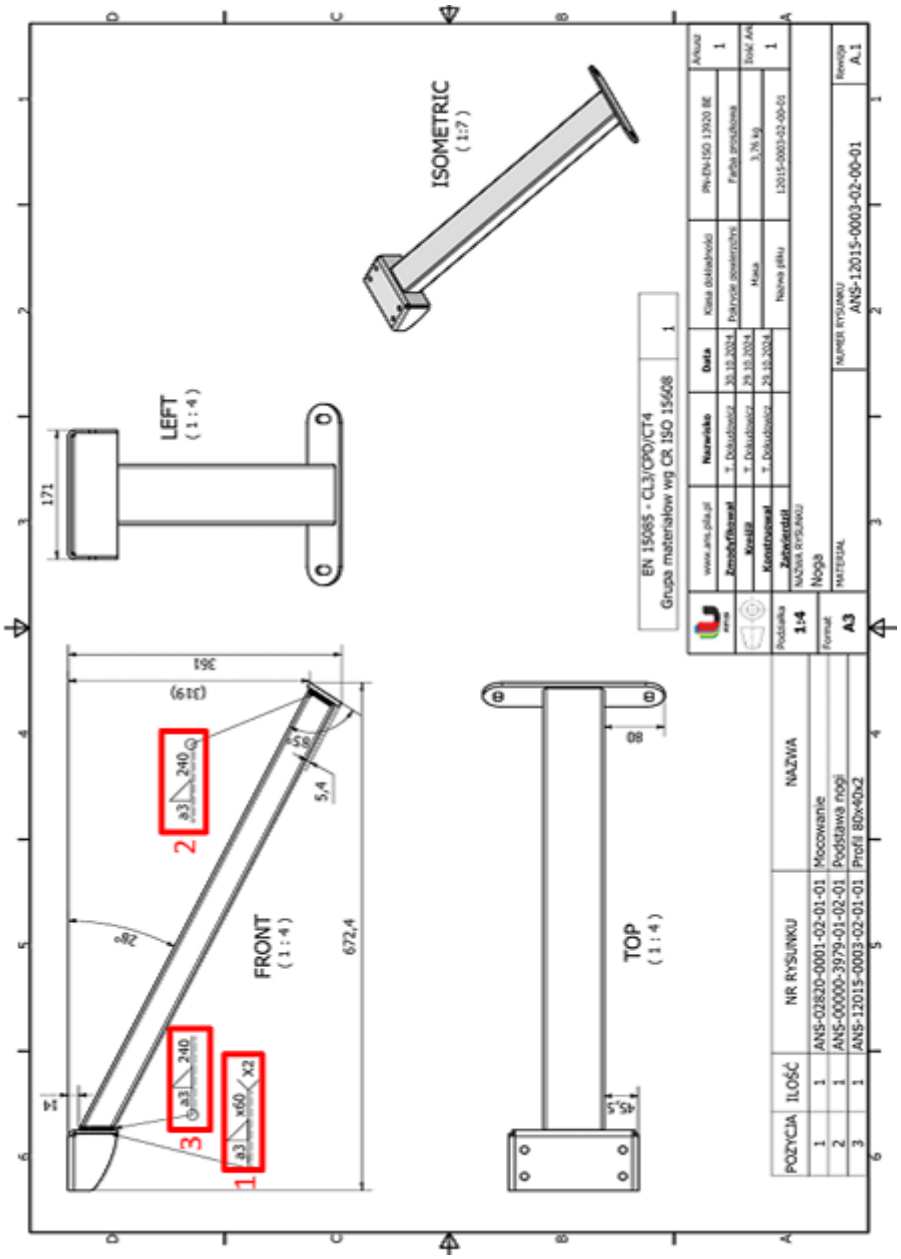

Fig. 11. Designation of welds subject to visual and macroscopic examination of the finished product

3. Test results and conclusion

Visual tests did not identify any major readings and confirmed that the weld requirements were met in accordance with the data contained in the assembly drawing of the finished product. VT testing generates the lowest cost and is widely used for quality control at production stations by welders and quality control personnel.

More detailed are macroscopic examinations which showed excessive protrusion of the tested welds. To avoid this type of inconsistency and maintain proper fusion of the weld into the material, the welder should increase the speed of the blowpipe.

4. Literature

1. Dobrowolski Z.: Podręcznik spawalnictwa. Wydawnictwo WNT, Warszawa 1978.
2. Grabowska M., Mikołajczyk J.: Zastosowanie tomografii komputerowej CAT w inżynierii materiałowej. Application of CAT scanning for materials engineering. Postępy w Inżynierii Mechanicznej [Developments in Mechanical Engineering]; 2017, nr 9 (5), s. 15÷26, p-ISSN: 2300-3383; Wydawnictwa Uczelniane Uniwersytetu Technologiczo-Przyrodniczego w Bydgoszczy, Poland. **http://wu.utp.edu.pl/oferta,8,1**
3. Grabowska M., Mikołajczyk J., Basiak S.: Zastosowanie tomografii komputerowej CAT w nieniszczących badaniach teowych złączy spawanych. Application of cat scanning in non-destructive testing of welded t-joints. Postępy w Inżynierii Mechanicznej [Developments in Mechanical Engineering]; 2018, nr 11 (6), s. 31÷44, p-ISSN: 2300-3383; Wydawnictwa Uczelniane Uniwersytetu Technologiczno-Przyrodniczego w Bydgoszczy, Poland. **http://wu.utp.edu.pl/oferta,8,1**
4. Hillar J., Jarmoszuk S.: Technologia. Spawalnictwo. Wydawnictwa Szkolne i Pedagogiczne, Warszawa 1987.
5. Hillar J.: Spawanie gazowe. Wiadomości specjalistyczne. Wydawnictwo ZZDZ, nr M-120.
6. https://stalpact.pl/stal-235jr-kluczowe-parametry-i-wlasciwosci/
7. https://www.inzynier-spawalnik.pl/spawalnosc-stali
8. Jarmoszuk S.: Spawanie elektryczne. Wiadomości specjalistyczne. Wydawnictwo ZZDZ, nr M-121.
9. Jarmoszuk S.: Spawanie w osłonie argonu elektrodą wolframową. Wydawnictwo ZZDZ, nr M-158.
10. Jarmoszuk S.: Spawanie w osłonie dwutlenku węgla. Wydawnictwo ZZDZ, nr M-157.
11. Michalski R.: Zgrzewanie oporowe. Poradnik. Wydawnictwa Naukowo-Techniczne. Warszawa 1970.
12. Mistur L.: Spawanie gazowe i elektryczne. Wydawnictwa Szkolne i Pedagogiczne. Warszawa 1983.
13. Norma PN-86/H-84018. Stal niskostopowa o podwyższonej wytrzymałości. Gatunki.
14. Norma PN-75/H-84019. Stal węglowa konstrukcyjne wyższej jakości ogólnego przeznaczenia. Gatunki.
15. Norma PN-72/H-84020. Stal węglowa konstrukcyjna zwykłej jakości ogólnego przeznaczenia. Gatunki.
16. Norma PN-75/H-84024. Stal do pracy przy podwyższonych temperaturach. Gatunki.
17. Norma PN-71/H-86020. Stal odporna na korozję (nierdzewna i kwasoodporna). Gatunki.
18. Norma PN-71/H-86022. Stal żaroodporna. Gatunki.
19. Norma PN-75/M-69703. Spawalnictwo. Wady złączy spawanych. Nazwy i określenia (zmiana 1, Biul. PKNiM nr 9/76, poz. 85).
20. Norma PN-78/M-69760. Spawalnictwo. Badania skłonności do tworzenia zimnych pęknięć w złączach spawanych łukowo.
21. Norma PN-79/M-69761. Spawalnictwo. Metody badań skłonności do tworzenia pęknięć krystalizacyjnych w spoinach stalowych złączy spawanych łukowo.
22. Norma PN-72/M—69770. Radiografia przemysłowa. Radiogramy spoin czołowych w złączach doczołowych ze stali. Wymagania jakościowe i wytyczne wykonania.
23. Norma PN-74/M-69771. Spawanie. Wady złączy doczołowych wykrywane badaniami radiograficznymi. Nazwy i określenia (zmiana 1, Biul. PKNiM nr 9/76, poz. 85).

24. Norma PN-87/M-69772. Spawalnictwo. Klasyfikacja wadliwości złączy spawanych na podstawie radiogramów.
25. Norma PN-85/M-69775. Spawalnictwo. Wadliwość złączy spawanych. Oznaczenia klasy wadliwości na podstawie oględzin zewnętrznych.
26. Norma PN-77/M-70001. Przemysłowe badania radiograficzne. Wskaźniki jakości obrazu. Wymagania.
27. Norma PN-75/M-70020. Badania nie niszczące. Metody radiologiczne. Nazwy i określenia.
28. Norma PN-76/M-70050. Badania nie niszczące. Metody ultradźwiękowe. Nazwy i określenia.
29. Norma PN-75/M-70051. Badania nie niszczące metodami ultradźwiękowymi. Wzorzec kontrolny W1.
30. Norma PN-74/M-70052. Badania nie niszczące. Metody penetracyjne. Nazwy i określenia.
31. Norma PN-75/M-70054. Badania nie niszczące metodami ultradźwiękowymi. Wzorzec kontrolny W2.
32. Norma PN-77/M-70055. Badania nie niszczące. Metody ultradźwiękowe. Badanie spoin w złączach doczołowych.
33. Norma PN-75/M-70056. Badania nie niszczące metodami ultradźwiękowymi. Wzorce mikrosekundowe.
34. Norma PN-86/M-69707. Spawalnictwo. Zasady wykonywania próbnych złączy spawanych lub zgrzewanych.
35. Norma PN-78/M-69710. Spawalnictwo. Próba statyczna rozciągania doczołowych złączy spawanych lub zgrzewanych.
36. Norma PN-80/M-69714. Spawalnictwo. Próba statyczna rozciągania złączy ze spoinami pachwinowymi.
37. Norma PN-57/M-69715. Spawanie. Próba statyczna rozciągania złącza nakładkowego z pachwinowymi spoinami poprzecznymi.
38. Norma PN-57/M-69716. Spawanie. Próba statyczna rozciągania złącza nakładkowego z pachwinowymi spoinami podłużnymi.
39. Norma PN-78/M-69720. Spawalnictwo. Próby zginania doczołowych złączy spawanych lub zgrzewanych.
40. Norma PN-70/M69733. Spawalnictwo. Próba udarności złączy spawanych lub zgrzewanych doczołowo.
41. Norma PN-69/M-69734. Próba starzenia stalowych płaskich złączy spawanych doczołowo.
42. Norma PN-58/M69740. Spawanie. Próba łamania płaskiego złącza doczołowego o grubości powyżej 4 mm.
43. Norma PN-58/M-69741. Spawanie. Próba łamania złącza kątowego ze spoiną pachwinową.
44. Norma PN-58/M-69742. Spawanie. Próba łamania złącza nakładkowego ze spoiną pachwinową.
45. Norma PN-64/M-69751. Próba twardości złączy spawanych i zgrzewanych.
46. Norma PN-76/M-69783. Spawalnictwo. Próby statyczne ścinania i rozciągania zgrzein liniowych.
47. Norma PN-67/M-69790. Próby statyczne rozciągania i ścinania złączy lutowanych.
48. Norma PN-65/M-69013. Spawanie gazowe stali niskowęglowych i niskostopowych. Rowki do spawania.
49. Norma PN-75/M-69014. Spawanie lukowe elektrodami otulonymi stali węglowych i niskostopowych. Przygotowanie brzegów do spawania.

50. Norma PN-73/M-69015. Spawanie łukiem krytym stali węglowych i niskostopowych. Przygotowanie brzegów do spawania.
51. Norma PN-74/M-69016. Spawanie w osłonie dwutlenku węgla stali węglowych i niskostopowych. Przygotowanie brzegów do spawania.
52. Norma PN-65/M-69017. Spawanie argonowe elektroda nietopliwą stali stopowych. Rowki do spawania.
53. Norma PN-67/M-69018. Spawanie żużlowe stali węglowych i niskostopowych. Rowki do spawania.
54. Norma PN-69/M-69019. Spawanie doczołowe rur stalowych. Rowki do spawania.
55. Norma PN-70/M-69023. Spawanie łukowe stali platerowanych stalą odporną na korozje. Wytyczne projektowania i wykonywania złączy spawanych.
56. Norma PN-70/M-69024. Spawanie łukowe aluminium i jego stopów elektrodą wolframową w osłonie argonu. Przygotowanie brzegów do spawania.
57. Norma PN-70/M-69025. Spawanie gazowe miedzi. Przygotowanie brzegów do spawania.
58. Norma PN-72/M-69026. Spawanie łukowe miedzi w osłonie argonu elektrodą wolframową. Przygotowanie brzegów do spawania.
59. Norma PN-73/M-69027. Spawanie łukowe aluminium i jego stopów elektrodą topliwą w osłonie argonu. Przygotowanie brzegów do spawania.
60. Norma PN-78/M-69028. Spawalnictwo. Spawanie łukowe miedzi w osłonie argonu elektrodą topliwą. Przygotowanie brzegów do spawania.
61. Norma PN-76/M-69070. Spawalnictwo. Urządzenia do mechanizacji spawania. Nazwy i określenia.
62. Norma PN-61/M-69100. Spawalnictwo. Źródła prądu do ręcznego spawania łukowego. Klasyfikacja.
63. Norma PN-75/M-69101. Spawalnictwo. Szpule elektrodowe do automatów i półautomatów spawalniczych. Główne wymiary.
64. Norma PN-75/M-69104. Automaty i półautomaty do spawania łukiem krytym i w osłonie gazów ochronnych elektrodą topliwą. Nazwy i określenia.
65. Norma PN-75/M-69105. Spawalnictwo. Półautomaty spawalnicze do spawania łukowego w osłonie gazu ochronnego elektrodą topliwą. Ogólne wymagania i badania.
66. Norma PN-79/M-69106. Spawalnictwo. Automaty spawalnicze. Ogólne wymagania i badania.
67. Norma PN-83/M-69108. Spawalnictwo. Źródło energii elektrycznej do spawania łukowego. Nazwy i określenia.
68. Norma PN-69/M-69124. Elektrody wolframowe do celów spawalniczych.
69. Norma PN-76/M-69160. Spawalnictwo. Osłony twarzy przed promieniowaniem łuku spawalniczego. Tarcze spawalnicze.
70. Norma PN-80/M-69161. Spawalnictwo. Uchwyty elektrodowe do spawania ręcznego izolowane.
71. Norma PN-79/M-69010. Wyroby z węgli uszlachetnionych. Elektrody spawalnicze.
72. Norma PN-85/E-81106. Spawalnictwo. Jednostanowiskowe transformatory spawalnicze. Wymagania i badania.
73. Norma PN-74/M-69102. Spawalnictwo. Przecinarki do cięcia termicznego. Dokładność odwzorowania.
74. Norma PN-74/M-69103. Spawalnictwo. Przecinarki półautomatyczne do cięcia tlenem stali. Wymagania i badania.
75. Norma PN-80/M-69107. Spawalnictwo. Przecinarki do cięcia termicznego. Nazwy i określenia.
76. Norma PN-80/M-69180. Spawalnictwo. Palniki, oznaczenia i cechowanie.

77. Norma PN-81/M-69181. Spawalnictwo. Dysze palników gazowych. Określenia, podział i oznaczenia.
78. Norma PN-76/M69182. Spawalnictwo. Palniki do spawania gazowego i cięcia tlenem. Wymagania i badania.
79. Norma PN-75/M-69200. Spawalnictwo. Wytwornice acetylenowe. Podział.
80. Norma PN-76/M-69202. Spawalnictwo. Zawory bezpieczeństwa.
81. Norma PN-75/M-69210. Zbiorniki transportowe do gazów. Barwy rozpoznawcze i oznakowanie.
82. Norma PN-79/M-69221. Butle do gazów. Butle stalowe do gazów.
83. Norma PN-76/M-69222. Butle do gazów. Butle stalowe bez szwu.
84. Norma PN-82/M-69223. Butle do gazów. Gwinty stożkowe. Wymiary i tolerancje.
85. Norma PN-60/M-69224. Butle do gazów. Gwinty Whitwortha o średnicach 21,8 i 24,3 mm.
86. Norma PN-80/M-69225. Butle do gazów. Gwint Whitwortha o średnicy 80 mm.
87. Norma PN-63/M-69226. Butle do gazów. Gwint stożkowy metryczny.
88. Norma PN-67/M-69227. Zawory butlowe do acetylenu VA1.
89. Norma PN-81/M-69228. Butle do gazów. Zawory do butli. Wymagania i badania.
90. Norma PN-81/M-69229. Butle do gazów. Złącza zaworów butlowych.
91. Norma PN-74/M-69240. Reduktory spawalnicze. Główne wskaźniki.
92. Norma PN-80/M-69242. Spawalnictwo. Reduktory do tlenu.
93. Norma PN-77/M-69243. Spawalnictwo. Reduktory butlowe do gazów płynnych.
94. Norma PN-78/M-69244. Spawalnictwo. Reduktory do acetylenu.
95. Norma PN-72/M-69260. Spawalnictwo. Króćce do przyłączenia węży gumowych. Główne wymiary.
96. Norma PN-71/M-69261. Spawalnictwo. Przyłączki i złączki do węży gumowych.
97. Norma PN-76/M-69774. Spawalnictwo. Cięcie gazowe stali węglowych o grubości 5÷100 mm. Jakość powierzchni cięcia.
98. Norma PN-63/M-74905. Opaski zaciskowe przewodów giętkich.
99. Norma PN-77/C-94250.47. Węże gumowe. Węże tłoczne gumowe ze wzmocnieniem tekstylnym do tlenu.
100. Norma PN-77/C-94250.48. Węże gumowe. Węże tłoczne ze wzmocnieniem tekstylnym do acetylenu.
101. Norma BN-68/4122-02. Zawory butlowe do tlenu technicznego VT1.
102. Norma PN-67/M-69350. Topniki spawalnicze. Klasyfikacja.
103. Norma PN-81/M-69354. Spawalnictwo. Topniki do gazowego spawania miedzi, mosiądzów, brązów, aluminium i stopów aluminium.
104. Norma PN-73/M-69355. Topniki do spawania i napawania łukiem krytym.
105. Norma PN-67/M-69356. Topniki do spawania żużlowego.
106. Norma PN-76/M-69400. Spoiwa cynowo-ołowiowe do lutowania miękkiego. Gatunki.
107. Norma PN-80/M-69411. Spawalnictwo. Spoiwa srebrne do lutowania.
108. Norma PN-73/M-69412. Spawalnictwo. Druty do gazowego i łukowego metalizowania natryskowego.
109. Norma PN-70/M-69413. Spoiwa miedziane, mosiężne, brązowe i niklowe do spawania i lutowania.
110. Norma PN-75/M-69414. Spawalnictwo. Spoiwa do spawania aluminium i stopów aluminium.
111. Norma PN-77/M-69420. Spawalnictwo. Spoiwa stalowe do spawania i napawania.
112. Norma PN-74/M-69430. Spawalnictwo. Elektrody stalowe otulone do spawania i napawania. Ogólne wymagania i badania.

113. Norma PN-77/M-69433. Spawalnictwo. Elektrody stalowe otulone do spawania stali węglowych i niskostopowych.
114. Norma PN-74/M-69434. Elektrody otulone do spawania stali niskostopowych przeznaczonych do pracy w podwyższonych temperaturach.
115. Norma PN-79/M-69435. Spawalnictwo. Elektrody stalowe do spawania stali wysokostopowych.
116. Norma PN-74/M-69436. Elektrody stalowe do napawania.
117. Norma PN-57/M-69451. Spawanie. Spoiwa. Pręty żeliwne.
118. Norma PN-64/M-69708. Spawalnictwo. Próby mechaniczne stopiwa.
119. Norma PN-57/M-69712. Spawanie. Próba statyczna rozciągania materiału spoiny.
120. Norma PN-58/M-69717. Spawanie gazowe. Próba statyczna rozciągania stopiwa.
121. Norma PN-58/M-69730. Spawanie gazowe. Próba udarności stopiwa.
122. Norma PN-82/C-23050. Karbid.
123. Norma PN-71/C-84905. Acetylen rozpuszczony.
124. Norma PN-61/C-84908. Wodór techniczny sprężony.
125. Norma PN-70/C-84910. Tlen sprężony (zmiana Biul. PKNiM nr 10/76, poz. 93).
126. Norma PN-72/C-84912. Azot sprężony techniczny.
127. Norma PN-82/C-96000. Przetwory naftowe. Gazy węglowodorowe (płynne C_3-C_4).
128. Norma PN-77/M-69000. Spawalnictwo. Spawanie metali. Nazwy i określenia.
129. Norma PN-84/M-69001. Spawalnictwo. Spajanie metali i procesy pokrewne. Podział.
130. Norma PN-75/M-69002. Spawalnictwo. Pozycje spawania. Klasyfikacja i oznaczenia.
131. Norma PN-87/M-69008. Spawalnictwo. Klasyfikacja konstrukcji spawanych.
132. Norma PN-87/M-6990/01. Spawalnictwo. Egzaminy spawaczy i zgrzewaczy. Postanowienia ogólne.
133. Norma PN-87/M-69900/02. Spawalnictwo. Podstawowy egzamin spawacza.
134. Norma PN-87/M-69900/03. Spawalnictwo. Ponadpodstawowy egzamin spawacza.
135. Norma PN-87/M-69900/04. Spawalnictwo. Egzamin spawacza-operatora.
136. Norma PN-87/M-69900/05. Spawalnictwo. Egzamin zgrzewacza.
137. Norma PN-87/M-69900/06. Spawalnictwo. Egzamin rozszerzający oraz sprawdzający spawacza i zgrzewacza.
138. Norma PN-79/M- 01134. Rysunek techniczny maszynowy. Uproszczenia rysunkowe. Zasady oznaczania spoin.
139. Norma PN-64/M-01138. Rysunek techniczny maszynowy. Połączenia spawane i powierzchnie napawane (zmiana Biul. PKN nr 6/67, poz. 67).
140. Norma PN-64/M-01139. Rysunek techniczny maszynowy. Połączenia zgrzewane i lutowane (bez lutowania). Biul. PKNiM nr 28/76.
141. Norma PN-83/N-01635. Rysunek techniczny. Uproszczenia rysunkowe. Połączenia nitowane, lutowane, klejone i zszywane.
142. Norma PN-64/B-01043. Rysunek konstrukcyjny budowlany. Konstrukcje stalowe.
143. Norma PN-81/M-Z-53201. Sprzęt ochrony osobistej oczu. Optyczne filtry i szybki ochronne. Ogólne wymagania i badania.
144. Norma PN-73/Z-53205. Sprzęt ochrony osobistej oczu. Szybki ochronne przeciwodpryskowe.
145. Pałasz J.: Poradnik spawacza gazowego. Wydawnictwa Naukowo-Techniczne. Warszawa 1986.
146. Piwowar S.: Spawanie i zgrzewanie elektryczne. Wydawnictwa Szkolne i Pedagogiczne. Warszawa 1981.
147. Piwowar S.: Kontrola procesów spawalniczych. Wydawnictwa Naukowo-Techniczne, Warszawa 1979.

148. Piątek P.: Spawanie (materiały dydaktyczne). Wydawnictwo SANNORT, Sandomierz, 2014.
149. Pikulik K.W., Mikołajczyk J.: The influence of the welding current on the air pollution emissions. Wpływ prądu spawania na emisję zanieczyszczeń powietrza. Postępy w Inżynierii Mechanicznej [Developments in Mechanical Engineering]; 2019, nr 14 (7), s. 33-46, p-ISSN: 2300-3383; Wydawnictwa Uczelniane Uniwersytetu Technologiczno-Przyrodniczego im. J. J. Śniadeckich w Bydgoszczy, Poland.
http://yadda.icm.edu.pl/baztech/element/bwmeta1.element.baztech-2faf200b-3010-4192-9fd0-062f53b49d38
150. Pikulik K.W., Mikołajczyk J.: Determination of emission of iron oxides from the welding process on the basis of mathematical models. Welding Technology Review; 2021, vol. 93, No 2, s. 35-43, p-ISSN: 0033-2364; e-ISSN: 2449-7959;
http://www.pspaw.wip.pw.edu.pl/index.php/pspaw/article/view/1132
DOI: 10.26628/wtr.v93i2.1132
151. Praca zbiorowa: Poradnik inżyniera spawalnictwa. Wydawnictwa Naukowo-Techniczne. Warszawa 1983.
152. Radomski T., Ciszewski A.: Lutowanie. Wydawnictwa Naukowo-Techniczne. Warszawa 1985.
153. Syrek S., Mikołajczyk J.: Analiza matematyczna podstawowych wymiarów złącza spawanego. **W:** Logistyka w ratownictwie 2022 / pod redakcją Andrzeja Chudzikiewicza i Andrzeja Krzyszkowskiego. Radom : Instytut Naukowo-Wydawniczy "Spatium", 2022; s. 169-190, p-ISBN: 978-83-67033-57-2; e-ISBN: 978-83-67033-70-1.
154. Syrek S., Mikołajczyk J.: Modele liniowe wpływu częstotliwości prądu spawania na grubość spoiny. **W:** MIK-21 : Międzynarodowa Innowacyjność i Konkurencyjność w XXI wieku : aspekty innowacyjne / redakcja naukowa Radosław Luft. Lublin: Fundacja Innowacji i Nowoczesnych Technologii INOTECH, 2022. Radom : nakładem Instytutu Naukowo-Wydawniczego "Spatium", 2022; s. 153-170, p-ISBN: 978-83-67033-43-5;
e-ISBN: 978-83-67033-44-2;
http://inw-spatium.pl/wp-content/uploads/2022/09/MIK-21-2022-Aspekty-innowacyjne-2.pdf
155. Syrek S., Mikołajczyk J.: Modele liniowe wpływu częstotliwości prądu spawania na szerokość spoiny. Obróbka Metalu; 2022, nr 4, s. 24-31,
p-ISSN: 2081-7002; **https://obrobkametalu.tech/**
156. Szustakowski J.: Poradnik spawacza elektrycznego. Wydawnictwa Naukowo-Techniczne, Warszawa 1977.

Testing characteristic parameters of a railway track during the passage of rail vehicles

mgr inż. Mariusz Rusin

Bydgoszcz University of Science and Technology

Faculty of Mechanical Engineering

https://orcid.org/0009-0006-4358-3375

corresponding e-mail: rusin-mariusz@wp.pl

Abstract: The paper presents issues related to the repair and assessment of the railway tracks condition. As a repair method discussed is the process of hard-facing of railway turnouts. It is stated in the paper that both the rolling stock and railway infrastructure constitute one thing that secures proper operation of the railway communication system and should not be discussed separately. They both influence each other, i.e. for example, fast trains will not run fast if there is no appropriate infrastructure for them and vice versa.

Keywords: railway track diagnostics, vibrations, dynamic loads, vision methods

1. Introduction

Modern technology of the 21st century has brought achievements that change our lives in many aspects. These technologies not only impact our everyday lives but also open the door to a future full of opportunities and challenges.

Rail transport is one of the main modes of transport and it plays a key role in passenger and freight transport. As technology and available products develop, railways are expected to ensure the reliability of railway infrastructure and increase safety and speed on railway systems. In Poland, increasing the speed of freight trains to 120 km/h and passenger trains to 200 km/h and increasing the axle load to 25 t/axle is associated with a number of challenges and requirements for the railway infrastructure and rolling stock [1, 2, 3, 4, 5, 6].

The paper presents tests of characteristic parameters of a railway track during the passage of rail vehicles, as well as the analysis of the tests carried out. Generally available technologies and free software were used, which allowed effective and economical track diagnostics. The vision method, thanks to its simplicity and extensive analytical capabilities, is a modern approach to assessing the technical condition of railway infrastructure.

The paper highlights the importance of modern diagnostic systems, such as vision measurements, vibration analyzers and real-time monitoring systems. Diagnostics allows for early detection of track defects, which translates into improved safety and reduced maintenance costs [1, 2, 3, 4, 5, 6].

The literature review and research conducted stress that parameters of a railway track are crucial for its behavior during the passage of rail vehicles. It also indicates the need for further research on the optimization of these parameters in order to meet the growing requirements related to speed, load and safety of rail transport [1, 6, 7, 8, 9].

Railway surface and track diagnostics is an area that has undergone significant development over the decades, with its origins as an organised discipline dating back to the 1980s. At that time, the first comprehensive studies were created which constituted the foundation for modern diagnostic methods in Poland [1, 2, 8, 9, 13, 15, 36, 186, 187].

The key challenge for railways around the world is to increase train speeds, optimize the costs of transported cargo and passengers, and ensure the reliability of rolling stock and tracks. The most important thing is the safety of the traffic and entire diagnostic process. At train speeds above 120 km/h, the aim is to automate diagnostics and eliminate direct measurement work on active tracks performed by men. With the increase in train speed, new problems with the operation of the entire system emerged [1, 3, 6, 9, 11, 186, 187, 194, 197].

Many scientific minds around the world are focusing their efforts on solving key problems related to the development of rail transport. Their work includes innovative technological solutions, process optimization and increasing safety and efficiency.

In China, scientists are intensively studying the problem of wheel polygonization, which generates significant economic losses for both railway operators and infrastructure managers. This phenomenon leads to increased wear of track components and rolling stock, and also increases maintenance and repair costs. Other problems include corrugation of the rails with wavelengths ranging from 20 mm to 80 mm, as well as vibration modes and wave propagation. Currently, work is underway to develop effective methods to minimize this phenomenon [1, 3, 4, 6, 9,14,15,16].

Nowadays, railway vehicles are manufactured so that they are adapted to make the diagnosis of the condition of railway tracks. They are used to carry out a detailed

analysis of track parameters, such as geometry, condition of sleepers, fastenings, corrugation and rail wear. These vehicles are equipped with advanced measurement systems, including laser sensors, accelerometers, high-resolution cameras and ultrasonic systems, which enable precise fault detection and assessment of the technical condition of infrastructure. Carrying out diagnostics using these systems make it possible to detect problems early, which translates into increased rail traffic safety and optimisation of track maintenance costs. The quality and safety of railway infrastructure require regular and timely diagnosis of its parameters and characteristics. At present, infrastructure diagnostics is carried out using modern measurement systems, developed specifically to examine its technical condition. Without systematic and accurate diagnostics, it is impossible to effectively and efficiently ensure high-quality railway infrastructure and the services it provides. Experimental studies were conducted focusing on the use of numerous, inexpensive inertial devices to assess ride comfort and monitor the condition of railway tracks. This approach allows to create distributed measurement systems that, thanks to their low price, can be widely used in practice. Inertial devices record dynamic parameters such as acceleration and vibrations, which enables the analysis of track quality and the identification of potential problems affecting passenger comfort and operational safety [7, 11, 12, 13].

Many scientific works on railways focus on developing mathematical models, conducting comprehensive analyses and deriving theoretical formulas. Two main groups can be distinguished in the track corrugations. The first includes cases in which the so-called "wavelength-setting mechanism" results from the resonance of the vehicle's unsprung mass on the track stiffness, known as P2 resonance, or from the rail resonance in which its vibrations resemble the behavior of a beam mounted on sleepers. The second group of corrugations highlights the differences between the results of tensile and fatigue tests, both in terms of their values and the details of their execution. This demonstrates the limitations of static test systems in assessing the durability of connections after their installation on tracks exposed to impact in the area of end posts. None of the tested joints were completely crack-resistant, even when unrealistic stress levels were applied. These tests also aim at improving the pearlitic microstructure of steel to increase its mechanical properties such as strength, ductility and hardness. Hardness, measured on the Brinell scale (BHN) has proven particularly useful in differentiating the behavior of different grades of rail and wheel steel. Moreover, a clear relationship has been demonstrated between increased hardness resulting from the microstructure and improved wear resistance [4, 5, 8, 10, 16, 18, 19, 29, 197].

When it comes to railway infrastructure in any country, it falls into two main categories:

- Railroads and rail lines:

This category covers instructions related to the construction, maintenance and operation of railway infrastructure, including tracks, sleepers, rails, turnouts and other track elements. It also includes regulations on traffic organization, safety on trails and rules of conduct in the event of infrastructure failure [2, 4, 6, 8, 12, 13, 19, 29, 36, 186, 187, 196].

- Railway vehicles:

The instructions in this group cover the operation, maintenance and diagnostics of railway vehicles such as locomotives, wagons and specialized vehicles. They contain detailed technical guidelines, safety standards and procedures for dealing with breakdowns and servicing rolling stock.

Both categories are crucial for ensuring efficient and safe operation of the railway, and obeying their instructions is essential in the daily work of railway staff [1, 2, 4, 6, 8, 9, 11, 14, 15, 36, 186].

Research on railway track parameters during the passage of rail vehicles is described in detail in the technical literature but it often lacks a comprehensive approach that would present the problem from general to specific. Currently, measurements are carried out using advanced technologies, such as modern measuring devices, image recording systems and advanced mathematical analyses.

Still, many studies focus solely on one aspect, either the railway track or the rolling stock wheel. This approach limits the possibility to fully understand the phenomena and mechanisms leading to wheel deformation or track damage. It exposes the infrastructure and rolling stock management to losses and threatens general safety.

To obtain reliable results and effectively identify the causes of problems, a systems approach is necessary that takes into account the interdependencies in the entire track-vehicle system being studied. Only through a comprehensive analysis will it be possible to diagnose the real causes of phenomena, not just their symptoms. This approach will allow to develop more effective solutions that will prevent the degradation of railway infrastructure and rolling stock components.

As a starting point for diagnostic tests in the field of railways, it is worth adopting classic publications from the 1980s, which describe diagnostic problems in detail. Although they may seem outdated, they provide a solid theoretical foundation that covers key issues related to the analysis of railway track parameters, rolling stock and related phenomena. Using these publications as a starting point gives a deeper understanding of fundamental problems that still remain relevant [15, 16, 186, 187, 194, 195, 196, 197].

Modern technologies and scientific advances provide an excellent opportunity to update this research. The integration of new measurement methods, such as advanced monitoring systems, artificial intelligence in data analysis, 3D imaging technologies, and predictive systems, can significantly increase the precision of diagnostics and enable faster fault detection. Thanks to this, the combination of classical concepts with modern technologies provides enormous potential for the development of effective diagnostic methods that will respond to the contemporary challenges of rail transport [7, 9, 11, 36, 186, 187, 195].

The year 2050 promises to be a breakthrough in the context of implementing cutting-edge technologies and using advanced technical knowledge in the transport sector. In particular, the development of artificial intelligence (AI) technologies, automation, traffic management systems, and innovative materials and infrastructure solutions will be crucial for further improving rail transport. These technologies will increase the efficiency, safety and comfort of travel, and will provide a better integration of various modes of transport, enabling a smoother flow of goods and passengers [10, 11, 12, 13, 27, 36, 186, 187].

2. Criteria and analysis of railway traffic

To carry out the tests, a measurement method based on vision techniques will be used, and the analysis of traffic be performed using Tracker software. The following limit parameters have been adopted on Polish railways for the design of the superstructure of the track which must be characterized by appropriate strength to ensure the transfer of specific loads:

The railway superstructure should be designed to be strong enough to withstand at least the following loads:

- *vertical loads:*

- static vertical axle load force P ≥ 250 kN,
-quasi-static vertical force of the wheel: Qqst ≥ 155 kN,
measurement methods used, numerical methods,
the sum of the vertical forces of the wheel action, which are the sum of the quasi-static vertical force of the wheel action and the dynamic wheel action: ΣQ ≥ 350 kN (in exceptional situations: individual cases ΣQ ≥ 500 kN),

- *cross-bending loads:*

- quasi-static transverse force of the wheel: Yqst ≥ 60 kN,
- sum of transverse forces of the wheel action: ΣY ≥ 100 kN,

- *longitudinal loads:*

- force resulting from acceleration and braking (0.25·P; a ≤ 2.5 m/s2): Zb ≥ 60 kN/axle,
- forces arising from temperature changes (ΔT≤35 K, A60E1=7670 mm2): Ztemp = 665 kN/rail
- force generated during emergency braking: ZBEC = 360 kN/train
- total longitudinal force taking into account the forces arising from changes of temperaturę and during acceleration and braking not less than: ZΣ ≥ 1200 kN/rail.

The paper analyzes the dynamic vertical force, which plays a key role in assessing interactions between a rail vehicle and railway surface.

Another important parameter in the design and operation of railway infrastructure is the permissible axle load of wagons which affects the durability of the surface, traffic safety and transport capacity. The maximum permissible axle loads of freight wagons depend on their geometric characteristics. Based on the reference loads presented in Fig. 1, Fig. 2, Fig. 3, Fig. 4 and Fig. 5, line classes and their corresponding permissible parameters can be presented.

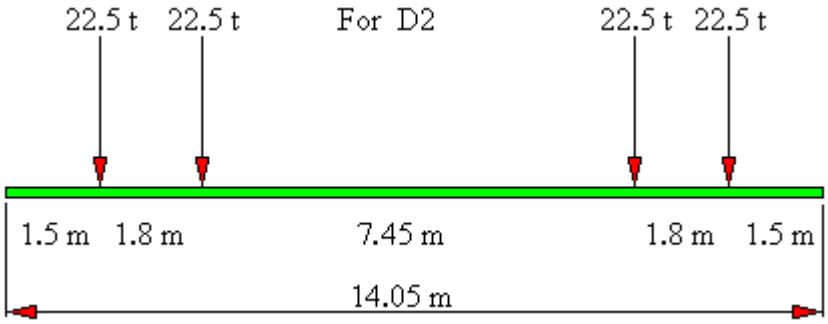

Fig. 1. Geometric characteristics of the reference load representing line class D2; axle load 221 [kN/axle] (22.5 t/axle); linear load 63 [kN/m] (6.4 t/m)

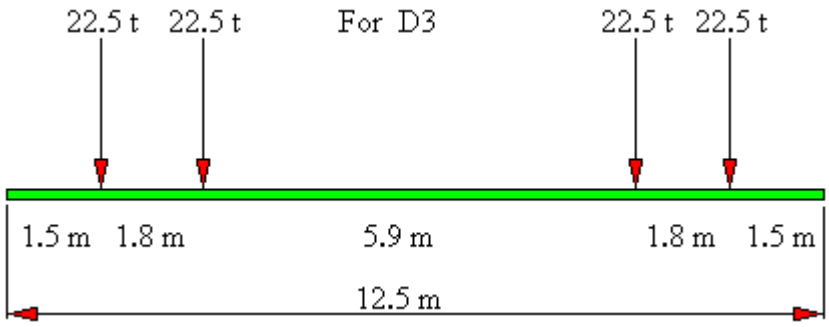

Fig. 2. Geometric characteristics of the reference load representing line class D3; axle load 221 [kN/axle] (22.5 t/axle); linear load 71 [kN/m] (7.2 t/m)

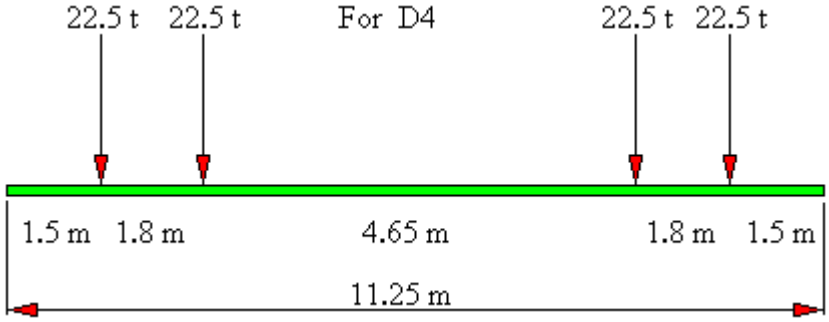

Fig. 3. Geometric characteristics of the reference load representing line class D4; axle load 221 [kN/axle] (22.5 t/axle); linear load 78 [kN/m] (8.0 t/m)

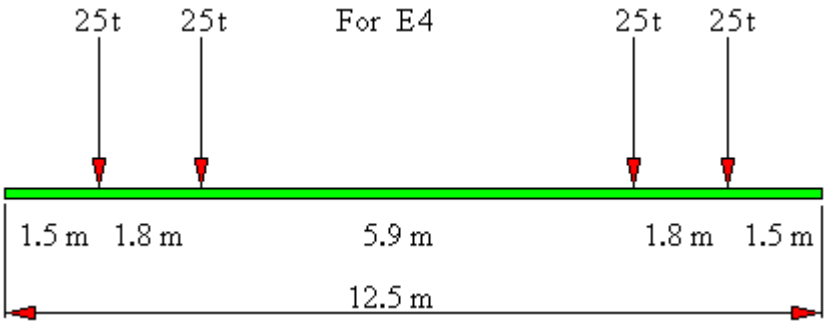

Fig. 4. Geometric characteristics of the reference load representing line class E4; axle load 245 [kN/axle] (25.0 t/axle); linear load 78 [kN/m] (8.0 t/m)

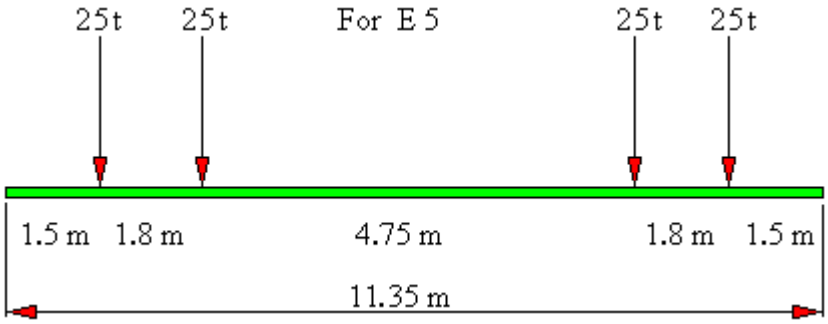

Fig. 5. Geometric characteristics of the reference load representing line class E5; axle load 245 [kN/axle] (25.0 t/axle); linear load 86 [kN/m] (8.8 t/m)

Fig. 6 shows a diagram of a railway wagon axle with the following elements specified: axle journal, wheel, wheel seat, hub and hub overhang. This diagram is helpful in analyzing the structure of the axle and its loads, taking into account the geometric and mechanical properties of individual elements. The wheel hub and wheel seat must be properly designed to withstand the dynamic loads resulting from vehicle movement. The axle journal is a key element that transfers loads to the bearings, which affects the operation of the entire running gear.

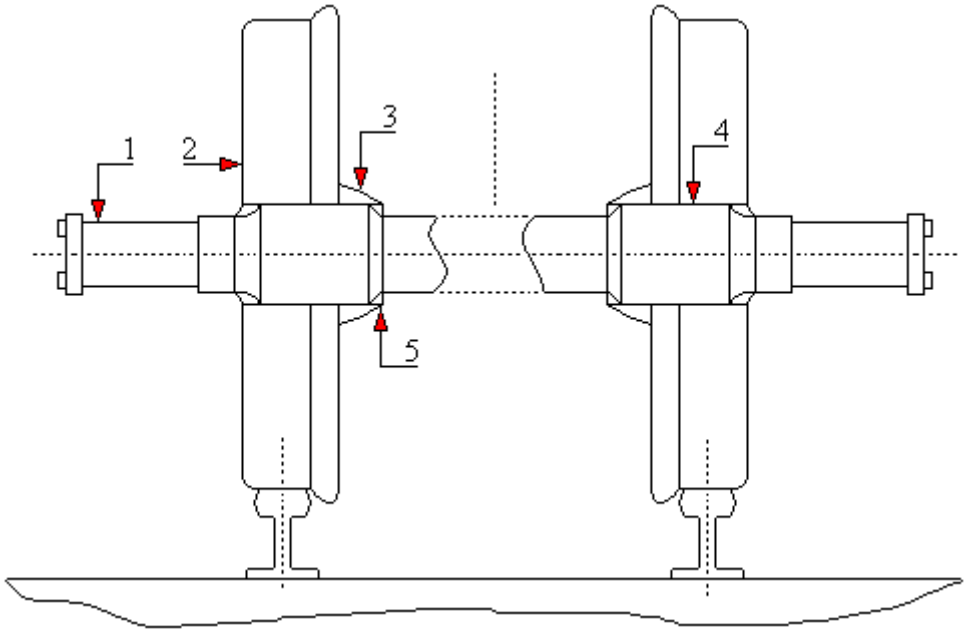

Fig. 6. Wheel set
1 – axle journal; 2 – wheel; 3 – hub; 4 – wheel seat; 5 – hub overhang

Every railway vehicle must have a Technical Condition Document *[DSU]*. This is a document that contains detailed information about the technical condition of a railway vehicle, including data on its construction, equipment, repairs, inspections and any modifications carried out. The DSU document is crucial for ensuring the safety of railway operations because it allows to have control over the technical condition of the vehicle and its compliance with standards and legal requirements.

The DSU document contains detailed information about the structure, dimensions, materials and repair history of a railway vehicle, which enables advanced analyses, construction of technical models and the optimization of design and maintenance processes.

The standard gauge of railway sleepers in Poland is 0.60 m, and the diameter of the wheels of railway rolling stock is: 920 mm, 940 mm, 960 mm, 1000 mm. The ideal theoretical wheel diameter is 956 mm. With a wheel diameter of 956 mm, a full rotation of the wheel allows to cover a distance of 3 meters. A distance of 3 meters corresponds to 5 sleepers in the track (3 m ÷ 0.60 m = 5 sleepers). This means that each wheel makes one full rotation every five sleepers, which might be important for uniform wear of wheels and rails.

Awareness of key technical information, such as sleeper spacing, wheel

dimensions and design parameters of railway vehicles, is essential for carrying out precise measurements, analyses and calculations. This data forms the foundation on which more advanced simulations and computer models are based.

With the appropriate quality of research, access to modern technologies and software, as well as financial possibilities, one can obtain very accurate and reliable results. These resources enable analyses to be performed that take into account various variables and conditions, such as dynamic loads, material wear, structural fatigue, and interactions between the vehicle and railway infrastructure.

Advanced computer models, based on data contained in documents such as DSUs, combined with reference load parameters of the railway track, make it possible to predict vehicle behavior in various conditions, which enables the optimization of the structure, improvement of safety and efficiency of the operation of rolling stock and railway infrastructure. Ultimately, well-planned studies and calculations based on solid data lead to reliable results that can significantly improve the quality of rail transport.

3. Traffic analysis with Tracker

Tracker is a free program for the analysis of video, designed for learning physics and mechanics. It allows to track the movement of objects in video recordings and perform measurements such as position, speed, acceleration and trajectory. Using a video recording, one can track the movements of track elements (rails, sleepers) during the passage of rail vehicles.

Traffic analysis with Tracker is divided into three main phases. The first phase is to prepare the equipment and determine the objects and measurement points.
The second phase is the process of image recording, downloading and calibrating it using software. The third phase is the analysis of results, graphs and their presentation.

- ***Phase 1: Preparing the equipment and establishing measurement points***

A video can be recorded using various recording devices, such as a camera built into a mobile phone, tablet, camera or high-speed digital camera. A key element of preparing a video is ensuring good visibility of the point whose movement we want to analyze. For this purpose it is necessary to ensure an appropriate background that will not distract or interfere with the visibility of the measurement point, and to clearly mark the point on the tested object. It is also important that the measured distances on the film match the actual dimensions, which requires precise calibration of the film before analysis. Fig. 7 shows marked measurement points on the rail at a distance of 2.5 m.

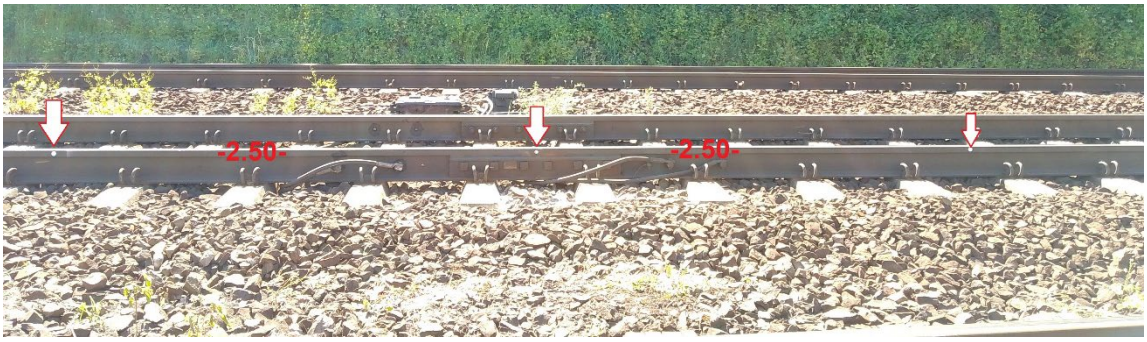

Fig. 7. Measurement base

The measurement points (Fig. 8) were permanently marked on the surface of the railway rail head using paint and a specially prepared template. This process was intended to ensure a precise and permanent marking that would remain visible throughout the experiment, regardless of atmospheric conditions or any vibrations or oscillations occurring in the environment. The paint was chosen to contrast with the rail color, making it easier to recognize both in the recording and during subsequent video analysis. The most commonly used paints are quick-drying, abrasion-resistant and resistant to external factors such as moisture and UV radiation. This makes the markings permanent and does not require re-application during the experiment.

Fig. 8. Measuring point

The image was recorded using the Hammer Energy 2 phone which is characterized by a solid construction and high resistance to mechanical damage, making it an ideal tool for work in difficult field conditions. The device was mounted on an aluminum construction tripod, which ensured stability and precision during recording. The Hammer Energy 2 phone is equipped with a camera with sufficient resolution to capture the details necessary to analyze the movement of measuring points. Thanks to the built-

in image stabilization function and the ability to manually set recording parameters (such as focus, white balance or exposure), this device allows you to obtain high-quality recordings, which are crucial for the accuracy of subsequent analysis. Additionally, this phone is waterproof and dustproof (IP68 certified), which ensures reliability in field conditions, such as near railway tracks.

The aluminum construction tripod (Fig. 9) was chosen for its durability and because it can be put stably on uneven ground. The tripod allows for height and angle adjustment, which allows precise positioning of the phone in relation to the tested object – in this case, a railway rail with marked measurement points. Fig. 9 shows the connection of the tripod and phone using a universal clamp.

Fig. 9. Aluminum tripod with a mounted phone

- ***Phase 2: The process of image recording, downloading and calibration using Trackers software***

An important element of this stage is the selection of an appropriate place to carry out measurements of the tested object. One should take into account the stability of the surface on which the camera tripod will be placed. This stability is crucial because even minimal vibrations can affect the quality of the recording and the accuracy of subsequent analysis. An ideal location is a level, paved surface near the track, from which the entire experimental scene can be captured in the camera frame.

The visibility of reference markers on the track is crucial for correct image scale calibration. These markers must be clear and clearly visible in the recording because only then it will be possible to have a precise representation of the actual distances in the image pixels. Adequate lighting and the absence of visual obstacles (e.g. shadows, vegetation) are essential for markers to be legible throughout the recording.

Before a rail vehicle passes, image recording should be started to capture both the beginning and end of the object's movement. It is important that the camera is fully stable before recording begins, which minimizes the risk of vibration interference. If you are recording with a phone or digital camera, it is worth making sure that the device is properly mounted on a tripod and that all locking mechanisms are tightened.

Transferring the recording from the camera to the computer is the next important step. This process involves connecting the device to a computer via a USB cable or using a memory card. After transferring the file, please make sure that the recording has been saved correctly and does not contain any technical errors such as missing fragments or image distortions. Converting a video file to a format supported by Tracker, e.g. MP4 or AVI is necessary if the recording was saved in another format. You can use free tools like HandBrake or VLC Media Player for this purpose. Conversion should be performed while maintaining the original image quality so as not to negatively affect the precision of the analysis. Loading the recording into Tracker allows you to start traffic analysis. Once you have imported your video file, you need to ensure that all key elements, such as metering points and reference markers, are visible in the frame throughout the recording.

Setting the scale based on the reference markers is the next step. For example, if markers are placed on the track at 2.5 meter intervals, you must define in the program how many image pixels correspond to this distance. This will make it possible to convert distances into real units. Fig. 10 shows a screenshot illustrating one of the key steps described in the analysis process. The screenshot shows the Tracker interface with the imported recording and settings made.

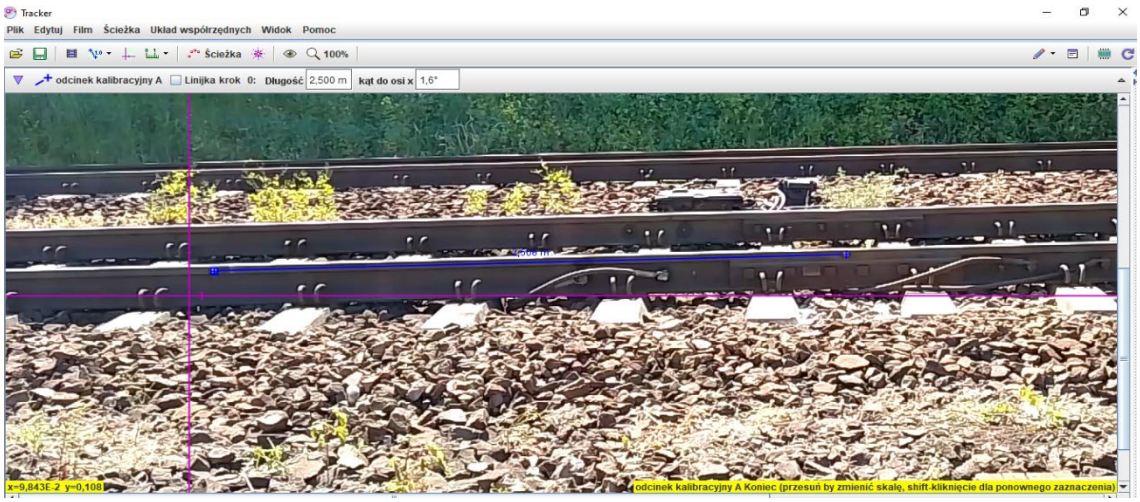

Fig. 10. Image calibration in Tracker

Defining a coordinate system in Tracker allows for a precise movement analysis. The X axis should be positioned along the track, allowing the analysis of horizontal

movement, while the Y axis should be positioned perpendicular to the track, allowing to carry out the analysis of vertical movement. The coordinate system setting must be adjusted to the camera orientation and track layout in the recording so that the analysis is consistent with real-world conditions.

The next step is tracking points which can be done manually or automatically depending on your preferences and the tools available in Tracker. Point tracking involves determining the trajectory of the object's movement which in this case is marked on the track using previously placed reference markers. Fig. 11 shows a screenshot illustrating the process of manually tracking a point in Tracker.

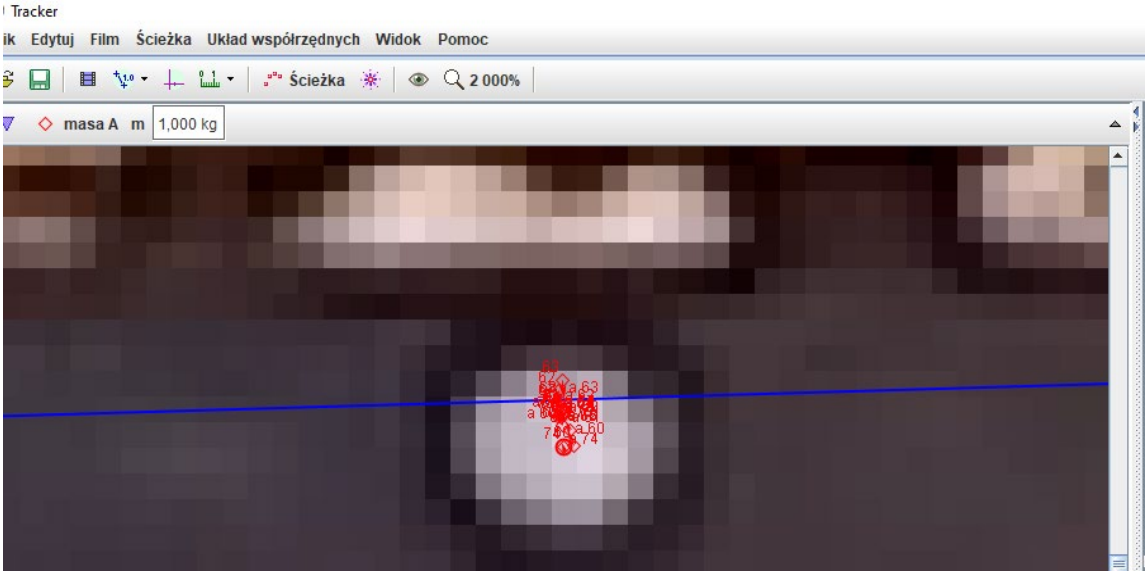

Fig. 11. Illustration of a manual tracking process in Tracker

In manual tracking, the Tracker user must manually identify and mark the position of a point in each video frame.
This process involves:

1. **Selecting a point in the image:** The user indicates places on the screen that correspond to selected measurement points (e.g. on a rail) in each video frame.
2. **Manually moving a point:** After selecting a point in one frame, Tracker automatically moves to the next frame and the user must re-select the point's position in the new image. This process repeats for each video frame.
3. **Trajectory analysis:** After selecting points in the appropriate frames, the program generates a motion trajectory, taking into account the position of the point in time.

Manual tracking is time-consuming but gives a lot of control over point selection, which is useful when measurement points are difficult to track automatically (e.g., in the case of fast motion or image noise).

Auto tracking in Tracker is the process by which the program automatically identifies and tracks selected points in each frame of the video. The program is based on algorithms that detect motion and analyze changes in the image, which allows automatic

assignment of points in subsequent video frames. Below is the sequence of actions you need to take to properly perform automatic tracking:

1. **Selecting starting points:** The user selects a point or area in the first frame to be tracked, and the program automatically identifies that point in subsequent frames.
2. **Application of the tracking algorithm:** Tracker uses algorithms such as optical flow analysis to track the movement of a point based on its visual characteristics, such as color, shape, or contrast with the background.
3. **Error correction:** If the algorithm encounters difficulties (e.g. due to changes in lighting, image noise or too fast movement), the user can manually correct the trajectory in selected frames.

Automatic tracking is faster and less time-consuming than manual tracking, but may require adjustments, especially in difficult conditions.

- ***Phase 3: Analysis of results, graphs and their presentation***

When analyzing the movement of rail vehicles on a railway track, it is crucial to present the results in the form of graphs and visualizations that enable accurate interpretation of the data and identification of potential problems with the track infrastructure.

In particular, there are three main types of charts:

1. Position vs. Time is a graph that shows changes in the object's position in space as time passes. It is one of the fundamental representations of motion in physics and dynamic analysis, especially in the context of the movement of rail vehicles on a track. In this chart:

-the horizontal axis (X) represents time (t), usually expressed in seconds (s),

-the vertical axis (Y) represents the position of the object in a given spatial axis, e.g. in the horizontal (X) or vertical (Y) direction, depending on which position is being analyzed.

In the case of railway track analysis, the position versus time graph (Fig.12) can represent changes in vehicle position along the track, which makes it possible to:

-track the vehicle's trajectory,

-identify track irregularities that may affect the vehicle's position.

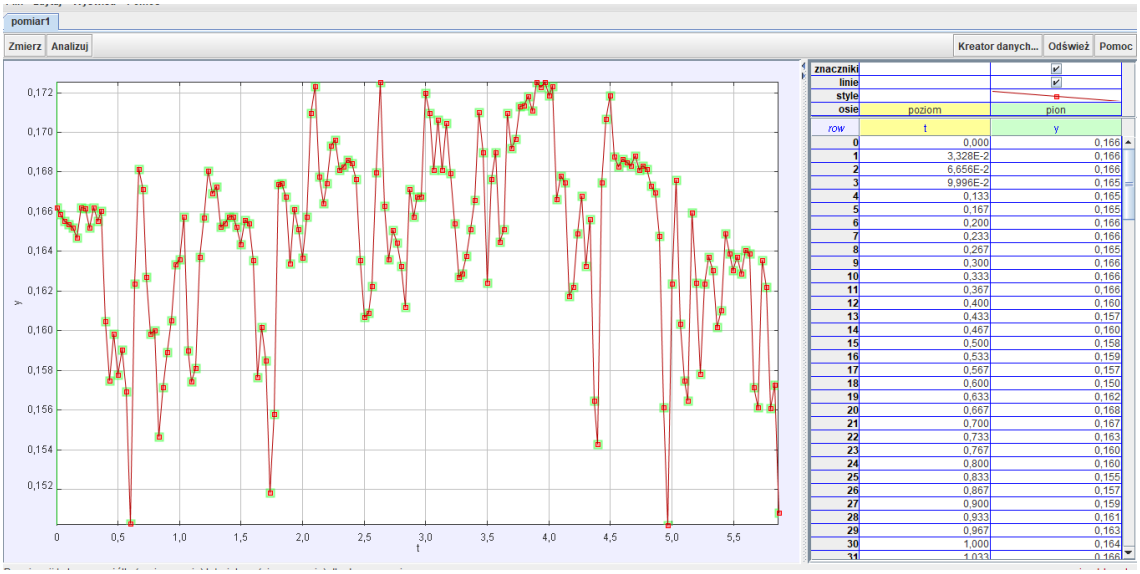

Fig. 12. Position vs.Time graph

2. Velocity vs Time is a graph (Fig.13) that shows changes in the object's velocity as time passes. This is a key relationship in traffic analysis, especially in the context of rail vehicles because it allows to conduct the assessment of traffic dynamics and the impact of various factors on its course.

In this chart:

-the horizontal axis (X) represents time (t), usually expressed in seconds (s),

-the vertical axis (Y) represents the velocity (v), expressed in speed units of meters per second (m/s).

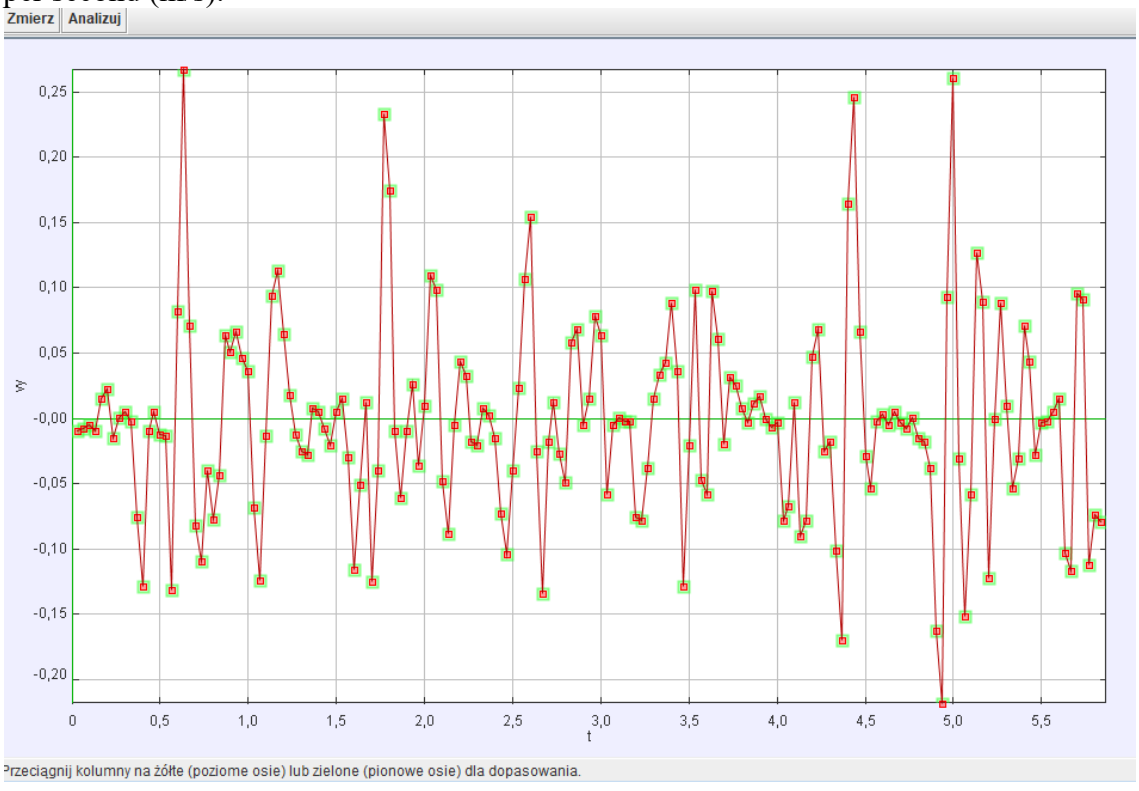

Fig. 13. Velocity vs. Time graph

3. Acceleration vs. Time is a graph (Fig.14) that shows changes in the object's acceleration as time passes. Acceleration is a measure of the change in velocity of an object per unit of time and is a key parameter in the motion analysis, especially in the context of rail vehicle dynamics. In this chart:

-the horizontal axis (X) represents time (t), usually expressed in seconds (s),

-the vertical axis (Y) represents the acceleration (a), expressed in acceleration units of meters per square second (m/s^2).

Changes in acceleration may indicate the presence of dynamic forces that affect the vehicle while in motion. An increase in acceleration may indicate sudden acceleration, which may be the result of track irregularities, such as damage to rails or railway sleepers.

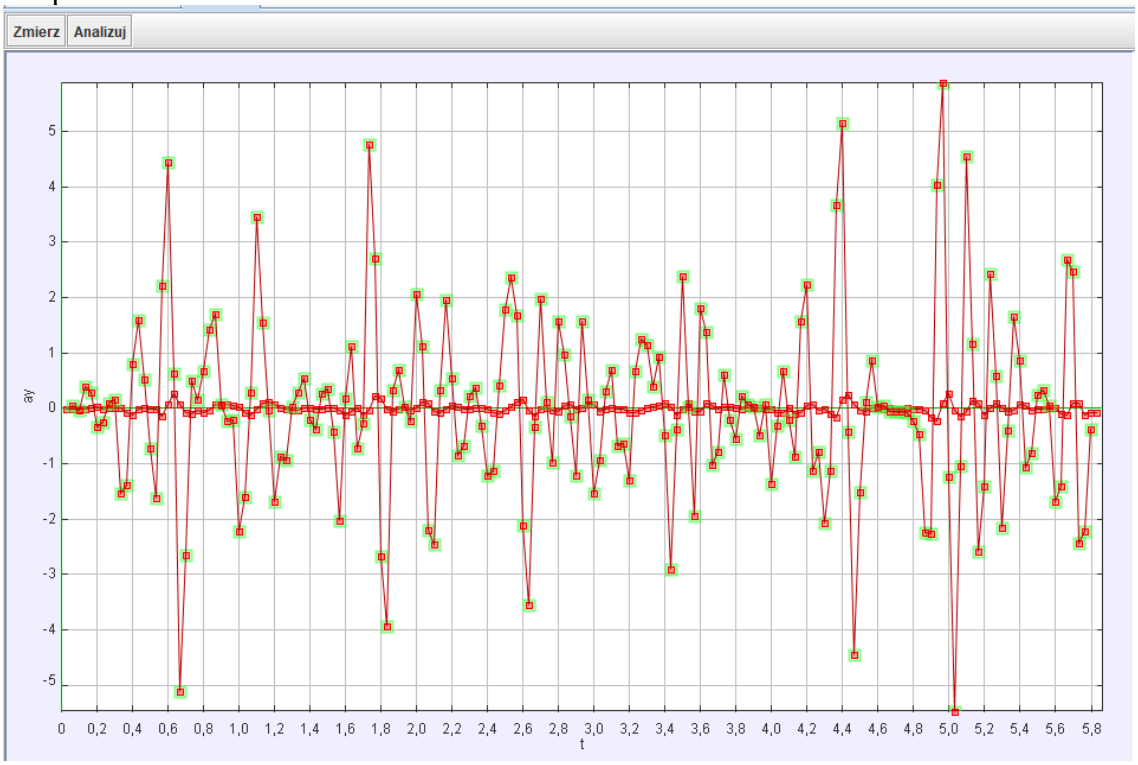

Fig. 14. Acceleration vs. Time graph

The analysis results allow to carry out the assessment of the impact of dynamic loads on the track. These loads can lead to track deformations such as rail cracks, sleeper wear, or uneven track levels. By analyzing vehicle movement it is possible to identify places where such problems occur and assess how loads affect the comfort and safety of travelling by train.

Tracker is an advanced tool for measuring and analyzing physical properties, particularly useful in scientific research, engineering, and education. In its work it focuses on three key parameters:

- position vs. time function,
- speed vs. time function,
- acceleration vs. time function.

Acceleration analysis allows us to study the dynamics of a system, the influence of resisting forces, friction and phenomena such as resonance.

Using the collected data, Tracker allows to carry out the calculation of resonance and other dynamic properties. Resonance, occurring when the excitation frequency coincides with the natural frequency of the system, leads to a sudden increase in the vibration amplitude. The analysis of position, velocity and acceleration makes it possible to:

- determine the natural frequencies of systems,
- study the effect of damping on dynamics,
- assess the stability of systems under dynamic conditions.

The Tracker program is widely used in classical mechanics, biomechanics and the analysis of advanced engineering structures. It provides a precise modeling, prediction of the behavior of dynamic systems, and optimization and diagnostics of mechanical systems.

The Tracker program enables precise dynamic analysis of railway tracks and rail vehicle movement by generating graphs of displacement, velocity and acceleration as a time function and calculating parameters such as vibration amplitude, frequency and extreme values of displacements. Its applications include comparing results for different vehicle types, assessing the effect of running speed on track dynamics, analysing track deformation caused by the passage of heavy freight trains, studying vibrations in areas with complex track geometry such as turnouts, as well as testing modern high-speed trains. The Tracker is distinguished by its low cost, precise measurements, multifunctionality and the ability to visualize results in the form of graphs and animations, which facilitates their interpretation. Thanks to these features, it is an excellent tool for research in railway engineering and education, allowing a comprehensive assessment of the dynamic parameters of the track and rail vehicles.

The human eye, one of the most advanced organs in nature, is the inspiration for many technologies, including those related to rail transport. Combining the natural ability to perceive precisely using eyes with modern technologies and engineering experience may be a key element in the development of future transport systems. The human eye not only enables us to recognize details and react quickly to changing conditions but also adapts to different lighting and traffic conditions, which is invaluable in the context of safety and comfort of travelling.

4. Author’s own testing

The tests were conducted on the basis of seven recordings of passing rail vehicles in three different locations thanks to which it was possible to obtain a diverse and representative data set. This allowed to take into account the variability of train traffic parameters in various conditions, such as the specificity of the railway infrastructure, location environment or the variety of train types.

In order to ensure confidentiality and limit the possibility of identifying the location of railway infrastructure, letter markings were used, i.e. the measurement locations were named as locations A, B and C, respectively.

The recordings and measurements were carried out in accordance with the agreed schedule and in compliance with appropriate safety measures, both in terms of protecting critical infrastructure and complying with regulations regarding work on railway premises. The collected materials are used to conduct research and analysis.

The smartphone myPhone Hammer Energy 2 Eco was used to record images during the tests and make a video recording at a speed of 30 frames per second [fbs]. This means that the time interval between subsequent frames is dt=0.033 s (1/30s). The recorded video recordings were used for traffic analysis using the Tracker program. This analysis was conducted on a computer equipped with an Intel Core i-7 3537U CPU @ 2.0 GHz, running a 64-bit operating system. The computer has 8 GB of RAM, which ensures adequate performance for processing and analyzing video data.

- ***First testing***

The test site is the bonded-prestressed joint in the track. This joint is particularly exposed to high loads because it is the place where two rails are connected by means of rail joint bars fastened with screws. For research purposes, the location of this connection was designated as site A. Rail deflection measurements were carried out under actual dynamic load resulting from the passage of a railway vehicle.

- ***Second testing***

Location marked B is a straight section of track that is characterized by uniform mechanical properties.

- ***Third testing***

Location marked C is another straight section of track where rail deflection measurements were taken. Unlike locations A and B, the tests at location C were aimed at assessing rail deflection under conditions slightly different from location B (taking into account the different degree of wear of the track fastening elements).

- ***Fourth testing***

The fourth test was carried out again at location B, i.e. on a straight section of the track. Unlike previous tests that analyzed rail deflection under the influence of vehicles passing at a certain speed, in this case the focus was on the effect of the transition from static to dynamic load (a train was recorded at a standstill, which then started moving after some time).

- ***Fifth testing***

The fifth test was carried out again at location B, i.e. on a straight section of the track. This was the third test at this location.

- ***Sixth testing***

The sixth test was also conducted at location B. Thanks to carrying out the next measurement it was possible to more accurately track trends in rail deflection during the passage of the same type of train.

- ***Seventh testing***

The seventh test was carried out again at location B, i.e. on the straight section of track where the previous fourth, fifth and sixth tests were also carried out. The aim of the next measurement was to check the repeatability of results for the same type of railway vehicle.

5. Analysis of results

The tests were carried out at three different track locations: A, B and C. At each of these locations changes in rail deflection were recorded during the passage of railway vehicles. The Tracker program was used to analyze the results, which enabled the calculation of the rail deflection value in [mm] and the speed of passing trains. The measurements allowed the identification of differences in track reactions at individual locations. The fastest speed was recorded during test No. 3, which indicates the highest dynamics of train movement in this series of measurements. In test No. 4, the train initially remained stationary and was then recorded at the moment of starting, which allowed to conduct the analysis of the transition from static to dynamic load.

Data analysis allowed to assess the dynamics of rail vehicles movement and their impact on rail deflection in various operating conditions, as well as to compare differences between individual locations. Particular attention was paid to comparing the results from individual locations:

- ***Location A*** – covers the bonded-prestressed joint in the track which is particularly exposed to high loads and may show higher deflection values,
- ***Location B*** – a straight section of track where several tests were carried out, including measurements of rail deflection at different train speeds and analysis of the effect of transition from static to dynamic load (in the fourth test, where the train first stood still and then moved),
- ***Location C*** – is also located on a straight section of track, which allows comparison of rail deflection values under different operating conditions.

The highest speed was measured in Test No. 3, which resulted in a rail deflection of 5 mm. The highest maximum rail deflection was recorded in test No. 1, which may be due to the location of the bonded-prestressed joint. The highest average rail deflection occurs in test No. 4, which may be the result of the transition from static to dynamic load. The initial moment of starting the train causes an uneven distribution of forces on the rail. Test No. 2, No. 5, No. 6 and No. 7 concern the same type of light train, which may explain having similar rail deflection values in these cases. The light weight of the train means less stress on the track and, consequently, limited rail deflection. Table 1 presents the test results.

Table 1. Summary of test results

Test No.	Location	Maximum rail deflection [mm]	Average rail deflection [mm]	Train speed [km/h]
1	A	18	2	91
2	B	9	3	34
3	C	5	2	132
4	B	2	7	0→25
5	B	3	0	38
6	B	6	0	38
7	B	3	0	38

6. Conclusion

Based on the conducted tests, the following conclusions can be drawn:

- The railway track bends under the influence of a passing railway vehicle. The amount of deflection is a key indicator of the technical condition of the track and track bed.
- An increased track deflection value indicates a deteriorating technical condition of the track and track bed. This may be the result of degradation of construction materials, weakening of the track bed structure or excessive wear of the rails or sleepers.
- Greater track deflection can be observed at critical track connections such as bonded-prestressed rail joints, rail joint bar connections, or turnouts.
- When designing railway vehicles, their basic parameters must be adapted to the characteristics of the railway track. In particular, it is important to take into account the wheelset gauge of the pivot pins and car wheelset gauge. Adjusting these parameters to multiples of the railway sleeper spacing will minimize dynamic impacts and increase the durability of the track infrastructure.
- The radius and size of railway wheels should be adjusted to the gauge of railway sleepers in order to reduce the polygonization of rolling stock wheels, improve the uniformity of pressure on rails and increase the durability of both the wheels and the track.
- Conduct research focusing on modeling dynamic interactions between vehicles and tracks, analyzing wheel-rail contact geometry, and monitoring long-term infrastructure wear to optimize its durability and safety. Using numerical methods, and processing large data sets with results visualization, it is possible to precisely diagnose the technical condition of tracks and vehicles.
- In Poland, testing should be initiated of using additional damping in concrete sleepers using rubber mats stuck to their bottom. This solution effectively reduces the dynamic forces transmitted to the track bed, which contributes to increasing the durability of the infrastructure, reducing noise and vibrations, as well as improving the comfort of train travel and operational safety.
- Research and technological trials should be initiated on applying a Nikasil coating to the rail head in order to strengthen its surface. This type of rails can be used in areas particularly exposed to wear, such as tight curves, areas near

platforms or sections before railway signals, which will extend their service life and reduce maintenance costs.

- The use of visual testing technologies in railway infrastructure should be widespread and standardized. These systems enable automatic monitoring of the condition of tracks, rails, turnouts and other infrastructure elements, which increases the efficiency of diagnostics, enables faster detection of defects and contributes to improved safety and optimized maintenance costs.

7. Literature

1. Bałuch H.: Odkształcenia trwałe rozjazdów w profilu na tle odkształceń torów. *Przegląd Kolejowy Drogowy*, 1970, Nr 8.
2. Bałuch H.: Zróżnicowanie odkształceń sprężystych nawierzchni S-60. Przegląd Kolejowy Drogowy, 1973, Nr 20.
3. Bałuch H.: Diagnostyka nawierzchni kolejowej. Wydawnictwa Komunikacyjne i Łączności, Warszawa, 1978.
4. Bałuch H.: Rozkłady naprężeń mierzonych w stopkach szyn i ich wpływ na obliczenia naprężeń maksymalnych. *Drogi Kolejowe*, 1979, Nr 10.
5. Bałuch H.: Doskonalenie napraw nawierzchni i zasad utrzymania dróg kolejowych w świetle ostatnich badań naukowych. *Drogi Kolejowe*, 1987, Nr 6.
6. Bałuch H. i inni: Metoda oceny stanu toru i planowania napraw powierzchni na podstawie wyników pomiarów drezyny EM-120. Prace CNTK, Nr 32, 14/12, Warszawa 1988.
7. Basiewicz T.: O strukturze tzw. współczynnika dynamicznego szybkości nawierzchni kolejowej. *Przegląd Drogowy*, 1967.
8. Basiewicz T.: Nawierzchnia kolejowa z podkładami betonowymi. Wydawnictwa Komunikacyjne i Łączności, Warszawa, 1969.
9. Basiewicz T., Bałuch H. i inni: Przystosowanie kolei do zwiększonych szybkości i dużych przewozów. Wydawnictwa Komunikacyjne i Łączności, Warszawa, 1969.
10. Bogdaniuk B.: Badania nierówności powierzchni tocznej szyn. *Drogi Kolejowe*, 1981r., Nr 5-6.
11. Bednarek W.: Analiza wpływu współczynników sprężystego podłoża dwuparametrowego na ugięcie podkładu kolejowego. Zeszyty Naukowo-Techniczne STTK RP, Oddział w Krakowie, Nr 2 (101), Kraków, 2013.
12. Bukowski M., Gradkowski K.: Dodatkowe obciążenia podtorza od mikrogeometrycznych nierówności podłużnych toru. *Drogi Kolejowe*, 1987, Nr 4-5.
13. Ciesielski R.: Ocena szkodliwości wpływów dynamicznych w budownictwie. Wydawnictwo Arkady, Warszawa, 1973.
14. Czyczuła W.: Możliwości przeprowadzenia przyspieszonej stabilizacji podsypki. *Drogi Kolejowe*, 1989, Nr 9.
15. Czyczuła W., Sromicki K., Ptak T.: Ocena możliwości wykorzystania pomiarów wskaźnika spokojności biegu pociągów do badania stanu toru. *Drogi Kolejowe*, 1988, Nr 3.
16. Czyczuła W.: Eksploatacyjna stabilność drogi kolejowej. Monografia 126. Zakład Graficzny Politechniki Krakowskiej im. Tadeusza Kościuszki, Kraków, 1992.
17. Dobrowolski Z.: Podręcznik spawalnictwa. Wydawnictwo WNT, Warszawa 1978.
18. Friszman M. A.: Tor kolejowy i jego współpraca z pojazdami. Wydawnictwa Komunikacyjne i Łączności, Warszawa, 1983.

19. Gryczmański M., Kłosek K., Sękowski J.: Efektywne metody wzmocnienia podtorza kolejowego na terenach górniczych. *Drogi Kolejowe*, 1987, Nr 12.
25. Jędrzejczyk D., Mikołajczyk J.: Defining the correlation between the cutting speed and roughness parameter Rz. **W:** MIK-21 : Międzynarodowa Innowacyjność i Konkurencyjność w XXI wieku : aspekty innowacyjne / redakcja naukowa Radosław Luft. Lublin : Fundacja Innowacji i Nowoczesnych Technologii INOTECH, 2022. Radom : nakładem Instytutu Naukowo-Wydawniczego "Spatium", 2022; s. 39-46, p-ISBN: 978-83-67033-43-5; e-ISBN: 978-83-67033-44-2; **http://inw-spatium.pl/wp-content/uploads/2022/09/MIK-21-2022-Aspekty-innowacyjne-2.pdf**
26. Jeske T., Przedecki T., Rosiński B.: Mechanika gruntów. Państwowe Wydawnictwa Naukowe, Warszawa, 1966.
27. Kanis J., Urda J.: Socio-Economic Benefits of the Project Diagnostic Vehicle for Rail Defectoscopy in the Slovak Republic. ISSN 2352-1465, Year 2024.
28. Kisiel F., Dmitruk S., Lysik B.: Zarys reologii gruntów. Wydawnictwo Arkady, Warszawa, 1969.
29. Kisilowski J. i inni: Modelowanie i analiza dynamiki układu mechanicznego tor-pojazd. Państwowe Wydawnictwa Naukowe, Warszawa, 1982.
30. Latoś H., Mikołajczyk J.: Effect of partial wear of the tool point on the selected indicator of the machining process. **W:** Logistyka w ratownictwie 2023 / pod redakcją Andrzeja Chudzikiewicza i Anny Stelmach. Radom: Instytut Naukowo-Wydawniczy "Spatium", 2023, Poland; s. 195-210, p-ISBN: 978-83-67033-95-4; e-ISBN: 978-83-67033-96-1.
31. Latoś H., Mikołajczyk J.: Thickness of the machined layer at milling with single-edge straight blades with an angle of $\lambda s \neq 0°$. **W:** MIK-21 : Międzynarodowa Innowacyjność i Konkurencyjność w XXI wieku : Aspekty innowacyjne / redakcja naukowa dr Łukasz Wojtowicz. Lublin: Fundacja Innowacji i Nowoczesnych Technologii INOTECH : nakładem Instytutu Naukowo-Wydawniczego "Spatium", 2023, Poland; s. 23-27, p-ISBN: 978-83-67033-89-3; e-ISBN: 978-83-67033-90-9.
32. Latoś H., Mikołajczyk J., Konarski J., Mikołajczyk T.: Turning using self-induced vibration. **W:** MIK-21 : Międzynarodowa Innowacyjność i Konkurencyjność w XXI wieku : aspekty innowacyjne / redakcja naukowa dr Łukasz Wojtowicz, 2023, Poland; s. 187-200, p-ISBN: 978-83-67033-89-3; e-ISBN: 978-83-67033-90-9.
33. Latoś H., Mikołajczyk J.: Vibration in machining. **W:** Logistyka w ratownictwie 2023 / pod redakcją Andrzeja Chudzikiewicza i Anny Stelmach. Radom: Instytut Naukowo-Wydawniczy "Spatium", 2023, Poland; s. 187-194, p-ISBN: 978-83-67033-95-4; e-ISBN: 978-83-67033-96-1
34. Latoś H., Mikołajczyk J.: The effect of feed rate on the roughness of machined surface. **W:** Szkoła Logistyki 2024 / redakcja naukowa Janusz Zawiła-Niedźwiecki, Adam Płaczek. Radom: Instytut Naukowo-Wydawniczy "Spatium", 2024, Poland; s. 217-226, p-ISBN: 978-83-68026-07-8; e-ISBN: 978-83-68026-08-5.
35. Makowski J.: Wzmocnienie torowiska linii kolejowych przeznaczonych do jazdy z duża szybkością. Problemy Kolejnictwa, 1977, Wydawnictwo Komunikacyjne i Łączności, Warszawa.
36. Megna G., Bracciali A., Mandal N.: Design, wheel-rail interaction and testing of an innovative reinforced smooth transition insulated rail joint. ISSN 0043-1648, Year 2023.
38. Mikołajczyk J.: Wpływ dodatków smarowych na transformację warstwy wierzchniej. Piła : Wydawnictwo Państwowej Wyższej Szkoły Zawodowej im.

Stanisława Staszica, 2017r., Poland. 215, [1] s., p-ISBN: 978-83-62617-76-0; www.ans.pila.pl
39. Mikołajczyk J.: Analiza statystyczna zmiany poboru mocy podczas procesu zużywania. Statistical analysis of the power variation of tribotester as a resultat of the wear process. Autobusy. Technika, Eksploatacja, Systemy Transportowe; 2019, nr 10-11, s. 83-88, p-ISSN: 1509-5878; e-ISSN: 2450-7725;
http://yadda.icm.edu.pl/yadda/element/bwmeta1.element.baztech-21189602-884a-4d1a-bb60-9edaeae4af8d
40. Mikołajczyk J.: Influence of consumables on the amount of power consumption of kinematic vapor of conformal contact. Wpływ PE na pobór mocy pary kinematycznej o styku konforemnym. Postępy w Inżynierii Mechanicznej [Developments in Mechanical Engineering]; 2019, nr 13 (7), s. 39-50, p-ISSN: 2300-3383; Wydawnictwa Uczelniane Uniwersytetu technologiczno-Przyrodniczego im. J. J. Śniadeckich w Bydgoszczy, Poland.
http://yadda.icm.edu.pl/baztech/element/bwmeta1.element.baztech-2faf200b-3010-4192-9fd0-062f53b49d38
41. Mikołajczyk J.: Statistical analysis of the mass variation of samples as a result of the wear process. Analiza statystyczna zmiany masy próbek w wyniku procesu zużywania. Postępy w Inżynierii Mechanicznej [Developments in Mechanical Engineering]; 2019, nr 13 (7), s. 51-61, p-ISSN: 2300-3383; Wydawnictwa Uczelniane Uniwersytetu Technologiczno-Przyrodniczego im. J. J. Śniadeckich w Bydgoszczy, Poland.
http://yadda.icm.edu.pl/baztech/element/bwmeta1.element.baztech-2faf200b-3010-4192-9fd0-062f53b49d38
42. Mikołajczyk J.: Tribotestery : budowa i przeznaczenie. Piła: Wydawnictwo Państwowej Wyższej Szkoły Zawodowej im. Stanisława Staszica, 2019, Poland; 160 s., e-ISBN: 978-83-62617-90-6;
https://wydawnictwo.pwsz.pila.pl/files/Tribotestery.pdf
43. Mikołajczyk J.: Determining the energy validity of the Kostetsky's hypothesis on the basis of models for relative motion velocity v = 0.08 m/sec. Developments in Mechanical Engineering; 2020, nr 16 (8), s. 17-29, p-ISSN: 2720-0639; Wydawnictwa Uczelniane Uniwersytetu Technologiczno-Przyrodniczego im. J. J. Śniadeckich w Bydgoszczy, Poland.
DOI: 10.37660/dme.2020.16.8.2
44. Mikołajczyk J.: Finding the correlation between wear of samples kinematic pair of conformal contact and electric power consumption. Postępy w Inżynierii Mechanicznej [Developments in Mechanical Engineering]; 2020, nr 15 (8), s. 59-68, p-ISSN: 2300-3383; Wydawnictwa Uczelniane Uniwersytetu Technologiczno-Przyrodniczego im. J. J. Śniadeckich w Bydgoszczy, Poland.
https://dme.utp.edu.pl/art/15(8)2020/59.pdf
DOI: 10.37660/dme.2020.15.8.6
45. Mikołajczyk J.: The effect of temperature lag on the value of power-temperature correlation for frictional pair of conformal contact. Postępy w Inżynierii Mechanicznej [Developments in Mechanical Engineering]; 2020, nr 15 (8), s. 79-86, p-ISSN: 2300-3383; Wydawnictwa Uczelniane Uniwersytetu Technologiczno-Przyrodniczego im. J. J. Śniadeckich w Bydgoszczy, Poland.
https://dme.utp.edu.pl/art/15(8)2020/79.pdf
DOI: 10.37660/dme.2020.15.8.8
46. Mikołajczyk J.: Określenie na podstawie modeli zmiany masy próbek w wyniku procesu zużywania. **W:** Szkoła Logistyki 2021 / redakcja naukowa Janusz Zawiła-

Niedźwiecki, Piotr Korneta. Radom : Instytut Naukowo-Wydawniczy "Spatium", 2021; s. 167-174, Poland; p-ISBN: 978-83-66550-75-9;
e-ISBN: 978-83-66550-89-6.
47. Mikołajczyk J.: A method of determining mathematical models of a seizure test of friction pairs. **W:** MIK-21 : Międzynarodowa Innowacyjność i Konkurencyjność w XXI wieku : aspekty innowacyjne / redakcja naukowa Radoslaw Luft. Lublin : Fundacja Innowacji i Nowoczesnych Technologii INOTECH, 2022. Radom : nakładem Instytutu Naukowo-Wydawniczego "Spatium", 2022; s. 7-24, p-ISBN: 978-83-67033-43-5;
e-ISBN: 978-83-67033-44-2.
http://inw-spatium.pl/wp-content/uploads/2022/09/MIK-21-2022-Aspekty-innowacyjne-2.pdf
48. Mikołajczyk J.: Friction machines. Piła: Wydawnictwo Akademii Nauk Stosowanych im. Stanisława Staszica, 2022, Poland; 488 s.,
e-ISBN: 978-83-62617-96-8.
https://wydawnictwo.ans.pila.pl/files/FRICTION_MACHINES.pdf
49. Mikołajczyk J., Jędrzejczyk D.: Określenie korelacji między prędkością skrawania a parametrem chropowatości Ra. Obróbka Metalu; 2022, nr 3, s. 11-15, p-ISSN: 2081-7002; **https://obrobkametalu.tech/**
50. Mikołajczyk J.: Determination of the modified coefficient of variation from the number of samples. **W:** MIK-21 : Międzynarodowa Innowacyjność i Konkurencyjność w XXI wieku : Aspekty innowacyjne / redakcja naukowa dr Łukasz Wojtowicz. Lublin: Fundacja Innowacji i Nowoczesnych Technologii INOTECH : nakładem Instytutu Naukowo-Wydawniczego "Spatium", 2023, Poland; s. 111-122,
p-ISBN: 978-83-67033-89-3; e-ISBN: 978-83-67033-90-9.
51. Mikołajczyk J.: Effect of cutting speed on the shape of the machined surface profile. Mebutra; 2023, nr 1, s. 47-63, Wydawnictwo Akademii Nauk Stosowanych im. S. Staszica w Pile, Piła 2023, Poland.
https://online.fliphtml5.com/vliuj/yunw/ p=48
52. Mikołajczyk J.: Friction Machines II. Piła: Wydawnictwo Akademii Nauk Stosowanych im. Stanisława Staszica w Pile, 2023, Poland; 598 s.,
p-ISBN: 978-83-67684-00-2;
https://wydawnictwo.ans.pila.pl/files/FRICTION_MACHINES_V_ANS_PILA.pdf
53. Mikołajczyk J.: Temperature as a parameter for assessing the work of a friction pair. **W:** Szkoła Logistyki 2023 / redakcja naukowa Janusz Zawiła-Niedźwiecki, Katarzyna Białczak. Radom: Instytut Naukowo-Wydawniczy "Spatium", 2023, Poland; s. 101-107, p-ISBN: 978-83-67033-75-6; e-ISBN: 978-83-67033-58-9.
54. Mikołajczyk J.: A method of determining mathematical models of a seizure test of friction pairs. **W:** MIK-21 : Międzynarodowa Innowacyjność i Konkurencyjność w XXI wieku : aspekty innowacyjne / redakcja naukowa Radoslaw Luft. Lublin : Fundacja Innowacji i Nowoczesnych Technologii INOTECH, 2022. Radom : nakładem Instytutu Naukowo-Wydawniczego "Spatium", 2022; s. 7-24, p-ISBN: 978-83-67033-43-5;
e-ISBN: 978-83-67033-44-2.
http://inw-spatium.pl/wp-content/uploads/2022/09/MIK-21-2022-Aspekty-innowacyjne-2.pdf
186. Recko J.: Wpływ zmian parametrów geometryczno-konstrukcyjnych toru na wielkość oddziaływań pojazdu szynowego. *Drogi Kolejowe*, 1987, Nr 3.
187. Ruta P.: Drgania belki na inercyjnym podłożu sprężystym obciążonej siłą ruchomą. Rozprawy inżynierskie, 1987, t. 35, z. 1.
188. Syrek S., Mikołajczyk J.: Analiza matematyczna podstawowych wymiarów złącza spawanego. **W:** Logistyka w ratownictwie 2022 / pod redakcją Andrzeja

Chudzikiewicza i Andrzeja Krzyszkowskiego. Radom : Instytut Naukowo-Wydawniczy "Spatium", 2022; s. 169-190, p-ISBN: 978-83-67033-57-2;
e-ISBN: 978-83-67033-70-1.
189. Syrek S., Mikołajczyk J.: Modele liniowe wpływu częstotliwości prądu spawania na grubość spoiny. **W:** MIK-21 : Międzynarodowa Innowacyjność i Konkurencyjność w XXI wieku : aspekty innowacyjne / redakcja naukowa Radosław Luft. Lublin: Fundacja Innowacji i Nowoczesnych Technologii INOTECH, 2022. Radom : nakładem Instytutu Naukowo-Wydawniczego "Spatium", 2022; s. 153-170,
p-ISBN: 978-83-67033-43-5; e-ISBN: 978-83-67033-44-2;
http://inw-spatium.pl/wp-content/uploads/2022/09/MIK-21-2022-Aspekty-innowacyjne-2.pdf
190. Syrek S., Mikołajczyk J.: Modele liniowe wpływu częstotliwości prądu spawania na szerokość spoiny. Obróbka Metalu; 2022, nr 4, s. 24-31, p-ISSN: 2081-7002; **https://obrobkametalu.tech/**
192. Semrau A.: Syntetyczna ocena utrzymania torów dla potrzeb planowania napraw nawierzchni. Problemy Kolejnictwa, z. 75, Wydawnictwo Komunikacyjne i Łączności, Warszawa, 1977.
193. Siewczyński L.: Zagadnienia współpracy nawierzchni kolejowej z podtorzem gruntowym. Politechnika Poznańska, Seria Rozprawy, Nr 66, Poznań, 1974.
194. Sokolov S. I. i inni: Badania dynamiki i wytrzymałości wagonów pasażerskich. Wydawnictwa Komunikacyjne i Łączności, Warszawa, 1983.
195. Szczepański W.: Stany graniczne i kinematyka ośrodków sypkich. Państwowe Wydawnictwa Naukowe, Warszawa, 1974.
196. Sysak J.: Podtorze a modernizacja dróg żelaznych. Wydawnictwo Poznańskiego Towarzystwa Przyjaciół Nauk, Wydział V – Nauk Technicznych, Poznań 1969, Tom I, Zeszyt 5.
197. Towpik K.: Badania zmienności charakterystyk nawierzchni kolejowej ze szczególnym uwzględnieniem wpływu działania maszyn torowych. Wydawnictwo Politechniki Poznańskiej, Seria Rozprawy, Nr 137, Poznań, 1982.
198. Zandecki R., Kmita C., Mikołajczyk J.: Mathematical models of the surface layer microhardness for a selected grade of ion nitrided steel. **W:** Szkoła Logistyki 2022. Radom : Instytut Naukowo-Wydawniczy "Spatium", 2022, Poland; s. 203-216, Materiały z IX Konferencji Naukowej "Szkoła Logistyki 2022";
p-ISBN: 978-83-67033-33-6; e-ISBN: 978-83-67033-34-3.

The impact of ergonomic directional modules on reducing stress and improving safety among drivers with laterality disorders

dr inż. Piotr STANOWSKI
Department of Transport
Stanisław Staszic State University of Applied Sciences in Piła, Poland
https://orcid.org/0000-0003-3776-7427
corresponding e-mail: pstanowski@ans.pila.pl

inż. Natalia NIEMIEC
Department of Transport
Stanisław Staszic State University of Applied Sciences in Piła, Poland
https://orcid.org/0009-0000-0758-3833

inż. Bartosz GRYKA
Department of Transport
Stanisław Staszic State University of Applied Sciences in Piła, Poland
https://orcid.org/0009-0003-2075-0095

Gustaw STANOWSKI
Department of Mechanical Engineering
Stanisław Staszic State University of Applied Sciences in Piła, Poland
https://orcid.org/0009-0005-2207-6932

Streszczenie

Dezorientacja w rozróżnianiu strony prawej i lewej (LRI - Left-Right Identification) to realny w stresujących warunkach jazdy istotny problem bezpieczeństwa ruchu drogowego, mogący prowadzić do błędnych manewrów i wypadków [2, 6]. W odpowiedzi na to wyzwanie, opracowano ergonomiczne moduły kierunkowe (znaczniki "L" i "R") montowane na słupkach "A" pojazdu. Niniejsze badanie miało na celu ocenę skuteczności tego rozwiązania w redukcji stresu i poprawie bezpieczeństwa. Metodyka obejmowała badanie ankietowe na reprezentatywnej próbie 400 kierowców (uczących się i początkujących), dobranej techniką losowego doboru warstwowego na podstawie danych Centralnej Ewidencji Pojazdów i Kierowców (CEPiK) z lat 2022-2024 [14]. Kluczowe wyniki wykazały, że 53,8% respondentów (215 osób) skorzystało zasadniczo z zamontowanych modułów, co potwierdza główną hipotezę badawczą o ich skuteczności podczas radzenia sobie w stresujących

sytuacjach [4, 7]. Analiza statystyczna (test χ^2) nie wykazała istotnych różnic w występowaniu problemu LRI między płciami ($\chi^2 = 0{,}84$, df = 1, $p > 0{,}05$). Dodatkowo, innowacyjność rozwiązania polega na nieinwazyjnym montażu i optymalnej ergonomii znaczników [5, 8]. Wnioski wskazują, że proponowane rozwiązanie jest skutecznym narzędziem redukującym stres i zwiększającym bezpieczeństwo w ruchu drogowym u osób z zaburzeniami lateralizacji, jednocześnie wyznaczając kierunek dla dalszych badań nad zintegrowanymi systemami wspomagania [6, 8].

Słowa kluczowe: dezorientacja prawo-lewo, moduły kierunkowe, bezpieczeństwo ruchu drogowego, zaburzenia lateralizacji, stres kierowcy, badanie ankietowe.

Abstract

Disorientation in distinguishing left from right (LRI - Left-Right Identification) under stressful driving conditions constitutes a significant road safety problem, potentially leading to erroneous maneuvers and accidents. In response to this challenge, ergonomic directional modules (markers "L" and "R") mounted on vehicle "A" pillars were developed. This study aimed at evaluating the effectiveness of this solution in reducing stress and improving safety. The methodology involved a survey conducted on a representative sample of 400 drivers (trainees and beginners), selected using stratified random sampling based on data from the Central Vehicle and Driver Registration Database (CEPiK) from 2022-2024. Key results showed that 53.8% of respondents (215 individuals) utilized the installed modules, confirming the main research hypothesis regarding their effectiveness in coping with stressful situations. Statistical analysis (χ^2 test) showed no significant differences in LRI occurrence between genders ($\chi^2 = 0.84$, df = 1, $p > 0.05$). Additionally, the innovation of the solution lies in its non-invasive mounting and optimal ergonomics of the markers. The conclusions indicate that the proposed solution is an effective tool for reducing stress and enhancing road safety among individuals with laterality disorders, while also setting a direction for further research on integrated assistance systems.

Keywords: left-right disorientation, directional modules, road safety, laterality disorders, driver stress, survey study.

1. Introduction

Ensuring road safety remains a key social challenge. One of the often overlooked risk factors is the difficulty in quickly and correctly distinguishing between the right and left side, especially in situations requiring an immediate decision [2, 6]. This problem, related to laterality disorders, may lead to incorrect maneuvers, collisions or accidents [4, 6]. The impulse to conduct the study was direct observation of this phenomenon among drivers, indicating an urgent need to develop practical support.

The subject of the issue is a comprehensive analysis of the impact of using ergonomic driving direction markings on road safety, with particular emphasis on special right-left markings in vehicles. The main goal is to investigate the influence of laterality disorders on the frequency of the problem with distinguishing sides in novice drivers in real traffic conditions and to develop and analyze the effectiveness of the proposed solution in the form of directional modules [5, 7].

The following hypotheses were formulated:

- **The main hypothesis** assumes that the installation of directional modules significantly helped the tested drivers to cope with a stressful situation resulting from incorrect recognition of the right and left side while driving a vehicle [4, 5].

- **H1 Hypothesis** suggests that the failure to distinguish between the sides causes stress more often in women than in men [7, 8].

- **H2 Hypothesis** indicates that the stress associated with the lack of ability to distinguish between left and right direction is correlated with the reluctance to drive in the future [6, 8].

- **H3 Hypothesis** asserts that the problem is particularly common among people aged 18-25 in whom the laterality process may not be fully completed and driving experience is limited [2, 3].

- **H4 Hypothesis** states that the problem is not related to gender and affects women and men to a similar extent [1, 6].

2. Literature review (analysis of laterality disorders)

Laterality is defined as a functional asymmetry or the tendency of certain cognitive processes to be dominated by one hemisphere of the brain over the other [4, 5]. The literature on the subject also uses terms such as "asymmetry" or "functional dominance." There are three types of laterality: homogeneous (the side of the body corresponding to the dominant hemisphere), heterogeneous (crossed), and weak [6].

The sources of laterality disorders have a neurobiological basis. Gender is one of the key factors, with studies indicating significant differences in functional brain asymmetry between the sexes [2, 8]. Developing a functional advantage on one side of the body is a gradual process, and early diagnosis is crucial to minimize the consequences in later life [1, 3]. Dysfunctions of brain centers, especially the right hemisphere, may lead to disturbances in spatial awareness and disorientation, manifested by, among others, hemispheric neglect and difficulties in localizing sounds [7, 9].

In the context of road traffic safety (RTD), problems with identifying the left and right side are not uncommon in the healthy population; it is estimated that 14.6% of people report insufficient skills in this area [10]. During driving, where quick decisions are required, the top-down representation of one's own body is a key mechanism in determining sides. Disturbances of this process, intensified by stress and environmental factors typical of road traffic (time pressure, complexity of road situations), constitute a real threat on the road [2, 6].

Additionally, studies on the late effects of laterality, including left-handedness, show that they can affect various aspects of functioning, including motor and perceptual skills [6, 11], which directly translates into driver competence.
In the context of research on laterality, it is also important to understand how various environmental and neurobiological factors may influence the development of laterality in children, which may be important in the context of early intervention and therapy [12, 13].

3. Concept and design of directional modules

The main design assumptions for directional modules embraced their universal use in any vehicle and minimization of eye refraction and interference with the driver's field of vision [4, 5]. The optimal installation location was found to be the vehicle's "A" pillars, i.e. the extreme elements of the body structure vertically limiting the windshield area which ensure constant access to information with minimal need for visual accommodation [6]. This location minimizes the risk of driver distraction while driving [2, 8].

The project was developed in cooperation with national psychologists and driving instructors to identify problems related to spatial orientation and reduce the driver's cognitive load [1, 3]. The module consists of a round base and three-dimensional letters "L" and "R". The colours applied guarantee immediate associative and intuitive recognition of the direction [5, 7]. The shape, and in particular the precisely designed inclination of the marker, was developed based on ergonomic studies to optimize the visual angle [6, 8]. The choice of the "L" and "R" symbols was based on the principles of cognitive ergonomics; they are universal, internationally recognized symbols that minimize the time needed for interpretation compared to more complex symbols. The production was carried out in the university laboratory of Mechanical Engineering Department using a high-quality 3D printing method from PLA/ABS materials, which ensures adequate durability and readability while maintaining low production costs.

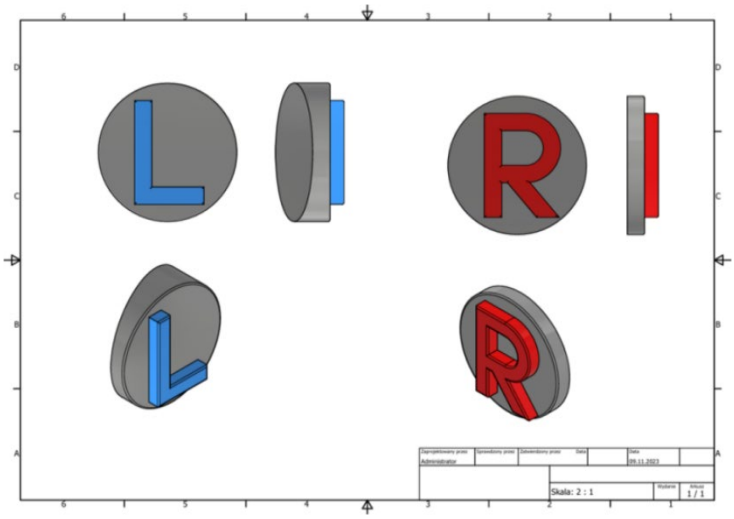

Fig. 1. 3D models of the directional markers ("L" and "R") applied, shown in projections: front, side and axonometric.

High-quality, non-invasive 3M VHB (Very High Bond) double-sided tape was used to mount the directional modules. This tape provides a durable, stable and vibration-resistant connection which is crucial for the safety and functionality of the orientation marker [2, 4]. Additionally, its non-invasive nature allows its easy disassembly without damaging the vehicle's structure, which is important for user convenience and maintaining the vehicle's value.

The device works by providing fast, precise and reliable directional information. Thanks to this, drivers can reduce the risk of errors in spatial orientation, especially in stressful conditions, which significantly improves safety in road traffic [6, 7]. Directional

modules provide practical support that directly helps in making quick decisions while driving, minimizing the impact of laterality disorders on driver behavior [5, 8].

4. Methodology of testing the impact of markings

The study was conducted in the form of a survey containing seven closed multiple-choice questions, addressed to people who drove a vehicle with the installed module.

• Number of respondents and representativeness

400 people participated in the study. The required number of participants was calculated based on data from the Central Register of Vehicles and Drivers (CEPiK) from years 2022-2024, which for the population of young drivers gave a representative sample of 382 people with a confidence level of 95% and a maximum error of 5% [14]. The collected sample (N=400) meets the criteria of representativeness. The sample was selected using a stratified random sampling technique, taking into account proportions by gender, age and experience of drivers from the CEPiK database.

• Spatial scope and respondent characteristics

The study covered the following poviats: Pilski and Wągrowiecki poviats, selected driving schools were invited to participate and the vehicles were equipped with directional markers. The research group was characterized based on the following criteria:

- Gender: The sample included 182 women (45.5%), 164 men (41%) and 54 people (13.5%) who did not reveal their gender [6].

- Age: The largest group were respondents aged 18-25 (59%, 236 people). Respondents aged 26-45 constituted 27% (108 people), and the smallest group (14%, 56 people) were people aged 46 and older [2, 3].

- **Driving experience:** 55% of respondents (220 people) identified themselves as "learners" and 45% (180 people) as "beginners" [7]. Additionally, the analysis included the factor of driving experience as a potential moderating variable. All participants met the criterion of having a valid category "B" driving license or being in the process of training for this category [14].

• Survey questionnaire The questionnaire consisted of seven closed, multiple-choice questions aimed at analyzing the scale of laterality problem, the presence of stress, reluctance to drive and the effectiveness of the proposed solution. Before the main study, a pilot survey was conducted to verify the clarity of questions and finalize the form [5].

• Statistical analysis

To verify the research hypotheses, statistical analysis was used using the chi-square test (χ^2) for nominal variables and correlation analysis. For all tests, the significance level was set at $\alpha = 0.05$. The analysis was performed using Statistica 13.3 software.

5. Research results (module impact analysis)

The study results reveal a significant scale of the left-right disorientation problem and its consequences, which are described in detail below.

“Problem with identifying right and left sides” (Question No. 4)

Confusion:

- Almost half of the respondents (44%) indicated that they always (22%) or very often (37%) noticed a problem with identifying the right and left side while driving [1].
- The rate of 37% (those indicating "very often") was identical among both men and women.
- The χ^2 test did not show any statistically significant differences in the frequency of LRI problem between genders ($\chi^2 = 0.84$, df = 1, $p > 0.05$).
- This problem was rarely or never indicated by 30% and 12% of respondents, respectively, mainly people under 20 and over 50.

“Presence of stress due to disorientation” (Question No. 5)

Stress:

- More than half of the participants (52.8%, 211 people) selected the answer "Yes", confirming that they experienced stress due to this problem [2].
- 25.5% (102 people) chose the "No" option, and 21.8% (87 people) indicated that the feeling of stress depends on the situation (answer "It depends").

“Reluctance to drive” (Question No. 6)

Reluctance:

- As many as 41% of respondents (164 people) declared reluctance to drive due to left-right side disorientation (answer "Yes") [2]. This result indicates serious psychological and social consequences of the LRI problem, beyond the maneuver error itself.
- 20.5% (82 people) selected "No", while 38.5% (154 people) stated that the decision depends on the circumstances (answer "Sometimes").

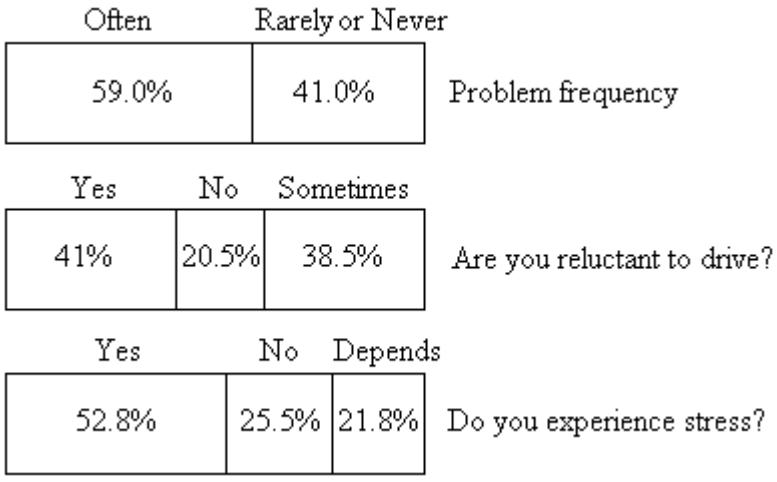

Fig. 2. Cumulative bar chart (100%) showing the relationship between the occurrence of a problem and its consequences among the surveyed individuals

The key conclusion regarding the effectiveness of the solution, based on the answers provided in **question No. 7**, is as follows:

Using Modules:

- A total of 53.8% of respondents (215 people) declared that they did use the accessories helping to identify the right and left side, offered by the installed modules [1].
- 25.5% (102 respondents) responded that the use of modules depended on the circumstances [2].
- 20.8% (83 respondents) did not use the accessory module [3].

The analysis of the reasons for not using the modules among 20.8% of respondents indicates several potential factors: lack of awareness of the existence of the LRI problem among some drivers, shame associated with admitting difficulties, preference to rely on one's own skills or insufficient promotion of the solution during the survey.

6. Discussion and verification of hypotheses

A detailed analysis of the results in the context of presented hypotheses allowed their verification. The table below summarizes this process.

Table 1. Verification of research hypotheses

Hypothesis	*Content*	*Verification*	*Grounds*
Main	Installing directional modules helped in coping with a stressful situation.	**Confirmed**	53.8% of respondents (215 people) used the accessories, which directly indicates the effectiveness of the solution. An additional 25.5% made their use dependent on the circumstances, suggesting that modules' usefulness depend on the situation. It should be noted, however, that the survey allows for conclusions about correlation, not causation - the declared use of the modules is associated with a positive perception of stress reduction and support in making decisions.
H1	Inability to distinguish between the sides causes stress more often in women than in men.	**Rejected**	The χ^2 test did not show any statistically significant differences in the frequency of LRI problem between genders ($\chi^2 = 0.84$, df = 1, $p > 0.05$). The identical percentage of men and women experiencing the problem "very often" (37%) provides strong evidence of no significant gender differences.
H2	The stress associated with the lack of ability to distinguish between left and right direction is correlated with the reluctance to drive.	**Confirmed**	The high percentage of people experiencing stress (52.8%) correlates with declarations of reluctance to drive (41%). Moreover, 38.5% of respondents made their reluctance dependent on the circumstances, which confirms the relationship between stressful disorientation and negative attitudes towards driving.
H3	The problem mainly affects people aged 18–25.	**Partially confirmed**	As many as 59% of respondents belonged to this group and they were the ones who most often declared difficulties, which confirms that this is a particularly susceptible group. However, the problem is not limited to this group, as it also occurs among older drivers (14% over 46 years of age), which indicates its broader nature.
H4	The problem is not related to gender.	**Confirmed**	The identical percentage of men and women experiencing the problem "very often" (37%) and the lack of statistical significance in the χ^2 test provide strong evidence for the lack of significant differences between genders in the occurrence of laterality disorders in the context of driving, which is confirmed by studies [1, 4].

• Limitations of the survey study

The main limitation of the study is its cross-sectional nature which prevents to make conclusions about the causality of the observed relationships. Despite the sample representativeness, the survey covered a limited geographical area, which may affect the generalizability of results [1, 4]. Furthermore, reliance on respondents' declarations may have introduced some degree of measurement error.

7. Final conclusions and further research directions

Accessory units in the form of ergonomic directional markers have proven helpful for most people struggling with laterality disorder. The fact that 53.8% of respondents actively used them, and another 25.5% used them depending on the situation, is a strong argument for the effectiveness of the solution in reducing stress and increasing the sense of safety in road traffic [2, 5].

The study results indicate that simple passive markers can be a more universal and cheaper solution compared to complex support systems, which is particularly important in the context of mass implementation. At the same time, 20.8% of respondents did not use the module, which indicates the need for further educational activities promoting such solutions and work on increasing their intuitiveness and accessibility [3, 6].

The survey encourages further development in this area, in particular towards technological integration, research on the combination of simple directional modules with advanced assistance systems such as GPS navigation or sign recognition systems, as well as possible connections with vehicle turn signals in order to create an automated, adaptive support system [5, 7]. It is worth emphasizing, however, that simple solutions often have the advantage of lower costs, greater reliability and wider availability.

Long-term studies using neuroimaging methods such as fMRI should also be conducted to better understand the neural correlates of the modules' effect on stress reduction and improvement of executive functions in drivers [8]. Moreover, it is worth analyzing the costs of implementing the solution on a mass scale compared to the potential social benefits, such as reducing the costs of road accidents [2,6]. It will also be important to monitor whether the use of modules changes positively over time as drivers gain experience [1, 3].

8. Bibliography

1. Mroziak, J. (1996). Zaburzenia spostrzegania. Agnozje. W: A. Herzyk & D. Kądzielawa (Red.) *Zaburzenia w funkcjonowaniu człowieka* (s. 11-52). Lublin: Wydawnictwo UMCS.
2. Mroziak, J. (1992). *Równoważność i asymetria półkul mózgowych*. Warszawa: Wydawnictwo Naukowe PWN.
3. Banasik, K. (2021). Znaczenie symetrii i asymetrii ludzkiego ciała w rozwoju mowy i motoryki dziecka. *Edukacja Elementarna w Teorii i Praktyce*, 16(5), 137-146. https://doi.org/10.35765/eetp.2021.1663.10

4. Hodgetts, S., & Hausmann, M. (2022). Sex/Gender Differences in Brain Lateralisation and Connectivity. *Current Topics in Behavioral Neurosciences*, 55, 1-25. https://doi.org/10.1007/7854_2022_303
5. Kurkowski, Z. (2018). *Lateralizacja słuchowa – wybrane problemy diagnozy i terapii*. Lublin: Wydawnictwo Polskie Towarzystwo Logopedyczne.
6. Gołyszny, M. (2021). Mózgowe (neuronalne) korelaty leworęczności: przyczyny i manifestacje z perspektywy neuronauk i nauk pedagogicznych. *Kwartalnik Pedagogiczny*, 66(2), 145-162. https://doi.org/10.19265/kp.2021.2.17.322
7. Kimura, D. (1967). Functional asymmetry of the brain in dichotic listening. *Cortex*, 3(2), 163-168.
8. Hellige, J. B. (1993). *Hemispheric asymmetry: What's right and what's left*. Cambridge, MA: Harvard University Press.
9. Mack, C., & Uomini, N. (2022). Modulation of behavioural laterality in wild New Caledonian crows (Corvus moneduloides): Vocalization, age and function. *Laterality: Asymmetries of Body, Brain and Cognition*, 27(4-6), 341-362. https://doi.org/10.1080/1357650X.2022.2098969
10. Ogata, H., Tanaka, H., & Hachisuka, K. (1999). Sound lateralisation in patients with left or right cerebral hemispheric lesions: Relation with unilateral visuospatial neglect. *Journal of Neurology, Neurosurgery & Psychiatry*, 67(4), 487-492.
11. Làdavas, E., & Pavani, F. (1998). Neuropsychological evidence of the functional integration of visual, auditory and proprioceptive spatial maps. *Neuroreport*, 9(6), 1195-1200.
12. Patel, K., Stotter, J., Pali, M. C., & Giannopulu, I. (2024). Imagine going left versus imagine going right: Whole body motion on the lateral axis. *Scientific Reports*, 14, 13933. https://doi.org/10.1038/s41598-024-57220-w
13. Kroliczak, G., & Przybylski, Ł. (2024). Handedness and the control of human technology and language. *Humanities and Social Sciences Communications*, 11, 1457. https://doi.org/10.1057/s41599-024-03985-4
14. Centralna Ewidencja Pojazdów i Kierowców. (2024). *Prawa jazdy wydane w latach 2022-2024*. Portal Gov.pl. Pozyskano z: https://www.gov.pl/web/cepik

Analysis of the security situation in the Pilski district

dr hab. inż. Piotr GORZELAŃCZYK

Department of Transport

Stanisław Staszic State University of Applied Sciences in Piła, Poland

https://orcid.org/0000-0001-9662-400X

corresponding e-mail: piotr.gorzelanczyk@ans.pila.pl

Abstract

Road safety remains one of the key challenges of transport policy at the local, regional, and national levels. Effective improvement of safety requires a reliable diagnosis based on the analysis of empirical data, taking into account both temporal and spatial conditions as well as the causes of road accidents. The aim of this article is to provide a comprehensive analysis of road safety in the Pilski district in the years 2018–2024.

The research material consisted of data from the police Accident and Collision Record System (SEWIK), covering 9,010 road incidents, including 265 accidents, 186 people slightly injured, 99 people seriously injured, and 58 fatalities [1]. The study used descriptive, structural, and comparative analysis methods, as well as an index-based assessment of the severity of incidents. The analysis covered the dynamics of changes in the number of incidents, their temporal and spatial distribution, environmental conditions, road infrastructure characteristics, and causes of incidents.

The results indicate that there was no clear trend towards improved road safety during the period analyzed and that there were significant differences in the severity of the consequences of events depending on the type of area and the time of their occurrence. Incidents outside built-up areas are characterized by particularly high mortality rates, while in urban areas, the high total number of incidents predominates. The analysis of the causes confirmed the dominant role of driver errors, especially failure to give way and speeding. Unprotected road users, especially pedestrians, are highly susceptible to serious injuries.

The results of the study provide a basis for formulating targeted recommendations for local road safety policy and can be used as a tool to support the decision-making process in safety management at the District level.

Keywords: road safety; road accidents; statistical analysis; local safety; SEWIK; accident victims; risk factors.

1. Introduction

Road safety has been one of the key challenges of transport policy and public health for many years, both globally and locally. Road accidents are among the leading causes of premature death and permanent injury, while generating significant social and economic costs. Despite technological advances, the development of driver assistance systems, and improvements in infrastructure standards, the scale of road traffic hazards remains a significant problem, especially in areas with a diverse functional and spatial structure.

The literature on the subject emphasizes that effective measures to improve road safety require a multidimensional approach, including analysis of human, infrastructural, environmental, and organizational factors. Increasingly, emphasis is also being placed on the importance of research conducted at the regional and local levels, which allows for the identification of specific conditions in a given area that are not visible in aggregated analyses at the national or provincial level. Local road safety assessments provide the basis for designing targeted interventions and the rational allocation of public funds.

The Piła, located in the northern part of the Wielkopolska Province, is characterized by significant spatial and functional diversity. The area includes both the city of Piła, which serves as the local administrative and communication center, and rural municipalities, where traffic is less intense but often has higher speed limits. The route of roads of various technical classes, including sections with a transit function, contributes to the occurrence of various traffic hazards, which makes the Pilski District an interesting subject for empirical research.

An analysis of data from 2018–2024 shows that a total of 9,010 road incidents were recorded in the Pilski District, including 265 accidents in which 343 road users were injured and 58 people were killed. This scale, when compared to the number of inhabitants and the structure of the road network, justifies the need for an in-depth analysis in terms of both quantity and quality. It is particularly important to identify the factors influencing the severity of road traffic incidents, including the role of speed, the type of road users, and environmental conditions.

Research conducted in Poland to date indicates that the behavior of road users, especially drivers, remains a key risk factor. Errors such as failure to give way or driving at speeds inappropriate for traffic conditions are consistently identified as the main causes of serious and fatal accidents. At the same time, there are significant variations in risk depending on the time of day, day of the week, and type of area, which confirms the validity of temporal and spatial analyses in road safety research.

The aim of this article is to provide a comprehensive analysis of road safety in the Pilski district in 2018–2024, with particular emphasis on the dynamics of changes in the number of incidents, the structure of victims, and temporal, spatial, and causal conditions. The author aims to identify areas of increased risk and the dominant mechanisms leading to road accidents with the most serious consequences. The results obtained may provide important decision-making support for local authorities, road administrators, and institutions responsible for shaping local road safety policy.

2. Literature review

The issue of RTS has been addressed in numerous articles. Pałegą [2] found road traffic risk indicators. At the provincial level, Wachnicka examined the variables influencing RTS (3). Rafalski examined RTS in Poland with a focus on large goods vehicles [4]. Furthermore, studies have investigated the causes of traffic accidents [5, 6]. Gądek-Hawlena and Los examined professional drivers' risky driving behaviours and evaluated the impact of heavy

vehicle solutions on RTS [7, 8]. Publications [11, 12] and books [9, 10] also provide general information on RTS. Road accident data also address this subject [1]. The work of [13–36] also addressed issues related to road safety.

With the exception of 2020 and the ongoing pandemic, Poland's automobile market has been expanding gradually. In 2022, there were 26,457,659 passenger cars registered [1]. Ten years ago, this figure stood at 18,744,412. Additionally, the number of cars per 1,000 people is increasing annually. According to the European Automobile Manufacturers Association (ACEA), Poland ranked 15th in Europe in 2011 with 470 cars per 1,000 people. According to the most recent data, Poland is set to top the European rankings in 2024, with the number rising to 703 cars per 1,000 people [37].

According to ACEA data, the average age of cars on Polish roads is over 15 years, compared to 12.3 years for the entire EU. This was certainly made possible by Poland's admission to the Schengen region and its membership of the European Union. Consequently, mass car imports began and international trade flourished [38].

3. Research hypotheses

Hypothesis H1 assumes that in the analyzed period 2018–2024, there is no clear downward trend in the number of road accidents in the Pilski district, despite the observed annual fluctuations. This hypothesis will be verified on the basis of an analysis of the linear trend in the total number of road accidents as a function of time. The average annual rate of change in the number of incidents and the sign and statistical significance of the trend function's direction coefficient were adopted as indicators. In addition, the interannual variability index will be used to assess the stability or instability of safety levels in subsequent years.

Hypothesis H2 assumes that road accidents in built-up areas are characterized by lower mortality than accidents occurring outside built-up areas, with a higher total number of accidents. To verify this hypothesis, a mortality rate indicator will be used, defined as the number of fatalities per 100 road accidents, calculated separately for built-up and non-built-up areas. In addition, the accident severity index, understood as the share of seriously injured and fatal victims in the total number of victims, will be used. A comparison of the values of the indices will allow for an assessment of the significance of the differences between these two types of areas.

Hypothesis H3 refers to the temporal variation in the risk of road accidents and assumes that the highest incidence of serious and fatal accidents occurs in the afternoon and on weekends, with particular emphasis on Saturdays. Verification of this hypothesis will be based on an analysis of the hourly and weekly distribution of accidents involving seriously injured and fatalities. The following indicators will be used: the percentage of serious and fatal accidents in a given time period in relation to all accidents, and the accident concentration index, which allows for the identification of periods of increased risk.

Hypothesis H4 assumes that the dominant causes of road accidents in the Pilski district are errors made by drivers, in particular failure to give way and failure to adjust speed to traffic conditions, and that these accidents are characterized by increased severity of consequences. This hypothesis will be verified by analyzing the structure of the causes of events and calculating the severity index for each category of causes. This index will be defined as the number of seriously injured and fatalities per 100 incidents in a given cause category. This will allow for an assessment of which driver behaviors generate the greatest risk of serious consequences.

Hypothesis H5 concerns a particularly vulnerable group of road users and assumes that, despite the relatively low number of incidents, pedestrians involved in road accidents suffer a

high rate of injury severity compared to other road users. Verification of this hypothesis will be based on a comparison of the severity rate of pedestrian injuries with analogous rates for drivers and passengers of vehicles. The severity rate will be defined as the proportion of seriously injured and fatal victims in the total number of victims in a given group of road users.

The hypotheses formulated in this way and the corresponding verification indicators enable an unambiguous assessment of road safety in the Pilski district and provide a solid methodological basis for further analysis of the results and their interpretation in the context of road safety management practice.

4. Materials and methods

The empirical basis for this study was a collection of data on road incidents recorded in the Pilski district between 2018 and 2024. The data came from the police Accident and Collision Recording System (SEWIK) and covered the entire population of road incidents recorded during the analyzed period, without sampling. A total of 9,010 road traffic incidents were analyzed, including 265 accidents in which 343 road users were injured and 58 people were killed.

The scope of the data included both quantitative and qualitative information describing road incidents. In particular, time variables (year, month, day of the week, time of the incident), spatial variables (District, municipality, town, street, intersection), environmental characteristics (weather and lighting conditions), road infrastructure features (type of accident location, road geometry, type of intersection, presence of traffic lights, speed limit), as well as information on road users, including vehicle type, age of victims, and type and severity of injuries. The data also made it possible to identify the direct causes of incidents, with particular emphasis on causes attributable to drivers, pedestrians, and factors beyond the control of road users.

The analysis of the research material was carried out in several complementary stages. In the first stage, a descriptive analysis was performed, including the determination of the number of incidents, accidents, and victims by degree of injury on an annual basis. This allowed for the assessment of the dynamics of changes in road safety over time and the identification of periods with an increased or decreased number of incidents. This was followed by structural analyses, which determined the distribution of incidents by month, day of the week, and hour, enabling an assessment of seasonality and daily and weekly risk patterns.

The next stage of the study focused on the spatial analysis of road incidents. The incidents were aggregated by municipality, town, and street, which allowed for the identification of areas with the highest concentration of incidents and accidents. Particular attention was paid to the city of Piła, where more than half of all road incidents in the District were recorded, as well as to selected transport routes and intersections characterized by a high frequency of collisions and accidents. This analysis was diagnostic in nature and provided the basis for identifying potential areas of increased risk.

An important element of the methodology was the assessment of the severity of road accident consequences. For this purpose, structural indicators were used, such as the share of seriously injured and fatal victims in the total number of victims, as well as the mortality rate calculated as the number of fatalities per 100 road accidents. These indicators were analyzed by built-up and non-built-up areas, type of accident location, speed limit, and lighting conditions, which made it possible to assess the impact of infrastructure and environmental factors on the scale of the consequences of accidents.

As part of the verification of research hypotheses, an analysis of the causes of road accidents was also carried out. The causes were classified according to the division used in the SEWIK system and then assessed in terms of frequency of occurrence and severity of consequences. Particular attention was paid to causes related to driver behavior, such as failure to give way and speeding, which in the analyzed data set were characterized by both high frequency and a significant share in accidents with the most serious consequences.

All analyses were secondary research and were carried out on aggregated data, maintaining the definitional consistency of variables throughout the analyzed period. The methodology adopted allows both for the assessment of the current state of road safety in the Pilski district and for the identification of key risk areas that may form the basis for further prognostic research and preventive measures at the local level.

Table 1. Road accidents and their consequences in the Pilski district in 2018–2024 [1]

Year	Number of Road Incidents	Number of Road Accidents	Number of Incidents with Minor Injuries	Number of Incidents with Serious Injuries	Number of Incidents with Fatalities
2018	1 382	50	40	16	12
2019	1 460	42	31	19	9
2020	1 241	34	24	10	5
2021	1 290	34	24	15	9
2022	1 163	38	25	11	8
2023	1 168	41	26	20	5
2024	1 306	26	16	8	10
Total	**9 010**	**265**	**186**	**99**	**58**

Table 2. Road accidents by month in the Pilski district (total for 2018–2024) [1]

Month	Number of Road Incidents	Number of Road Accidents	Number of Incidents with Minor Injuries	Number of Incidents with Serious Injuries	Number of Incidents with Fatalities
January	703	15	9	5	5
February	630	11	5	4	5
March	714	14	7	9	4
April	658	21	18	6	6
May	800	18	10	9	5
June	740	19	16	4	1
July	765	19	16	8	4
August	790	27	18	5	7
September	807	33	27	5	6
October	826	28	13	14	8
November	712	28	20	15	5
December	865	32	27	15	2
Total	**9 010**	**265**	**186**	**99**	**58**

Table 3. Road accidents by day of the week in the Pilski district [1]

Day of the week	Number of Road Incidents	Number of Road Accidents	Number of Incidents with Minor Injuries	Number of Incidents with Serious Injuries	Number of Incidents with Fatalities
Monday	1 452	36	25	16	6
Tuesday	1 359	43	21	19	15
Wednesday	1 327	41	28	10	10
Thursday	1 484	27	23	9	4
Friday	1 458	41	34	15	6
Saturday	1 123	50	35	18	15
Sunday	807	27	20	12	2
Total	**9 010**	**265**	**186**	**99**	**58**

Table 4. Road accidents by type of area in the Pilski district [1]

Type of area	Number of Road Incidents	Number of Road Accidents	Number of Incidents with Minor Injuries	Number of Incidents with Serious Injuries	Number of Incidents with Fatalities
Built-up area	6 417	141	95	43	11
Unbuilt area	2 593	124	91	56	47
Total	**9 010**	**265**	**186**	**99**	**58**

Table 5. Selected causes of road accidents and their consequences in the Pilski district [1]

Cause of the incident	Number of Road Incidents	Number of Road Accidents	Number of Incidents with Minor Injuries	Number of Incidents with Serious Injuries	Number of Incidents with Fatalities
Failure to yield right of way	1 806	58	56	15	4
Speeding	1 282	54	34	26	19
Hitting a pedestrian	262	76	36	31	11
Head-on collision	232	26	23	15	15

Table 6. Road accident victims by type of road user in the Pilski district [1]

Type of participant	Number of Incidents with Minor Injuries	Number of Incidents with Serious Injuries	Number of Incidents with Fatalities	Total
Passenger car	84	48	36	168
Bicycle	34	6	3	43
Motorcycle and moped	15	10	6	31
Other participants	16	3	2	21
Total	**149**	**68**	**47**	**264**

Table 7. Road accidents by time of day in the Pilski district (2018–2024) [1]

Time of day	Number of Road Incidents	Number of Road Accidents	Number of Incidents with Minor Injuries	Number of Incidents with Serious Injuries	Number of Incidents with Fatalities
00:00–05:59	824	29	19	14	9
06:00–11:59	2 476	61	42	18	11
12:00–17:59	3 584	108	79	42	23
18:00–23:59	2 126	67	46	25	15
Total	**9 010**	**265**	**186**	**99**	**58**

Table 8. Road accidents by lighting conditions in the Pilski district [1]

Lighting conditions	Number of Road Incidents	Number of Road Accidents	Number of Incidents with Minor Injuries	Number of Incidents with Serious Injuries	Number of Incidents with Fatalities
Daytime	5 712	148	104	46	21
Dusk, dawn	624	24	18	9	4
Nighttime – illuminated road	1 741	57	40	24	14
Nighttime – insufficient lighting	933	36	24	20	19
Total	**9 010**	**265**	**186**	**99**	**58**

Table 9. Road accidents by weather conditions in the Pilski district [1]

Weather conditions	Number of Road Incidents	Number of Road Accidents	Number of Incidents with Minor Injuries	Number of Incidents with Serious Injuries	Number of Incidents with Fatalities
Good weather conditions	6 521	183	127	69	36
Rain	1 541	41	31	17	9
Snowfall / slippery conditions	648	25	18	8	7
Fog / strong wind	300	16	10	5	6
Total	**9 010**	**265**	**186**	**99**	**58**

Table 10. Road accidents by type of location in the Pilski district [1]

Type of location	Number of Road Incidents	Number of Road Accidents	Number of Incidents with Minor Injuries	Number of Incidents with Serious Injuries	Number of Incidents with Fatalities
Intersection	3 842	89	71	25	11
Straight section of road	3 967	142	91	63	39
Pedestrian crossing	402	81	38	32	11
Other locations	799	53	42	17	7
Total	**9 010**	**265**	**186**	**99**	**58**

Table 11. Road accidents by type of intersection in the Pilski district [1]

Type of intersection	Number of Road Incidents	Number of Road Accidents	Number of Incidents with Minor Injuries	Number of Incidents with Serious Injuries	Number of Incidents with Fatalities
Equivalent	1 284	33	26	9	4
With right of way	1 936	42	37	14	5
With traffic lights	622	14	8	2	1
Roundabout	489	7	6	1	1
Total	**4 331**	**96**	**77**	**26**	**11**

Table 12. Road accidents by speed limit at the scene of the accident in the Pilski district [1]

Speed limit	Number of Road Incidents	Number of Road Accidents	Number of Incidents with Minor Injuries	Number of Incidents with Serious Injuries	Number of Incidents with Fatalities
do 50 km/h	5 938	133	94	41	14
60–70 km/h	1 247	42	29	18	9
80–90 km/h	1 428	63	38	27	21
> 90 km/h	397	27	25	13	14
Total	**9 010**	**265**	**186**	**99**	**58**

5. Results

Between 2018 and 2024, a total of 9,010 road incidents were recorded in the Pilski District, including 265 accidents. The annual analysis shows clear fluctuations in the number of incidents, with no clear downward trend throughout the entire period analyzed. The highest number of incidents was recorded in 2019 (1,460), while the lowest was in 2022 (1,163). In 2023–2024, an increase in the number of incidents was observed again, confirming the unstable nature of changes in road safety (Table 1).

The observed fluctuations, including the decline in the number of incidents in 2020–2021, may be partly related to mobility restrictions, but the fact that this trend did not continue in subsequent years confirms the validity of hypothesis H1.

The monthly analysis indicates a clear seasonality of road incidents. The highest number of incidents was recorded in the autumn and winter months, particularly in December (865) and October (826). The lowest values occurred in February (630) and April (658) (Table 2).

The weekly distribution confirms significant risk variation. The highest number of accidents and fatalities was recorded on Saturdays, which indicates an increased risk on non-working days (Table 3). These results confirm hypothesis H3 concerning the concentration of serious accidents on weekends.

The vast majority of road accidents occurred in built-up areas (71.2%), but an analysis of the consequences indicates a significantly higher mortality rate for accidents outside built-up areas (Table 4). The values obtained clearly confirm hypothesis H2 and indicate the key role of speed and the nature of infrastructure outside urban areas.

An analysis of the causes of accidents showed that errors made by drivers were the most common. The most frequently identified causes were failure to give way (1,806 accidents) and speeding (1,282 accidents). At the same time, these causes were characterized by a high number of seriously injured and fatal victims (Table 5).

The high proportion of fatalities in incidents related to speed and head-on collisions confirms hypothesis H4.

An analysis of the structure of victims shows that pedestrians and cyclists, despite their smaller numbers, have a high injury severity rate. The situation is particularly unfavorable for pedestrians, among whom the proportion of seriously injured and fatal victims is higher than in the case of passenger car users (Table 6).

The results confirm hypothesis H5 and indicate the particular vulnerability of unprotected road users to the serious consequences of road accidents.

Table 7 shows that the highest number of road incidents and their consequences occur in the afternoon (12:00–17:59), with 3,584 incidents, 108 accidents, and 23 fatalities recorded. This is the period of highest traffic activity, which indicates a significant impact of traffic intensity on the safety of road users. The fewest accidents and casualties were recorded at night (00:00–05:59), which may be due to lower traffic intensity, despite higher mortality per incident due to limited visibility.

The highest number of incidents and accidents occurred during the day, which corresponds to the natural activity of drivers, but the high number of fatalities occurs in conditions of insufficient night lighting (19 fatalities in 933 incidents), which highlights the risk associated with limited visibility (Table 8).

Table 9 shows that most road incidents occurred in good weather conditions (6,521 incidents), but a significant number of fatalities also occur in difficult weather conditions, especially in fog or strong winds (6 fatalities in 300 incidents), which indicates that not only the number of incidents but also the conditions conducive to accidents have an impact on their severity.

Analysis of Table 10 shows that the highest risk of serious accident consequences occurs on straight sections of road (63 seriously injured and 39 fatalities), even though the number of incidents is comparable to that at intersections. Pedestrian crossings show a relatively high number of accidents (81 accidents out of 402 incidents), which indicates a particular risk for pedestrians in this type of location.

Table 11 specifies the risk of accidents at intersections: intersections with right of way generate the most incidents and accidents (1,936 incidents and 42 accidents), while roundabouts are the least dangerous (489 incidents and 7 accidents), which may suggest the effectiveness of this type of infrastructure in reducing the number of accidents.

Table 12 shows the relationship between speed limits and accident consequences. The highest number of incidents occurs at speed limits of up to 50 km/h, which corresponds to increased traffic in urban areas. In contrast, the highest number of fatalities occurs on sections with speeds above 90 km/h (14 fatalities in 397 incidents), which indicates a higher accident mortality rate at higher speeds.

In summary, the data suggests that the main factors influencing the severity of road accidents in the Pilski district are: time of day (traffic activity), lighting conditions (especially at night), weather conditions (difficult conditions increase the risk of casualties), the location of the accident (straight sections and pedestrian crossings), and the speed limit. A combination of these factors allows us to identify priority areas for improving road safety, such as road lighting, speed limits in critical areas, and intersection infrastructure.

6. Discussion

An analysis of data on road accidents in the Pilski district between 2018 and 2024 confirms that road safety remains a complex problem, with no clear trend towards improvement. Annual fluctuations in the number of incidents, including a decline in 2020–2021 and an increase in subsequent years, indicate significant instability in safety levels, which may be partly related to mobility restrictions during the COVID-19 pandemic, but the lack of a sustained downward trend confirms hypothesis H1. Comparing these results with the national literature, there is consistency with the observations of other researchers who point

out that local changes in the number of accidents do not always reflect national trends, and the impact of random and seasonal factors may mask the effect of preventive measures.

Spatial analysis and area characteristics showed significant variation in risk depending on the type of development. Although most incidents occurred in built-up areas (71.2%), the highest mortality and proportion of seriously injured victims occurred outside the city, which clearly confirms hypothesis H2. These results highlight the key role of speed and road geometry in undeveloped areas. The data suggest that interventions to reduce speed and improve road infrastructure outside urban areas could significantly reduce serious accidents.

An analysis of the causes of incidents revealed a predominance of driver errors, in particular failure to give way and driving at speeds inappropriate for traffic conditions, which confirms hypothesis H4. The high proportion of these causes in the most serious incidents indicates the need to focus educational activities, enforce regulations, and implement infrastructure solutions that minimize the risk of driver errors, e.g., by installing speed bumps or traffic lights in critical locations.

The time analysis confirmed hypothesis H3, indicating that the highest risk of serious and fatal accidents occurs in the afternoon and on weekends, with particular emphasis on Saturdays. This observation is consistent with previous studies indicating that traffic intensity and driver fatigue during these periods increase the likelihood of road incidents. These results suggest that preventive measures, such as speed checks and information campaigns, should be targeted at specific time periods.

An analysis of road users showed that pedestrians and cyclists are highly vulnerable to serious injuries, confirming hypothesis H5. The results indicate that safety interventions for vulnerable road users, including improvements to pedestrian crossing infrastructure, segregation of pedestrian and bicycle traffic, and speed limits in high-risk areas, are key to reducing the number of casualties.

Further conclusions are drawn from the analysis of environmental and infrastructure conditions. The high number of casualties in poorly lit roads at night and on straight road sections confirms the importance of visibility and road geometry for the severity of accidents. In addition, the results indicate that not only weather conditions, but also location and speed limits have a key impact on the consequences of accidents. The highest number of fatalities occurred on sections with speed limits above 90 km/h, confirming the importance of speed control and restrictions where the risk of serious accidents is greatest.

In the context of planning preventive measures, the results suggest the need for a multidimensional approach including: infrastructure modernization (especially intersections and pedestrian crossings), improved road lighting, speed limits in critical areas, and educational and control measures targeting drivers. In addition, local diagnosis enables better allocation of public funds in a targeted manner, in line with identified areas of increased risk.

In summary, the study shows that local road safety analyses provide valuable information not only about the number of incidents, but also about the mechanisms leading to their most serious consequences. These results can serve as a basis for shaping effective safety policies at the District level and are also a starting point for further prognostic and evaluative research.

An analysis of road accidents in the Pilski district between 2018 and 2024 indicates an unstable level of road safety, with no clear downward trend in the number of accidents. Most accidents occur in built-up areas, but the most serious consequences, including high mortality, are recorded outside cities. The main causes of accidents are driver errors, especially failure to give way and driving at speeds inappropriate for traffic conditions. Pedestrians and cyclists are particularly vulnerable road users, exposed to serious injuries. The risk of accidents is strongly correlated with the time of day and week, lighting and weather conditions, and the nature of the road infrastructure, including the type of road section and speed limit.

The results confirm the validity of a multidimensional approach to road safety analysis and indicate the need for targeted preventive measures tailored to local conditions.

7. Recommendations

1. Speed reduction and infrastructure improvement on roads outside built-up areas – especially on straight sections with high mortality rates. Introduction of speed bumps, protective barriers, and clear speed limit signage.
2. Improving safety for pedestrians and cyclists – modernizing pedestrian crossings, segregating pedestrian and bicycle traffic, increasing visibility (lighting, traffic lights, vertical and horizontal signage).
3. Optimization of intersections – introduction of roundabouts or traffic lights where there is a high number of accidents, especially involving pedestrians, in order to reduce the risk of collisions.
4. Control and enforcement of traffic regulations – focusing on drivers who fail to give way and exceed speed limits; periodic intensification of controls in the afternoons and at weekends.
5. Improvement of lighting conditions – especially on roads outside cities, in areas with a high number of night-time accidents, in order to reduce the fatal consequences of incidents.
6. Educational activities – information campaigns and training for drivers, pedestrians, and cyclists, with particular emphasis on the risks associated with speeding and inattention in traffic.
7. Seasonal and temporal risk analysis – monitoring and adjusting preventive measures in months with an increased number of incidents and in the afternoons and at weekends.
8. Use of local data for safety policy planning – further predictive and evaluative research, targeting high-risk areas and specific types of road users.

8. References

1. Road accidents - Sttisstics [online] [accessed 2026-01-23]. Available from: https://sewik.pl/
2. Palega, M. Traffic safety in Poland in the light of road accidents and their consequences. *Buses: technique, exploitation, transport systems*. 2017. 18, no. 12
3. Wachnicka, J. Research on factors influencing road traffic safety in provinces *Transport Miejski i Regionalny* 4/2012.
4. Rafalski, L. Safety of road traffic in Poland with special reference to heavy vehicles Conference: *Safety in road and rail transport* At: Warsaw. Volume: 1 https://doi.org/10.13140/2.1.1013.5683
5. Klepacki, B., Koper, B. Road safety in the opinion of its participants. Science notebooks. *Warsaw University of Life Sciences in Warsaw Economics and Organization of Logistics* 3 (3) 2018
6. Gądek-Hawlena, T., Los, M. Modern solutions in heavy duty vehicles and their impact *Science notebooks. Warsaw University of Life Sciences in Warsaw Economics and Organization of Logistics 3* (3) 2018
7. Orłowski, Ł., Wszeborowski, R. Safety in road traffic. *Safety in Road Traffic Logistic Systems of the Army* 53/2020. https://doi.org/10.37055/slw/133858
8. Yannis G., Papadimitriou E. Road Traffic Safety, *International Encyclopedia of Transport,* 2021, https://doi.org/10.1016/B978-0-08-102671-7.10613-X

9. Bąk-Gajda, D., Bąk, J. *Psychology of Transport and Road Traffic Safety*, Difin 2010. 11.
10. Wicher, J. *Car and road safety*, Publishing House of Communication and Communications, Warsaw 2012.
11. Wojtas, A., Szkoda, M. Analysis of selected factors affecting safety in road traffic, *Buses* 2018, no. 6, p. 1149.
12. Zbyszyński, M. Safety of Unprotected Road Traffic Participants - Present and Future Status, *Motor Transport Magazine*. 2017. vol. 1 pp. 49-64.
13. Golakiya, H. D., Chauhan, R., Dhamaniya, A. Evaluating safe distance for pedestrians on urban midblock sections using trajectory plots. *European TransportTrasporti* Europei. 2020. Issue 75. Paper no 2. ISSN 1825- 3997.
14. Wachowiak, P., Gorzelańczyk, P., Kalina, T. Analysis of the effectiveness of shock absorbers in the light of Polish and Slovak regulations. *Coaches. Technika, Eksploatacja, Systemy Transportowe* 2018, vol. 220, no. 6, pp. 764-770
15. Gorzelańczyk, P., Górniak, W. Assessment of the technical condition of tires for forklifts used in internal transport by examining damage and operating conditions. *Engineering Sciences and Technologies*. 2019, no. 2 (33), pp. 44-59.
16. Ashish, Mhaske, S. Y. (2023). Road Safety Audit (RSA) Guidelines of Selected Nations - a Comparative Review. *Journal of Road Safety,* 34(4), 42-50. https://doi.org/10.33492/ JRS-D-23-209291
17. Eskandari Torbaghan, M., Sasidharan, M., Reardon, L., Muchanga-Hvelplund, L. C. W. (2022). Understanding the potential of emerging digital technologies for improving road safety. *Accident Analysis Prevention,* 166, 106543. https://doi.org/10.1016ZJ.AAP.2021.106543
18. Giribabu, D., Ghosh, K., Hari, R., Chadha, I., Rathore, S., Kumar, G., Roy, S., Joshi, N. K., Bharadwaj, P., Bera, A. K., Srivastav, S. K. (2024). Road accidents on Indian National highways, ambulance reachability and transportation of injured to trauma facility: Survey-based introspection of golden hour. *Journal of Family Medicine and Primary Care,* 13(2), 704-712. https://doi.org/10.4103/jfmpc. jfmpc_1832_23
19. Joshi, E., Gautam, P., Khadka, A., Pilkington, P., Parkin, J., Joshi, S. K., Mytton, J. (2022). Experience of living near a highway in Nepal: Community perceptions of road dangers in Makwanpur district. *Journal of Transport and Health,* 24. https://doi.org/10.1016/j. jth.2022.101337
20. Katsarov, I., Penkov, S. (2023). Application of artificial intelligence in road network inventory and network-wide road safety assessment. *IOP Conference Series: Materials Science and Engineering,* 1297(1), 012020. https://doi. org/10.1088/1757-899x/1297/1/012020
21. Kaul, A., Altaf, I. (2022). Vanet-TSMA: A traffic safety management approach for smart road transportation in vehicular ad hoc networks. International Journal of Communication Systems, 35(9). https://doi.org/10.1002/ dac.5132
22. Regmi, M. B. (2021). What does it Take to Improve Road Safety in Asia? *Journal of Road Safety,* 32(4), 29-39. https://doi.org/10.33492/JRS-D-21-00040
23. Shafiq, S., Dahal, S., Siddiquee, N. K. A., Dhimal, M., Jha, A. K. (2020). Existing Laws to Combat Road Traffic Injury in Nepal and Bangladesh: A Review on Cross Country Perspective. In *Journal of Nepal Health Research Council* (Vol. 17, Issue 4, pp. 416-423). NLM (Medline). https://doi.org/10.33314/jnhrc. v17i4.2363
24. Tiwari, H., Luitel, S. (2023). Re-orienting towards Safer Roads Infrastructure in Nepal. *Journal of Recent Activities in Infrastructure Science,* 8(3), 14-26. https://doi.org/10.46610/jorais.2023. v08i03.003
25. Toriumi, A., Abu-Lebdeh, G., AlhajyaseeN, W., Christie, N., Gehlert, T., Mehran, B.,

Mussone, Shawky, M., Tang, K., Nakamura, H. (2022). A multi-country survey for collecting and analyzing facts related to road traffic safety: Legislation, enforcement, and education for safer drivers. *IATSS Research,* 46(1), 14-25. https://doi.org/10.1016/j.iatssr.2022.01.004

26. Wei, L., Li, Z., Gong, J., Gong, C., Li, J. (2021). *Autonomous Driving Strategies at Intersections: Scenarios, State-of-the-Art, and Future Outlooks.* https://doi.org/10.1109/ITSC48978.2021.9564518
27. Tomasch, E.; Gstrein, G. Correlation of Road Safety Criteria with Occupant Safety Criteria in Impacts on Crash Cushions. *Infrastructures* 2024, *9*, 136. https://doi.org/10.3390/infrastructures9080136
28. Ziegler, J.; Unger, T.; Spitzhüttl, F.; Malcyk, A. *Anforderungen an Schutzeinrichtungen neben der Fahrbahn*; Unfallforschung der Versicherer: Berlin, Germany, 2022.
29. Meng, Y.; Untaroiu, C. Numerical investigation of occupant injury risks in car-to-end terminal crashes using dummy-based injury criteria and vehicle-based crash severity metrics. *Accid. Anal. Prev.* 2020, *145*, 105700.
30. Tomasch, E.; Gstrein, G. Impacts on Crash Cushions—Analysis of the Safety Performance of Passenger Cars with Improved Safety Equipment Compared with Test Vehicles Based on Assessment Criteria as Defined in EN 1317. *Infrastructures* 2024, *9*, 59.
31. Tomasch, E.; Heindl, S.F.; Gstrein, G.; Sinz, W.; Steffan, H. Assessment of the Effectiveness of Different Safety Measures at Tunnel Lay-Bys and Portals to Protect Occupants in Passenger Cars. *Infrastructures* 2021, *6*, 81.
32. Davidović, J., Antić, B., & Pešić, D. (2024). The importance of road safety inspection for the improvement of pedestrian safety in traffic. Journal of Road and Traffic Engineering, 70(2), 45-51. https://doi.org/10.31075/PIS.70.02.06
33. Семченко, Н. О., Ніколаєнко, І. В., Маслак, Г. В., & Хара, М. В. (2024). Оцінювання динаміки зміни показників безпеки руху в україні. *Транспортні системи та технології перевезень*, (28), 52–59. https://doi.org/10.15802/tstt2024/312024
34. Alokwu Stella O., Ewuim Ngozi C., Obi Emeka F. and Asoya Nkem P. Human Approach to Road Safety Administration in Nigeria'sFederal Road Safety Commission. International Journal of Academic Multidisciplinary Research (IJAMR)ISSN: 2643-9670Vol. 5 Issue 8, August - 2021, Pages: 92-97. www.ijeais.org/ijamr92
35. Delmondes Chaves, Gustavo Vinicius. Governmental Expenditures and the Challenges to Improve Road Safety in Brazil. Journal of Public Administration and Governance, [S.l.], v. 14, n. 2, p. Pages 125-141, nov. 2024. ISSN 2161-7104. doi:http://dx.doi.org/10.5296/jpag.v14i2.22370.
36. Gustavo Vinicius Delmondes Chaves Governmental Expenditures and the Challenges to Improve Road Safety in Brazil. Journal of Public Administration and Governance ISSN 2161-7104 2024, Vol. 14, No. 2
37. Automotive indexes in the EU, by country and vehicle type. [online] [accessed 2022-01-21]. Available from: https://www.acea.be/statistics/tag/category/vehicles-per-capita-by-country/
38. PZMOT. [online] [accessed 2022-01-21]. Available from: https://www.pzpm.org.pl/content/download/2591/10569/file/park%20pojazdow%20PL%201990_2018.pdf

ISSN 3071-9216

Wydawca | Published by: Akademia Nauk Stosowanych im. Stanisława Staszica w Pile
ul. Podchorążych 10, 64-920 Piła
Katedra Inżynierii Mechanicznej, Budynek J, pok. 33 (adres siedziby redakcji)
www.ans.pila.pl
https://wydawnictwo.ans.pila.pl